Mécanismes de régulation impliqués dans la résistance aux antibiotiques chez Mycobacterium abscessus

Matthias Richard

THÈSE POUR OBTENIR LE GRADE DE DOCTEUR DE L'UNIVERSITÉ DE MONTPELLIER

En Microbiologie

École doctorale CBS2

Unité de recherche : Pathogénie Mycobactérienne et Nouvelles Cibles Thérapeutiques

Mécanismes de régulation impliqués dans la résistance aux antibiotiques chez *Mycobacterium abscessus*

Présentée par Matthias RICHARD
Le 25 novembre 2019

Sous la direction de Laurent KREMER

Devant le jury composé de

Stéphane CANAAN, Directeur de Recherche, Laboratoire d'Ingénierie des Systèmes Macromoléculaires	Président du jury
Jean-Luc MAINARDI, Professeur, Institut de Recherche des Cordeliers	Rapporteur
Franck BIET, Directeur de Recherche, INRA Val de Loire	Rapporteur
Hélène MARCHANDIN, Professeur, Université de Montpellier-CHU de Nîmes	Examinateur
Ruben HARTKOORN, Chargé de Recherche, Institut Pasteur de Lille	Examinateur
Laurent KREMER, Directeur de Recherche, Institut de Recherche en Infectiologie de Montpellier	Directeur de thèse

UNIVERSITÉ DE MONTPELLIER

Remerciements

Je remercie grandement les membres de mon jury,

Le Professeur Jean-Luc Mainardi et le Docteur Franck Biet,

Pour avoir accepté d'évaluer mon manuscrit de thèse en tant que rapporteurs.

Le Professeur Hélène Marchandin et le Docteur Ruben Hartkoorn,

Pour avoir accepté d'évaluer mon travail de thèse en tant qu'examinateurs.

Le Docteur Stéphane Canaan,

D'avoir fait l'honneur de présider mon jury de thèse.

J'adresse de chaleureux remerciements à toutes les personnes de l'équipe de recherche parmi laquelle j'ai fait partie ces 3 ans et demi,

Le Docteur Laurent Kremer mon directeur de thèse,

D'avoir guidé et supervisé en me faisant confiance ainsi qu'en me permettant de développer un esprit critique et scientifique, à qui j'adresse l'expression de ma profonde gratitude.

Le Docteur Mickael Blaise,

De m'avoir enseigné toutes ces techniques de biochimie et de cristallogenèse.

Le Docteur Albertus Viljoen,

De m'avoir permis d'acquérir autant de connaissances en matière de biologie moléculaire.

Mais également nos collaborateurs,

Le Docteur Stéphane Canaan et le Docteur Jean-François Cavalier,

D'avoir grandement participés à la publication de mon premier article en tant que premier auteur.

Ainsi que les membres de mon comité de suivi de thèse,

Le Docteur Edouard Tuaillon et le Docteur Alain Baulard,

De m'avoir aiguillé et conseillé les deux premières années de ma thèse.

Un grand merci également à tous mes collègues de l'IRIM, dont beaucoup sont devenus des amis par la suite,

De m'avoir fait passer autant de bons moments intra comme hors institut, scientifiques ou non.

Et bien sûr je remercie infiniment ma famille, *mes parents et mes frères,* ***mes amis,*** *d'Ardèche mais aussi de Montpellier et bien plus loin encore,* ***et mes proches,*** *Ana Victoria,* ***de m'avoir soutenu pendant cette aventure.***

Table des matières

Index des Figures et de la Table

Å : angström

AAC(2') : aminoglycoside 2'-acétyltransférase

ABC : ATP-binding cassette

ADN : acide désoxyribonucléique

AMK : amikacine

ARN : acide ribonucléique

ARNr : ARN ribosomique

ARNt : ARN de transfert

AT-Hook : domaine riche en adénosine et thymine

ATP : adénosine triphosphate

ATS : American Thoracic Society

AZM : azithromycine

BDQ : bédaquiline

BPCO: broncho-pneumopathies chroniques obstructives

CoA : coenzyme A

CLSI : Clinical & Laboratory Standards Institute

CLR : clarithromycine

CFTR : cystic fibrosis transmembrane conductance regulator

CFX : céfoxitine

CFZ : clofazimine

cMBT : carboxymycobactine

CMI : Concentration minimale inhibitrice

DAT : diacyle tréhalose

DNA_{op} : ADN opérateur / ADN cible

DTT : dithiothréitol

Eis : enhanced intracellular survival

EMB : éthambutol

Erm : erithromycine resistance methylase

ESAT6 : early secretory antigenic target of 6 kDa

ESX : ESAT6 secretionsystems

ETH : éthionamide

ETZ : electron translucent zone

facteur σ : facteur sigma

FAD : flavine adénine dinucléotide

GC% : taux de guanine – cytosine

GDND : glycosyl diacylated nonadecyl diol

GPL : glycopeptidolipide

Gram - : Gram négative

Gram + : Gram positive

GW-rich : domaine riche en glycine – tryptophane

h-α : hélices-α

HTH : helix – turn – helix

IDSA : Infectious Diseases Society of America

IL : interleukine

IFN : interféron

INH : isoniazide

IPM : imipénème

KAN : kanamycine

Kb : mille paires de base

kDa : kilo dalton

LAM : lipoarabinomannane

LBP : ligand binding pocket

LM : lipomannane

LNZ : linézolide

LPS : lipopolysaccharide

MALDI-TOF : matrix-assisted laser desorption/ionisation – time of flight

MarR : multiple antibiotic resistance regulator

MATE : multidrug and toxic compound extrusion

Mb : un million de paires de bases

MBT : mycobactine

MEW : mycolic ester wax

MCL : mycobactérie à croissance lente

MCR : mycobactérie à croissance rapide

MDR-Tb : tuberculose multi résistante

MFX : moxifloxacine

MFP : membrane fusion-like protein

MMDAG : monomeromycolyl diacylglycerol

MmpL : mycobacterial membrane protein large

MmpS : mycobacterial membrane protein small

MNC : minocycline

MNT : mycobactérie non-tuberculeuse

MQ : ménaquinone

NAD : nicotinamide adénine dinucléotide

NAG : N-acétylglucosamine

NAM : N-acétylmuramique

NDH-2 : NADH oxydoréductase de type II

NGM : N-glycolylmuramique

OMF : outer-membrane factor

OMS : Organisation Mondiale de la Santé

PAT polyacyle tréhalose

pb : paire de base

PCR : polymerase chain reaction

PDIM : phthiocerol dimycocerosate

PHE : public health England

PIM : phosphatidyl-*myo*-inositol mannoside

Pks : polykétide synthase

PL : phospholipide

PMF : force proto-motrice

PMA : pays les moins avancés

qRT-PCR : quantitative real-time PCR

R : rough / rugueux

RGO : reflux gastro-œsophagien

RND : resistance nodulation cell division

ROS : reactive oxygen species

S : smooth / lisse

SARM : *Staphylococcus aureus* résistant à la méthicilline

SCFM : synthetic cistyc fibrosis sputum

SGL : sulfoglycolipide

SL : sulfolipide

SMR : small multidrug resistance

SNC : système nerveux central

SMARt : small molecule aborting resistance

SPM : streptomycine

TAC : thiacétazone

TACa : analogues structuraux du TAC

TBM : tobramycine

TDM : tréhalose dimycolate

TDZ : tédizolide

TetR : tetracycline repressor

TGC : tigécycline

TLR : toll-like receptor

TM : transmembranaire

TMM : tréhalose monomycolate

TNF : tumor necrosis factor

TPP : tréhalose polyphléate

Whi : white mutants

WHO : world health organisation

ZF : zebrafish/poisson-zèbre

Introduction

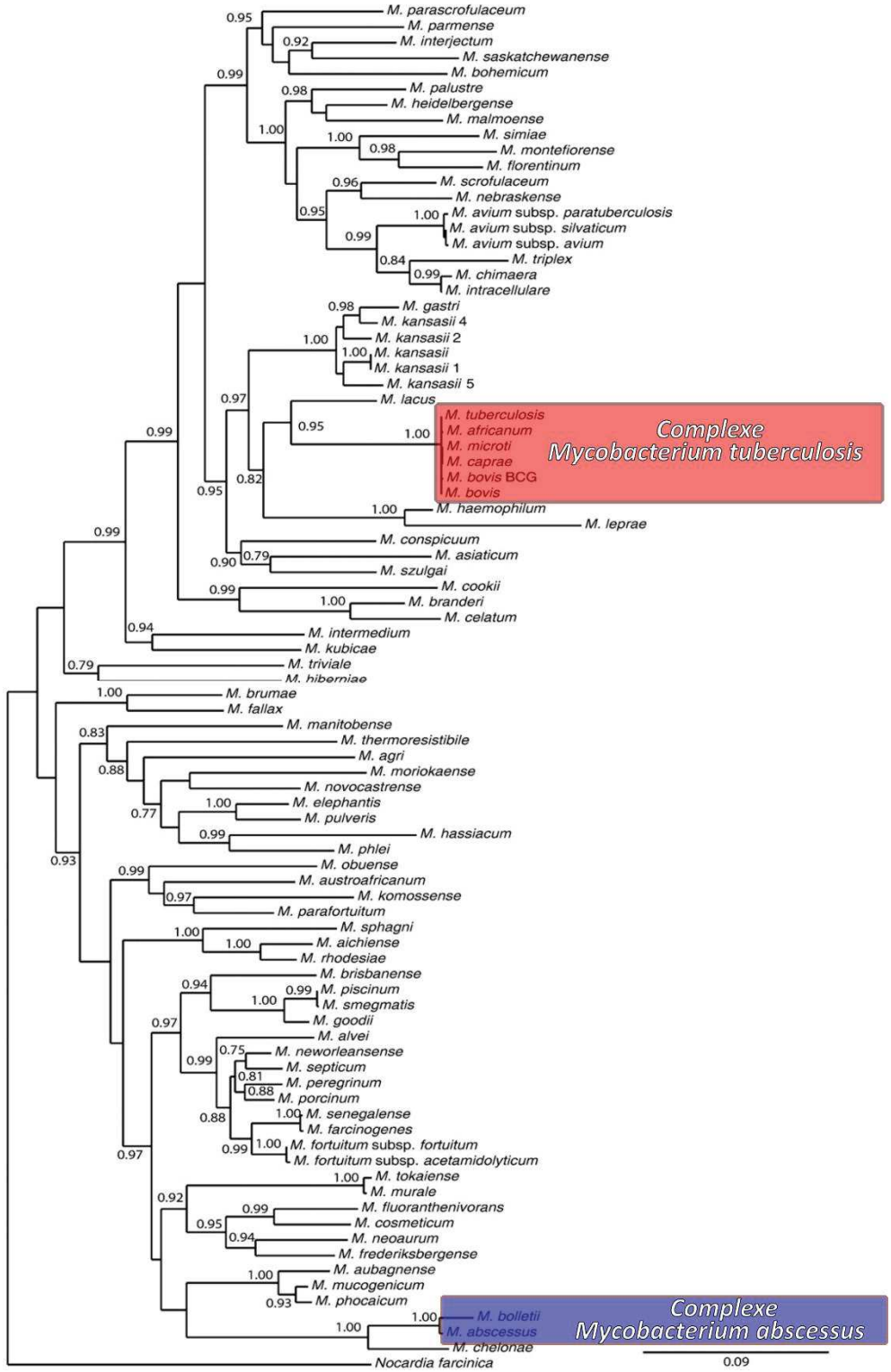

Figure 1. Arbre phylogénétique basé sur l'analyse de la séquence complète de 7 gènes (*ARN16S*, *hsp65*, *rpoB*, *smpB*, *sodA*, *tmRNA* et *tuf*) sur 87 espèces de mycobactéries. *Nocardia farcinica* a été utilisée comme *outgroup*. La bar représente 0,09 substitution de nucléotide par site (Adapté de Mignard et Flandrois 2008).

1) Phylogénie et niches écologiques :

Les mycobactéries appartiennent au phylum des *actinobacteria*. Ces bactéries, pour la plupart des Gram positives (Gram +), sont des microorganismes saprophytiques que l'on retrouve dans l'eau et le sol sous forme solide ou en aérosol mais également chez toute une variété d'organismes supérieurs. La notoriété de ces organismes leur vient principalement du fait que certains d'entre eux sont de grands producteurs d'antibiotiques de différentes classes comme les macrolides, les aminoglycosides, les rifamycines, les tétracyclines, les β-lactamines et les glycopeptides (Genilloud 2017). Ces antibiotiques ainsi que leurs dérivés sont aujourd'hui largement utilisés en clinique. Les mycobactéries ne produisent aucune classe d'antibiotiques et sont connues pour des raisons bien plus funestes, car étant notamment responsables de maladies comme la lèpre et la tuberculose. Elles appartiennent à la famille des *Mycobacteriaceae*, au sein du sous-ordre des *Corynebacterineae* et de l'ordre des *Actinomycetales*. La phylogénie mycobactérienne a évolué ces dernières années grâce à l'ajout de 6 gènes très conservés (*hsp65*, *rpoB*, *smpB*, *sodA*, *tmRNA* et *tuf*) au séquençage de l'*ARNr 16S*, qui était utilisé seul auparavant (Mignard et Flandrois 2008). Les techniques de séquençage à haut débits permettant une analyse complète du génome y ont aussi contribuées. On dénombre à ce jour près de 200 espèces de mycobactéries (http://www.bacterio.net/mycobacterium.html) dont la grande majorité sont des bactéries environnementales non-pathogènes. On parle ici de MycobactériesNon-Tuberculeuses (MNT) qui s'opposent aux bactéries appartenant au complexe de *Mycobacterium tuberculosis* (Figure 1). Cependant, certaines de ces MNT se révèlent capables d'infecter plusieurs espèces animales comme des poissons, des amphibiens, des oiseaux ainsi qu'une grande variété de mammifères incluant des animaux d'élevage (bovins, chèvres et moutons) et également l'homme (Medjahed et al. 2010)(Palmer et al. 2011). Cette grande variété de niches écologiques auxquelles ont été exposées ces bactéries se traduit par une forte capacité d'adaptation. Cette force est le reflet d'un large arsenal génétique pour à la fois compétiter avec d'autres microorganismes (résistances aux antibiotiques, acquisition de nutriments) et manipuler leurs éventuels hôtes lors du processus infectieux (survie intramacrophagique, manipulation du système immunitaire et latence).

2) Caractéristiques microbiologiques et génétiques :

Une des grandes spécificités des mycobactéries est leur importante masse lipidique, près de 40 % du contenu cellulaire, que l'on retrouve principalement dans la paroi, qui renferme également

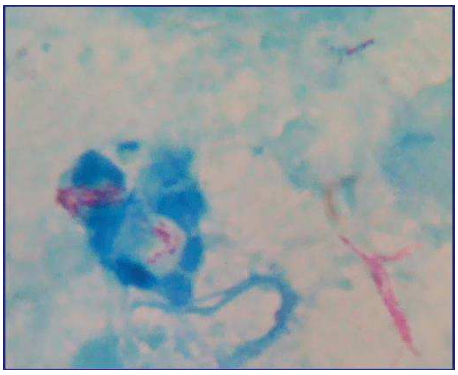

Figure 2. Coloration de mycobactéries par la technique de Ziehl-Neelsen. Les bacilles sont colorés en rose car leurs parois très hydrophobiques ont retenu la fuschine phénylée. Les structures bleues peuvent être des polynucléaires ou des cellules épithéliales.

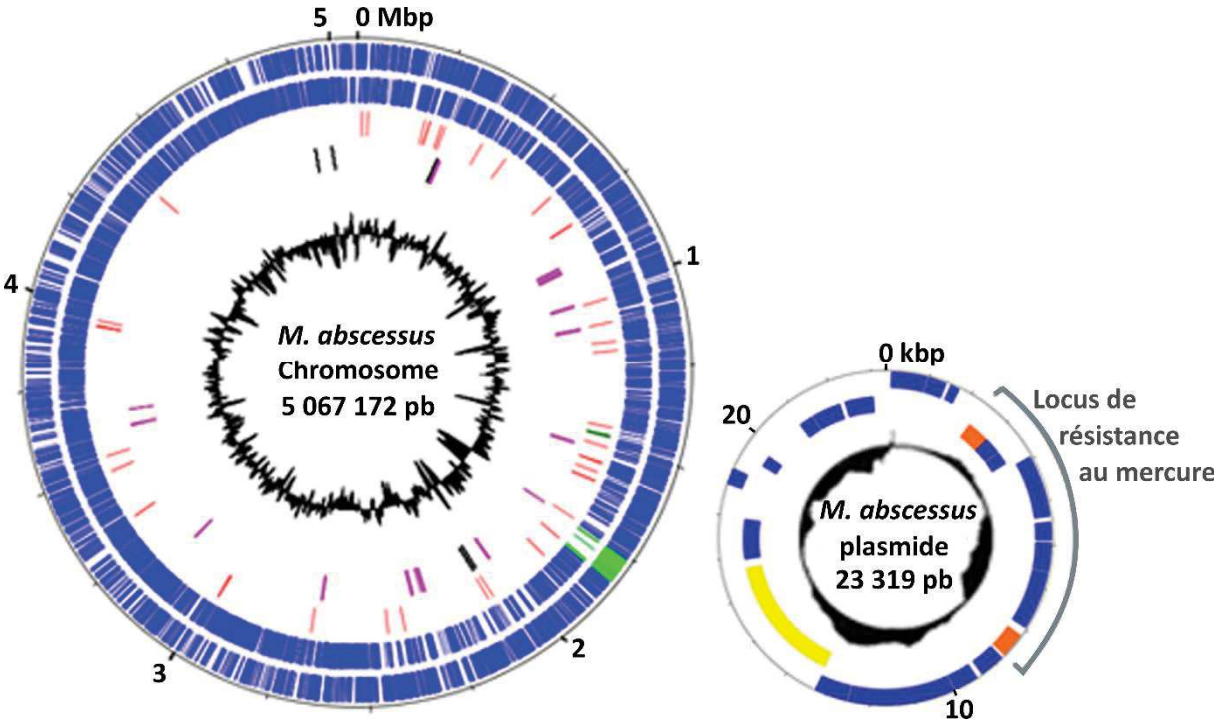

Figure 3. Cartes génétiques du chromosome et du plasmide circulaires de *M. abscessus* CIP104536^{T}. En ce qui concerne le chromosome, le cercle bleu le plus externe montre les gènes mycobactériens transcrits dans le sens de l'annotation génomique. Le cercle bleu sous-jacent montre les gènes mycobactériens transcrit en anti-sens. Les gènes phagiques sont en verts. En partant de l'extérieur, les troisième et quatrième cercles représentent les ARNt et les ARNr. Le plasmide est annoté de la même façon que le chromosome. Les parties oranges et jaune codent pour des recombinases et des éléments nécessaires à la conjugaison du plasmide. Les cercles noirs au centre représentent le GC%. (Adapté de Ripoll et al. 2009)

une grande variété de sucres et de protéines (Chiaradia et al. 2017). Les mycobactéries sont les seulesà répondre à la coloration de Ziehl-Neelsen grâce à leurs propriétés acido-alcoolo-résistantes (Vilchèze et Kremer 2017). Cette technique est basée sur la capacité des bactéries à retenir un colorant phéniqué, la fuschine, à la suite d'un lavage avec un mélange acido-alcoolique. La rétention de la fuschine est due à la grande hydrophobicité de la paroi des mycobactéries et leur donnera une couleur rose (Figure 2). Tout autre type de bactéries sera décoloré, étant donné le manque de glycolipides permettant de piéger ce colorant. Une étape supplémentaire consiste à ajouter du bleu de méthylène donnant l'aspect visuel caractéristique de cette coloration, bacilles rouges si l'échantillon est positif, sur fond bleu. Cette coloration s'effectue sur un frottis qui sera ensuite examiné au microscope. Ces mycobactéries sont des bacilles d'une taille comprise entre 1 et 4μm de long pour un diamètre de 0,3 à 0,5μm, non-flagellés et non-sporulants avec un métabolisme à aérobie strict (Cook et al. 2009). Parmi les actinomycètes, le genre *Mycobacterium* a le plus haut taux de Guanine et de Cytosines (GC%) au sein de leurs ADN. Egalement appelé coefficient de Chargaff, ce GC% serait synonyme de meilleure stabilité de d'ADN et des structures dérivant de l'ARN, comme les ARNr et les ARNt. L'environnement dans lequel un phylum a évolué est en majeure partie responsable de ce plus ou moins haut GC% (Foerstner et al. 2005). Leurs génomes sont sous formes d'un chromosome circulaire d'une taille comprise entre 3,27 millions de paires de base (Mb) pour *M. leprae TN* et 7,69 Mb pour *M. brisbanense UM_WWY*, appartenant au complexe de *M. fortuitum* (Wee et al. 2017). La taille du génome est généralement signe de capacité d'adaptation. *M. leprae* a un génome extrêmement réduit qui reflète son mode de vie uniquement intracellulaire. Le génome de *M. abscessus* compte un peu plus de 5 Mb supplémentées par un plasmide de 23 000 paires de bases (Kb), avec un GC% de respectivement 64 et 68 % (Ripoll et al. 2009) (Figure 3). Cet élément génétique mobile, identique à 99,9% à celui de *M. marinum*, contient un locus de résistance au mercure encodant pour des gènes permettant de soit exporter activement les ions Hg^{2+}, soit de les réduire sous leur forme Hg qui diffuseront librement vers l'extérieur du cytoplasme (Barkay et al. 2003)(Schué et al. 2009). La haute conservation de séquences entre ces deux plasmides atteste de la cohabitation dans un environnement commun des deux espèces. Ce type de plasmide confère une capacité accrue à résister aux désinfectants et rend les bactéries plus susceptibles de provoquer des infections nosocomiales *via* la contamination de matériel chirurgical.

3) Les parois bactériennes :

Les procaryotes sont divisés en deux groupes distincts, en en se basant toujours sur la composition de leurs enveloppes. On utilise cette fois-ci encore une coloration réalisée sur frottis, appelée Coloration de Gram. Les étapes en elles-mêmes diffèrent de lacoloration de Ziehl-Neelsen mais le principe en est très similaire et repose toujours sur le niveau d'hydrophobicité de la paroi.

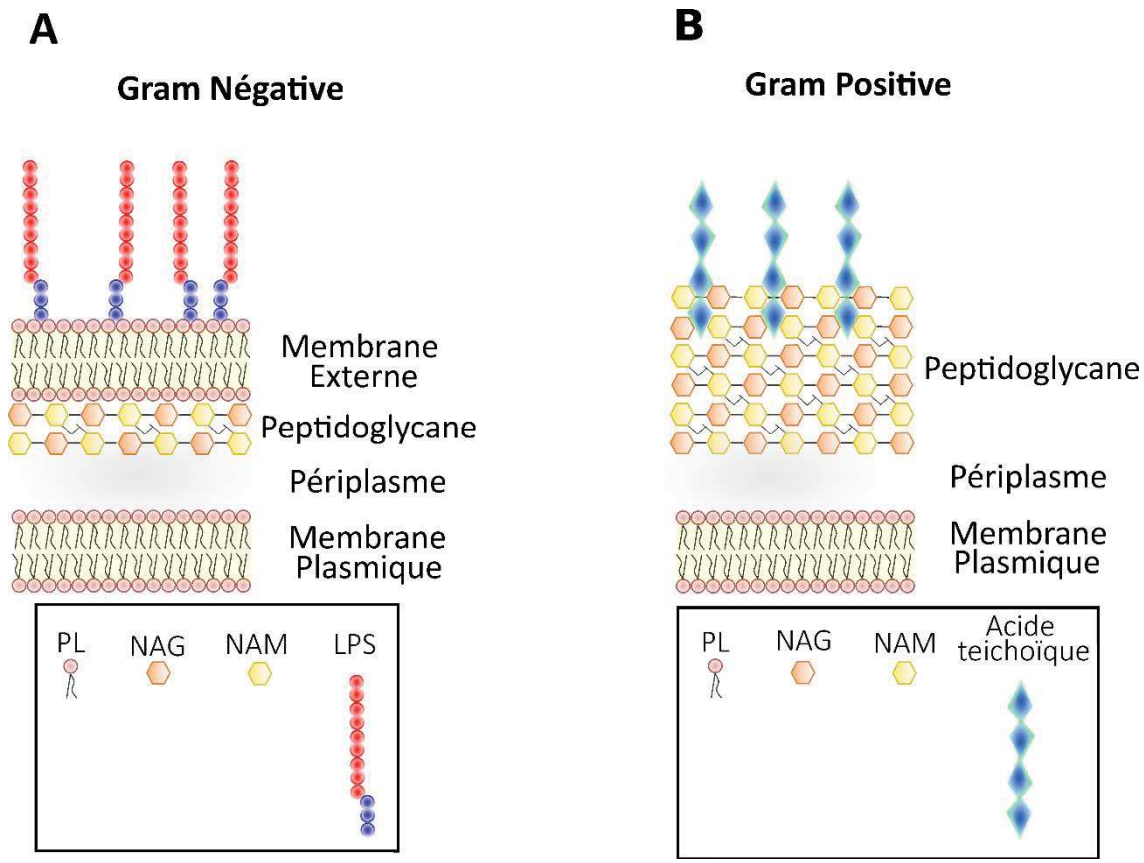

Figure 4. Représentation schématique des parois bactérienne des Gram – et des Gram +. (A) La paroi des bactéries Gram – comporte un fine couche de peptidoglycane entre la membrane plasmique classique et une membrane externe au sein de laquelle sont insérés différents facteurs de virulence comme le LPS. (B) Les bactéries Gram + possèdent uniquement une épaisse couche de peptidoglycane au-dessus de leur membrane plasmique, sont insérés dans ce peptidoglycane des facteurs de virulence comme les acides teichoïques. PL, phospholipide ; NAM, N-acétylmuramique ; NAG, N-acétylglucosamine ; LPS, lipopolysaccharides (Adapté de Gutiérrez et al. 2018).

3a) La paroi des Gram – :

Les bactéries à Gram –, qui apparaissent en rose, possèdent une fine couche de peptidoglycane, également appelée muréine. Il s'agit d'un polymère composé d'une partie glucidique comprenant une molécule d'acide N-acétylmuramique (NAM) rattachée par une liaison β 1 – 4 osidique à une molécule de N-acétylglucosamine (NAG). Cette unité glycosidique est liée dans le cytoplasme à une chaine de 5 acides aminés pouvant être soit lévogyres (L), comme c'est fréquemment le cas pour le résidu alanine en position 1, soit dextrogyres (D), une conformation unique aux bactéries, ou encore non-chirales comme l'acide méso-diaminopimélique. Après avoir été transloquées du cytoplasme vers le feuillet extérieur de la membrane plasmique, deux de ces unités sont liées entre elles *via* leurs chaines peptidiques par des enzymes appelées D, D-transpeptidases. Cette dernière étape de transpeptidation achève la synthèse de l'unique couche de peptidoglycane située dans le périplasme entre la membrane plasmique et une membrane externe. On retrouve dans ce dernier feuillet de nombreuses molécules importantes pour la virulence comme les lipopolysaccharides (LPS)(Beveridge 1999)(Figure 4A).

3b) La paroi des Gram + :

Les bactéries à Gram +, violettes suite à la coloration, ne possèdent pas de membrane externe mais une très épaisse couche de peptidoglycane. La muréine est cette fois-ci constituée de plusieurs couches consécutives toujours liées entre elles par les mêmes liaisons peptidiques, faisant penser à une organisation en maille qui donne une forte rigidité à la paroi de ces bactéries. Cette partie de la paroi est également riches en facteurs de virulence mais sont différents de ceux des Gram –, comme par exemple les acides teichoïques (Brownet al. 2013)(Figure 4B).

3c) La paroi mycobactérienne :

L'enveloppe mycobactérienne est unique en son genre de par sa complexité et sa composition excluant donc les mycobactéries des Gram – et +.

Insérés dans la partie extérieure de la bicouche phospholipidique formant la membrane plasmique se trouvent des glycolipides comme le Phosphatidyl-*myo*-Inositol Mannoside (PIM) et ses dérivés, du LipoMannane (LM) et du LipoArabinoMannane (LAM).

Au-dessus se dresse un large périplasme suivi d'une couche de peptidoglycane liée de manière covalente à un polysaccharide appelé arabinogalactane, lui-même estérifié par de longues molécules d'acides mycoliques. Le LAM se retrouve jusque dans la couche de la paroi mycobactérienne.

Le peptidoglycane mycobactérien se démarque de celui retrouvé chez les autres bactéries car il ne contient pas uniquement du NAG et du NAM mais aussi de l'acide N-glycolylmuramique (NGM)

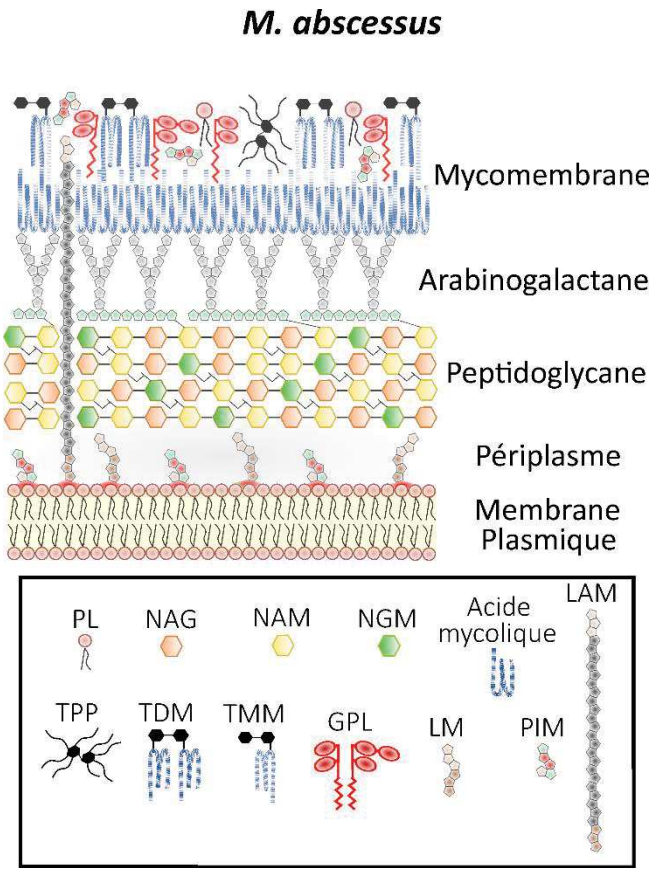

Figure 5. Organisation schématique de la paroi mycobactérienne de *M. abscessus*. On retrouve attachés à la membrane plasmique dans le périplasme du LM, du PIM et du LAM. Le LAM se retrouvera jusque dans la mycomembrane. Le peptidoglycane est composé de NAG, NAM et de NGM. Le TMM, le TDM, le TPP, les GPL mais également du LIM et du PIM se retrouvent insérés entre des molécules d'acides mycoliques dans le feuillet externe de la mycomembrane. PL, phospholipide ; NAM, N-acétylmuramique ; NAG, N-acétylglucosamine ; NGM, N-glycolylmuramique ; LM, lipomannane ; LAM, lipoarabinomannane ; PIM, phosphatidyl-*myo*-inositol mannoside ; TPP, tréhalose polyphléate ; TMM, tréhalose monomycolate ; TDM, tréhalose dimycolate ; GPL, glycopeptidolipide (Adapté de Gutiérrez et al. 2018).

(Mahapatra et al. 2005). Les unités glycosidiques sont néanmoins toujours reliées par des liaisons β 1 – 4 osidiques. La présence de N-glycolylation dans le peptidoglycane mycobactérien pourrait en réalité le renforcer et le rendre encore plus résistant que celui des Gram + (Alderwick et al. 2015). Une autre particularité du peptidoglycane mycobactérien est la nature des ponts peptidiques reliant les différentes unités glycosidiques. En effet, contrairement aux autres genres bactériens, les mycobactéries utilisent majoritairement un autre type de transpeptidase, les L, D-transpeptidases, identifié la première fois en 2002 chez la bactérie *Enterococcus faecium* (Mainardi et al. 2002). *M. tuberculosis* utilise ce type de transpeptidases majoritairement lorsqu'il rentre en phase stationnaire (80% du peptidoglycane est issu de ces L, D-transpeptidases) alors que chez *M. abscessus*, autour de 70% de son peptidoglycane est synthétisé par ces L, D-transpeptidases, indifféremment de la phase de croissance (Lavollay et al. 2008)(Lavollay et al. 2011).

L'arabinogalactane est donc un polysaccharide constitué d'arabinose et de galactose. Plus précisément, la partie galactane est une chaine de 30 molécules de D-galactofuranosyles liée covalemment au peptidoglycane *via* une molécule de L-rhamnose. Cette chaine galactane est reliée de manière covalente à 3 domaines tricosamériques chacun composés de 23 molécules de D-arabinofuranosyles (Alderwick et al. 2015).

Les acides mycoliques, uniques aux mycobactéries, sont de longues molécules pouvant compter jusqu'à 90 carbones chez *M. tuberculosis*. Ils estérifient entreautre la partie terminale de l'arabinogalactane. On retrouve 3 types d'acides mycoliques, les alphas, methoxys et ketos-acides mycoliques au sein desquels est intercalé une immense variété de lipides et glycolipides complexes ayant un rôle structural et participant à la virulence des bacilles. Cet ensemble de composés exotiques forme le feuillet interned'une structure plus exposéeau milieu extérieur appelée mycomembrane. Du tréhalose peut être greffé à ces acides mycoliques par les membres du complexe Antigène 85 et former du Tréhalose MonoMycolate (TMM) et du Tréhalose DiMycolate (TDM) également appelé « *cord factor* ». Le TDM est le glycolipide le plus abondant de la mycomembrane. A la fois très immunogène, il participe aussi dans la survie des bactéries dans l'hôte infecté(Thanna et Sucheck 2016). D'autres molécules sont également présentes comme du DiAcyle Tréhalose (DAT), du PolyAcyle Tréhalose (PAT) , des Sulfo/SulfoGlycoLipides (SL/SGL) et Phthiocerol DIMycocerosate (PDIM)(Abrahams et Besra 2018). On y retrouve du PIM mais aussi du LAM qui joueront ici un important rôle dans l'inactivation des macrophages et dans la neutralisation des composés réactifs de l'oxygène (ROS pour Reactive Oxygen Species)(Mishra et al. 2011). Tous ces lipides, glycolipides et dérivés forment le feuillet externe de la mycomembrane chez *M. tuberculosis*. *M. abscessus* ne possède pas de DAT, PAT et SL mais un autre glycolipide, leTréhalose PolyPhléates

(TPP). *M. abscessus*, comme également *M. smegmatis* et *M. avium*, peut posséder des GlycoPeptidoLipides (GPL) impliqués aussi dans la virulence (Figure 5).

Une capsule peut être retrouvée au-dessus de la mycomembrane chez certaines mycobactéries pathogènes, notamment chez *M. tuberculosis* et *M. marinum* (Daffé et Marrakchi 2019). Elle est composée d'un mélange de protéines ainsi que de mannane, glucane et d'arabinomanne qui sont respectivement des polymères de mannose, glucose et d'arabinose/mannose.

Cet ensemble varié de molécules complexes fait de la paroi mycobactérienne une structure extrêmement hydrophobe et robuste qui représente une première barrière physique à de nombreux antibiotiques, notamment ceux de nature hydrophile qui ne peuvent la pénétrer que s'il y a transport actif vers l'intérieur du cytoplasme. Cette structure offre égalementaux mycobactéries la capacité de résister à de fortes variations de températures et de pH.

4) Classification de Runyon :

Dès 1959, une observation visuelle et temporelle a permis à Ernest Runyon de proposer une classification faisant la séparation entre deux grands types de mycobactéries, celles à croissance rapide (MCR) et celles à croissance lente (MCL). Les MCR forment des colonies sur milieu solide en moins de 7 jours correspondant à un temps de génération ; i.e. période pendant laquelle un bacille donne naissance à deux nouvelle bactéries à la suite d'une réplication par fission binaire ; inférieure à 6 heures. Les MCL ont un temps de génération supérieur à 6 heures et mettent donc plus de 7 jours pour former des colonies. Il a ensuite discriminé au sein des MCL trois sous-catégories :

- Les non-chromogènes dont les colonies ne sont pas pigmentées,
- Les scotochromogènes qui développent une pigmentation dans l'obscurité,
- Les photochromogènes qui ont besoin d'une source lumineuse pour devenir pigmentées.

Cette classification a été par la suite appuyée par les nouvelles techniques de génétique et de séquençage.

5) Mycobactéries à croissance lente :

Les MCL sont généralement des pathogènes dont le plus connu est *M. tuberculosis*. Cette mycobactérie également appelé Bacille de Koch, d'après sa découverte par Robert Koch en 1882, est l'agent étiologique de la tuberculose. Cette maladie, dont les preuves moléculaires les plus anciennes ont été rapportées jusqu'en 600 avant JC (Donoghue et al. 2010), est encore un problème de santé publique majeur à l'échelle mondiale avec près de 10 millions de nouveaux cas annuels et presque 2 millions de décès (WHO 2018). Plus de 250 000 de ces décès sont dus à des souches multi résistantes

(MDR-Tb) aux traitements disponibles, incitant au développement de nouveaux antibiotiques et stratégies thérapeutiques (WHO 2017). Cette bactérie provoque généralement une pathologie pulmonaire mais des formes osseuses et des méningites peuvent se produire. D'autres MCL provoquant des maladies pulmonaires existent comme les bactéries du complexe *M. avium* mais sont retrouvées généralement chez des personnes avec des problèmes pulmonaires préexistants ou un système immunitaire affaibli (Daley 2017). Certaines de ces MCL provoquent des types d'infection plus variés, notamment dans les régions tropicales d'Afrique, comme *M. ulcerans* responsable de l'ulcère de Buruli qui se caractérise par une importante nécrose d'une plaie infectée (van der Werf et al. 2005).

6) Mycobactéries à croissance rapide :

Les MCR sont des bactéries environnementales qui peuvent parfois se transformer en pathogènes opportunistes si les facteurs environnementaux appropriés sont réunis. Un de ces facteurs est le statut immunitaire/pathologique du patient (Cowman et al. 2019). Mais un prérequis à la mise en place de l'infection est bien sûr un contact physique avec ces microorganismes. Il se trouve que ces contacts sont en réalités très fréquents car on retrouve des MCR dans les systèmes de plomberies domestiques (Falkinham 2011) ainsi que dans les jardins ou même la terre de rempotage (Thomson et al. 2013)(De Groote et al. 2006). Des études récentes ont d'ailleurs mis en évidence une transmission possible de patient à patient, particulièrement dans les infrastructures de santé (Bryant et al. 2016). Ces MCR cibleront préférentiellement l'appareil pulmonaire mais sont capables d'infecter n'importe quelle partie du corps. Les MCR pathogènes les plus souvent isolées sont *M. fortuitum*, *M. kansasii* ainsi que le complexe *M. abscessus*.

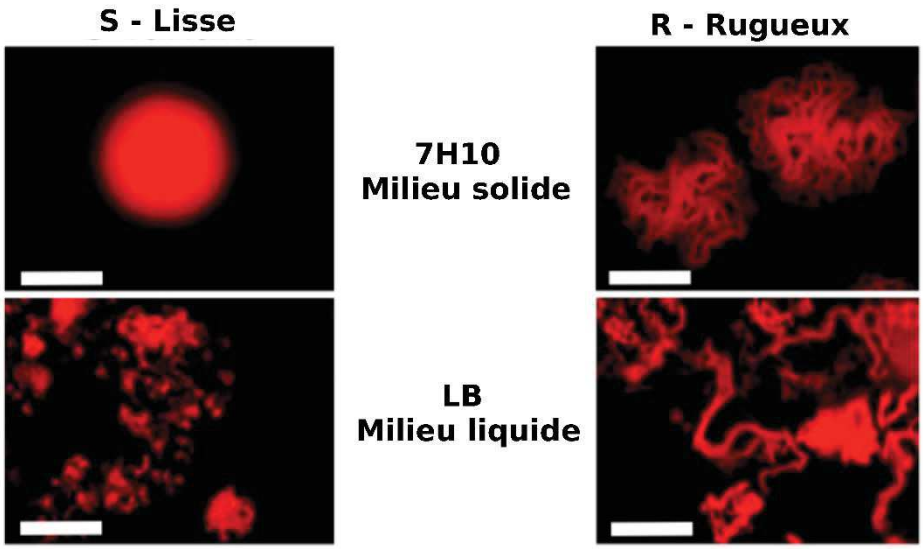

Figure 6. Les différents morphotypes de *M. abscessus* en milieu liquide et en milieu solide.Le morphotype S (colonne de gauche) forme des colonies lisses et rondes sur 7H10 et des petits amas répartis de manière homogène en culture liquide. Le morphotype R (colonne de droite) s'organise en chainettes sur la périphérie de ses colonies très déshydratées sur 7H10 et forme des agrégats volumineux en culture liquide. L'échelle est ici de 1 mm (Adapté de Bernut et al. 2014).

Chapitre II) Mycobacterium abscessus, généralités

1) Histoire et présentation du complexe :

Isolé pour la toute première fois en 1953 chez une patiente présentant un abcès au genou, *M. abscessus* a d'abord été rattaché à *M. chelonae* formant un groupe au sein du complexe *M. fortuitum* jusqu'en 1970. Il a ensuite fallu attendre 1992 pour que *M. abscessus* soit séparé de *M. chelonae* et qu'il soit considéré comme une espèce bactérienne à part entière. A l'heure actuelle, le complexe *M. abscessus* contient trois sous-espèces, *M. abscessus abscessus, M. abscessus massiliense* et *M. abscessus bolletii* (Tortoli et al. 2016)(Adekambi et al. 2017). Cette séparation taxonomique devrait impérativement êtreprise en compte lors du choix de l'antibiothérapie car ces espèces répondent différemment aux antibiotiques constituant la thérapie (Benwill et Wallace 2014).

2) Les différents morphotypes et leurs répercutions :

M. abscessus présente deux morphotypes qui peuvent être différenciés visuellement sur la simple observation de l'aspect des colonies sur milieu solide. Cette simple différence morphologique a un impact fort sur leur physiologie et physiopathologie respective. Il est donc possible de se retrouver face à des colonies rondes dites « *Smooth* » (S) ayant un aspect lisse et crémeux. Les autres colonies observables, « *Rough* » (R), sont très rugueuses, semblent être déshydratées et sont organisées en structures serpentines sur leur périphérie. En milieu liquide, le variant S est présent sous la forme de suspensions relativement homogènes quand on le compare au variant R qui forme de gros agrégats (Bernut et al. 2014)(Figure 6).

La capacité à former des biofilms confère aux bactéries un énorme avantage en termes de survie, transmission et pathogénicité. Un biofilm est défini par l'agrégation de cellules planctoniques dans une matrice auto-sécrétéesur une surface solide. Ce comportement est temporaire et pourrait s'apparenter à un style de vie multicellulaire en réponse à différents signaux environnementaux. Ce biofilm procure aux bactéries la capacité de coloniser des niches écologiques variées. Ce phénomène peut également favoriser la persistance et la transmission à un nouvel hôte, notamment pour les bactéries pathogènes retrouvées dans les conduits d'aération, les robinets, ou même les instruments chirurgicaux (Bryant et al. 2016). La formation de biofilms peut également se produire au sein d'un hôte infecté et conférera aux bactéries la capacité de contourner les défenses immunitaires et de mieux tolérer un traitement antibiotiques (Baker et al. 2017)(Fennelly et al. 2016). Le morphotype R était considéré comme incapablede former des biofilms, mais Clary et al. ont récemment fourni de nouvelles données permettant de réfuter en partie cette observation. En effet, il semblerait que la capacité d'agrégation du variant R donne au biofilm un aspect plus cireux que le variant S, mais les deux morphotypes semblent capables de s'organiser en biofilm de même taille et de même densité.

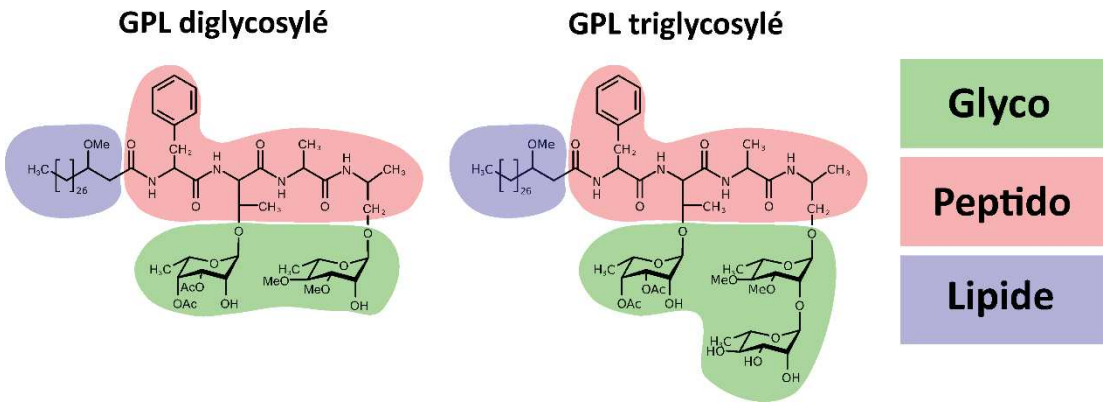

Figure 7. Structures des différents GPL produits par *M. abscessus*. Le GPL triglycosylé est plus soluble que sa version diglycosylé (Adapté de Gutiérrez et al. 2018).

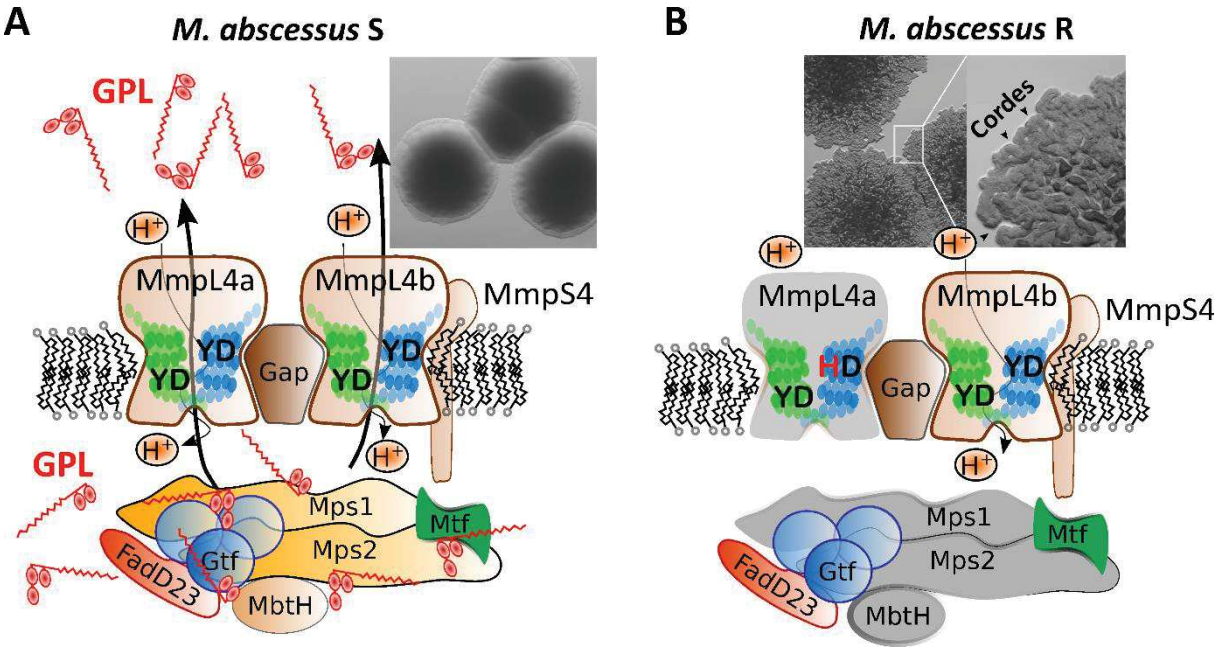

Figure 8. Les GPL influencent le morphotype de *M. abscessus*. Représentation schématique de la voie de biosynthèse et du système de transport des GPL chez le morphotype S (A) et chez le morphotype R (B). Les gènes retrouvés mutés chez le variant R sont en gris. Le résidu tyrosine 842 substitué par une histidine de *mmpL4a* chez *M. abscessus bolletii* est ici représenté en rouge. Cette mutation mène à un arrêt de la force proto-motrice et au transport des GPL ayant pour conséquence la transition vers le morphotype R (Adapté de Gutiérrez et al. 2018).

En revanche, le morphotype S est lui considéré comme mobile car il peut glisser (*sliding motility*) vers les bords d'une boite de pétrie, alors que le morphotype R en est incapable (Howard et al. 2006). Ces phénomènes d'agrégation et de mobilité seraient en grande partie dus à la présence chez le variant S, et à son absence chez le variant R, de GPL présents dans le feuillet externe de la mycomembrane (Recht et al. 2000). Comme son nom l'indique, cette molécule comprend une partie lipidique, composée d'une mixture d'acide gras de chaine carbonée allant de 28 à 30 atomes, qui est reliée à un noyau peptidique soit diglycosilé soit triglycosilé, ce dernier exhibant une plus forte polarité (Gutiérrez et al. 2018)(Figure 7). Le morphotype R ne possède pas de GPL car on retrouve dans son génome des mutations dans le locus de biosynthèse de ces molécules (Pawlik et al. 2013) et dans le complexe transmembranaireimpliqué dans leur export (Bernut, Viljoen, et al. 2016)(Figure 8).

Ces GPL sont responsables de l'aspect lisse du morphotype S. Leur absence chez le variant R provoque la formation de « cordes », qui sont en réalitéles structures serpentines observées en périphérie des colonies sur milieu solide et qui affectent fortement la virulence de ce morphotype (Howard et al. 2006)(Bernut et al. 2014)(Halloum et al. 2016). Ce phénomène de « *cording* » chez *M. abscessus* est également dû à une autre molécule, le TPP (Llorens-Fons et al. 2017). Le *cording* est défini comme une agrégation tridimensionnelle latérale ou au niveau des pôles des bacilles incapables de se séparer après réplication. Ce trait microbiologique confère au morphotype R une hypervirulence retrouvée majoritairement chez les patients souffrant d'infections pulmonaires aiguës (Catherinot et al. 2009)(I. K. Park et al. 2015). A l'opposé, le morphotype S serait plus une forme environnementale colonisante retrouvée dans des plaies infectées après contact direct (Jönsson et al. 2007).

3) Physiopathologie, infection du macrophage par le morphotype S :

Les GPL influencent fortement la réponse phagocytaire des macrophages à *M. abscessus.* Le morphotype S est phagocyté individuellement et les GPL vont permettre de retarder l'importante réponse pro-inflammatoire en empêchant notamment la production initiale d'InterLeukine-8 (IL) (Davidson et al. 2011). Les GPL recouvrent les agonistes des Toll-Like Receptor-2 (TLR) présents à la surface des bacilles et empêchent toute interaction avec les récepteurs membranaires de l'inflammation (Rhoades et al. 2009). Ceci va limiter le recrutement de nouveaux macrophages et la

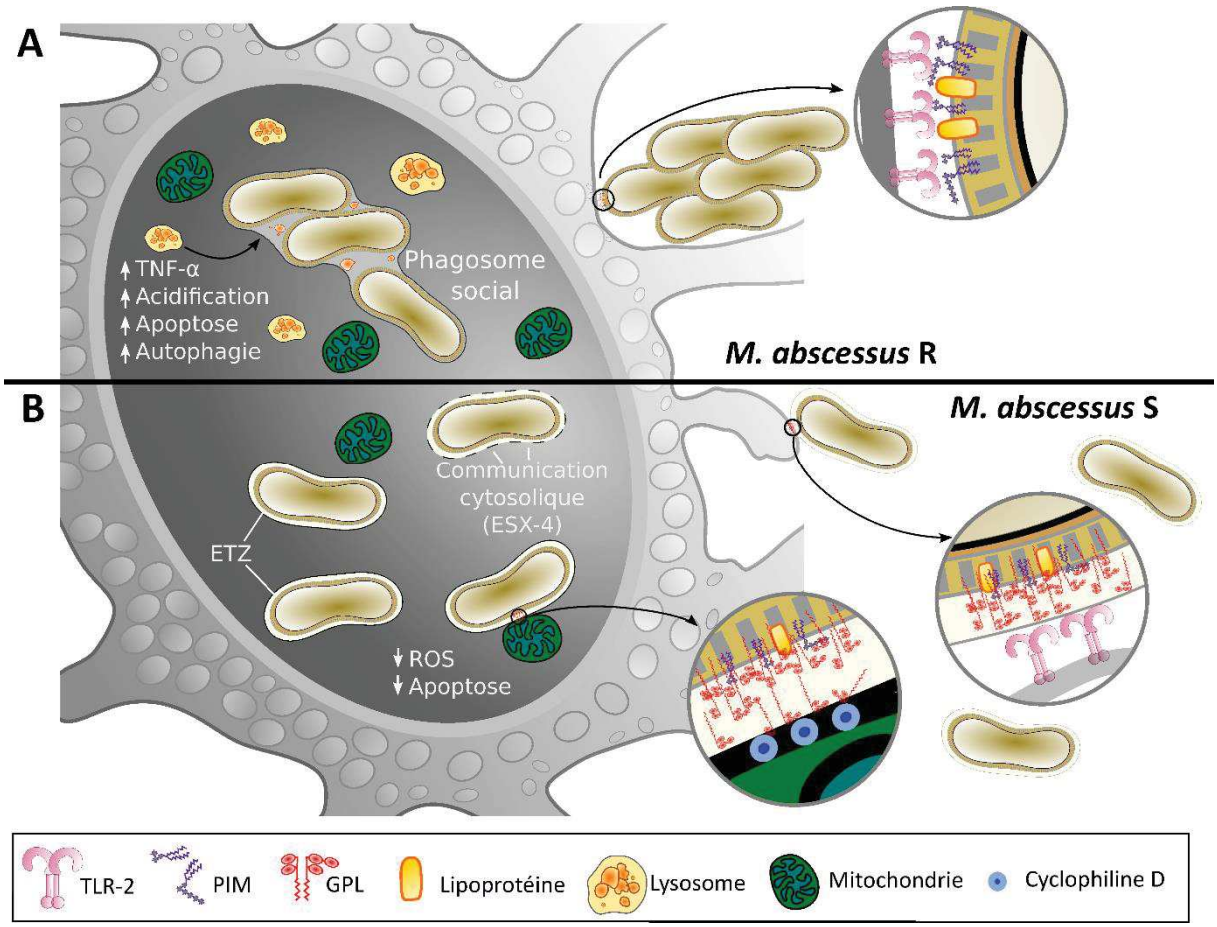

Figure 9. Infection du macrophage par le morphotype R et S. (A) Chez le variant R, l'exposition des agonistes du TLR-2 comme le PIM_2 et des lipoprotéines vont provoquer une forte réponse inflammatoire menant à une infection sévère due une surproduction de ROS et à l'augmentation de l'apotose et de l'autophagie. (B) Les GPL présents chez le variant S vont recouvrir les agonistes de TLR-2 et vont permettre une communication cellulaire avec le macrophage résultant en un contrôle de l'infection. TLR-2, toll-like receptor 2 ; PIM, phosphatidyl-*myo*-inositol mannoside ; TNF-α, tumor necrosis factor alpha ; ETZ, electron translucent zone ; ROS, reactive oxygen species (Adapté de Gutiérrez et al. 2018).

surproduction d'autres cytokines pro-inflammatoires qui conduiraient à une réponse exacerbée puis à une mort cellulaire. Une fois internalisés, les GPL vont de nouveau former une barrière physique mais cette fois-ci entre la membrane du phagosome et la paroi mycobactérienne. Ce phénomène est visible par microscopie électronique et est caractérisé par une zone non-colorée par les électrons appelée « Electron Tranfslucent Zone » (ETZ)(Roux et al. 2016). Les GPL permettent également de bloquer la fusion avec les lysosomes ainsique la production de ROS ce qui permet de contrôler l'infection. Les GPL participeront à l'inhibition de l'apoptose en interagissant à travers la membrane phagosomaleavec la cyclophiline D de la mitochondrie (Whang et al. 2017). Le bacille va ensuite continuer de moduler la réponse macrophagique en bloquant l'acidification du phagosome grâce à l'établissemen td'une communication avec le cytoplasme médiée par les ystème de sécrétion de type VII ESX-4 (Laencina et al. 2018). Cet ensemble de mécanismes va permettre au variant S d'établir une niche de réplication sécurisée et stable au court du temps (Figure 9A). Mais une fois la charge bactérienne intracellulaire trop importante, les macrophages entrent en apoptose, libérant les bacilles dans le milieu extracellulaire qui seront de nouveau phagocytés et qui entameront alors un nouveau cycle infectieux.

4) Physiopathologie, infection du macrophage par le morphotype R :

Les cordes mycobactériennes exhibées par le variant R sont un véritable défi pour les cellules phagocytaires (Figure 9B). Ces structures sont parfois longues de plus d'une centaine de micromètres et excédent largement la taille des macrophages qui ne peuvent donc pas phagocyter ces bactéries. Chez le variant R dépourvu de GPL, les agonistes du TLR-2 comme le PIM et certaines lipoprotéines ne sont plus masqués et déclenchent une forte réponse inflammatoire (Roux et al. 2011). Néanmoins, il arrive que de plus petits agrégats bacillaires ne se forment et soient phagocytés, donnant naissance à un phagosome « social » (Roux et al. 2016). Ces bacilles vont être incapables d'empêcher la fusion phagolysosomale et donc son acidification. Il n'y aura également pas d'inhibition de l'autophagie et de l'apoptose comme c'est la cas pour le variant Saugmentant ainsi la lyse des macrophages (Whang et al. 2017). Il se produit en parallèle une production exacerbée de cytokines pro-inflammatoires comme le Tumoral Necrosis Factor α (TNF- α), qui se traduira par une activation des autres macrophages à proximité et une escalade de la production de ces molécules qui reflètera le caractère hypervirulent du variant R de *M. abscessus* (Figure 9B).

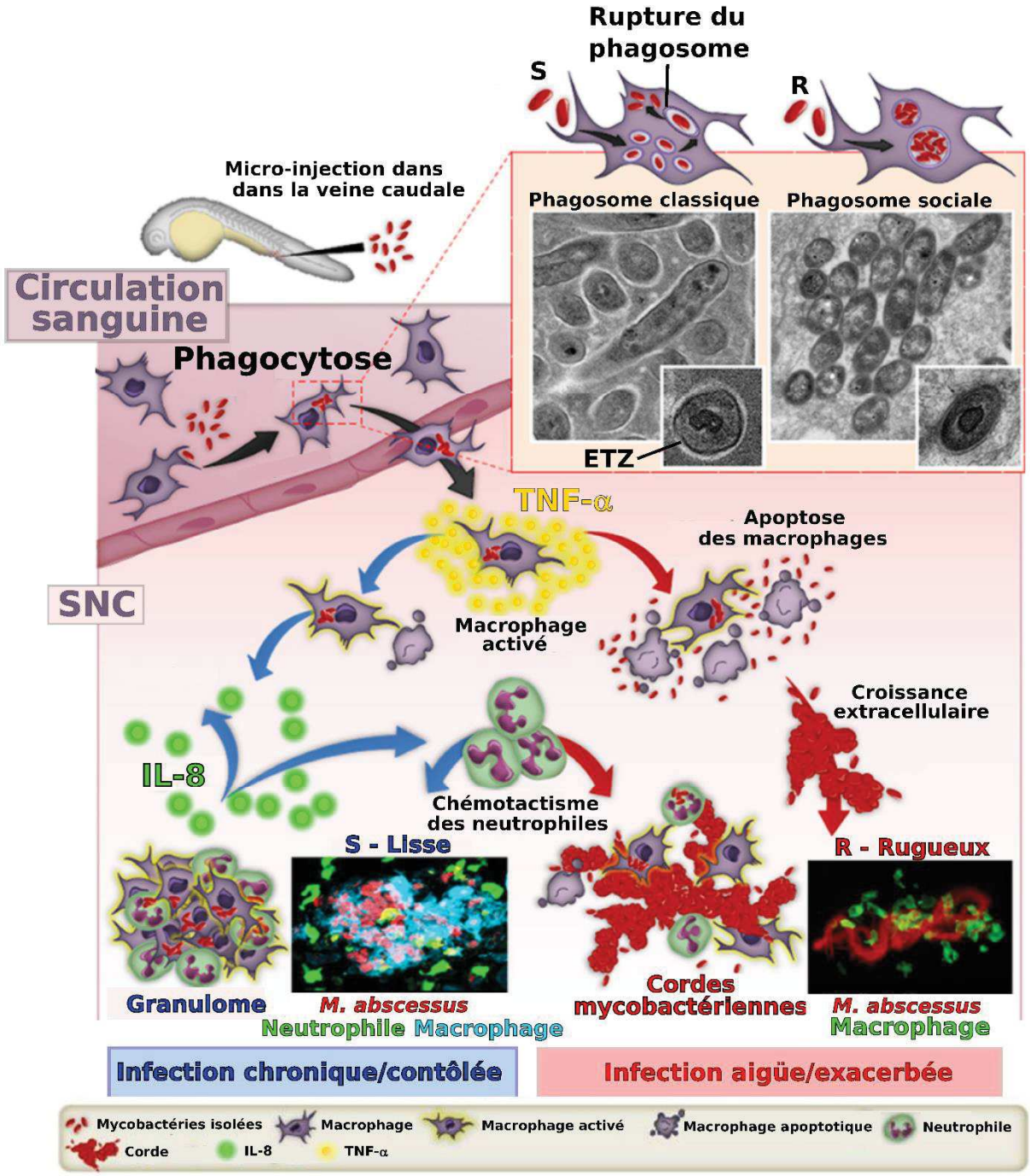

Figure 10. Infection des morphotypes S et R chez le zebrafish. L'infection provoquée par le morphotype S (partie de gauche) est contenu au sein de structures immunologiques appelées granulome ce qui conduit à une infection chronique et contrôlée. Le morphotype R (partie de droite) va lyser les macrophages, se développer extracellulairement en produisant des cordes mycobactériennes et provoquer une infection aigüe conduisant à la mort du zebrafish. (Adapté de Bernut et al. 2017)

5) Physiopathologie, infection chez le poisson-zèbre :

Le *Dario rerio*, poisson-zèbre ou encore zebrafish (ZF) est un excellent modèle pour suivre en temps réel les interactions hôte-pathogène. L'embryon de ce poisson, endémique d'Inde, est un excellent outil pour disséquer les processus infectieux viraux et bactériens dû au fait :

- qu'il possède une immunité innée proche de celle de l'homme avec des macrophages etdes neutrophiles jusqu'à quatre semaines de développement (Torraca et al. 2014),
- qu'il est aisément modifiable génétiquement ce qui permet la génération de cellulesimmunitaires fluorescentes (Torraca et Mostowy 2018),
- que sa transparence optique permet l'utilisation de méthodes de microscopie non-invasives offrant la possibilité de suivre l'interaction entre des bactéries et cellules immunitaires exprimant différents fluorophores (Bernut et al. 2017).

Le ZF a été largement utilisé dans le cadre de l'étude de la physiopathologie de *M. abscessus* et a mis en exergue le même phénotype infectieux que chez le macrophage. Mais ce modèle a également permis de découvrir chez les deux morphotypes un tropisme neuronal (Bernut et al. 2014). Après micro-injection de *M. abscessus* dans le système circulatoire *via* la veine caudale, les bacilles vont être phagocytés par des macrophages circulants. Ces cellules immunitaires font offices de cheval de Troie et fournissent aux bactéries un moyen de transport à travers la barrière hémato-encéphalique du Système Nerveux Central (SNC) et se retrouver dans le cerveau et la moelle épinière.

5a) Le morphotype S, infection chronique chez le poisson-zèbre :

L'infection des macrophages du ZF par le variant S se déroule de la même manière que lors d'une infection *in vitro* (« **Chapitre II) *Mycobacterium abscessus*, généralités**, **3) Physiopathologie, infection du macrophage par le morphotype S »**). La différence est qu'icion retrouve d'autres types cellulaires présents chez le ZF, comme les neutrophiles. Les cycles infectieux ; i.e. phagocytose – apoptose – phagocytose ; vont se produire dans le SNC ou potentiellement toujours au site d'injection. Le relargage du contenu cellulaire et des cytokines du macrophage après son apoptose va provoquer l'activation d'autres macrophages à proximité qui produiront à leur tour du TNF-α mais aussi désormais de l'IL-8. Les neutrophiles vont être recrutés grâce à cette IL-8 et s'agglutiner aux macrophages. Cette structure immunologique pluricellulaire a pour but d'emprisonner les bacilles extracellulaires et les phagocytes infectés afin de limiter la dissémination de l'infection. Ces édifices sont appelés granulomes et permettent de contrôler l'infection (Figure 10, partie de gauche). Les phagocytes au centre du granulome vont rentrer en apoptose ce qui permet la création d'un compartiment hermétique empêchant la propagation des bactéries vers le milieu extérieur. On assistera ici à une infection contrôlée, qualifiée de chronique (Bernut, Nguyen-Chi, et al. 2016).

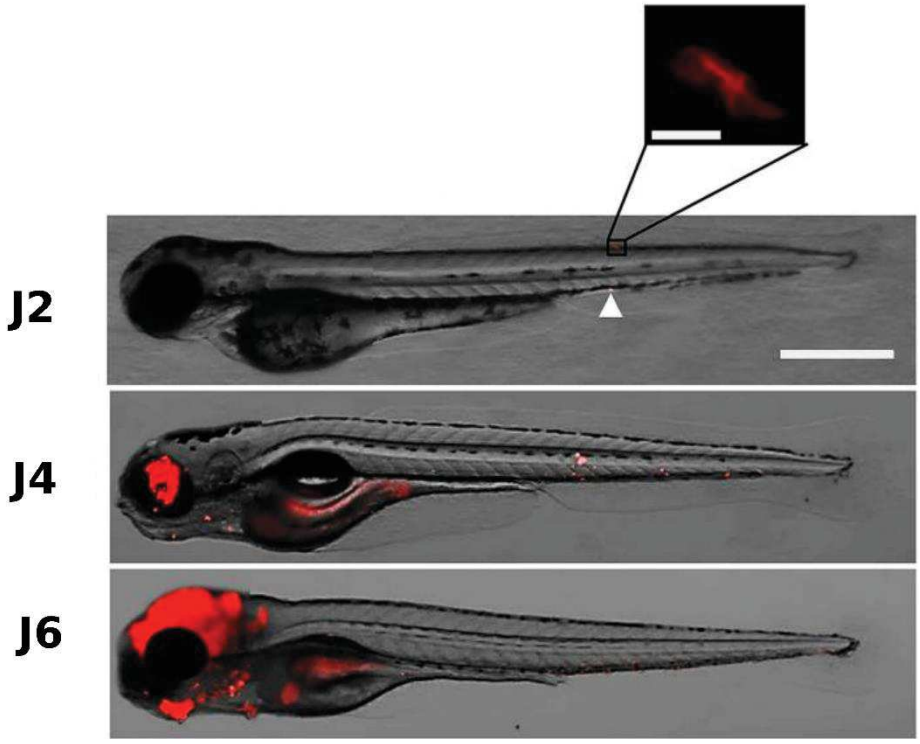

Figure 11. Formation d'abcès dans le système nerveux central d'un embryon de zebrafish. Suivi spatiotemporelle d'une infection non-traitée par le morphotype R de *M. abscessus* montrant l'évolution 2, 4 et 6 jours après injection (J2, J4 et J6 respectivement). A J2, le triangle blanc pointe la présence de petits agrégats de bacille et l'encadré montre la genèse de cordes mycobactérienne. La barre d'erreur représente 200 μm (Adapté de Dupont et al. 2017).

5b) Le morphotype R, infection aigüe chez le poisson-zèbre :

Avec le morphotype R, les premiers macrophages infectés entrent rapidement et massivement en apoptose. Les neutrophiles et macrophages établissent de nombreux granulomes dans le SNC et à travers l'ensemble de l'embryon. Cependant les bacilles se répliquent trop rapidement et de manière anarchique dans le milieu extracellulaire formant alors des cordes démesurées empêchant de nouvelles phagocytoses (Bernut et al. 2014)(Figure 10, partie de droite). Ceci a pour conséquence un orage cytokinique qui mènera à une dégradation des tissus proches et à la formation d'abcès (Figure 11). Ces événements sont caractérisés comme étant la phase aigüe de l'infection qui entraînera la mort de l'embryon de ZF.

6) Symptômes et épidémiologie des infections extrapulmonaires à *M. abscessus* :

M. abscessus est une des principales MNT à provoquer des infections extrapulmonaires qui se caractériseront par des atteintes cutanées et des tissus mous (Lee et al. 2015). Elles provoquent généralement des nodules pourpres, des abcès et des lésions ulcératives, qui dans 45% des cas surviennent après un acte opératoire (Chadha et al. 1998).

La contamination de matériels chirurgicaux invasifs, comme les aiguilles, représentent le principal accès à travers la barrière cutanée. La réalisation de tatouage (Bechara et al. 2010) ou les injections de silicone sont également mises en causes (Fox et al. 2004). La localisation de ces infections dépend aussi de la nature des opérations et des instruments contaminés. Des cas à *M. abscessus* ont été répertoriés après des transplantations cardiaques (Richey et al 2013) ou des poses de prothèses (Eid et al. 2007).

Mais le matériel chirurgical n'est pas toujours mis en cause. Plusieurs épidémies ont été provoquées par l'injection de solutions contaminées. L'exemple le plus frappant s'est produit en Colombie entre 1992 et 1993, où parmi 2000 personnes injectées avec un anesthésique local, la lidocaïne, 205 ont développé des abcès cutanés ou des cellulites dus à *M. abscessus* (Villanueva et al. 1997).

Bien qu'étant plus rares, des infections disséminées à *M. abscessus* peuvent se produire chez des personnes souffrant de maladies génétiques immunosuppressives, chez des personnesâgées ou sous traitement immunosuppresseurs comme lors d'une chimiothérapie. Les personnes avec une grande partie de l'épiderme endommagée, comme les grands brûlés, sont également sujetes à ce genre d'infections nosocomiales (Vaghaiwalla et al. 2014). Dans certains cas, *M. abscessus* est capable d'avoir le même tropisme que chez le ZF et va provoquer des infections du SNC s'il parvient à traverser la barrière hémato-encéphalique (Lee et al. 2012)(Giovannenze et al. 2018).

7) Symptômes et épidémiologies des infections pulmonaires à *M. abscessus* :

Comme pour les infections de la peau et des tissus mous, des cas d'infections pulmonaires à *M. abscessus* sont répertoriés sur tous les continents même si l'incidence varie d'une région à une autre. Par exemple, la proportion d'infection à *M. abscessus* parmi les MNT est de seulement 13,3% en Chine, contre 45, 52 et 56 % aux Etats-Unis, en France et au Royaume-Uni respectivement (Mougari et al. 2016). La plupart des infections pulmonaires à *M. abscessus* sont d'ordres chroniques et caractérisées par une toux récurrente et persistante, une dyspnée, une hémoptysie, une production excessive de mucus, le tout accompagné de fièvre et de perte de poids. La maladie peut ensuite progresser sous la forme de bronchectasie nodulaire ou la forme fibro-cavitaire, qui est le pronostic le plus sévère. En l'absence de traitement, cette dernière forme peut provoquer un déclin des fonctions respiratoires dû à la formation de larges cavités et d'une fibrose qui réduira irrémédiablement le tissu pulmonaire (National Organisation for Rare Disorders, 2015 - 2018). Environ un tiers des personnes souffrant d'infections pulmonaires à *M. abscessus* sont *apriori* en bonne santé (Griffith et al. 1993), sans pathologie pulmonaire sous-jacente, mais il existe plusieurs maladies chroniques qui sont menacées par une surinfection par cette MNT.

8) Facteurs de risques, les troubles pulmonaires chroniques d'origines environnementales et non génétiques :

Les troubles pulmonaires chroniques d'origines environnementales augmentant le risque d'infection à *M. abscessus* sont variés et provoquent tous une inflammation du système respiratoire. Ces facteurs déclenchants incluent par exemple :

- les pneumoconioses, qui sont des inflammations des poumons pouvant mener à une fibrose suite à l'inhalation de particules minérale comme la silice, l'amiante ou le charbon (American Lung Association,2018).
- les Broncho-Pneumopathies Chroniques Obstructives (BPCO) regroupant deux pathologies, la bronchite chronique et l'emphysème. Ce dernier est caractérisé par une dégradation du septa, qui est la paroi des alvéoles pulmonaires (National Health Service 2017).
- les séquelles pulmonaires liées à une tuberculose antérieure.
- les syndromes de reflux gastro-œsophagien (RGO), où les patients vont régulièrement subir des remontées gastriques voire des vomissements. Le contenu acide de l'estomac favorisera alors une inflammation de l'œsophage (Won-Jung Koh et al. 2007).

9) Facteurs de risques, les troubles pulmonaires chroniques d'origine génétique, cas de la mucoviscidose :

La maladie génétique qui prédispose le plus aux infections pulmonaires à *M. abscessus* est la mucoviscidose. C'est une maladie autosomale récessive avec une prévalence estimée de 1 cas toutes les 2500 naissances dans la population caucasienne globale, même si cette valeur peut osciller d'une région à une autre (Leitch et Rodgers 2013). Elle est due à des mutations du gène *cftr* localisé sur le chromosome 7 encodant pour la protéine Cystic Fibrosis Transmembrane conductance Regulator (CFTR). A ce jour, plus de 1000 altérations génétiques différentes ont été identifiées, donnant naissanceà 6 classes de mutations distinctes. Néanmoins, une d'entre elles prédomine la délétion de classe 2 de l'acide aminé phénylalanine en position 508 (Ratjen et Döring 2003). La fonction de cette protéine est le transport des ions chlorures à travers la membrane apicale de cellules épithéliales de plusieurs organes comme le foie, le pancréas, l'appareil génital, les sinus et les poumons. Le système respiratoire représente l'organe le plus débilitant de la maladie. Le non-adressage du canal CFTR à la membrane apicale des cellules épithéliales pulmonaires provoque un épaississement et un changement de composition du mucus présent dans les bronches. Cela empêchela fonction muco-ciliaire normaleconduisant à une accumulation accrue de mucus ce qui aboutira à une forte détresse respiratoire.Ce mucus pathologiquereprésente un environnement propice à la prolifération de *M. abscessus*. Cependant, ce n'est pas l'espèce bactérienne que l'on retrouve le plus fréquemment. Elle est précédée, dans cet ordre-ci, par les bactéries *Pseudomonas aeruginosa*, *Staphylococcus aureus* Résistant à la Méthicilline (SARM), *Heamophilus influenzae* et *Stenotrophomonas maltophilia* (Surette 2014).

Le contenu modifié de ce mucus est primordial pour la mise en place de l'infection bactérienne. Premièrement, ce mucus est très riche en cytokines pro-inflammatoires et déficient en IL-10 (une cytokine anti-inflammatoire) ce qui va promouvoir l'infection de *P. aeruginosa* dans le modèle souris (Chmiel et al. 1999). Deuxièmement, le canal CFTR non-fonctionnel conduit à une augmentation de la concentration en NaCl du mucus, qui a pour effet d'inactiver les défensines et leur pouvoir bactéricide(Smith et al. 1996). Enfin, il a été montré *in vitro* que les propriétés anoxiques de ce mucus perturbent le fonctionnement normal des neutrophiles qui ne peuvent plus combattre efficacement une infection à *P. aeruginosa* (Worlitzsch et al. 2002).

Ces canaux CFTR ont également un rôle à jouer dans l'élimination des pathogènes. Chez une personne saine, les canaux CFTR des cellules épithéliales pulmonaires vont servir de récepteur et permettre l'internalisation de *P. aeruginosa* et son élimination(Pier et al. 1996). Les cellules épithéliales possédant des canaux CTFR défectueuxne sont pas capables d'internaliser ce pathogène et de le détruire. Les bactéries se retrouvent alors libres dans le mucus et continuent de se multiplier (Pier et al. 1996). Plus récemment, il a été démontré que dans le modèle zebrafish, que les

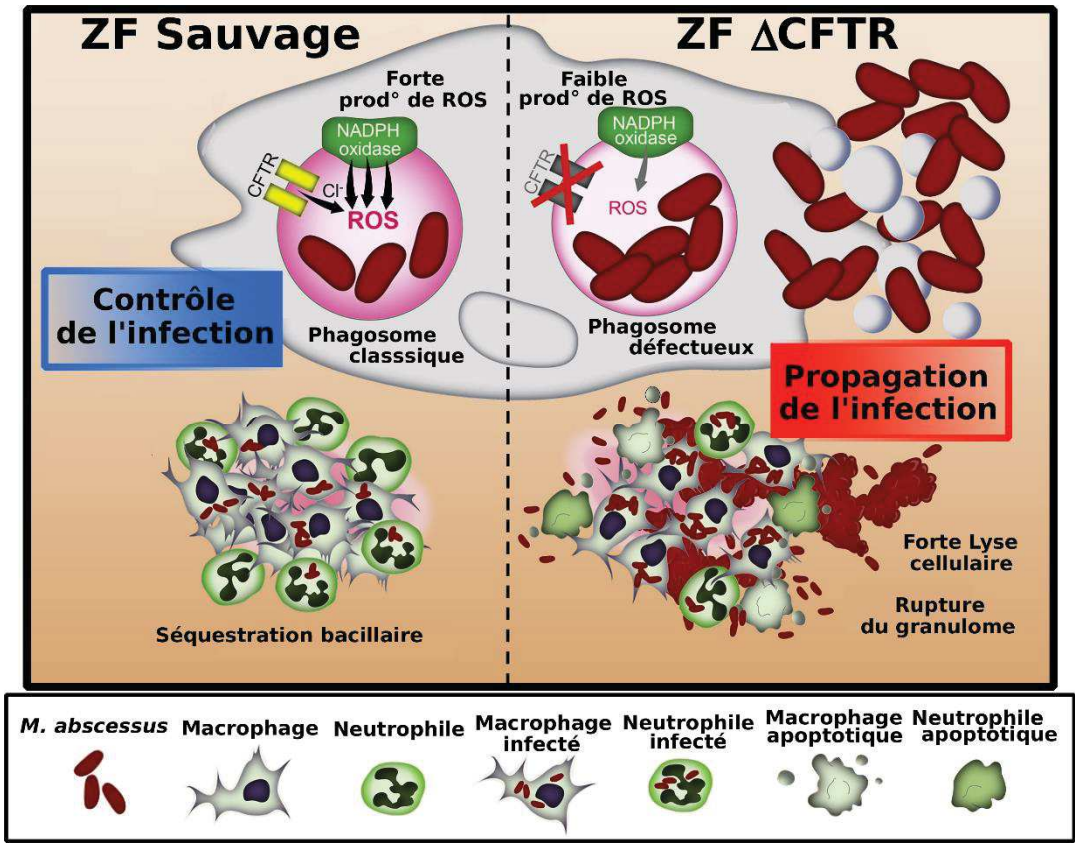

Figure 12. Les macrophages Δ*cftr* ne sont plus en mesure de contrôler l'infection de *M. abscessus*. (Partie de gauche) Forte production de ROS dans le phagosome médiée par la NADPH oxidase et favorisée par l'import de Cl^- menant à la mort des bacilles. Le chimiotactisme des neutrophiles est efficace et conduit à la formation d'un granulome. (Partie de droite) Les canaux CFTR mutés ne sont plus en mesure de favoriser la production de ROS. Les bactéries se divisent jusqu'à la lyse du macrophage. Le chimiotactisme des neutrophiles est altéré et la formation du granulome échoue. Les bacilles se multiplient extracellulairement et provoque d'importants dégâts tissulaires menant à la mort du zebrafish. ZF, zebrafish ; ROS, reactive oxygen species (Adapté de Bernut et al. 2019).

transporteurs CFTR jouent un rôle primordial dans l'élimination intracellulaire de *M. abscessus* (Bernut et al. 2019). En effet, les canaux CFTR vont permettre l'entrée des ions chlorures dans les phagosomes permettant une forte production de ROS par la NADPH oxydase ce qui permettra d'éliminer les bactéries internalisées (Figure 12). Cependant, chez des embryons de ZF Δ*cftr*, les bactéries phagocytées ne sont pas détruites. Elles lyseront les cellules infectées et se multiplieront dans le milieu extracellulaire. Dans ce contexte génétique, les deux morphotypes provoqueront une forte mortalité des larves de ZF.

Chez une personne atteinte de mucoviscidose, l'épaisseur du mucus rend l'expectoration très délicate. Les bactéries pathogènes comme *M. abscessus* se retrouvent alors bloquées dans un environnement où tout semble être propice pour qu'elles prolifèrent.

10) Détection des infections à *M. abscessus*, les différentes méthodes de diagnostic :

Les méthodes de diagnostic varient selon les pays qui sont dépendants des moyens financiers à disposition. Un diagnostic rapide et surtout précis est un des éléments clefs pour le traitement efficace d'une infection à *M. abscessus*.

Les« Pays les Moins Avancés » (PMA) ne disposent pas des toutes dernières techniques de séquençage/génotypage et de spectrométrie de masse permettant de reconnaitre une infection causée par *M. abscessus* d'une autre mycobactériose. Le personnel de santé ne peut donc uniquement compter sur un examen des symptômes cliniques (décrits en section « **Chapitre II) *Mycobacterium abscessus*, généralités** , **7) Symptômes et épidémiologie des infections pulmonaires à *M. abscessus*** ») ouune coloration de Ziehl-Neelsen (Sarro et al. 2018). L'utilisation restreinte de ces méthodes de diagnostic soulève un grave problème dans ces PMA. Il s'agit en effet la plupart du temps de région où la tuberculose est endémique, comme en Afrique ou en Inde, où l'on sous-estime l'incidence des infections à *M. abscessus* et aux autres MNT (Maiga et al. 2012). Il est impossible de différencier une tuberculose d'une autre mycobactériose avec ces deux techniques et les médecins vont alors traiter ces patients pour une tuberculose au lieu d'une MNT. Ceci a de graves répercussions envers le patient mais aussi sur le point de vue économique. Les MNT et plus particulièrement *M. abscessus* sont totalement résistantes aux traitements anti-tuberculeux de base. Les patients sont donc traités avec des thérapies longues, inefficaces et coûteuses. Ils souffrent la plupart du temps des effets secondaires liés aux antibiotiques et l'infection continue de se propager et de causer d'importantes lésions engageant le pronostic favorable à une guérison. Un examen radiographique ou un scanner de la cage thoracique peuvent aussi être pratiqués. Cependant, cette méthode ne permet pas de distinguer avec certitude *M. abscessus* d'une autre MNT étant données

les caractéristiques communes observées :

- une bronchiectasie bilatérale.
- la présence d'opacités réticulonodulaires.
- et la présence de cavités dans les parties supérieures des lobes pulmonaires.

Suite à un examen radiographique positif à la présence d'une infection par une MNT, un examen microbiologique (Koh et al 2014) peut être réalisé selon les critères de l'Infectious Diseases Society of America (IDSA) et de l'American Thoracic Society (ATS) qui sont basés sur des cultures positives issues d'un lavage des bronches, de biopsies pulmonaires et d'expectorations couplées à une observation histologique d'une inflammation granulomateuse.

Un séquençage des gènes de ménages *rpoB*, *hsp65* et *rrs* (ARN 16S) permet d'identifier avec certitude une infection par 7 MNT parmi lesquelles font parties les espèces du complexe *M. abscessus* ainsi que *M. avium*, *M. chelonae*, *M. chimera* et *M. intracellulare*. Ce kit, GenoType NTM-DR (Hain Lifescience, Nehren, Allemagne), permet également d'identifier, au sein du complexe *M. abscessus*, le profil de résistance pour : (i) les macrolides en séquençant les gènes *erm(41)* et de l'*ARNr 23S*, (ii) pour les aminoglycosides *via* le séquençage del'*ARNr 16S*. La discrimination entre les trois sous-espèces *M. abscessus* est possible car la protéine Erm(41) est tronquée chez la sous-espèce *M. massiliense*. Cette enzyme va méthyler de l'A2058 de l'ARNr 23S de la grande sous-unité ribosomique et le protéger des macrolides. Le séquençage d'*erm(41)* permet de détecter un polymorphisme nucléotidique bien particulier chez les sous-espèces *M. abscessus* et *M. bolletii*, une mutation en position 28 (T28C), qui rend Erm(41) non-fonctionnelle (Brown-Elliott et al. 2015). Le séquençage de l'*ARNr 23S* permet de détecter pour ces 7 MNT un polymorphisme nucléotidique sur l'A2058 ciblée par les macrolides. Les mutations dans l'ARNr 16S comme celle du résidu A1408 rendent ces 7 MNT résistantes aux aminoglycosides et sont donc recherchées par séquençage (Kehrmann, Kurt, et al. 2016)(Mougari et al. 2017). Il est donc primordial d'identifier quelle sous-espèce de *M. abscessus* est responsable de l'infection car chaque membre de complexe répond différemment aux antibiotiques.

La spectrométrie de masse de type MALDI-TOF (Matrix-Assisted Laser Desorption/Ionisation – Time Of Flight) est une technique très présente en milieu hospitalier qui permet une identification rapide du pathogène responsable de l'infection (Kehrmann, Wessel, et al. 2016)(Sriram et al. 2018). Des marqueurs de résistance peuvent également être ajoutés au panel de détection ainsi que des souchiers d'isolats cliniques permettant une identification très précise et voire même de suivre le déroulement d'une épidémie. Ces caractéristiques techniques permettent de diminuer grandement les risques de diagnostics erronés entrainant des traitements inadéquats.

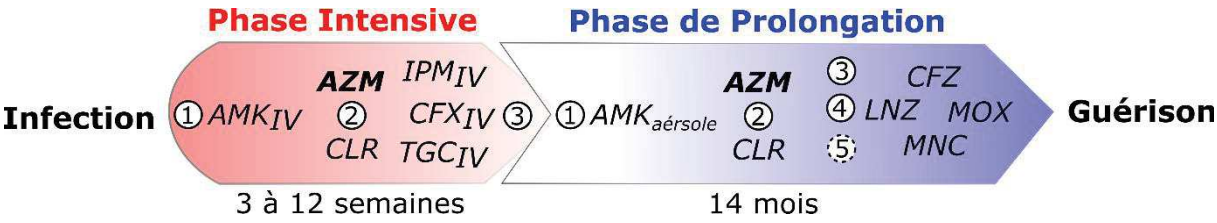

Figure 13. Antibiothérapie dans le cadre d'infections pulmonaires par le complexe *M. abscessus*.
La phase intensive est composée d'une dose journalière de macrolide comme de la clarithromycine (CLR) ou préférablement de l'azithromycine (AZM), d'amikacine (AMK), et d'un des antibiotiques suivant : céfoxitine (CFX), tigécycline (TGC) ou imipénème (IPM). Cette phase est recommandée pour une durée de 3 à 12 semaines, en tenant compte de la sévérité des symptômes et de la tolérance des effets indésirables. La phase de prolongation comprend toujours une dose journalière d'AZM de préférence et d'AMK administrée cette fois-ci en aérosol. Ajoutés à ce cocktail, on retrouve pris par voie orale 2 à 3 des antibiotiques suivants : clofazimine (CFZ), moxifloxacine (MOX), linézolide (LNZ) et minocycline (MNC). Cette phase de prolongation s'étend sur une période de 14 mois et l'utilisation de ces molécules est relative à la susceptibilité aux antibiotiques de la souche incriminée. Cette susceptibilité est définie par la valeur de la Concentration Minimal Inhibitrice (CMI) de chaque antibiotique. Néanmoins ces recommandations semblent relativement arbitraires et pourraient toujours mener à une utilisation inappropriée d'antibiotiques (Citation de Floto et al. 2016 « guided but not dictated by drug susceptibility testing » i.e. l'utilisation des antibiotiques cités ci-dessus). IV, intraveineuse ; voie d'administration non précisée = voie orale (Adapté de Floto et al. 2016).

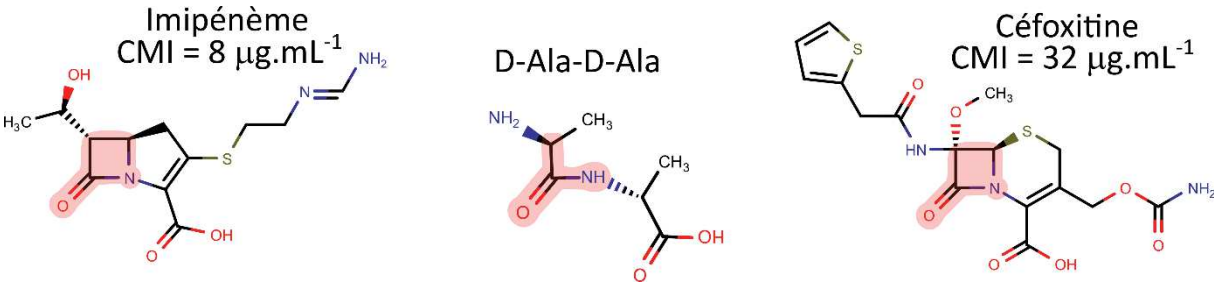

Figure 14. Structures des β-lactamines utilisées dans le traitement de *M. abscessus*. Le D-Ala-D-Ala, substrat des D, D-transpeptidases, est représenté au centre. La partie du substrat imitée par les β-lactamines *via* leurs noyaux β-lactames est encadrée en rouge pour l'imipénème (à gauche) et la céfoxitine (à droite).

1) Présentation de l'antibiothérapie dite « classique » :

Les recommandations pour le traitement d'une infection pulmonaires à *M. abscessus* ont été pendant plusieurs années basées sur une trithérapie s'étalant sur une période de 12 mois composée d'une β-lactamine, d'un aminoglycoside, tous deux administrés par voie parentérale, ainsi que d'un macrolide administré par voie orale. C'est dans l'optique d'optimiser cette trithérapie chez les personnes souffrant de mucoviscidose que s'est réuni en 2016 un consortium entre l'US Cystic Fibrosis Fondation et l'European Cystic Fibrosis Society. Il en a émergé une stratégie thérapeutique préconisant un traitement divisé en deux parties, la phase « intensive » et la phase de « prolongation » comprenant chacune différentes combinaisons d'antibiotiques (Floto et al. 2016) (Figure 13). Un régime antibiotique similaire peut être envisagé chez des personnes ne souffrant pas de mucoviscidose. Ce traitement peut être accompagné d'actes chirurgicaux qui paraissent améliorer l'issue des traitements (Jeon et al. 2009)(Jarand et al. 2011).

1a) Les β-lactamines :

La céfoxitine (CFX) est une céphalosporine semi-synthétique de deuxième génération. Son activité bactéricide est due à l'inhibition du stade final de la biosynthèse du peptidoglycane, un composé essentiel de la paroi mycobactérienne. La CFX rentre en compétition avec le substratd'une classe d'enzymes appelées « D, D-transpeptidases » (Figure 14). Ces enzymes également désignées Protéines Liant la Pénicilline (PLP)(Sauvage et al. 2008), sont présentes dans la partie externe de la membrane plasmique et tournées vers le périplasme (Luthra et al. 2018). Les β-lactamines ont donc de manière générale structure proche du substrat des PLP, le dipeptide D-alanyl-D-alanine. Leur stratégie d'inhibition est donc basée sur un mimétisme de substrat qui provoquera l'arrêt de la synthèse du peptidoglycane (Kohanski et al. 2010).

L'imipénème (IPM) est également une β-lactamine semi-synthétique mais appartient à la famille des carbapénèmes. L'IPM va inhiber les L, D-transpeptidases avec un mécanisme similaire mais avec une meilleure activité *in vitro* (Dubée et al. 2015).

1b) Les aminoglycosides :

L'amikacine (AMK) est un 2-deoxystreptamine aminoglycoside et également une molécule semi-synthétique dérivée de la kanamycine A (KAN A)(Figure 15A). Cet antibiotique interagit avec

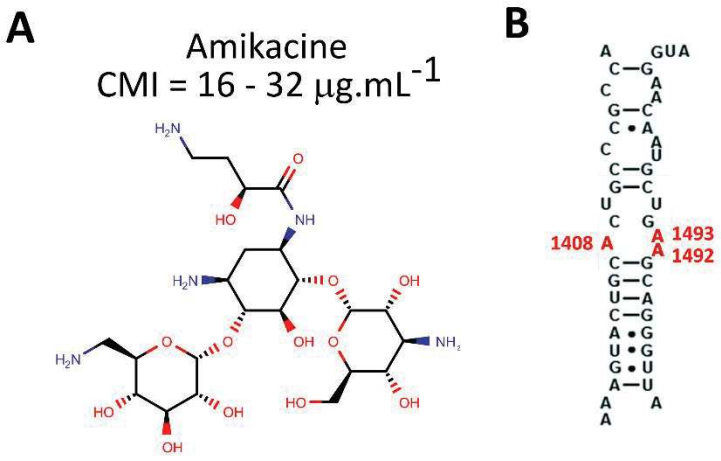

Figure 15. Structures de l'amikacine (A) et de la région qu'elle cible dans l'ARNr 16S (B). Les nucléotides du site-A ciblés par l'amikacine sont en rouge (Adapté de Sarpe et al. 2019)

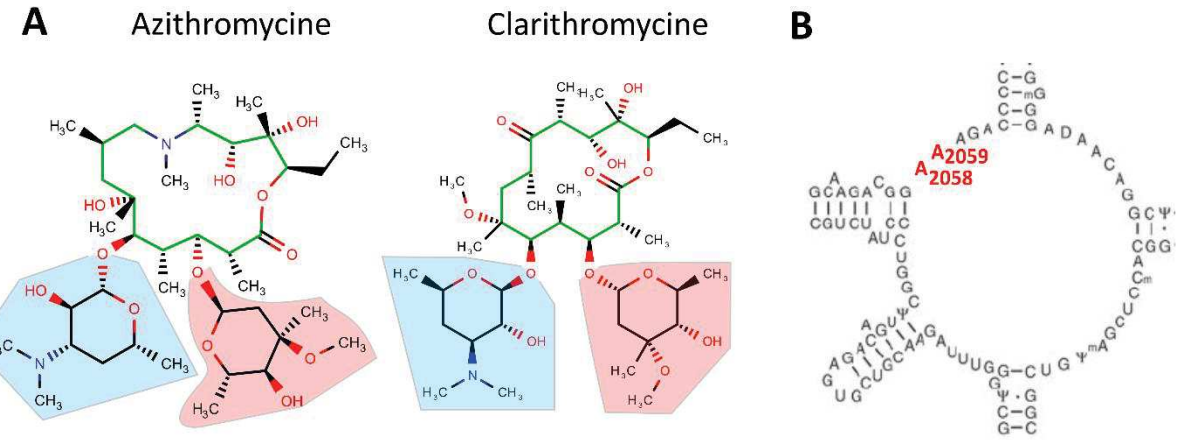

Figure 16. Structure de l'azithromycine et de la clarithromycine (A) ainsi que de la région qu'elles ciblent dans l'ARNr 23S (B). Les cycles lactones sont en vert, les sucres désosamines et cladinoses sont encadrés en bleu et en rouge respectivement. Les adénines de la boucle centrale du domaine V de l'ARNr 23S ciblées par ces macrolides sont marqués en rouge (Adapté de Douthwaite 2001).

l'ARNr 16S de la petite sous-unité du ribosome (30S). Les aminoglycosides étant des antibiotiques polycationiques et l'ARNr 16S chargé négativement (Shakil et al. 2008), l'AMK va former des liaisons électrostatiques avec les adénines en position 1408 (A1408), 1492 (A1492) et 1493 (A1493) responsables de l'activité de *decoding,* perturbant l'entrée du bon ARNt dans le site A (O'Sullivan et al. 2018)(Dudek et al. 2014)(Figure 15B). Ceci provoque l'incorporation d'aminoacides ne correspondant pas à l'ARNm. Ces erreurs de traduction mènent à la synthèse de protéines mal repliées ce qui génère alors un fort stress oxydatif et membranaire (Kohanski et al. 2010). Afin d'éviter les effets secondaires liés à l'injection intraveineuse d'AMK comme la perte de l'ouïe et la toxicité rénale, cette antibiotique peut être administré en aérosol, notamment lors de la phase de continuité (Yagi et al. 2017).

1c) Les macrolides :

Dérivés de l'érythromycine, la clarithromycine (CLR) et l'azithromycine (AZM) sont des antibiotiques d'hémisynthèses qui diffèrent principalement par le nombre d'atomes composant leur cycle lactone, 14 et 15 respectivement (Figure 16A). Cette classe d'antibiotiques cible également la synthèse protéique mais en interagissant cette fois avec l'ARNr 23S de la grande sous-unité ribosomale (50S), plus précisément avec la boucle du centre peptidyltransférase dans le domaine V (Figure 16B). La CLR et l'AZM vont former des liaisons hydrogènes réversibles avec deux nucléotides, l'A2058 et l'A2059 *via* leur sucre désosamine (Garza-Ramos et al. 2001). Ces deux antibiotiques établiront également des interactions électrostatiques avec d'autres nucléotides de cette région du ribosome qui forment la sortie d'un tunnel par lequel sort la chaine polypeptidique néo-synthétisée. Ceci aura pour conséquence d'empêcher la translocation, c'est-à-dire la formation du pont peptidique entre la protéine en cours de synthèse et le nouvel acide aminé porté par l'ARNt. *M. abscessus abscessus* et *M. abscessus bolletii* sont de manière générale naturellement résistant à ces macrolides (Nash et al. 2009). Néanmoins, ces molécules peuvent s'avérer efficaces lorsqu'elles sont utilisées en combinaison, particulièrement contre la sous-espèce *M. abscessus massiliense* (Zhang et al. 2017). L'AZM possède une demi-vie plus élevée que la CLR et ne provoque pas d'interaction médicamenteuse avec les autres antibiotiques présents dans l'antibiothérapie contre *M. abscessus* (Periti et al. 1992). Cependant, Renna et al. ont tiré la sonnette d'alarme quant à l'utilisation à long terme d'AZM, particulièrement chez les personnes souffrant de mucoviscidose. Tout d'abord, il arrive que l'AZM soit administrée pour ses propriétés immunomodulatrices et non pas pour traiter une infection. Les doses données sont subinhibitrices et peuvent donc permettre la sélection de MNT résistantes aux macrolides (Levy et al. 2008). Ces même propriétés immunomodulatrices vont bloquer l'autophagie, la fusion phagolysosomale et l'élimination des bacilles dépendante de la

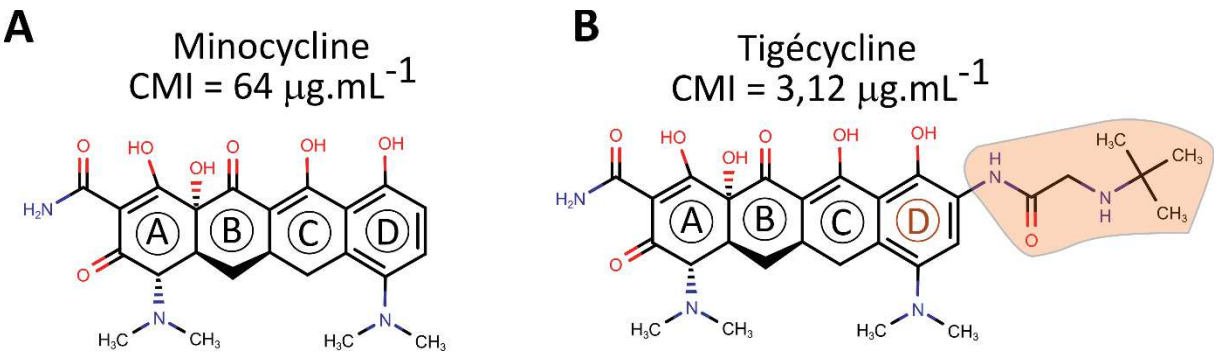

Figure 17. Structures de la minocycline (A) et de la tigécycline (B). La chaine 2-tert-butylglycylamido en position C9 du cycle aromatique D de la tigécycline est encadrée en orange.

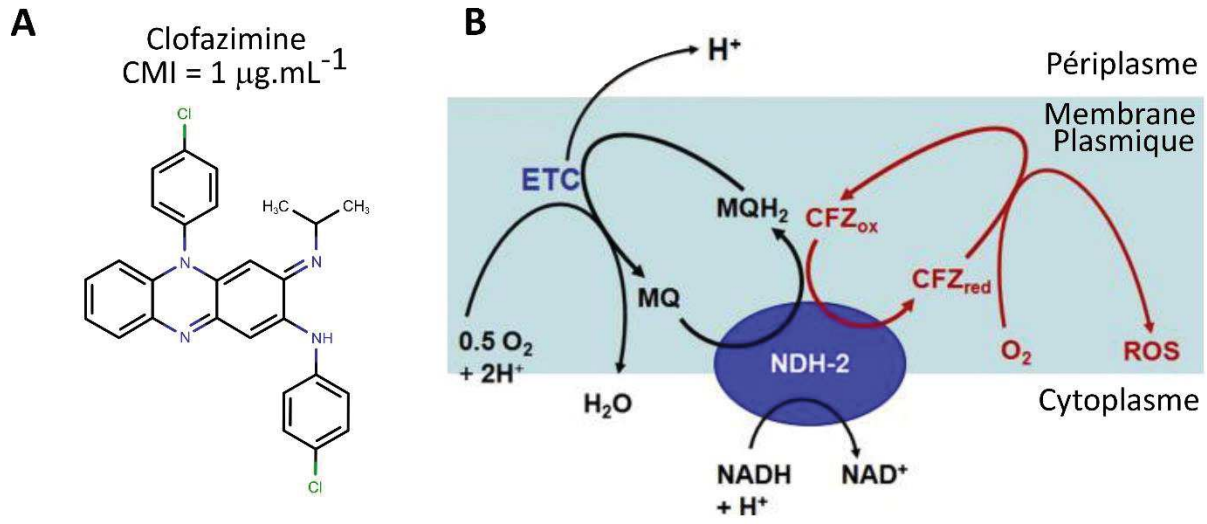

Figure 18. Structure de la clofazimine (A) et représentation schématique de sa voie d'activation (B). La NDH-2 catalyse le transfert d'H^+ du NADH à la ménaquinone (MQ) qui participera ensuite dans le transfert d'électrons vers les autres oxydoréductases de la chaine respiratoire mycobactérienne avec comme réaction finale la réduction de O_2 en H_2O et une sortie d'H^+ vers le périplasme. Cette étape terminale générera une force proton motrice indispensable à la synthèse d'ATP. La CFZ est activée sous sa forme réduite par la NDH-2 *via*le NADH également. La CFZ_{red} interagira ensuite avec les molécules d'O_2 obtenues en bout de chaine respiratoire pour conduire à la production de ROS nocifs pour la bactérie. La production de ROS va ré-oxyder de manière non-enzymatique la CFZ qui pourra à nouveau être réactivée par la NDH-2. Ainsi la CFZ subit une réactivation redox cyclique menant à la production croissante de ROS. ETC, electron transport chain ; MQ, ménaquinone ; CFZ, clofazimine ; ROS, reactive oxygen species ; ox, oxydée ; red, réduite (Adapté de Yano et al. 2011).

production d'IFN-γ et de TNF-α par les macrophages. Autant de facteurs combinés qui favorisent la colonisation par les MNT (Renna et al. 2011).

1d) Les tétracyclines :

La minocycline (MNC) est une tétracycline de deuxième génération qui ne possède généralement pas une très bonne activité *in vitro* contre *M. abscessus.* Son utilisation en deuxième phase de traitement contre les infections pulmonaires ne doit être envisagée que contre des souches sensibles. De plus, les récents travaux de Ruth et al. de 2018 rapportent la même inefficacité aussi bien seule qu'en combinaison avec d'autres antibiotiques *in vitro*.

La tigécycline (TGC) est cependant elle un des seuls analogues de tétracycline possédant une activité antimicrobienne contre *M. abscessus*. Cette glycylcycline administrée en intraveineuse possède un très bon taux d'absorption et d'accumulation intracellulaire en faisant donc un bon candidat pour lutter contre les infections mycobactériennes (Ferro et al. 2016). La TGC est la seule de toutes les tétracyclines prescrites à posséder une chaine 2-tert-butylglycylamido en position C9 de son cycle aromatique D (Figure 17). Cette particularité structurale lui confèrerait la capacité de résister à l'efflux actif et à l'inactivation enzymatique que subit cette classe d'antibiotiques chez *M. abscessus* (Rudra et al. 2018). Comme les autres types de tétracyclines, la MNC et la TGC vont bloquer la traduction en interagissant avec la sous-unité 30S du ribosome et empêcher l'entrée des aminocayl-ARNt dans le site-A du centre peptidyltransférase provoquant l'arrêt de la synthèse protéique.

1e) Les phénazines :

La clofazimine (CFZ), autrefois utilisée pour traiter la lèpre mais faisant partie actuellement du régime thérapeutique anti-MDR-Tb (Mirnejad et al. 2018) est toujours en cours d'évaluation clinique pour son efficacité contre *M. abscessus*. C'est une molécule de synthèse appartenant à la famille des phénazines. Cet antibiotique considéré comme bactériostatique possède aussi de bonnes propriétés anti-inflammatoires ce qui lui donne l'occasion de se retrouver dans le traitement de certaines maladies non-infectieuses comme le lupus et le psoriasis (Sanchez 2000). Le mécanisme d'action de la CFZ contre *M. abscessus* n'est pas décrit. Néanmoins, il a été montré chez *M. smegmatis* que la CFZ est une pro-drogue nécessitant d'être bio-activée par la NADH oxydoréductase de type II (NDH-2) insérée dans le feuillet interne de la membrane plasmique (Yano et al. 2011). Cette bio-activation mène à une importante production de ROS pouvant s'avérer fatale pour le bacille (Figure 18B).

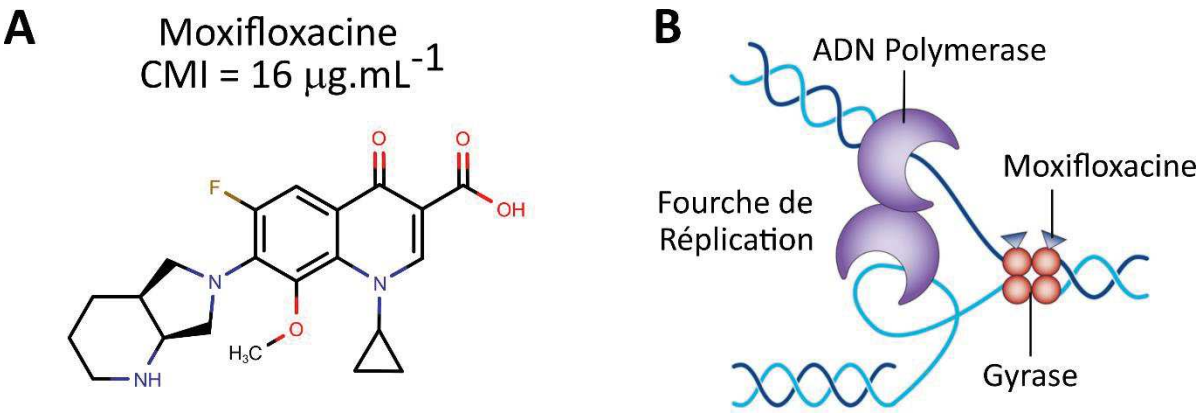

Figure 19. Structure de la moxifloxacine (A) et représentation schématique de son interaction avec l'ADN gyrase lors de la réplication de l'ADN (B). L'ADN gyrase va désenrouler l'ADN en générant des coupures temporaires de la double-hélice permettant à l'ADN polymérase de répliquer le matériel génétique. La moxifloxacine va former un complexe avec l'ADN et l'ADN gyrase ce qui provoquera un arrêt de la réplication et laissera l'ADN clivé. Ces cassures de l'ADN généreront un fort stress oxydatif déclenchant la mort cellulaire (Adapté de Kohanski et al. 2010).

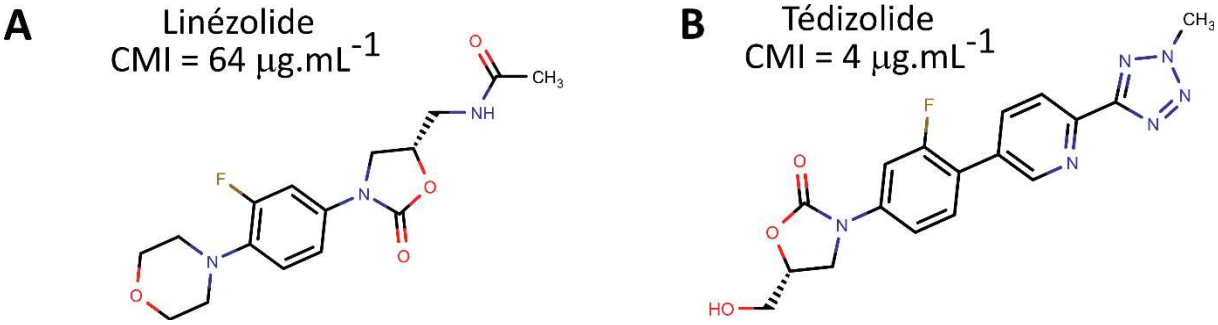

Figure 20. Structure du linézolide (A) et du tédizolide (B)

1f) Les fluoroquinolones :

La moxifloxacine (MXF) est une fluoroquinolone de quatrième génération retrouvée en phase de continuité dans le traitement de *M. abscessus*. Cet antibiotique peut être administré par voie orale, parentérale mais aussi de manière locale mais aussi pour un traitement ophtalmologique.

Cette molécule de synthèse dérive de l'acide nalidixique découvert en 1962 (Figure 19A). Elle va interagir avec les sous-unités α de l'ADN gyrase/Topoisomérase II lorsqu'elle forme un complexe avec l'ADN (Figure 19B). Cette enzyme est essentielle et a pour rôle de « dénouer » les super enroulements du chromosome bactérien causés lors de la réplication de l'ADN et de la progression de la fourche de réplication. Elle agit également sur une autre enzyme structurellement proche de l'ADN gyrase, la topoisomérase IV. Cette enzyme est impliquée dans les derniers stades de la réplication en séparant les deux chromosomes néo-synthétisés avant leurs ségrégations dans les deux cellules filles. L'interaction de la MOX avec ces deux complexes enzyme-ADN aboutiraau même résultat: cassure des chromosomes bactériens et lyse du bacille. Malgré l'efficacité des fluoroquinolones, l'Agence Européenne du Médicament recommande de limiter leur utilisation afin de prévenir l'émergence de résistance comme ce fut le cas pour les fluoroquinolones de deuxième et troisième générations (Kowalski et al. 2003) mais aussi à cause de leurs effets secondaires (Francisco 2018).

1g) Les oxazolidinones :

Il s'agit d'une autre classe de molécules intégrées dans la deuxième phase de l'antibiothérapie contre *M. abscessus*, dont fait partie le LNZ. Ce sont des composés organiques de synthèse hétérocycliques qui vont bloquer la synthèse protéique. La LNZ va interagir de manière non-covalente avec les nucléotides uraciles 2504 (U2504), 2506 (U2506), 2585 (U2585) et les résidus A2451 et A2503 de l'ARNr 23S chez la bactérie *Deinococcus radiodurans* (Wilson et al. 2008). Ces nucléotides sont proches de l'interface 50S/30S et l'interaction du LNZ va bloquer la formation du complexe d'initiation 70S. Ces antibiotiques peuvent être administrés par voie orale ou par intraveineuse. Le tédizolide (TDZ), un analogue structural du LNZ a une très bonne activité contre un large panel d'isolats cliniques de *M. abscessus in vitro* (Compain et al. 2018) (Figure 20). Le TDZ semble également être une molécule très prometteuse lorsqu'elle est utilisée en combinaison contre *M. abscessus* (Le Run et al. 2019).

2) Présentation des autres possibilités thérapeutiques:

Malgré les associations possibles entre ces différentes classes d'antibiotiques avec des cibles subcellulaires variées, 40 % des traitements de *M. abscessus* aboutissent à un échec thérapeutique (Koh et al. 2014). Les cliniciens ont donc parfois recours à des antibiotiques peu communs et sans

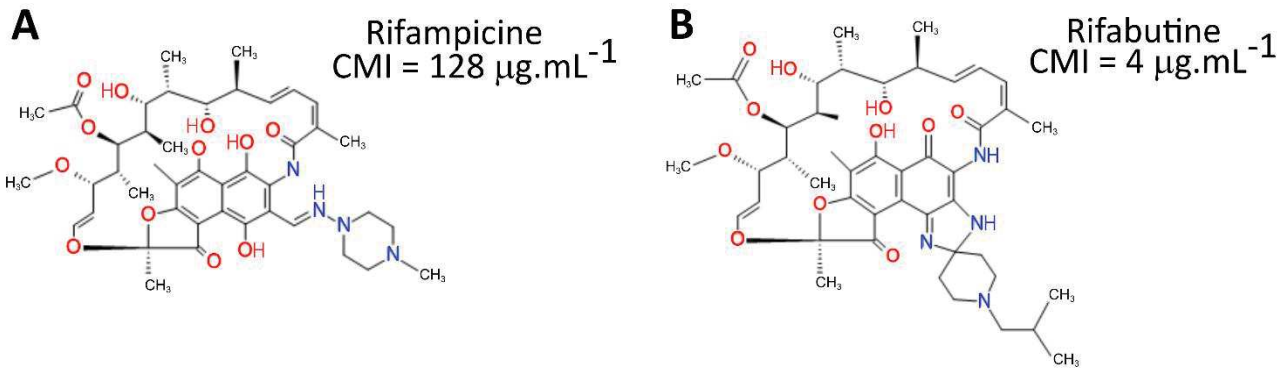

Figure 21. Structure de la rifampicine (A) et de son dérivé la rifabutine (B).

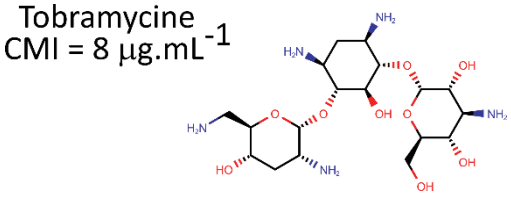

Figure 22. Structure de la tobramycine.

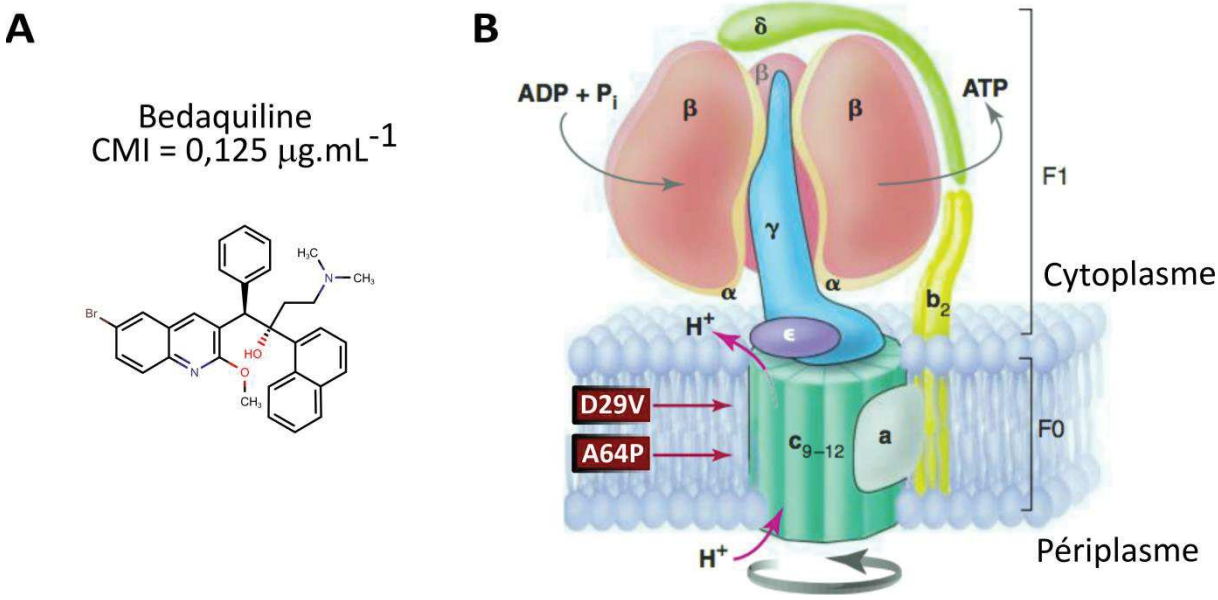

Figure 23. Structure de la bédaquiline (A) et représentation schématique de sa cible, l'ATP synthase (B). L'ATP synthase est constituée d'une partie cytoplasmique F_1 et d'une partie transmembranaire F_0. Les sous-unités c sont arrangées en disques symétriques capables de rentrer en rotation grâce à la force proto-motrice, qui est nécessaire par la suite pour la synthèse d'ATP. Les mutations D29V et A64P confèrent à *M. abscessus* de hauts niveau de résistance (Adapté de Cole et Alzari 2005).

précédents d'utilisations contre les MNT, mais dont l'utilisation est approuvée pour le traitement d'autres bactérioses.

2a) Les rifamycines :

La rifabutine est une rifamycine semi-synthétique, une variété d'antibiotiques appartenant à la classe des ansamycines. Cette nouvelle molécule a récemment montré une activité antimicrobienne bien supérieure contre *M. abscessus* que la molécule de laquelle elle dérive, la rifampicine (Rominski, Roditscheff, et al. 2017)(Aziz et al. 2017)(Figure 21). Cet antibiotique, administré par voie orale, va inhiber la synthèse d'ARN catalysée par l'ARN polymérase. Les mécanismes par lesquels la rifabutine interagit avec l'ARN polymérase ne sont pas décrits mais il est probable qu'elle opère de la même manière que la rifampicine. Ces antibiotiques,*via* des interactions de type van der Waals avec la sous-unité β de l'ARN polymérase,vont bloquer le sillon par lequel l'enzyme entre en contact avec l'ADN (Campbell et al. 2001). De plus, la rifabutine semble avoir un fort potentiel synergique *in vitro* avec d'autres antibiotiques utilisés contre *M. abscessus* (Le Run et al. 2018)(Cheng et al. 2019).

2b) Les aminoglycosides non-conventionnels :

La tobramycine (TBM) est un autre 2-deoxystreptamine aminoglycoside qui peut aussi être utilisé contre *M. abscessus*. Comme l'AMK, elle peut être administrée par voie orale et parentérale mais également localement pour traiter des infections oculaires. La TBM agit de la même manière que l'AMK sur la sous-unité 30S du ribosome en se liant aux mêmesrésidus A1492 et A1493 (Yang et al. 2006). La TBR est légèrement plus efficace que l'AMK*in vitro* mais sa sensibilité aux enzymes dégradant les aminoglycosides est différente ce qui limite son utilisation (Rominski, Selchow, et al. 2017)(Figure 22).

2c) Les diarylquinolines :

C'est en 2012 que la bédaquiline (BDQ) fait son arrivée dans le traitement des souches de MDR-Tb. Comme la CFZ, son utilisation est envisagée pour traiter *M. abscessus* et son efficacité est en cours d'évaluation. *A contrario*, la BDQ n'a pas un effet bactéricide chez *M. abscessus* mais est extrêmement active *in vitro* (Dupont et al. 2017). La BDQ est un antibiotique de synthèse appartenant à la famille des diarylquinolines qui est administrée par voie orale (Figure 23A). Elle va inhiberl e complexe enzymatique membranaire F_0-F_1 ATP synthase. Les cibles de la BDQ sont les sous-unités c, qui forment un anneau transmembranaire par lesquels transitent les protons nécessaires à la production d'ATP. Plus précisément, la BDQ interagirait avec les résidus acide

Table 1) Récapitulatif des études menées *in vitro/in vivo* depuis 2005 contre le complexe *M. abscessus.*

	Combinaison antibiotiques/inhibiteurs	Type d'étude	Nb de Souches	Résultats obtenus	Réf.
1	Clarithromycine + linézolide	*In vitro*	2	100%	Cremades et al. 2009
2	Clarithromycine + tigécycline	*In vitro*	20	65% *M. massiliense*	Zhang et al. 2017
				25%	
		In vitro	31	80.6%	Huang et al. 2013
3	Clarithromycine + vancomycine	*In vitro*	12	100%	Mukherjee et al. 2017
4	Clarithromycine + moxifloxacine	*In vitro*	28	39.3% *M. massiliense*	Choi et al. 2012
			26	3.8%/65.4%	
		macrophage	15	33.3% *M. massiliense*	
				6.6%/66.7%	
		souris	6	50% *M. massiliense*	
			7	71.4% *M. abscessus*	
		In vitro	20	85% *M. massiliense*	Zhang et al. 2017
				5%/45% *M. abscessus*	
5	Azithromycine + moxifloxacine	*In vitro*	28	35.7% *M. massiliense*	Choi et al. 2012
			26	3.8%/46.2%	
		macrophage	15	20% *M. massiliense*	
				6.6%/40.0%	
		souris	6	50% *M. massiliense*	
			7	71.4% *M. abscessus*	
6	Clarithromycine + linézolide + moxifloxacine/gatifloxacine/lévofloxacine	*In vitro*	2	100%	Cremades et al. 2009
7	Clarithromycine + ciprofloxacine + rifabutine	*In vitro*	2	100%	Cremades et al. 2009
8	Imipénème + clarithromycine	*In vitro*	21	43%	Miyasaka et al. 2007
9	Imipénème + lévofloxacine	*In vitro*	21	29%	Miyasaka et al. 2007
10	Amikacine + clofazimine	*In vitro*	40	100%	Shen et al. 2010
		In vitro	77	80.5%	van Ingen et al. 2012
11	Amikacine + linézolide	*In vitro*	32	53.1% *M. massiliense*	Zhang et al. 2018
				37.5%	
12	Tigécycline + clofazimine	*In vitro*	19	42%	Singh et al. 2014

aspartique 32 (D32) et alanine 64 (A64)(Dupont et al. 2017)(Figure 23B). Il en résulte un blocage de la rotation de l'anneau formé par toutes les unités c arrêtant la production d'ATP (Preiss et al. 2015). La BDQ semble également avoir une seconde cible chez *M. tuberculosis*, la sous-unité ε de l'ATP synthase (Kundu et al. 2016).

3) Associations d'antibiotiques et synergies pour le traitement de *M. abscessus* :

L'association d'antibiotiques permet l'éradication de germes multi-résistants en élargissant leurs spectres individuels et prévient les poly-infections. Les doses d'antibiotiques administrées lors d'une thérapie ne sont forcément réduites comme c'est le cas *in vitro* et les doses dictées par les autorités sanitaires de chaque antibiotique sont respectées (Auboyer et al. 2000). Ainsi il peut en résulter une cumulation d'effets indésirables très handicapants menant à l'abandon du traitement. Certains antibiotiques vont également avoir une pharmacocinétique différente chez l'homme et perdre en efficacité. Ceci explique pourquoi les données sur les synergies entre différents antibiotiques fluctuent entre les études *in vitro* et les études *in vivo*. Par définition, une synergie entre deux ou plusieurs antibiotiques résulte en un meilleur effet antibactérien que le cumul des effets de chaque antibiotique utilisé séparément. Il est donc préférable d'utiliser des antibiotiques avec des cibles distinctes afin de cumuler le pouvoir antimicrobien de chaque molécule.

Les études de l'efficacité de combinaisons antibiotiques sur patients sont peu abondantes. L'une d'elle (Choi et al. 2011) a mis en évidence une synergie visible entre une bithérapie MOX/CLR comparée à une combinaison AMK/CLR dans le cadre d'infections cutanées causées par *M. abscessus*. La convalescence des patients étaient également plus courtes avec l'utilisation de MOX et CLR.

Les informations sur les synergies antibiotiques *in vitro* sont largement plus conséquentes que celles faites *in vivo*. L'ensemble de ces synergies testées contre *M. abscessus* est récapitulé en Table 1. Certaines de ces combinaisons étant plus originales ou novatrices sont décrites ci-dessous.

L'une d'elle inclut l'utilisation de TDZ. Le Run et al. ont récemment démontré *in vitro* ainsi que dans un modèle macrophage une synergie du TZD avec l'IPM et la rifabutine en combinaison avec un inhibiteur de β-lactamases de dernière génération, l'avibactam. De plus, la rifabutine et le TDZ ont été utilisés à des concentrations sériques, ce qui encourage leur évaluation clinique contre *M. abscessus*.

Similaire à la stratégie incluant l'avibactam, le vérapamil (VPM), un inhibiteur de courant calcique membranaire, permet d'optimiser les antibiotiques ciblant les voies métaboliques dépendantes des gradients électrochimiques comme les pompes à efflux ou l'ATP synthase. Le VPM seul est inactif mais en combinaison avec la BDQ présente un fort effet synergique contre des isolats

13	Tigécycline + linézolide	*In vitro*	32	**31.3%** *M. massiliense*	Zhang et al. 2018
				21.9%	
		drosophile	1	**100%**	Oh et al. 2014
14	Tigécycline + teicoplanine	*In vitro*	1	**100%**	Aziz et al. 2018
15	Rifampicine + doripénème/biapénème	*In vitro*	1	**100%**	Kaushik et al. 2015
16	Rifabutine + imipénème	*In vitro*	13	**100%**	Cheng et al. 2019
17				**69%**	
18	Rifabutine + tigécycline	*In vitro*	13	**77%** *M. massiliense*	
19				**69%** *M. massiliense*	
20	Rifabutine + tigécycline + clarithromycine	*In vitro*	7	**71%**	Pryjma et al. 2018
21	Avibactam + amoxicilline	*In vitro*	17	**100%**	Dubée et al. 2015
		macrophage	1	**100%**	
		ZF		**100%**	
22	Avibactam + céftaroline	*In vitro*	1	**100%**	Lefebvre et al. 2016
		macrophage		**100%**	
23	Avibactam + imipenème + amikacine	*In vitro*	1	**100%**	Lefebvre et al. 2017
		macrophage		**100%**	
		ZF		**100%**	
24	Avibactam + tébipénème/ertapénème/panipénème	*In vitro*	29	**100%**	Kaushik et al. 2017
25	Avibactam + doripénème/faropénème/ merépenème/biapénème	*In vitro*	29	**55–75.9%**	Kaushik et al. 2017
26	Avibactam + céfalotine/Céfuroxime céfamandole/céftriaxone	*In vitro*	1	**100%**	Dubée et al. 2015
27	Acide clavulanique + meropénème	*In vitro*	1	**100%**	Kaushik et al. 2015
28	Vérapamil + bédaquiline	*In vitro*	18	**100%** *M. abscessus sensu lato*	Viljoen et al. 2019
		macrophage	1	**100%**	

Synergie, FICI < 0,5 ; **Antagonisme**, FICI > 2 ; FICI = FICA + FICB, Fractionnal Inhibitory Concentration Index (FICI). FICA est égale à la valeur de la CMI d'un antibiotique A utilisé en combinaison avec un autre antibiotique divisée par la valeur de la CMI de l'antibiotique A seul. FICB est équivalent à FICA pour l'antibiotique B. Lorsque le nom de l'espèce n'est pas spécifié dans la colonne « Résultats obtenu », c'est qu'il s'agit de *M. abscessus sensu stricto* (Adapté de Wu et al. 2018).

cliniques de *M. abscessus in vitro.* Cet effet est également observé au sein de macrophages infectés, mettant en avant l'intérêt de cette combinaison contre *M. abscessus* (Viljoen et al. 2019). La résistance inductible aux macrolides chez les sous-espèces *M. abscessus* et *M. bolletii* est un réel frein à l'utilisation de cette classe de molécules qui est un pilier dans le traitement de ces mycobactérioses. Cependant, la vancomycine, un antibiotique glycopeptidique ciblant la synthèse de la paroi, est en réalité efficace en combinaison avec la CLR. Cette combinaison est même effective contre des souches dont la résistance aux macrolides a été induite antérieurement (Mukherjee et al. 2017). Chez ces deux sous-espèces, ce système de résistance inductible est en partie responsable du faible taux de succès thérapeutique, avoisinant les 25 % (Jarand et al. 2011). Cette combinaison mériterait également une évaluation clinique, d'autant plus que la vancomycine est un antibiotique approuvé par les administrations sanitaires.

Chapitre IV) L'Antibiorésistance chez M. abscessus

1) Polymorphisme nucléotidique, génétique et mutations acquises :

L'antibiorésistance innée de *M. abscessus* est due, en plus de l'imperméabilité de sa paroi, à un fort polymorphisme génétique retrouvé soit sur les cibles de certains antibiotiques soit sur les gènes codants les enzymes responsables de leurs activations. La résistance intrinsèque aux antituberculeux de première intention est un bon exemple de ce polymorphisme génétique comme c'est le cas pour l'éthambutol (EMB). Cet antibiotique cible les arabinosyltransférases produites par l'opéron *embCAB* qui sont impliquées dans l'arabinosylation de l'arabinogalactane et du LAM (Zhang et al. 2003). Deux substitutions d'acides aminés ont un rôle dans la résistance à l'EMB. La présence de résidus glutamine et méthionine en position 303 et 304 de la protéine ciblée par cet antibiotique EmbB confère de haut niveau de résistance à *M. abscessus* et à d'autres mycobactéries (Nessar et al. 2012). *M. tuberculosis* possède des résidus isoleucine et leucine à ces positions 303 et 304, le rendant sensible à cet antibiotique (Alcaide et al 1997).

La résistance aux fluoroquinolones de deuxième et troisième génération est aussi due à un polymorphisme génétique de leurs cibles, les gènes *gyrA* et *gyrB*, encodant les deux sous-unités de l'ADN gyrase (Guillemin et al. 1998). Les résidus, selon la numérotation faite chez *E. coli*, alanine en position 83 (A83) dans le gène *gyrA*, ainsi qu'une arginine et qu'une asparagine en position 447 (R447) et 464 (N464) dans le gène *gyrB* respectivement, sont critiques. En effet, la substitution de ces aminoacidespar les résidus d'*E. coli* chez *M. tuberculosis*, qui possède le même polymorphisme de résistance que *M. abscessus*, provoque une sensibilité du bacille de Koch (Matrat et al. 2008).

Un autre exemple de polymorphisme génétique responsable de résistance intrinsèque à un antituberculeux de première ligne est celui de l'isoniazide (INH) et du gène *katG*, codant pour une catalase/péroxydase. L'INH est une pro-drogue inactive qui doit être péroxydée par KatG. Les dérivés de l'INH produits se lient au NADH cytoplasmique. Ce complexe va par la suite inhiber InhA, une énoyle réductase faisant partie du complexe enzymatique FAS-II impliquée dans la synthèse desprécurseurs des acides mycoliques (Wiseman et al. 2010). Cette bio-activation de l'INH ne se produit pas chez *M. abscessus*. KatG est présente et fonctionnelle mais elle est incapable de transformer l'INH en métabolite actif (Luthra et al. 2018).

Ce défaut de bio-activation est aussi observé pour un antibiotique utilisé dans le traitement de MDR-Tb, l'éthionamide (ETH). Cette molécule est un dérivé structural de l'INH qui va également

inhiber la synthèse d'acides mycoliques en ciblant InhA. L'ETH est activé par la monooxygénase EthA chez *M. tuberculosis* (Dover et al. 2007). L'EthA de *M. abscessus* n'est pas capable d'activer l'ETH mais cette enzyme est fonctionnelle car elle active d'autres antibiotiques de la même classe, le thiacétazone (TAC) et ses dérivés (Halloum et al. 2017). La résistance au TAC chez *M. abscessus* est due à une redondance fonctionnelle de sa cible, la déhydratase HadBC. Ces phénomènes de redondances fonctionnelles transforment les cibles initiales essentielles en cibles secondaires, et l'effet antibiotique est alors perdu. L'autre déhydratase résistante au TAC, MAB_4780, remplit la fonction de HadBC lorsqu'elle est inhibée par le TAC (Halloum et al. 2016).

Les mutations chromosomiques spontanées sur les cibles des antibiotiques après une exposition trop courte ou après des concentrations trop faibles représentent également un mécanisme majeur d'émergence de résistances chez *M. abscessus*. Cependant, il convient également de prendre compte le fait qu'une infection bactérienne est provoquée par une population génétiquement très hétérogène. Si le traitement n'est donc par exemple pas administré de manière régulière et ponctuelle, l'irrégularité de la prise d'antibiotique va dans un premier temps éliminer les populations sensibles. Les sous-populations résistantes résiduelles, possédant à la fois des mutations conférant une résistance sans impacter le métabolisme basal vont alors émerger, se multiplier et occuper le vide laissé par l'élimination des populations sensibles. L'émergence de ces souchesrésistantes mènent éventuellement à l'échec thérapeutique (Blair et al. 2015). Ces altérations génétiques sont rencontrées lors de thérapies basées sur l'utilisation de plusieurs classes d'antibiotiques comme les macrolides, les aminoglycosides et les fluoroquinolones.

En ce qui concerne les macrolides, aucune information n'est disponible sur la différence de pouvoir mutagène entre la CLR et l'AZM. Les mutations semblent toutes se produire sur le gène cible *rrl* codant pour l'ARNr 23S. Les mutations apparaissent au niveau des nucléotides responsables des liaisons hydrogènes avec ces antibiotiques, en l'occurrence les nucléotides A2058 et A2059.Ces événements mutagènes sont néanmoins très rares, plus particulièrement sur le résidu A2059 (Carvalho et al. 2018). Il semblerait cependant que le taux de mutations soit plus important chez *M. massiliense*, cette dernière ne possédant pas de système de résistance inductible *via* méthylation de l'ARNr 23S car Erm(41) est tronquée (Liu et al. 2017). Le peu de souches *M. abscessus sensu stricto* ayant mutées possèdent probablement un polymorphisme nucléotidique délétère comme la substitution classique T28C, rendant Erm(41) non-fonctionnelle (Nash et al. 2009). La sous-espèce *M.massiliense* et le séquovar T28 sont donc soumis à une importante pression de sélection pouvant expliquer ces mutations chromosomiques sur le gène *rrl*. Vraisemblablement, en présence d'un système de résistance inductible très efficace, *M. abscessus abscessus* et *M. abscessus bolletii* n'acquerront aucune mutation. Tous les 2-deoxystreptamines aminoglycosides ne vont pas interagir

avec exactement les mêmes nucléotides de l'ARNr 16S. Néanmoins, tous vont avoir ont une forte affinité pour l'A1408, qui est l'un des quatre nucléotides les plus communément mutés, avec les A1492, A1493 et la G1494 (Shakil et al. 2008)(Prammananan et al. 1998)(M. Wu et al. 2019). Comme pour le gène *rrl* et la résistance constitutive aux macrolides, cette mutation ne semble pas être un événement fréquent. Ceci est potentiellement dû en partie à des mécanismes de résistances inductibles inhérents à cette classe d'antibiotiques. *M. abscessus* possède des enzymes modifiant directement ces antibiotiques et des pompes à efflux les expulsant du cytoplasme (Hurst-Hess et al. 2017)(Pryjma et al. 2017). Un type de mutation original a été identifié chez des isolats cliniques de *M. tuberculosis* et entraîne une résistance à la KAN. Il s'agit cette fois-ci de mutation non pas sur le gène cible mais dans son promoteur. Le gène en question, Rv2416c, code pour une acétyltransférase impliquée dans la survie intramacrophagique (Zaunbrecher et al. 2009). Les mutations dans le promoteur vont entrainer une surexpression de cette protéine qui est également capable de bio-inactiver certains des 2-deoxystreptamines aminoglycosides.

Le polymorphisme génétique responsable de la résistance intrinsèque de *M. abscessus* aux fluoroquinolones de deux- et troisième générations, A83 pour *gyrA* et R447-N463 pour *gyrB*, ne semble pas empêcher l'activité antimycobactérienne de la MXF. Quarante souches appartenant au complexe *M. abscessus* considérées comme résistantes à la MXF ont été séquencées pour les gènes *gyrA* et *gyrB*. Ces séquençages n'ont révélé aucune mutation pour l'ADN gyrase (Kim et al. 2018). Cet antibiotique cible également la topoisomérase IV, il serait donc, *a minima*, nécessaire de séquencer les gènes encodant cette enzyme, *parC* et *parE*, voire d'effectuer un séquençage complet du génome pour incriminer l'apparition de mutation dans ce phénotype de résistance.

A ce jour concernant la BDQ, aucune mutation dans le gène *atpE* chez des isolats cliniques de *M. abscessus* n'a été rapporté dans la littérature. Cependant, des mutations dans ce gène générées au sein de notre laboratoire ont offert une forte résistance *in vitro* rendant *M. abscessus* 250 fois plus résistant (Dupont et al. 2017). Au vu de l'énorme avantage en termes de résistance apportées par ses mutations qui n'ont apparemment ni coût réplicatif ni coût métabolique pour les bactéries, on ne peut omettre la possibilité qu'une telle sous-population existe d'ores et déjà ou qu'elle soit susceptible d'apparaitre.

2) Les enzymes modifiant / inactivant les antibiotiques :

Les enzymes capables d'inactiver les antibiotiques en les modifiant chimiquement ont une grande place dans l'arsenal enzymatique constituant le résistome de *M. abscessus*. Leurs mécanismes d'action ainsi que leurs cibles sont variés limitant ainsiles options thérapeutiques.

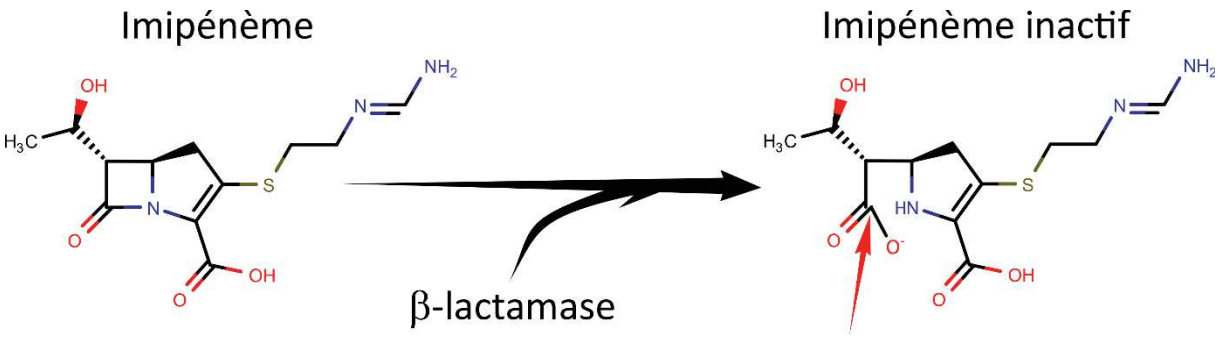

Figure 24. Exemple de dégradation d'une β-lactamine par une β-lactamase. La flèche rouge indique où se situe la dégradation effectuée par une β-lactamase sur l'imipénème (Adapté de Zhai et al. 2012)

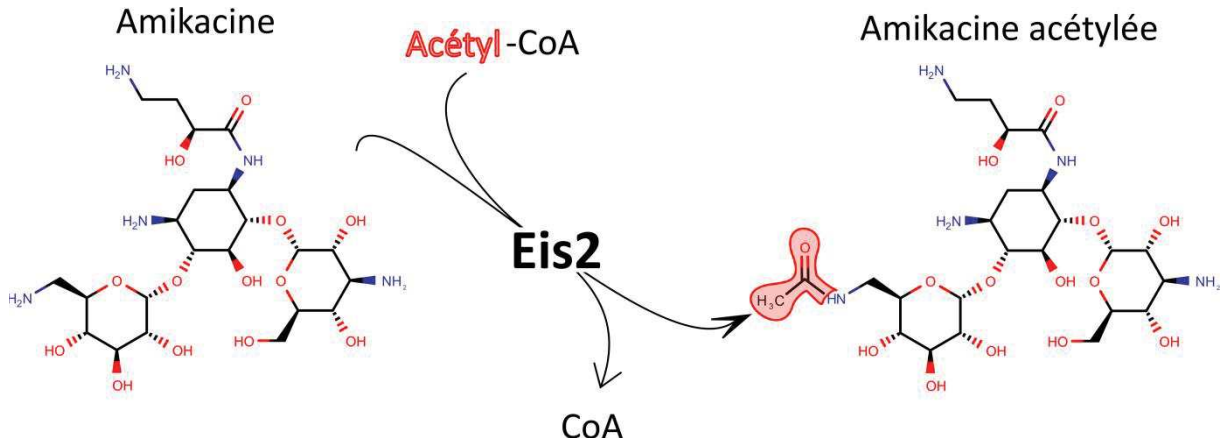

Figure 25. Inactivation enzymatique de l'amikacine par Eis2. Cette N-acétyltransférase transfert un acétyle d'une molécule d'acétyl-CoA sur le groupement amine situé en position 2' du cycle 1 de certains 2-deoxystreptamines aminoglycosides (Adapté de Tran et al. 2018).

2a) Les β-lactamines :

Une seule β-lactamase a été à ce jour caractérisée chez *M. abscessus*, MAB_2875, également appelée Bla_*Mab*, est une β-lactamase de classe A. Il existe quatre classes de β-lactamases (A – B – C – D) séparées en fonction de leurs séquences en acides aminés et par la présence de certains motifs conservés (Bush 2013). Toutes agissent sur le noyau β-lactame des pénicillines, céphalosporines et carbapénèmes (Figure 24). Bla_*Mab* possède une très grande variabilité de substrats, exprimant à la fois une activité pénicillinase, céphalosporinase et carbapénèmase, tout en conservant une très bonne efficacité en présence d'inhibiteurs classiques de β-lactamases comme le clavulanate ou le tazobactam (Soroka et al. 2014). L'IPM est un substrat de Bla_*Mab* mais il semblerait que cette β-lactamine soit en réalité dégradée très lentement, ce qui rend son utilisation clinique toujours possible. La CFX n'est pas un substrat de Bla_*Mab*. La présence d'un groupement méthoxyle (OCH_3) sur le C7 du noyau β-lactame de la CFX la protège probablement de la dégradation par Bla_*Mab*, comme c'est le cas pour la témocilline (Soroka et al. 2014).

2b) Les aminoglycosides :

Chez *M. abscessus,* trois enzymes sont responsables de la résistance aux aminoglycosides. Deux d'entre elles, AAC(2') et Eis2, produits respectifs des gènes *MAB_4395* et *MAB_4532c*, sont des N-acétyltransférases tandis que la troisième est la phosphotransférase MAB_2385 (Luthra et al. 2018). Ces trois enzymes vont modifier de manière covalente des groupements amines clefs de la structure des aminoglycosides diminuant fortement l'affinité de ces antibiotiques pour l'ARNr 16S de la petite sous-unité du ribosome (Blair et al. 2015).

AAC(2'), pour Aminoglycoside 2'-ACétyltransférase, va transférer un groupement acétyle d'une molécule d'acétyle Coenzyme-A (CoA) sur le groupement amine situé en position 2' du cycle 1 de certains 2-deoxystreptamines aminoglycosides (Maurer et al. 2015). Cette enzyme modifie aussi la gentamicine C, la dibékacine, la tobramycine ainsi que la KAN B. L'inactivation génétique de *MAB_4395* provoque une sensibilité pour les antibiotiques ci-dessus (Rominski, Selchow, et al. 2017).

Les protéines Eis (Enhanced Intracellular Survival) sont présentes de manière globale chez les mycobactéries mais aussi chez les Gram +. Eis chez *M. tuberculosis*, en plus d'être aussi impliquée dans la résistance aux aminoglycosides, joue un rôle dans la survie intramacrophagique grâce à son activité acétyltransférase. Eis va bloquer les processus d'autophagie, de maturation phagosomale, de production de cytokines pro-inflammatoires et d'apoptose en inhibant des voies signalétiques dépendantes des ROS (Shin et al. 2010)(K. H. Kim et al. 2012). Même si l'homologie de séquence entre Eis *de M. tuberculosis* et Eis2 de *M. abscessus* est modérée (28 %), la superposition de leurs

structures cristallographiques atteste de la similarité des deux protéines (Ung et al. 2019). Des travaux menés avec l'aide d'un mutant *eis2* chez *M. abscessus* a également montré un déclin dans la survie intracellulaire dans des modèles amibien et macrophagique (Dubois et al. 2019). Il se peut donc qu'Eis2 de *M. abscessus* agisse de la même manière qu'Eis de *M. tuberculosis*. Concernant la résistance au 2-deoxystreptamines aminoglycosides, Eis2 va inactiver, comme AAC(2'), la KAN B, mais aussi la KAN A, l'AMK, l'hygromycine B et la capréomycine en acétylant le premier groupement amine de ces antibiotiques. Un mutant Δ*eis2* est largement plus sensible à ces cinq antibiotiques en comparaison avec la souche parentale. Eis1, un autre homologue présent chez *M. abscessus*, ne semble pas jouer un rôle dans la résistance à cet classe d'antibiotiques là (Rominski, Schulthess, et al. 2017). Eis1 est peut-être impliquée dans d'autres processus cellulaires comme la compaction du chromosome bactérien. Cette fonction est remplie par Eis chez *M. tuberculosis*, toujours grâce à son activité acétyltransférase (Ghosh et al. 2016).

La dernière enzyme MAB_2385, est une 3''-O-phosphotransférase responsable de l'inactivation de la streptomycine (SPM), membre de l'autre sous-classe des aminoglycosides, les streptidines. Dal Molin et al. ont identifié *MAB_2385* comme étant le plus proche homologue de *aph(3'')-Ic*, une phosphotransférase connue pour être responsable de la résistance à la SPM chez *M. fortuitum* (Ramón-García et al. 2006). Ils ont ensuite montré à l'aide d'une étude génétique basée sur un mutant Δ*MAB_2385* et de complémentation fonctionnelle chez *M. smegmatis* que ce gène est en effet responsable de la résistance intrinsèque à la SPM chez *M. abscessus*. Le mutant Δ*MAB_2385* était 16 fois plus sensible à la SPM que la souche sauvage. Une analyse phylogénétique a révélé la présence d'autres acétyltransférases (*MAB_0247c*, *MAB_0404c*, *MAB_0745*, *MAB_4235c* et *MAB_4324c*) et phosphotransférases (*MAB_0163c*, *MAB_0313c*, *MAB_0327*, *MAB_0951* et *MAB_1020*) assez proches génétiquement pour pouvoir être aussi impliquées dans la résistance aux aminoglycosides et/ou dans la survie intracellulaire (Luthra et al. 2018).

2c) Les ryfamicines :

La rifabutine exhibe une forte activité antibactérienne car elle est capable de contourner les mécanismes de résistance intrinsèque qui touchent les autres rifamycines comme la rifampicine et la rifapentine. Ces antibiorésistances sont conférées par deux types d'inactivations enzymatiques distinctes (Ganapathy et al. 2019).

La rifampicine et la rifapentine sont sujettes à l'auto-oxydation à l'extérieur et l'intérieur de *M. abscessus* car elles possèdent une hydroquinone (groupements hydroxyles en position C1 et C4 du cycle naphtyle) ce qui n'est pas le cas de la rifabutine (Buss et al. 1977)(Figure 26A). La présence

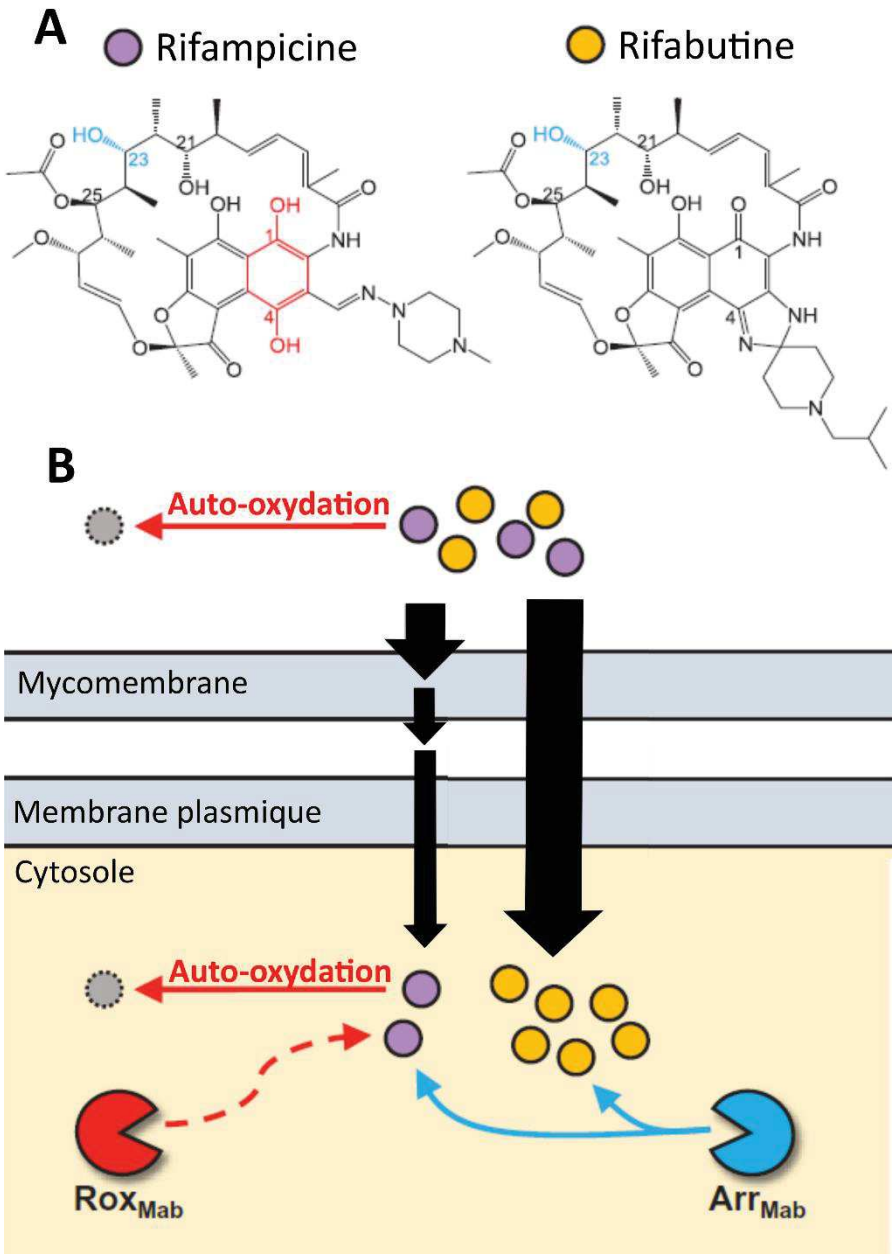

Figure 26. La rifabutine possède des propriétés structurales lui conférant une meilleure absorption ainsi qu'une meilleure résistance à l'auto-oxidation et aux dégradations enzymatiques. (A) Le C23 ADP-ribosylée modifié par Arr_{Mab} est marqué en bleu sur les structures de la rifampicine et de la rifabutine. Le cycle naphtoquinone responsable de l'auto-oxydation et de la dégradation par Rox_{Mab} est marqué en rouge sur la structure de la rifampicine. (B) La rifabutine pénètre de manière plus efficace la paroi mycobactérienne que la rifampicine et possède alors une meilleure pharmacocinétique. La rifabutine n'est pas sensible à l'auto-oxydation de Rox_{Mab} mais ces deux rifamycines sont sensibles à Arr_{Mab} (Adopté de Ganapathy et al 2019).

(Koteva et al. 2018)(Figure 26B). La meilleure accumulation cytoplasmique, la résistance à l'auto-oxydation et à la monooxyénation par Rox_{Mab} explique le meilleur pouvoir antibactérien de la rifabutine par rapport aux autres rifamycines (Ganapathy et al. 2019). Le mécanisme de résistance majeur concernant toutes les rifamycines, en moindre mesure pour la rifabutine, est leur inactivation enzymatique par l'ADP-ribosyltransférase Arr_{Mab} encodée par le gène *MAB_0591* (Rominski, Roditscheff, et al. 2017)(Figure 26B). La suppression chromosomique d'Arr_{Mab} rend *M. abscessus* extrêmement sensible à la rifampicine et à la rifapentine et son expression hétérologue chez deux organismes naturellement sensibles à ces rifamycines, *E. coli* et *M. tuberculosis*, rend ces deux bactéries très résistantes (Rominski, Roditscheff, et al. 2017). Chez *M. smegmatis*, Arr_{Mab} modifie chimiquement le C23 de la rifampicine (Baysarowich et al. 2008). La rifabutine possède le même C23 que les autres rifamycines sensibles mais elle est en réalité moins efficacement ADP-ribosylée par Arr_{Mab}. Il est alors probable que d'autres parties de la molécule ont un rôle dans la résistance à l'inactivation enzymatique, comme pour Rox_{Mab} et le cycle napthoquinone. En réalité Rominski et al. ont prouvé que des modification du C25 permettent d'augmenter l'activité antimicrobienne des rifamycines. La grande taille de ces molécules ne leurs permet pas d'être activement absorbées par des porines et elles doivent donc traverser la membrane plasmique de manière passive (Lambert 2002). La meilleure accumulation de la rifabutine est possiblement due à des différences structurales qui ne sont pas présentes chez les autres rifamycines et favoriseraient la diffusion à l'intérieur de la bactérie. Ainsi, une optimisation structurale des rifamycines parait être une option attractive dans le développement de nouveaux antibiotiques.

2d) Les tétracyclines :

La TGC est un autre bel exemple de modifications structurales conférant une résistance à un mécanisme d'inactivation enzymatique intrinsèque. Cette glycylcycline possèdeune chaine 2-tert-butylglycylamido qui la protège de la FAD-dépendante (Flavine Adénine Dinucléotide) monooxygénase MabTetX (*MAB_1496*) de *M. abscessus* (Rudra et al. 2018). Rudra et al. ont démontré l'hydroxylation de la tétracycline et de la doxycycline chez *M. abscessus* par MabTeTX et sa délétion rend la bactérie 20 fois plus sensible à ces deux antibiotiques, soulignant l'importance de l'activité intrinsèque de cette enzyme. L'expression de MabTetX est régulée par le répresseur de transcription $MabTetR_X$. Cette protéine codée par le gène *MAB_1497c*, appartient à la superfamille des régulateurs TetR. En l'absence de son ligand, en l'occurrence les antibiotiques de la famille des tétracyclines, $MabTetR_X$ va réprimer sa propre expression ainsi que celle de MabTetX en se liant à une séquence d'ADN cible située en amont de l'opéron *MAB_1497c*/*MAB_1496c*. Une fois à l'intérieur de la bactérie, les tétracyclines vont interagir avec $MabTetR_X$, qui libèrera son ADN cible à

la suite d'un réarrangement conformationnel ce qui mènera à l'expression de l'opéron *MAB_1497c*/*MAB_1496c* (Rudra et al. 2018). La TGC est actuellement la seule glycylcycline utilisée dans la thérapie contre *M. abscessus* mais deux autres composés, l'éravacycline et l'omadacycline sont en cours d'évaluation et exhibent une efficacité *in vitro* similaire à la TGC (Kaushik et al. 2019).

3) Les enzymes protégeant la cible des effecteurs, le cas d'Erm(41) et des macrolides :

La littérature ne recense qu'une seule protéine capable de protéger *M. abscessus* en modifiant biochimiquement la cible d'une classe d'antibiotiques. Il s'agit de la méthyltransférase Erm(41) protégeant la boucle du centre peptidyltransférase par méthylation de l'ARNr 23S de la grande sous-unité ribosomale (Maurer et al. 2014). « Erm » est l'acronyme de « Erythromycin Resistance Methylase », ces gènes sont présents chez d'autres genres bactériens,notamment chez les staphylococci et les streptococci ainsi que chez *Campylobacter* mais, contrairement à *M. abscessus*, sont généralement portés sur des éléments génétiques mobiles de types plasmidiques (Schroeder et Stephens 2016)(Bolinger et Kathariou 2017)(Feßler et al. 2018). Ces enzymes catalysent sur l'atome d'azote N6 de l'adénine en position A2058 de l'ARNr 23S le transfert de un ou deux groupements méthyles depuis de la S-adénosyl-L-méthionine. Cette réaction va produire de la S-adénosyl-homocystéine et ces groupements méthyles vont briser la liaison hydrogène entre le C2'-OH du sucre désosamine des macrolides et l'A2058. La gêne stérique occasionnée par cette simple ou double méthylation va gravement diminuer l'affinité de ces antibiotiques. Il a été rapporté chez plusieurs espèces bactériennes Gram - et Gram +, notamment *S. aureus*, que la diméthylation offre un moyen de résistance plus efficace que la monométhylation contre les macrolides mais aussi contre les lincosamides et la streptogramine B (Weisblum 1995)(Maravić 2004). C'est en 2009 que Nash et al. ont fourni la première, mais aussi la plus complète, des études sur la résistance inductible aux macrolides *via* Erm(41) chez *M. abscessus*. Ils ont montré que comme *S. aureus* et sa diméthyltransférase ErmC, *M. abscessus* est résistant aux macrolides, aux lincosamides et àla streptogramine B, supportant l'hypothèse d'une activité N, N6-diméthyltransférase d'Erm(41). Les gènes *erm* ne sont pas présents chez toutes les mycobactéries, comme par exemple chez *M. chelonae*, contre qui les macrolides sont théoriquement efficaces en l'absence de mutation chromosomique du gène *rrl*. On retrouve néanmoins ces gènes *erm* chez *M. tuberculosis*, *M. smegmatis*, *M. fortuitum* et *M. margeritense*. En termes de phylogénie, *erm(41)* est plus proche d'*erm(37)* de *M. tuberculosis* et leurs séquences sont très différentes des trois autres espèces. La position d'*erm(41*) sur le chromosome est également unique suggérant que *M. abscessus* aurait acquis ce gène indépendamment des autres mycobactéries, probablement à la suite d'un transfert horizontalde matériel génétique provenant d'une autre bactérie(Nash et al. 2009). Chez la sous- espèce *M. massiliense*, *erm(41)* est tronquée, un segment de 198 nucléotides situés au centre du gène a disparu, réduisant le cadre de lecture de 522 à 324 pb.

Une hypothèse est que suite à l'absence de pression de sélection, la bactérie a tout simplement perdu une partie de son patrimoine génétique n'en ayant pas l'utilité, rendant cette protéine non-fonctionnelle. Contrairement à certaines autres bactéries où l'expression des gènes *erm* est constitutive, la résistance de *M. abscessus* aux macrolides est un phénomène inductible et qui augmente de manière quasi- exponentielle au fil du temps (Maravić 2004)(Maurer et al. 2014). En effet, la CMI de la CLR et de l'AZM doit être évaluée sur 14 jours car, lorsqu'on la détermine de manière classique au bout de 3 ou 4 jours, sa valeur varie entre de 1 et 32 $\mu g.mL^{-1}$ alors qu'elle est ensuite supérieure à 256 $\mu g.mL^{-1}$ au bout de 14 jours. Il existe une relation entre pouvoir inductible des macrolides et la présence dans leur structure d'un sucre, le cladinose (Douthwaite 2001). Cependant, la télithromycine, un macrolide de la sous-classe des kétolides ne possède pas de cladinose mais subit quand même ce phénomène de résistance inductible (Nash et al. 2009). Chez *M.tuberculosis* et *M. abscessus*, cette induction est directement liée à la présence de l'activateur de transcription WhiB7 (Burian et al. 2012)(Ramón-García et al. 2013) (Hurst-Hess et al. 2017). Les gènes *whiB* sont propres aux actinomycètes, les autres bactéries résistantes aux macrolides doivent donc posséder d'autres stratégies de régulation. L'absence de ces activateurs de transcription peut également expliquer le caractère constitutif de l'expression des gènes *erm* chez certains de ces organismes.

4) Export actif par des pompes à efflux :

Les pompes à efflux sont des protéines transmembranaires abondantes chez les mycobactéries. Elles sont responsables de l'homéostasie de la cellule bactérienne en réalisant l'export de composés majeurs de la paroi, de facteurs de virulence ainsi que de toxines et de leurs possibles métabolites. Ces protéines ont donc une large variété de substrats, ce qui peut parfois leurs permettre d'expulser hors du cytosol, une ou plusieurs classes d'antibiotiques aux structures éloignées en plus de leur substrat premier. La perméabilité ajustable de la paroi mycobactérienne par ces pompes à efflux représente un premier mécanisme de résistance intrinsèque de plus ou moins grande efficacité (Louw et al. 2009). Ce phénomène d'export n'est pas à l'heure actuelle aussi bien décrit chez *M. abscessus* que chez d'autres bactéries, mais il a déjà été démontré qu'il concerne le LNZ et des dérivés structuraux du TAC. L'export de l'AMK et possiblement d'AZM et de rifamycines seraient dus à un seul transporteur transmembranaire MAB_1409c (MAB_{Tap}) appartenant à la famille MFS (Major Facilitator Superfamily), un homologue de la pompe à efflux Tap de *M. tuberculosis*. La fonction première de Tap chez *M. bovis* BCG et vraisemblablement comme chez d'autres mycobactéries n'est pas l'efflux d'antibiotiques. Son rôle principal est en réalité de détoxifier le cytoplasme après le début de l'entrée en phase stationnaire (Ramón-García et al. 2012).

4a) L'export de l'amikacine :

L'efflux de cet aminoglycoside chez *M. abscessus* implique une fois de plus l'activateur de transcription WhiB7. Hurst-Hess et al. ont identifié par RNA-Seq le régulome complet de WhiB7 et ont généré un mutant Δ*whiB7*/*MAB_3508c* chez *M. abscessus*. Ils ont alors identifié MAB_{Tap} comme une cible de WhiB7 et la délétion de *MAB_3508c* rend *M. abscessus* 4 fois plus sensible à l'AMK. L'acétyltransférase Eis2 est aussi sous le contrôle de WhiB7. Des isolats cliniques résistant à l'AMK possédaient à la fois des mutation du gène *rrs* mais égalementune surexpression des transcrits de *whiB7* et de MAB_{Tap} ou une surexpression de *eis2* (Wu et al. 2019). Il semblerait donc que la résistance à l'AMK soit multifactorielle chez *M. abscessus*, combinant à la fois export basal, mutation chromosomique et inactivation enzymatique.

4b) Le cas des rifamycines et de l'azithromycine :

L'implication de MAB_{Tap} dans l'export de ces deux familles de molécules ne repose pour le moment sur aucunes données expérimentales mais plutôt sur lescomparaisons de degrés d'homologie entre protéines. Tap est responsable de l'export de la RFP chez *M. tuberculosis* (Szumowski et al. 2013). D'après sa grande homologie de structure secondaire avec MAB_{Tap} (Schmalstieg et al. 2012), Ganapathy et al. suggèrent que MAB_{Tap} exporte de la rifampycine et de la rifabutine chez *M. abscessus*. La perméase de *M. avium*, MAV_1406 est impliquée dans l'export d'AZM et partage aussi un bon degrés d'homologie avec MAB_{Tap} (Schmalstieg et al. 2012). Ces deux phénomènes d'efflux sont possibles mais ne mèneraientprobablement qu'à de faibles niveaux de résistances basales, étant donné la présence de systèmes de résistance beaucoup plus performants.

4c) L'export du linézolide :

Classiquement, la résistance au LNZ est associée à la présence de mutations dans sa cible, le gène *rrl* codant l'ARNr 23S. Cependant chez *M. abscessus*, il semblerait que dans 25% des cas, cette résistance ne soit pas due à des mutations du gène cible mais plutôt dans des régulateurs de transcription potentiels (Ye et al. 2019). Toutes ces souches surproduisaient les transcrits de deux pompes à efflux, l'une appartenant aussi à la famille MFS comme MAB_{Tap}, LmrS, et l'autre est un transporteur de la famille RND (Resistance Nodulation cell Division), le MmpL MAB_4746. *M. abscessus* acquiert potentiellement des mutations dans des répresseurs qui ne sont alors plus en mesure de réguler ces deux pompes à efflux qui extrudent le LNZ.

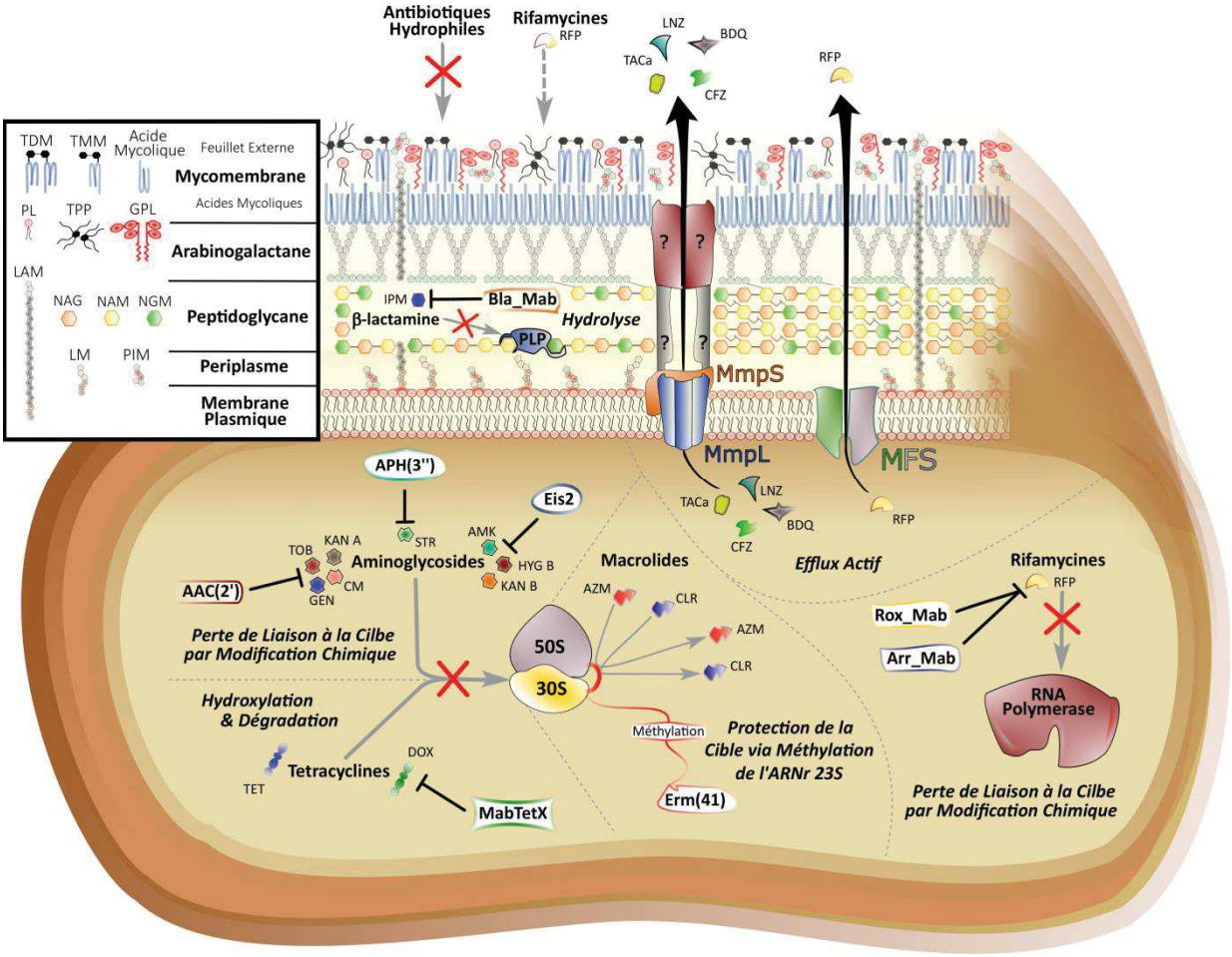

Figure 27. Mécanismes majeurs de résistance aux antibiotiques chez *M. abscessus*. *M. abscessus* est résistant à une large variété d'antibiotiques appartenant à de nombreuses différentes familles. La paroi mycobactérienne représente un premier facteur déterminant dans la résistance antibiotique. Son hydrophobicité empêche l'entrée d'antibiotiques hydrophiles et diminue l'absorption des molécules plus hydrophobes comme les rifamycines. Différentes familles de pompes à efflux sont responsables de la résistance innée et acquise de *M. abscessus*. Les MmpS/MmpL appartenant à la famille RND, sont impliqués dans la résistance au LNZ, aux TACa, à la CFZ et à la BDQ ainsi que MAB_{Tap}, membre de la famille MFS, étant responsable de l'export de la RFP. *M. abscessus* possède également tout un arsenal d'enzymes modifiant soit les antibiotiques, soit les cibles de ces antibiotiques. La monooxygénase Rox_Mab et l'ADP-ribosyltransférase Arr_Mab sont capables d'inactiver les rifamycines comme la RFP. La phosphotransférase APH(3'') inactive la STR. L'acétyletransférase AAC(2') inactive la TOB, KAN A, CM et GEM. L'autre acétyltransférase Eis2 inactive quant à elle l'AMK, l'HYG B et la KAN B. Bla_Mab est une β-lactamase responsable de l'hydrolyse de nombreuses β-lactamines parmi lesquelles figure l'IMP. Les tétracyclines classiques sont également dégradées, cette fois-ci par la monooxygénase MabTetX. Erm(41) est à ce jour la seule enzyme identifiée chez *M. abscessus* qui confère une résistance en protégeant la cible d'un antibiotique. Cette enzyme va méthyler l'adénine 2058 de l'ARNr 23S de la grande sous-unité ribosomale, diminuant l'affinité des macrolides comme l'AZM et la CLR. GPL, glycopeptidolipide ; LAM, lipoarabinomannane ; LM, lipomannane ; NAG,N-acétylglucosamine ; NAM, N-acétylmuramique ; NGM, N-glycolylmuramique ; PIM, phosphatidyl-*myo*-inositol mannoside ; PL, phospholipide ; TPP, tréhalose polyphléate ; TMM, tréhalose monomycolate ; TDM, tréhalose dimycolate ; AMK, amikacine ; MFS, major facilitator superfamily ; MmpS/L, mycobacterial membrane protein small/large ; RND, resistance – nodulation – cell division ; AZM, azithromycine ; BDQ, bédaquiline ; CFZ, clofazimine ; CM, capréomycine ; DOX, doxycycline ; GEN, gentamycine C ; HYG B, hygromycine B ; IPM, imipénème ; KAN, kanamycine ; LNZ, linézolide ; RFP, rifampycine ; STR, streptomycine ; TACa, analogues de thiactétazone ; TET, tétracycine ; TOB, tobramycine. (Adaptée de Gutiérrez et al. 2018, Luthra et al. 2018)

4d) L'export des analogues structuraux du TAC :

L'optimisation structurale du TAC a notamment généré trois analogues désignés D6, D15 et D17 avec une très bonne activité antibactérienne contre à la fois *M. tuberculosis* et *M. abscessus* (Halloum et al. 2017). Cette étude a révélé que la surexpression du transporteur MmpS/MmpL codé par l'opéron *MAB_4383c*/*MAB_4382c* était due à des mutations dans un régulateur de transcription situé juste en amont. Des mutants spontanés à ces dérivés exhibent de très hauts niveaux de résistances à D6, D15 et D17 parfois supérieurs à un facteur de 20 à 30. Ces phénotypes sont en parfaite corrélation avec l'importante production des transcrits de la pompe à efflux MAB_4383c/MAB_4382c.

Un schéma récapitulant la majorité de ces mécanismes de résistance est présenté Figure 27.

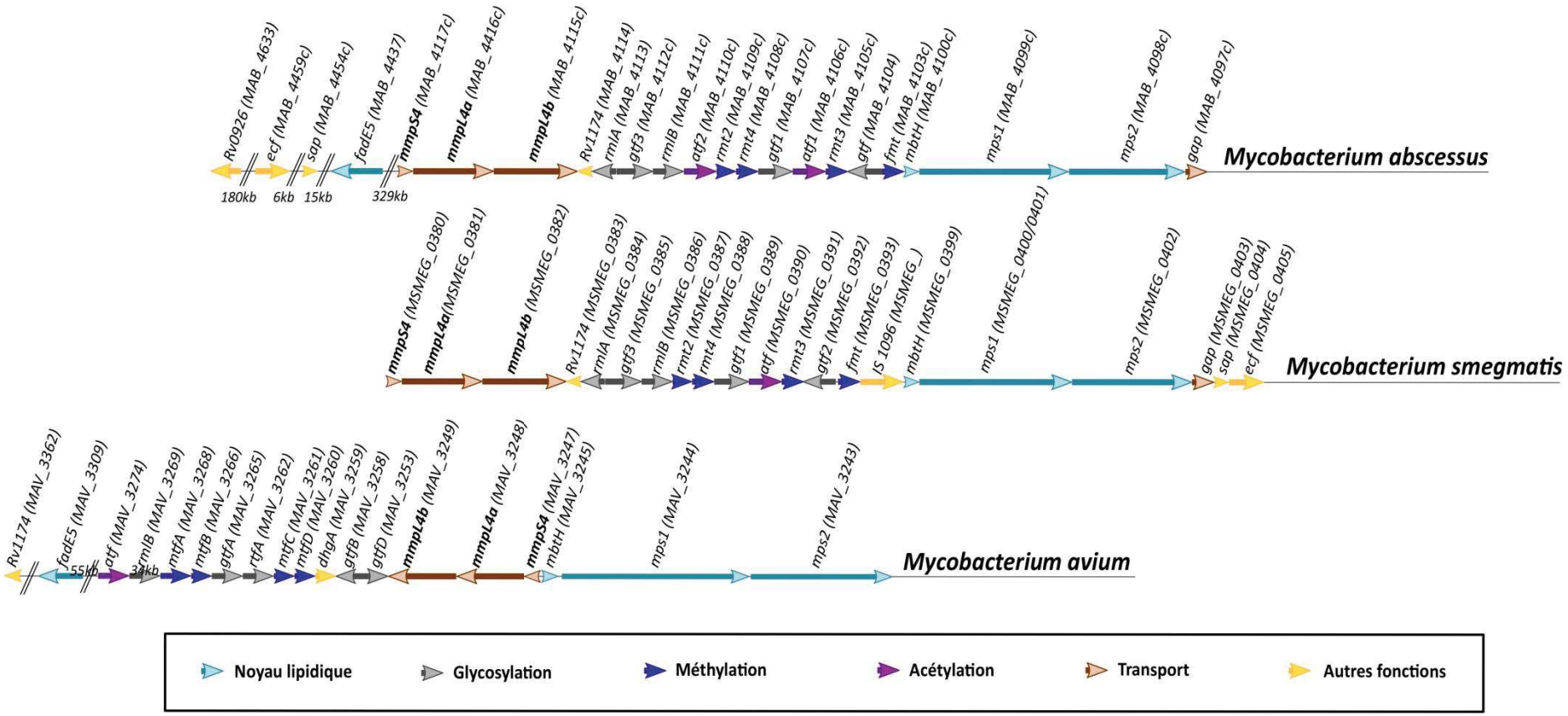

Figure 28. Organisation génomique des locus *gpl* de *M. abscessus*, *M. smegmatis* et *M. avium* (Adapté de Gutiérrez et al. 2018)**.**

Chapitre V) Les Transporteurs Transmembranaires MmpL

1) Propriétés génétiques :

Les *mmpL* sont exclusifs aux mycobactéries, mais on retrouve des orthologues relativement proches de ces gènes chez d'autres actinomycètes, notamment chez le genre *Corynebacterium*, *Rhodococcus* et *Nocardia*. Ces trois genres bactériens possèdent des lipides ayant une structure proche de celle des acides mycoliques mycobactériens (Nataraj et al. 2015). Chez les mycobactéries, les *mmpL* sont des gènes de grande taille, près de 3000 pb. On retrouve également en opéron avec certains *mmpL* des gènes de plus petite taille, d'environ 500 pb, appelés Mycobacterial Membrane Protein Small (*mmpS*). L'hypothèse est que ces protéines épaulent les MmpL dans leur rôle de transport mais ne sont pas indispensables étant donné qu'ils ne sont pas retrouvés à proximité de tous les *mmpL*. En effet, *M. tuberculosis* possède 13 *mmpL*, mais seulement 4 *mmpS*, supposément co-transcrits avec *mmpL1*, *mmpL2*, *mmpL4* et *mmpL5* (Chalut 2016). La même observation est faite pour *M. abscessus*, qui possède 24 *mmpS* et 31*mmpL* (Viljoen et al. 2017). Une caractéristique frappante liée à l'environnement génomique des *mmpL* est de la présence de gènes impliqués dans la biosynthèse des molécules que ces protéines exportent. Chez *M. tuberculosis*, les MmpL connus pour leurs implications dans le transport de lipides retrouvés dans la paroi sont plus ou moins proches de gènes codants des Polyketides Synthases (*pks*), indispensables à la synthèse de lipides complexes, à l'exception de MmpL3 et 11 (Chalut 2016). Le locus impliqué dans la production et l'export des GPL est le mieux caractérisé chez *M. abscessus* et reflète avec fidélité ce qui est observé chez *M. tuberculosis* (Gutiérrez et al. 2018). L'opéron composé de *mmpS4–mmpL4a–mmpL4b* responsable de l'export de ces molécules est entouré de gènes impliqués dans la biosynthèse et l'assemblage de parties glucidique, peptidique et lipidique composant les GPL. Il a été démontré chez *M. smegmatis* qu'une autre protéine accessoire est impliquée dans la translocation des GPL au travers de la membrane plasmique (Sondén et al. 2005). Il s'agit de la protéine Gap, dont le gène est situé à l'extrémité du locus *gpl* chez *M. abscessus*. Il est fort probable que d'autres protéines accessoires jouent un rôle primordial d'assistance dans le transport effectué par les MmpL. Il existe une certaine synténie dans la répartition des *mmpL* au sein du génome des mycobactéries. Des exemples convaincants montrent que si ces loci sont conservésentre deux espèces, alors la fonction du transporteur et les molécules qu'il exporte sont présentes chez ces dernières. Ceci est le cas pour le locus de *mmpL3* qui est strictement conservé parmi les espèces *M. tuberculosis*, *M. leprae*, *M. avium*, *M. marinum* et *M. abscessus* (Viljoen et al. 2017). Ces observations étaient anticipées étant donné que *mmpL3* est le seul MmpL essentiel chez les mycobactéries, ce qui en fait donc une cible thérapeutique extrêmement intéressante. Le locus GPL est très conservé entre *M. abscessus*, *M. avium* et *M. smegmatis*, trois espèces productrices de GPL (Gutiérrez et al. 2018)(Figure 28).

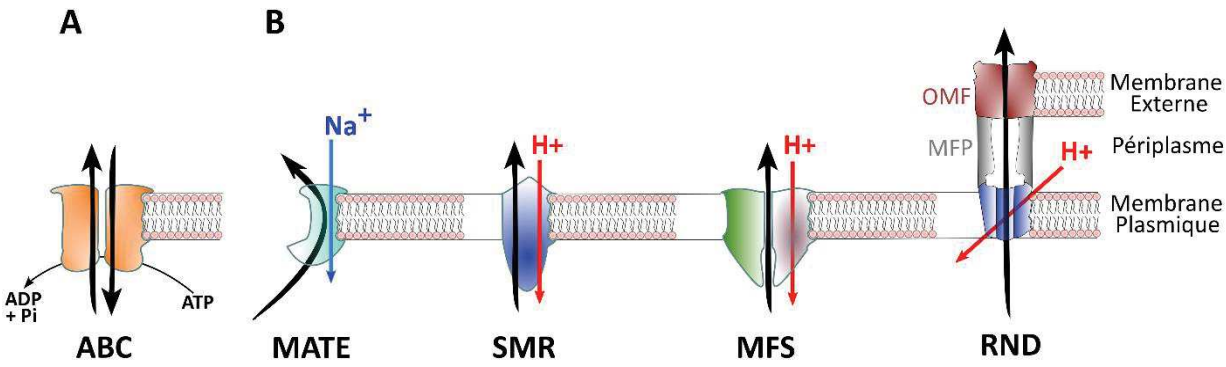

Figure 29. Représentations schématiques des deux superfamilles de transporteurs retrouvées chez les mycobactéries. (A) Les transporteurs primaires ABC utilisent l'hydrolyse de l'ATP pour transporter à travers la membrane plasmique leurs substrats et sont des homodimères ou des hétérodimères. (B) Les transporteurs MATE sont les seuls à utiliser un gradient de sodium afin d'expulser leurs substrats du cytoplasme et sont monomériques. Les transporteurs SMR, MFS et RND utilisent la PMF pour extruder leurs substrats vers le milieu extérieur et sont respectivement des monomères, des homodimères ou des hétérodimères et des systèmes tripartites. ABC, ATP-binding cassette ; MATE, multidrug and toxic coupound extrusion ; SMR, small multidrug resistance ; RND, resistance nodulation cell division ; MFP, membrane fusion-like protein ; OMF, outer-membrane factor, PMF, force proto-motrice (Adapté de Lubelski et al. 2007).

A l'opposé, la non-conservation entre espèces de ces blocs synténiques résultent en une perte de fonction de ces *mmpL*. Par exemple ce locus *gpl* est éparse chez les espèces où ces molécules sont absentes, comme chez *M. tuberculosis* ou encore *M. leprae* (Viljoen et al. 2017). La fonction et la nature des molécules exportées par les MmpL sont très peu connues chez *M. abscessus*. Cependant, il est possible d'acquérir des informations préliminaires, voire même de prédire la fonction de certains de ces transporteurs, à l'aide d'études phylogénétiques et bio-informatiques. Un exemple de ce type d'approche est la recherche de séquencesd'acides aminés bien précises parmi les protéines Pks. Ces séquences d'aminoacides sont caractéristiques du lipide que les Pks synthétisent (Yadav et al. 2003).

2) Propriétés biochimiques et structurales :

Les pompes à efflux bactériennes peuvent être séparées en deux superfamilles présentes chez tous les procaryotes. Cette différenciation est basée sur la façon dont elles se procurent l'énergie nécessaire au transport actif de leurs substrats.

La première est la superfamille des transporteurs ABC (ATP-Binding Cassette), également appelée transporteur primaire (Figure 29A). Ces protéines transmembranaires vont obtenir de l'énergie en fixant et hydrolysant l'ATP *via* leur domaine cytoplasmique (Locher 2009). Ces transporteurs vont généralement importer à l'intérieur du cytosol des nutriments hydrophiles comme des aminoacides ou des sucres mais aussi des ions ainsi que des sidérophores. Ces transporteurs expulsent également des molécules toxiques ou antigéniques.

La seconde, celle des transporteurs secondaires, regroupe 4 familles de protéines qui tirent leur énergie d'un gradient électrochimique dû à différente concentration de sodium ou de proton de part et d'autre de la membrane expulsant tous types de substrats hors du cytoplasme (Lubelski et al. 2007)(Figure 29B). Un seul type de transporteur utilise un gradient de sodium, il s'agit des MATE (Multidrug And Toxic compound Extrusion). Les trois autres type de transporteurs secondaires utilisent tous les trois la force proto-motrice (PMF) entre le milieu extérieur et le cytoplasme pour expulserleurs substrats et sont donc séparés par rapport à leurs caractéristiques structurales. On retrouve donc les transporteurs MFS, comme MAB_{Tap}, les transporteurs SMR (Small multiDrug Resistance) et les transporteurs RND dont les MmpL font partis, L'organisation des RND est plus complexe et la PMF s'effectue grâce à un gradient de proton entre le périplasme et le cytosol. Ce sont des systèmes tripartites, composé d'une protéine périplasmique MFP (Membrane Fusion-like Protein) qui relierait le transporteur transmembranaire homotrimèrique à une protéine insérée dans la membrane externe appelée OMF (Outer-Membrane Factor). Ils sont absents chez les Gram +.

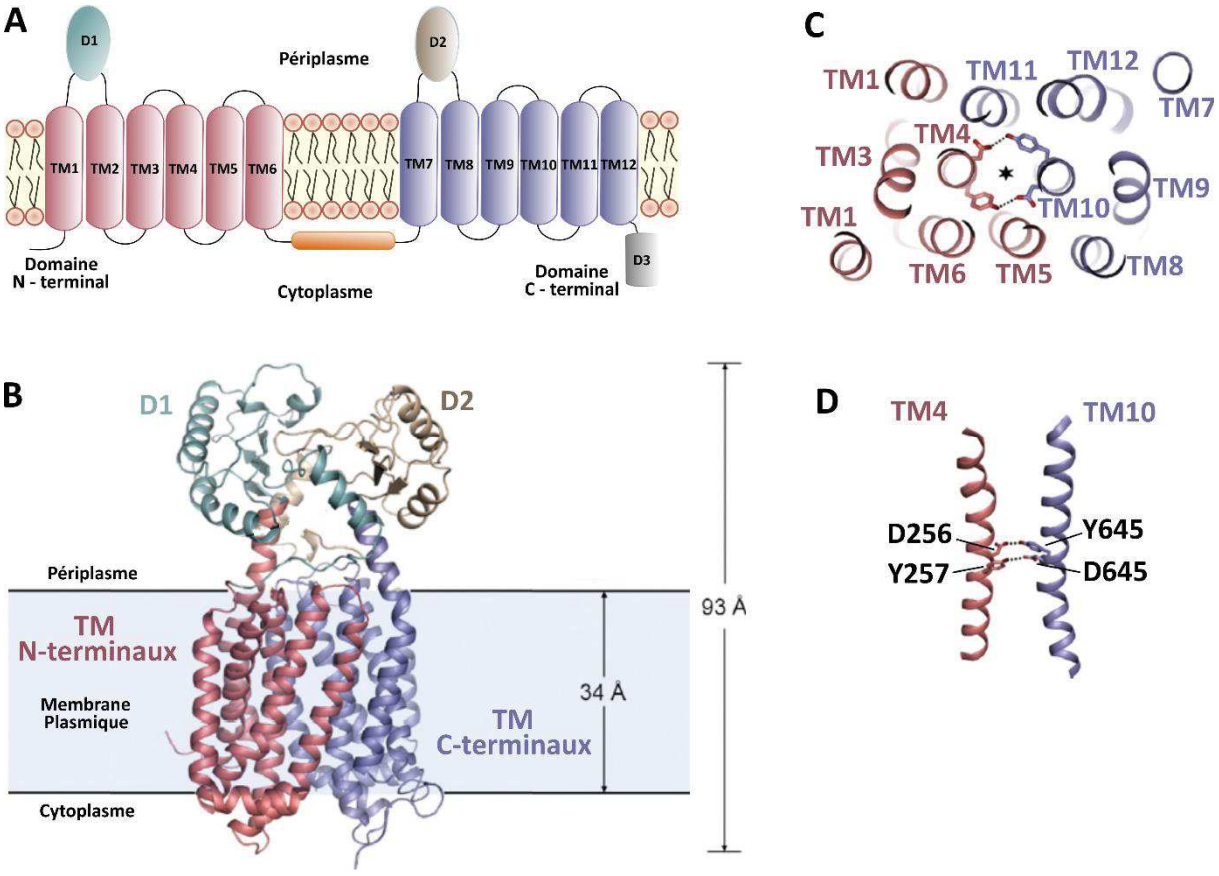

Figure 30. Organisation structurale des MmpL. Schéma représentant les 6 domaines transmembranaires N-terminaux en rouge (TM1-6) et les 6 domaines transmembranaires C-terminaux en bleu (TM7-12). Les domaines périplasmiques D1 et D2 sont représentés en turquoise et beige respectivement. L'hélice cytoplasmique reliant les domaines N- et C-termini est en orange et le domaine cytoplasmique D3 en gris. (B) Structure 3D de MmpL de *M. smegmatis* reprenant le même code couleur que décrit en (A). (C) Organisation spatiale des 12 domaines transmembranaires avec le TM4 et le TM10 formant un canal. (D) Positionnement des résidus critiques D256 et Y257 pour le TM4 et Y646 et D645 pour le TM10 responsables du transport des électrons (Adapté de Viljoen et al. 2017 et de Zhang et al. 2019)

Les connaissances sur la présence avérée de ces protéines MFP et OMF pour les MmpL n'est pas démontrée expérimentalement mais est cependant très probable et pourrait inclure certaines lipoprotéines (Melly et Purdy 2019). Les prédictions faites après analyses de la séquence des MmpL et de leurs homologies avec d'autres transporteurs RND proposent qu'ils soient composés de 11 ou 12 hélices transmembranaires (TM1 à TM12)(Figure 30A). On retrouve deux domaines périplasmiques (D1 et D2) situés entre les TM1 et 2 et les TM7 et 8. Il a été proposé que ces régions solubles aient un rôle dans la liaison et le transport des substrats (Chim et al. 2015). Le domaine N-terminal contient entre 5 et 6 TM et la partie C-terminale est composée de 6 TM. La jonction entre les domaines N et C terminaux est due à la présence d'une hélice cytoplasmique positionnée parallèlement à la membrane plasmique. La partie C-terminale est cytoplasmique (D3)(Viljoen et al. 2017). L'ensemble de ces hypothèses a été fortement appuyé récemment grâce à l'obtention de la structure 3D à très haute résolution de MmpL3 de *M. smegmatis* (Zhang et al. 2019)(Figure 30B). Le passage des protons créant la PMF nécessaire au transport des substrats hors du cytoplasme est relié par des résidus aspartate et tyrosine extrêmement conservés parmi les TM4 et TM10 des MmpL (Figure 30C). C'est grâce à une combinaison d'études génétique et bio-informatique que Bernut et al. ont pu mettre en avant l'importance des résidus D265 du TM4 et de la paire D625 – Y626 du TM10 dans le relais des protons à travers MmpL4a pour le transport des GPL chez *M. bolletii*. Ils ont aussi démontré l'importance des résidus D251 du TM4 et de la paire D640 – Y641 du TM10 de MmpL3 de *M. tuberculosis* à l'aide d'expériences de complémentation fonctionnelle. Chez *M. smegmatis*, la cristallographie aux rayons X de MmpL3 révèle deux paires aspartate – tyrosine. Il s'agit des paires D256 – Y257 et D645 – Y646 situées respectivement dans les TM4 et TM10 (Zhang et al. 2019)(Figure 30D).

3) Rôles et fonctions des MmpL :

Ces données restent éparses concernant *M. abscessus*, mais seront affinées prochainement compte tenu de l'évolution des techniques de lipidomiques et de génétiques appliquées spécialement à ces mycobactéries. C'est chez *M. tuberculosis* que les informations à ce sujet sont les plus importantes, avec les fonctions de 6 protéines MmpL identifiées sur un total de 13 transporteurs. Les rôles les plus connus mais aussi les plus étudiés concernent en général le transport de lipides majeurs à travers la paroi mycobactérienne, l'import passif de fer, l'export de sidérophores et d'antibiotiques.

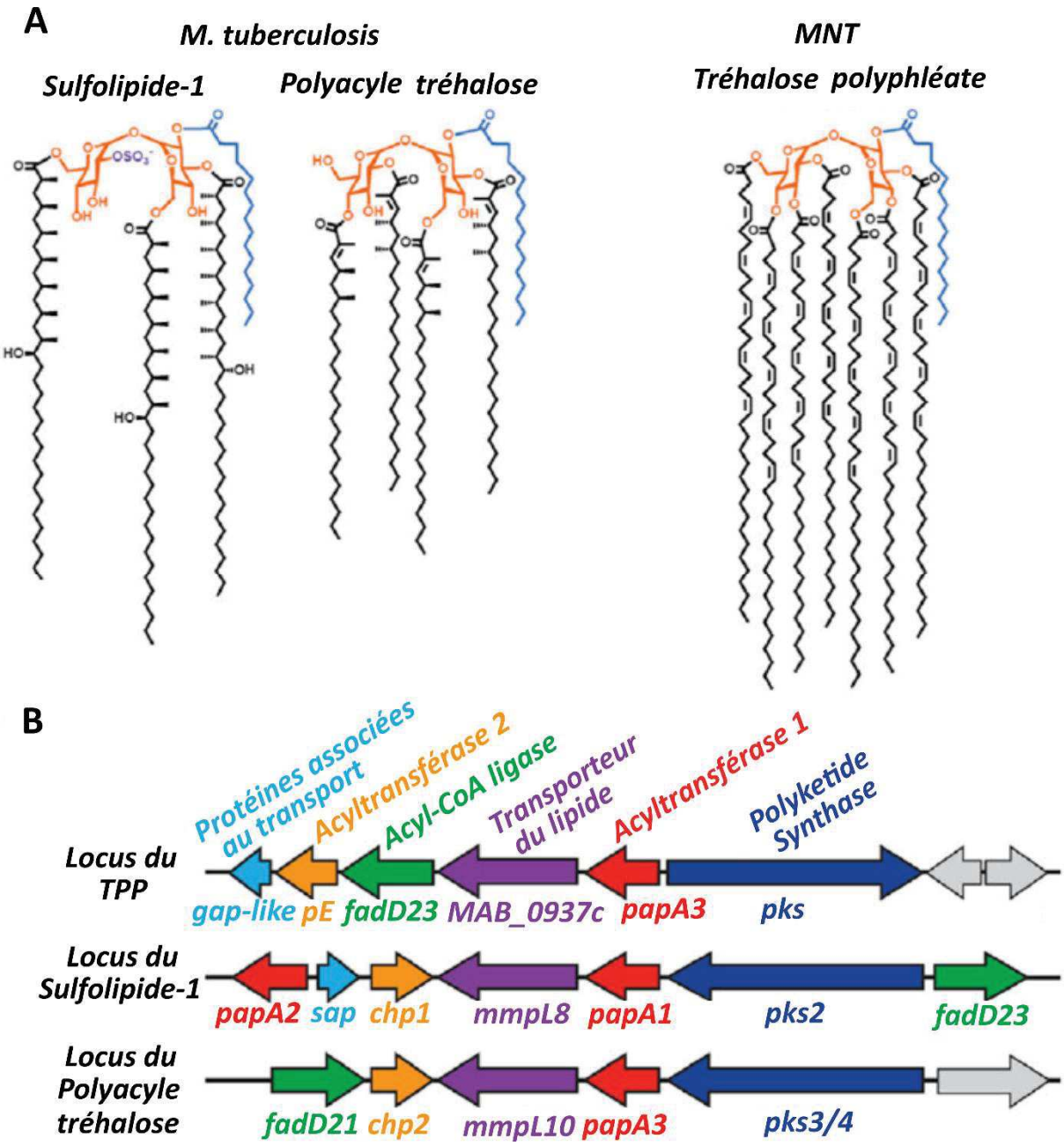

Figure 31. Le tréhalose polyphléate de MNT semble être une chimère structurale (A) et génétique (B) entre le sulfolipide-1 et le polyacyle tréhalose de *M. tuberculosis*. (B) En partant du haut, l'opéron codant pour les gènes responsables de la production des TPP chez *M. abscessus*, les deux locus suivant sont responsables de la production des sulfolipide-1 et polyacyle tréhalose ches *M. tuberculosis. MAB_0937 c'*est un homologue proche de gène de MmpL10 qui transporte les polyacyles tréhaloses (Adapté de Seeliger et Moody 2016).

3a) Export des lipides :

En ce qui concerne le transport de lipides chez *M. abscessus*, l'implication de trois MmpL a été confirmée avec certitude.

MmpL3, pour le transport du TMM, est encodée par le gène *MAB_4508*. L'utilisation d'une nouvelle classe d'inhibiteurs et l'étude du profile lipidique en découlant ont montré une accumulation du TMM cytoplasmique ainsi qu'une disparition concomitante de TDM et de la mycolylation de l'arabinogalactane, confirmant le rôle de « MmpL3 » du gène *MAB_4508* (Dupont et al. 2016).

L'opéron *MAB_4117c – MAB_4116c – MAB_4115c* responsable de la formation du complexe MmpS4 – MmpL4a – MmpL4b transportant les GPL hors du cytosol a également été bien caractérisé. Ce rôle de transporteur des GPL est également élucidé chez *M. smegmatis* et *M. avium* (Gutiérrez et al. 2018).

Le troisième est le MmpL encodé par le gène *MAB_0855* qui est responsable du transport d'un lipide exclusivement retrouvé chez *M. chelonae* et chez le complexe *M. abscessus*. Un mutant Δ*MAB_0855* perd en grande partie sa capacité de survie intracellulaire dans un modèle amibien, macrophagique et *in vivo* chez le zebrafish. Ceci est dû à l'absence d'un glycolipide unique, le GDND (Glycosyl Diacylated Nonadecyl Diol), sans qui une adhésion optimale au macrophage et une dégradation de la membrane phagolysosomale n'est possible. Cette dégradation n'ayant pas lieu, la communication avec le cytoplasme est impossible et il n'y a donc pas inhibition de la réponse immunitaire, ce qui réduit fortement la capacité de survie intramacrophagique (Dubois et al. 2018). Le TPP est un glycolipide composé d'une molécule de tréhalose sulfatée et multi-acylée de très grande taille que l'on retrouve uniquement chez les MNT. Ces lipides sont synthétisés par un opéron « *fadE5-gap-like* » conservé parmi les MNT (Seeliger et Moody 2016). Chez *M. smegmatis*, les délétions du *mmpL* de l'opéron et de l'acyltransférase *pE* provoquent une disparition du TPP de la mycomembrane (Burbaud et al. 2016). Ce même groupe a également montré que chez *M. abscessus* la délétion de *pE* a le même effet. L'organisation génomique de ces deux loci *fadE5-gap-like* est très conservée entre ces deux MNT, il est donc très probable que le MmpL MAB_0937c de ce locus chez *M. abscessus* soit responsable de l'export des TPP. La génération d'un mutant *MAB_0937c* permettrait d'affirmer son rôle avec certitude. La fonction des TPP, étant donné leur taille et leur hydrophobicité, est avant tout structurale mais pourrait aussi être impliquée dans le *cording* du morphotype R et donc son hypervirulence (Llorens-Fons et al. 2017). Le TPP pourrait être décrit comme un hybride structural de SL-1 et de PAT (PentAcyl Trehalose), une sorte d'araignée à 8 pattes (*eight-legged spider*) comme aiment à l'appeler Seeliger et Moody (Figure 31A). C'est en effet comme si ces deux lipides complexes avaient fusionnés pour produire cet imposant glycolipide. L'opéron

fadE5-gap-like des TPP possède un mélange de gènes que l'on retrouve seulement dans le locus de SL-1 et celui de PAT, comme par exemple *fadD23* et *papA3* respectivement (Figure 31B).

En plus de MmpL3 chez *M. tuberculosis*, MmpL7 transporte les PDIM vers la mycomembrane. Le PDIM a un rôle important dans la virulence et l'imperméabilité de la paroi mycobactérienne mais aussi dans la résistance à des détergents (Camacho et al. 2001).

Le SL-1 fait partie de la même famille de glycolipides que le TPP mais est lui organisé autour d'une molécule de tréhalose sulfatée et tetra-acylée. Ce glycolipide est capable de moduler la réponse immunitaire de l'hôte en altérant la maturation phagolysosomale, la production de ROS et de cytokines et serait vraisemblablement transporté par MmpL8 (Converse et al. 2003)(Seeliger et al. 2012).

Belardinelli et al. ont démontré que leDAT est transporté par MmpL10 et se retrouvera alors comme le PAT dans la mycomembrane. Ils proposent que le PAT soit formé dans le périplasme à partir de trois molécules de DAT par une réaction de transestérification réalisée par l'acyltransférase Chp2 qui produira également trois molécules de monoacyle-tréhalose. Le PAT n'est donc pas exporté par MmpL10 mais résulte d'un produit de la translocation de DAT par ce transporteur.Le DAT et le PAT modulent aussi la réponse immunitaire orchestrée par le macrophage en agissant sur le phagosome en bloquant son acidification (Passemar et al. 2014). Grâce à un mécanisme original de recyclage, ces tréhaloses polyacylés vont indirectement détoxifier le cytoplasme de leur hôte et limiter son stress métabolique (Lee et al. 2013). Une fois phagocyté, les principaux nutriments accessibles à *M. tuberculosis* sont les acides gras et le cholestérol. Leurs dégradations par ces mycobactéries vont générer du propionyl-CoA, dont les intermédiaires métaboliques peuvent se révéler toxiques à long terme. Les bacilles vont alors incorporer ce propionyl-CoA dans la chaine de biosynthèse du DAT en l'utilisant pour estérifier le tréhalose. Ces molécules participent donc indirectement à un autre mécanisme de survie intramacrophagique.

Pacheco et al. ont mis en évidence chez *M. smegmatis* l'importance de MmpL11 de *M. tuberculosis* dans le transport des MMDAG (MonoMeromycolyl DiAcylGlycerol) et MEW (Mycolic Ester Wax) grâce à des expériences de complémentation fonctionnelle. Ce MmpL11 estimpliqué dans la formation de biofilms.

3b) Système d'acquisition du fer

Le fer est un nutriment essentiel à la survie des mycobactéries comme de tout être vivant. Au cours de l'infection, le système immunitaire de l'hôte va tenter de priver au maximum l'accès au fer des pathogènes. Mais les mycobactéries ont su s'adapter en devenant capables de récupérer ce fer

libre dans la lumière phagosomale ou associé à des structures de stockage, comme des gouttelettes lipidiques. La stratégie pour palier à cette privation de fer est axée autour de l'import/export de sidérophores : la MycoBacTine (MBT) et la CarboxyMycoBacTine (cMBT), qui vont chélater, séquestrer les cations à leur proximité (Sandhu et Akhter 2017). Les MBT et cMBT sont transportées par les systèmes MmpS4-MmpL4 et MmpS5-MmpL5 chez *M. tuberculosis*. Wells et al. en sont parvenus à ces conclusions grâce à un travail colossal comprenant de multiples inactivations géniques ainsi que des études biochimiques, structurales et *in vivo* chez la souris. Ils ont pu également déduire que *mmpS4* et *mmpS5* sont impliqués dans la synthèse de ces sidérophores et seraient également des adaptateurs périplasmiques pour l'ancrage de leurs MmpL respectifs. Les bacilles mutés présentaient des défauts de croissance sur milieu limité en fer et la mortalité des souris infectées avec ces mutants était nulle même au bout de 180 jours. Le système par lequel les sidérophores retournent jusqu'aux mycobactéries n'a pas encore été découvert. Il a été montré que MmpL3 et MmpL11, avec l'aide de la protéine Rv0203, ont la capacité d'importer le fer endogène lié à des cofacteurs de l'hôte jusqu'à l'intérieur du cytoplasme (Owens et al. 2013). Les sidérophores ainsi que leurs transporteurs semblent tous comme MmpL3 être des candidats de choix dans le développement de nouveaux pharmacophores.

Le ou lesquels des *mmpS* et/ou *mmpL* impliqués dans l'homéostasie du fer n'ont pas encore été identifiés chez *M. abscessus*. Cependant quatre *mmpL*, dont les rôles n'ont pas encore été définis, organisés en deux clusters *MAB_4116c – MAB_4115c* et *MAB_4704c – MAB_4703c* sont phylogénétiquement proches de *mmpL4* de *M. tuberculosis* et pourraient alors remplir la fonction d'exporter les sidérophores.

3c) Export d'antibiotiques :

A l'exception des travaux publiés faisant corps avec cette thèse, peu d'informations sont disponibles sur le rôle des MmpL dans l'export d'antibiotiques chez *M. abscessus*. L'une de ces études a été le pilier de l'article 1 présent dans ces travaux de thèse. Il s'agit de l'étude réalisée par Halloum et al. impliquantun homologue de *mmpS5*/*mmpL5* de *M. tuberculosis*, la pompe à efflux *MAB_4383c*/*MAB_4382c* conférant une résistance aux TACa. (Partie détaillée en section « **Chapitre IV) L'Antibiorésistance chez *M. abscessus*, 4d) Export actif des analogues structuraux du TAC** »)

L'autre étude impliquant un MmpL dans l'export d'antibiotiques est celle deYe et al. qui ont mis en avant l'implication du MmpL MAB_4746 dans la résistance au LNZ (discutée dans la section « **Chapitre IV) L'Antibiorésistance chez *M. abscessus*, 4e) Export du linézolide** »)

Concernant *M. tuberculosis*, deux MmpL sont impliqués dans l'efflux d'antibiotiques, parmi lesquels MmpS5/MmpL5, responsable de l'export d'azole, de CFZ et de BDQ ainsi que le transporteur des PDIM, MmpL7, exportant hors de la bactérie l'INH.

Historiquement, le premier MmpL impliqué dans la résistance à un antibiotique est MmpL7. Pasca et al. en 2005 ontattribué ce rôle à ce transporteur en introduisant le MmpL7 de *M. tuberculosis* chez *M. smegmatis*, ce qui provoqua une forte augmentation de sa résistance à l'INH.

C'est ensuite en 2009 que MmpS5/MmpL5 a été incriminé dans la résistance aux azoles, des molécules de petites tailles généralement utilisées dans le traitement d'infections fongiques (Milano et al. 2009). Les mutants spontanés qu'ils ont générés exprimaient des niveaux de résistance modérés, 4 et 8 fois supérieurs à la souche sauvage. Leurs analyses ont révélé un haut taux d'expression des transcrits de MmpS5/MmpL5, liés à des mutations dans le régulateur de transcription juxtaposé *Rv0678*, appartenant à la famille MarR (Multiple antibiotic resistance Regulator). En 2014, Hartkoorn et al. ont mis en avant la résistance croisée à deux antibiotiques d'intérêts thérapeutiques majeurs dans le traitement de MDR-Tb, la CFZ et la BDQ. Ils ont utilisé la même stratégie en générant des mutants spontanés qui possédaient encore une fois tous des mutations dans *Rv0678*. Les niveaux de résistance observés étaient similaires. MmpS5/MmpL5 de *M. tuberculosis* et MAB_4383c/MAB_4382c de *M. abscessus* sont des homologues mais ne partagent apparemment pas la même spécificité de substrats. La force respective de leurs promoteurs peut jouer un rôle déterminant dans le contraste observé entre les deux niveaux de résistance.

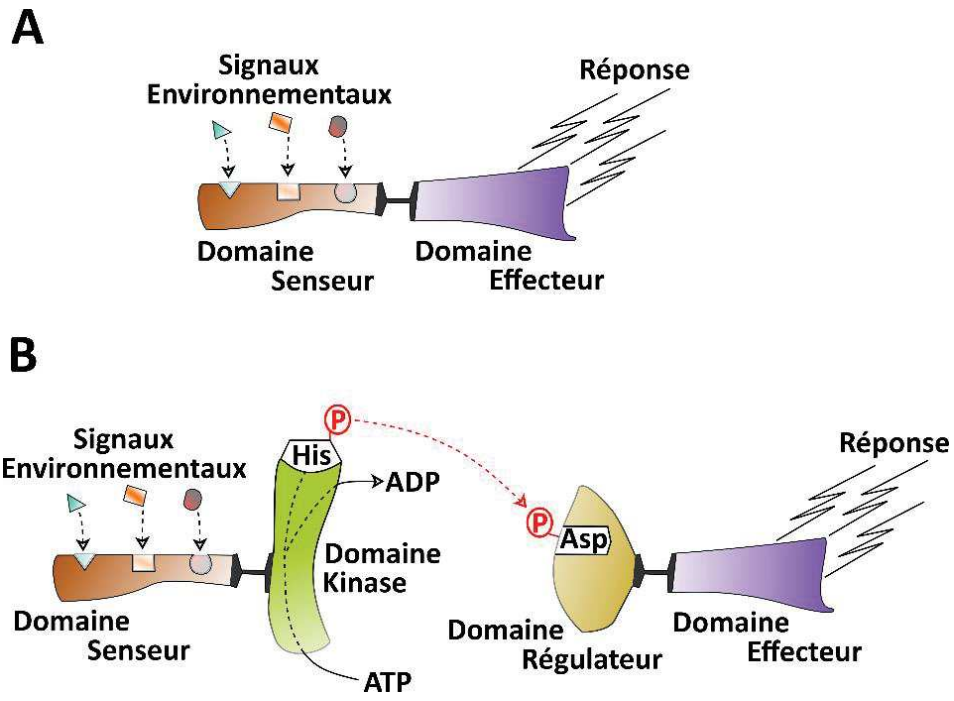

Figure 32. Représentation schématique des deux principaux types de système de régulation procaryotique. (A) Système à un composant. Une seule protéine comporte à la fois un domaine senseur et un domaine effecteur. Chaque domaine peut être en N- ou C-terminal. (B) Système à deux composants. La première protéine du système est composée d'un domaine senseur et d'un domaine kinase qui peut s'auto-phosphoryler à partir d'ATP sur un résidu histidine de son sous-domaine phosphotransferase. Ce phosphate sera ensuite transféré sur un résidu aspartate de la deuxième protéine du système aux propriétés régulatrices (Adapté de Ulrich et al 2005).

Chapitre VI) La Régulation des Mécanismes de Résistance aux Antibiotiques

Le profil d'expression génique de n'importe quelle forme de vie varie régulièrement en fonction du stade de croissance et ceci grâce à des systèmes de régulation fins et complexes, y compris pour des organismes pouvant paraitre moins évolués comme les procaryotes. Ces phénomènes de régulation se produisent en réponse à un stress environnemental et à un besoin métabolique. Ils se matérialisent par une transduction de ces signaux exogènes ou endogènes et se manifestent soit par une activation, soit par une inactivation de la transcription de gènes clefs. Ces mécanismes sont le résultat d'une longue optimisation évolutive qui procure une réponse rapide etadaptée. Chez une bactérie et particulièrement en présence d'un antibiotique, lamise en place rapide du mécanisme de résistance approprié est une condition*sine qua non* à la survie du microorganisme, avant que ces molécules antimicrobiennes ne causent trop de dégâts.La mise en place de ce processus a un coût énergétique, plus spécialement dans le cas de la synthèse de grosses molécules comme les MmpL, et doit donc être finement contrôlé.

1) La superfamille des régulateurs de transcription TetR :

Les bactéries répondent aux signaux environnementaux qu'elles rencontrent grâce à deux grands groupes de régulateurs, les systèmes à un composant et les systèmes à deux composants (Figure 31). Comme l'indique leur nom, les systèmes à un composant sont constitués d'une seule protéine, qui contient à la fois une partie effectrice et une partie senseur. La partie effectrice interagit avec l'ADN cible du régulateur et la partie senseur reconnaitun ligand spécifique. Il existe une relation entre localisation de la partie effectrice et l'action du régulateur. En effet, il semblerait que les protéines avec le site de liaison à l'ADN situé en N-terminal seraient des répresseurs de transcription. A l'inverse, un site de liaison à l'ADNà l'extrémité C-terminale serait le reflet d'une activité activatrice (Cuthbertson et Nodwell 2013). Ces fonctions « senseur & effecteur » sont attribuées à deux protéines chez les systèmes à deux composants. Le signal adéquat déclenche un transfert de phosphate entre la protéine histidine kinase senseur au niveau d'un résidu aspartate situé dans la région régulatrice de la protéine effectrice. Ce phosphotransfert a pour conséquence de leverl'inhibition de la protéine effectrice qui pourra assurer sa fonction régulatrice (Hoch 2000). Les informations sont plus nombreuses concernant les systèmes à deux composants, cependant, ce sont les systèmes à un composant qui sont les plus abondants parmi les bactéries. Ces derniers sont constitués de plusieurs superfamilles, dont celle des TetR.

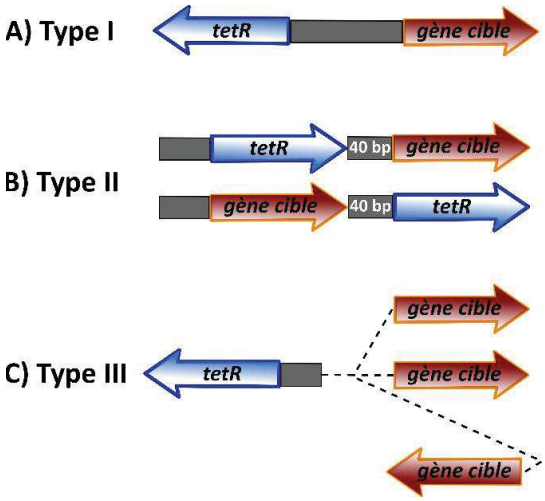

Figure 33. Organisation génomiques des *tetR* et de leurs gènes cibles. (A) Les TetR de type I. Le *tetR* et le gène cible sont voisins et orientés de manière opposée sur le génome. (B) Les TetR de type II. Le *tetR* est soit en aval soit en amont son gène cible dans la même orientation génomique, avec une région intergénique les séparant de moins de 40 bp. (C) Les TetR de type III. Le *tetR* est situé soit juste à côté soit à distance de son gène cible sur le chromosome (Adapté de Cuthbertson et Nodwell 2013).

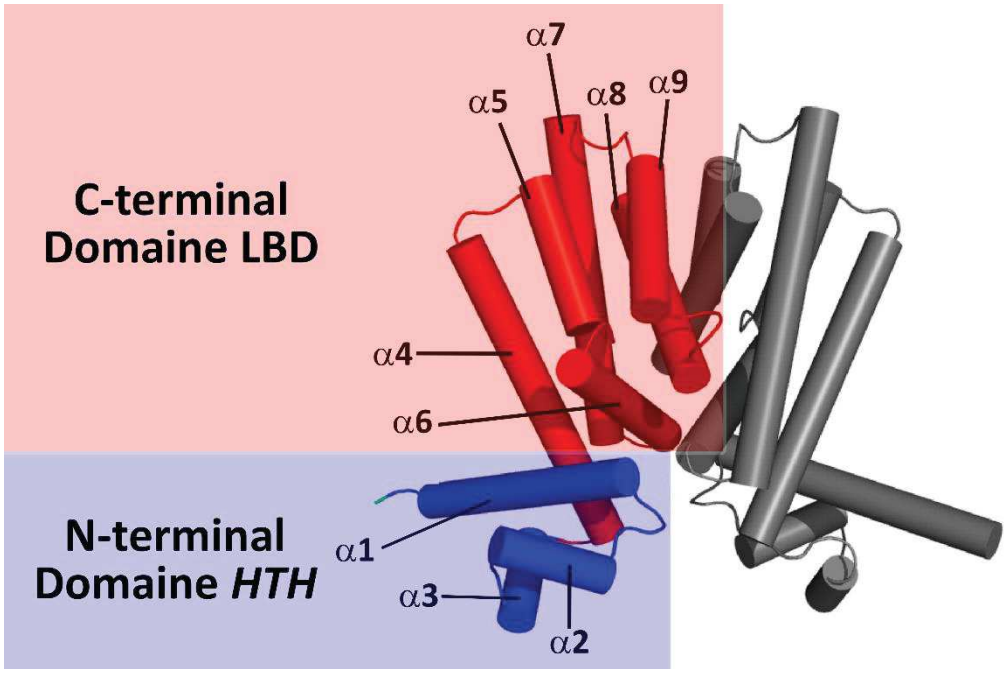

Figure 34. Schéma de l'organisation structurale d'un régulateur TetR. Structure du TetR Rha06780 de *Rhodococcus sp.* RHA1. Les hélices-a sont représentées par des cylindres. En rouge, les hélices 1, 2 et 3 formant le domaine de liaison à l'ADN. En bleu, on retrouve les hélices 4, 5, 6, 7, 8 et 9 qui forment le domaine de liaison au ligand et de dimèrisation. Le deuxième monomère est totalement gris. HTH : Helix – Turn – Helix ; LBD : Ligand Binding Domain (Adapté de Yu et al. 2010)

1a) Propriétés génétiques :

Ces protéines sont en quasi-totalité des répresseurs de transcription. Le premier du genre a été identifié en 1966 chez *E. coli*, et contrôle l'expression de la pompe à efflux TetA, impliquée dans la résistance intrinsèque à la tétracycline, d'où le nom de TetR (Tetracycline Repressor)(Izaki etal. 1966). Les TetR peuvent être classifiés en fonction de leur orientation génomique et de celle du ou des gènes qu'ils contrôlent (Cuthbertson et Nodwell 2013) . On retrouve alors trois types de régulateur TetR. Ceux de type I, où le régulateur et le gène cible sont voisins, séparés par région intergénique non-codante, et qui possède une orientation génomique opposée (Figure 33A). Les TetR de type II, qui possèdent la même orientation génomique que le gène dont ils contrôlent l'expression.Le TetR peut être soit en amont soit en aval de son gène cible. La région intergéniquesituée entre eux deuxdoit être de moins de 40 pb, la taille minimum d'un promoteur mycobactérien (Newton-Foot et Gey van Pittius 2013)(Figure 33B). Il est possible pour les TetR de type I et II de se baser sur ces critères génomiques pour prédire la relation régulateur – gène cible. Cependant, pour les TetR de type III, il est impossible de se baser sur les mêmes paramètres génétiques. Ces TetR peuvent réguler des gènes voisins comme des gènes dispersés sur le chromosome (Figure 33C). Le nombre de ces régulateurs est extrêmement variable d'une espèce à l'autre, en particulier chez les mycobactéries. La quantité de TetR présents sur le génome est, comme pour le nombre de MmpL, le reflet de la capacité d'adaptation et de mode de vie intra/extracellulaire. Par exemple *M. leprae*, pathogène intracellulaire strict aux nombres de gènes réduit, et *M. tuberculosis*, possèdent 13 et 49 régulateurs TetR respectivement. *M. abscessus* ainsi que *M. smegmatis*, tous deux des MNT environnementales, disposent respectivement de 138 et 137 gènes *tetR* sur leurs génomes. Les gènes *tetR* mesurent environ 660 pb codants donc pour des protéines d'approximativement 220 aminoacides.

1b) Propriétés biochimiques et structurales :

Les membres de la superfamille de régulateurs TetR sont des homodimères, chacun composés de 9 à 10 hélices-α (h-α)(Figure 34). Le domaine N-terminus régit les interactions avec l'ADN cible tandis que le domaine C-terminus est responsable de la reconnaissance du ou des ligands ainsi que des interactions monomère – monomère. Le domaine N-terminal est très conservé et est composé de trois h-α d'une longueur totale moyenne de 41 acides aminés (h1, h2, et h3)(Yu et al. 2010). L'h1 a un rôle d'interaction avec le petit sillon de l'ADN mais sert principalement de connexion entre les domaines N/C-termini en liant les h4 et les h6 (Le et al. 2011). Les h2 et h3 vont former le domaine structural typique de liaison à l'ADN des systèmes à un composant, le motif hélice – coude – hélice (HTH pour Helix – Turn – Helix). Ce motif va se comporter comme une pince ou une tenaille et

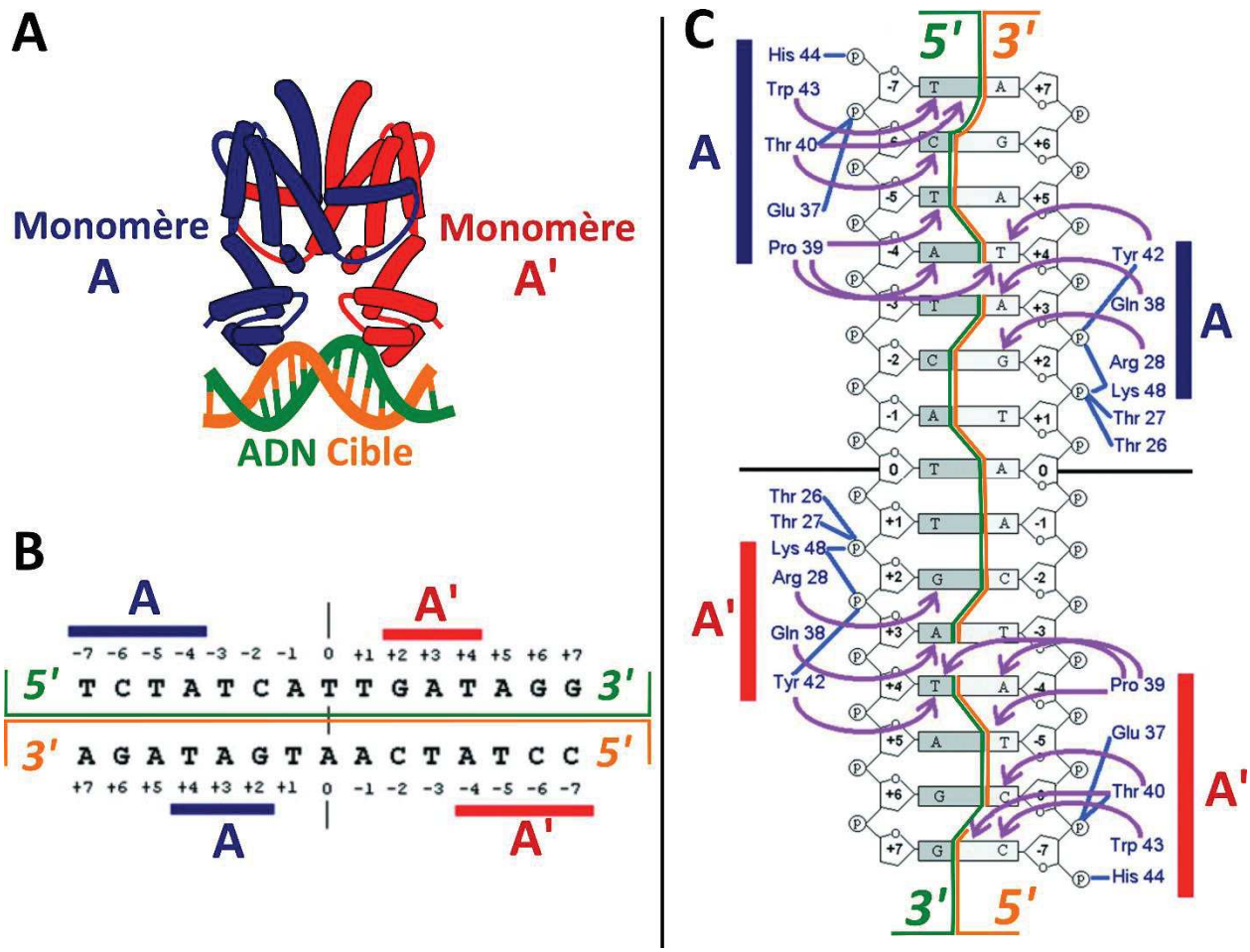

Figure 35. Interaction d'un dimère du TetR d'*E. coli* avec son ADN cible. (A) Représentation schématique du monomère A en bleu et du monomère A' en rouge du même dimère interagissant avec l'ADN cible. (B) Site d'interaction des domaines HTH des monomères A et A' avec le DNA_{op}. (C) Spécificité et nature des liaisons des aminoacides des domaines HTH avec les bases nucléotidiques (flèches violettes) ou avec les phosphates du squelette d'ADN (flèches bleues)(Adapté de Ramos et al. 2005).

aller se verrouiller sur l'ADN cible. L'h3 ainsi que l'h3', appartenant au deuxième monomère, vont participer à la majorité des contacts avec l'ADN en s'insérant dans les grand sillons adjacents (Schumacher et al. 2002). Ramos et al. proposent grâce à un alignement d'acides aminés de plusieurs TetR que les résidus 37, 39 et 43 (annotation du TetR d'*E. coli*) de cette h3 soient primordiaux pour les contacts régulateurs – DNA car ils sont conservés parmi les séquences analysées. Les h2 déforment la structure en double-hélice et permettent aux h3 de s'orienter parallèlement aux grands sillons de l'ADN pour maximiser les contacts spécifiques (Bhukya et Anand 2017). Les contacts TetR – ADN peuvent être deux types. Les acides aminés chargés de domaine HTH, comme les résidus arginines, vont interagir avec les phosphates chargés négativement de l'ADN (PO_4^{3-}) par des liaisons hydrogènes par exemple. D'autres aminoacides comme des tyrosines présentes dans le domaine HTH vont former les liaisons dites « base-spécifique » *via* des interaction hydrophobes ou électrostatiques (Ramos et al. 2005). Cependant, les acides aminés n'ont pas de rôle arbitraire pour l'un ou l'autre type d'interaction. La composition, l'organisation du domaine HTH et la séquence d'ADN va guider le mode d'interaction et pas forcément la nature de l'aminoacide. Un aminoacide peut alors établir soit des liaisons avec les PO_4^{3-} du squelette de l'ADN soit avec une base nucléotidique. Ceci est très bien illustré par les données cristallographiques du complexe régulateur – ADN du TetR d'*E. coli* (Orth et al. 2000)(Figure 34).

Le domaine C-terminal est quant à lui beaucoup moins conservé et reflète la diversité des ligands reconnue par chaque TetR. Les h5 et h7 ainsi que les boucles les reliant vont former un triangle qui sera la poche de reconnaissance du ligand du TetR (LBP pour Ligand Binding Pocket). La nature de ces ligands est aussi variée que les voies métaboliques et les fonctions que ces TetR remplissent. Ils peuvent être substrats de molécules toxiques comme des antibiotiques mais aussi d'ions, de sucres, de protéines, de lipides ainsi que de leurs dérivés potentiels. La nature des aminoacides présents dans cette poche va déterminer le type de ligands qui ira s'y nicher. Néanmoins, il n'est pas possible d'affirmer que telle ou telle molécule est le ligand d'un TetR juste en se basant simplement sur la composition de sa LBP même s'il existe cependant une corrélation. QacR contrôle la pompe à efflux de type MFS QacA responsable de multi-résistances antibiotiques chez *S. aureus*. Plusieurs co-structures de ces régulateurs ont été obtenues avec des antibiotiques cationiques, où les interactions avec les résidus chargés négativement de la LBP étaient prédominantes (Cuthbertson et Nodwell 2013). La stoechiométire des substrats au sein de la LBD est également variable, comme c'est le cas pour LfrR de *M. smegmatis* qui accommode une molécule de proflavine ou de fluoroquinolone (Bellinzoni et al. 2009) alors que ActR de *S. coelicolor* accueille soit deux molécules d'actinorhodine, soit quatre molécules du précurseur biosynthétique de cet antibiotique (Willems et al. 2008).

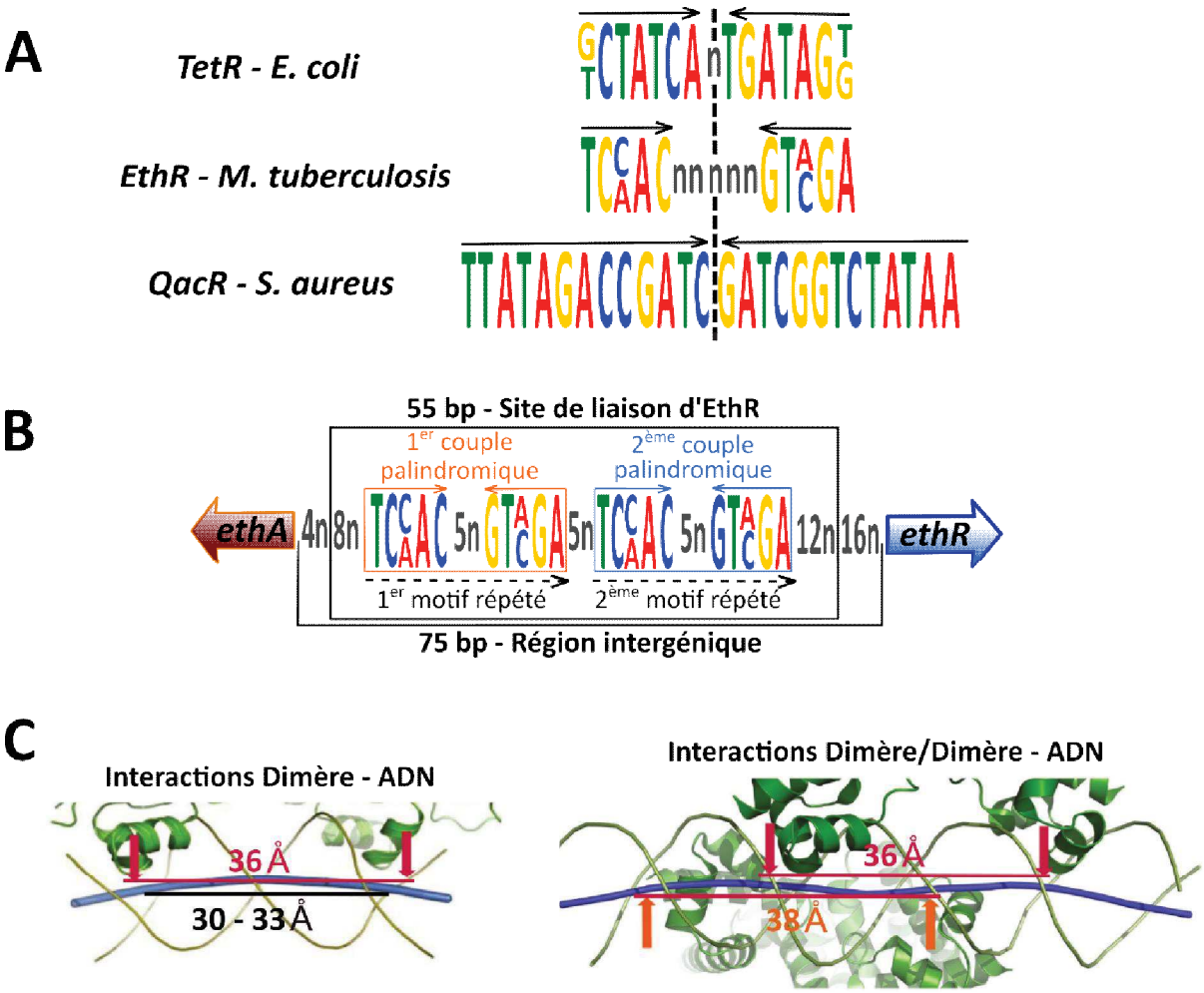

Figure 36. Structure de l'ADN cible d'un TetR. (A) Exemple de palindromes et de leurs architectures. Le DNA_{op} de TetR d'*E. coli* est composé d'un palindrome dégénéré d'une base sur ses extrémités. Il est composé de 15 pb avec un spacer de un nucléotide. Le DNA_{op} d'EthR de *M. tuberculosis* est composé de deux couples de palindromes dégénérés de 15 pb avec des spacers de 5 nucléotides. Le DNA_{op} de QacR de *S. aureus* est un palindrome parfait de 26 pb sans aucun spacer. (B) Représentation schématique de la région intergénique d'EthR. Les deux couples de palindrome sont indiqués en orange et bleu clair. Ils sont séparés par 5 nucléotides et forment deux motifs répétés orientés dans le même sens. Ces motifs sont indiqués en pointillé. La région de 55 pb protégée par EthR suite à la digestion à la DNase I est encadrée. (C) Représentation 3D des déformations que subi la double-hélice d'ADN suite à l'interaction avec un TetR (Adapté de Bhukya et Anand 2017).

Les h8, h9 et éventuellement l'h10, vont former l'interface de dimérisation connectant les deux monomères. Ces h5, 7, 8, 9 voire 10 forment une grappe au sein de laquelle les substrats peuvent pénétrer la LBP de manière latérale, apicale ou frontale (Cuthbertson et Nodwell 2013).

1c) Structure de l'ADN cible et réarrangements conformationnels :

L'ADN cible ou ADN opérateur (DNA_{op}) est de taille et de composition très variable. De manière générale, les TetR reconnaissent des séquences palindromiques ou des motifs répétés inversés, qui sont en réalité des palindromes dégénérés. Ces régulateurs se lient la plupart du temps à des séquences d'ADN d'environ 15 nucléotides, où les motifs palindromiques sont séparés ou non par un ou plusieurs nucléotides (Figure 36A). Ces nucléotides entre les palindromes sont appelés *spacers*, et peuvent être particulièrement longs. EthR de *M. tuberculosis* est impliqué dans la résistance à l'ETH et au TAC en contrôlant l'expression de monooxygénase EthA qui transforme ces deux pro-drogues en métabolites actifs. Une analyse par digestion à la DNase I de la région intergénique située entre *ethA* et *ethR* a révélé que la liaison d'EthR sur ce fragment d'ADN protégeait une région de 55 pb (Engohang-Ndong et al. 2004). Ce DNA_{op} contient deux couples de palindromes dégénérés de 15 nucléotides séparés par un *spacer* de 5 pb. Ces deux couples de palindromes forment deux séquences répétées orientées dans la même direction (Figure 36B). Les TetR vont également influencer la morphologie de la double hélice d'ADN et l'impacter différemment selon la stœchiométrie avec leurs DNA_{op}. Lorsqu'un seul dimère interagit avec le DNA_{op}, ces h2 vont modifier la courbure de la double hélice en induisant un léger arc de cercle. Cette déformation permet d'optimiser l'orientation des h3 dans les grands sillons. Cette courbure unidirectionnelle provoque le passage d'un pas entre deux grands sillons de 36 Å à 30-33 Å et empêche l'appareillement d'un autre dimère sur le brin d'ADN opposé (Bhukya et Anand 2017). Lorsque deux TetR se lient à leurs motifs cibles, ils se retrouvent de part et d'autre de l'ADN et exercent donc un effet de force opposée. Les h2 remplissent toujours le même rôle ce qui mène à une courbure bidirectionnelle moins prononcée, allant de 36 à 38 Å (Bhukya et al. 2014). L'un comme l'autre vont modifier dans leur intérêt la conformation optimale de l'ADN-B (Figure 36C). Le mode de liaison dimère – dimère est généralement synonyme de grande spécificité du régulateur pour son DNA_{op}, alors que l'autre type d'interaction mettant en jeu un seul dimère suggérerait une certaine plasticité du régulateurpour sa cible et donc une implication possible dans la régulation de plusieurs gènes.

Les protéines TetR elles-mêmes subissent un réarrangement structural quand les apoprotéines sont en conformation avec l'ADN ou quand elles sont sous formes libres liées au substrat. Cette allostérie est le résultat d'un mouvement dit de « balancier » ou de « pendule » des

trois premières h-α vers l'extérieur lorsqu'elles relâchent le DNA_{op} suite à l'arrivée du ligand dans la LBP. On parle alors d'état relaxé, où les domaines HTH sont éloignés les uns des autres résultant en une perte de complémentarité de structure avec la double hélice d'ADN. Le mouvement est déclenché principalement par l'h4 interagissant avec l'h1 mais aussi par l'h6, qui sont responsables de la transduction du signal entre les domaines LBP et HTH. Ce balancier des HTH est réalisé suite à la disparition et formation de liaison hydrogène entre les h8, 9 et 10 mais aussi suite à des déroulements de la structure hélicoïdale des h4, h5 et h6 (Cuthbertson et Nodwell 2013)(Bhukya et Anand 2017).

1d) Rôles et fonctions :

La quasi-totalité des voies métaboliques chez les bactéries peuvent contenir une étape régulée par une protéine de la superfamille des TetR. Ces régulateurs sont donc impliqués dans l'antibiorésistance, les métabolismes lipidiques, protéiques, de cofacteurs, du sucre et de l'azote ainsi que dans le *quorum sensing* (Cuthbertson et Nodwell 2013).

Le rôle des TetR dans l'antibiorésistance peut être séparé en deux classes. La première classe constitue les TetR impliqués dans l'antibiorésistance chez les bactéries productrices d'antibiotiques. La deuxième classe est composée des TetR impliqués dans l'antibiorésistance chez les bactéries non-productrices d'antibiotiques.

La première classe regroupe principalement des actinomycètes appartenant au genre *Streptomyces*. L'un d'entre eux est ActR qui contrôle la pompe à efflux ActA sous le contrôle du produit final, l'actinorhobine, et de certains de ses précurseurs métaboliques (Tahlan et al. 2007). Le contrôle de la pompe à efflux par les produits intermédiaires de la chaine de biosynthèse permet à la bactérie de s'assurer que le mécanisme de résistance sera en place une fois le produit final obtenu. Ce genre de mécanismes permet à ces bactéries productrices résistantes d'éliminer les bactéries sensibles voisines ce qui leurs confère un fort avantage adaptatif. Certains de ces TetR, en plus de réguler une protéine transmembranaire impliquée dans l'efflux de l'antibiotique produit, régule des enzymes impliquées dans la biosynthèse et la maturation des précurseurs métaboliques des produits finaux. C'est le cas de LanK chez la bactérie *S. cyanogenus* S136 qui produit la landomycine A. En plus de la pompe à efflux LanJ, ce TetR contrôle l'expression du gène *lanZ1*, codant pour une épimérase impliquée dans les stades tardifs de glycosylation de la landomycine A (Ostash et al. 2008).

Les TetR impliqués dans l'antibiorésistance de classe 2 sont également très repandus et peuvent être le fruit de transfert horizontaux entre bactéries productrices résistantes et bactéries non-productrices sensibles. Chez ces dernières devenues résistantes, on retrouve la plupart du temps

plus de multi-résistances que de mono-résistance. Le couple TetR contrôlant TetA chez *E. coli* est uniquement responsable de l'export de la tétracycline. Mais toujours chez *E. coli*, un régulateur impliqué dans des multi-résistances est AcrR contôlant la pompe à efflux multi-substrat AcrAB, un transporteur RND, la familledont font partis les MmpL. Des mutations ponctuelles situées dans le gène d'*acrR* provoquent la surexpression de la pompe à efflux AcrAB chez des isolats cliniques d'*E. coli* résistants aux fluoroquinolones (Gibson et al. 2010). A l'inverse, la délétion du gène *ethR* mène à une surexpression de la monooxygénase EthA chez *M. bovis* BCG ce qui conduit à une hypersensibilité à l'ETH (Baulard et al. 2000). Cela laisse à penser que des molécules capables de déréprimer les TetR impliqués dans l'activation de pro-drogue seraient de nouveaux pharmacophores originaux. Ce type de molécules, appelées « *boosters* », ont d'ores et déjà prouvé leurs efficacité *in vitro* et *in vivo* contre des isolats cliniques MDR-Tb en combinaison avec l'ETH (Blondiaux et al. 2017). Des mutations dans *ethA* provoquent une résistance accrue à l'ETH chez *M. tuberculosis* car cette enzyme n'est plus en mesure d'activer cet antibiotique le laissant sous sa forme de pro-drogue. Cependant, la combinaison d'ETH et d'une molécule de synthèse de la famille des spiroisoxazoline désignée SMARt-420 (Small Molecule Aborting Resistance) augmente la sensibilité des souches résistantes à l'ETH. Cette combinaison a complétement éradiqué les bacilles chez un modèle murin. Ceci est due à la présence d'un système auxiliaire *ethA2 – ethR2* dans la même conformation génomique qu'*ethA – ethR*. EthR2 est un régulateur de la famille TetR et EthA2 est ici oxydoreductase, elle aussi capable de bio-activer l'ETH. Une étude biochimique a révélé que ce deuxième système est indépendant de EthA – EthR, que les deux régulateurs TetR se lient uniquement à leurs ADN cibles respectifs. SMARt-420 va se positionner dans la LBP d'EthR2 qui déréprimera EthA2 activant alors l'ETH. La présence d'un système homologue à celui-ci n'est pas connue chez *M. abscessus*, mais ces travaux ouvrent des perspectives sur de nouvelles stratégies thérapeutiques originales.

2) La famille de régulateur WhiB :

Cette famille de protéines est restreinte aux actinobactéries. Comme la superfamille des TetR, ces protéines sont en charge de la régulation de nombreuses voies métaboliques impliquées dans la réponse à des stress environnementaux, des changements morphologiques et au coursdes différentes phases de croissance. Ces gènes ont été identifiés il y a presque 50 ans grâce à l'observation microscopique de colonies blanches (*whi* pour « white mutants ») ou grises de *S. coelicolor* capables ou incapables de sporuler respectivement (Chater 1972). C'est donc la fonction de sporulation chez cette bactérie gouvernée par le gène *whiB* qui a d'abord été étudiée dans le détail.

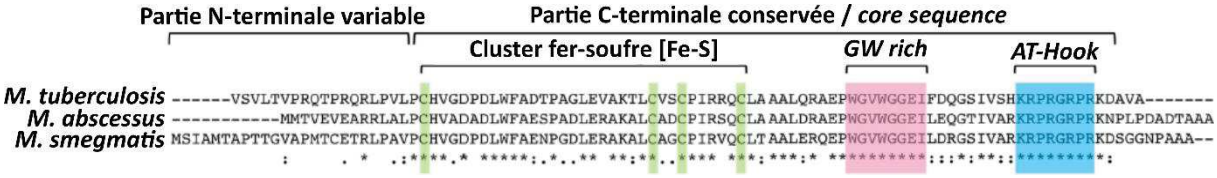

Figure 37. Alignement des séquences d'acides aminés de WhiB7 de mycobactéries. Alignements protéiques de WhiB7 de *M. tuberculosis*, *M. abscessus* et *M. smegmatis* mettant en avant le caractère conservé de la partie C-terminale. Les résidus marqués d'un astérisque (*) sont ultra-conservés, comme les 4 cystéines du cluster fer-soufre, les glycines, tryptophanes et autres acides aminés composant le domaine *GW rich* ainsi que les arginines et lysines de l'*AT-Hook* (Adapté de (Hurst-Hess et al 2017).

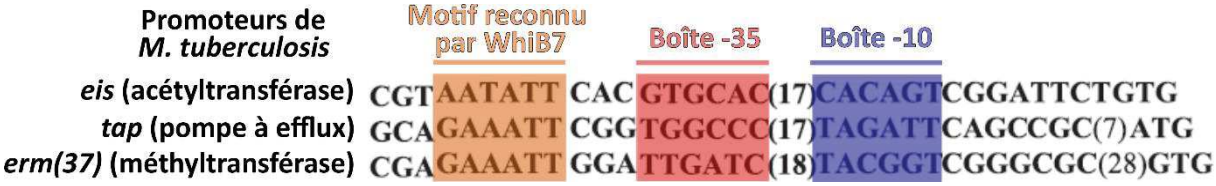

Figure 38. Alignement nucléotidique des séquences promotrices contrôlées par WhiB7 chez *M. tuberculosis*. L'alignement des promoteurs d'*eis*, de *tap* et d'*erm(37)* responsable, respectivement, des résistances aux aminoglycosides, aux rifamycines et aux macrolides révèle l'organisation typique des gènes contrôlés par WhiB7. Un motif riche en AT en orange, situé à 3 nucléotides de la boite -35 en rouge. La boite -10 est colorée en bleu, et est située à 17-18 nucléotides de la boite -35 (Adapté de Burian et al. 2012).

2a) Propriétés génétiques :

Des paralogues de ces gènes *whiB* ont ensuite été identifiés au sein d'autres genres bactériens, comme chez les mycobactéries. Que ce soit chez les streptomycètes ou les mycobactéries, les gènes *whiB*ont une taille comprise entre 250 et 400 pb. Chez *M. tuberculosis*, 7 gènes de type *whiB* ont été identifiés contre 6 chez *M. abscessus*. A l'inverse des *mmpL* et des *tetR*, le nombre de gènes *whiB* ne paraît pas être relié à la capacité d'adaptation, étant donné que *M. leprae* possède 5 homologues potentiels sur son génome (Morris et al. 2005).

2b) Propriétés biochimiques et structurales :

Ces gènes de tailles réduites produisent des polypeptides de petites tailles, 94 acides aminés pour le WhiB7 de *M. abscessus*. Ces protéines sont partiellement très conservées parmi les mycobactéries mais également au sein d'autres genres comme *Rhodococcus* et *Streptomyces* (Hurst-Hesset et al 2017). La région N-terminale est moins conservée et de taille variable que le reste de la protéine qui est appelée « *core sequence* » (Figure 37). Cette *core sequence* est composée d'un cluster fer-souffre où quatre résidus cystéines sont absolument conservés dans toutes les séquences. Ces cystéines sont capables de lier deux ou quatre atomes de fer et deux ou quatre de soufre ([2/4Fe – 2/4S]) en fonction de leur état oxydatif (Ramón-García et al. 2013). Si ce cluster fer-soufre ne lie aucun de ces deux atomes, les cystéines vont former des ponts intramoléculaires provoquant un réarrangement structural avec un impact sur la fonction de régulation. Les formes [2/4Fe – 2/4S] ne sont pas forcément les configurations protéiques capables de lier l'ADN et inversement. On retrouve ensuite une partie riche en glycine – tryptophane (GW-rich) et la partie responsable de l'interaction, de l'hameçonnage de domaines riches en adénosine et thymine de l'ADN cible (AT-Hook). Ces motifs sont tous les deux hautement conservés. Le domaine GW-rich forme un feuillet bêta qui sera en contact avec les acides aminés chargés positivement composant l'AT-Hook, des arginines et des lysines. Ce domaine de liaison en C-terminal attribue classiquement une fonction d'activateur au système à un composant. Cependant, chez *M. tuberculosis*, les protéines WhiB peuvent être des répresseurs comme par exempleWhiB1 ou des activateurs comme WhiB2, 3, 4 et 7 (Burian et al. 2012). Les protéines WhiB activatrices vont alors interagir avec différents facteurs sigmas (σ). La préférence pour tel ou tel facteur σ est liée à l'architecture du promoteur en amont du gène (Newton-Foot et Gey van Pittius 2013). Ces protéines WhiB se lieraient aux parties C-terminales de leurs facteurs σ respectifs etcatalyseraient la transcriptiondes régulons par l'ARN polymérase. La taille et la séquence de ces motifs riches en AT sont variables d'un gène et d'une espèce à l'autre. En règle générale, ils sont composés de 5-6 pb situés à 3 nucléotides en amont de la boîte hexamèrique -35 du promoteur, comme illustré pour les gènes *erm(37)*, *eis* et *tap* de *M. tuberculosis* (Burian et al 2012)(Figure 38). Chez les mycobactéries, la distance entre la boîte -35 et la boîte -10 détermine le type de facteur σqui interagira avec ce promoteur (Newton-Foot et Gey van Pittius 2013).

2c) Rôles et fonctions :

Chez *M. abscessus*, c'est le gène *whiB7* qui est principalement étudié étant donné son implication dans les processus de multi-résistances intrinsèques aux antibiotiques. Deux études récentes rapportent l'enrôlement de WhiB7 dans la résistance de *M. abscessus* à l'AMK, à la CLR, à la TGC mais aussi à la TBM, à la gentamicine et au chloramphénicol (Hurst-Hess et al 2017)(Pryjma et al. 2017). Des études de RNA-seq comparant l'expression des gènes entre une souche sauvage et un mutant Δ*whiB7* ont révélé que le régulon de *whiB7* s'étend à plus de 120 gènes, suggérant un rôle global de WhiB7 dans l'homéostasie de cette MNT (Hurst-Hess et al 2017). Pryjma et al. proposent un antagonisme *in vitro* entre la CLR avec l'AMK à des doses subinhibitrices. En effet une faible concentration de CLR induit une résistance croisée à l'AMK.

En revanche chez *M. tuberculosis*, les fonctions des 7 gènes *whiB* sont connues. Plusieurs de ces protéines partagent des rôles similaires comme dans la virulence au sein du macrophage ainsi que les différentes phases de croissance et la persistance. C'est le cas par exemple de WhiB1, 2 et 3 qui sont surexprimés lors de la phase stationnaire.

WhiB1 est également impliqué dans la survie intramacrophagique et la possible réactivation des bacilles après une infection latente (Smith et al. 2010). En effet, WhiB1 contrôle l'expression du gène *rpfA*, un facteur de croissance nécessaire à la sortie de la phase de latence (Kana et al. 2008).

WhiB2 est aussi surexprimé en phase stationnaire ainsi qu'en carence de nutriments et en présence de molécules ciblant la paroi mycobactérienne comme l'EMB (Geiman et al. 2006).

WhiB3 s'active également lors d'un stress nutritif et oxydatif que l'on retrouve en phase de latence (Singh et al. 2007). Il catalyse aussi l'anabolisme de lipides nécessaires à la pathogénicité de *M. tuberculosis* dans le macrophage *via* l'utilisation du propionate pour la synthèse de certains glycolipides comme le DAT (Singh et al. 2009).

WhiB4 est lui exprimé tout au long des phases de croissance et joue un rôle dans la virulence mais aussi dans la dissémination de l'infection. Un mutant Δ*whiB4* montre une hypervirulence dans le système pulmonaire mais un défaut de dissémination des bactéries jusqu'à la rate chez un modèle murin (Chawla et al. 2012).

WhiB5 est quant à lui seulement exprimé en phase exponentielle de croissance mais semble répondre à des agents provoquant un stress membranaire (Geiman et al. 2006). Comme WhiB1, cette protéine aurait un rôle dans la réactivation et la reprise de croissance après une infection latente (Casonato et al. 2012). Le régulon de WhiB5 est important puisqu'il contient au moins 58 gènes identifiés. Parmi ses candidats, on retrouve les gènes codant les systèmes de sécrétion de

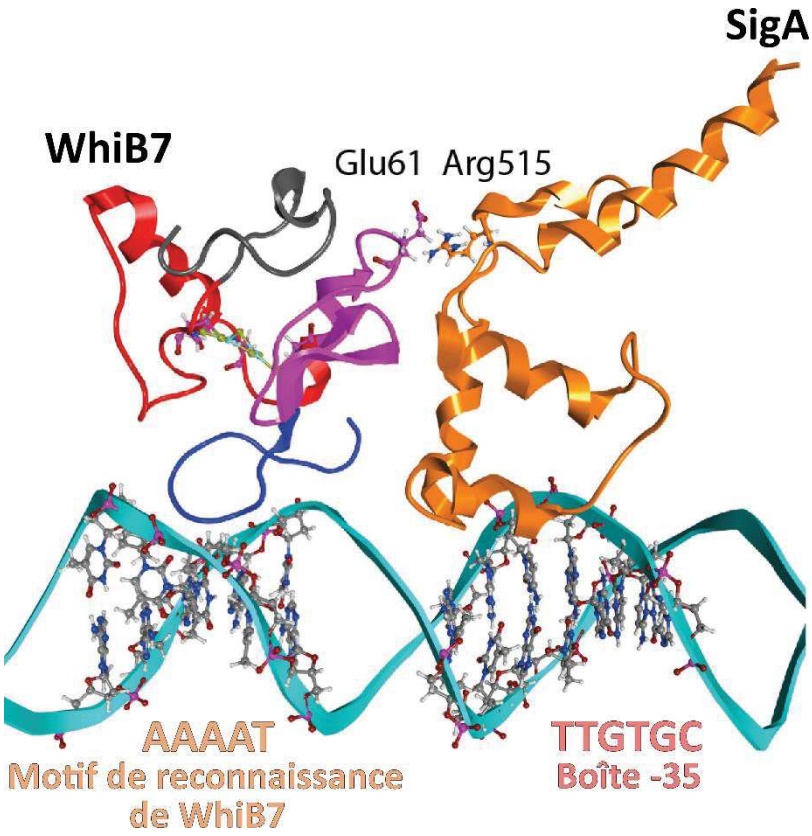

Figure 39. Modèle de prédiction d'interaction du complexe WhiB7 – SigA lié à l'ADN cible. L'interaction du résidu Glu61 de WhiB7 avec le résidu Arg515 de la région 4,2 C-terminale de SigA a été déterminée expérimentalement. La région N-terminale, le cluster fer-soufre, l'AT-Hook et la région intermédiaire située en ces deux derniers domaines sont colorés en gris, rouge, bleu et rose respectivement. La région 4 du facteur SigA d'*E. coli* a été utilisée dans ce modèle et est colorée en doré (PDB : 4IGC_X)(Adapté de Burian et al. 2013).

type VII ESX-2 et ESX-4, des protéines nécessaire à la survie au sein de cellules dendritiques et de macrophages (Mendum et al. 2015).

WhiB6 est aussi surexprimé en conditions de stress membranaire par exemple après exposition au SDS, à de l'éthanol et après un choc thermique (Geiman et al. 2006). Cette protéine semble aussi activer l'expression d'un système de sécrétion de type VII, cette fois-ci ESX-1 (Wiseman et al. 2010). ESX-1 est responsable de la sécrétion d'antigènes majeurs liés à la virulence de *M. tuberculosis*. Les pertes de virulence des souches de *M. bovis* BCG et *M. microti* utilisées dans les vaccins anti-tuberculeux sont liées à des mutations dans locus d'*esx-1* (Pym et al. 2002).

Le rôle de WhiB7 est identique chez *M. abscessus* et chez *M. tuberculosis*. Une approche biochimique a permis de montrer que WhiB7 interagit avec la partie C-terminal du facteur végétatif SigA pour améliorer le niveau de transcription des gènes cibles (Burian et al 2013)(Figure 39). Cette interaction serait due à la région située entre le cluster fer-soufre et l'AT-Hook. L'activation n'est pas uniquement dépendante de la présence d'antibiotiques ciblant le ribosome. Ce régulateur s'active au moment de l'entrée en phase stationnaire ou en absence de fer, comme par exemple à l'intérieur d'un phagosome (Homolka et al. 2010). Des conditions entraînant une réduction du potentiel redox du cytoplasme suivie d'un stress oxydatif peut provoquer en théorie une activation de WhiB7. Burian et al. le démontrèrent simplement en mesurant le niveau d'expression de l'ARNm par qRT-PCR de *whiB7* en présence d'antibiotiques couplés soit à un agent réducteur soit à un agent oxydatif, respectivement du DiThioThréitol (DTT) ou du diamide. Le DTT couplé à une très faible concentration d'érythromycine augmente fortement le niveau de transcrits de *whiB7* alors que le diamide en stoppe la production. Ceci reflète expérimentalement le changement de la balance redox du mycothiol dans le cytoplasme de la bactérie. Le mycothiol est aux actinomycètes ce qu'est le glutathion chez les Gram - et les eucaryotes. C'est un agent réducteur qui permet entre autre de se débarrasser des ROS lorsqu'il est retrouvé en grande quantité sous sa forme réduite. En plus des gènes de résistance présents dans le régulon de *whiB7*, ce mécanisme d'oxydoréduction participe à la lutte contre les antibiotiques en inactivant la production de radicaux libres que ces antimicrobiens engendrent indirectement (Rawat et al. 2002).

Améliorer la compréhension des mécanismes qui régissent l'antibiorésistance intrinsèque chez *M. abscessus* est primordial pour :

- le développement de nouveaux pharmacophores biologiquement actifs,
- la découverte de nouvelles cibles médicamenteuses,
- l'élaboration de nouvelles stratégies thérapeutiques utilisant les antibiotiques dont l'utilisation est déjà approuvée.

Mes travaux de thèse s'inscrivent dans le domaine de la recherche fondamentale. Ces recherches se sont, dans un premier temps, axées sur des transporteurs membranaires impliqués dans l'efflux d'antibiotiques, dont les principaux objectifs ont consisté à :

- identifier les antibiotiques potentiellement expulsés par *M. abscessus*,
- identifier le ou les transporteurs MmpL impliqués dans ce processus,
- décrire les mécanismes de régulation de ces pompes à efflux,
- proposer de nouveaux marqueurs de résistance à certains antibiotiques.

Trois études comprenant des approches biochimique, génétique et structurale ont permis de disséquer les mécanismes de résistance basale de trois couples TetR – MmpS/MmpL impliqués dans la résistance à trois classes d'antibiotiques différentes. Nous avons tout d'abord identifié le système MAB_4384 – MAB_4383c/MAB_4382c, responsable de l'export des analogues du TAC (**Article 1**). Nous avons également décrit et attribué la résistance croisée à la CFZ et à la BDQ à deux couples MmpS/MmpL, les paires MAB_2300/MAB_2301 (**Article 2**) et MAB_1135c/MAB_1134c (**Article 3**), toutes deux régulées par le même TetR MAB_2299c.

La deuxième partie de ma thèse a porté sur la résistance inductible aux macrolides chez *M. abscessus*. Ce phénomène, encore très mal compris, est d'autant plus problématiqueque les macrolides sont la pierre angulaire de la thérapie anti – *M. abscessus*. Les objectifs ont consisté à :

- identifier les éléments nécessaires à l'activation de cet événement inductible,
- comparerl'activité antimicrobienne et la cinétique de l'induction de l'AZM et de la CLR,
- mettre en évidence et observer ce phénomène de résistance induite dans un modèle animal, l'embryon de zebrafish.

Nous avons confirmé *via* une étude génétique et biochimique l'implication de WhiB7 dans l'activation de cette résistance et nous avons également clôturé le débat sur les effets respectifs de l'AZM et de la CLR en démontrant que l'AZM n'est pas un meilleur antibiotique que la CLR *in vitro*. Ces deux macrolides induisent également la résistance*in vivo* chez le zebrafish. Ces travaux ont aussi souligné la complexité de cette cascade de régulation qui a pour répercussion un antagonisme entre l'AMK et ces deux macrolides.

Résultats

Article 1

« **Mechanistic and Structural Insights Into the Unique TetR-Dependant Regulation of a Drug Efflux Pump in *Mycobacterium abscessus*.** » Richard M, Gutiérrez AV, Viljoen A, Ghigo E, Blaise M, Kremer L. Front Microbiol. 2018 Apr 5; Vol 9 Article 649.

La récente optimisation chimique du TAC a permis d'obtenir une nouvelle génération d'analogues structuraux (TACa) à la fois efficaces contre *M. abscessus* et *M. tuberculosis* (Coxon et al. 2013). Une étude antérieure menée dans l'équipe a mis en avant un lien entre la résistance aux TACa et la présence de mutations dans le régulateur TetR MAB_4384 qui s'accompage d'une augmentation des transcrits de la pompe à efflux de type MmpS/MmpL MAB_4383c/MAB_4382c (Halloum et al. 2017). Sur la base d'une approche biochimique incluant la technique d'EMSA, nos travaux ont permis de prouver l'interaction physique du TetR MAB_4384 avec un motif palindromique situé en amont de l'opéron *MAB_4383c/MAB_4382c*. Des EMSA réalisés avec des protéines mutées sur des résidus spécifiques ont permis de démontrer le rôle de ces acides aminés dans la capacité du régulateur TetR à se lier à son ADN cible. Par ailleurs, des substitutions nucléotidiques dans le motif palindromique ont permis de démontrer la spécificité de MAB_4384 pour sa séquence cible. Une étude génétique basée sur l'utilisation du gène rapporteur *lacZ* sous le contrôle de la séquence promotrice de *MAB_4383c/MAB_4382c* a mis en lumière la force de ce promoteur, permettant ainsi d'expliquer les hauts niveaux de résistance observés dans les souches de *M. abscessus* devenues spontanément résistantes aux TACa. Les expériences menées avec cette souche rapportrice suggèrent également un export basal et intrinsèque des TACa *via* l'activité de pompe à efflux de MAB_4383c/MAB_4382c. La résolution de la structure cristallographique de MAB_4384 combinée à des expériences de *docking in silico* des TACa au sein de son domaine LBP suggèrent fortement la possibilité d'une expression accrue de la pompe à efflux lorsque ces molécules se fixent sur le régulateur TetR. L'ensemble de ces résultats met en avant, pour la premières fois, un mécanisme de régulation et d'expression basal de pompes à efflux de la famille MmpL impliqué dans la résistance aux antibiotiques chez *M. abscessus*.

frontiers in Microbiology

ORIGINAL RESEARCH
published: 05 April 2018
doi: 10.3389/fmicb.2018.00649

Mechanistic and Structural Insights Into the Unique TetR-Dependent Regulation of a Drug Efflux Pump in *Mycobacterium abscessus*

Matthias Richard[1], Ana Victoria Gutiérrez[1,2], Albertus J. Viljoen[1], Eric Ghigo[3], Mickael Blaise[1] and Laurent Kremer[1,4]**

[1] CNRS UMR 9004, Institut de Recherche en Infectiologie de Montpellier, Université de Montpellier, Montpellier, France, [2] Unité de Recherche, Microbes, Evolution, Phylogeny and Infection, Institut Hospitalier Universitaire Méditerranée Infection, Marseille, France, [3] Centre National de la Recherche Scientifique, Campus Joseph Aiguier, Marseille, France, [4] Institut National de la Santé et de la Recherche Médicale, Institut de Recherche en Infectiologie de Montpellier, Montpellier, France

OPEN ACCESS

Edited by:
Thomas Dick,
Rutgers University, United States

Reviewed by:
Peter Sander,
Universität Zürich, Switzerland
Kyle Rohde,
University of Central Florida,
United States

***Correspondence:**
Mickael Blaise
mickael.blaise@irim.cnrs.fr
Laurent Kremer
laurent.kremer@irim.cnrs.fr

Specialty section:
This article was submitted to Antimicrobials, Resistance and Chemotherapy, a section of the journal Frontiers in Microbiology

Received: 13 February 2018
Accepted: 20 March 2018
Published: 05 April 2018

Citation:
Richard M, Gutiérrez AV, Viljoen AJ, Ghigo E, Blaise M and Kremer L (2018) Mechanistic and Structural Insights Into the Unique TetR-Dependent Regulation of a Drug Efflux Pump in Mycobacterium abscessus. Front. Microbiol. 9:649. doi: 10.3389/fmicb.2018.00649

Mycobacterium abscessus is an emerging human pathogen causing severe pulmonary infections and is refractory to standard antibiotherapy, yet few drug resistance mechanisms have been reported in this organism. Recently, mutations in *MAB_4384* leading to up-regulation of the MmpS5/MmpL5 efflux pump were linked to increased resistance to thiacetazone derivatives. Herein, the DNA-binding activity of MAB_4384 was investigated by electrophoretic mobility shift assays using the palindromic sequence $IR_{S5/L5}$ located upstream of *mmpS5/mmpL5*. Introduction of point mutations within $IR_{S5/L5}$ identified the sequence requirements for optimal binding of the regulator. Moreover, formation of the protein/$IR_{S5/L5}$ complex was severely impaired for MAB_4384 harboring D14N or F57L substitutions. $IR_{S5/L5}$*/lacZ* reporter fusions in *M. abscessus* demonstrated increased β-galactosidase activity either in strains lacking a functional MAB_4384 or in cultures treated with the TAC analogs. In addition, X-ray crystallography confirmed a typical TetR homodimeric structure of MAB_4384 and unraveled a putative ligand binding site in which the analogs could be docked. Overall, these results support drug recognition of the MAB_4384 TetR regulator, alleviating its binding to $IR_{S5/L5}$ and steering up-regulation of MmpS5/MmpL5. This study provides new mechanistic and structural details of TetR-dependent regulatory mechanisms of efflux pumps and drug resistance in mycobacteria.

Keywords: ***Mycobacterium abscessus,*** **TetR regulator, MmpL, efflux pump, structure, thiacetazone analogs, EMSA**

INTRODUCTION

Mycobacterium abscessus is a rapid growing mycobacterium (RGM) that has recently become an important health problem (Mougari et al., 2016). This non-tuberculous mycobacterial (NTM) pathogen can cause serious cutaneous, disseminated or pulmonary infections, particularly in cystic fibrosis (CF) patients. In CF patients, infection with *M. abscessus* is correlated with a decline in lung function and poses important challenges during last-resort lung transplantation (Esther et al., 2010; Smibert et al., 2016). An epidemiological study has recently documented the prevalence

and transmission of *M. abscessus* between hospital settings throughout the world, presumably *via* fomites and aerosols and uncovered the emergence of dominant circulating clones that have spread globally (Bryant et al., 2016). In addition, *M. abscessus* exhibits innate resistance to many different classes of antimicrobial agents, rendering infections with this microorganism extremely difficult to treat (Nessar et al., 2012; van Dorn, 2017). Recent studies have started to unveil the basis of the multi-drug resistance characterizing *M. abscessus,* uncovering a wide diversity of mechanisms or regulatory networks. These involve, for example, the induction of the *erm(41)* encoded 23S rRNA methyltransferase and mutations in the 23S *rRNA* that lead to clarithromycin resistance (Nash et al., 2009), the presence of a broad spectrum β-lactamase that limits the use of imipenem (Dubée et al., 2015; Lefebvre et al., 2016, 2017) or the presence of *eis2,* encoding an acetyl-transferase that modifies aminoglycosides, specifically induced by *whiB7*, which contributes to the intrinsic resistance to amikacin (Hurst-Hess et al., 2017; Rominski et al., 2017b). Other studies reported the role of the ADP-ribosyltransferase MAB_0591 as a major contributor to rifamycin resistance (Rominski et al., 2017a) whereas MAB_2385 was identified as an important determinant in innate resistance to streptomycin (Dal Molin et al., 2018).

Recently, we reported the activity of a library of thiacetazone (TAC) derivatives against *M. abscessus* and identified several compounds exhibiting potent activity against a vast panel of clinical strains isolated from CF and non-CF patients (Halloum et al., 2017). High resistance levels to these compounds were linked to mutations in a putative transcriptional repressor MAB_4384, together with a strong up-regulation of the divergently oriented adjacent locus encoding a putative MmpS5/MmpL5 transporter system. That ectopic overexpression of MmpS5/MmpL5 in *M. abscessus* also increased the minimal inhibitory concentration (MIC) to analogs of TAC further suggested that these two proteins may act as an active efflux pump which was sufficient to confer drug resistance (Halloum et al., 2017). In addition to uncovering new leads for future drug developments, this study also highlighted a novel mechanism of drug resistance in *M. abscessus*. Unexpectedly, an important difference relies on the fact that, in *M. tuberculosis*, MmpS5/MmpL5 acts as a multi-substrate efflux pump causing low resistance levels to antitubercular compounds such as clofazimine, bedaquiline, and azoles (Milano et al., 2009; Andries et al., 2014; Hartkoorn et al., 2014) whereas the *M. abscessus* strains overexpressing MmpS5/MmpL5 are very resistant to the TAC analogs but fail to show cross-resistance against clofazimine or bedaquiline (Halloum et al., 2017). This implies that, despite their high primary sequence identity, the MmpS5/MmpL5 orthologs from *M. tuberculosis* and *M. abscessus* do not share the same substrate specificity. Moreover, whereas Rv0678, the cognate regulator of MmpS5/MmpL5 in *M. tuberculosis* belongs to the MarR family (Radhakrishnan et al., 2014), MAB_4384 is part of the TetR family of regulators and the change in the transcriptional level of *mmpS5/mmpL5* was much more pronounced in the *M. abscessus* mutants than in the *M. tuberculosis* mutants (Milano et al., 2009; Hartkoorn et al., 2014).

The TetR transcriptional regulatory factors are common single component signal transduction systems found in bacteria. These proteins possess a conserved helix-turn-helix (HTH) signature at the N-terminal of the DNA-binding domain as well as a ligand binding domain (LBD) located at the C-terminal part (Cuthbertson and Nodwell, 2013). They often act as repressors and interact with a specific DNA target to prevent or abolish transcription in the absence of an effector. In contrast, the binding of a specific ligand to the LBD induces structural changes, conducting the dissociation of the repressor from the target DNA, and the subsequent transcription of the TetR-regulated genes. Being largely associated with resistance to antibiotics and regulation of genes coding for small molecule exporters, TetR regulators also govern expression of antibiotic biosynthesis genes, quorum sensing and in distinct aspects in bacterial physiology/virulence (Cuthbertson and Nodwell, 2013). A recent global analysis indicated that the TetR regulators represent the most abundant class of regulators in mycobacteria, the vast majority remaining uncharacterized (Balhana et al., 2015). In order to provide new insight into the mechanism of gene regulation by TetR regulators in mycobacteria and to describe a new and specific drug resistance mechanism in *M. abscessus*, we focused our efforts on the molecular and structural characterization of the MAB_4384-dependent regulation of MmpS5/MmpL5.

In this study, a combination of genetic and biochemical analyses was applied to determine the specificity of this regulatory system in *M. abscessus* and to describe the contribution of key residues that are important in driving the DNA-binding of MAB_4384 to its operator. We report also the crystal structure of the MAB_4384 TetR regulator. Overall, the results provide new insights into the regulation of members of the MmpL family and on a novel mechanism of drug resistance in *M. abscessus*.

MATERIALS AND METHODS

Plasmids, Strains, Growth Conditions, and Reagents

The *Mycobacterium abscessus* subsp. *abscessus* CIP104536^T reference strain and all derived mutant strains are listed in Supplementary Table S1. Strains were grown in Middlebrook 7H9 broth (BD Difco) supplemented with 0.05% Tween 80 (Sigma-Aldrich) and 10% oleic acid, albumin, dextrose, catalase (OADC enrichment; BD Difco) (7H9$^{T/OADC}$) at 30°C or in Sauton's medium in the presence of antibiotics, when required. On plates, colonies were selected either on Middlebrook 7H10 agar (BD Difco) supplemented with 10% OADC enrichment (7H10^{OADC}) or on LB agar. For drug susceptibility testing, cultures were grown in Cation-Adjusted Mueller-Hinton Broth (CaMHB; Sigma-Aldrich). The TAC analogs D6, D15, and D17 were synthesized as reported previously (Coxon et al., 2013) and dissolved in DMSO. Other antibiotics were purchased from Sigma-Aldrich.

Cloning of Wild-Type and Mutated MAB_4384 and Site-Directed Mutagenesis

MAB_4384 was PCR-amplified from *M. abscessus* CIP104536^T purified genomic DNA using the *MAB_4384_full* primers (Supplementary Table S2) and Phusion polymerase (Thermo Fisher Scientific). The amplicon was cloned into pET32a restricted with KpnI and HindIII (New England Biolabs), enabling the introduction of *MAB_4384* in frame with the thioredoxin and poly-histidine tags as well as a Tobacco Etch Virus protease (TEV) cleavage site between the N-terminus of MAB_4384 and the tags. The *MAB_4384* alleles harboring the g40a (D14N) and t169c (F57L) mutations were PCR-amplified using the primers described above and using the purified genomic DNA of the two spontaneous resistant *M. abscessus* strains to TAC analogs reported previously (Halloum et al., 2017). The double mutant carrying both g40a and t169c mutations was obtained from the *MAB_4384* (g40a) allele using the PCR-driven primer overlap extension method (Aiyar et al., 1996). Briefly, two separate PCR reactions were set up using Phusion polymerase. The first was generated using the forward primer *MAB_4384_full* Fw and a reverse internal primer *MAB_4384_DM* Rev harboring the nucleotide substitution responsible for the mutation. The second PCR was set up with an internal forward primer *MAB_4384_DM* Fw overlapping the internal reverse primer *MAB_4384_DM* Rev and with the original reverse primer *MAB_4384_full* Rev. PCR products were purified, annealed and amplified by a last PCR amplification with the *MAB_4384_full* primers. All mutated genes were cloned into pET32a, as described for wild-type *MAB_4384*.

Expression and Purification of MAB_4384 Variants

The various pET32a-derived constructs containing either the wild-type or the mutated *MAB_4384* gene alleles were used to transform *Escherichia coli* strain BL21 Rosetta 2 (DE3) (Novagen). Cultures were grown in Luria-Bertani (LB) medium containing 200 μg/mL ampicillin and 30 μg/mL chloramphenicol until an optical density at 600 nm (OD_{600}) of between 0.6 and 1.0 was reached. Liquid cultures were then placed on icy water for 30 min prior to the addition of 1 mM isopropyl β-D-1-thiogalactopyranoside (IPTG) and incubation for an additional 20 h at 16°C. Bacteria were then collected by centrifugation (6,000 × *g*, 4°C, 60 min) and the pellets were resuspended in lysis buffer (50 mM Tris-HCl pH 8, 200 mM NaCl, 20 mM imidazole, 5 mM β-mercaptoethanol, 1 mM benzamidine). Cells were opened by sonication and the lysate clarified by centrifugation (28,000 × *g*, 4°C, 45 min) and subjected to a first step of nickel affinity chromatography (IMAC) (Ni-NTA Sepharose, GE Healthcare Life Sciences). After elution, the protein was dialyzed overnight at 4°C in a buffer containing 50 mM Tris-HCl pH 8, 200 mM NaCl, 5 mM β-mercaptoethanol and TEV protease (1 mg of protease/50 mg of total protein) to cleave the thioredoxin and histidine tags from the recombinant proteins. The dialyzed preparations were purified again by IMAC, followed by an anion exchange chromatography step (HiTrap Q Fast Flow, GE Healthcare Life Sciences) as well as a final polishing step using size exclusion chromatography (SEC) (Sephadex^{TM} 75 10/300 GL, GE Healthcare Life Sciences) and a buffer containing 50 mM Tris-HCl pH 8, 200 mM NaCl and 5 mM β-mercaptoethanol.

The selenomethionine-substituted protein was expressed in the methionine auxotroph *E. coli* strain B834 (DE3) (Novagen). A 1L culture was grown very densely in LB medium containing 200 μg/mL ampicillin for 36 h at 37°C. Bacteria were harvested by centrifugation and the pellets resuspended in minimal medium A without antibiotic and methionine traces (M9 medium, trace elements, 0.4% glucose, 1 μM $MgSO_4$, 0.3 mM $CaCl_2$, biotin and thiamine at 1 μg/mL). After an additional wash in medium A, the bacterial pellet was resuspended in 6L of medium A containing 200 μg/mL ampicillin and incubated for 2 h at 37°C. Finally, S/L selenomethionine was added at a final concentration of 100 μg/mL. After 30 min of incubation, expression of the protein was induced with 1 mM IPTG for 5 h at 37°C. The protein was purified using a protocol similar to the one used for the proteins expressed in the *E. coli* strain BL21 Rosetta 2(DE3).

Determination of Oligomeric States of MAB_4384 by Size Exclusion Chromatography

The oligomeric state of MAB_4384 and MAB_4384:DNA complex in solution were assessed on an ENrich^{TM} SEC 650 size exclusion column (Bio-Rad) run on an ÄKTA pure 25M chromatography system (GE Healthcare Life Science). The protein, DNA or protein:DNA complex were eluted with 50 mM Tris-HCl pH 8, 200 mM NaCl and 5 mM β-mercaptoethanol at a flow rate of 0.4 mL/min at 4°C. MAB_4384 (dimer) was concentrated to 3.9 mg/mL, while DNA was at 2.8 mg/mL and complexes were formed at different protein(dimer)/DNA molar ratios of 1:1, 2:1, 3:1. The molecular weights were determined based on a calibration curve generated using the Gel Filtration Markers Kit (Sigma-Aldrich) for proteins ranging from 12,400 to 200,000 Da. The column void volume was assessed with the elution peak of dextran blue. The apparent mass was obtained by plotting the partition coefficient K_{av} against the log values of the molecular weights of the standard proteins.

Disruption of *MAB_4384* and *mmpL5* in *M. abscessus*

To generate *MAB_4384* and *mmpL5* knock-out mutants, internal fragments of the genes were PCR-amplified using Phusion polymerase and the specific oligonucleotide sets: *MAB_4384*::pUX1 Fw with *MAB_4384*::pUX1 Rev and *mmpL5*::pUX1 Fw with *mmpL5*::pUX1 Rev, respectively, digested with NheI and BamHI and ligated to NheI-BamHI-linearized pUX1 (Supplementary Table S1), a suicide vector specifically designed to perform gene inactivation in *M. abscessus* (Viljoen et al., 2018). Electrocompetent *M. abscessus* was transformed with the plasmids pUX1-*MAB_4384* and pUX1-*mmpL5* and plated on 250 μg/mL kanamycin LB plates. After 5 days of incubation at 37°C, red fluorescent colonies were selected and gene disruption resulting from homologous recombination

between the plasmid DNA and the target genes was confirmed by PCR and sequencing with appropriate primers (Supplementary Table S2).

Quantitative Real-Time PCR

Isolation of RNA, reverse transcription and qRT-PCR were done as reported earlier (Halloum et al., 2017) using the primers listed in Supplementary Table S2.

Drug Susceptibility Assessment

The MICs were determined according to the CLSI guidelines (Woods et al., 2011), as reported earlier (Halloum et al., 2017).

Electrophoretic Mobility Shift Assays

First, a typical DNA binding motif recognized by the TetR regulator, often composed of palindromic sequences or inverted repeats, was identified *in silico* within the intergenic region located between *MAB_4384* and the *MAB_4383c (mmpS5$_{Mabs}$)/MAB_4382c (mmpL5$_{Mabs}$)* gene cluster, hereafter referred to as IR$_{S5/L5}$, using the MEME Suite 4.20.0 online tool[1] (Bailey et al., 2009). A 45 bp double stranded DNA fragment (Probe 1) containing the 27 bp palindromic sequence was labeled with fluorescein at their 5′ ends (Sigma-Aldrich). Increasing amounts of purified MAB_4384 protein were co-incubated with 280 nM of the fluorescein-labeled probes in 1X Tris Base/acetic acid/EDTA (TAE) buffer for 1 h at room temperature. The samples were then subjected to 6% native polyacrylamide gel electrophoresis for 30 min at 100 V in 1X TAE buffer. Gel shifts were visualized by fluorescence using an Amersham Imager 600 (GE Healthcare Life Sciences). All additional modified probes listed Supplementary Table S2 and used in this study were synthetized and used in electrophoretic mobility shift assay (EMSA) assays, as described above.

Construction of β-Galactosidase Reporter Strains and β-Gal Assays

The *lacZ* reporter gene encoding the β-galactosidase was amplified from the *E. coli* HB101 using primers listed in Supplementary Table S2. The amplicon was cloned into pMV261 cut with BamHI and HindIII, thus yielding pMV261_P$_{hsp60}$_*lacZ*. The 208 bp intergenic region IR$_{S5/L5}$ was amplified by PCR using *M. abscessus* CIP104536^T genomic DNA and the *MAB_4384*_P$_{S5/L5}$ primers (Supplementary Table S2) and subsequently cut with XbaI and BamHI. The *hsp60* promoter was removed from pMV261_P$_{hsp60}$_*lacZ* construct by restriction using XbaI and BamHI and replaced with IR$_{S5/L5}$, thus creating pMV261_P$_{S5/L5}$_*lacZ*. A promoterless pMV261_*lacZ* construct was also generated by removing the *hsp60* promoter from the pMV261_P$_{hsp60}$_*lacZ* with BamHI and XbaI, blunting the overhang extremities using the T4 DNA Polymerase and self-religation.

The β-galactosidase activity of the *M. abscessus* strains carrying either wild-type or mutated *MAB_4384* alleles and the various β-gal reporter constructs was monitored streaking the strains directly on 7H10^{OADC} agar plates supplemented with 100 μg/mL kanamycin and 50 μg/mL X-gal (Sigma-Aldrich). The quantification of the β-gal activity was also assayed in liquid medium using a protocol adapted from Miller's method. Briefly, a 10 mL culture in Sauton's medium supplemented with 0.025% tyloxapol was grown until the OD_{600} reached 0.6–1. Cultures were collected by centrifugation (4,000 × *g* for 10 min at 4°C) and the bacterial pellets were resuspended in 700 μL 1X phosphate-buffered saline (PBS) prior to mechanical lysis by bead beating (3 min treatment, 30 Hz). Lysates were finally centrifuged at 16,000 × *g* for 10 min at 4°C. 10 μL of clarified lysate were co-incubated 30 min at 37°C with 100 μL of reaction buffer (60 mM Na_2HPO_4, 40 mM NaH_2PO_4, 10 mM KCl, 1 mM $MgSO_4$, 50 mM β-mercaptoethanol) in 96-well plates. Enzymatic reactions were initiated by adding 35 μL of 2-Nitrophenyl β-D-galactopyranoside (ONPG, Sigma-Aldrich) at 4 mg/mL and absorbance was recorded at 420 nm at 34°C using a Multimode Microplate Reader POLARstar Omega (BMG Labtech). The β-galactosidase specific activity ($SA_{\beta-Gal}$) was calculated using the following formula: $SA_{\beta-Gal}$ = ($Absorbance_{420nm}$ × min^{-1})/(OD_{280nm} × liter of culture). To test the β-gal-induction by the TAC analogs, the drugs were added directly to the cultures grown in Sauton's medium (OD_{600} = 0.6–1) and incubated with slow shaking for 96 h at 37°C. The β-gal activity was determined as described above.

Crystallization, Data Collection, and Refinement

The MAB_4384 crystals were grown in sitting drops in MR Crystallization Plates (Hampton Research) at 18°C by mixing 1.5 μl of protein solution concentrated to 4.7 mg/mL with 1.5 μl of reservoir solution made of 100 mM sodium cacodylate pH 6.5, 200 mM $MgCl_2$, 16% PEG 8000 and 5% DMSO. Crystals were briefly soaked in 100 mM Cacodylate buffer pH 6.5, 200 mM $MgCl_2$, 16% PEG 8000, 5% DMSO and 10% PEG 400 prior to being cryo-cooled in liquid nitrogen. The selenomethionine-substituted MAB_4384 crystals were obtained in sitting drops in 96-well SWISSCI MRC plates (Molecular Dimension) at 18°C by mixing 0.8 μl of protein solution concentrated to 2.5 mg/mL with 0.8 μl of reservoir solution consisting of 35% (v/v) 1,4 dioxane. Crystals were cryo-cooled without any additional cryo-protection. Data were processed with *XDS* and scaled and merged with *XSCALE* (Kabsch, 2010). Data collection statistics are presented in **Table 1**. The MAB_4384 structure was solved by the single wavelength anomalous dispersion method. *AutoSol* from the *Phenix* package was used to solve the structure (Adams et al., 2010). Twelve of the fourteen potential selenium sites in the asymmetric unit were found using a resolution cutoff of 3.4 Å for the search of the Se atoms. After density modification, a clear electron density map for the two TetR monomers allowed initial model building. The resulting partial model was used to perform molecular replacement with the 1.9 Å native dataset using *Phaser* (McCoy et al., 2007) from the *Phenix* package (Adams et al., 2010). *Coot* (Emsley et al., 2010) was used for manual rebuilding while structure refinement and validation were performed with

[1]http://meme-suite.org

TABLE 1 | Data collection and refinement statistics.

	MAB_4384 native	Selenium peak
Data collection statistics		
Beamline	ESRF-ID30B	ESRF-ID30B
Wavelength (Å)	0.979	0.979
Resolution range (Å)	36.5–1.9 (1.96–1.9)	47–2.3 (2.38–2.3)
Space group	P 1 21 1	P 1 21 1
Unit cell (Å,°)	40.8 100.8 56.0 90 105.8 90	41.4 99.3 55.7 90 106.9 90
Total reflections	73028 (7378)	126590 (12013)
Unique reflections	31705 (3193)	18983 (1849)
Multiplicity	2.3 (2.3)	6.7 (6.5)
Completeness (%)	92.1 (93.4)	98.6 (98.1)
Mean I/sigma (I)	11.09 (1.06)	11.66 (1.36)
Wilson B-factor (Å^2)	33.9	46.02
R-meas	0.06 (0.92)	0.13 (1.21)
CC1/2	0.99 (0.51)	0.97 (0.67)
CC*	1 (0.82)	0.99 (0.89)
Data refinement statistics		
Reflections used in refinement	31695 (3193)	
Reflections used for R-free	2000 (201)	
R-work	0.184 (0.312)	
R-free	0.213 (0.351)	
Number of non-H atoms	3460	
Macromolecules	3178	
Solvent	282	
Protein residues	402	
RMS bonds (Å)	0.002	
RMS angles (°)	0.45	
Ramachandran favored (%)	98.99	
Ramachandran allowed (%)	1.01	
Ramachandran outliers (%)	0.00	
Rotamer outliers (%)	0.95	
Average B-factor (Å^2)	43.6	
Macromolecules	43.2	
Solvent	47.6	
PDB accession number	5OVY	

The values in parenthesis are for the last resolution shell.

the *Phenix* package (Adams et al., 2010). The statistics for data collection and structure refinement are displayed in **Table 1**. Figures were prepared with PyMOL[2]. The atomic coordinates and the structure factors for the reported MAB_4384 crystal structure has been deposited at the Protein Data bank (accession number 5OVY).

Docking of TAC Analogs Into the Ligand Binding Site

Docking studies was performed with *PyRx* (Dallakyan and Olson, 2015) running *AutoDock Vina* (Trott and Olson, 2010). Search was done with grid dimensions of 39.45, 39.05, 29.25 Å and origin coordinates at $x = -17.8$, $y = 6.9$, $z = 0.63$. The search was performed on chain B of the crystal structure of MAB_4384 without any additional model modification.

[2]www.pymol.org

RESULTS

MAB_4384 Specifically Regulates Susceptibility to TAC Analogs in *M. abscessus*

We recently showed that mutations in the MAB_4384 regulator were associated with the transcriptional induction of the divergently oriented adjacent genes coding for an MmpS5/MmpL5 efflux pump and accounting for high resistance levels toward various TAC analogs (Halloum et al., 2017). To gain more insight into this drug resistance mechanism in *M. abscessus,* detailed genetic, functional and structural characterizations of the MAB_4384 regulator were undertaken. First, the expression profile of 19 *mmpL* genes was analyzed by qRT-PCR using the *M. abscessus* D15_S4 strain which possesses an early stop codon in *MAB_4384* resulting in high resistance levels to the TAC analogs D6, D15 and D17 (MIC > 200 μg/mL), presumably due to derepression of the MmpS5/MmpL5 efflux pump machinery (Halloum et al., 2017). The results clearly showed a pronounced increase in the expression level of *MAB_4382c* (*mmpL5*) mRNA in D15_S4 in comparison to the wild-type strain as reported previously, while no marked effect on the remaining *mmpL* genes was detected **(Figure 1A)**. The expression levels of *tgs1*, encoding the primary triacylglycerol synthase responsible for the accumulation of triglycerides in *M. abscessus* (Viljoen et al., 2016) was included as unrelated gene control. As expected, expression of *tgs1* stayed unchanged **(Figure 1A)**. To further confirm these results, the *MAB_4384* and *MAB_4382c* genes were inactivated by homologous recombination using the recently developed genetic tool dedicated to facilitate gene disruption in *M. abscessus* (Viljoen et al., 2018), as illustrated in Supplementary Figures S1A,B. The mutant strain, designated *MAB_4384*::pUX1, failed to show morphological changes (Supplementary Figure S1C) and grew similarly to its parental strain and the *MAB_4382c*::pUX1 mutant (Supplementary Figure S1D), suggesting that *MAB_4384* does not play a significant role under normal *in vitro* conditions. However, this mutant exhibited high resistance levels to D6, D15, and D17 (MIC > 200 μg/mL, corresponding to >8-, >32-, and >16-fold-increases in MIC levels, respectively) (**Table 2**) similarly to our previous results for D15_S4 (Halloum et al., 2017), thus validating the expected phenotype of the strain. Analysis of the transcriptional profile of all 19 *mmpL* genes in *MAB_4384*::pUX1 confirmed the results obtained in the D15_S4 strain **(Figure 1B)**. Interestingly, expression of *MAB_4384* itself was significantly induced in *MAB_4384*::pUX1, **(Figure 1C)**, albeit lower than the expression level of *mmpL5*, thus indicating that MAB_4384 is self-regulated.

Overall, these results suggest that MAB_4384 is a unique and highly specific regulator controlling expression of *mmpL5* in *M. abscessus*, which was strongly up-regulated in the absence of MAB_4384.

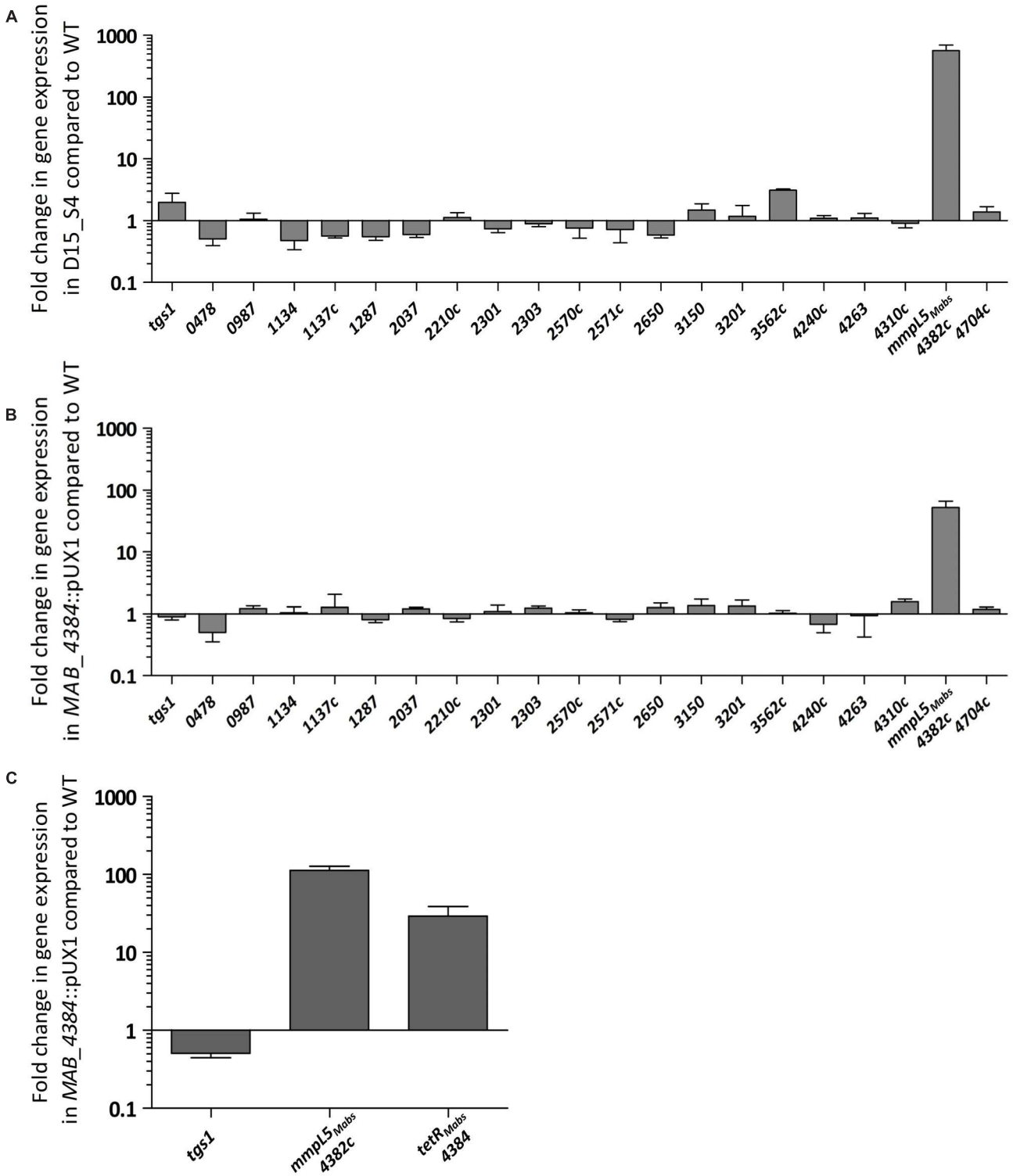

FIGURE 1 | MAB_4384 is a specific repressor of the *mmpS5/mmpL5* locus in *M. abscessus*. Transcriptional profile of 19 *mmpL* in *M. abscessus* expressed in fold induction relative to expression in the wild-type strain (CIP104536^T) in **(A)** the D15_S4 spontaneous mutant resistant to TAC analogs containing a stop codon in *MAB_4384* and in **(B)** *MAB_4384*::pUX1 in which *MAB_4384* has been disrupted by homologous recombination. *tgs1* was included as a non-relevant control gene. Error bars indicate standard deviation. **(C)** Expression of MAB_*4384* in *M. abscessus.* Fold induction levels of *MAB_4384* were calculated in *MAB_4384*::pUX1 relative to the parental strain. Error bars indicate standard deviation. Relative gene expression was calculated using the $\Delta\Delta$Ct method with correction for PCR efficiency. Data is representative of three independent experiments.

TABLE 2 | Drug susceptibility profile of *M. abscessus* S strains inactivated in either *MAB_4384* (*tetR* gene) or *MAB_4382c* (*mmpL5* gene).

	MIC (μg/mL)				
Strain	**D6**	**D15**	**D17**	**CFZ**	**BDQ**
CIP104536^T	25	6.2	12.5	1.6	0.05
MAB_4384::pUX1	>200	>200	>200	1.6	0.05
MAB_4382c::pUX1	12.5	6.2	6.2	1.6	0.05

The MIC (μg/mL) was determined in CaMH medium. Data are representative of three independent experiments. CFZ, clofazimine; BDQ, bedaquiline.

MAB_4384 Negatively Regulates Expression of *mmpS5/mmpL5*

The pMV261_$P_{S5/L5}$_*lacZ* plasmid was constructed, containing the β-galactosidase gene as a reporter in *M. abscessus* to further confirm the negative regulation of MAB_4384 on the target gene (*mmpS5/mmL5* locus) expression. To do this, the 208 bp intergenic region located between *MAB_4384* and *mmpS5/mmpL5* **(Figure 2A)**, designated $IR_{S5/L5}$, was cloned upstream of *lacZ*. pMV261_$P_{S5/L5}$_*lacZ* was subsequently introduced in parental smooth (S) and rough (R) variants of *M. abscessus* as well as in three different strains carrying single point mutations in MAB_4384 (M1A, F57L, and D14N), previously selected for their high resistance phenotype to TAC analogs (Halloum et al., 2017). In addition, pMV261_P_{hsp60}_*lacZ* allowing constitutive expression of *lacZ* under the control of the strong *hsp60* promoter was produced. As expected, pMV261_P_{hsp60}_*lacZ* led to high expression of *lacZ* in the wild-type strain and in the mutants compared to the promoter-less plasmid, as evidenced by the production of intense blue colonies and a strong β-Gal activity (**Figure 2B**). In contrast, whereas $IR_{S5/L5}$ resulted in very low expression of LacZ in the wild-type strains, characterized by a pale blue color on plates and low β-Gal activity in liquid-grown cultures, a pronounced *lacZ* induction was detected in all three mutant strains (**Figure 2B**). Strikingly, the *lacZ* expression levels in these strains was almost comparable to the one observed in the pMV261_P_{hsp60}_*lacZ*-containing strains.

Overall, these results indicate that expression of *lacZ* is strongly repressed in the presence of an intact MAB_4384 regulator and that under derepressed conditions, the promoter driving expression of *mmpS5/mmpL5* appears almost as strong as the *hsp60* promoter.

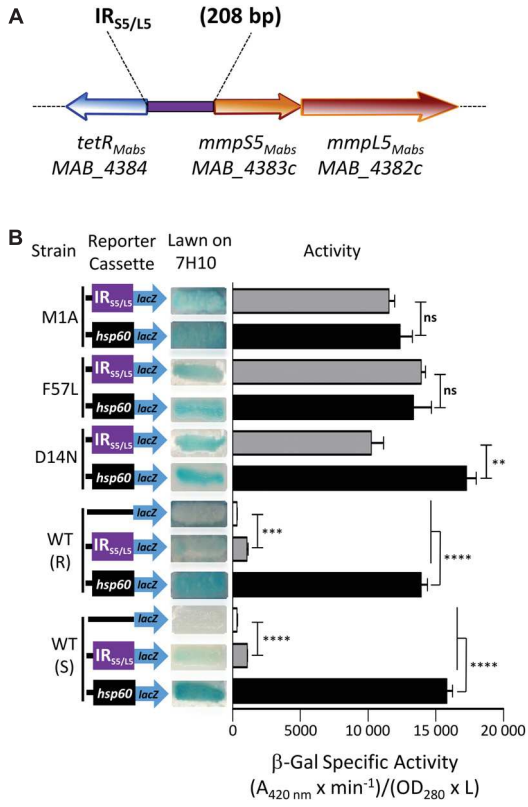

FIGURE 2 | Identification of a MAB_4384-dependent regulatory promoter region in *M. abscessus*. **(A)** Schematic representation of the genome organization of *MAB_4384* and the *mmpS5/mmpL5* gene cluster in *M. abscessus* with the purple rectangle indicating the $IR_{S5/L5}$ intergenic region cloned upstream of the *lacZ* reporter construct. **(B)** The effect of MAB_4384 on *mmpS5/mmpL5* expression was assayed by constructing a plasmid with the *lacZ* reporter under control of $IR_{S5/L5}$. A positive control plasmid consisting of the constitutive expression of *lacZ* under the control of the *hsp60* promoter and a negative control consisting of a promoter-less *lacZ* were also generated. All constructs were introduced into wild-type smooth (S) and rough (R) variants as well as into three different strains harboring single point mutations in MAB_4384 (M1A, D14N and F57L replacements). Exponentially growing *M. abscessus* cultures were streaked onto 7H10 plates containing 100 μg/mL kanamycin and 50 μg/mL X-gal. The plates were subsequently incubated for 3–4 days at 37°C and visualized for their appearance with respect to white-to-blue coloration. The β-galactosidase specific activity ($SA_{\beta-Gal}$) was quantified in liquid cultures using ONPG as a substrate. Results were obtained from three independent experiments and the error bars represent standard deviation. The capped lines indicate the groups compared. For statistical analysis, the Student's *t*-test was applied with ns, **, ***, **** indicating non-significant, $p < 0.01$, $p < 0.001$, and $p < 0.0001$, respectively.

MAB_4384 Binds to a Palindromic Sequence Within $IR_{S5/L5}$

Motif-based sequence analysis using MEME (Bailey et al., 2009) revealed the presence of a 27 bp segment within the divergently oriented $IR_{S5/L5}$ intergenic region and harboring a palindromic sequence **(Figure 3A)**. To test whether this motif represents a DNA binding site for MAB_4384, EMSA was first performed using increasing concentrations of purified MAB_4384 expressed in *E. coli* in the presence of a 45 bp fragment of $IR_{S5/L5}$ (Probe 1; **Figure 3B**) carrying extra nucleotides flanking the palindromic sequence. Under these conditions, a DNA–protein complex was seen **(Figure 3C)**. To confirm the specificity of the binding, a competition assay with increasing concentrations of the corresponding unlabeled probe (cold probe) was carried out, leading to a dose-dependent decrease of the DNA–protein complex **(Figure 3C)**. In addition, in the presence of an excess of a non-related labeled probe, the shift was maintained, thus indicating that a specific protein–DNA complex was seen only when MAB_4384 was incubated with DNA containing the specific inverted repeat sequence. To better define the

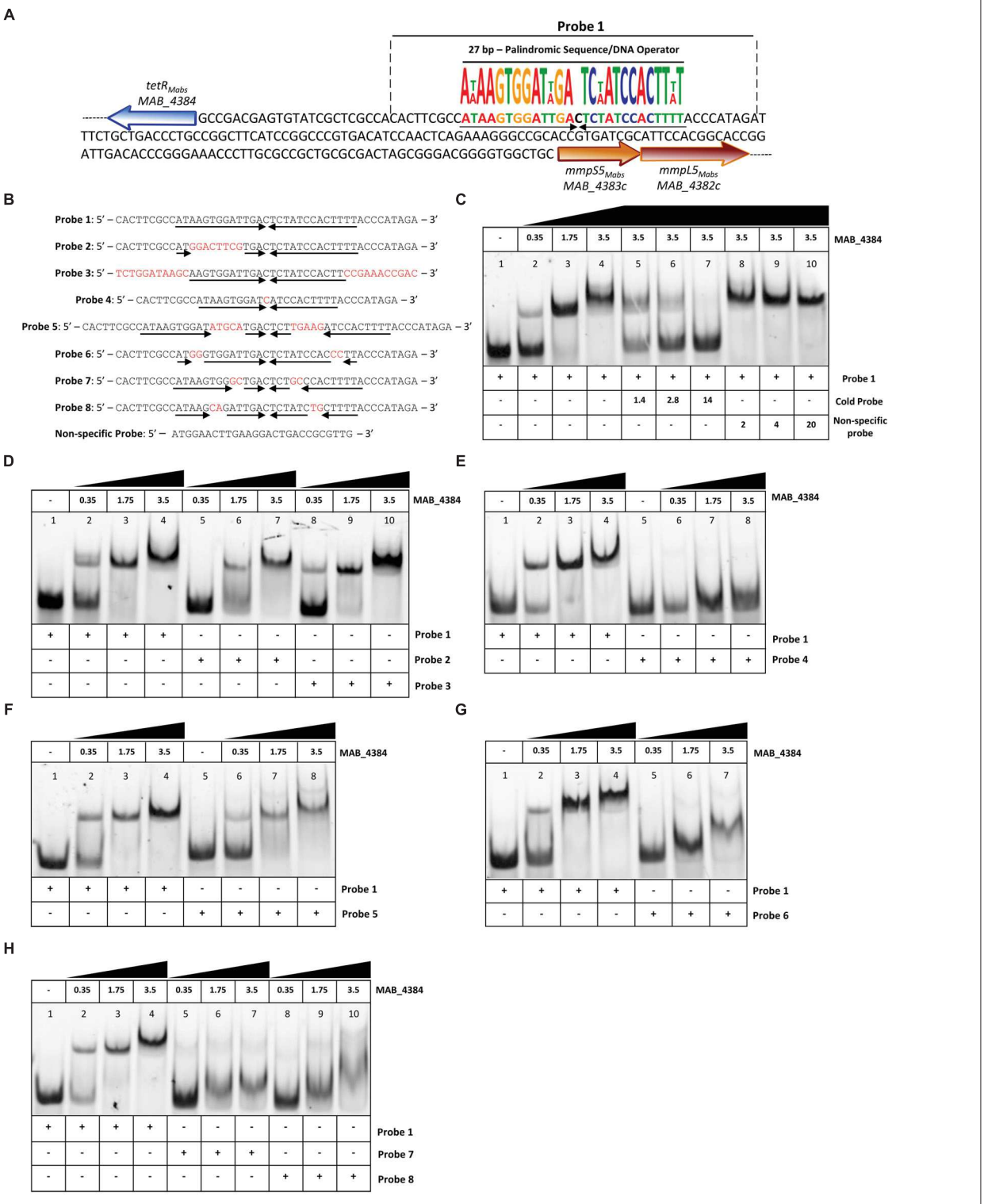

FIGURE 3 | Binding activity of MAB_4384 to a palindromic region within $IR_{S5/L5}$. **(A)** DNA sequence of $IR_{S5/L5}$ and representation of the operator composed of a 27 bp region containing two degenerated inverted sequences of 13 nucleotides each (black arrows) and separated by a one nucleotide spacer. The probe used to perform the EMSA is delimited by dotted lines (Probe 1). **(B)** DNA sequences of all the various 5′ fluorescein-labeled probes used in this study. **(C)** EMSA and competition assay using probe 1. Protein and DNA concentrations are expressed in μM. In competition assays, the concentration of Probe 1 was fixed at 280 nM. Gel shifts were revealed by fluorescence emission. **(D–H)** EMSA using Probes 2 to 8, each time compared to the shift profile obtained with Probe 1. Experiments were reproduced three times with similar results.

minimal motif and the importance of the nucleotides involved in recognition and binding of the protein, a large set of fluorescein-labeled probes differing in their size and/or sequence were next assayed **(Figure 3B).** In the presence of Probe 2, in which only the right inverted sequence was conserved, a delay in the DNA shift was observed (partial in the presence of 1.75 μM of protein as compared to the reaction in the presence of Probe 1). Shifts using Probe 3, where the extra nucleotides surrounding the palindromic sequence were changed randomly were comparable to those obtained with Probe 1 **(Figure 3D)**, indicating that the extra-palindromic sequence does not influence protein binding. With Probe 4, where the inverted repeats were shortened by six nucleotides, the formation of the DNA–protein complex was severely impeded even with the highest concentration of protein tested (3.5 μM) **(Figure 3E)**. Increasing the spacer between the two inverted repeats by 10 nucleotides (Probe 5) negatively impacted the shift **(Figure 3F)**. Substitutions of two nucleotides at the extremities in each repeat sequence (Probe 6) was accompanied by a pronounced shift alteration **(Figure 3G)** and similar results were obtained when di-nucleotide substitutions occurred at other positions within the conserved palindromic sequence (Probes 7 and 8) **(Figure 3H)**.

Overall, these results confirm that a strict preservation of this inverted sequence and space separating these two motifs are crucial for binding of MAB_4384 to its target.

Asp14 and Phe57 Are Critical for Optimal DNA-Binding Activity of MAB_4384

Multiple primary sequence alignments of the MAB_4384 N-terminus with other TetR regulators with known three-dimensional structures indicate that the N-terminus Asp14 residue is well conserved in several other Tet regulators **(Figure 4A)**. Similarly, Phe57 was also found to be part of a highly conserved stretch of amino acids in these proteins, although, in some instances, Phe was replaced by bulky/hydrophobic residues **(Figure 4A)**. The importance of the conservation of these two residues for the function of MAB_4384 and presumably also for that of the other TetR regulators, was next assessed by EMSA using the purified MAB_4384 mutated variants. As compared to the shift profile with wild-type MAB_4384, the production of the DNA–protein complex was severely impaired in the presence of either MAB_4384 (D14N) **(Figure 4C)** or MAB_4384 (F57L) **(Figure 4D)** and fully abrogated in the presence of the double mutant (D14N/F57L) **(Figure 4E)**.

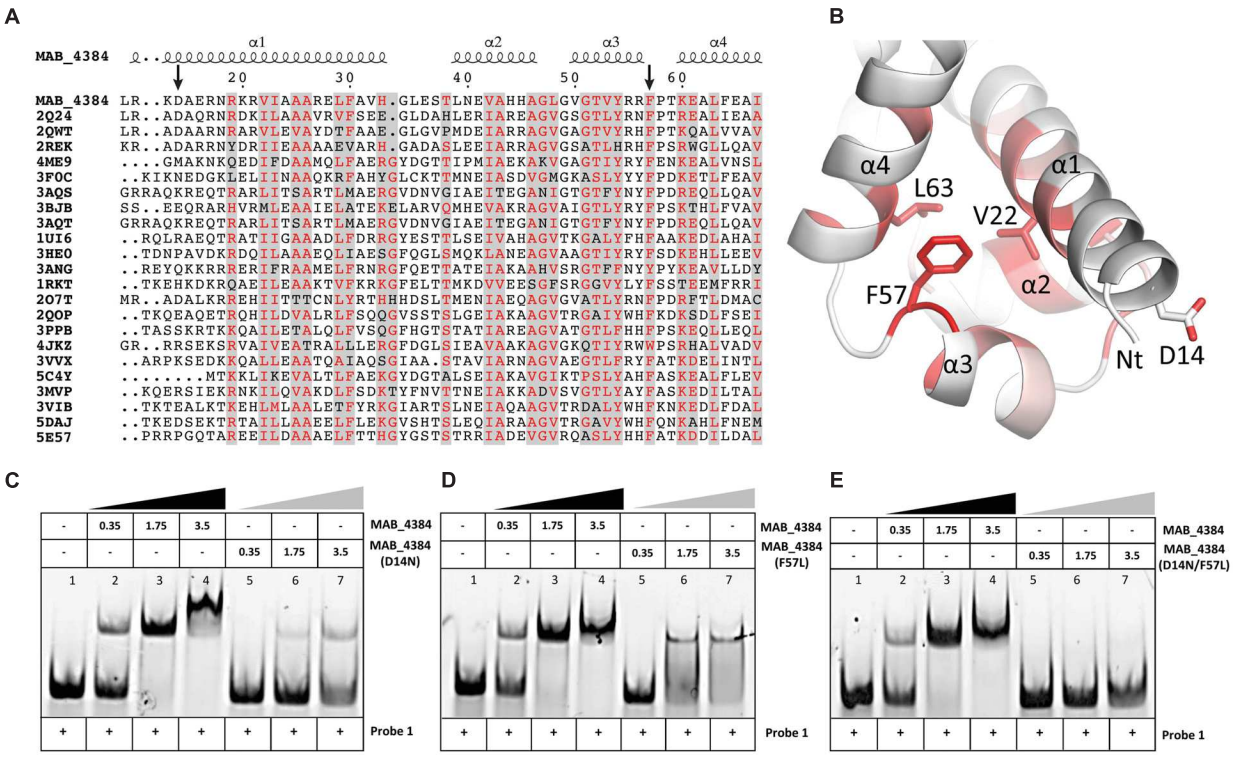

FIGURE 4 | D14N and F57L mutations abrogate binding of MAB_4384 to its palindromic DNA target. **(A)** Multiple primary sequence alignments of MAB_4384 N-terminus with other TetR family members whose crystal structures are known (PDB code indicated) from different microorganisms showing the conservation of the Asp14 and Phe57 residues (indicated with black arrows). **(B)** Mapping of the mutations on the crystal structure of MAB_4384, the degree of residue conservation (obtained from the sequence alignment in **A**) is represented by the coloration, from white (low conservation) to red (high conservation). **(A,B)** Were prepared using the ENDscript server (http://endscript.ibcp.fr/ESPript/ENDscript/). EMSA were performed using increasing concentrations (in μM) of the purified MAB_4384 (D14N) **(C)**, MAB_4384 (F57L) **(D)** or MAB_4384 (D14N/F57L) **(E)** in the presence of Probe 1. Wild-type MAB_4384 was included as a positive control in each assay. The concentration of Probe 1 was fixed at 280 nM. Gel shifts were revealed by fluorescence emission. Three independent experiments were performed with similar results.

Overall, these results support the importance of both residues in the DNA-binding capacity of MAB_4384 and the impaired ability of the mutants to bind to the operator is in agreement with the derepression of *lacZ* transcription in the *M. abscessus* strains carrying the D14N or F57L mutations **(Figure 2B)**.

Oligomeric States of MAB_4384 and MAB_4384:DNA in Solution

To further characterize the MAB_4384:DNA complex formation, we next assessed its stability in solution by SEC **(Figure 5)**. The oligomeric state of MAB_4384 in solution has an apparent 42.6 kDa molecular weight as compared to its 24.7 kDa theoretical molecular mass calculated from its primary sequence, thus highlighting the dimeric state of MAB_4384 in solution. MAB_4384 (dimer) was next incubated with the non-fluorescent DNA Probe 1 **(Figure 3A)** in a 1:1 molar ratio. A stable complex elution peak at 12.6 mL clearly shifted from the elution peak of MAB_4384 and DNA alone **(Figure 5)**, allowing deduction of the molecular mass of the protein:DNA complex at 102 kDa. As the DNA alone in solution appeared on SEC as a 24.5 kDa molecule, these results strongly suggest the existence of two MAB_4384 dimers bound to one DNA molecule as such a complex would possess a molecular mass of 109.7 kDa (2×42.6 kDa + 24.5 kDa). This 2-to-1 binding mode was further corroborated by the fact that an elution peak corresponding to free DNA can be seen at 14.4 mL when we mixed the MAB_4384 dimer and DNA in a 1:1 ratio. Moreover, increasing the molar ratio of the MAB_4384 dimer:DNA complex (2:1 and 3:1) did not yield larger protein:DNA complexes (data not shown), suggesting that, at a 1:1 molar ratio, the operator is already saturated by the protein. This observation is not unique as two TetR dimers have been shown to bind their DNA targets in other microorganisms, such as in *Staphylococcus aureus* (Grkovic et al., 2001) or in *Thermus thermophilus* (Agari et al., 2012).

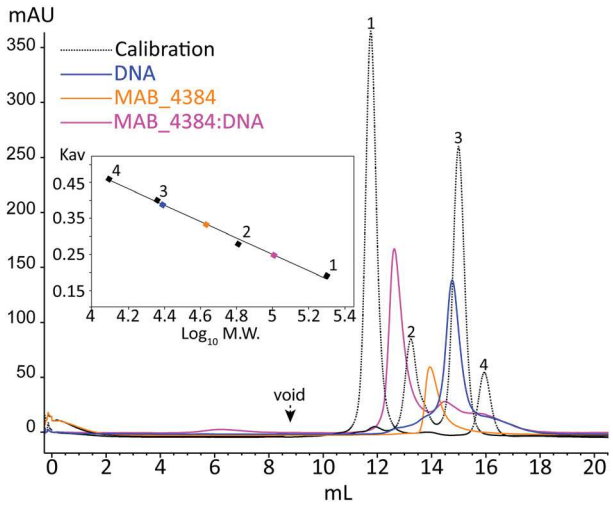

FIGURE 5 | Oligomerization of MAB_4384 and the MAB_4384:DNA complex in solution. The oligomeric states of MAB_4384 alone or complexed to its DNA target were determined by size exclusion chromatography. The elution profile of the proteins, used for the calibration is displayed as a dashed black line. Calibration was established using β-amylase (200 kDa) (1), bovine serum albumin (66 kDa) (2), carbonic anhydrase (29 kDa) (3), and cytochrome C (12.4 kDa) (4), eluting with estimated volumes of 11.7, 13.2, 14.9, 15.9 mL, respectively. The void volume was determined with the elution volume (8.8 mL) of dextran blue. MAB_4384 (dimer) was at a concentration of 3.9 mg/mL. The elution profiles of MAB_4384 dimer, DNA target and MAB_4384 bound to the DNA target are shown in orange, blue, and pink and their respective elution peaks were at 13.9, 14.7, and 12.6 mL. K_{av} indicates the partition coefficient.

Crystal Structure of MAB_4384

To understand, at a molecular basis, how the D14N or F57L mutations generate resistance to TAC analogs, we first crystallized and determined the X-ray structure of MAB_4384. Although the structure of the protein could not be solved by molecular replacement, the phase problem was overcome with the SAD method using crystals of selenomethionine-substituted MAB_4384 **(Table 1)**. The crystal structure of the native protein was subsequently solved with the partial model obtained from the SAD data and refined to a resolution of 1.9 Å. The asymmetric unit contains two subunits. Chain A was modeled from residues Asp14 to Thr213, indicating that the first thirteen residues, one residual Gly residue from the tag and the last eight residues in the C-terminus were not visible in the electron density. Chain B showed also disordered regions as the first ten residues, one Gly residue from the tag in N-terminus as well as the last nine residues in the C-terminus, could not be modeled. Analysis of the crystal packing using the *PISA* server (Krissinel and Henrick, 2007) predicted the existence of a stable homodimer formed within the crystal, consistent with other TetR regulators (Cuthbertson and Nodwell, 2013) and with the SEC profile of MAB_4384 in solution **(Figure 5)**.

The two subunits are very similar as their superposition leads to a root mean square deviation (r.m.s.d.) of 0.53 Å over 198 aligned residues. The N-terminus comprises the DNA binding domain (DBD), followed by the LBD. The DBD is composed of three α-helices α1: residues 12–33, α2: 39–46, and α3: 50–56, where helices 2 and 3 form a helix-turn-helix (HTH) motif. The LBD is made of seven α-helices, α4: 60–82, α5: 88–104, α6: 107–114, α7: 121–143, α8: 155–170, α9: 178–188, and α10: 205–211 **(Figure 6A)**. The surface of dimerization of about 1,700 $Å^2$ is mediated by 31 residues mainly from helices α8 and α9 of each subunit and involves numerous interactions notably five salt bridges, fourteen hydrogen bonds and van der Waals interactions.

Interestingly, we noticed the presence of extra electron density in the LBD of chain B in a rather hydrophobic pocket **(Figure 6B)**. Although we could not interpret this density, we hypothesize that it may correspond to a compound present in the crystallization solution, such as PEG. Search for structural homologs in the PDBeFold server indicated that the closest structure to MAB_4384 corresponds to the LfrR TetR transcriptional regulator from *Mycobacterium smegmatis* bound to proflavin (PDB id : 2V57) (Bellinzoni et al., 2009) with an r.m.s.d. of 2.6 Å and sharing 16% primary sequence identity with MAB_4384. However, only one subunit of each structure could

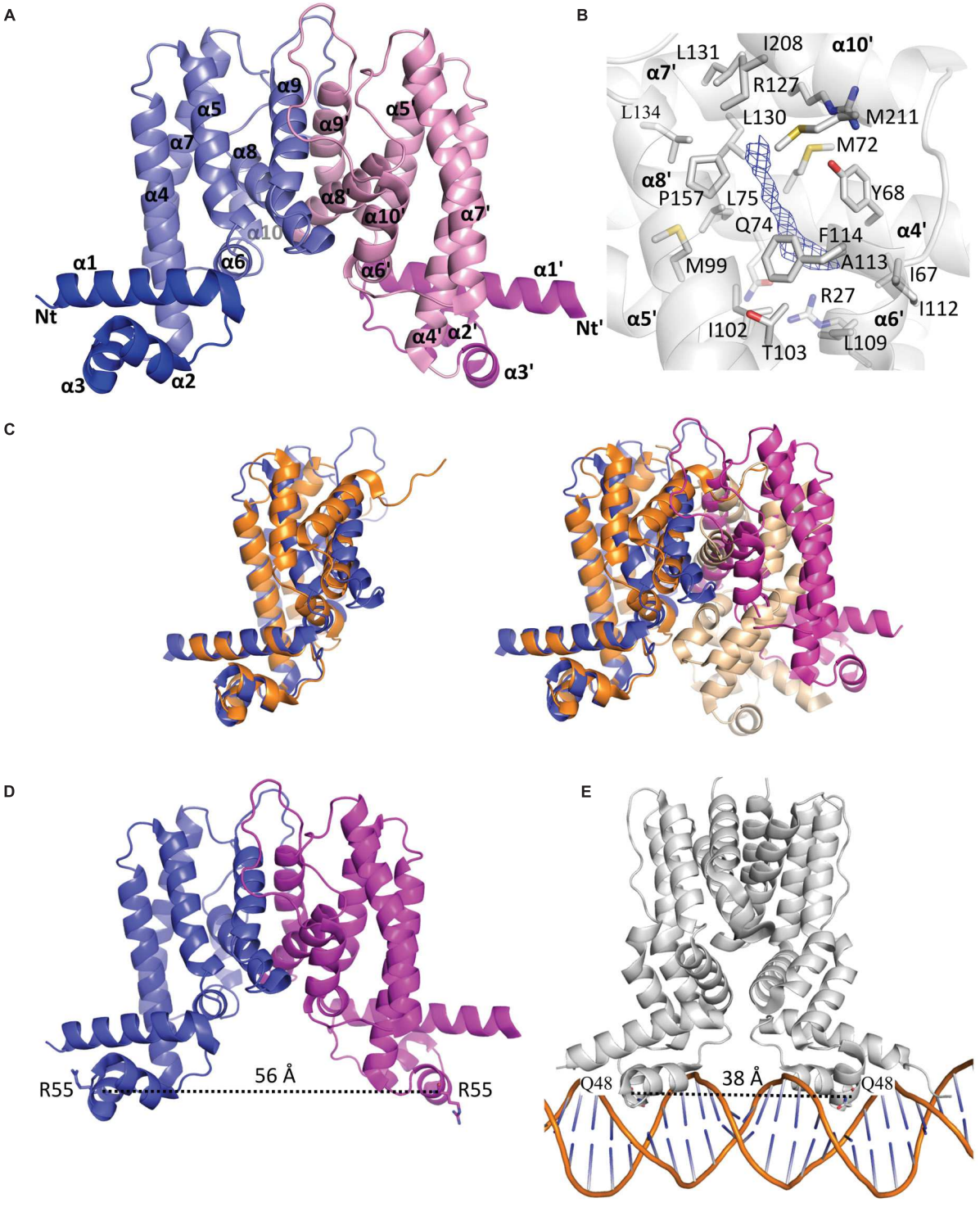

FIGURE 6 | The homodimeric crystal structure of MAB_4384. **(A)** Overall structure of the MAB_4384 dimer displayed as cartoon representation. The LBDs of each subunit are colored in slate and pink while the DNA binding domains are colored in blue and magenta. Helices are indicated by the α signs followed by numbers, Nt and Ct stands for N-terminus and C-terminus and ' is for chain B. **(B)** Putative ligand binding pocket in the LBD of MAB_4384. The Fo-Fc simulated annealed omit map contoured at 3 σ level is shown in blue. Residues that are 4 Å around the electron density blob and that are potential amino acids of the ligand binding site are shown as sticks. **(C)** Structural comparison of MAB_4384 with the crystal structure of the *M. smegmatis* LfrR repressor (PDB id: 2V57). The left panel represents the superposition of one monomer of MAB_4384 (in blue) on one monomer of LfrR (in orange). The superposition of the two homodimers is shown on the right panel, the two subunits of MAB_4384 are in blue and magenta and the two monomers of LfrR are in orange and wheat. **(D,E)** The figures compare the distance between the two DNA binding domains in MAB_4384 **(D)** and in the crystal structure of the *M. smegmatis* TetR Ms6564 protein bound to its DNA target (PDB id: 4JL3).

be superposed as the overall dimers differed largely **(Figure 6C)**. LrfR represses the expression of the LfrA efflux pump (Buroni et al., 2006) and mediates resistance to ethidium bromide, acriflavine, and fluoroquinolones (Takiff et al., 1996).

Due to the occurrence of an extra electron density within the LBD of MAB_4384 and that the closest structure of MAB_4384 is LfrR in its ligand bound form, it is very likely that MAB_4384 was crystallized in its open conformation, i.e., its derepressed form that is not able to interact with DNA. This was assessed by determining the distance between two residues from the DBD susceptible to interact with DNA. Residues Arg55 from chains A and B are about 56 Å apart **(Figure 6D)**. In comparison, the distances between the equivalent residues in various TetR:DNA complexes are largely reduced. In the TetR:DNA complex (PDB id: 4PXI) from *Streptomyces coelicolor* this distance is 45 Å (Bhukya et al., 2014), in the TetR:DNA complex from *M. smegmatis* (PDB id: 4JL3) (Yang et al., 2013) **(Figure 6E)**, *E. coli* (PDB id: 1QPI) (Orth et al., 2000), *Corynebacterium glutamicum* (PDB id: 2YVH) (Itou et al., 2010) or *Staphylococcus aureus* (PDB id: 1JT0) (Schumacher et al., 2002) the distances are 38 Å, 30 Å, 42 Å, and 37 Å, respectively. From these results it can be inferred that the DBDs of MAB_4384 are too far from each other to bind to the DNA groove. These observations combined with the presence of an unidentified ligand in the LBD strongly suggest that the MAB_4384 structure is in an open conformation.

Structural Basis of the Resistant Phenotype of the Mutants

To determine the impact of the mutations in the spontaneous resistant *M. abscessus* mutants, the D14N and F57L residues were mapped on the crystal structure of MAB_4384. Asp14 is located at the beginning of helix α1 and is conserved in several TetR protein members **(Figures 4A,B)**. Residues from helix α1 are often found in contact with DNA as seen in several TetR:DNA crystal structures. Nonetheless, due to the acidic nature of Asp, it is more likely that this residue repulses DNA. We, therefore, hypothesize that it may instead contribute to the correct positioning of other residues located in its close vicinity. Alternatively, repulsion may promote important interactions of DNA with other residues. Indeed, in other collected datasets at lower resolution (data not shown), Asp14 was found to establish a salt bridge interaction, thereby stabilizing the side chain of Arg17 that could interact with DNA. In the absence of a crystal structure of MAB_4384 bound to DNA it is, however, difficult to convincingly affirm the impact of the D14N substitution. However, neither the repulsion of DNA nor the establishment of a salt bridge would be possible if Asn is present instead of Asp, presumably explaining the loss of DNA binding activity of the TetR D14N mutant.

The role of Phe57 situated on helix α3 is more obvious as this position appears always occupied by bulky residues (Phe, Tyr, or Trp) in numerous TetR proteins **(Figure 4A)**. The side chain of Phe57 contacts the side chains of Val22 from helix α1 and Leu63 from helix α4 **(Figure 4B)**. Phe57 is very likely to perform an important structural role in stabilizing the DBD. Replacement with a less bulky side chain such as Leu would abolish these contacts with helices α1 and α4 residues, thus perturbing the overall structural fold of this domain and suppressing the DNA-binding capacity of MAB_4384.

Drug Recognition of MAB_4384 Induces Expression of MmpS5/MmpL5

TetR regulators can respond to small molecules and the best characterized member of this family of regulators is *E. coli* TetR itself. It confers resistance to tetracycline by regulating the expression of the tetracycline TetA efflux pump (Hillen and Berens, 1994). When tetracycline binds to TetR, the regulator loses affinity for the operators, conducting derepression of *tetA* and extrusion of tetracycline out of the bacteria (Lederer et al., 1995). To investigate whether TAC derivatives could bind to the LBD of MAB_4384, *in silico* docking was performed. Despite using a large grid box covering the entire LBD, all three compounds seem to be accommodated by the same binding pocket **(Figure 7A)**. Interestingly, this pocket positioned exactly where the extra electron density was seen in the LBD **(Figure 6B)**. All the compounds bind with similar energies in the aforementioned hydrophobic binding pocket. A slightly stronger interaction for the most hydrophobic derivative D17 was nonetheless observed. D17 and D6 that seem to bind stronger are more hydrophobic and in their best docking poses their thiosemicarbazide group is differently oriented as compared to D15.

Next, we determined whether expression of *mmpS5/mmpL5* can be conditionally induced by the substrates that are extruded by the efflux pump system. This was achieved by determining the effect of the D6, D15, and D17 analogs on LacZ production using the pMV261_$P_{S5/L5}$_*lacZ* reporter strain in *M. abscessus* incubated in Sauton's medium with various drug concentrations consisting of 1X, 2.5X, and 5X the MIC for D15 and of 0.5X, 1X, and 2.5X for D6 and D17. Kinetic studies indicated that optimal expression was obtained after 96 h of treatment (data not shown). The LacZ assay showed that transcription was induced by the TAC analogs in a dose-dependent manner whereas non-related drugs such as amikacin or the DMSO control had no effects **(Figure 7B)**. In comparison with the basal transcriptional level in Sauton's medium (no drug control), the addition of TAC derivatives in the cultures resulted in a reproducible 2.5- to 5-fold increase in the detection of β-Gal activity with D17 being the most potent inducer at 2.5X MIC. However, ethionamide, an antitubercular drug that, like the TAC and TAC analogs, requires to be activated by the EthA monooxygenase (Baulard et al., 2000; DeBarber et al., 2000; Dover et al., 2007; Halloum et al., 2017) failed to induce *lacZ* at 5X MIC (previously determined at 16 μg/ml). Induction of *lacZ* by D17 treatment was further confirmed at a transcriptional level from the pMV261_$P_{S5/L5}$_*lacZ* cultures treated with 2.5× MIC of D17 for 8 h **(Figure 7C**, left). This effect was specific to D17 as no gene induction was observed in the DMSO-treated cultures. Consistently, transcription profiling of *mmpS5* and *mmpL5* in the D17-exposed cultures clearly showed a marked induction level as compared to the DMSO-treated cultures and no effect on *tgs1* expression **(Figure 7C**, right).

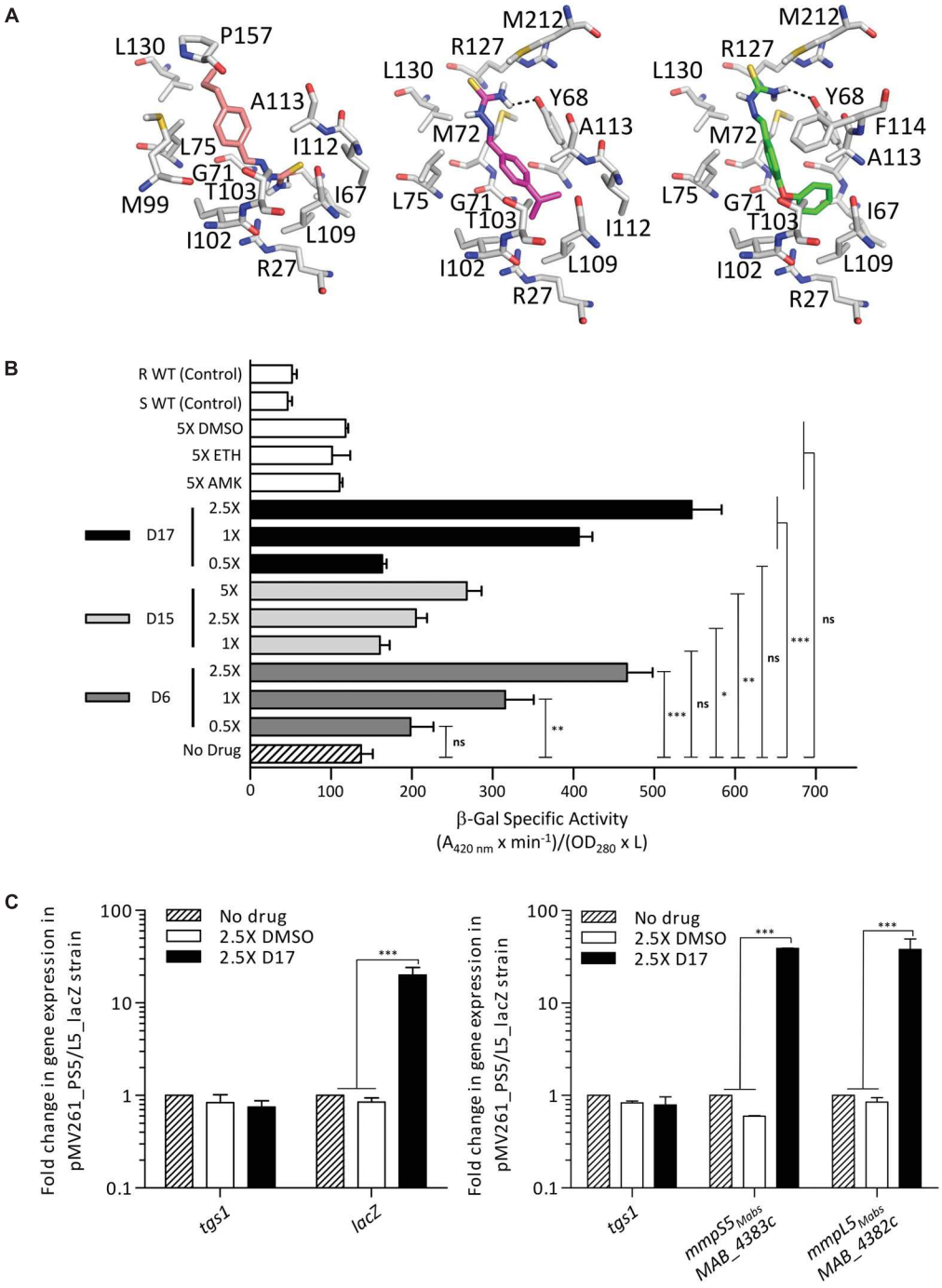

FIGURE 7 | $IR_{S5/L5}$ can be induced by structural analogs of thiacetazone. **(A)** Docking of TAC derivatives in the ligand binding site of MAB_4384. All the residues involved in van der Waals, hydrophobic bonds or hydrogen bonds (in black dashes) are displayed as sticks. D15 in salmon has a binding energy of $\Delta G = -6.6$ kcal/mol, D6 in magenta has a $\Delta G = -7.3$ kcal/mol, and D17 seems to bind slightly stronger with a $\Delta G = -8.3$kcal/mol. **(B)** Conditional induction of *lacZ* by structural analogs of TAC in *M. abscessus*. Induction of β-Gal activity in wild-type *M. abscessus* S carrying pMV261_$P_{S5/L5}$_*lacZ* was assayed using mid-log phase cultures incubated with increasing drug concentrations varying from 1X to 5X the MIC for D15 and varying from 0.5X to 2.5X the MIC for D6 and D17. Inductions were performed for 96 h at 37°C. The β-galactosidase specific activity ($SA_{\beta-Gal}$) was quantified in liquid cultures using ONPG as a substrate. Amikacin (AMK) and ethionamide (ETH) were included as unrelated drug controls. **(C)** Transcriptional profile of *lacZ* in the *M. abscessus* pMV261_$P_{S5/L5}$_*lacZ* reporter strain exposed to 2.5X the MIC of D17 for 8 h (left). *tgs1* was included as a non-relevant control. Replacing D17 by an equal volume of DMSO had no effect on *lacZ* transcription. Transcriptional induction of $mmpS5_{Mabs}$ and $mmpL5_{Mabs}$ following exposure to 2.5X the MIC of D17 for 8 h (right). Results were obtained from three independent experiments and the error bars represent standard deviation. For statistical analysis the Student's *t*-test was applied with ns, *, **, ***, **** indicating non-significant, $p < 0.05$, $p < 0.01$, $p < 0.001$, and $p < 0.0001$, respectively.

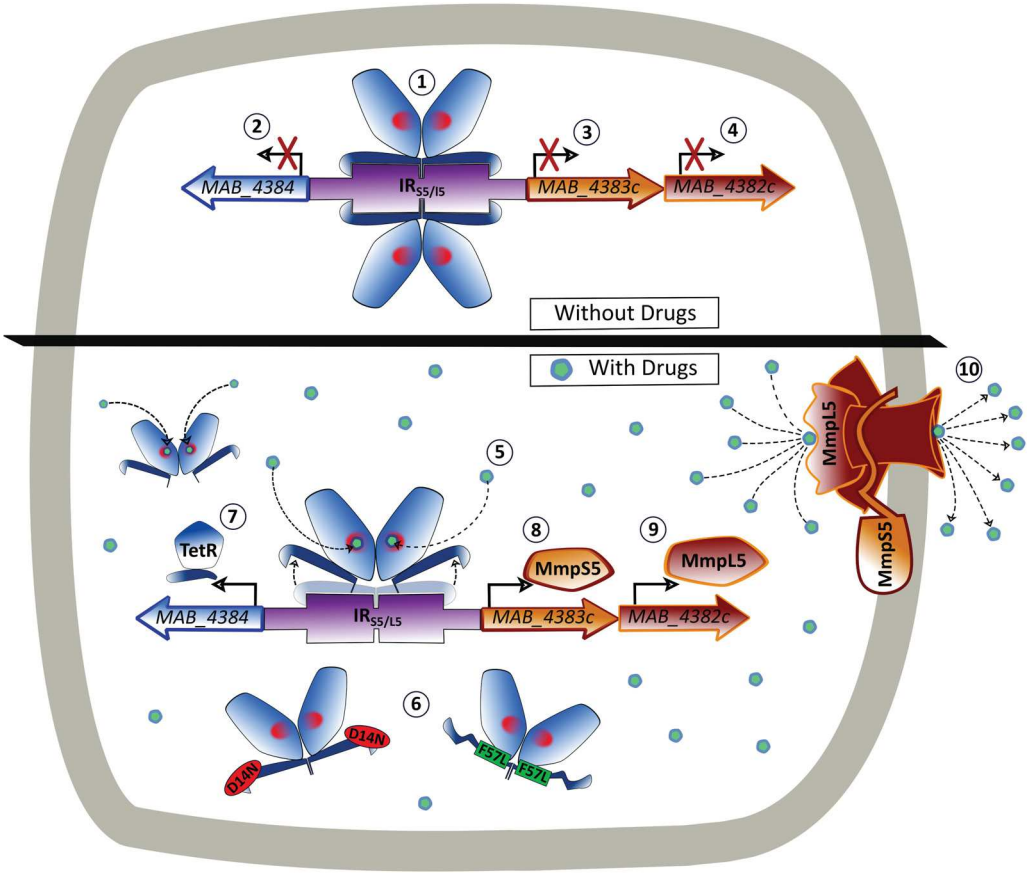

FIGURE 8 | Model of the binding of MAB_4384 to its operator and regulation of the MmpS5/MmpL5 efflux pump machinery. In the absence of drug, two MAB_4384 dimers bind to their DNA operator located in the intergenic region ($IR_{S5/L5}$) between the divergently transcribed *MAB_4384* (encoding the TetR regulator) and *MAB_4383c/MAB_4382c* (encoding the MmpS5/MmpL5 efflux pump) (1). This action represses the transcription of *MAB_4384* (2), *MAB_4383c* (3) and *MAB_4382c* (4), predisposing the bacteria to drug susceptibility. When the TAC derivatives bind to MAB_4384 (5) or if MAB_4384 harbors the D14N or F57L mutations (6), the regulator loses affinity for the operator, leading to derepression of *MAB_4384* itself (7), *MAB_4383c* (8) and *MAB_4382c* (9). This triggers high levels of expression of the MmpS5/MmpL5 complex in the plasma membrane and the subsequent export of the TAC analogs outside the bacteria (10), reducing susceptibility to the compounds.

Together, these results support the view that TAC analogs, which are substrates of MmpS5/mmpL5, are also effectors of MAB_4384-induced transcription of *mmpS5/mmpL5*.

DISCUSSION

Herein, a combination of genetic, biochemical and structural studies was used to demonstrate that MAB_4384 is part of the TetR family of regulators, which represses the transcriptional expression of the MmpS5/MmpL5 efflux pump. MAB_4384 belongs to the type I class TetR family of regulators, characterized by a divergent orientation to one of the adjacent target genes (Cuthbertson and Nodwell, 2013). In *M. tuberculosis,* MmpS5/MmpL5 is under the control of the MarR repressor Rv0678 (Radhakrishnan et al., 2014) and mutations in this regulator leads to drug resistance (Andries et al., 2014; Hartkoorn et al., 2014; Zhang et al., 2015). EMSA indicated a direct binding of Rv0678 to the intergenic region located between *mmpS5* and *Rv0678*. However, shifts were also found using the promoter regions of *mmpS2-mmpL2*, *mmpS4-mmpL4,* and *Rv0991-Rv0992* (Radhakrishnan et al., 2014), suggesting that a single regulator can control expression of several *mmpS/mmpL* loci. Our analysis indicates that, despite the fact that *M. abscessus* possesses the highest number of *mmpL* genes among all mycobacterial species studied (Viljoen et al., 2017), the MAB_4384 regulator is highly specific to the *mmpS5/mmpL5* pair as demonstrated by the lack of transcriptional regulation of a large set of *mmpL* genes and the presence of a unique inverted DNA sequence target that was not found elsewhere in the chromosome. This unique trait might also be reflected by the modest structural homology of MAB_4384 with other TetR crystal structures. The tight regulation and the high specificity of interaction with its target DNA, however, cannot be solely explained on the basis of the MAB_4384 crystal structure and the structure of the MAB_4384:DNA complex is, therefore, greatly warranted to dissect these underlying mechanisms. Nevertheless, our structural analysis underscores the strategy employed by *M. abscessus* to acquire mutations

impacting the DNA-binding capacity or the folding/stability of the DBD of MAB_4384 to become resistant.

EMSA and *lacZ* reporter fusions confirmed that D14N and F57L mutations, alleviating the DNA-binding activity of MAB_4384, cause a strong up-regulation of *mmpS5/mmpL5* gene expression, in agreement with our previous qRT-PCR analyses (Halloum et al., 2017). This leads to extrusion of the TAC derivatives out of the cells, contributing to the high MIC values for TAC derivatives against these mutants, as illustrated in **Figure 8**. Expression of multi-drug resistant efflux pumps can also be conditionally induced using structurally diverse substrates (Kaatz and Seo, 1995; Rosenberg et al., 2003; Buroni et al., 2006). This induction is caused by the direct interaction of these substrates with the repressors, interfering with binding of the repressors to their target operators and resulting in increased expression of the pumps. Here, we show inducible β-galactosidase activity following treatment with D6, D15, or D17, a mechanism that is very likely to be meditated by MAB_4384. This view is reinforced by the fact that docking studies highlighted the possibility that all three analogs could be accommodated in the LBD of the protein, which perfectly coincided with the extra electron density observed. Since, the LBD are remote from the DBD, the derepression of TetR family regulators involves allosteric mechanisms that include conformational changes transmitted largely within the same subunit (Ramos et al., 2005). The interaction of ligands with the LBD captures a conformational state where the DBD is repositioned relative to the LBD in a way that the dimer is prevented from binding to its target DNA. However, definitive proof of this mechanism awaits the elucidation of the crystal structure of the D17-bound form of MAB_4384, as reported for instance with the hexadecyl octanoate-bound EthR repressor (Frénois et al., 2004) or the LfrR regulator complexed with proflavine (Bellinzoni et al., 2009). Lack of inducible *lacZ* expression in *M. abscessus* cultures exposed to amikacin, for which mutations in 16S rRNA represent a major mechanism of resistance (Prammananan et al., 1998), indicates that MmpL5-mediated efflux cannot mediate resistance toward this antibiotic in line with the lack of cross-resistance toward amikacin observed for TAC derivative-spontaneous resistant mutants (Halloum et al., 2017). The specificity of the MAB_4384-driven resistance mechanism described herein is further supported by the lack of *lacZ* induction during exposure to ETH, that similarly to TAC and TAC analogs, requires bio-transformation by EthA, whose expression is also dependent on the EthR regulator belonging to the TetR family (Baulard et al., 2000; Engohang-Ndong et al., 2004; Halloum et al., 2017). Together, these findings strongly suggest that when TAC analogs bind to MAB_4384, the regulator loses affinity for its DNA target, resulting in up-regulation of *mmpS5/mmpL5* and export of the drugs from the cells **(Figure 8)**. These results also point out the selectivity of this efflux-based mechanism. Indeed, no change in the MIC of clofazimine or bedaquiline were noticed in a *MAB_4384*-disrupted strain, which appears intriguing as MmpL5 has been reported as a multi-substrate efflux pump responsible for low-level resistance to both of these drugs in *M. tuberculosis* (Hartkoorn et al., 2014). The LBD of MAB_4384 potentially can accommodate bulky molecules and might thus indicate that MAB_4384 is involved in efflux of other types of compounds in addition to TAC analogs. However, we could neither dock clofazimine nor bedaquiline in the LBD of MAB_4384 (not shown). Several reasons can be put forth to explain these species-specific variations. In *M. tuberculosis*, expression of MmpL5 is under the control of a MarR regulator rather than a TetR regulator. Alternatively, we have previously reported the occurrence in *M. abscessus* of three *mmpS5/mmpL5* paralogs (Halloum et al., 2017), thus, it remains possible that either of the two remaining genes may participate in co-resistance to these drugs in *M. abscessus*.

The highly pronounced expression of *lacZ* under derepressed conditions found in the M1A, F57L, or D14N mutant strains, almost at levels similar to those driven by the strong and constitutive *hsp60* promoter, confirmed the very high expression levels of *mmpS5* and *mmpL5* detected by qRT-PCR and probably explains the very high level of resistance of the mutants (MIC $>$ 200 μg/mL). This contrasts also with findings where MmpL5 mediates only low-levels of resistance in *M. tuberculosis* (Andries et al., 2014; Hartkoorn et al., 2014), presumably because expression of *mmpL5* is driven by a weaker promoter than in *M. abscessus*. That *mmpS5/mmpL5* expression is tightly controlled suggests that the MmpS5/MmpL5 machinery may exert an important function in the assembly and/or maintenance of the cell wall by exporting a yet unidentified lipid, as already reported for several MmpL transporters in *M. tuberculosis* (Chalut, 2016; Viljoen et al., 2017). Alternatively, they may participate in adaptation during the infection process. However, the growth curves of the wild-type or the strain constitutively expressing high levels of MmpL5 (due to the M1A mutation in MAB_4384) were comparable *in vitro*. In addition, microinjections of the different strains were done in the zebrafish embryo, an animal model previously developed to study the early events of the *M. abscessus* infection (Bernut et al., 2014, 2015). No differences in virulence were noticed between the wild-type and MAB_4384 (M1A) strains (Supplementary Figure S2). Interestingly, the *mmpS5/mmpL5* locus was found to be induced when *M. abscessus* was exposed to a defined, synthetic medium that mimics the composition of CF sputum (Miranda-CasoLuengo et al., 2016). This may be part of a complex adaptive transcriptional response to the mucus layer of the CF airways that leads to the chronic infections of *M. abscessus*.

In summary, this study provides new functional and structural insights into TetR-dependent regulation of MmpL efflux pumps in mycobacteria. Considering the exceptionally high abundance of TetR transcriptional regulators (more than 130) as well as the important MmpL repertoire (around 30) in *M. abscessus*, one can anticipate that mechanisms similar to the one described here are exploited by this pathogen to express its intrinsic resistance level to other antibiotics.

ETHICS STATEMENT

Zebrafish experiments were done at IRIM, according to European Union guidelines for handling of laboratory animals

(http://ec.europa.eu/environment/chemicals/lab_animals/home_en.htm) and approved by the Direction Sanitaire et Vétérinaire de l'Hérault and Comité d'Ethique pour l'Expérimentation Animale de la Région Languedoc Roussillon (CEEA-LR) under the reference CEEA-LR-1145.

AUTHOR CONTRIBUTIONS

MR, AVG, AV, MB, and LK acquired and analyzed the data. EG, MB, and LK wrote the manuscript. LK conceived and designed the study.

FUNDING

This work was supported by the Fondation pour la Recherche Médicale (FRM) (grant number DEQ20150331719 to LK; grant number ECO20160736031 to MR) and by the InfectioPôle Sud for funding the Ph.D. Fellowship of AVG.

ACKNOWLEDGMENTS

The authors wish to thank G. S. Coxon for the generous gift of the TAC analogs. The crystallographic data were collected on beamline ID30B at the European Synchrotron Radiation Facility (ESRF), Grenoble, France. The authors are grateful to Local Contact at the ESRF for providing assistance in using beamline ID30B.

SUPPLEMENTARY MATERIAL

The Supplementary Material for this article can be found online at: https://www.frontiersin.org/articles/10.3389/fmicb.2018.00649/full#supplementary-material

REFERENCES

Adams, P. D., Afonine, P. V., Bunkóczi, G., Chen, V. B., Davis, I. W., Echols, N., et al. (2010). *PHENIX*: a comprehensive Python-based system for macromolecular structure solution. *Acta Crystallogr. D Biol. Crystallogr.* 66, 213–221. doi: 10.1107/S0907444909052925

Agari, Y., Sakamoto, K., Kuramitsu, S., and Shinkai, A. (2012). Transcriptional repression mediated by a TetR family protein, PfmR, from *Thermus thermophilus* HB8. *J. Bacteriol.* 194, 4630–4641. doi: 10.1128/JB.00668-12.

Aiyar, A., Xiang, Y., and Leis, J. (1996). Site-directed mutagenesis using overlap extension PCR. *Methods Mol. Biol.* 57, 177–191. doi: 10.1385/0-89603-332-5:177

Andries, K., Villellas, C., Coeck, N., Thys, K., Gevers, T., Vranckx, L., et al. (2014). Acquired resistance of *Mycobacterium tuberculosis* to bedaquiline. *PLoS One* 9:e102135. doi: 10.1371/journal.pone.0102135

Bailey, T. L., Boden, M., Buske, F. A., Frith, M., Grant, C. E., Clementi, L., et al. (2009). MEME SUITE: tools for motif discovery and searching. *Nucleic Acids Res.* 37, W202–W208. doi: 10.1093/nar/gkp335

Balhana, R. J. C., Singla, A., Sikder, M. H., Withers, M., and Kendall, S. L. (2015). Global analyses of TetR family transcriptional regulators in mycobacteria indicates conservation across species and diversity in regulated functions. *BMC Genomics* 16:479. doi: 10.1186/s12864-015-1696-9

Baulard, A. R., Betts, J. C., Engohang-Ndong, J., Quan, S., McAdam, R. A., Brennan, P. J., et al. (2000). Activation of the pro-drug ethionamide is regulated in mycobacteria. *J. Biol. Chem.* 275, 28326–28331. doi: 10.1074/jbc.M003744200

Bellinzoni, M., Buroni, S., Schaeffer, F., Riccardi, G., De Rossi, E., and Alzari, P. M. (2009). Structural plasticity and distinct drug-binding modes of LfrR, a mycobacterial efflux pump regulator. *J. Bacteriol.* 191, 7531–7537. doi: 10.1128/JB.00631-09

Bernut, A., Dupont, C., Sahuquet, A., Herrmann, J.-L., Lutfalla, G., and Kremer, L. (2015). Deciphering and imaging pathogenesis and cording of *Mycobacterium abscessus* in zebrafish embryos. *J. Vis. Exp.* 103:53130. doi: 10.3791/53130

Bernut, A., Herrmann, J.-L., Kissa, K., Dubremetz, J.-F., Gaillard, J.-L., Lutfalla, G., et al. (2014). *Mycobacterium abscessus* cording prevents phagocytosis and promotes abscess formation. *Proc. Natl. Acad. Sci. U.S.A.* 111, E943–E952. doi: 10.1073/pnas.1321390111

Bhukya, H., Bhujbalrao, R., Bitra, A., and Anand, R. (2014). Structural and functional basis of transcriptional regulation by TetR family protein CprB from *S. coelicolor* A3(2). *Nucleic Acids Res.* 42, 10122–10133. doi: 10.1093/nar/gku587

Bryant, J. M., Grogono, D. M., Rodriguez-Rincon, D., Everall, I., Brown, K. P., Moreno, P., et al. (2016). Emergence and spread of a human-transmissible multidrug-resistant nontuberculous mycobacterium. *Science* 354, 751–757. doi: 10.1126/science.aaf8156

Buroni, S., Manina, G., Guglierame, P., Pasca, M. R., Riccardi, G., and De Rossi, E. (2006). LfrR is a repressor that regulates expression of the efflux pump LfrA in *Mycobacterium smegmatis*. *Antimicrob. Agents Chemother.* 50, 4044–4052. doi: 10.1128/AAC.00656-06

Chalut, C. (2016). MmpL transporter-mediated export of cell-wall associated lipids and siderophores in mycobacteria. *Tuberclosis* 100, 32–45. doi: 10.1016/j.tube.2016.06.004

Coxon, G. D., Craig, D., Corrales, R. M., Vialla, E., Gannoun-Zaki, L., and Kremer, L. (2013). Synthesis, antitubercular activity and mechanism of resistance of highly effective thiacetazone analogues. *PLoS One* 8:e53162. doi: 10.1371/journal.pone.0053162

Cuthbertson, L., and Nodwell, J. R. (2013). The TetR family of regulators. *Microbiol. Mol. Biol. Rev.* 77, 440–475. doi: 10.1128/MMBR.00018-13

Dal Molin, M., Gut, M., Rominski, A., Haldimann, K., Becker, K., and Sander, P. (2018). Molecular mechanisms of intrinsic streptomycin resistance in *Mycobacterium abscessus*. *Antimicrob. Agents Chemother.* 62:e01427-17. doi: 10.1128/AAC.01427-17

Dallakyan, S., and Olson, A. J. (2015). Small-molecule library screening by docking with PyRx. *Methods Mol. Biol.* 1263, 243–250. doi: 10.1007/978-1-4939-2269-7_19

DeBarber, A. E., Mdluli, K., Bosman, M., Bekker, L. G., and Barry, C. E. (2000). Ethionamide activation and sensitivity in multidrug-resistant *Mycobacterium tuberculosis*. *Proc. Natl. Acad. Sci. U.S.A.* 97, 9677–9682. doi: 10.1073/pnas.97.17.9677

Dover, L. G., Alahari, A., Gratraud, P., Gomes, J. M., Bhowruth, V., Reynolds, R. C., et al. (2007). EthA, a common activator of thiocarbamide-containing drugs acting on different mycobacterial targets. *Antimicrob. Agents Chemother.* 51, 1055–1063. doi: 10.1128/AAC.01063-06

Dubée, V., Bernut, A., Cortes, M., Lesne, T., Dorchene, D., Lefebvre, A.-L., et al. (2015). β-Lactamase inhibition by avibactam in *Mycobacterium abscessus*. *J. Antimicrob. Chemother.* 70, 1051–1058. doi: 10.1093/jac/dku510

Emsley, P., Lohkamp, B., Scott, W. G., and Cowtan, K. (2010). Features and development of coot. *Acta Crystallogr. D Biol. Crystallogr.* 66, 486–501. doi: 10.1107/S0907444910007493

Engohang-Ndong, J., Baillat, D., Aumercier, M., Bellefontaine, F., Besra, G. S., Locht, C., et al. (2004). EthR, a repressor of the TetR/CamR family implicated in ethionamide resistance in mycobacteria, octamerizes cooperatively on its operator. *Mol. Microbiol.* 51, 175–188. doi: 10.1046/j.1365-2958.2003.03809.x

Esther, C. R., Esserman, D. A., Gilligan, P., Kerr, A., and Noone, P. G. (2010). Chronic *Mycobacterium abscessus* infection and lung function decline

in cystic fibrosis. *J. Cyst. Fibros.* 9, 117–123. doi: 10.1016/j.jcf.2009.12.0001

Frénois, F., Engohang-Ndong, J., Locht, C., Baulard, A. R., and Villeret, V. (2004). Structure of EthR in a ligand bound conformation reveals therapeutic perspectives against tuberculosis. *Mol. Cell* 16, 301–307. doi: 10.1016/j.molcel.2004.09.020

Grkovic, S., Brown, M. H., Schumacher, M. A., Brennan, R. G., and Skurray, R. A. (2001). The staphylococcal QacR multidrug regulator binds a correctly spaced operator as a pair of dimers. *J. Bacteriol.* 183, 7102–7109. doi: 10.1128/JB.183.24.7102-7109.2001

Halloum, I., Viljoen, A., Khanna, V., Craig, D., Bouchier, C., Brosch, R., et al. (2017). Resistance to thiacetazone derivatives active against *Mycobacterium abscessus* involves mutations in the MmpL5 transcriptional repressor MAB_4384. *Antimicrob. Agents Chemother.* 61:11e01225-17. doi: 10.1128/AAC.02509-16

Hartkoorn, R. C., Uplekar, S., and Cole, S. T. (2014). Cross-resistance between clofazimine and bedaquiline through upregulation of MmpL5 in *Mycobacterium tuberculosis*. *Antimicrob. Agents Chemother.* 58, 2979–2981. doi: 10.1128/AAC.00037-14

Hillen, W., and Berens, C. (1994). Mechanisms underlying expression of Tn10 encoded tetracycline resistance. *Annu. Rev. Microbiol.* 48, 345–369. doi: 10.1146/annurev.mi.48.100194.002021

Hurst-Hess, K., Rudra, P., and Ghosh, P. (2017). *Mycobacterium abscessus* WhiB7 regulates a species-specific repertoire of genes to confer extreme antibiotic resistance. *Antimicrob. Agents Chemother.* 61:e01347-17. doi: 10.1128/AAC.01347-17

Itou, H., Watanabe, N., Yao, M., Shirakihara, Y., and Tanaka, I. (2010). Crystal structures of the multidrug binding repressor *Corynebacterium glutamicum* CgmR in complex with inducers and with an operator. *J. Mol. Biol.* 403, 174–184. doi: 10.1016/j.jmb.2010.07.042

Kaatz, G. W., and Seo, S. M. (1995). Inducible NorA-mediated multidrug resistance in *Staphylococcus aureus*. *Antimicrob. Agents Chemother.* 39, 2650–2655. doi: 10.1128/AAC.39.12.2650

Kabsch, W. (2010). Integration, scaling, space-group assignment and post-refinement. *Acta Crystallogr. D Biol. Crystallogr.* 66, 133–144. doi: 10.1107/S0907444909047374

Krissinel, E., and Henrick, K. (2007). Inference of macromolecular assemblies from crystalline state. *J. Mol. Biol.* 372, 774–797. doi: 10.1016/j.jmb.2007.05.022

Lederer, T., Takahashi, M., and Hillen, W. (1995). Thermodynamic analysis of tetracycline-mediated induction of Tet repressor by a quantitative methylation protection assay. *Anal. Biochem.* 232, 190–196. doi: 10.1006/abio.1995.0006

Lefebvre, A.-L., Dubée, V., Cortes, M., Dorchêne, D., Arthur, M., and Mainardi, J.-L. (2016). Bactericidal and intracellular activity of β-lactams against *Mycobacterium abscessus*. *J. Antimicrob. Chemother.* 71, 1556–1563. doi: 10.1093/jac/dkw022

Lefebvre, A.-L., Le Moigne, V., Bernut, A., Veckerlé, C., Compain, F., Herrmann, J.-L., et al. (2017). Inhibition of the β-lactamase BlaMab by avibactam improves the *in vitro* and *in vivo* efficacy of imipenem against *Mycobacterium abscessus*. *Antimicrob. Agents Chemother.* 61:e02440-16. doi: 10.1128/AAC.02440-16

McCoy, A. J., Grosse-Kunstleve, R. W., Adams, P. D., Winn, M. D., Storoni, L. C., and Read, R. J. (2007). *Phaser* crystallographic software. *J. Appl. Crystallogr.* 40, 658–674. doi: 10.1107/S0021889807021206

Milano, A., Pasca, M. R., Provvedi, R., Lucarelli, A. P., Manina, G., Ribeiro, A. L., et al. (2009). Azole resistance in *Mycobacterium tuberculosis* is mediated by the MmpS5-MmpL5 efflux system. *Tuberclosis* 89, 84–90. doi: 10.1016/j.tube.2008.08.003

Miranda-CasoLuengo, A. A., Staunton, P. M., Dinan, A. M., Lohan, A. J., and Loftus, B. J. (2016). Functional characterization of the *Mycobacterium abscessus* genome coupled with condition specific transcriptomics reveals conserved molecular strategies for host adaptation and persistence. *BMC Genomics* 17:553. doi: 10.1186/s12864-016-2868-y

Mougari, F., Guglielmetti, L., Raskine, L., Sermet-Gaudelus, I., Veziris, N., and Cambau, E. (2016). Infections caused by *Mycobacterium abscessus*: epidemiology, diagnostic tools and treatment. *Expert Rev. Anti Infect. Ther.* 14, 1139–1154. doi: 10.1080/14787210.2016.1238304

Nash, K. A., Brown-Elliott, B. A., and Wallace, R. J. (2009). A novel gene, *erm(41)*, confers inducible macrolide resistance to clinical isolates of *Mycobacterium abscessus* but is absent from *Mycobacterium chelonae*. *Antimicrob. Agents Chemother.* 53, 1367–1376. doi: 10.1128/AAC.01275-08

Nessar, R., Cambau, E., Reyrat, J. M., Murray, A., and Gicquel, B. (2012). *Mycobacterium abscessus*: a new antibiotic nightmare. *J. Antimicrob. Chemother.* 67, 810–818. doi: 10.1093/jac/dkr578

Orth, P., Schnappinger, D., Hillen, W., Saenger, W., and Hinrichs, W. (2000). Structural basis of gene regulation by the tetracycline inducible Tet repressor-operator system. *Nat. Struct. Biol.* 7, 215–219. doi: 10.1038/73324

Prammananan, T., Sander, P., Brown, B. A., Frischkorn, K., Onyi, G. O., Zhang, Y., et al. (1998). A single 16S ribosomal RNA substitution is responsible for resistance to amikacin and other 2-deoxystreptamine aminoglycosides in *Mycobacterium abscessus* and *Mycobacterium chelonae*. *J. Infect. Dis.* 177, 1573–1581. doi: 10.1086/515328

Radhakrishnan, A., Kumar, N., Wright, C. C., Chou, T.-H., Tringides, M. L., Bolla, J. R., et al. (2014). Crystal structure of the transcriptional regulator Rv0678 of *Mycobacterium tuberculosis*. *J. Biol. Chem.* 289, 16526–16540. doi: 10.1074/jbc.M113.538959

Ramos, J. L., Martínez-Bueno, M., Molina-Henares, A. J., Terán, W., Watanabe, K., Zhang, X., et al. (2005). The TetR family of transcriptional repressors. *Microbiol. Mol. Biol. Rev.* 69, 326–356. doi: 10.1128/MMBR.69.2.326-356.2005

Rominski, A., Roditscheff, A., Selchow, P., Böttger, E. C., and Sander, P. (2017a). Intrinsic rifamycin resistance of *Mycobacterium abscessus* is mediated by ADP-ribosyltransferase MAB_0591. *J. Antimicrob. Chemother.* 72, 376–384. doi: 10.1093/jac/dkw466

Rominski, A., Selchow, P., Becker, K., Brülle, J. K., Dal Molin, M., and Sander, P. (2017b). Elucidation of *Mycobacterium abscessus* aminoglycoside and capreomycin resistance by targeted deletion of three putative resistance genes. *J. Antimicrob. Chemother.* 72, 2191–2200. doi: 10.1093/jac/dkx125

Rosenberg, E. Y., Bertenthal, D., Nilles, M. L., Bertrand, K. P., and Nikaido, H. (2003). Bile salts and fatty acids induce the expression of *Escherichia coli* AcrAB multidrug efflux pump through their interaction with Rob regulatory protein. *Mol. Microbiol.* 48, 1609–1619. doi: 10.1046/j.1365-2958.2003.03531.x

Schumacher, M. A., Miller, M. C., Grkovic, S., Brown, M. H., Skurray, R. A., and Brennan, R. G. (2002). Structural basis for cooperative DNA binding by two dimers of the multidrug-binding protein QacR. *EMBO J.* 21, 1210–1218. doi: 10.1093/emboj/21.5.1210

Smibert, O., Snell, G. I., Bills, H., Westall, G. P., and Morrissey, C. O. (2016). *Mycobacterium abscessus* complex - a particular challenge in the setting of lung transplantation. *Expert Rev. Anti Infect. Ther.* 14, 325–333. doi: 10.1586/14787210.2016.1138856

Takiff, H. E., Cimino, M., Musso, M. C., Weisbrod, T., Martinez, R., Delgado, M. B., et al. (1996). Efflux pump of the proton antiporter family confers low-level fluoroquinolone resistance in *Mycobacterium smegmatis*. *Proc. Natl. Acad. Sci. U.S.A.* 93, 362–366. doi: 10.1073/pnas.93.1.362

Trott, O., and Olson, A. J. (2010). AutoDock Vina: improving the speed and accuracy of docking with a new scoring function, efficient optimization, and multithreading. *J. Comput. Chem.* 31, 455–461. doi: 10.1002/jcc.21334

van Dorn, A. (2017). Multidrug-resistant *Mycobacterium abscessus* threatens patients with cystic fibrosis. *Lancet Respir. Med.* 5:15. doi: 10.1016/S2213-2600(16)30444-1

Viljoen, A., Blaise, M., de Chastellier, C., and Kremer, L. (2016). MAB_3551c encodes the primary triacylglycerol synthase involved in lipid accumulation in *Mycobacterium abscessus*. *Mol. Microbiol.* 102, 611–627. doi: 10.1111/mmi.13482

Viljoen, A., Dubois, V., Girard-Misguich, F., Blaise, M., Herrmann, J.-L., and Kremer, L. (2017). The diverse family of MmpL transporters in mycobacteria: from regulation to antimicrobial developments. *Mol. Microbiol.* 104, 889–904. doi: 10.1111/mmi.13675

Viljoen, A., Gutiérrez, A. V., Dupont, C., Ghigo, E., and Kremer, L. (2018). A simple and rapid gene disruption strategy in *Mycobacterium abscessus*: on the design and application of glycopeptidolipid mutants. *Front. Cell. Infect. Microbiol.* 8:69. doi: 10.3389/fcimb.2018.00069

Woods, G. L., Brown-Elliott, B. A., Conville, P. S., Desmond, E. P., Hall, G. S., Lin, G., et al. (2011). *Susceptibility Testing of Mycobacteria, Nocardiae and Other Aerobic Actinomycetes: Approved Standard*, 2nd Edn. Wayne, PA: Clinical and Laboratory Standards Institute.

Yang, S., Gao, Z., Li, T., Yang, M., Zhang, T., Dong, Y., et al. (2013). Structural basis for interaction between *Mycobacterium smegmatis* Ms6564, a TetR family master regulator, and its target DNA. *J. Biol. Chem.* 288, 23687–23695. doi: 10.1074/jbc.M113.468694

Zhang, S., Chen, J., Cui, P., Shi, W., Zhang, W., and Zhang, Y. (2015). Identification of novel mutations associated with clofazimine resistance in *Mycobacterium tuberculosis*. *J. Antimicrob. Chemother.* 70, 2507–2510. doi: 10.1093/jac/dkv150

Conflict of Interest Statement: The authors declare that the research was conducted in the absence of any commercial or financial relationships that could be construed as a potential conflict of interest.

Supplementary Information

Mechanistic and structural insights into the unique TetR-dependent regulation of a drug efflux pump in *Mycobacterium abscessus*

Matthias Richard[1], Ana Victoria Gutierrez[1,3], Albertus Viljoen[1], Eric Ghigo[4], Mickael Blaise[1,*] and Laurent Kremer[1,2,*]

[1]Institut de Recherche en Infectiologie de Montpellier (IRIM), Université de Montpellier, CNRS UMR 9004, Montpellier, France.
[2]INSERM, IRIM, 34293 Montpellier, France.
[3]Unité de Recherche Microbes, Evolution, Phylogeny and Infection (MEPHI), Institut Hospitalier Universitaire Méditerranée-Infection, Cedex 05, 13385 Marseille, France.
[4]CNRS, Campus Joseph Aiguier, 31 Chemin Joseph Aiguier, 13009 Marseille, France.

[*]To whom correspondence should be addressed:
Tel: (+33) 4 34 35 94 47; E-mail: laurent.kremer@irim.cnrs.fr; mickael.blaise@irim.cnrs.fr

Running title: TetR-dependent regulation of MmpL expression in *M. abscessus*.

Keywords: *Mycobacterium abscessus,* TetR regulator, MmpL, efflux pump, structure, thiacetazone analogues, EMSA.

Table S1. List of bacterial strains and plasmids used in this study.

Name	Description/genotype	Marker	Reference
Strains			
M. abscessus S	*Mabs sensu stricto*, strain CIP104536^T, smooth	_	Laboratoire de Référence des Mycobactéries
M. abscessus R	*Mabs sensu stricto*, strain CIP104536 ^{T}, rough	_	Laboratoire de Référence des Mycobactéries
M. abscessus S Δ*mmpL5*	*Mabs* mutant obtained by recombination in the smooth parental strain CIP104536^T	Kan	This study
M. abscessus R Δ*mmpL5*	*Mabs* mutant obtained by recombination in the rough parental strain CIP104536^T	Kan	This study
M. abscessus S Δ*MAB_4384*	*Mabs* mutant obtained by recombination in the smooth parental strain CIP104536^T	Kan	This study
M. abscessus R Δ*MAB_4384*	*Mabs* mutant obtained by recombination in the rough parental strain CIP104536^T	Kan	This study
M. abscessus D15_S6	*Mabs* smooth strain containing a D14N point mutation in MAB_4384 and resistant to TAC analogues	_	Halloum et al., 2017
M. abscessus D15_S7	*Mabs* smooth strain containing a F57L point mutation in MAB_4384 and resistant to TAC analogues	_	Halloum et al., 2017
M. abscessus D15_R1	*Mabs* rough strain containing a M1A point mutation in MAB_4384 and resistant to TAC analogues	_	Halloum et al., 2017
E. coli HB101	*F$^-$ mcrB mrr hsdS20(rB$^-$ mB$^-$) recA13 leuB6 ara-14 proA2 lacY1 galK2 xyl-5 mtl-1 rpsL20(SmR) glnV44 λ-*	Stp	MCLAB
E. coli XL1-Blue	*recA1 endA1 gyrA96 thi-1 hsdR17 supE44 relA1 lac* [F′ *proAB lacI*qZΔ*M15* Tn*10* (Tetr)].	Tet	Stratagene
E. coli BL21(DE3) Rosetta2	F$^-$ *ompT hsdS*$_B$(r_B^- m_B^-) *gal dcm* (DE3) pRARE2 (Cam^R)		Novagen
Plasmids			
pET32a	Vector for high-level expression of proteins fused with an N-terminal thioredoxin protein and a His tag	Amp	Novagen
pET32a_*MAB_4384*	pET32a in which *MAB_4384* is cloned in fusion with the thioredoxin/His tag sequence and containing a TEV cleavage site before MAB_4384 to remove the tags fusion	Amp	This work
pET32a_MAB_*4384(D14N)*	pET32a_*MAB_4384* carrying the D14N mutation in MAB_4384	Amp	This work

pET32a_MAB_*4384(F57L)*	pET32a_*MAB_4384* carrying the F57L mutation in MAB_4384	Amp	This work
pET32a_MAB_*4384(D14N/F57L)*	pET32a_*MAB_4384* carrying the double D14N/F57L mutation in MAB_4384	Amp	This work
pUX1	Suicide construct designed for single cross-over in mycobacteria	Kan	Viljoen et al. 2017, in preparation
pUX1_*MAB_4384*	pUX1 designed to inactivate *MAB_4384* in *M. abscessus*	Kan	This study
pUX1_*mmpL5*	pUX1 designed to inactivate *mmpL5* in *M. abscessus*	Kan	This study
pMV261	Multi-copy *E. coli*/mycobacterial shuttle vector. Cloned genes are under the control of the constitutive *hsp60* promoter	Kan	(53)
pMV261_*lacZ*	pMV261 containing the promoterless *lacZ* reporter gene	Kan	(53)
pMV261_P_{hsp60}_*lacZ*	pMV261_*lacZ* carrying the *hsp60* promoter region cloned upstream of *lacZ*	Kan	(53)
pMV261_$P_{S5/L5}$_*lacZ*	pMV261_*lacZ* carrying the promoter region of *mmpS5/mmpL5* cloned upstream of *lacZ*	Kan	This study

Amp, ampicillin; Kan, kanamycin; Tet, Tetracycline; Stp, streptomycin

Table S2: Oligonucleotides used in this study. Fw and Rev stand for forward and reverse, respectively.

Primers	5' to 3' sequence
Cloning in pET32a	
MAB_4384_full	Fw: TCA GGG TAC C*GA GAA TCT GTA CTT CCA GGG A* GT GAA CGG CCG TGA AGT GGC GCA TC (KpnI , Tobacco Etch Virus [TEV] cleavage site in in italic) Rev: GAG AAA GCT TGA GAC GCA GTG ACA GTG AGC (HindIII))
MAB_4384_DM	Fw: GTG TAC CGC CGC **C**TT CCC ACG AAA (substituted nucleotide in bold) Rev: TTT CGT GGG AA**G** GCG GCG GTA CAC (substituted nucleotide in bold)
Cloning in pMV261_*lacZ* derivatives	
HB101_lacZ	Fw: TAT ATA GGA TCC GAT GAC CAT GAT TAC GGA TTC ACT GGC C (BamHI) Rev: TAT AGC AAG CTT TAC GCG AAA TAC GGG CAG ACA TGG (HindIII)
*MAB_4384_* $P_{S5/L5}$	Fw: *TCT AGA* GCC GAC GAG TGT ATC GCT CG (XbaI) Rev: *GGA TCC* CGC AGC CAC CCC GTC CCG CT (BamHI)
Cloning in pUX1	
*MAB_4384::*pUX1	Fw: GAG AGA GCT AGC CCT TTT CGA GGC AAT TTA CG (NheI) Rev: GAG AGA GGA TCC CGG TAA GCA CTC CGA AGA AG (BamHI) Conf: CGT AAC CGG AAG CGT GTA ATC
*mmpL5::*pUX1	Fw: TCAG GGA TCC GGC AAC TGC CGT CAT TAA CT Rev: GAG AGC TAG CCC GGT CGT TAT AGG TGG TGT Conf: CGG GTT CAT CTT GGC TTT AGA
Sequencing	
pMV5'	CGC CCG GCC AGC GTA AGT AGC
pMV3'	GCC TGG CAG TCG ATC GTA CG
pMV3' Ext	TTG AGA CAC AAC GTC GCT TT
NheIpUX1	ACGGCATGGACGAGCTGTAC
qRT-PCR	
sigA	Fw: CAC ATG GTC GAG GTC ATC AA Rev: TGG ATT TCC AGC ACC TTC TC
MAB_4384	Fw: CGT AAC CGG AAG CGT GTA ATC Rev: GGA AAG CGG CGG TAC AC
MAB_3551C (tgs1)	Fw: CAC CGT CTA CTA CGG AAT CAA C Rev: TGC GCA GCC TCC AAT AAT
MAB_0478	Fw: CCACTCCGCAGATGATTACT Rev: GCGATGGTGGCATGAAATAG
MAB_0987c	Fw: CCGCCTATCAGACGATGTATAAG Rev: CGTGTGAACGACAGACAGAA
MAB_1134c	Fw: CCGGAAGGTCTTTCGCATATC Rev: CGAGTTCGATCTTGGCATCTT
MAB_1137c	Fw: CTCGGGCTACCTCAATAACATC Rev: GCCTTGTGGCGGTAGATAAA
MAB_1287	Fw: AACAACAGCTCCACCAACT Rev: CTCCTTGACGTCCTCGATATTC

MAB_2037	Fw: GGGACAATGGAGGAGATGAAG Rev: GTGCGGTTCCCAGTAGTAATAG
MAB_2210c	Fw: CCAAGCGGTACAAGGCATTA Rev: GCTGACCATCTCGGCTATTT
MAB_2301	Fw: CAGCTCCATCCCATTCCTTATC Rev: TCGGCCTGGACCTTCATA
MAB_2303	Fw: ACATTCTCTGTCCCGATCATTC Rev: GTGCTCTTTACCGACCTCTTC
MAB_2570c	Fw: GGCTCAAGGAAGTAATGGAGAA Rev: GTGTGGCTCCCAATACAGATAG
MAB_2571c	Fw: CTCTTGTTGGCGTGTTGATTAC Rev: CGAACGACGAGATTCCAATGA
MAB_2650	Fw: GAAAGCGGACTCGGGTATTT Rev: TTGGGCTTGTATGTCGGAAG
MAB_3150	Fw: ACTGGTCATCCTGGTGATTG Rev: CATCCGCCTTCGTCATACTT
MAB_3201	Fw: CCGATTCTCGATACCCATTCTC Rev: GTGCTGCTTGATCACTGTTTC
MAB_3562c	Fw: GGGAGTTTGTTCGGGCTATT Rev: GCACCCACCATGACGATAAT
MAB_4240c	Fw: CTCGATGAAGGAGATGGGAAAG Rev: GCTCGATCAACGCCGAATA
MAB_4263	Fw: CTGATTCCGACCTCGATGATG Rev: GCCGATGAAGAAGATGGAGTAG
MAB_4310c	Fw: AAGCCCAACAGCAAGAATTG Rev: GAATACATCGGGCGGTAGATAG
MAB_4382c	Fw: GGGCTATCACACCACCTAT Rev: CGGGTTCATCTTGGCTTTA
MAB_4383c	Fw: GTCATGCATTTACGCACCAAC Rev: CGAAGACCTCATACGTCACAAC
MAB_4704c	Fw: CTCGGCAATCTGGGATTCATAG Rev: CTCTTGGTATCGCCCAGTAAAG
LacZ	Fw: CCAACGTGACCTATCCCATTAC Rev: TTCCTGTAGCCAGCTTTCATC
Eletrophoretic Mobility Shift Assay (EMSA)	
Probe 1	Fw: CAC TTC GCC *ATA AGT GGA TTG ACT CTA TCC ACT TTT* ACC CAT AGA (Fluorescein in 5') Rev :TCT ATG GGT AAA AGT GGA TAG AGT CAA TCC ACT TAT GGC GAA GTG
Probe 2	Fw: CAC TTC GCC **ATG GAC TTC GTG A**C*T CTA TCC ACT TTT* ACC CAT AGA (Fluorescein in 5') Rev: TCT ATG GGT AAA AGT GGA TAG AGT CAC GAA GTC CAT GGC GAA GTG
Non-specific probe	Fw: ATG GAA CTT GAA GGA CTG ACC GCG TTG (Fluorescein in 5') Rev: CAA CGC GGT CAG TCC TTC AAG TTC CAT
Probe 3	Fw:**TCT GGA TAA *GC***A AGT GGA TTG ACT CTA TCC ACT ***TCC*** **GAA ACC GAC** Rev: GTC GGT TTC GGA AGT GGA TAG AGT CAA TCC ACT TGC TTA TCC AGA

Probe 4	Fw: CAC TTC GCC *ATA AGT GGA T***C***A TCC ACT TTT* ACC CAT AGA (Fluorescein in 5’) Rev: TCT ATG GGT AAA AGT GGA TGA TCC ACT TAT GG C GAA GTG
Probe 5	Fw: CACT TCG CC*A TAA GTG GAT* **ATG CA***T GA*C *TCT C***TG AAG** *ATC CAC TTT T*AC CCA TAG A (Fluorescein in 5’) Rev: TCT ATG GGT AAA AGT GGA TCT TCA GAG AGT CAT GCA TAT CCA CTT ATG GCG AAG TG
Probe 6	Fw: CAC TTC GCC *AT***G G***GT GGA TTG ACT CTA TCC AC***C C***TT* ACC CAT AGA (Fluorescein in 5’) Rev: TCT ATG GGT AAG GGT GGA TAG AGT CAA TCC ACC CAT GGC GAA GTG
Probe 7	Fw: CAC TTC GCC *ATA AGT GG***G C***TG ACT CT***G C***CC ACT TTT* ACC CAT AGA (Fluorescein in 5’) Rev: TCT ATG GGT AAA AGT GGG CAG AGT CAG CCC ACT TAT GGC GAA GTG
Probe 8	Fw: CAC TTC GCC *ATA AG***C A***GA TTG ACT CTA TC***T G***CT TTT* ACC CAT AGA (Fluorescein in 5’) Rev: TCT ATG GGT AAA AGC AGA TAG AGT CAA TCT GCT TAT GGC GAA GTG

[a]Restriction sites are underlined and specified inside brackets.

[b]Mutagenized bases are shown in bold.

[c]Inverted palindromes are shown in italic on the 5’ primer.

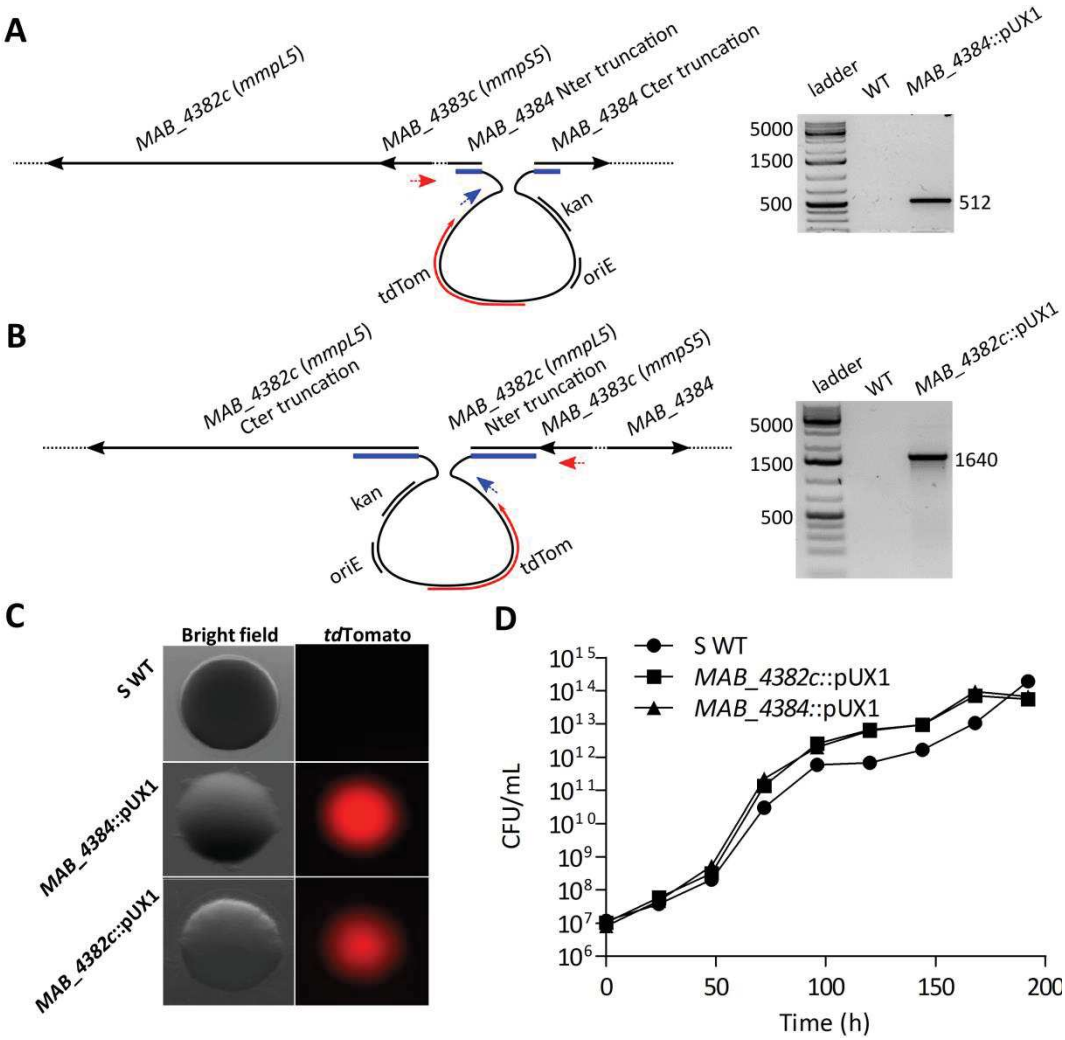

Figure S1. Generation of *M. abscessus* mutants with interruptions in *MAB_4384* and *MAB_4382c* (*mmpL5*). The strategy involves the production of suicide vectors that homologously recombine within targeted genes and carrying a kanamycin cassette as well as a *td*Tomato marker for a rapid screening of transformants having undergone gene disruption (Viljoen et al. 2018). The schematic representation of disrupted *MAB_4384* **(A)** and *MAB_4382c* **(B)** is shown. Proper gene disruption was confirmed by PCR analyses after selection of the red fluorescent colonies **(C)** obtained after transformations. Specific sets of primers were designed to only amplify a band of the expected size in the mutant strains. Blue arrows represent primers that hybridize within the inserted plasmid whereas red arrows correspond to primers only hybridizing within the chromosome. Sizes of the PCR products were analyzed on agarose gels and further sequenced to confirm the gene disruption. **(D)** *In vitro* growth of the parental *M. abscessus* S strain and its *MAB_4384::*pUX1 and *MAB_4382c::*pUX1 derivatives. Bacteria were grown in 7H9 broth supplemented with ADC and 0.05% Tween 80. Growth was monitored by determining the CFU/ml at different time points.

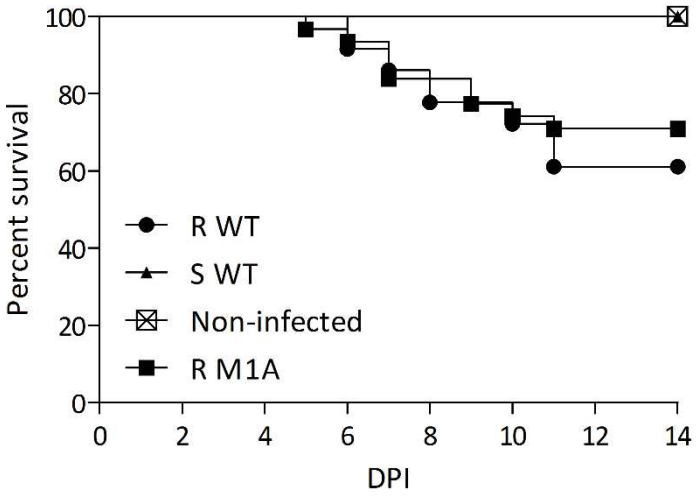

Figure S2. Survival curves of *M. abscessus* strains in zebrafish embryos. Embryos were infected intravenously the wild-type smooth (S) (350 CFU), rough (R) (220 CFU) or MAB_4384(M1A) mutant (280 CFU) strains expressing tdTomato as reported earlier (Bernut et al., 2014, 2015). Groups of uninfected fishes were also included as controls. Dead embryos succumbing from infection were monitored on a daily basis up to 14 days post-infection (dpi). Results are representative of two independent experiments.

All zebrafish experiments were approved by the Direction Sanitaire et Vétérinaire de l'Hérault et Comité d'Ethique pour l'Expérimentation Animale de la région Languedoc Roussillon under the reference CEEA-LR-1145.

Article2

« **Mutations in the MAB_2299c TetR Regulator Confer Cross-Resistance to Clofazimine and Bedaquiline in *Mycobacterium abscessus*.** » Richard M*, Gutiérrez AV*, Viljoen A, Rodriguez-Rincon D, Roquet-Baneres F, Blaise M, Everall I, Parkhill J, Floto RA, Kremer L (* = Contribution équivalente)Antimicrob Agents Chemother. 2018 December 21; Volume 63 Issue 1.

La bédaquiline (BDQ) et la clofazimine (CFZ) sont actuellement utilisées dans le traitement de tuberculoses multi-résistantes et sont évaluées cliniquement pour leurs utilisations dans la thérapie contre *M. abscessus*. La sélection de mutants spontanés résistants à la CFZ a révélé la présence de mutations dans le régulateur TetR codé par *MAB_2299c*. De façon surprenante, ces mêmes souches étaient également co-résistantes à la BDQ et toutes présentaient une augmentation modérée des ARNm de *MAB_2300/MAB_2301* codant pour une potentielle pompe à efflux de type MmpS/ MmpL. De la même façon que précédemment pour le régulateur TetR MAB_4384 (voir **Article 1**), l'utilisation d'EMSA a permis d'identifier une longue séquence palindromique située en amont de *MAB_2300/MAB_2301* et de prouver l'interaction physique de ce régulateur TetR avec ce segment d'ADN cible. La présence d'un complexe TetR/ADN stable isolé par gel filtration a confirmé la liaison spécifique de cette protéine avec ce motif palindromique. Des substitutions nucléotidiques au sein du motif provoquent un échec dans la formation de ce complexe. Par ailleurs, un variant de MAB_2299c présentant une mutation dans le domaine HTH n'est également plus capable de former un complexe avec l'ADN cible, démontrant ainsi l'importance de ce résidu dans la liaison du régulateur à l'ADN. Le développement d'une nouvelle technique de délétion génique basée sur un évènement de double recombinaison homologue, combinant une première étape de sélection de colonies fluorescentes et d'une seconde étape de contre-sélection en présence d'isoniazide a permis de générer les mutants non-marqués Δ*MAB_2299c* et Δ*MAB_2299c* – Δ*MAB_2300/2301*. Ces souches mutées ont permis de confirmer le rôle de MAB_2300/MAB_2301 dans la résistance intrinsèque de *M. abscessus* à la CFZ et la BDQ. Cette nouvelle technique de génétique représente un outil très performant ouvrant la possibilité de déléter simultanément de nombreux gènes et d'étudier leur fonction biologique ainsi que leur contribution dans la virulence et/ou résistance aux antibiotiques chez *M. abscessus*.

AMERICAN SOCIETY FOR MICROBIOLOGY | Antimicrobial Agents and Chemotherapy®

MECHANISMS OF RESISTANCE

Mutations in the MAB_2299c TetR Regulator Confer Cross-Resistance to Clofazimine and Bedaquiline in *Mycobacterium abscessus*

Matthias Richard,[a] Ana Victoria Gutiérrez,[a,c] Albertus Viljoen,[a] Daniela Rodriguez-Rincon,[d] Françoise Roquet-Baneres,[a] Mickael Blaise,[a] Isobel Everall,[e] Julian Parkhill,[e] R. Andres Floto,[d] Laurent Kremer[a,b]

[a]Institut de Recherche en Infectiologie de Montpellier (IRIM), Université de Montpellier, CNRS UMR 9004, Montpellier, France
[b]INSERM, IRIM, Montpellier, France
[c]Unité de Recherche Microbes, Evolution, Phylogeny and Infection (MEPHI), Institut Hospitalier Universitaire Méditerranée-Infection, Marseille, France
[d]Molecular Immunity Unit, Department of Medicine, University of Cambridge, MRC Laboratory of Molecular Biology, Cambridge, United Kingdom
[e]Wellcome Trust Sanger Institute, Hinxton, United Kingdom

ABSTRACT New therapeutic approaches are needed against *Mycobacterium abscessus*, a respiratory mycobacterial pathogen that evades efforts to successfully treat infected patients. Clofazimine and bedaquiline, two drugs used for the treatment of multidrug-resistant tuberculosis, are being considered as alternatives for the treatment of lung diseases caused by *M. abscessus*. With the aim to understand the mechanism of action of these agents in *M. abscessus*, we sought herein to determine the means by which *M. abscessus* can develop resistance. Spontaneous resistant strains selected on clofazimine, followed by whole-genome sequencing, identified mutations in *MAB_2299c*, encoding a putative TetR transcriptional regulator. Unexpectedly, mutants with these mutations were also cross-resistant to bedaquiline. MAB_2299c was found to bind to its target DNA, located upstream of the divergently oriented *MAB_2300-MAB_2301* gene cluster, encoding MmpS/MmpL membrane proteins. Point mutations or deletion of *MAB_2299c* was associated with the concomitant upregulation of the *mmpS* and *mmpL* transcripts and accounted for this cross-resistance. Strikingly, deletion of *MAB_2300* and *MAB_2301* in the *MAB_2299c* mutant strain restored susceptibility to bedaquiline and clofazimine. Overall, these results expand our knowledge with respect to the regulatory mechanisms of the MmpL family of proteins and a novel mechanism of drug resistance in this difficult-to-treat respiratory mycobacterial pathogen. Therefore, *MAB_2299c* may represent an important marker of resistance to be considered in the treatment of *M. abscessus* diseases with clofazimine and bedaquiline in clinical settings.

KEYWORDS EMSA, MmpL, *Mycobacterium abscessus*, TetR regulator, bedaquiline, clofazimine, drug resistance mechanisms, efflux pumps

Mycobacterium abscessus is an emerging nontuberculous mycobacterium (NTM) commonly associated with contaminated traumatic skin wounds or postsurgical soft tissue infections (1). Among the rapid growers, *M. abscessus* also represents the most frequently isolated species in cystic fibrosis (CF) patients, with a prevalence of 3% to 6% in this population (2), or in patients with other underlying lung disorders, such as non-CF bronchiectasis and chronic obstructive pulmonary disease (COPD), resulting in nodular and cavitary granulomas and persistent lung infection (3–6). CF patients with chronic *M. abscessus* infection have higher rates of lung function decline than those with no NTM infections (7). Recent surveys have identified *M. abscessus* to be a major threat in many CF centers worldwide (5), and this alarming situation is worsened by

Citation Richard M, Gutiérrez AV, Viljoen A, Rodriguez-Rincon D, Roquet-Baneres F, Blaise M, Everall I, Parkhill J, Floto RA, Kremer L. 2019. Mutations in the MAB_2299c TetR regulator confer cross-resistance to clofazimine and bedaquiline in *Mycobacterium abscessus*. Antimicrob Agents Chemother 63:e01316-18. https://doi.org/10.1128/AAC.01316-18.

Address correspondence to Laurent Kremer, laurent.kremer@irim.cnrs.fr.

M.R. and A.V.G. contributed equally to this article.

Received 20 June 2018
Returned for modification 3 August 2018
Accepted 9 October 2018
Accepted manuscript posted online 15 October 2018
Published 21 December 2018

epidemiological studies documenting the transmission of dominant circulating *M. abscessus* clones that have spread globally between hospitals (8). In addition, lung infections caused by *M. abscessus* remain extremely difficult to treat, mainly because of its natural resistance to most currently available antibiotics (9). The prognosis of pulmonary infections is poor, particularly in the context of CF, with a cure rate of 30% to 50%, in spite of lengthy courses of antibiotics often complemented by surgery (10). In contrast to many other NTM infections, antibiotherapy against *M. abscessus* often fails, leading to lasting sputum culture positivity, and no antibiotic regimen reliably cures these infections (3, 11–14).

There is an important medical need to discover and develop more efficient and safer treatments to fight against *M. abscessus*. The proposed strategy for fueling a drug pipeline can rely on (i) *de novo* drug discovery to identify new pharmacophores and targets, (ii) repurposing of known drugs as new treatments of *M. abscessus* infections, or (iii) the repositioning of antibiotics that act against pharmacologically validated targets but that have been developed for the treatment of other infectious diseases (15). Among the repositioned drugs over which there is increasing interest, clofazimine (CFZ) and bedaquiline (BDQ) are currently being evaluated in clinical trials for their activities against *M. abscessus* pulmonary infections.

The riminophenazine clofazimine (CFZ) is a lipophilic agent with cationic amphiphilic properties used as an antileprosy drug and currently repurposed as an antituberculosis (anti-TB) drug (16). CFZ also has unique characteristics, such as a slow metabolic elimination, preferential accumulation inside macrophages, and a low incidence of drug resistance (16). In *M. tuberculosis*, CFZ acts as a prodrug which is reduced by the NADH dehydrogenase (Ndh2) and, upon spontaneous reoxidation by O_2, releases reactive oxygen species (ROS) (17), explaining why high levels of resistance to CFZ are rare. Due to the recent widespread emergence of *M. abscessus*, there has been a renewed interest in the repurposing of CFZ for the treatment of *M. abscessus* infections. *In vitro* studies reported the efficacy of CFZ in multidrug regimens for the treatment of *M. abscessus* infections, in which it showed synergistic activity with amikacin (18) or tigecycline (19). CFZ was also found to prevent the regrowth of *M. abscessus* exposed to clarithromycin and amikacin (13). Although CFZ has increasingly been used in the treatment of lung diseases in clinical practice (10, 20), only limited data on its effectiveness are available. In one study, CFZ was found to be safe, reasonably tolerated, and active when given orally for the treatment of NTM infections, including *M. abscessus* infections, and was proposed to be an alternative drug for the treatment of NTM diseases (21). In another study, CFZ-containing regimens also showed improved treatment outcomes in patients with pulmonary diseases due to *M. abscessus* (22).

BDQ is a diarylquinoline antibiotic that has been approved by the Food and Drug Administration and the European Medicines Agency for the treatment of multidrug-resistant tuberculosis (MDR-TB) (23). BDQ acts by targeting the c subunit of the essential F_oF_1 ATP synthase (24–27), and studies have also proposed that it may inhibit the ATP synthase via another mechanism involving the ε subunit of the enzyme, in addition to binding to its c subunit (28, 29). BDQ exhibits very low MICs against various NTM, including *M. abscessus* clinical isolates from CF and non-CF patients (27, 30, 31), but despite being an excellent growth inhibitor at low doses, it lacks bactericidal activity against *M. abscessus* (27). Studies in immunocompromised mouse models led to conflictual conclusions, reporting, on the one hand, a benefit of BDQ in reducing bacterial loads in gamma interferon knockout mice (32) and, on the other hand, no decrease in the bacillary loads in the lungs or an inability to prevent death in nude mice (33). However, BDQ is highly efficient in reducing pathophysiological signs, such as abscesses and cords in *M. abscessus*-infected zebrafish, and in protecting zebrafish larvae from death (27). The mode of action of BDQ in *M. abscessus* relies on rapid ATP depletion and was demonstrated by genetically transferring single point mutations into *atpE*, which conferred high levels of resistance to the drug (27). Preliminary results of studies using BDQ as salvage therapy for pulmonary infections with *M. avium* or *M. abscessus* suggested that BDQ has clinical activity but its efficacy appears to be

TABLE 1 Drug susceptibility profiles and genotypes of 6 spontaneous CFZ-resistant *M. abscessus* strains[a]

Strain	MIC_{99} (μg/ml)			Mutation in *MAB_2299c*	
	CFZ	BDQ	AMK	SNP/indel	Amino acid change
Wild type	4	0.5	8		
CFZ-R1	8	2	8	T119G	L40W
CFZ-R3	8	2	8	C276del	P92fs
CFZ-R4	8	2	8	G541T	E181stop
CFZ-R6	8	2	8	ins318A	D106fs
CFZ-R7	8	2	8	T452C	L151P
CFZ-R9	8	2	8	G643A	G215S

[a]The mutants were derived from the ATCC 199177 S parental strain and selected in the presence of CFZ. MIC_{99} values were determined on Middlebrook 7H10 agar. Single nucleotide polymorphisms (SNP) and/or indels were identified in *MAB_2299c*. The corresponding amino acid changes are also indicated. CFZ, clofazimine; BDQ, bedaquiline; AMK, amikacin; del, deletion; ins, insertion; fs, frameshift.

relatively moderate, as suggested by a low sputum culture conversion rate (34). Therefore, the clinical utility of BDQ against *M. abscessus* infections requires more studies.

To further delineate the mechanism of action of CFZ and BDQ in *M. abscessus*, we sought to determine how *M. abscessus* develops resistance to these agents. Herein, mutations were identified in a new TetR regulator, MAB_2299c. These mutations were associated with low levels of resistance to both CFZ and BDQ. Genetic and biochemical analyses were applied to determine the specificity of this regulatory system in *M. abscessus* and to describe the contribution of a key residue important in driving the DNA-binding activity of MAB_2299c to its operator. The results expand our knowledge with respect to the regulatory mechanisms of the MmpL family of efflux pumps and on a novel mechanism of drug resistance in *M. abscessus*.

RESULTS

Mutations in *MAB_2299c* confer coresistance to CFZ and BDQ. With the aim of identifying the mechanism of resistance to CFZ in *M. abscessus*, 6 spontaneous CFZ-resistant mutants were first reared in passages of the reference *M. abscessus* ATCC 19977 S strain in liquid medium containing increasing concentrations of CFZ and then isolated on solid 7H11 medium supplemented with oleic acid-albumin-dextrose-catalase (OADC) ($7H11^{OADC}$ medium). All 6 resistors exhibited low resistance levels (MIC, 8 μg/ml) compared to the resistance level of the parental strain (MIC, 4 μg/ml) (Table 1). Spontaneous resistant mutants arose at a frequency of $\approx 2 \times 10^{-7}$. Whole-genome sequencing identified mutations in the *MAB_2299c* locus in all 6 mutants, which were subsequently confirmed by PCR amplification and Sanger sequencing. This approach identified single nucleotide polymorphisms (SNP) in mutants CFZ-R1 (L40W replacement), CFZ-R4 (stop codon), CFZ-R7 (L151P replacement), and CFZ-R9 (G215S replacement), as well as a single nucleotide deletion in CFZ-R3 or a single nucleotide insertion in CFZ-R6 leading to frameshift mutations (Table 1). These observations converge to a prominent role of MAB_2299c in the CFZ resistance phenotype. Interestingly, all 6 CFZ-resistant mutants were also coresistant to BDQ with MIC levels of 2 μg/ml, corresponding to a 4-fold increased MIC compared to that for the parental strain (Table 1). In contrast, all mutants remained susceptible to amikacin (AMK). These results imply that mutations in *MAB_2299c* confer cross-resistance to CFZ and BDQ but not to AMK, pointing out a unique resistance mechanism.

***MAB_2299c* encodes a TetR repressor controlling expression of a specific MmpS/MmpL pair.** Sequence alignments and BLAST analyses indicated that *MAB_2299c* encodes a putative TetR transcriptional regulator. TetR family members possess a conserved N-terminal helix-turn-helix (HTH) DNA-binding domain and a C-terminal ligand regulatory domain and are commonly associated with antibiotic resistance by regulating expression of genes coding for multidrug resistance efflux pumps (35). Interestingly, the two gene pairs (*MAB_2300-MAB_2301* and *MAB_2302-MAB_2303*)

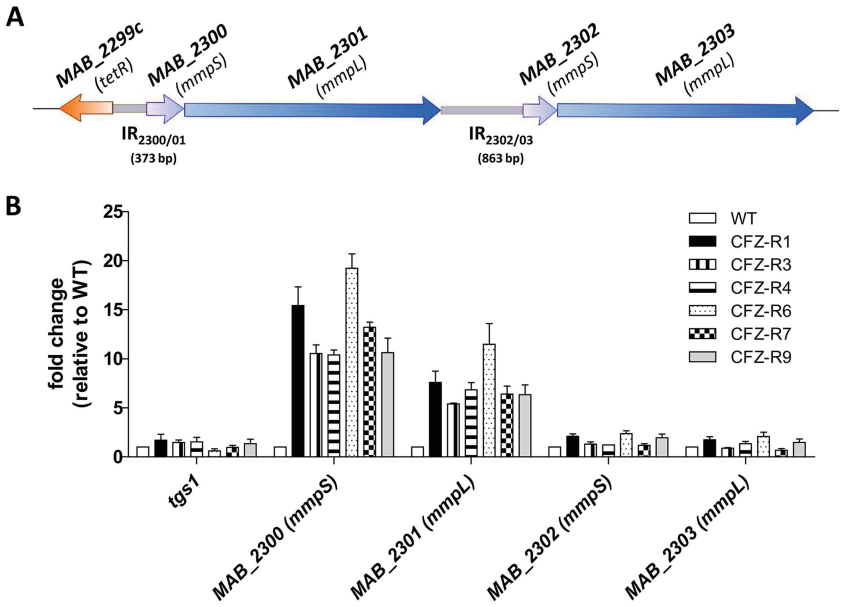

FIG 1 *MAB_2299c* regulates expression of the *MAB_2300-MAB_2301* locus. (A) Schematic representation of the genetic environment of *MAB_2299c* and its two adjacent *mmpS-mmpL* gene pairs (*MAB_2300-MAB_2301* and *MAB_2302-MAB_2303*). The sizes and positions of the two intergenic regions ($IR_{2300/01}$ and $IR_{2302/03}$) are indicated. (B) Transcriptional expression of the *MAB_2300-MAB_2303* genes in the parental *M. abscessus* strain and in 6 spontaneous CFZ-resistant mutants harboring mutations in *MAB_2299c*. The results are expressed as the fold change in mRNA levels between the mutant strains and the parental strain. Error bars indicate the standard deviation. Relative gene expression was calculated using the $2^{-\Delta\Delta CT}$ threshold cycle (C_T) method with PCR efficiency correction. The data are representative of those from three independent experiments.

adjacent to *MAB_2299c* and transcribed in the opposite direction code for MmpS (*MAB_2300* and *MAB_2302*) and MmpL (*MAB_2301* and *MAB_2303*) integral membrane proteins (Fig. 1). MmpL proteins are part of the superfamily of resistance, nodulation, and division (RND) transporters and were reported to act as efflux pumps for azoles, CFZ, and BDQ in *M. tuberculosis* (36, 37) and for thiacetazone analogues in *M. abscessus* (38, 39).

To explore whether the TetR regulator MAB_2299c controls the expression of the neighboring *mmpS* and *mmpL* genes, quantitative reverse transcription-PCR (qRT-PCR) was first performed both in the parental *M. abscessus* S strain and in the 6 CFZ- and BDQ-resistant derivatives harboring the various *MAB_2299c* alleles. The results clearly showed the induction of both the *MAB_2300* and the *MAB_2301* transcripts in all 6 mutants (Fig. 1B). The expression levels of *tgs1*, which encodes the triacylglycerol synthase, involved in the synthesis and accumulation of triglycerides in *M. abscessus* (40), and which was included as an unrelated gene control, were found to remain unchanged in the various strains tested (Fig. 1B). In contrast, no induction of the expression levels of *MAB_2302* and *MAB_2303* transcripts was observed in the different mutant strains (Fig. 1B). This suggests that MAB_2299c represses expression of only the *MAB_2300-MAB_2301* (*mmpS-mmpL*) pair.

MAB_2299c binds to a palindromic sequence upstream of *MAB_2300*. Using MEME, a motif-based sequence analysis tool (41), a 64-bp DNA segment within the 373-bp intergenic region between *MAB_2299c* and *MAB_2300* ($IR_{2300/01}$) harboring two palindromic sequences as well as two degenerated repeat motifs was identified (Fig. 2A). To test whether this 64-bp fragment represents a DNA-binding site for MAB_2299c, electrophoretic mobility shift assays (EMSA) were performed using increasing concentrations of purified MAB_2299c in the presence of the corresponding labeled fragment (probe A; Fig. 2B). Under these conditions, a DNA-protein complex was detected. The specificity of binding was demonstrated in a competition assay by adding increasing concentrations of the corresponding unlabeled DNA fragment (cold

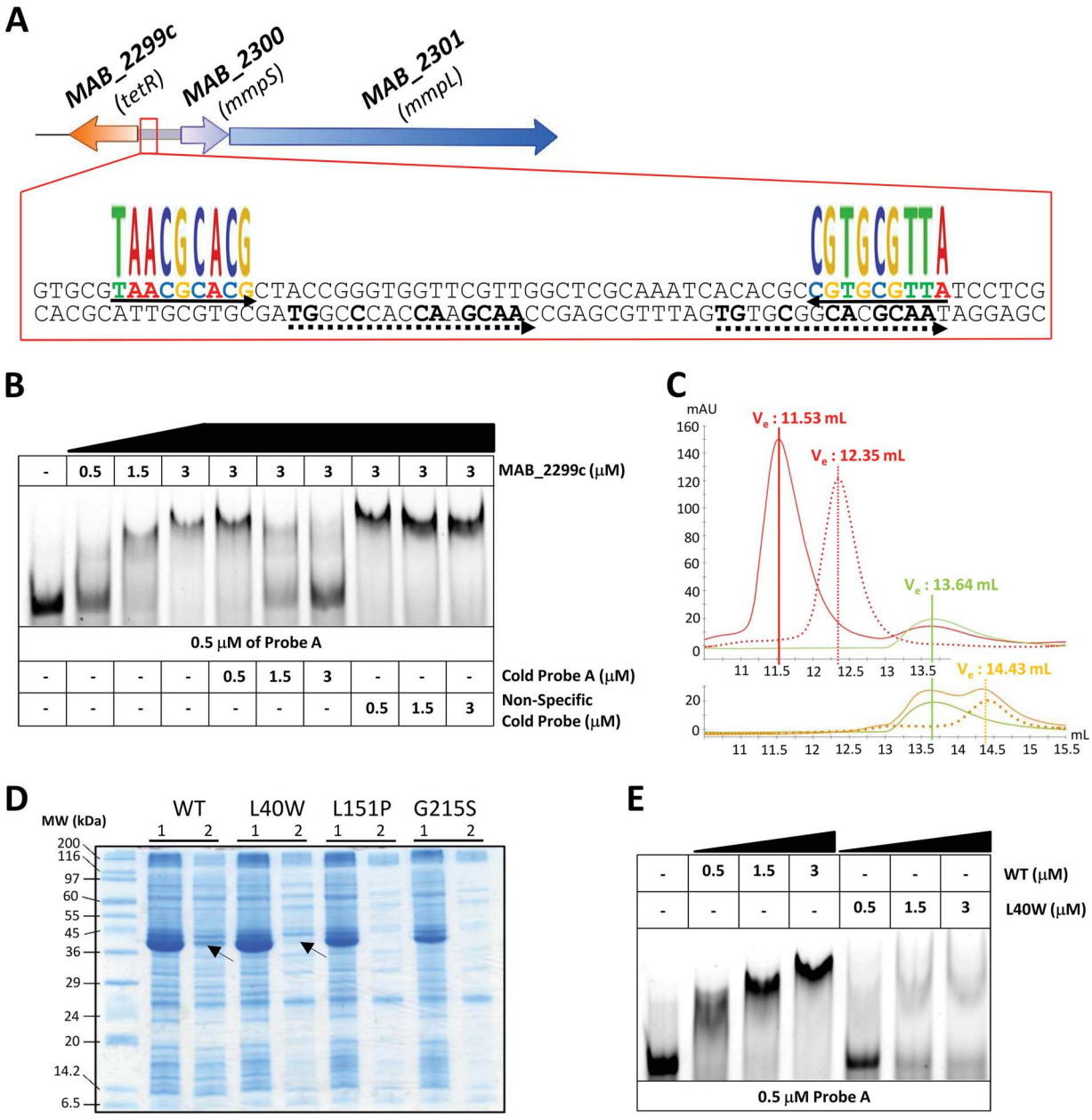

FIG 2 Binding activity of MAB_2299c to the intergenic region upstream of *MAB_2300-MAB_2301*. (A) Schematic representation of the 64-bp DNA operator identified within $IR_{2300/01}$ corresponding to the sequence of probe A. The oligonucleotides recognized by MAB_2299c are composed of two palindromes (underlined by arrows) and two degenerated double repeats (underlined by dashed arrows). (B) EMSA and competition assays using probe A and purified MAB_2299c. Gel shifts were revealed by fluorescence emission using a 5′ fluorescein-labeled probe A. (C) Gel filtration profiles of free probe A, free MAB_2299c, and the TetR-DNA complex. Probe A (red dotted line) and *MAB_2299c* (green line) were isolated individually by size exclusion chromatography and displayed elution volumes (V_e) of 12.35 ml and 13.64 ml, respectively. When mixed together, a stable MAB_2299c-probe A complex (red line) with an elution volume of 11.53 ml was observed. The MAB_4384-specific palindromic sequence (orange dotted line) eluted at 14.43 ml. However, when mixed together with MAB_2299c, no protein-DNA complex was formed and both the DNA and protein were eluted separately (orange line) as two distinct peaks, with the elution volumes corresponding exactly to those for the MAB_4384 palindrome and MAB_2299c protein alone. mAU, milli-absorbance units. (D) Expression of the various MAB_2299c variants in *E. coli*. Lanes 1, total crude extract; lanes 2, clarified/soluble extract. The theoretical molecular mass of MAB_2299c-6His-TrxA is 41,420 Da. MW, molecular weight. (E) Impaired DNA-binding activity of the MAB_2299c L40W mutant, as shown by EMSA using either the soluble MAB_2299c (WT) or MAB_2299c (L40W) protein. Gel shifts were revealed by the fluorescence emission thanks to fluorescein-labeled probe A.

probe), which led to a dose-dependent decrease in DNA-protein complex formation (Fig. 2B). Moreover, the shift was maintained in the presence of an excess of a nonrelated probe, further indicating that a specific protein-DNA complex was formed only when the TetR regulator was incubated with DNA containing its specific target.

These results were also confirmed by size exclusion chromatography (SEC), where the MAB_2299c-probe A complex eluted at 11.53 ml and could be readily separated from the protein alone (which eluted at 13.64 ml) or the DNA target (which eluted at 12.35 ml) (Fig. 2C, top). In contrast, no protein-DNA complex was eluted when MAB_2299c was incubated with the DNA target from MAB_4384, a previously characterized TetR regulator in *M. abscessus* (38, 39) (Fig. 2C, bottom), further highlighting the specificity of the MAB_2299c/$IR_{2300/01}$ interaction. In addition, the pronounced shift impairment using mutated derivatives of probe A lacking either the palindromic sequence (ΔPalin) or the degenerated double repeats (ΔDR), generated by replacing the original sequences with random nucleotides, suggests that both the palindrome and the double repeats are required for the optimal binding of MAB_2299c to its operator (see Fig. S1 in the supplemental material).

Screening of the entire 863-bp $IR_{2302/03}$ located upstream of the second *mmpS-mmpL* pair (Fig. 1A) using MEME failed to identify inverted repeats that looked similar to the ones found in $IR_{2300/01}$, suggesting that the regulator is unlikely to recognize a DNA-binding sequence in the upstream region of *MAB_2302-MAB_2303*. To confirm this hypothesis, EMSAs were done by incubating increasing concentrations of MAB_2299c with 3 overlapping probes covering the entire $IR_{2302/03}$ region (Fig. S2A). Even at the highest protein concentration tested, no protein-DNA complexes were observed with either of the three probes (Fig. S2B). These results are in agreement with the qRT-PCR results (Fig. 1B) and support the view that MAB_2299c is unable to bind to $IR_{2302/03}$ and to regulate the expression of this second *mmpS-mmpL* pair.

Overall, these results confirm the strict DNA sequence requirements for the optimal binding of MAB_2299c to $IR_{2300/01}$.

Leu40 is critical for optimal DNA-binding activity of MAB_2299c. To get insights into the mechanisms by which the different point mutations in CFZ-R1, CFZ-R7, and CFZ-R9 confer resistance to CFZ and BDQ, the three corresponding *MAB_2299c* alleles were cloned into pET32a and introduced into *E. coli* for expression. Figure 2D shows that although the 3 mutated proteins were highly expressed, only a very small fraction of the L40W protein was found in the soluble fraction, whereas the vast majority of the L151P and G215S mutants remained insoluble. Despite many attempts and by using large *E. coli* cultures, we failed to obtain enough soluble L151P and G215S proteins for subsequent purification but succeeded in generating the L40W derivative in a soluble form. Due to its localization within the N-terminal domain of the TetR regulator, known to participate in the DNA-binding activity of the protein (35), we addressed whether the L40W substitution conferring resistance to CFZ and BDQ affects the DNA-binding activity of MAB_2299c. EMSAs were therefore performed using purified MAB_2299c (L40W) and probe A. Compared to the shift profile with wild-type (WT) MAB_2299c, the formation of the DNA-protein complex was severely impaired in the presence of the mutated protein, even at high protein concentrations (Fig. 2E).

Overall, these results support the importance of Leu40 in the DNA-binding capacity of MAB_2299c and explain the reduced ability of the mutants to bind to the operator region, in agreement with the derepression of *MAB_2300-MAB_2301* transcription in the CFZ-R1 *M. abscessus* strain carrying the L40W substitution (Fig. 1B).

An unmarked deletion of *MAB_2299c* leads to upregulation of the *MAB_2300-MAB_2301* efflux pump and coresistance to CFZ and BDQ. Because point mutations or premature stop codons in the *MAB_2299c* mutants did not prevent the altered proteins from interacting with other protein partners/DNA sequences and eventually generating aberrant phenotypes, we further confirmed the contribution of *MAB_2299c* in the profile of susceptibility/resistance to CFZ and BDQ by generating an *M. abscessus* deletion mutant. To achieve this aim, we first improved a flexible suicide vector that we previously created, pUX1 (43), by cloning into it the *M. tuberculosis katG*, which was recently demonstrated as an efficient counterselectable marker in *M. abscessus* in the presence of isoniazid (INH) (42). Through the positive selection afforded by kanamycin resistance and tdTomato markers and the negative selection afforded by *katG*, this

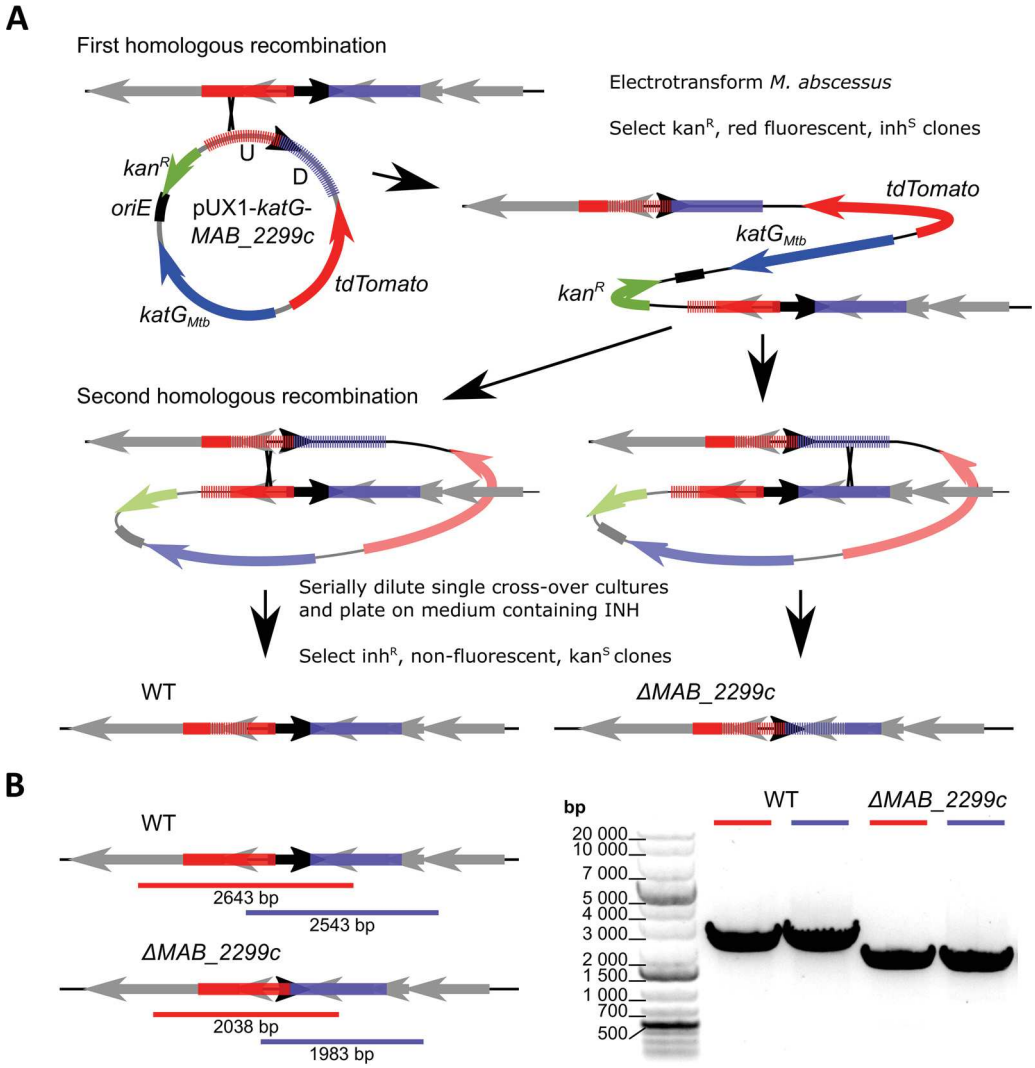

FIG 3 Generation of an unmarked *MAB_2299c* deletion mutant in *M. abscessus*. (A) Line drawing illustrating the general protocol followed to ascertain the Δ*MAB_2299c* mutant. $katG_{Mtb}$, *M. tuberculosis katG*. (B) (Left) Line drawing of the genomic context in the *M. abscessus* WT and Δ*MAB_2299c* mutant that also illustrates the PCR strategy followed to confirm the deletion of *MAB_2299c*. Red and blue bars, the PCR products obtained during the screening of potential mutant clones; black arrow, *MAB_2299c*. (Right) A gel confirming the Δ*MAB_2299c* genotype. The red and blue bars correspond to the amplicons obtained in the left panel. These amplicons were subjected to sequencing analysis to confirm the correct deletion of the *MAB_2299c* gene.

vector, pUX1-*katG*, could be used in a two-step homologous recombination procedure to generate scarless unmarked deletion mutants in *M. abscessus*. The different steps of this method leading to an unmarked *MAB_2299c* deletion are depicted in Fig. 3A. As a first step, sequences of approximately 1 kb directly upstream and downstream of a 560-bp internal fragment of the 666-bp *MAB_2299c* open reading frame were cloned adjacently into pUX1-*katG*. After transformation of *M. abscessus* with pUX1-*katG-MAB_2299c*, colonies that had undergone a first homologous recombination between the plasmid and the bacterial chromosome either up- or downstream of the *MAB_2299c* gene were easily identified by their red fluorescence against a large background of colonies spontaneously resistant to the selective antibiotic. After a single passage in liquid culture without kanamycin, the *MAB_2299c* single-crossover clones were serially diluted and the dilutions were plated on INH-containing solid medium. Clones that were INH resistant, nonfluorescent, and kanamycin sensitive arose at an approximate frequency of 10^{-4} to 10^{-3} CFU/ml. These clones were selected and subsequently

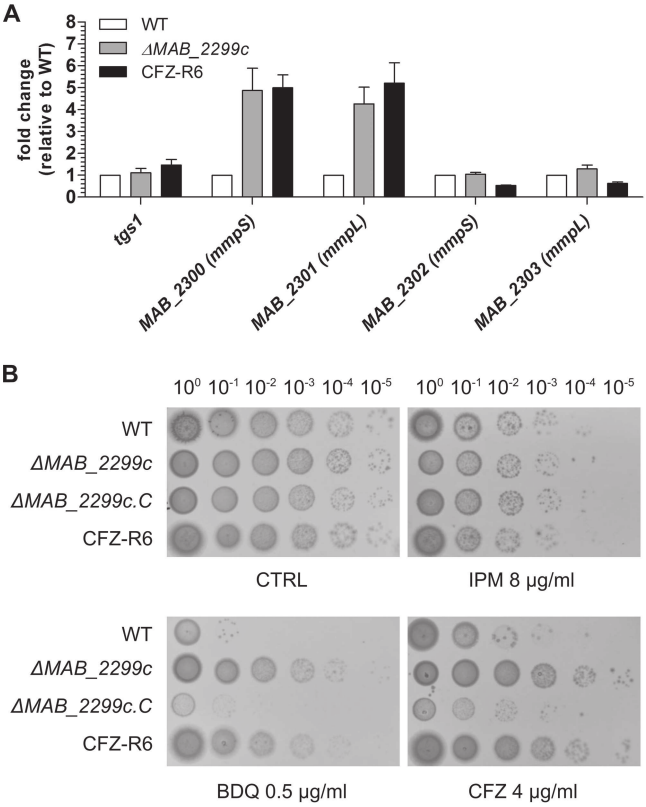

FIG 4 Deletion of *MAB_2299c* confers resistance to both CFZ and BDQ. (A) Results of a qRT-PCR experiment showing the induction levels of the *mmpS-mmpL* (*MAB_2300-MAB_2301*) pair but not *MAB_2302-MAB_2303* when *MAB_2299c* is deleted from the *M. abscessus* genome. (B) Profile of the susceptibility or resistance of *M. abscessus* WT, *M. abscessus* Δ*MAB_2299c*, and the complemented derivative of Δ*MAB_2299c* (Δ*MAB_2299c.C*) to BDQ, CFZ, or IPM. Five microliters of 10-fold serially diluted bacterial suspensions of exponentially growing cultures was spotted on Middlebrook 7H10 plates in the absence (control [CTRL]) or presence of drugs at the indicated concentrations. The plates were incubated at 37°C for 4 days.

genotyped to confirm the correct unmarked deletion of *MAB_2299c* by PCR/sequencing analysis (Fig. 3B). No observable changes in the colony morphology or in the *in vitro* growth rate were noticed in this unmarked deletion mutant, subsequently designated Δ*MAB_2299c* (Fig. S3). Δ*MAB_2299c* was then subjected to qRT-PCR analysis. The results in Fig. 4A clearly show a 5-fold increase in the transcription level of *MAB_2300* and *MAB_2301*, but not that of *MAB_2302* and *MAB_2303*. Interestingly, these induction levels were comparable to those found in CFZ-R6. In agreement with the qRT-PCR results performed using the various CFZ spontaneous mutants, the *MAB_2299c* gene deletion did not affect expression of the *MAB_2302-MAB_2303* pair. As expected, the CFZ and BDQ susceptibility pattern of the Δ*MAB_2299c* mutant was comparable to that of CFZ-R6 (Fig. 4B). Importantly, both the Δ*MAB_2299c* and CFZ-R6 mutants displayed enhanced growth on agar supplemented with 0.5 μg/ml BDQ or 4 μg/ml CFZ (Fig. 4B, bottom), whereas, under the same conditions, the growth of the parental *M. abscessus* strain was severely inhibited. That this resistance phenotype was restricted to CFZ and BDQ only was supported by the similar growth and susceptibility to imipenem (IPM) of all strains. As anticipated, complementation of the Δ*MAB_2299c* mutant by introducing a pMV261-*MAB_2299c* construct (leading to Δ*MAB_2299c*.C) fully restored susceptibility to both CFZ and BDQ (Fig. 4B). In contrast, the susceptibility profile of the Δ*MAB_2299c* mutant to anti-TB front-line drugs (INH, ethambutol, or rifampin) was comparable to that of the WT and complemented strains (Table S3). Together, these results confirm the importance of MAB_2299c in resistance to CFZ and BDQ.

Deletion of *MAB_2300-MAB_2301* in the Δ*MAB_2299c* mutant restores susceptibility to CFZ and BDQ. To address whether resistance to CFZ and BDQ is directly

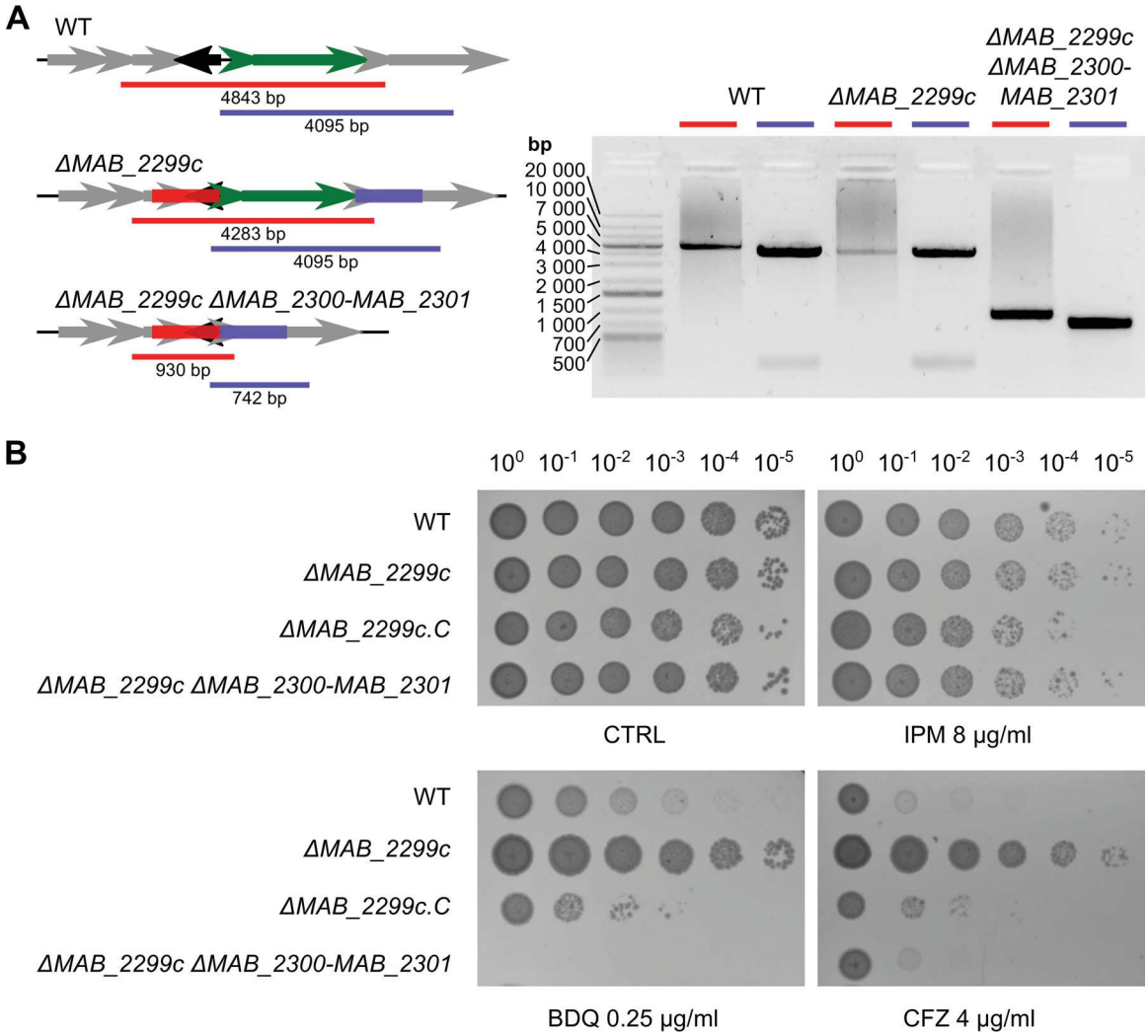

FIG 5 Deletion of *MAB_2300* and *MAB_2301* in Δ*MAB_2299c* restores sensitivity to CFZ and BDQ. (A) Line drawing (left) of the *MAB_2299c-MAB_2301* genomic context in the *M. abscessus* WT, Δ*MAB_2299c*, and Δ*MAB_2299c* Δ*MAB_2300-MAB_2301* strains. Also illustrated is the PCR strategy followed to confirm the deletion of *MAB_2300* and *MAB_2301*. Black arrow, *MAB_2299c*; small and large green arrows, *MAB_2300* and *MAB_2301*, respectively. (B) Profile of susceptibility of the Δ*MAB_2299c* Δ*MAB_2300-MAB_2301* triple-knockout strain to BDQ, CFZ, or IPM compared to the other strains reared in this study. Five microliters of 10-fold serially diluted bacterial suspensions obtained from exponentially growing cultures was spotted on Middlebrook 7H10 plates in the absence (control [CTRL]) or presence of drugs at the indicated concentrations. The plates were incubated at 37°C for 4 days.

mediated by an MmpS/MmpL-dependent efflux machinery which is induced in Δ*MAB_2299c*, both *MAB_2300* and *MAB_2301* were deleted in the Δ*MAB_2299c* mutant. The simultaneous knockout of *MAB_2300* and *MAB_2301* in the unmarked *MAB_2299c* deletion mutant was achieved using a strategy similar to the one used to construct the Δ*MAB_2299c* mutant. The Δ*MAB_2299c* Δ*MAB_2300-MAB_2301* genotype of this triple-knockout mutant was confirmed by PCR, as illustrated in Fig. 5A. Importantly, whereas the susceptibility of the triple mutant to CFZ was reverted to WT levels, the MIC of BDQ for this mutant was even lower than the MIC observed for the WT strain (Fig. 5B and Table S3). This indicates that abolition of the MAB_2300-MAB_2301 efflux pump system rendered the Δ*MAB_2299c* mutant sensitive to both drugs. As expected, the triple mutant's sensitivity to IPM remained similar to that of the Δ*MAB_2299* progenitor (Fig. 5B and Table S3).

Overall, these results suggest that both CFZ and BDQ are specific substrates of the MAB_2301 (MmpL) efflux pump and that the sole deletion of this MmpS/MmpL system is sufficient to reverse the CFZ and BDQ resistance phenotype of the Δ*MAB_2299c* mutant.

DISCUSSION

M. abscessus has recently emerged as one of the most clinically relevant NTM (8, 14) and accounts for more than 80% of all pulmonary infections caused by rapidly growing mycobacteria (44). It poses a serious threat, particularly in patients suffering from lung disorders, such as CF or bronchiectasis (14, 44). Occasional fatalities due to *M. abscessus* infections (44, 45) can be a result of the extreme difficulty with the treatment of patients as a result of the intrinsic and broad antibiotic resistance of this bacterium conferred by an impermeable cell envelope, the presence of drug-modifying enzymes and a large abundance of efflux pumps (3, 11, 46). Therefore, to reach an unmet medical need in the treatment of *M. abscessus* diseases, the repositioning of the anti-TB drugs CFZ and BDQ has recently been evaluated in retrospective case series, although data related to their mode of action and/or resistance mechanisms in *M. abscessus* remain scarce.

In this study, whole-genome sequencing of *in vitro*-selected mutants showing cross-resistance to CFZ and BDQ identified mutations in *MAB_2299c* that were subsequently confirmed by PCR/sequencing. MAB_2299c belongs to the TetR family of transcriptional regulators, representing the most abundant family of regulators in mycobacteria (47). In line with the general observation that 60% of TetR regulators are divergently oriented with the genes that they control, *MAB_2299c* was found in the opposite orientation relative to that of its *MAB_2300* and *MAB_2301* target genes. That the different point mutations identified (L40W, L151P, and G215S) were associated with similar fold increases in the upregulation of *MAB_2300-MAB_2301* in the mutants carrying premature stop codons suggested a loss of DNA-binding activity, resulting in derepression of *MAB_2300-MAB_2301* gene expression. This hypothesis was confirmed by EMSA, which clearly demonstrated an impaired DNA-binding activity of the L40W mutant, with Leu40 being located in the N-terminal domain, which carries the DNA-binding activity in TetR regulators (35). The L151P and G215S mutated proteins, albeit being expressed in high yields in *E. coli*, remained largely insoluble, suggesting that the L151 and G215 residues play a role in the folding and/or stability of the MAB_2299c multimer. Therefore, substitution of these important residues is very likely to affect the overall structure of the regulator and, consequently, its biological function. During preparation of the manuscript, an independent study identified mutations in several genes, including *MAB_2299c*, in CFZ-resistant *M. abscessus* strains selected *in vitro* (48). Whereas most mutations conferred a loss of function caused by indels or stop codons, three amino acid replacements differing from ours were found, namely, C110Y, H173R, and A214S. Interestingly, the mutation at position A214 is located next to G215, found in our study, further emphasizing an important role of this region in the activity/structure of the regulator. However, despite the lack of any mechanistic data regarding the involvement of these mutations in the function of MAB_2299c and in MmpS/MmpL expression and a potential link with BDQ resistance, the study by Chen et al. (48) strongly supports our findings regarding the implication that MAB_2299c is a major determinant of resistance to CFZ and BDQ. Our results are also reminiscent of those of previous work describing a similar cross-resistance to both BDQ and CFZ identified by a whole-genome sequencing comparison of initial and relapse isolates of *Mycobacterium intracellulare* which occurred during a trial of BDQ as salvage therapy for *M. intracellulare* lung disease (49). Mutations in MmpT5, another TetR member controlling expression of the adjacent *mmpS5-mmpL5* drug efflux operon, was identified as the cause for this cross-resistance. Susceptibility testing indicated that *mmpT5* mutations are associated with 2- to 8-fold increases in MICs for BDQ and CFZ (49).

MAB_2300-MAB_2301 encodes an MmpS/MmpL efflux pump system which is separated by an intergenic region from *MAB_2302-MAB_2303*, encoding a second putative efflux pump system. Whether MAB_2299c controls the expression of the first, the second, or both MmpS/MmpL pairs was addressed by qRT-PCR. Our results clearly indicate that only *MAB_2300-MAB_2301* is under the control of MAB_2299c, and this specificity of regulation was further confirmed by functional complementation exper-

iments with a *MAB_2299c* deletion mutant. Restoration of the CFZ and BDQ susceptibility profile to WT levels was achieved following ectopic expression of MAB_2299c in the deletion mutant. Strikingly, deletion of the *MAB_2300-MAB_2301* locus in Δ*MAB_2299c* abrogated the resistance to both drugs, thus suggesting that the MmpS/MmpL machinery encoded by *MAB_2300-MAB_2301* acts as a multisubstrate efflux pump that is responsible for the drug resistance phenotype in *M. abscessus*. Similarly, studies in *M. tuberculosis* showed resistance to azoles, CFZ, and BDQ involving a wide set of mutations in *Rv0678*, encoding a transcriptional regulator from the MarR family, causing overexpression of the MmpS5/MmpL5 efflux pump (36, 37, 50–52). In addition, the level of resistance to both drugs in the *M. tuberculosis Rv0678* mutants was similar to that found in the *M. abscessus MAB_2299c* mutants. To explain why the MAB_2300/MAB_2301 pair participates in BDQ and CFZ extrusion while the MAB_4383c/MAB_4382c pair that we previously identified to be the closest ortholog in *M. abscessus* of MmpS5/MmpL5, rather, excludes thiacetazone derivatives and not BDQ and CFZ (38), we performed multiple-sequence alignments and subsequent sequence identity determination of the nucleotide and protein sequences of the 17 MmpS/MmpL pairs encoded by the *M. abscessus* genome (see Table S4 in the supplemental material). The identity scores at both the nucleotide and protein levels supported our previous observations that MAB_4383c/MAB_4382c is the closest orthologous pair to MmpS5/MmpL5 from *M. tuberculosis*. Interestingly, considering the protein sequence identity, MAB_2301 is the second closest ortholog to MmpL5 from *M. tuberculosis* after MAB_4382c, explaining the functional similarity in CFZ and BDQ export. However, a full explanation of the differences in substrate specificity that exist between MmpS5/MmpL5 orthologs/paralogs will rely on the elucidation of the high-resolution three-dimensional structures of MmpS5/MmpL5 alone and, more pertinently, in complex with their substrates. Given the very high relatedness between MAB_2300/MAB_2301 and other MmpS-MmpL pairs in *M. abscessus* (Table S4), one cannot exclude the possibility that other MmpS-MmpL efflux pumps mediate cross-resistance to CFZ and BDQ. This can be investigated thanks to the new suicide vector pUX1-*katG*, described in this study, which allows the easy and rapid generation of scarless genetic alterations in the *M. abscessus* chromosome, facilitated by the presence of the brightly red fluorescent tdTomato positive selectable marker and the KatG counterselectable marker.

In *M. tuberculosis*, efflux inhibition using efflux pump inhibitors such as verapamil or reserpine decreases the MICs of BDQ and CFZ *in vitro* (52, 53). Whether these inhibitors would also potentiate the effect of CFZ and/or BDQ in resistant *M. abscessus* strains remains to be established. However, in both organisms, the resistance levels were low and were about 4-fold greater than those of their parental strains. This may be linked to the low induction level of the *MAB_2300-MAB_2301* gene cluster under derepressed conditions (in the *MAB_2299c* mutants or deletion strain). This also contrasts with the very high induction level reported previously for *mmpS5-mmpL5* in mutants or a deletion strain of *MAB_4384*, which also accounted for very high levels of resistance to thiacetazone analogues (38, 39). Overall, these observations, combined with the fact that *M. abscessus* possesses a very large *mmpL* repertoire (54) and also a high abundance of TetR transcriptional regulators, allow us to speculate that similar drug resistance mechanisms are employed by this pathogen to express its natural pattern of resistance to many more antimicrobial agents.

In summary, this study adds new functional and mechanistic insights into the TetR-dependent regulation mechanisms responsible for cross-resistance to CFZ and BDQ in *M. abscessus*, which may have important clinical implications. Future studies should help to elucidate whether the emergence of *MAB_2299c* variants occurs during BDQ or CFZ treatment in patients with *M. abscessus* lung disease.

MATERIALS AND METHODS

Strains, growth conditions, and reagents. All *M. abscessus* strains used in this study are listed in Table S1 in the supplemental material. The strains were grown in Middlebrook 7H9 broth (BD Difco) supplemented with 0.05% Tween 80 (Sigma-Aldrich) and 10% oleic acid, albumin, dextrose, catalase (OADC enrichment; BD Difco) ($7H9^{T/OADC}$) at 30°C (unless otherwise stated) or in Sauton's medium in the

presence of antibiotics, when required. On plates, colonies were selected on Middlebrook 7H10 or 7H11 agar (BD Difco) supplemented with 10% OADC enrichment (7H10^{OADC} or 7H11^{OADC}, respectively) or on LB agar. All drugs were purchased from Sigma-Aldrich.

Drug susceptibility testing. MICs were determined on cation-adjusted Mueller-Hinton broth using the microdilution method or on Middlebrook 7H10^{OADC} agar plates. The MIC_{99} was defined as the minimal drug concentration required to inhibit 99% growth and was recorded by counting the colonies obtained after 3 to 4 days of incubation at 30°C. All experiments were done on three independent occasions. The frequency of spontaneous resistance was determined by counting the number of resistant colonies growing on 7H10^{OADC} and 7H11^{OADC} agar supplemented with 8 μg/ml CFZ after plating 5×10^7 CFU.

Generating clones resistant to clofazimine. Resistance to CFZ was induced by subjecting an *M. abscessus* ATCC 19977 susceptible clone to sub-MICs of the antibiotic. The bacteria were grown in 7H9 supplemented with albumin-dextrose-catalase (ADC; 10%) and glycerol (0.04%) containing sub-MICs of CFZ for 5 days. The bacteria were then spun in a centrifuge at 3,000 $\times$ *g* and washed with phosphate-buffered saline. Bacteria that grew at the highest concentration of CFZ were used to inoculate new cultures containing increasing concentrations of CFZ. The bacteria were then grown in 7H9 supplemented with ADC (10%) and glycerol (0.04%) without CFZ for 5 days and streaked on 7H11 agar plates supplemented with OADC (10%) and glycerol (0.04%) containing CFZ. Single colonies isolated from these plates were subjected to MIC determinations and DNA extraction and sequencing. All growth was done at 37°C.

Whole-genome sequencing and target identification. DNA from six spontaneous resistant mutants and one susceptible isolate was sequenced on an Illumina MiSeq platform, producing 150-bp paired-end reads. The raw reads were subsequently mapped to the *M. abscessus* reference genome using the BWA-MEM algorithm (55). Variants were called using the SAMtools (v.1.2) and BCFtools (v.1.2) packages and the parameters described previously (56, 57). Single nucleotide polymorphisms (SNP) were identified in *MAB_2299c*, and confirmation of these mutations was done by PCR amplification and sequencing.

DNA constructs. All constructs used in this study are listed in Table S1. For expression of MAB_2299c in *E. coli*, *MAB_2299c* was PCR amplified from pure genomic DNA of *M. abscessus* CIP104536^T using primers MAB_2299c_Fw and MAB_2299c_Rv (Table S2) and Phusion polymerase (Thermo Fisher Scientific). The allele carrying the L40W mutation was amplified from strain CFZ-R1 using the same primers. The PCR products were then cloned into pET32a that had been cut with KpnI and HindIII, allowing introduction of thioredoxin and polyhistidine tags at the N terminus of the protein. A tobacco etch virus (TEV) cleavage site was also incorporated before the 1st amino acid of the protein to remove the N-terminal tags from the rest of the protein. To complement the *M. abscessus* Δ*MAB_2299c* mutant, *MAB_2299c* was PCR amplified using the Compl_MAB_2299c primers (Table S2), digested with EcoRI, and ligated into pMV261 that had been digested with MscI and EcoRI, allowing the constitutive overexpression of *MAB_2299c* under the control of the *hsp60* promoter, thus yielding pMV261-*MAB_2299c* (Table S1).

Quantitative real-time PCR. Isolation of RNA, reverse transcription, and qRT-PCR were done as reported earlier (38), using the primers listed in Table S2.

Expression and purification of MAB_2299c variants. The *E. coli* BL21(DE3) strain (New England Biolabs) containing the pRARE2 vector was transformed with the pET32a constructs containing either the wild-type (WT) or the mutated *MAB_2299c* gene harboring the L40W mutation. Protein expression was done in lysogeny broth (LB) medium containing 200 μg/ml ampicillin and 30 μg/ml chloramphenicol. When an optical density at 600 nm of 0.6 to 1 was reached, the cultures underwent a 30-min cold shock in icy water prior to protein synthesis induction with 1 mM isopropyl-β-D-1-thiogalactopyranoside (IPTG). Cultures were then grown for 20 h at 16°C prior to centrifugation (6,000 $\times$ *g*, 4°C, 20 min). Bacterial pellets were resuspended in lysis buffer (50 mM Tris-HCl, pH 8, 200 mM NaCl, 20 mM imidazole, 1 mM benzamidine, 5 mM β-mercaptoethanol), and the cells were disrupted by sonication before the lysates were clarified by an additional centrifugation (16,000 $\times$ *g*, 4°C, 45 min). Proteins were then purified by a first ion metal affinity chromatography (IMAC) step (Ni-nitrilotriacetic acid Sepharose; GE Healthcare Life Sciences). To remove the two N-terminal tags (thioredoxin, His tag), the eluted proteins were mixed in a 1:50 ratio with the TEV protease and dialyzed overnight at 4°C against 50 mM Tris-HCl, pH 8, 200 mM NaCl, and 5 mM β-mercaptoethanol. The dialyzed proteins were subjected to a second IMAC step before being further dialyzed against a buffer consisting of 50 mM Tris-HCl, pH 8, and 5 mM β-mercaptoethanol. The proteins were then purified by cation exchange chromatography (HiTrap SP Sepharose Fast Flow; GE Healthcare Life Sciences) and eluted in the same buffer using a linear NaCl gradient. Size exclusion chromatography (SEC; ENrich SEC 650; Bio-Rad) was then performed using an elution buffer containing 50 mM Tris-HCl, pH 8, 200 mM NaCl, and 5 mM β-mercaptoethanol to generate highly pure proteins.

EMSA. Using the MEME suite 4.20.0 online tool, a DNA operator of 64 nucleotides containing two perfect palindromes and a degenerated double repeat sequence was identified within the intergenic region between *MAB_2299c* and *MAB_2300*. Thus, the 64-bp double-stranded sequence (probe A) was labeled at the 5′ end with fluorescein (Sigma-Aldrich) and incubated for 1 h at room temperature in 1$\times$ Tris base-acetic acid-EDTA (TAE) buffer with increasing amounts of MAB_2299c or MAB_2299c (L40W). After 30 min of electrophoresis in 1$\times$ TAE buffer at 100 V, gel shifts were revealed by fluorescence using an Amersham Imager 600 imager (GE Healthcare Life Sciences). This native DNA operator as well as mutated probes are listed in Table S2. The 373-bp intergenic region located between *MAB_2299c* and *MAB_2300* and the three overlapping probes covering the entire intergenic region between *MAB_2301*

and *MAB_2302* (Table S2) were amplified using a similar strategy and subjected to electrophoretic mobility shift assays (EMSA) using purified MAB_2299c.

Isolation of the MAB_2299c-probe A complex by SEC. Protein-DNA complex formation was assessed by high-performance liquid chromatography (HPLC) using an Akta Pure 25M chromatography system (GE Healthcare Life Sciences) on an ENrich SEC 650 column (Bio-Rad). The DNA alone, the protein alone, and the protein-DNA mixture were eluted at 4°C at a flow rate of 0.4 ml/min in a buffer containing 50 mM Tris-HCl, pH 8, 200 mM NaCl, 5 mM β-mercaptoethanol. Probe A (60 μg) and MAB_2299c (186 μg) were independently loaded onto the column. A mixture of 60 μg probe A and 186 μg MAB_2299c was coincubated for 1 h at room temperature and loaded onto the column. As a negative control, 21 μg of a 45-bp DNA operator targeted by the TetR regulator MAB_4384 was coincubated with 186 μg MAB_2299c and loaded onto the column.

Generation of *MAB_2299c* and *MAB_2300-MAB_2301* recombination plasmids. To generate pUX1-*katG*, used to perform gene disruption by two-step homologous recombination, the *M. tuberculosis katG* gene was first PCR amplified using the overlap extension mutagenesis approach (58) to introduce a synonymous mutation in the gene, removing an NheI restriction site. Briefly, two separate PCR mixtures containing either the primer set katG_outer_Fw and katG_inner_Rev or the primer set katG_inner_Fw and katG_outer_Rev, purified genomic DNA from *M. tuberculosis*, and Phusion polymerase (Thermo Fisher Scientific) were set up. The PCR products were purified and added (10 ng each) to a new Phusion polymerase PCR mixture without any primers or genomic DNA. This mixture was then subjected to two cycles of 95°C for 30 s, 55°C for 2 min, and 72°C for 3 min before the outer primers were added and 25 more cycles of 95°C for 10 s, 55°C for 30 s, and 72°C for 2 min were performed. The final PCR product was AvrII digested and ligated to AvrII-XmnI-linearized pUX1 to produce pUX1-*katG*. To generate pUX1-*katG-MAB_2299c*, the same overlap extension approach with outer and inner primers was first used to generate a single fused PCR amplicon containing 1-kb up- and downstream sequences of *MAB_2299c* so that it effectively carried a 560-bp deletion in the 666-bp *MAB_2299c* open reading frame. This PCR product was NheI digested and ligated to NheI-XmnI-linearized pUX1-*katG* to produce pUX1-*katG-MAB_2299c*. The pUX1-*katG-MAB_2300-MAB_2301* plasmid used to make a Δ*MAB_2299c* Δ*MAB_2300-MAB_2301* triple-knockout mutant was made using the same approach.

Unmarked deletions of *MAB_2299c* and *MAB_2300-MAB_2301* in *M. abscessus*. The generation of an unmarked *MAB_2299c* deletion in *M. abscessus* relied on two separate homologous recombination events. First, highly electrocompetent *M. abscessus* was transformed with pUX1-*katG-MAB_2299c*, as previously described (43). Kanamycin-resistant (growing at 200 μg/ml), red fluorescent colonies were selected, and the broth was cultured in the presence of kanamycin and subjected to PCR screening using either the primer set MAB_2299c_U_scrn_Fw and MAB_2299c_U_scrn_Rev or the primer set MAB_2299c_D_scrn_Fw and MAB_2299c_D_scrn_Rev (Table S2). Based on the PCR product sizes obtained using the two primer sets, clones that had undergone a single homologous recombination event in either the upstream or the downstream sequence flanking *MAB_2299c* were identified. Positive clones were washed to remove the antibiotics, cultured for 4 h in the absence of antibiotic, and then 10-fold serially diluted, and the dilutions were plated on 7H10 agar plates containing 50 μg/ml isoniazid (INH). INH-resistant, nonfluorescent colonies were restreaked on plates without selective antibiotics to obtain single colonies that were used to inoculate the broth cultures. These cultures were confirmed to be kanamycin sensitive and used to extract and purify genomic DNA, which was subsequently used to perform the same PCR screening described above to identify clones that had undergone a second homologous recombination event effectively deleting 85% of the *MAB_2299c* open reading frame from the *M. abscessus* genome. The PCR products were sequenced, and special attention was paid in the subsequent analyses of the sequencing data to verify the correct junctions between cloned sequences and chromosomal sequences to exclude the possibility of spurious PCR amplification products. The Δ*MAB_2299c* Δ*MAB_2300-MAB_2301* triple-knockout mutant was reared in a similar way, with the only difference being that the Δ*MAB_2299c* strain was the progenitor strain transformed with pUX1-*katG-MAB_2300-MAB_2301*.

SUPPLEMENTAL MATERIAL

Supplemental material for this article may be found at https://doi.org/10.1128/AAC.01316-18.

SUPPLEMENTAL FILE 1, PDF file, 1.3 MB.

ACKNOWLEDGMENTS

This work was supported by the Fondation pour la Recherche Médicale (FRM) (grant number DEQ20150331719 to L.K.; grant number ECO20160736031 to M.R.); the InfectioPôle Sud, which funded the Ph.D. fellowship of A.V.G.; the Wellcome Trust (098051, 107032AIA); and the Cystic Fibrosis Trust (to D.R.-R., I.E., J.P., and R.A.F.).

The funders had no role in study design, data collection and interpretation, or the decision to submit the work for publication.

We have no conflict of interest to declare.

REFERENCES

1. Singh M, Dugdale CM, Solomon IH, Huang A, Montgomery MW, Pomahac B, Yawetz S, Maguire JH, Talbot SG. 2016. Rapid-growing mycobacteria infections in medical tourists: our experience and literature review. Aesthet Surg J 36:NP246–NP253. https://doi.org/10.1093/asj/sjw047.
2. Roux A-L, Catherinot E, Ripoll F, Soismier N, Macheras E, Ravilly S, Bellis G, Vibet M-A, Le Roux E, Lemonnier L, Gutierrez C, Vincent V, Fauroux B, Rottman M, Guillemot D, Gaillard J-L, Herrmann J-L, for the OMA Group. 2009. Multicenter study of prevalence of nontuberculous mycobacteria in patients with cystic fibrosis in France. J Clin Microbiol 47:4124–4128. https://doi.org/10.1128/JCM.01257-09.
3. Medjahed H, Gaillard J-L, Reyrat J-M. 2010. *Mycobacterium abscessus*: a new player in the mycobacterial field. Trends Microbiol 18:117–123. https://doi.org/10.1016/j.tim.2009.12.007.
4. Griffith DE, Aksamit T, Brown-Elliott BA, Catanzaro A, Daley C, Gordin F, Holland SM, Horsburgh R, Huitt G, Iademarco MF, Iseman M, Olivier K, Ruoss S, von Reyn CF, Wallace RJ, Winthrop K, ATS Mycobacterial Diseases Subcommittee, American Thoracic Society, Infectious Diseases Society of America. 2007. An official ATS/IDSA statement: diagnosis, treatment, and prevention of nontuberculous mycobacterial diseases. Am J Respir Crit Care Med 175:367–416. https://doi.org/10.1164/rccm.200604-571ST.
5. Floto RA, Olivier KN, Saiman L, Daley CL, Herrmann J-L, Nick JA, Noone PG, Bilton D, Corris P, Gibson RL, Hempstead SE, Koetz K, Sabadosa KA, Sermet-Gaudelus I, Smyth AR, van Ingen J, Wallace RJ, Winthrop KL, Marshall BC, Haworth CS. 2016. US Cystic Fibrosis Foundation and European Cystic Fibrosis Society consensus recommendations for the management of non-tuberculous mycobacteria in individuals with cystic fibrosis: executive summary. Thorax 71:88–90. https://doi.org/10.1136/thoraxjnl-2015-207983.
6. Catherinot E, Roux A-L, Macheras E, Hubert D, Matmar M, Dannhoffer L, Chinet T, Morand P, Poyart C, Heym B, Rottman M, Gaillard J-L, Herrmann J-L. 2009. Acute respiratory failure involving an R variant of *Mycobacterium abscessus*. J Clin Microbiol 47:271–274. https://doi.org/10.1128/JCM.01478-08.
7. Esther CR, Esserman DA, Gilligan P, Kerr A, Noone PG. 2010. Chronic *Mycobacterium abscessus* infection and lung function decline in cystic fibrosis. J Cyst Fibros 9:117–123. https://doi.org/10.1016/j.jcf.2009.12.001.
8. Bryant JM, Grogono DM, Rodriguez-Rincon D, Everall I, Brown KP, Moreno P, Verma D, Hill E, Drijkoningen J, Gilligan P, Esther CR, Noone PG, Giddings O, Bell SC, Thomson R, Wainwright CE, Coulter C, Pandey S, Wood ME, Stockwell RE, Ramsay KA, Sherrard LJ, Kidd TJ, Jabbour N, Johnson GR, Knibbs LD, Morawska L, Sly PD, Jones A, Bilton D, Laurenson I, Ruddy M, Bourke S, Bowler IC, Chapman SJ, Clayton A, Cullen M, Daniels T, Dempsey O, Denton M, Desai M, Drew RJ, Edenborough F, Evans J, Folb J, Humphrey H, Isalska B, Jensen-Fangel S, Jönsson B, Jones AM, et al. 2016. Emergence and spread of a human-transmissible multidrug-resistant nontuberculous mycobacterium. Science 354:751–757. https://doi.org/10.1126/science.aaf8156.
9. Brown-Elliott BA, Nash KA, Wallace RJ. 2012. Antimicrobial susceptibility testing, drug resistance mechanisms, and therapy of infections with nontuberculous mycobacteria. Clin Microbiol Rev 25:545–582. https://doi.org/10.1128/CMR.05030-11.
10. Jarand J, Levin A, Zhang L, Huitt G, Mitchell JD, Daley CL. 2011. Clinical and microbiologic outcomes in patients receiving treatment for *Mycobacterium abscessus* pulmonary disease. Clin Infect Dis 52:565–571. https://doi.org/10.1093/cid/ciq237.
11. Nessar R, Cambau E, Reyrat JM, Murray A, Gicquel B. 2012. *Mycobacterium abscessus*: a new antibiotic nightmare. J Antimicrob Chemother 67:810–818. https://doi.org/10.1093/jac/dkr578.
12. Maurer FP, Bruderer VL, Ritter C, Castelberg C, Bloemberg GV, Böttger EC. 2014. Lack of antimicrobial bactericidal activity in *Mycobacterium abscessus*. Antimicrob Agents Chemother 58:3828–3836. https://doi.org/10.1128/AAC.02448-14.
13. Ferro BE, Srivastava S, Deshpande D, Pasipanodya JG, van Soolingen D, Mouton JW, van Ingen J, Gumbo T. 2016. Failure of the amikacin, cefoxitin, and clarithromycin combination regimen for treating pulmonary *Mycobacterium abscessus* infection. Antimicrob Agents Chemother 60:6374–6376. https://doi.org/10.1128/AAC.00990-16.
14. Griffith DE. 2014. *Mycobacterium abscessus* subsp *abscessus* lung disease: "trouble ahead, trouble behind. . . ." F1000Prime Rep 6:107. https://doi.org/10.12703/P6-107.
15. Wu M-L, Aziz DB, Dartois V, Dick T. 2018. NTM drug discovery: status, gaps and the way forward. Drug Discov Today 23:1502–1519. https://doi.org/10.1016/j.drudis.2018.04.001.
16. Reddy VM, O'Sullivan JF, Gangadharam PR. 1999. Antimycobacterial activities of riminophenazines. J Antimicrob Chemother 43:615–623. https://doi.org/10.1093/jac/43.5.615.
17. Yano T, Kassovska-Bratinova S, Teh JS, Winkler J, Sullivan K, Isaacs A, Schechter NM, Rubin H. 2011. Reduction of clofazimine by mycobacterial type 2 NADH:quinone oxidoreductase: a pathway for the generation of bactericidal levels of reactive oxygen species. J Biol Chem 286:10276–10287. https://doi.org/10.1074/jbc.M110.200501.
18. Shen G-H, Wu B-D, Hu S-T, Lin C-F, Wu K-M, Chen J-H. 2010. High efficacy of clofazimine and its synergistic effect with amikacin against rapidly growing mycobacteria. Int J Antimicrob Agents 35:400–404. https://doi.org/10.1016/j.ijantimicag.2009.12.008.
19. Singh S, Bouzinbi N, Chaturvedi V, Godreuil S, Kremer L. 2014. In vitro evaluation of a new drug combination against clinical isolates belonging to the *Mycobacterium abscessus* complex. Clin Microbiol Infect 20:O1124–O1127. https://doi.org/10.1111/1469-0691.12780.
20. Czaja CA, Levin AR, Cox CW, Vargas D, Daley CL, Cott GR. 2016. Improvement in quality of life after therapy for *Mycobacterium abscessus* group lung infection. A prospective cohort study. Ann Am Thorac Soc 13:40–48. https://doi.org/10.1513/AnnalsATS.201508-529OC.
21. Martiniano SL, Wagner BD, Levin A, Nick JA, Sagel SD, Daley CL. 2017. Safety and effectiveness of clofazimine for primary and refractory nontuberculous mycobacterial infection. Chest 152:800–809. https://doi.org/10.1016/j.chest.2017.04.175.
22. Yang B, Jhun BW, Moon SM, Lee H, Park HY, Jeon K, Kim DH, Kim S-Y, Shin SJ, Daley CL, Koh W-J. 2017. Clofazimine-containing regimen for the treatment of *Mycobacterium abscessus* lung disease. Antimicrob Agents Chemother 61:e02052-16. https://doi.org/10.1128/AAC.02052-16.
23. Matteelli A, Carvalho AC, Dooley KE, Kritski A. 2010. TMC207: the first compound of a new class of potent anti-tuberculosis drugs. Future Microbiol 5:849–858. https://doi.org/10.2217/fmb.10.50.
24. Andries K, Verhasselt P, Guillemont J, Göhlmann HWH, Neefs J-M, Winkler H, Van Gestel J, Timmerman P, Zhu M, Lee E, Williams P, de Chaffoy D, Huitric E, Hoffner S, Cambau E, Truffot PC, Lounis N, Jarlier V. 2005. A diarylquinoline drug active on the ATP synthase of *Mycobacterium tuberculosis*. Science 307:223–227. https://doi.org/10.1126/science.1106753.
25. Koul A, Dendouga N, Vergauwen K, Molenberghs B, Vranckx L, Willebrords R, Ristic Z, Lill H, Dorange I, Guillemont J, Bald D, Andries K. 2007. Diarylquinolines target subunit c of mycobacterial ATP synthase. Nat Chem Biol 3:323–324. https://doi.org/10.1038/nchembio884.
26. Haagsma AC, Podasca I, Koul A, Andries K, Guillemont J, Lill H, Bald D. 2011. Probing the interaction of the diarylquinoline TMC207 with its target mycobacterial ATP synthase. PLoS One 6:e23575. https://doi.org/10.1371/journal.pone.0023575.
27. Dupont C, Viljoen A, Thomas S, Roquet-Banères F, Herrmann J-L, Pethe K, Kremer L. 2017. Bedaquiline inhibits the ATP synthase in *Mycobacterium abscessus* and is effective in infected zebrafish. Antimicrob Agents Chemother 61:e01225-17. https://doi.org/10.1128/AAC.01225-17.
28. Biukovic G, Basak S, Manimekalai MSS, Rishikesan S, Roessle M, Dick T, Rao SPS, Hunke C, Grüber G. 2013. Variations of subunit {varepsilon} of the *Mycobacterium tuberculosis* F1Fo ATP synthase and a novel model for mechanism of action of the tuberculosis drug TMC207. Antimicrob Agents Chemother 57:168–176. https://doi.org/10.1128/AAC.01039-12.
29. Kundu S, Biukovic G, Grüber G, Dick T. 2016. Bedaquiline targets the ε subunit of mycobacterial F-ATP synthase. Antimicrob Agents Chemother 60:6977–6979. https://doi.org/10.1128/AAC.01291-16.
30. Pang Y, Zheng H, Tan Y, Song Y, Zhao Y. 2017. *In vitro* activity of bedaquiline against nontuberculous mycobacteria in China. Antimicrob Agents Chemother 61:e02627-16. https://doi.org/10.1128/AAC.02627-16.
31. Vesenbeckh S, Schönfeld N, Roth A, Bettermann G, Krieger D, Bauer TT, Rüssmann H, Mauch H. 2017. Bedaquiline as a potential agent in the treatment of *Mycobacterium abscessus* infections. Eur Respir J 49:1700083. https://doi.org/10.1183/13993003.00083-2017.
32. Obregón-Henao A, Arnett KA, Henao-Tamayo M, Massoudi L, Creissen E, Andries K, Lenaerts AJ, Ordway DJ. 2015. Susceptibility of *Mycobacterium*

abscessus to antimycobacterial drugs in preclinical models. Antimicrob Agents Chemother 59:6904–6912. https://doi.org/10.1128/AAC.00459-15.
33. Lerat I, Cambau E, Roth Dit Bettoni R, Gaillard J-L, Jarlier V, Truffot C, Veziris N. 2014. *In vivo* evaluation of antibiotic activity against *Mycobacterium abscessus*. J Infect Dis 209:905–912. https://doi.org/10.1093/infdis/jit614.
34. Philley JV, Wallace RJ, Benwill JL, Taskar V, Brown-Elliott BA, Thakkar F, Aksamit TR, Griffith DE. 2015. Preliminary results of bedaquiline as salvage therapy for patients with nontuberculous mycobacterial lung disease. Chest 148:499–506. https://doi.org/10.1378/chest.14-2764.
35. Cuthbertson L, Nodwell JR. 2013. The TetR family of regulators. Microbiol Mol Biol Rev 77:440–475. https://doi.org/10.1128/MMBR.00018-13.
36. Milano A, Pasca MR, Provvedi R, Lucarelli AP, Manina G, Ribeiro ALDJL, Manganelli R, Riccardi G. 2009. Azole resistance in *Mycobacterium tuberculosis* is mediated by the MmpS5-MmpL5 efflux system. Tuberculosis (Edinb) 89:84–90. https://doi.org/10.1016/j.tube.2008.08.003.
37. Hartkoorn RC, Uplekar S, Cole ST. 2014. Cross-resistance between clofazimine and bedaquiline through upregulation of MmpL5 in *Mycobacterium tuberculosis*. Antimicrob Agents Chemother 58:2979–2981. https://doi.org/10.1128/AAC.00037-14.
38. Halloum I, Viljoen A, Khanna V, Craig D, Bouchier C, Brosch R, Coxon G, Kremer L. 2017. Resistance to thiacetazone derivatives active against *Mycobacterium abscessus* involves mutations in the MmpL5 transcriptional repressor MAB_4384. Antimicrob Agents Chemother 61:e02509-16. https://doi.org/10.1128/AAC.02509-16.
39. Richard M, Gutiérrez AV, Viljoen AJ, Ghigo E, Blaise M, Kremer L. 2018. Mechanistic and structural insights into the unique TetR-dependent regulation of a drug efflux pump in *Mycobacterium abscessus*. Front Microbiol 9:649. https://doi.org/10.3389/fmicb.2018.00649.
40. Viljoen A, Blaise M, de Chastellier C, Kremer L. 2016. *MAB_3551c* encodes the primary triacylglycerol synthase involved in lipid accumulation in *Mycobacterium abscessus*. Mol Microbiol 102:611–627. https://doi.org/10.1111/mmi.13482.
41. Bailey TL, Boden M, Buske FA, Frith M, Grant CE, Clementi L, Ren J, Li WW, Noble WS. 2009. MEME Suite: tools for motif discovery and searching. Nucleic Acids Res 37:W202–W208. https://doi.org/10.1093/nar/gkp335.
42. Rominski A, Selchow P, Becker K, Brülle JK, Dal Molin M, Sander P. 2017. Elucidation of *Mycobacterium abscessus* aminoglycoside and capreomycin resistance by targeted deletion of three putative resistance genes. J Antimicrob Chemother 72:2191–2200. https://doi.org/10.1093/jac/dkx125.
43. Viljoen A, Gutiérrez AV, Dupont C, Ghigo E, Kremer L. 2018. A simple and rapid gene disruption strategy in *Mycobacterium abscessus*: on the design and application of glycopeptidolipid mutants. Front Cell Infect Microbiol 8:69. https://doi.org/10.3389/fcimb.2018.00069.
44. Griffith DE, Girard WM, Wallace RJ. 1993. Clinical features of pulmonary disease caused by rapidly growing mycobacteria. An analysis of 154 patients. Am Rev Respir Dis 147:1271–1278. https://doi.org/10.1164/ajrccm/147.5.1271.
45. Sermet-Gaudelus I, Le Bourgeois M, Pierre-Audigier C, Offredo C, Guillemot D, Halley S, Akoua-Koffi C, Vincent V, Sivadon-Tardy V, Ferroni A, Berche P, Scheinmann P, Lenoir G, Gaillard J-L. 2003. *Mycobacterium abscessus* and children with cystic fibrosis. Emerg Infect Dis 9:1587–1591. https://doi.org/10.3201/eid0912.020774.
46. Ripoll F, Pasek S, Schenowitz C, Dossat C, Barbe V, Rottman M, Macheras E, Heym B, Herrmann J-L, Daffé M, Brosch R, Risler J-L, Gaillard J-L. 2009. Non mycobacterial virulence genes in the genome of the emerging pathogen *Mycobacterium abscessus*. PLoS One 4:e5660. https://doi.org/10.1371/journal.pone.0005660.
47. Balhana RJC, Singla A, Sikder MH, Withers M, Kendall SL. 2015. Global analyses of TetR family transcriptional regulators in mycobacteria indicates conservation across species and diversity in regulated functions. BMC Genomics 16:479. https://doi.org/10.1186/s12864-015-1696-9.
48. Chen Y, Chen J, Zhang S, Shi W, Zhang W, Zhu M, Zhang Y. 2018. Novel mutations associated with clofazimine resistance in *Mycobacterium abscessus*. Antimicrob Agents Chemother 62:e00544-18. https://doi.org/10.1128/AAC.00544-18.
49. Alexander DC, Vasireddy R, Vasireddy S, Philley JV, Brown-Elliott BA, Perry BJ, Griffith DE, Benwill JL, Cameron ADS, Wallace RJ. 2017. Emergence of *mmpT5* variants during bedaquiline treatment of *Mycobacterium intracellulare* lung disease. J Clin Microbiol 55:574–584. https://doi.org/10.1128/JCM.02087-16.
50. Zhang S, Chen J, Cui P, Shi W, Zhang W, Zhang Y. 2015. Identification of novel mutations associated with clofazimine resistance in *Mycobacterium tuberculosis*. J Antimicrob Chemother 70:2507–2510. https://doi.org/10.1093/jac/dkv150.
51. Somoskovi A, Bruderer V, Hömke R, Bloemberg GV, Böttger EC. 2015. A mutation associated with clofazimine and bedaquiline cross-resistance in MDR-TB following bedaquiline treatment. Eur Respir J 45:554–557. https://doi.org/10.1183/09031936.00142914.
52. Andries K, Villellas C, Coeck N, Thys K, Gevers T, Vranckx L, Lounis N, de Jong BC, Koul A. 2014. Acquired resistance of *Mycobacterium tuberculosis* to bedaquiline. PLoS One 9:e102135. https://doi.org/10.1371/journal.pone.0102135.
53. Gupta S, Cohen KA, Winglee K, Maiga M, Diarra B, Bishai WR. 2014. Efflux inhibition with verapamil potentiates bedaquiline in *Mycobacterium tuberculosis*. Antimicrob Agents Chemother 58:574–576. https://doi.org/10.1128/AAC.01462-13.
54. Viljoen A, Dubois V, Girard-Misguich F, Blaise M, Herrmann J-L, Kremer L. 2017. The diverse family of MmpL transporters in mycobacteria: from regulation to antimicrobial developments. Mol Microbiol 104:889–904. https://doi.org/10.1111/mmi.13675.
55. Li H. 2013. Aligning sequence reads, clone sequences and assembly contigs with BWA-MEM. arXiv arXiv:1303-3997v2 [q-bio.GN].
56. Li H, Handsaker B, Wysoker A, Fennell T, Ruan J, Homer N, Marth G, Abecasis G, Durbin R, 1000 Genome Project Data Processing Subgroup. 2009. The sequence alignment/map format and SAMtools. Bioinformatics 25:2078–2079. https://doi.org/10.1093/bioinformatics/btp352.
57. Harris SR, Feil EJ, Holden MTG, Quail MA, Nickerson EK, Chantratita N, Gardete S, Tavares A, Day N, Lindsay JA, Edgeworth JD, de Lencastre H, Parkhill J, Peacock SJ, Bentley SD. 2010. Evolution of MRSA during hospital transmission and intercontinental spread. Science 327:469–474. https://doi.org/10.1126/science.1182395.
58. Aiyar A, Xiang Y, Leis J. 1996. Site-directed mutagenesis using overlap extension PCR. Methods Mol Biol 57:177–191. https://doi.org/10.1385/0-89603-332-5:177.

Table S1. List of bacterial strains and plasmids used in this study.

Name	Description/genotype	Marker	Reference
Strains			
M. abscessus S	*Mabs sensu stricto*, strain CIP104536^T, smooth	_	Laboratoire de Référence des Mycobactéries
M. abscessus R	*Mabs sensu stricto*, strain CIP104536 ^{T}, rough	_	Laboratoire de Référence des Mycobactéries
M. abscessus S	*Mabs sensu stricto*, strain ATCC 19977, smooth	_	ATCC
CFZ-R1	*M. abscessus* S harboring the L40W mutation in MAB_2299c, co-resistant to CFZ/BDQ	_	This study
CFZ-R3	*M. abscessus* S harboring a c276 deletion leading to a P92 frameshift mutation in MAB_2299c, co-resistant to CFZ/BDQ	_	This study
CFZ-R4	*M. abscessus* S harboring a g541t substitution leading to an early stop codon in position E181 in MAB_2299c, co-resistant to CFZ/BDQ	_	This study
CFZ-R6	*M. abscessus* S harboring a 318a insertion leading to a D106 frameshift mutation in MAB_2299c, co-resistant to CFZ/BDQ	_	This study
CFZ-R7	*M. abscessus* S harboring the L151P mutation in MAB_2299c, co-resistant to CFZ/BDQ	_	This study
CFZ-R9	*M. abscessus* S harboring the G215S mutation in MAB_2299c, co-resistant to CFZ/BDQ	_	This study
Δ*MAB_2299c*	*Mabs MAB_2299c* unmarked deletion mutant obtained by two-step homologous recombination in the smooth parental strain CIP104536^T	_	This study
Δ*MAB_2299c*.C	Δ*MAB_2299c* complemented with pMV261-*MAB_2299c*	Kan	This study
Δ*MAB_2299c* / Δ*MAB_2300-MAB_2301*	Δ*MAB_2299c* in which Δ*MAB_2300-2301* have been deleted by two-step homologous recombination.	_	This study
E. coli XL1 Blue	*endA1 gyrA96 recA1 thi-1 relA1 hsdR17 supE44 lac [F´ proAB lacIqZΔM15 Tn10 (Tetr)].*	Tet	Stratagene
E. coli BL21 (DE3) (pRARE2)	*gal dcm (DE3) F- ompT hsdSB(rB- mB-) transformed by our hand with the pRARE2 vector (CamR)*	Cam	New England Biolabs
Plasmids			

pET32a	Vector for high-level expression of proteins fused with an N-terminal thioredoxin protein and a 6×His tag.	Amp	Novagen
pET32a-*MAB_2299c*	pET32a in which *MAB_2299c* is cloned in fusion with the thioredoxin/His tag sequence and containing a TEV cleavage site before MAB_2299c to remove the tags.	Amp	This work
pET32a-*MAB_2299c_L40W*	pET32a into which the *MAB_2299c_L40W* gene is cloned.	Amp	This work
pUX1	Vector for targeted disruption through homologous integration, containing the brightly red fluorescent tdTomato marker for positive selection.	Kan, Hyg	(1)
pUX1-katG	Variant of pUX1 containing the *katG* gene of *M. tuberculosis* H37Rv as a counter-selectable marker in the presence of isoniazid and used for the generation of unmarked chromosomal alterations.	Kan, Hyg	This work
pUX1-katG-*MAB_2299c*	Variant of pUX1-katG containing adjacently cloned up- and downstream sequences (approximately 1 kb each) of the *MAB_2299c* open reading frame. Used to generate an unmarked deletion of *MAB_2299c* in *M. abscessus*.	Kan	This work
pUX1-katG-*MAB_2300-MAB_2301*	Variant of pUX1-katG containing adjacently cloned up- and downstream sequences (approximately 0.5 kb each) of the *MAB_2300-2301* operon. Used to generate an unmarked deletion of *MAB_2300* and *MAB_2301* in Δ*MAB_2299c*.	Kan	This work
pMV261	Multi-copy vector enabling the cloning into *E. coli* and the overexpression of genes under the control of the strong and constitutive *hsp60* promoter in mycobacteria.	Kan	(2)
pMV261-AflII	pMV261 vector where an AflII restriction site was inserted within the multi-cloning site.	Kan	(1)
pMV261-*MAB_2299c*	pMV261 overexpressing the TetR MAB_2299c under the control of the *hsp60* promoter.	Kan	This work

Amp, ampicillin; Kan, kanamycin; Tet, Tetracycline; Stp, streptomycin ; Cam, chloramphenicol.

References

1. Viljoen A, Gutiérrez, Ana Victoria, Dupont C, Ghigo E, Kremer L. 2018. A simple and rapid gene disruption strategy in Mycobacterium abscessus: on the design and application of glycopeptidolipid mutants. Front Cell Infect Microbiol 8:69.

2. Stover CK, de la Cruz VF, Fuerst TR, Burlein JE, Benson LA, Bennett LT, Bansal GP, Young JF, Lee MH, Hatfull GF. 1991. New use of BCG for recombinant vaccines. Nature 351:456–460.

Table S2: Oligonucleotides used in this study. Fw and Rv stand for forward and reverse, respectively.

Primers	5' to 3' sequence
Cloning in pET32a	
MAB_2299c_Fw (KpnI) (**TEV Cleavage Site**)	TATAGGTACC**GAGAATCTGTACTTCCAGGGA**GTGGCGCAACTGA CATTCCAACGCG
MAB_2299c_Rv (HindIII)	TCGTAAGCTTTTGGTTCGCCCAGGCGTACACGCGG
Cloning in pMV261	
Compl_MAB_2299c_Fw	CGCAACTGACATTCCAACGCGC
Compl_MAB_2299c_Rv (HindIII)	GAGAGAAAGCTTTTCTGGTGCACGTGAGAGTG
Generation of pUX1-*katG* and derivative constructs	
katG_outer_Fw	TATACCGGACTACGCCGAAC
katG_outer_Rev (AvrII)	GAGAGACCTAGGTGCATGAGCATTATCCCGTA
katG_inner_Fw	CCGGAGCCGCCAGCAACGGCT
katG_inner_Rev	AGCCGTTGCTGGCGGCTCCGG
MAB_2299c_outer_Fw	GAAGAACAGCAGCATCACGA
MAB_2299c_outer_Rev (NheI)	GAGAGAGCTAGCGACACCTTCGTTCACGGTTT
MAB_2299c_inner_Fw	AAAGAAGCGTCGCTCTGACCAGGCTGTTA
MAB_2299c_inner_Rev	GGTCAGAGCGACGCTTCTTTTCGTCAGTCC
MAB_2300-MAB_2301_outer_Fw	ACGCCTTAGCTTTTCCGTTT
MAB_2300-MAB_2301_outer_Rev (NheI)	GAGAGAGCTAGCGCAGATGTCAACAACCGATG
MAB_2300-MAB_2301_inner_Fw	TTGGATCCCGCAGCTCCGATCCGCGTGGT
MAB_2300-MAB_2301_inner_Rev	ATCGGAGCTGCGGGATCCAAGCCCGCTTC
PCR confirmation of *MAB_2299* knock-out	
MAB_2299c_U_scrn_Fw	GAAGATCGCGTAGTCGGTTC
MAB_2299c_U_scrn_Rev	ATCACCACAGATGACCCACA
MAB_2299c_D_scrn_Fw	CGCGTTTCATCAGGATCTTT
MAB_2299c_D_scrn_Rev	CTTTGGAGCATGGGCATATT
MAB_2300-MAB_2301_U_scrn_Fw	ATCACCACAGATGACCCACA
MAB_2300-MAB_2301_U_scrn_Rev	GTGCAGGAATTCTCATGCTG
MAB_2300-MAB_2301_D_scrn_Fw	GGAATCCGATCGGTAGTTGA
MAB_2300-MAB_2301_D_scrn_Rev	CGCTCATGCCGATTTCTTAG
Sequencing	
pMV5'	CGCCCGGCCAGCGTAAGTAGC
pMV3'	GCCTGGCAGTCGATCGTACG
pMV3' Ext	TTGAGACACAACGTCGCTTT
NheIpUX1	ACGGCATGGACGAGCTGTAC
qRT-PCR	
sigA	Fw: CACATGGTCGAGGTCATCAA Rev: TGGATTTCCAGCACCTTCTC
MAB_3551c (tgs1)	Fw: CACCGTCTACTACGGAATCAAC Rev: TGCGCAGCCTCCAATAAT
MAB_2300	Fw: GAGAAGCATGACCGACGACAAA Rev: CACACCCTTCCTTGTCGATGTAGTT
MAB_2301	Fw: CAGCTCCATCCCATTCCTTATC Rev: TCGGCCTGGACCTTCATA
MAB_2302	Fw: GAGATATTCGGCTCCACCAACATC

	Rev: CACAGATAGTTCACCTCACCCTTTGT
MAB_2303	Fw: ACATTCTCTGTCCCGATCATTC Rev: GTGCTCTTTACCGACCTCTTC
Eletrophoretic Mobility Shift Assay (EMSA)	
Probe A_Fw	GTGCGTAACGCACGCTACCGGGTGGTTCGTTGGCTCGCAAATCAC ACGCCGTGCGTTATCCTCG
Probe A_Rv	CACGCATTGCGTGCGATGGCCCACCAAGCAACCGAGCGTTTAGTG TGCGGCACGCAATAGGAGC
Probe B_Fw	CAGCTCCGATCCGCGTGGTGTCGG
Probe B_Rv	GCTAATTCTCAATGGTGCGATGCC
Probe C_Fw	TCGCCGCTAGTGGTGACGAACGAC
Probe C_Rv	TCAGGGAACTGTACATGTGTCGTC
Probe D_Fw	GCTTGTAGCTAACTAGGCTATTGC
Probe D_Rv	GACTAGTGGGATCCATACCCGCGT
Non-specific probe_Fw	CACTTCGCCATAAGTGGATTGACTCTATCCACTTTTACCCATAGA
Non-specific probe_Fw	TCTATGGGTAAAAGTGGATAGAGTCAATCCACTTATGGCGAAGTG
ΔPalin_Fw	GTGCGGCTACTTACCTACCGGGTGGTTCGTTGGCTCGCAAATCAC ACGCTCGCACGAGTCCTCG
ΔPalin_Rv	CACGCCGATGAATGGATGGCCCACCAAGCAACCGAGCGTTTAGT GTGCGAGCGTGCTCAGGAGC
ΔDR_Fw	GTGCGTAACGCACGCTTGATATACTGCTTAAGGCTCGCAAATCCT GACTTAGTGACCTTCCTCG
ΔDR_Rv	CACGCATTGCGTGCGAACTATATGACGAATTCCGAGCGTTTAGGA CTGAATCACTGGAAGGTCG

[a]Restriction sites are underlined and specified inside brackets.

Table S3. Drug susceptibility profile of *M. abscessus* CIP104536 and its various derivatives to IPM, BDQ, CFZ, INH, EMB or RIF. MIC_{99} (µg/ml) were visually determined on Middlebrook 7H10 agar after 4 days at 37°C.

Strain	MIC (µg/mL)					
	IPM	**BDQ**	**CFZ**	**INH**	**EMB**	**RIF**
CIP104536	4	0.25	2	>256	16	128
ΔMAB_2299c	4	1	8	>256	16	128
ΔMAB_2299c.C	4	0.25	2	>256	16	128
ΔMAB_2299c / ΔMAB_2300-MAB_2301	4	0.031	2	ND	ND	ND

IPM, imipenem; BDQ, bedaquiline; CFZ, clofazimine; INH, isoniazid; EMB, ethambutol; RIF, rifampicin. ND, not determined.

Table S4. Percentage of nucleotide or protein sequence identity (ID) between seventeen identified *M. abscessus mmpS-mmpL* couples and the *M. tuberculosis mmpS5-mmpL5* couple after multiple alignment using the MUSCLE algorithm.

MmpS/MmpL	Nucleotide ID[a]	MmpS ID	MmpL ID
Rv0677c-Rv0676c	100	100	100
MAB_0477-MAB_0478	75	35	44
MAB_0988c-MAB_0987c	79	46	57
MAB_1135c-MAB_1134c	80	49	60
MAB_2036-MAB_2037	75	38	52
MAB_2211c-MAB_2210c	73	36	38
MAB_2300-MAB_2301	**80**	**49**	**62**
MAB_2302-MAB_2303	**77**	**47**	**54**
MAB_2572c-MAB_2571c	75	41	20
MAB_2649-MAB_2650	77	41	52
MAB_3149-MAB_3150	80	54	61
MAB_3200-MAB_3201	73	35	42
MAB_3563c-MAB_3562c	77	38	51
MAB_4117c-MAB_4115c[b]	36	48	61, 59[b]
MAB_4262-MAB_4263	72	27	38
MAB_4311c-MAB_4310c	78	50	54
MAB_4383c-MAB_4384c	**82**	**61**	**68**
MAB_4705c-MAB_4703c[b]	35	51	60, 62[b]

[a]For nucleotide alignments and ID calculations, the sequence starting at the start codon of the *mmpS* gene and ending at the stop codon of the *mmpL* gene was used.
[b]*mmpS/mmpL* couples containing an additional mmpL in the operon. For MmpL protein sequence identity to $MmpL5_{Mtb}$ the % ID of the first MmpL is shown first followed by a comma and then the % ID of the second MmpL.

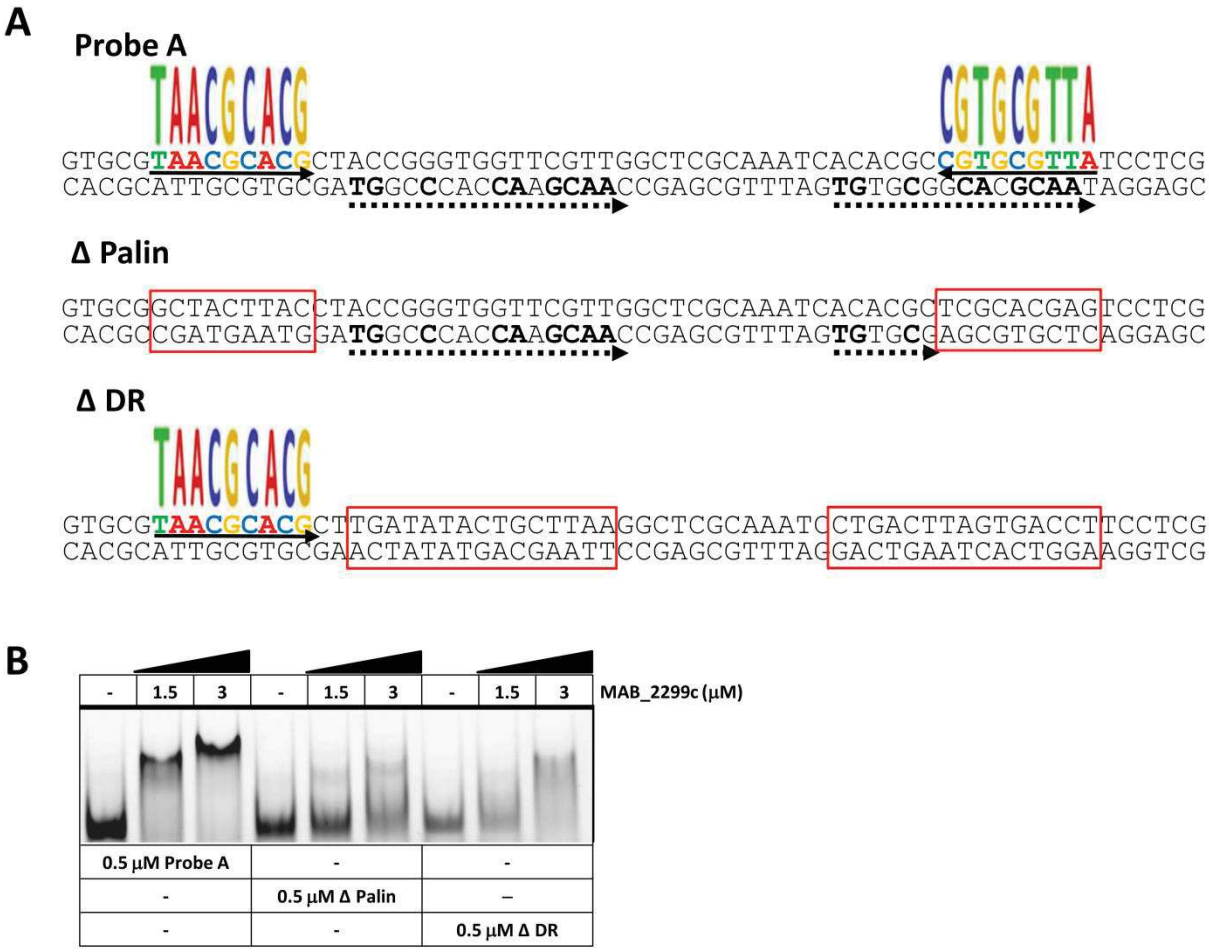

Fig. S1. Binding activity of MAB_2299c to mutated Probe A. (A) DNA sequences of Probe A and its two mutated derivatives, ΔPalin and ΔDR, where the conserved palindromes and the degenerated double repeats were replaced by random nucleotides, respectively. Conserved residues are in color for the palindromes and in bold for the double repeats. **(B)** EMSA using the Probes A, ΔPalin and ΔDR with purified MAB_2299c. Gel Shifts were revealed by fluorescence emission using the corresponding 5' fluorescein-labeled probes.

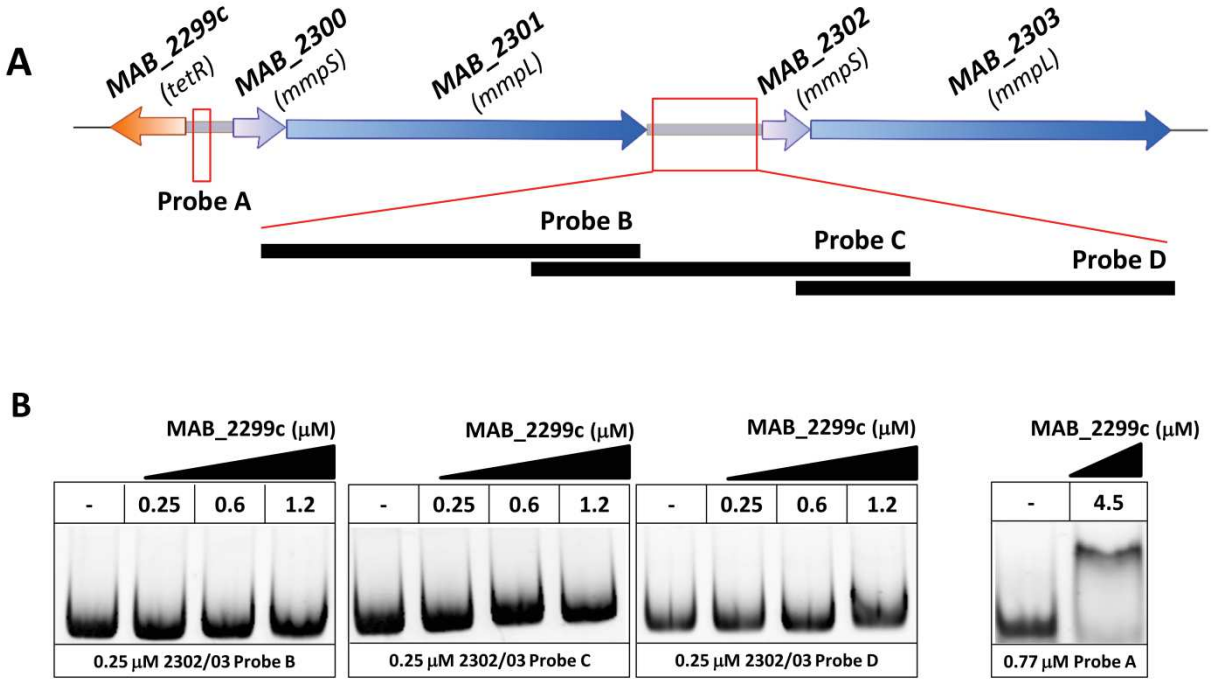

Fig. S2. (A) Schematic representation of the intergenic region $IR_{2302/03}$ present upstream of *MAB_2302/MAB_2303*. Due to its large size, this 893 bp region was divided into three 373 bp overlapping probes (Probes B – C – D). **(B)** EMSA using increasing concentrations of purified MAB_2299c with Probe A (left panel), Probe B (middle panel) or Probe C (right panel). Probe A was also included as a positive control (far right panel). Gel shifts were revealed by fluorescence emission using 5' fluorescein-labeled probes. Experiments were repeated three times with similar results.

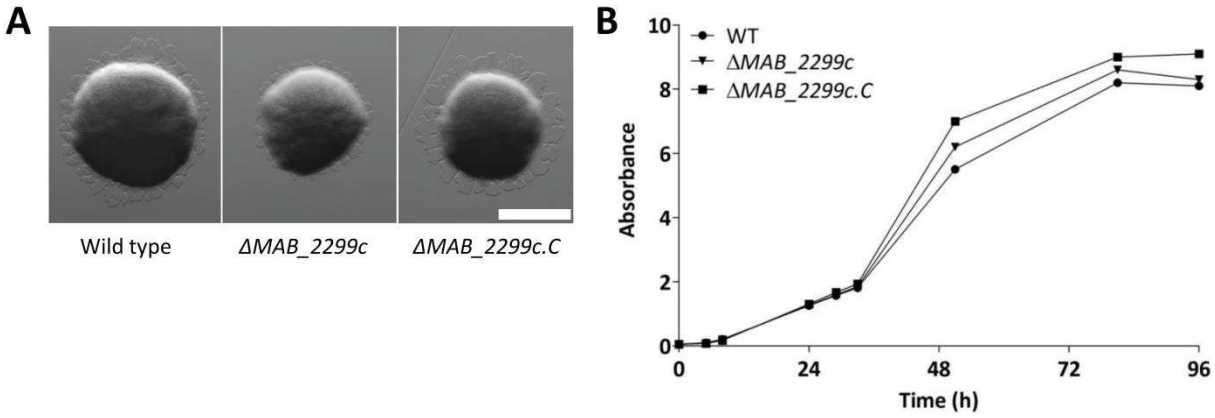

Fig. S3. Colony morphology **(A)** and *in vitro* growth **(B)** of parental *M. abscessus* WT CIP104536^T, *ΔMAB_2299c* and its complemented derivative *ΔMAB_2299c.C*. Bacteria were grown in 7H9 broth supplemented with OADC and 0.05% Tween 80. Growth was monitored by determining the OD_{600} at different time points. Scale bar corresponds to 150 µm.

Article 3

« **The TetR Family Transcription Factor MAB_2299c Regulates the Expression of Two Distinct MmpS-MmpL Efflux Pumps Involved in Cross-Resistance to Clofazimine and Bedaquiline in *Mycobacterium abscessus*.** ». Gutiérrez AV*, Richard M*, Roquet-Banères F, Viljoen A, Kremer L (* = contribution égale) Antimicrob Agents Chemother.2019 September 23 ; Volume 63 Issue 10.

L'abondance à la fois des régulateurs TetR et des protéines de type MmpL chez *M. abscessus* suggère fortement la possibilité que d'autres couples régulateur/MmpL soient impliqués dans l'export des antibiotiques. Une étude phylogénétique des protéines MmpL chez *M. abscessus* a révélé que la paire MmpS/MmpL codée par *MAB_1135c/MAB_1134c* résulterait d'une duplication génique de *MAB_2300/MAB_2301*. L'analyse *in silico* de la région intergénique située en amont de *MAB_1135c/MAB_1134c* a révélé la présence d'une séquence palindromique identique mais de taille totale plus courte que celle reconnue par MAB_2299c retrouvée en amont de *MAB_2300/MAB_2301* (voir **Article 2**). Des expériences d'EMSA entre MAB_2299c et cette nouvelle région palindromique ont montré que ce régulateur est également capable de se lier à la séquence d'ADN située en amont de *MAB_1135c/MAB_1134c*. Une analyse des transcrits de tous les *mmpL* issue du mutant Δ*MAB_2299c*a révélé un niveau plus élevé des ARNm de *MAB_2300/MAB_2301* sans surprise, mais aussi de *MAB_1135c*/*MAB_1134c* par rapport à la souche sauvage, suggérant que MAB_2299c agisse également comme répresseur sur la pompe à effluxMAB_1135c/MAB_1134c. Nous avons généré, grâce à notre nouvelle technique de mutagénèse pUX1-*katG* (**Article 2**) un quintuple mutant Δ*MAB_2299c* – Δ*MAB_2300/2301* – Δ*MAB_1135c/1134c* qui présente une hypersusceptiblité à la CFZ et à la BDQ. Ce phénotype a également été mis en évidence dans des macrophages humains infectés. L'ensemble de cette étude démontre que le régulome *MAB_2299c* – MAB_*2300/2301* – *MAB_1135c/1134c* joue un rôle dans la multi-résistance intrinsèque de *M. abscessus* à deux antibiotiques qui sont structuralement différents et actuellement en cours d'évaluation clinique dans le traitement des infections à *M. abscessus*. *MAB_2299c* pourrait donc représenter un marqueur de résistance à prendre en considération dans la détermination du profil de susceptibilité/résistance d'isolats cliniques issus de patients traités avec la BDQ et la CFZ.

AMERICAN SOCIETY FOR MICROBIOLOGY | Antimicrobial Agents and Chemotherapy®

MECHANISMS OF RESISTANCE

The TetR Family Transcription Factor MAB_2299c Regulates the Expression of Two Distinct MmpS-MmpL Efflux Pumps Involved in Cross-Resistance to Clofazimine and Bedaquiline in *Mycobacterium abscessus*

Ana Victoria Gutiérrez,[a] Matthias Richard,[a] Françoise Roquet-Banères,[a] Albertus Viljoen,[a]* Laurent Kremer[a,b]

[a]Institut de Recherche en Infectiologie de Montpellier (IRIM), Université de Montpellier, CNRS UMR 9004, Montpellier, France
[b]INSERM, IRIM, Montpellier, France

ABSTRACT *Mycobacterium abscessus* is a human pathogen responsible for severe respiratory infections, particularly in patients with underlying lung disorders. Notorious for being highly resistant to most antimicrobials, new therapeutic approaches are needed to successfully treat *M. abscessus*-infected patients. Clofazimine (CFZ) and bedaquiline (BDQ) are two antibiotics used for the treatment of multidrug-resistant tuberculosis and are considered alternatives for the treatment of *M. abscessus* pulmonary disease. To get insights into their mechanisms of resistance in *M. abscessus*, we previously characterized the TetR transcriptional regulator MAB_2299c, which controls expression of the *MAB_2300-MAB_2301* genes, encoding an MmpS-MmpL efflux pump. Here, *in silico* studies identified a second *mmpS-mmpL* (*MAB_1135c-MAB_1134c*) target of MAB_2299c. A palindromic DNA sequence upstream of *MAB_1135c*, sharing strong homology with the one located upstream of *MAB_2300*, was found to form a complex with the MAB_2299c regulator in electrophoretic mobility shift assays. Deletion of *MAB_1135c-1134c* in a wild-type strain led to increased susceptibility to both CFZ and BDQ. In addition, deletion of these genes in a CFZ/BDQ-susceptible mutant lacking *MAB_2299c* as well as *MAB_2300-MAB_2301* further exacerbated the sensitivity of this strain to both drugs *in vitro* and inside macrophages. Overall, these results indicate that *MAB_1135c-1134c* encodes a new MmpS-MmpL efflux pump system involved in the intrinsic resistance to CFZ and BDQ. They also support the view that MAB_2299c controls the expression of two separate MmpS-MmpL efflux pumps, substantiating the importance of *MAB_2299c* as a marker of resistance to be considered when assessing drug susceptibility in clinical isolates.

KEYWORDS EMSA, MmpL, *Mycobacterium abscessus*, TetR regulator, bedaquiline, clofazimine, drug resistance mechanisms, efflux pumps

Mycobacterium abscessus is a rapidly growing nontuberculous mycobacterium (NTM) and an emerging pathogen that causes sporadic outbreaks worldwide (1). The *M. abscessus* complex comprises three subspecies, *M. abscessus sensu stricto*, *Mycobacterium bolletii*, and *Mycobacterium massiliense* (2, 3), differing in their drug susceptibility profile and evolution (4). Genomic analyses indicated that, in addition to specific genes linked to mycobacterial virulence, other virulence genes found in *Pseudomonas aeruginosa* and *Burkholderia cepacia*, pathogens commonly isolated from the lungs of cystic fibrosis (CF) patients and acquired by horizontal transfer, are also present in *M. abscessus* (5, 6). Likewise, the *M. abscessus* complex represents the most important cause of pulmonary infections by rapidly growing NTM in patients with chronic lung diseases, such as bronchiectasis and CF (7, 8), which can result in nodular and cavitary granulomas and persistent lung infection (7–10). Patients with chronic *M. abscessus*

Citation Gutiérrez AV, Richard M, Roquet-Banères F, Viljoen A, Kremer L. 2019. The TetR family transcription factor MAB_2299c regulates the expression of two distinct MmpS-MmpL efflux pumps involved in cross-resistance to clofazimine and bedaquiline in *Mycobacterium abscessus*. Antimicrob Agents Chemother 63:e01000-19. https://doi.org/10.1128/AAC.01000-19.

Address correspondence to Laurent Kremer, laurent.kremer@irim.cnrs.fr.

* Present address: Albertus Viljoen, Louvain Institute of Biomolecular Science and Technology, Université Catholique de Louvain, Louvain-la-Neuve, Belgium.

A.V.G. and M.R. contributed equally to this work.

Received 14 May 2019
Returned for modification 23 June 2019
Accepted 19 July 2019
Accepted manuscript posted online 22 July 2019
Published 23 September 2019

infections present higher rates of pulmonary function decline than those without NTM infections (11). Recent epidemiological studies also documented the transmission of dominant circulating *M. abscessus* clones that have spread globally between hospitals (12), highlighting *M. abscessus* as a major threat in many CF centers worldwide (8).

A recent meta-analysis reported that the treatment success rate across all patients with *M. abscessus* pulmonary disease was 45.6%, reaffirming that treatment outcomes are unsatisfactory (13). *M. abscessus* treatment remains very challenging. The American Thoracic Society (ATS)/Infectious Disease Society of America recommend multidrug therapy that includes a macrolide and one or more parenteral drugs (amikacin plus cefoxitin or imipenem) (7). *M. abscessus* has developed a large panel of drug resistance mechanisms that considerably restrict the available antimicrobials to treat these infections (14–16). They include the acquisition of mutations in the target genes, intrinsic resistance to drugs attributed to low permeability of the *M. abscessus* cell envelope, defective drug-activating systems that convert prodrugs into metabolically active compounds, induction of drug export systems, and the expression of numerous enzymes that can modify either the drug target or the drug itself (15, 17). Overall, this leads to the phenomenal resistance level of *M. abscessus* to most classes of antibiotics used for treatment of other infectious diseases, such as macrolides, aminoglycosides, rifamycins, β-lactams, quinolones, and tetracyclines.

Fueling a drug pipeline to discover and develop improved and safer treatments for *M. abscessus* infections relies on *de novo* drug discovery to identify new pharmacophores as well as repositioning of antimicrobials acting against validated targets for other infectious diseases (18). In this context, the repositioning of clofazimine (CFZ) and bedaquiline (BDQ) is gaining increasing interest for the treatment of *M. abscessus* pulmonary disease. CFZ is an orally administered drug, originally approved for the treatment of leprosy, that is reduced by the type 2 NADH:quinone oxidoreductase, a key component in the electron transport chain (19). *In vitro* studies highlighted its advantages in multidrug regimens against *M. abscessus*, acting in synergism with amikacin (AMK) (20) or tigecycline (TIG) (21) and in preventing bacterial regrowth observed with clarithromycin or AMK alone (22). BDQ, approved by the Food and Drug Administration and the European Medicines Agency for the treatment of multidrug-resistant tuberculosis, is a diarylquinoline that targets the ATP synthase in *M. tuberculosis* (23). We and others showed that BDQ exhibits very low MICs against NTM, including clinical *M. abscessus* strains from CF and non-CF patients (24–26). However, despite being a potent growth inhibitor at low concentrations, BDQ lacks bactericidal activity against *M. abscessus* (26, 27). In the *M. abscessus* zebrafish model of infection, BDQ acts very efficiently by reducing the number and size of abscesses, which represent a marker of disease severity and uncontrolled infection (28), protecting the infected larvae from killing by *M. abscessus* (26). The mode of action of BDQ in *M. abscessus* relies on the rapid depletion of ATP, and the transfer of single point mutations into the chromosomal *atpE* locus conferred high resistance levels to BDQ (26). In addition to *atpE*, mutations associated with cross-resistance to CFZ and BDQ were recently uncovered in *MAB_2299c*, encoding a TetR-family transcription factor that controls the expression level of the MmpS-MmpL (MAB_2300-2301) efflux pump (29).

Considering the extremely high number of TetR regulators and MmpL proteins in *M. abscessus* (30), it remains possible that additional TetR-dependent MmpS-MmpL efflux pump systems contribute to the drug resistance profile of *M. abscessus* to CFZ and BDQ. In this study, we identified a new *mmpS-mmpL* gene cluster (*MAB_1135c-MAB_1134c*; termed *MAB_1135c-1134c*) whose expression is also dependent on the MAB_2299c TetR repressor. Genetic approaches were used to demonstrate that this gene cluster participates in cross-resistance to both CFZ and BDQ. These findings expand our current understanding about transcriptional regulation of the MmpS-MmpL efflux pumps in mycobacteria and mechanisms of drug resistance in one of the most difficult-to-treat mycobacterial species.

RESULTS

Identification of *MAB_1135c-1134c* as a close paralog of *MAB_2300-2301*. We recently demonstrated that mutations in the TetR regulator MAB_2299c lead to upregulation of the *MAB_2300-2301* gene cluster, encoding the MmpS-MmpL efflux pump membrane proteins accounting for cross-resistance to CFZ and BDQ in *M. abscessus* (29). With the objective to identify other potential MmpS-MmpL couples that are functionally homologous to MAB_2300-2301 and participate in CFZ/BDQ resistance, we performed a homology analysis of all *M. abscessus* MmpS and MmpL paralogs as well as all of the TetR family transcription factors present in close genomic vicinity to these MmpS-MmpL couples. This analysis identified MAB_1135c-1134c as the closest paralogous MmpS-MmpL couple to MAB_2300-2301 (Fig. 1A). In addition, the TetR protein MAB_1136, whose gene is located upstream of *MAB_1135c*, was uncovered as the closest homologue of MAB_2299c. Indeed, a comparison of the two loci that contain the *mmpS-mmpL* genes as well as their adjacent upstream (containing the *tetR* genes and their nucleotide target sequences) and downstream nucleotide sequences suggests that one of the two *tetR-mmpS-mmpL* clusters arose as a duplication of the other (Fig. 1B), representing these genes as potential candidates in CFZ/BDQ cross-resistance.

Expression of *MAB_1135c-1134c* is not controlled by the TetR regulator MAB_1136. Careful inspection of the genomic organization around the *MAB_1135c-1134c* locus indicated that *MAB_1136* is an adjacent and divergently orientated gene (Fig. 2A). To test the hypothesis that this potential regulator controls the expression of the *MAB_1135c-1134c* gene cluster, a *MAB_1136* deletion mutant was produced. This was achieved by using a recently developed strategy based on a new suicide vector, pUX1-*katG*, allowing easy and rapid generation of unmarked genetic deletions in the *M. abscessus* chromosome, facilitated by the presence of the brightly red fluorescent tdTomato positive selectable marker and the *katG* counterselectable marker (29, 31, 32). The selected INH-resistant, KAN-sensitive, and nonfluorescent clones were subsequently genotyped by PCR/sequencing analysis to confirm unmarked deletion of *MAB_1136* (Fig. 2A).

The drug susceptibility pattern of the Δ*MAB_1136* strain and its parental progenitor to imipenem (IPM; control drug), CFZ, and BDQ was next assessed by comparing growth on agar plates containing the corresponding drugs (Fig. 2B). The two strains displayed similar growth on agar supplemented with 16 μg/ml IPM, 0.125 μg/ml BDQ, or 1 μg/ml CFZ, indicating that the absence of *MAB_1136* does not influence the sensitivity of the strain to these compounds. These results were subsequently confirmed by the failure of the Δ*MAB_1136* strain to show an upshift in the MIC levels (Table 1). Hypothesizing that MAB_1136 represses transcriptional expression of *MAB_1135c-1134c*, quantitative reverse transcription-PCR (qRT-PCR) analysis was performed, which failed to show increased expression of *MAB_1134c* or *MAB_1135c* in the Δ*MAB_1136* strain (data not shown). Together, these results suggest that expression of *MAB_1135c-1134c* is not controlled by MAB_1136.

The TetR regulator MAB_2299c represses expression of *MAB_1135c-1134c*. As mentioned above, our *in silico* study revealed a high level of primary protein sequence identity between MAB_1136 and MAB_2299c (Fig. 1A), which might point to a role for the latter in transcriptional repression of *MAB_1135c-1134c* in the absence of such a function of the former. Interestingly, we recently identified MAB_2299c as a TetR transcriptional regulator that represses its *mmpS-mmpL* (*MAB_2300-2301*) target genes and found that different single-point mutations in MAB_2299c were associated with upregulation of the *MAB_2300-2301* efflux pump system, leading to cross-resistance to CFZ and BDQ (29). Therefore, to interrogate whether MAB_2299c regulates other target genes belonging to the MmpS-MmpL systems, qRT-PCR was performed on 30 *mmpL* genes identified in the *M. abscessus* chromosome (30) in a Δ*MAB_2299c* deletion mutant (29). This systematic analysis clearly indicated that, in addition to *MAB_2301*, identified previously (29), only one other *mmpL* gene (*MAB_1134c*) was upregulated in the Δ*2299c* strain (Fig. 3A).

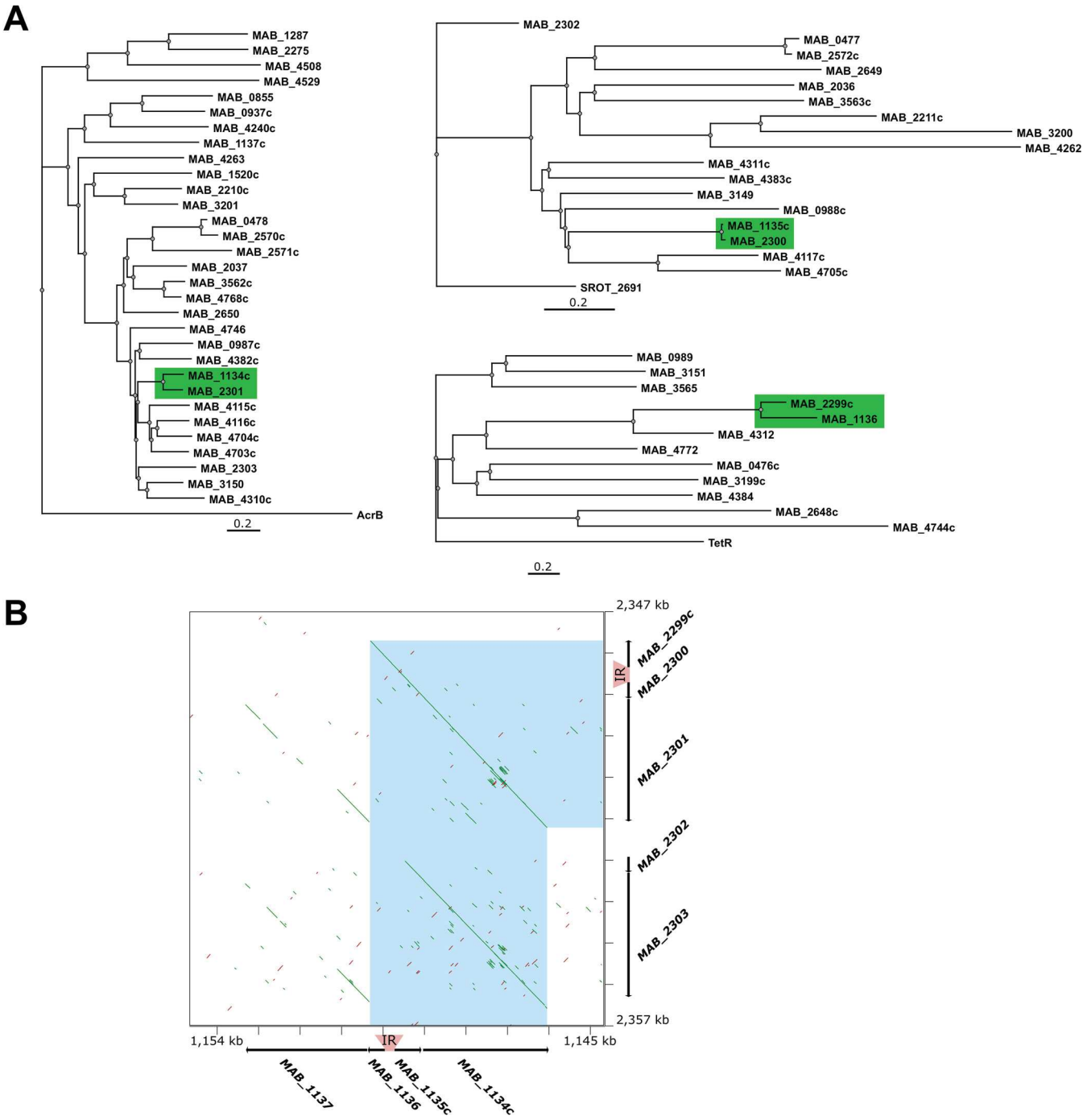

FIG 1 Closest paralogs of the MmpS-MmpL couple MAB_2300-2301, MAB_1135c-1134c, arose as a result of a gene duplication event. (A) Homology trees of all *M. abscessus* MmpL (left), all *M. abscessus* MmpS (top right), and several *M. abscessus* TetR/MarR family transcriptional regulators in close proximity to MmpS-MmpL couples (bottom right). The scale bar below each tree indicates 0.2 amino acid substitutions per site. The trees were rooted to *Escherichia coli* AcrB (MmpL) and TetR (transcriptional regulator) and *Segniliparus rotundus* MmpS ortholog SROT_2691 (MmpS). (B) Dot plot generated using the YASS genomic similarity tool (http://bioinfo.lifl.fr/yass/yass.php), showing nucleotide similarity between the *MAB_2299c-2300-2301* and the *MAB_1136-1135c-1134c* loci (highlighted by a light blue inverted-L-shaped box). Green lines indicate forward matches, and red lines indicate reverse matches. The intergenic regions (IR) between the *tetR* genes (*MAB_2299c* and *MAB_1136*) and the *mmpS* genes (*MAB_2300* and *MAB_1135c*) are highlighted by light gray trapezoidal boxes.

Increased transcription of both *mmpS-mmpL* gene clusters (*MAB_1135c-1134c* and *MAB_2300-2301*) was next confirmed by additional qRT-PCR analysis in both the parental *M. abscessus* smooth (S) strain and in the Δ*MAB_2299c* strain (Fig. 3B). Complementation of the Δ*MAB_2299c* strain by introducing the pMV261-*MAB_2299c* construct (Δ*MAB_2299c*.C) led to reduced transcriptional levels of both *mmpS-mmpL*

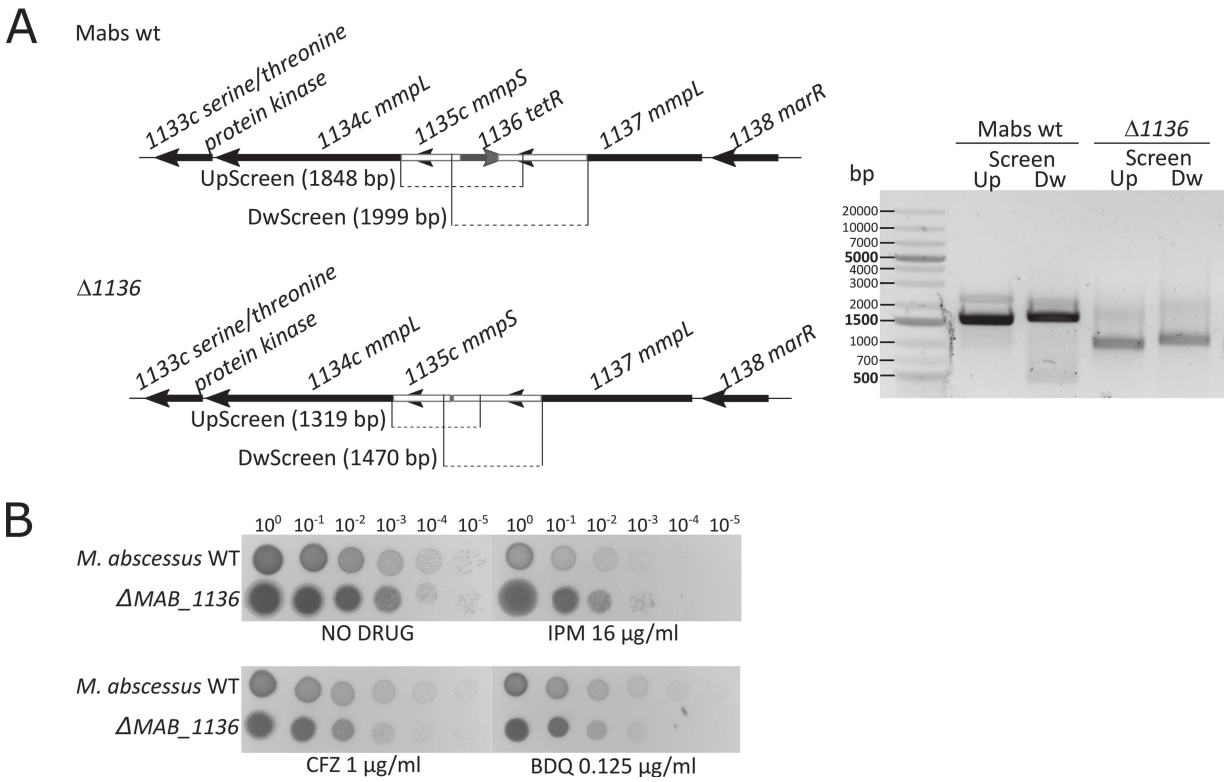

FIG 2 Deletion of *MAB_1136* does not confer resistance to CFZ or BDQ. (A) Genome organization of *MAB_1136* in *M. abscessus* and the screening approach used to confirm deletion of *MAB_1136*. White lines in the drawing represent the left and right arms flanking the region of *MAB_1136* targeted for deletion and exploited in the two-step homologous recombination procedure to generate the Δ*MAB_1136* strain. (Left) Dotted lines represent the size of the expected PCR products in *M. abscessus* WT and Δ*MAB_1136* strains. (Right) Gel migration profile of the amplicons in *M. abscessus* WT and Δ*MAB_1136* strains. All PCR products were purified and sequenced to confirm the *MAB_1136* deletion genotype. Up stands for upstream and Dw stands for downstream amplicons. (B) Susceptibility/resistance profiles of *M. abscessus* WT and Δ*MAB_1136* strains to various drugs. Five microliters of a 10-fold serially diluted bacterial suspension was spotted on 7H10^{OADC} alone or supplemented with 16 μg/ml imipenem (IPM), 1 μg/ml clofazimine (CFZ), or 0.125 μg/ml bedaquiline (BDQ). Growth was observed after 4 days of incubation at 37°C. All experiments were done on three independent occasions.

pairs, as anticipated. The expression levels of the unrelated control gene *tgs1*, encoding the triacylglycerol synthase involved in the synthesis and accumulation of triglycerides in *M. abscessus* (33), remained unchanged in the various strains tested. As anticipated, the 6 CFZ-resistant mutants harboring mutations in MAB_2299c and associated with upregulation of the *MAB_2300-2301* efflux pump system (29) also expressed higher transcriptional levels of *MAB_1135c* and *MAB_1134c* (see Fig. S1 in the supplemental material). Together, these results indicate that expression of both *MAB_2300-2301* and *MAB_1135c-1134c* gene couples is repressed by MAB_2299c under normal growth conditions.

TABLE 1 Drug susceptibility/resistance profile of WT CIP104536, Δ*MAB_2299c*, Δ*MAB_1135c-1134c*, Δ*MAB_2299c-2300-2301*, Δ*MAB_2299c-2300-2301-1135c-1134c*, and Δ*MAB_1136* strains to various drugs

Strain	MIC_{99} (μg/ml)							
	IPM[a]	AMK	EMB	CFZ	TIG	LNZ	MOX	BDQ
CIP104536	8	16	16	2	16	64	32	0.25
Δ*MAB_2299c*	8	16	16	4	16	64	32	0.5
Δ*MAB_1135c-1134c*	8	16	16	0.5	16	64	32	0.125–0.06
Δ*MAB_2299c-2300-2301*	8	16	16	0.5	16	64	32	0.03–0.015
Δ*MAB_2299c-2300-2301-1135c-1134c*	8	16	16	0.25	16	64	32	0.015–0.0075
Δ*MAB_1136*	8	16	16	1	ND	ND	ND	0.125

[a]MIC_{99} values were visually determined on Middlebrook 7H10 agar after 4 days at 37°C. IPM, imipenem; AMK, amikacin; BDQ, bedaquiline; CFZ, clofazimine; EMB, ethambutol; TIG, tigecycline; LNZ, linezolid; MOX, moxifloxacin; ND, not determined.

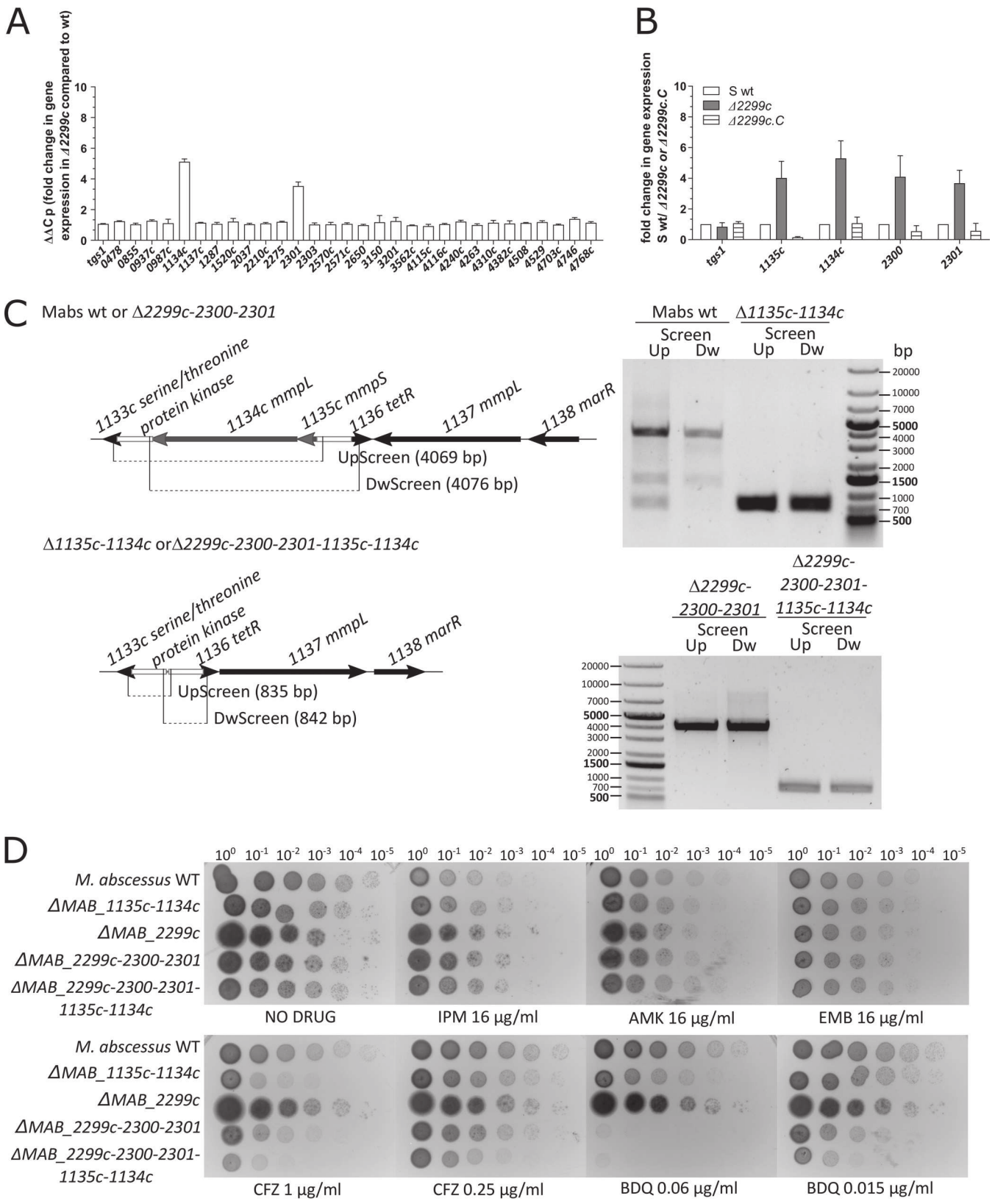

FIG 3 MAB_2299c represses expression of two distinct MmpS-MmpL efflux pump systems. (A) qRT-PCR analysis showing the transcriptional expression profile of 30 *mmpL* genes in the Δ*MAB_2299c* strain. (B) qRT-PCR analysis showing the transcriptional profiles of the *mmpS-mmpL* couples *MAB_1135c-1134c* and *MAB_2300-2301* in *M. abscessus* WT, the Δ*MAB_2299c* strain, and its Δ*MAB_2299c*.C complemented derivative. Results are expressed as fold induction levels in the mutant strains relative to levels of the parental strain. Error bars indicate standard deviations. Relative gene expression was calculated using the $2^{-\Delta\Delta CT}$ method with E correction. Data are representative of two independent experiments. (C) Genome organization of the *mmpS-mmpL* couple *MAB_1135c-1134c* in

(Continued on next page)

Unmarked deletion of the *MAB_1135c-1134c* efflux pump leads to increased susceptibility to CFZ and BDQ. Using the same strategy as that used to produce the Δ*MAB_1136* strain, a two-step homologous recombination procedure was first applied to generate a scarless deletion of *MAB_1135c-1134c* in the *M. abscessus* wild type (WT) (Fig. 3C, left). This unmarked deletion mutant, designated the Δ*MAB_1135c-1134c* strain, was subjected to PCR and sequencing analysis to confirm gene deletion (Fig. 3C, upper right). Although WT and Δ*MAB_1135c-1134c* strains displayed similar growth on agar without drugs or agar supplemented with 16 μg/ml IPM, AMK, or ethambutol (EMB), the mutant strain showed reduced growth in the presence of 1 μg/ml CFZ or 0.06 μg/ml BDQ (Fig. 3D). These results were confirmed by determination of the MIC values of CFZ and BDQ against the Δ*MAB_1135c-1134c* strain, which were almost 4 times lower than those of the parental strain (Table 1). Overall, this increased susceptibility to both drugs strongly suggests that MAB_1135c-1134c plays a role in intrinsic resistance to these compounds. That no differences in MIC values were observed with the unrelated drugs IPM, AMK, and EMB indicates that the drug efflux mechanism mediated by MAB_1135c-1134c is specific to CFZ and BDQ.

Since we previously demonstrated that a mutant lacking *MAB_2299c* and *MAB_2300-2301* was more sensitive to CFZ/BDQ, we next addressed whether the additional deletion of *MAB_1135c-1134c* in this mutant strain would further increase the susceptibility to these drugs. This was achieved by generating an unmarked deletion of *MAB_1135c-1134c* in the Δ*MAB_2299c-2300-2301* background (Fig. 3C). PCR analyses confirmed deletion of the genes, yielding a strain missing 5 genes: *MAB_2299c*, encoding the central transcriptional regulator, and its two pairs of *mmpS-mmpL* target genes. Whereas this quintuple mutant exhibited growth similar to that of the WT strain or the parental Δ*MAB_2299c-2300-MAB_2301* triple mutant in the absence of drugs (control plates) or in the presence of IPM, AMK, or EMB, it showed increased sensitivity to both CFZ and BDQ (Fig. 3D). The near absence of growth of the quintuple mutant in the presence of 0.06 μg/ml BDQ indicates that deletion of the second MmpS-MmpL couple further enhances the level of susceptibility of the strain. The MIC values of the quintuple mutant were 8-fold lower for CFZ and 16- to 32-fold lower for BDQ than those of the WT strain and 2-fold lower for both drugs compared to levels for the triple mutant lacking only one MmpS-MmpL pair (Table 1). The multiple deletion had no effect on the MIC of other drugs, including IPM, AMK, EMB, moxifloxacine (MOX), linezolid (LNZ), and tigecycline (TIG) (Table 1). As expected, the Δ*MAB_2299c* strain, in which both *MAB_2300-2301* and *MAB_1135c-1134c* are induced (Fig. 3B), failed to show growth inhibition in the presence of CFZ or BDQ (Fig. 3D) and displayed a 2-fold increased resistance to both drugs compared to that of the WT strain, as reported previously (29).

Collectively, these results indicate that both the *MAB_2300-2301* and the *MAB_1135c-1134c* efflux pump systems operate simultaneously in the resistance mechanism in *M. abscessus* against CFZ and BDQ.

MAB_2299c binds to a palindromic sequence upstream of *MAB_1135c*. We previously demonstrated that MAB_2299c binds to a palindromic sequence upstream of *MAB_2300*. That MAB_2299c also represses transcription of *MAB_1135c-1134c* suggested that it recognizes a conserved DNA-binding site located upstream of *MAB_1135c*. Using the MEME Suite software, we identified in the intergenic region upstream of *MAB_1135c* two palindromic sequences comprised of 7 nucleotides that

FIG 3 Legend (Continued)
M. abscessus and the screening approach for identification of Δ*MAB_1135c-1134c* in the *M. abscessus* WT and Δ*MAB_2299c-2300-2301* genetic backgrounds. White lines in the drawing represent the left and right arms of homology involved in two-step homologous recombination with the pUX1-*katG-MAB_1135c-1134c* suicide vector. Dotted lines represent the size of the expected PCR products in the WT and Δ*MAB_1135c-1134c* strains (left), along with the corresponding gel migration profile (right). All PCR products were purified and sequenced to confirm the *MAB_1135c-1134c* deletion genotype. (D) Susceptibility/resistance profiles of *M. abscessus* WT, Δ*MAB_2299c*, Δ*MAB_1135c-1134c*, Δ*MAB_2299c-2300-2301*, and Δ*MAB_2299c-2300-2301-1135c-1134c* strains to various drugs. Tenfold serially diluted bacterial suspensions were spotted (5 μl) on $7H10^{OADC}$ alone or supplemented with 16 μg/ml imipenem (IPM), 16 μg/ml amikacin (AMK), 16 μg/ml ethambutol (EMB), 0.25 μg/ml or 1 μg/ml clofazimine (CFZ), or 0.06 μg/ml or 0.015 μg/ml bedaquiline (BDQ). Growth was observed after 4 days of incubation at 37°C. All experiments were done on two separate occasions.

are fully conserved with those found in the DNA-binding site upstream of *MAB_2300* (Fig. 4A). However, a major difference between the two sequences relies on a short spacer between the two palindromic sequences upstream of *MAB_1135c* and a longer spacer between the two palindromic sequences upstream of *MAB_2300*.

To confirm binding of the regulator to this palindromic sequence, electrophoretic mobility shift assays (EMSAs) were done by incubating increasing concentrations of purified MAB_2299c with a 64-bp DNA segment containing the two palindromes identified upstream of *MAB_1135c* and labeled at its 5′ end with fluorescein (probe A). Under these conditions, a DNA-protein complex was detected and specificity of binding was demonstrated in a competition assay by adding increasing concentrations of the corresponding unlabeled DNA fragment (cold probe), which led to a dose-dependent decrease in DNA-protein complex formation (Fig. 4B). In the presence of an excess of unlabeled probe B, corresponding to a 64-bp DNA fragment containing the palindromic sequence found upstream of *MAB_2300*, previously reported to bind to MAB_2299c (29), a dose-dependent decrease in DNA-protein complex formation, similar to the one found with probe A, was noticed (Fig. 4B). This indicates that binding to probe A can be outcompeted by probe B, emphasizing the fact that MAB_2299c has the capacity to bind to both probes. However, in the presence of an excess of a nonrelated probe the shift was maintained, further indicating that a specific protein-DNA complex was formed only when the TetR regulator was incubated with DNA containing its specific target (Fig. 4B). In addition, a pronounced shift impairment was observed when the regulator was incubated with fluorescent probe C, a variant of probe A harboring multiple DNA substitutions within the palindromic sequence (Fig. 4C). This indicates that the TAACGCA/TGCGTTA motif in the palindrome (conserved in probes A and B) is required for optimal binding of MAB_2299c to its operator region.

***M. abscessus* lacking both MmpS-MmpL pairs is highly susceptible to CFZ or BDQ treatment in macrophages.** In the absence of drug treatment, all *M. abscessus* strains (WT, Δ*MAB_2299c*, Δ*MAB_1135c-1134c*, Δ*MAB_2299c-2300-2301*, and Δ*MAB_2299c-2300-2301-1135c-1134c* strains) grew similarly in 7H9$^{T/OADC}$ (Middlebrook 7H9 broth supplemented with 0.05% Tween 80 and 10% oleic acid, albumin, dextrose, catalase [OADC enrichment]) at 30°C (Fig. 5A), indicating that the multiple-gene deletion of the TetR regulator and its target genes does not influence mycobacterial growth. Exposure of WT cultures to 0.25 μg/ml BDQ (corresponding to 2× MIC) showed an important growth inhibition over the 4-day period of treatment with CFU numbers remaining constant over time, confirming the bacteriostatic effect of BDQ reported earlier (26) (Fig. 5A). As anticipated, growth of the Δ*MAB_2299c* strain was only partially inhibited, confirming the BDQ-resistant phenotype of the strain. However, deletion of either one or both MmpS-MmpL pairs in Δ*MAB_2299c* fully abrogated the BDQ resistance phenotype. Moreover, after 4 days of treatment, the CFU numbers of the MmpS-MmpL mutants were approximately 1 to 2 logs lower than those of the WT strain and the original inoculum, indicating that these strains in effect became susceptible to killing by BDQ (Fig. 5A). Similar growth profiles were obtained when the different strains were exposed to a lower concentration of BDQ (0.06 μg/ml) (data not shown).

The hypersusceptibility of the quintuple mutant to CFZ and BDQ *in vitro* prompted us to investigate whether this phenotype was maintained when bacteria reside inside the macrophage. However, this required us to first examine the potential cytotoxicity induced by the two drugs over a 48-h period of treatment in THP-1 macrophages. The cytotoxicity profiles of CFZ and BDQ were very different, with BDQ showing extremely poor cytotoxicity (no macrophage killing at concentrations up to 50 μg/ml), while CFZ exhibited toxicity with a 50% inhibitory concentration of 2.6 μg/ml (Fig. 5B). Macrophages next were infected with various *M. abscessus* strains at a multiplicity of infection (MOI) of 5. Following extensive washing and treatment with AMK to remove the extracellular bacilli, infected cells were either left untreated or were treated with low concentrations of drugs (1 μg/ml CFZ or 0.25 μg/ml BDQ) for 48 h. In the absence of drug treatment, all mycobacterial strains replicated in a comparable manner, with a 2-log increase in the intracellular CFU, except for Δ*MAB_2299c* and the quintuple

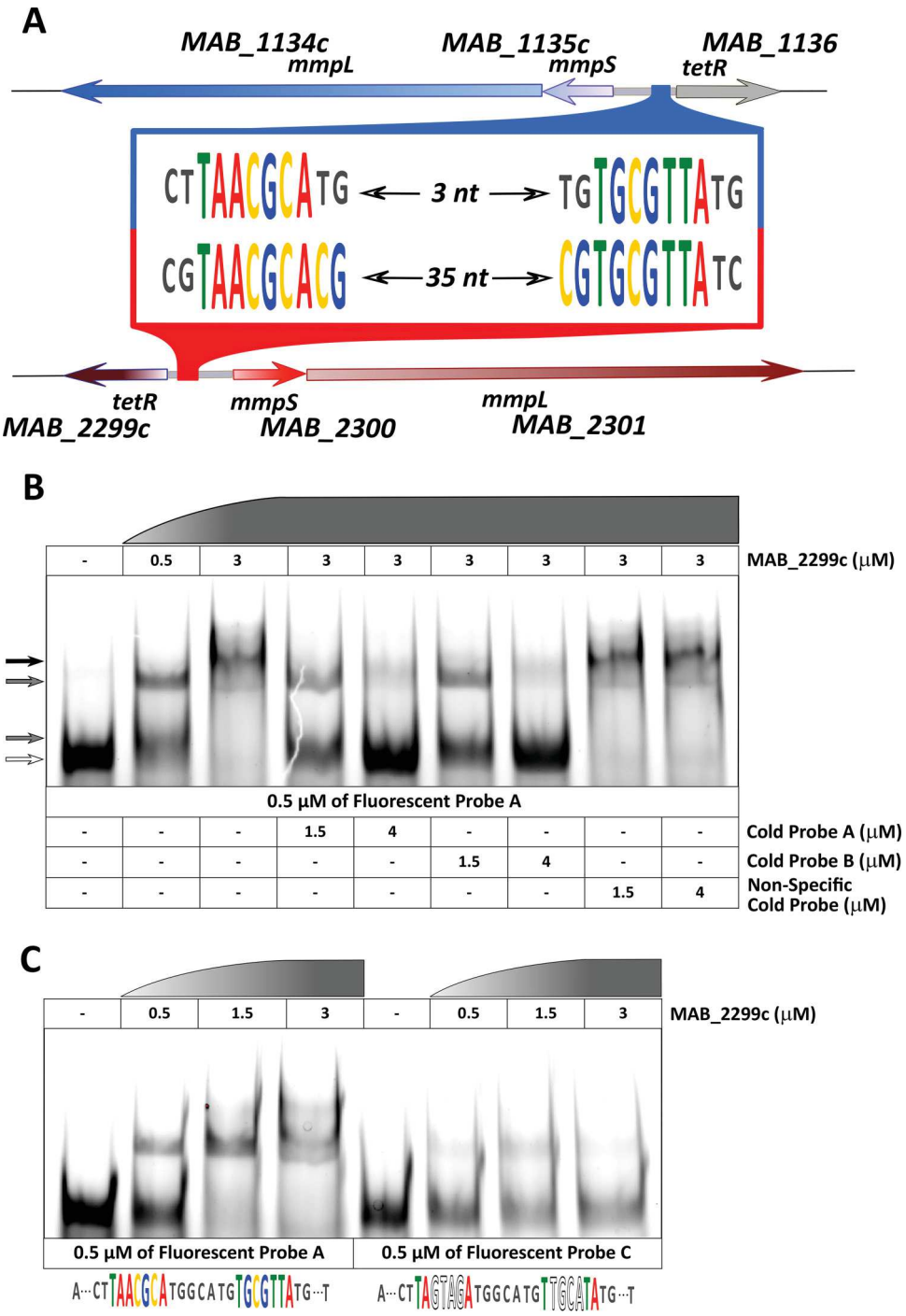

FIG 4 TetR regulator MAB_2299c binds to the intergenic region upstream of *MAB_1135c-1134c*. (A) Schematic representation of the DNA operators located upstream of *MAB_1135c-1134c* (comprising probe A) and *MAB_2300-2301* (comprising probe B). The palindromic sequences of 7 nucleotides in probe A are separated by a spacer and are identical to those found in probe B, in which they are separated by 35 nucleotides. (B) EMSA and competition assays using purified MAB_2299c and incubated with 5′ fluorescein-labeled probe A in the absence or presence of an excess of unlabeled probe A or probe B. A nonrelated probe was also included as a control of specificity of the TetR/DNA complex formed. Detection of the unbound or the complexed probe A was revealed by fluorescence emission. The white arrow indicates the DNA alone, gray arrows the formation of intermediate TetR/DNA complexes, and the black arrow the formation of a complete TetR/DNA complex. (C) Comparison of the EMSA pattern of MAB_2299c incubated with 5′ fluorescein-labeled probe A and probe C in which 4 of the central nucleotides forming the palindromic sequences of probe A were replaced by a random sequence, resulting in a clear defect in the formation of the TetR/DNA complex. The corresponding unbound and complexed probes were revealed by fluorescence emission.

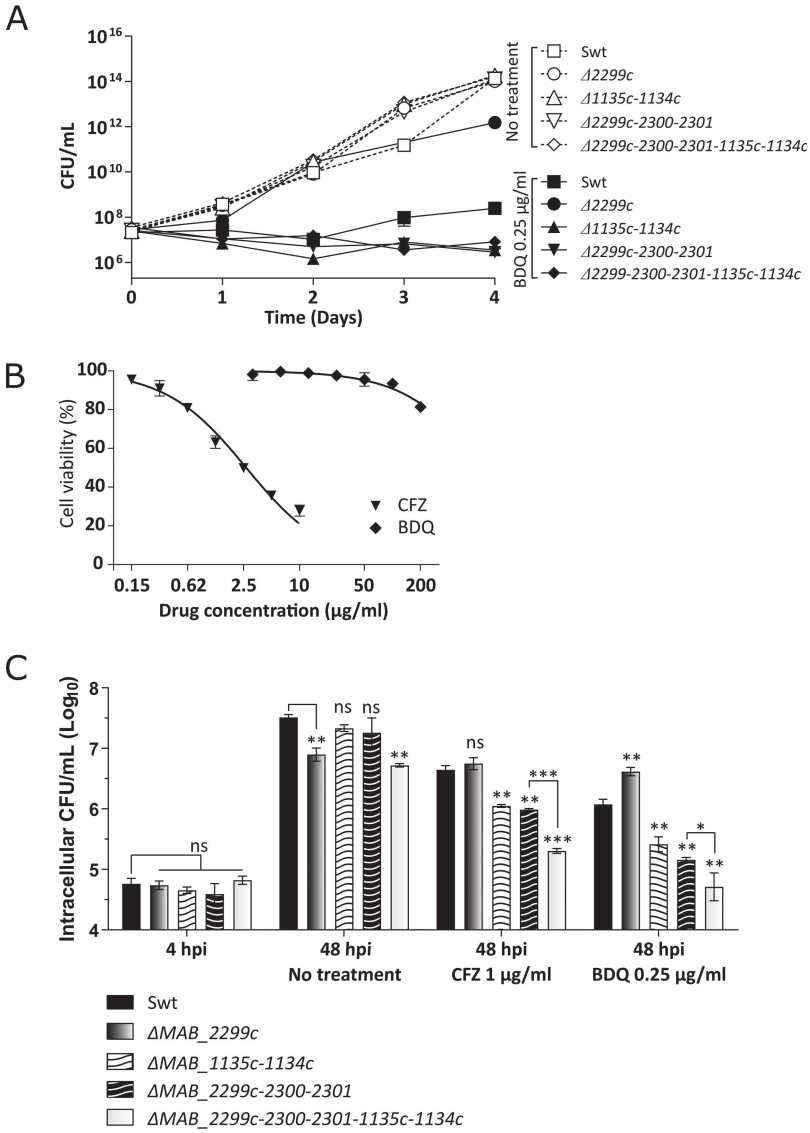

FIG 5 Activity of BDQ *in vitro* and in infected macrophages. (A) *M. abscessus* CIP104536^T WT and its mutant derivatives were either left untreated or exposed to 0.25 μg/ml BDQ in 7H9^{OADC} at 30°C. Bacterial suspensions were collected on a daily basis, diluted, plated on LB agar, and further incubated at 37°C for 4 days prior to CFU determination. Results are expressed as the means ± standard errors of the means from triplicates and are representative of two independent experiments. Ctrl, untreated cultures; Swt, smooth wild type. (B) Cytotoxicity assay of CFZ and BDQ toward THP-1 macrophages. Cells were treated for 48 h with increasing concentrations of CFZ or BDQ, and viability was determined using the CellTiter-Blue reagent. The percentage of cell survival was determined based on control cells incubated in DMSO-containing medium. (C) *M. abscessus*-infected THP-1 macrophages were exposed to either 1 μg/ml CFZ or 0.25 μg/ml BDQ for 2 days before they were lysed and plated for subsequent CFU enumeration. Histograms and error bars represent means and standard errors of the means calculated from three independent experiments. CFU numbers at 4 h postinfection reflect the sizes of the different inocula. For statistical analysis, Student's *t* test was applied. ns, *, **, and *** stand for nonsignificant, $P < 0.01$, $P < 0.001$, and $P < 0.0001$, respectively.

mutant, both showing a slight reduction in the number of intracellular CFU (Fig. 5C). The Δ*MAB_2299c* mutant, however, exhibited slightly higher CFU numbers in macrophages after 48 h of treatment with BDQ than with untreated macrophages, in agreement with its increased resistance phenotype to BDQ *in vitro*. Importantly, the *in vitro* CFZ/BDQ-susceptible Δ*MAB_1135c-1134c* and Δ*MAB_2299c-2300-2301* mutants were also more susceptible to CFZ and BDQ inside macrophages than the wild-type strain. Moreover, the quintuple mutant (lacking both efflux pump systems) exhibited an even

further increased sensitivity to CFZ and BDQ in macrophages compared to that of the triple mutant (lacking one efflux pump system only). Together, these results indicate that abrogating the functionality of multiple efflux pumps translates into additive effects, resulting in higher sensitivity to drugs *in vitro* and in infected host cells.

DISCUSSION

M. abscessus is intrinsically resistant to a wide range of antimicrobials, including most antitubercular drugs, posing a serious challenge for drug discovery. Hit rates in primary screens for *M. abscessus* are low, primarily because of the low level of susceptibility due to its expansive drug resistome (18). As environmental bacteria, NTM reside essentially in soil and water, and it is plausible that the selection pressure from antimicrobial-producing bacteria sharing the same biological niches have forced NTM to develop a wide diversity of resistance mechanisms, allowing them to survive in hostile environments. The antimicrobial resistome of *M. abscessus* results from mutations in antibiotic target genes or other related genes, mostly occurring during the prolonged course of treatment, as well as genes involved in intrinsic drug resistance mechanisms. Among the latter, efflux pump mechanisms, protecting bacteria against toxic compounds and promoting bacterial homeostasis by transporting toxins or metabolites to the extracellular environment (34), have drawn attention as important elements preventing the intracellular accumulation of drugs.

Resistance mechanisms associated with MmpL-derived efflux pump systems were recently identified in *M. abscessus*. In the case of thiacetazone analogs, mutations in the TetR repressor MAB_4384 led to upregulation of the adjacent genes encoding an MmpS-MmpL efflux pump system (35, 36). Increased expression of *MAB_4746*, encoding a member of the MmpL family, was also reported recently in LNZ-resistant isolates (37). In the case of CFZ, where CFZ-resistant strains demonstrated cross-resistance to BDQ (29), whole-genome sequencing analyses of the *in vitro*-selected resistors uncovered point mutations in MAB_2299c (29), a member of the TetR family of transcriptional regulators, representing the most abundant family of regulators in mycobacteria. These findings are supported by an independent study that also identified mutations in *MAB_2299c*, among other genes, in CFZ-resistant strain selected *in vitro* (38). It was originally shown that MAB_2299c regulates transcription of the *MAB_2300-2301* target genes, found in an orientation opposite that of *MAB_2299c* (29). Point mutations (L40W, L151P, and G215S) identified in the spontaneous resistant strains were correlated with a loss of DNA-binding activity of MAB_2299c, resulting in derepression of *MAB_2300-2301* (29) and *MAB_1135c-1134c* (this study) gene expression, leading to increased drug efflux and cross-resistance to CFZ and BDQ (29). In contrast to *MAB_2300-2301*, adjacent to *MAB_2299c*, *MAB_1135c-1134c* is located far from the regulator (Fig. 6). This indicates that MAB_2299c can act simultaneously on closely and distantly located target genes on the chromosome. That both efflux pump systems participate in CFZ and BDQ export strongly suggests that they are structurally and functionally related. This hypothesis was confirmed by the phylogenetic analysis that allowed us to identify *MAB_1135c-1134c*, along with *MAB_2300-2301*, products of a possible gene duplication event. That both MmpS-MmpL systems operate simultaneously was verified using multiple gene deletions thanks to the recent development of a suicide vector-based approach, which allows easy and rapid unmarked genetic alteration of the *M. abscessus* chromosome (29). While the triple mutant lacking the regulator and one efflux pump system (Δ*MAB_2299c-2300-2301*) was more sensitive to CFZ/BDQ than the WT progenitor, the quintuple mutant lacking the regulator and both efflux pump systems further gained in susceptibility to CFZ and BDQ treatment. To verify whether the two efflux pumps and MAB_2299c are widely distributed among *M. abscessus* clinical isolates or restricted to the CIP104536 type strain, a BLAST search for *MAB_2299c-2300-2301* and *MAB_1136-1135c-1134c* was performed (see Table S3 in the supplemental material). This revealed that both loci as well as their DNA operators are conserved in *M. bolletii*, *M. massiliense*, and *M. chelonae* and in all clinical isolates analyzed, suggesting that both efflux pump systems are present and presumably operating in all of these strains.

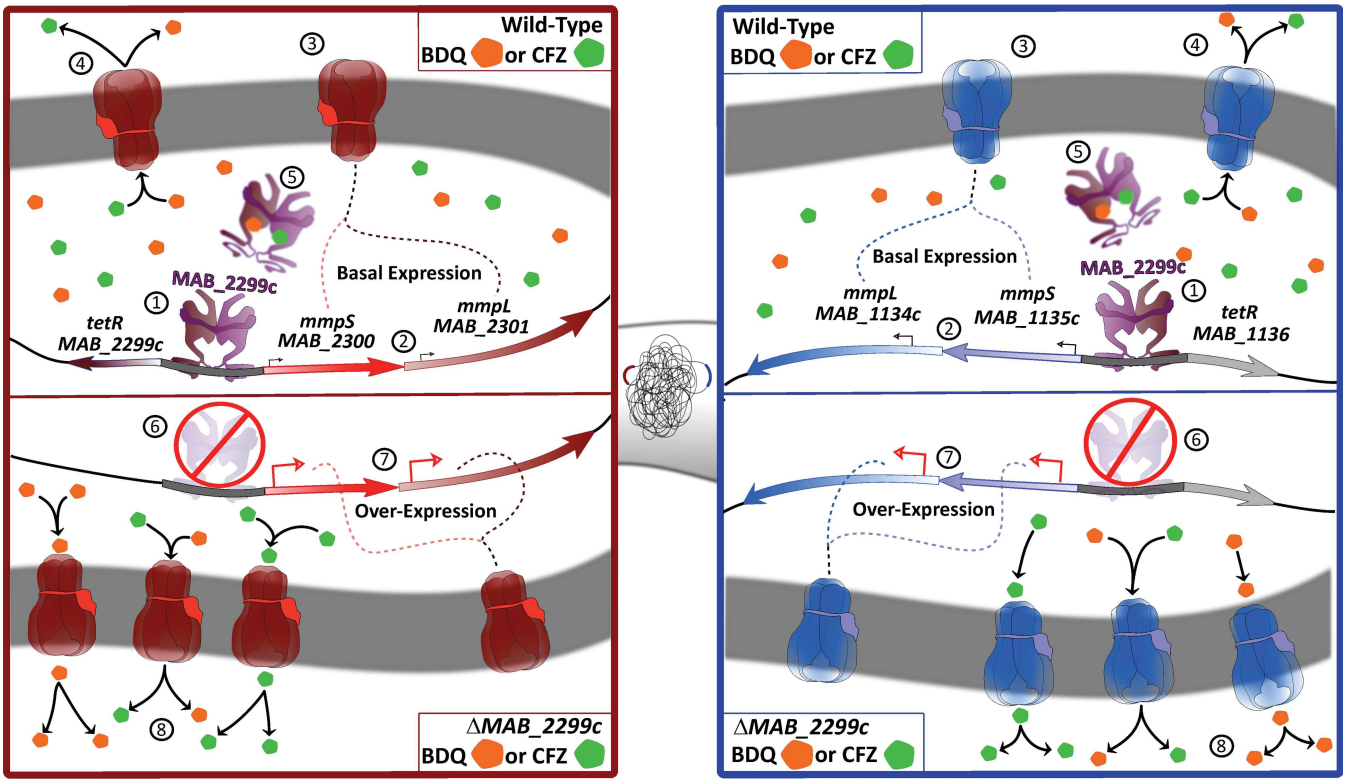

FIG 6 General schematic representing the mechanism of CFZ/BDQ resistance mediated by MAB_2299c-dependent MmpS-MmpL efflux pumps in *M. abscessus*. (1) Binding of MAB_2299c to the intergenic regions of *MAB_2300-2301* (left) and *MAB_1135c-1134c* (right). (2) Transcriptional repression of *MAB_2300-2301* (left) and *MAB_1135c-1134c* (right) allows only basal expression of the two efflux pumps. (3) Insertion of the two MmpS-MmpL efflux pumps into the plasma membrane. (4) Extrusion of CFZ and BDQ conferring intrinsic resistance to both drugs. (5) Possible interaction of the drugs with the TetR regulator, triggering its dissociation from the DNA operator and transcriptional derepression. (6) Lack of binding of the regulator to the intergenic regions either due to point mutations acquired in *MAB_2299c* under CFZ selective pressure *in vitro* or when *MAB_2299c* was inactivated through targeted deletion by homologous recombination. (7) Enhanced expression of the two drug efflux pumps and extrusion of CFZ and BDQ, leading to increased resistance levels to the drugs.

These results indicate that mutations in *MAB_2299c*, which can be easily selected on CFZ *in vitro* (29), affect the expression of two efflux pump systems, both contributing to the resistance mechanism. However, while our transcriptomic studies showed that only these two MmpS/MmpL pairs are regulated by MAB_2299c, one cannot exclude the possibility that additional MAB_2299c-independent MmpL proteins or unrelated efflux pump systems, such as members of the major facilitator superfamily or ATP-binding cassette (ABC) transporters, mediate cross-resistance to CFZ/BDQ. It also remains possible that MAB_2299c regulates other gene targets involved in various metabolic pathways and/or in intracellular survival of *M. abscessus* in macrophages. This hypothesis may be supported by a slightly reduced burden of the Δ*MAB_2299c* strain than the WT at 48 h postinfection in THP-1 cells in the absence of drug treatment (Fig. 5C).

We recently showed that verapamil improves the efficacy of BDQ activity against *M. abscessus* clinical isolates both *in vitro* and in macrophages (39). Interestingly, verapamil kept its capacity to potentiate the activity of BDQ even in *M. abscessus* mutants resistant to CFZ/BDQ (overexpressing both the MAB_2300-2301 and MAB_1135c-1134c efflux pumps), highlighting the value of the verapamil-BDQ combination in cases of low-level acquired resistance to BDQ in this mycobacterium. Importantly, the Δ*MAB_2299c-2300-2301* strain, in which this BDQ efflux pump was deleted, leading to increased BDQ sensitivity compared to that of WT *M. abscessus*, exhibited a further increase in sensitivity to BDQ in the presence of verapamil, suggesting that the mechanism whereby verapamil exerts its potentiating effect on BDQ activity is not dependent on this efflux pump, apparently excluding this efflux pump as the major target of verapamil. In fact, it was recently reported that verapamil targets membrane energetics in mycobacteria (40).

The inhibition by BDQ of the ATP synthase in mycobacteria was also previously shown to impact membrane energetics, an effect which is probably compounded when verapamil is also present (41). Our genetics data suggest that if a specific inhibitor of the two highly related CFZ/BDQ efflux pumps (MAB_2300-2301 and MAB_1135c-1134c) could be developed, such a compound given in combination with BDQ/CFZ and a molecule targeting membrane potential would provide an extremely potent therapeutic cocktail against *M. abscessus*.

We previously speculated that, given the large *mmpL* repertoire (30) and high abundance of TetR transcriptional regulators (42) found in *M. abscessus*, efflux-based mechanisms represent a general mechanism to express its natural resistance pattern to antimicrobial agents. The present study confirms this to be true, at least regarding CFZ and BDQ resistance. In summary, we provide here additional mechanistic insights into the TetR-dependent regulation of MmpL efflux pumps responsible for cross-resistance to CFZ and BDQ in *M. abscessus*, which may have important clinical implications. Overall, this study underpins *MAB_2299c* as a marker of resistance to be considered when assessing the drug susceptibility profile of *M. abscessus* clinical isolates. However, future studies should also be dedicated to investigating whether mutations in *MAB_2299c* occur in clinical isolates from patients treated with CFZ or BDQ.

MATERIALS AND METHODS

Strains, growth conditions, and reagents. Bacterial strains used in this study are listed in Table S1 in the supplemental material. *M. abscessus* was grown in Middlebrook 7H9 broth (BD Difco) supplemented with 0.05% Tween 80 (Sigma-Aldrich) and 10% oleic acid, albumin, dextrose, catalase (OADC enrichment; BD Difco) ($7H9^{T/OADC}$) at 30°C (unless otherwise stated) in the presence of antibiotics, when required. On plates, colonies were selected either on Middlebrook 7H10 agar (BD Difco) supplemented with 10% OADC enrichment ($7H10^{OADC}$) or on LB agar. All drugs were purchased from Sigma-Aldrich.

Drug susceptibility testing. The MIC, defined as the minimal drug concentration required to inhibit 99% growth (MIC_{99}), was recorded on Middlebrook $7H10^{OADC}$ agar after 3 to 4 days of incubation at 30°C. All experiments were done on three independent occasions.

Quantitative real-time PCR. Isolation of RNA, reverse transcription, and qRT-PCR were done as reported earlier (35) using the primers listed in Table S2 in the supplemental material.

Expression and purification of MAB_2299c variants. The *E. coli* BL21(DE3) strain (New England Biolabs) possessing pRARE2 was transformed with a pET32a derivative containing the wild-type *MAB_2299c* gene. Expression in *E. coli* and purification of MAB_2299c was performed as described earlier (29).

Electrophoretic mobility shift assays (EMSAs). Thanks to the MEME Suite 4.20.0 online tool, we identified a perfect pair of palindromes comprised of 7 nucleotides each and separated by a 7-nucleotide spacer within the intergenic region upstream of *MAB_1135c*. These palindromes are identical to the ones located between *MAB_2299c* and *MAB_2300*. A double-stranded DNA fragment of 64 bp containing the pair of palindromes labeled at their 5′ ends with fluorescein (probe A) was purchased from Sigma-Aldrich. The 5′ fluorescein probes (500 nM) were coincubated for 1 h at room temperature in 1× Tris base–acetic acid–EDTA (TAE) buffer with increasing amounts of purified MAB_2299c protein with or without excess concentrations of cold probes (unlabeled DNA fragments). Electrophoresis was performed for 30 min at 100 V in 1× TAE buffer, and fluorescence was revealed using a ChemiDoc Imaging System (Bio-Rad). Sequences of the probes are listed in Table S2.

Generation of the *MAB_1136c* and *MAB_1135c-1134c* recombination plasmids. The suicide vector pUX1-*katG* (29) was used to generate pUX1-*katG-MAB_1136*. To produce pUX1-*katG-MAB_1136*, genomic DNA from *M. abscessus*, Q5 polymerase (New England Biolabs), and the primers *MAB_1136_LA_Fw* and *MAB_1136_LA_Rev* were used to PCR amplify a left arm (LA). A similar PCR but with the primers *MAB_1136_RA_Fw* and *MAB_1136_RA_Rev* generated a right arm (RA). The purified LA and RA amplicons were added to a new PCR mix without any primers or genomic DNA. This reaction consisted of two cycles of 95°C for 30 s, 55°C for 2 min, and 72°C for 3 min prior to the addition of primers *MAB_1136_RA_Fw* and *MAB_1136_LA_Rev* and 25 additional cycles of 95°C for 10 s, 55°C for 30 s, and 72°C for 2 min. The 1.7-kb primer-overlap extension PCR product was restricted with NheI and MfeI and ligated to the NheI-MfeI-linearized pUX1-*katG*, yielding pUX1-*katG-MAB_1136*, designed to delete 530 bp (80%) of the *MAB_1136* open reading frame (Table S1).

The same approach was applied to generate pUX1-*katG-MAB_1135c-1134c*, using the primers *MAB_1135c-1134c_LA_Fw* and *MAB_1135c-1134c_LA_Rev* to produce the LA and the primers *MAB_1135c-1134c_RA_Fw* and *MAB_1135c-1134c_RA_Rev* to produce the RA. The ~1.4-kb primer overlap extension PCR product was restricted with NheI and MfeI and ligated to the NheI-MfeI-linearized pUX1-*katG*, yielding pUX1-*katG-MAB_1135c-1134c*, designed to delete 3,234 bp (96%) of the *MAB_1135c-1134c* gene cluster (Table S1).

Unmarked deletion in *M. abscessus*. Highly electrocompetent *M. abscessus* smooth (S) WT and S Δ*MAB_2299c-2300-2301* strains were prepared as reported earlier (31) and subsequently transformed with pUX1-*katG-MAB_1136* or pUX1-*katG-MAB_1135c-1134c*. Selection of bacteria having undergone the

first homologous recombination was done by screening for red fluorescent colonies on 7H10^{OADC} supplemented with 200 μg/ml kanamycin. To promote the second homologous recombination event, the selected clones were subcultured overnight in 7H9^{OADC} in the absence of kanamycin. Cultures were 10-fold serially diluted and plated onto 7H10^{OADC} containing 50 μg/ml isoniazid (INH) to select for INH-resistant, KAN-sensitive, and nonfluorescent colonies. Following genomic DNA preparation from such colonies, PCR screening was set up using primer sets binding upstream of the LA and inside the RA or binding inside the LA and downstream of the RA. Amplicons were subsequently sequenced to confirm the junction between LA and RA and the correct unmarked deletion of *MAB_1136* and *MAB_1135c-1134c*.

Macrophage infections. THP-1 macrophages were grown at 37°C in a 5% CO_2 incubator in RPMI 1640 supplemented with 10% FBS (RPMI^{FBS}) and differentiated for 48 h prior to infection with 20 ng/ml phorbol myristate acetate (PMA). *M. abscessus* strains were cultured at 37°C in 7H9^{OADC} until they reach the exponential growth phase and were harvested by centrifugation and resuspended in phosphate-buffered saline (PBS). Single-cell preparations were prepared by passing the bacterial suspension through a 26.5-gauge needle (~20 times) and then through a 5.0-μm filter (Merck Millipore). THP-1 cells (5×10^5 cells/ml) were then infected at an MOI of 5 and incubated at 37°C in the presence of 5% CO_2. After 2 to 3 h of incubation, cells were washed three times with PBS and refed with RPMI^{FBS} supplemented with 250 μg/ml AMK for 1 h in order to kill extracellular bacilli. Cells were washed three times with PBS and incubated for an additional 48 h with either RPMI^{FBS} alone (no treatment; control of intracellular growth), RPMI^{FBS} containing 1 μg/ml CFZ, or RPMI^{FBS} containing 0.25 μg/ml BDQ. For intracellular CFU determination, cells were washed three times with PBS, and 100 μl of 1% PBS-Triton X-100 was added to lyse the cells at day 0 and day 2. Lysis was stopped by adding 900 μl of PBS. Tenfold dilutions were plated onto LB agar, and colonies were counted after 5 days of incubation at 37°C.

Cytotoxicity assay. THP-1 macrophages (5×10^5 cells/ml) in 96–well flat-bottom culture microtiter plates were differentiated for 48 h with PMA, after which RPMI^{FBS} was replaced with 180 μl of fresh medium containing increasing concentrations of either CFZ (ranging from 0.15 to 10 μg/ml) or BDQ (ranging from 3.1 to 200 μg/ml). After 48 h of incubation at 37°C with 5% CO_2, 20 μl of CellTiter-Blue reagent (Promega) was added and cells were incubated for an additional 2 h. The optical density at 560 nm (OD_{560}) was recorded using a microplate reader. The percentage of cell survival was determined considering the control wells (cells incubated in dimethyl sulfoxide-containing medium).

Multiple alignments and synteny analysis. Primary protein sequences were retrieved from the KEGG website (https://www.genome.jp/kegg/), and multiple alignments of the sequences were done with the MUSCLE algorithm using its default parameters in the UniProt UGENE suite (43). Phylogenetic trees were constructed from the multiple-alignment data using the PHYLIP neighbor-joining tree-building method with default parameters of the UGENE suite. Nucleotide sequences were also retrieved from the KEGG website, and syntenic comparisons of these sequences were done on the YASS genomic similarity tool web server (http://bioinfo.lifl.fr/yass/yass.php).

Statistical analysis. All statistical analyses were performed using GraphPad Prism 5 (version 5.03; GraphPad Software). Student's *t* test was used for all comparisons. A *P* value of less than 0.05 was considered significant (ns, nonsignificant; *, $P < 0.05$; **, $P < 0.01$; ***, $P < 0.001$).

SUPPLEMENTAL MATERIAL

Supplemental material for this article may be found at https://doi.org/10.1128/AAC.01000-19.

SUPPLEMENTAL FILE 1, PDF file, 0.8 MB.

ACKNOWLEDGMENTS

This work was supported by the Fondation pour la Recherche Médicale (FRM) (grant number DEQ20150331719 to L.K.; grant number ECO20160736031 to M.R.) and the InfectioPôle Sud for funding the Ph.D. fellowship of A.V.G.

We have no conflicts of interest to declare.

REFERENCES

1. Davidson RM. 2018. A closer look at the genomic variation of geographically diverse *Mycobacterium abscessus* clones that cause human infection and disease. Front Microbiol 9:2988. https://doi.org/10.3389/fmicb.2018.02988.
2. Choo SW, Wee WY, Ngeow YF, Mitchell W, Tan JL, Wong GJ, Zhao Y, Xiao J. 2014. Genomic reconnaissance of clinical isolates of emerging human pathogen *Mycobacterium abscessus* reveals high evolutionary potential. Sci Rep 4:4061. https://doi.org/10.1038/srep04061.
3. Tan JL, Ngeow YF, Choo SW. 2015. Support from phylogenomic networks and subspecies signatures for separation of *Mycobacterium massiliense* from *Mycobacterium bolletii*. J Clin Microbiol 53:3042–3046. https://doi.org/10.1128/JCM.00541-15.
4. Tan JL, Ng KP, Ong CS, Ngeow YF. 2017. Genomic comparisons reveal microevolutionary differences in *Mycobacterium abscessus* subspecies. Front Microbiol 8:2042. https://doi.org/10.3389/fmicb.2017.02042.
5. Ripoll F, Pasek S, Schenowitz C, Dossat C, Barbe V, Rottman M, Macheras E, Heym B, Herrmann J-L, Daffé M, Brosch R, Risler J-L, Gaillard J-L. 2009. Nonmycobacterial virulence genes in the genome of the emerging pathogen *Mycobacterium abscessus*. PLoS One 4:e5660. https://doi.org/10.1371/journal.pone.0005660.
6. Le Moigne V, Belon C, Goulard C, Accard G, Bernut A, Pitard B, Gaillard J-L, Kremer L, Herrmann J-L, Blanc-Potard A-B. 2016. MgtC as a host-induced factor and vaccine candidate against *Mycobacterium abscessus* infection. Infect Immun 84:2895–2903. https://doi.org/10.1128/IAI.00359-16.
7. Griffith DE, Aksamit T, Brown-Elliott BA, Catanzaro A, Daley C, Gordin F, Holland SM, Horsburgh R, Huitt G, Iademarco MF, Iseman M, Olivier K, Ruoss S, von Reyn CF, Wallace RJ, Winthrop K, ATS Mycobacterial Diseases Subcommittee; American Thoracic Society, Infectious Disease Society of America. 2007. An official ATS/IDSA statement: diagnosis, treatment, and prevention of nontuberculous mycobacterial diseases. Am J

Respir Crit Care Med 175:367–416. https://doi.org/10.1164/rccm.200604-571ST.
8. Floto RA, Olivier KN, Saiman L, Daley CL, Herrmann J-L, Nick JA, Noone PG, Bilton D, Corris P, Gibson RL, Hempstead SE, Koetz K, Sabadosa KA, Sermet-Gaudelus I, Smyth AR, van Ingen J, Wallace RJ, Winthrop KL, Marshall BC, Haworth CS. 2016. US Cystic Fibrosis Foundation and European Cystic Fibrosis Society consensus recommendations for the management of non-tuberculous mycobacteria in individuals with cystic fibrosis: executive summary. Thorax 71:88–90. https://doi.org/10.1136/thoraxjnl-2015-207983.
9. Medjahed H, Gaillard J-L, Reyrat J-M. 2010. *Mycobacterium abscessus*: a new player in the mycobacterial field. Trends Microbiol 18:117–123. https://doi.org/10.1016/j.tim.2009.12.007.
10. Catherinot E, Roux A-L, Macheras E, Hubert D, Matmar M, Dannhoffer L, Chinet T, Morand P, Poyart C, Heym B, Rottman M, Gaillard J-L, Herrmann J-L. 2009. Acute respiratory failure involving an R variant of *Mycobacterium abscessus*. J Clin Microbiol 47:271–274. https://doi.org/10.1128/JCM.01478-08.
11. Esther CR, Esserman DA, Gilligan P, Kerr A, Noone PG. 2010. Chronic *Mycobacterium abscessus* infection and lung function decline in cystic fibrosis. J Cyst Fibros 9:117–123. https://doi.org/10.1016/j.jcf.2009.12.001.
12. Bryant JM, Grogono DM, Rodriguez-Rincon D, Everall I, Brown KP, Moreno P, Verma D, Hill E, Drijkoningen J, Gilligan P, Esther CR, Noone PG, Giddings O, Bell SC, Thomson R, Wainwright CE, Coulter C, Pandey S, Wood ME, Stockwell RE, Ramsay KA, Sherrard LJ, Kidd TJ, Jabbour N, Johnson GR, Knibbs LD, Morawska L, Sly PD, Jones A, Bilton D, Laurenson I, Ruddy M, Bourke S, Bowler IC, Chapman SJ, Clayton A, Cullen M, Daniels T, Dempsey O, Denton M, Desai M, Drew RJ, Edenborough F, Evans J, Folb J, Humphrey H, Isalska B, Jensen-Fangel S, Jönsson B, Jones AM, Katzenstein TL, Lillebaek T, MacGregor G, Mayell S, Millar M, Modha D, Nash EF, O'Brien C, O'Brien D, Ohri C, Pao CS, Peckham D, Perrin F, Perry A, Pressler T, Prtak L, Qvist T, Robb A, Rodgers H, Schaffer K, Shafi N, van Ingen J, Walshaw M, Watson D, West N, Whitehouse J, Haworth CS, Harris SR, Ordway D, Parkhill J, Floto RA. 2016. Emergence and spread of a human-transmissible multidrug-resistant nontuberculous mycobacterium. Science 354:751–757. https://doi.org/10.1126/science.aaf8156.
13. Kwak N, Dalcolmo MP, Daley CL, Eather G, Gayoso R, Hasegawa N, Jhun BW, Koh W-J, Namkoong H, Park J, Thomson R, van Ingen J, Zweijpfenning SMH, Yim J-J. 2019. *Mycobacterium abscessus* pulmonary disease: individual patient data meta-analysis. Eur Respir J 54:1801991. https://doi.org/10.1183/13993003.01991-2018.
14. Brown-Elliott BA, Nash KA, Wallace RJ. 2012. Antimicrobial susceptibility testing, drug resistance mechanisms, and therapy of infections with nontuberculous mycobacteria. Clin Microbiol Rev 25:545–582. https://doi.org/10.1128/CMR.05030-11.
15. Nessar R, Cambau E, Reyrat JM, Murray A, Gicquel B. 2012. *Mycobacterium abscessus*: a new antibiotic nightmare. J Antimicrob Chemother 67:810–818. https://doi.org/10.1093/jac/dkr578.
16. van Ingen J, Boeree MJ, van Soolingen D, Mouton JW. 2012. Resistance mechanisms and drug susceptibility testing of nontuberculous mycobacteria. Drug Resist Updat 15:149–161. https://doi.org/10.1016/j.drup.2012.04.001.
17. Luthra S, Rominski A, Sander P. 2018. The role of antibiotic-target-modifying and antibiotic-modifying enzymes in *Mycobacterium abscessus* drug resistance. Front Microbiol 9:2179. https://doi.org/10.3389/fmicb.2018.02179.
18. Wu M-L, Aziz DB, Dartois V, Dick T. 2018. NTM drug discovery: status, gaps and the way forward. Drug Discov Today 23:1502–1519. https://doi.org/10.1016/j.drudis.2018.04.001.
19. Yano T, Kassovska-Bratinova S, Teh JS, Winkler J, Sullivan K, Isaacs A, Schechter NM, Rubin H. 2011. Reduction of clofazimine by mycobacterial type 2 NADH:quinone oxidoreductase: a pathway for the generation of bactericidal levels of reactive oxygen species. J Biol Chem 286:10276–10287. https://doi.org/10.1074/jbc.M110.200501.
20. van Ingen J, Totten SE, Helstrom NK, Heifets LB, Boeree MJ, Daley CL. 2012. *In vitro* synergy between clofazimine and amikacin in treatment of nontuberculous mycobacterial disease. Antimicrob Agents Chemother 56:6324–6327. https://doi.org/10.1128/AAC.01505-12.
21. Singh S, Bouzinbi N, Chaturvedi V, Godreuil S, Kremer L. 2014. *In vitro* evaluation of a new drug combination against clinical isolates belonging to the *Mycobacterium abscessus* complex. Clin Microbiol Infect 20:O1124–O1127. https://doi.org/10.1111/1469-0691.12780.
22. Ferro BE, Meletiadis J, Wattenberg M, de Jong A, van Soolingen D, Mouton JW, van Ingen J. 2016. Clofazimine prevents the regrowth of *Mycobacterium abscessus* and *Mycobacterium avium* type strains exposed to amikacin and clarithromycin. Antimicrob Agents Chemother 60:1097–1105. https://doi.org/10.1128/AAC.02615-15.
23. Matteelli A, Carvalho AC, Dooley KE, Kritski A. 2010. TMC207: the first compound of a new class of potent anti-tuberculosis drugs. Future Microbiol 5:849–858. https://doi.org/10.2217/fmb.10.50.
24. Pang Y, Zheng H, Tan Y, Song Y, Zhao Y. 2017. *In vitro* activity of bedaquiline against nontuberculous mycobacteria in China. Antimicrob Agents Chemother 61:e02627-16. https://doi.org/10.1128/AAC.02627-16.
25. Vesenbeckh S, Schönfeld N, Roth A, Bettermann G, Krieger D, Bauer TT, Rüssmann H, Mauch H. 2017. Bedaquiline as a potential agent in the treatment of *Mycobacterium abscessus* infections. Eur Respir J 49:1700083. https://doi.org/10.1183/13993003.00083-2017.
26. Dupont C, Viljoen A, Thomas S, Roquet-Banères F, Herrmann J-L, Pethe K, Kremer L. 2017. Bedaquiline inhibits the ATP synthase in *Mycobacterium abscessus* and is effective in infected zebrafish. Antimicrob Agents Chemother 61:e01225-17. https://doi.org/10.1128/AAC.01225-17.
27. Ruth MM, Sangen JJN, Remmers K, Pennings LJ, Svensson E, Aarnoutse RE, Zweijpfenning SMH, Hoefsloot W, Kuipers S, Magis-Escurra C, Wertheim HFL, van Ingen J. 2019. A bedaquiline/clofazimine combination regimen might add activity to the treatment of clinically relevant non-tuberculous mycobacteria. J Antimicrob Chemother 74:935–943. https://doi.org/10.1093/jac/dky526.
28. Bernut A, Herrmann J-L, Kissa K, Dubremetz J-F, Gaillard J-L, Lutfalla G, Kremer L. 2014. *Mycobacterium abscessus* cording prevents phagocytosis and promotes abscess formation. Proc Natl Acad Sci U S A 111:E943–E952. https://doi.org/10.1073/pnas.1321390111.
29. Richard M, Gutiérrez AV, Viljoen A, Rodriguez-Rincon D, Roquet-Baneres F, Blaise M, Everall I, Parkhill J, Floto RA, Kremer L. 2019. Mutations in the MAB_2299c TetR regulator confer cross-resistance to clofazimine and bedaquiline in *Mycobacterium abscessus*. Antimicrob Agents Chemother 63:e01316-18. https://doi.org/10.1128/AAC.01316-18.
30. Viljoen A, Dubois V, Girard-Misguich F, Blaise M, Herrmann J-L, Kremer L. 2017. The diverse family of MmpL transporters in mycobacteria: from regulation to antimicrobial developments. Mol Microbiol 104:889–904. https://doi.org/10.1111/mmi.13675.
31. Viljoen A, Gutiérrez AV, Dupont C, Ghigo E, Kremer L. 2018. A simple and rapid gene disruption strategy in *Mycobacterium abscessus*: on the design and application of glycopeptidolipid mutants. Front Cell Infect Microbiol 8:69. https://doi.org/10.3389/fcimb.2018.00069.
32. Rominski A, Selchow P, Becker K, Brülle JK, Dal Molin M, Sander P. 2017. Elucidation of *Mycobacterium abscessus* aminoglycoside and capreomycin resistance by targeted deletion of three putative resistance genes. J Antimicrob Chemother 72:2191–2200. https://doi.org/10.1093/jac/dkx125.
33. Viljoen A, Blaise M, de Chastellier C, Kremer L. 2016. MAB_3551c encodes the primary triacylglycerol synthase involved in lipid accumulation in *Mycobacterium abscessus*. Mol Microbiol 102:611–627. https://doi.org/10.1111/mmi.13482.
34. Louw GE, Warren RM, Gey van Pittius NC, McEvoy CRE, Van Helden PD, Victor TC. 2009. A balancing act: efflux/influx in mycobacterial drug resistance. Antimicrob Agents Chemother 53:3181–3189. https://doi.org/10.1128/AAC.01577-08.
35. Halloum I, Viljoen A, Khanna V, Craig D, Bouchier C, Brosch R, Coxon G, Kremer L. 2017. Resistance to thiacetazone derivatives active against *Mycobacterium abscessus* involves mutations in the MmpL5 transcriptional repressor MAB_4384. Antimicrob Agents Chemother 61:e02509-16. https://doi.org/10.3389/fcimb.2018.00069.
36. Richard M, Gutiérrez AV, Viljoen AJ, Ghigo E, Blaise M, Kremer L. 2018. Mechanistic and structural insights into the unique TetR-dependent regulation of a drug efflux pump in *Mycobacterium abscessus*. Front Microbiol 9:649. https://doi.org/10.3389/fmicb.2018.00649.
37. Ye M, Xu L, Zou Y, Li B, Guo Q, Zhang Y, Zhan M, Xu B, Yu F, Zhang Z, Chu H. 2018. Molecular analysis of linezolid-resistant clinical isolates of *Mycobacterium abscessus*. Antimicrob Agents Chemother 63:e01842-18. https://doi.org/10.1128/AAC.01842-18.
38. Chen Y, Chen J, Zhang S, Shi W, Zhang W, Zhu M, Zhang Y. 2018. Novel mutations associated with clofazimine resistance in *Mycobacterium abscessus*. Antimicrob Agents Chemother 62:e00544-18. https://doi.org/10.1128/AAC.00544-18.
39. Viljoen A, Raynaud C, Johansen M, Roquet-Baneres F, Herrmann J-L, Daher W, Kremer L. 17 June 2019. Improved activity of bedaquiline by verapamil against *Mycobacterium abscessus in vitro* and in macrophages. Antimicrob Agents Chemother. https://doi.org/10.1128/AAC.00705-19.
40. Chen C, Gardete S, Jansen RS, Shetty A, Dick T, Rhee KY, Dartois V. 2018.

Verapamil targets membrane energetics in *Mycobacterium tuberculosis*. Antimicrob Agents Chemother 62:e02107-17. https://doi.org/10.1128/AAC.02107-17.
41. Lamprecht DA, Finin PM, Rahman MA, Cumming BM, Russell SL, Jonnala SR, Adamson JH, Steyn AJC. 2018. Turning the respiratory flexibility of *Mycobacterium tuberculosis* against itself. Nat Comm 7:12393. https://doi.org/10.1038/ncomms12393.
42. Balhana RJC, Singla A, Sikder MH, Withers M, Kendall SL. 2015. Global analyses of TetR family transcriptional regulators in mycobacteria indicates conservation across species and diversity in regulated functions. BMC Genomics 16:479. https://doi.org/10.1186/s12864-015-1696-9.
43. Okonechnikov K, Golosova O, Fursov M, Withers M, Kendall SL, UGENE Team. 2012. Unipro UGENE: a unified bioinformatics toolkit. Bioinformatics 28:1166–1167. https://doi.org/10.1093/bioinformatics/bts091.

Table S1. List of bacterial strains and plasmids used in this study.

Name	Description/genotype	Marker	Reference
Strains			
M. abscessus S	*Mabs sensu stricto*, strain CIP104536^T, smooth	_	Laboratoire de Référence des Mycobactéries
M. abscessus S Δ*MAB_2299c*	*Mabs MAB_2299c* unmarked deletion mutant obtained by two-step homologous recombination in the smooth parental strain CIP104536^T	_	(1)
M. abscessus S *ΔMAB_2299c.C*	*ΔMAB_2299c* complemented with *pMV261-MAB_2299c*	Kan	(1)
M. abscessus S Δ*MAB_2299c-2300-2301*	*Mabs MAB_2299c-2300-2301* unmarked deletion mutant obtained by two-step homologous recombination in the smooth parental strain Δ*MAB_2299c*	_	(1)
M. abscessus S Δ*MAB_1136*	*Mabs MAB_1136* unmarked deletion mutant obtained by two-step homologous recombination in the smooth parental strain CIP104536^T	_	This work
M. abscessus S Δ*MAB_1135c-1134c*	*Mabs MAB_1135c-1134c* unmarked deletion mutant obtained by two-step homologous recombination in the smooth parental strain CIP104536^T	_	This work
M. abscessus S Δ*MAB_2299c-2300-2301-1135c-1134c*	*Mabs MAB_2299c-2300-2301-1135c-1134c* unmarked deletion mutant obtained by two-step homologous recombination in the smooth parental strain Δ*MAB_2299c-2300-2301*	_	This work
E. coli XL1 Blue	*endA1 gyrA96 recA1 thi-1 relA1 hsdR17 supE44 lac [F´ proAB lacIqZΔM15 Tn10 (Tetr)].*	Tet	Stratagene
E. coli BL21 (DE3) (pRARE2)	*gal dcm (DE3) F- ompT hsdSB(rB- mB-) transformed with pRARE2*	CAM	New England Biolabs
Plasmids			
pET32a::*MAB_2299c*	pET32a in which *MAB_2299c* is cloned in fusion with the thioredoxin/His tag sequence and containing a TEV cleavage site before MAB_2299c to remove the fused tags.	Amp	(1)
pUX1-*katG*	Variant of pUX1 containing the *katG* gene of *M. tuberculosis* H37Rv as a counter-selectable marker in the presence of isoniazid and used for the generation of unmarked chromosomal alterations.	Kan, Hyg	(1)

pUX1-*katG-MAB_1136*	pUX1-*katG* containing the upstream and downstream sequences (approximately 1.7 kb) of *MAB_1136*.	Kan	This work
pUX1-*katG-MAB_1135c-1134c*	pUX1-*katG* containing the upstream and downstream sequences (approximately 1.4 kb) of *MAB_1135c-1134c.*	Kan	This work

Amp, ampicillin; Hyg, hygromycin; Kan, kanamycin; Tet, tetracycline; Stp, streptomycin; CAM, chloramphenicol.

REFERENCES

1. Richard M, Gutiérrez AV, Viljoen A, Rodriguez-Rincon D, Roquet-Baneres F, Blaise M, Everall I, Parkhill J, Floto RA, Kremer L. 2019. Mutations in the MAB_2299c TetR regulator confer cross-resistance to clofazimine and bedaquiline in *Mycobacterium abscessus*. Antimicrob Agents Chemother 63: e01316-18.

Table S2. Oligonucleotides used in this study. Fw and Rv stand for forward and reverse, respectively.

Primers	5' to 3' sequence
Generation of pUX1-*katG* and derivative constructs	
*MAB_1136*_RA_Fw (MfeI)	GAGAGACAATTGGAGCACCGATCCGAGTGTAT
*MAB_1136*_RA_Rv	GCGTCAACGTACGACTGGGACACCGACTT
*MAB_1136*_LA_Fw	TCCCAGTCGTACGTTGACGCTTGTTTTCCT
*MAB_1136*_LA_Rv (NheI)	GAGAGAGCTAGCCATGTTCTTCATCGCCTTCA
*MAB_1135c-1134c*_LA_Fw (NheI)	CAGAGCTAGCTGAACGGAGGTTTGCCATC
*MAB_1135c-1134c*_LA_Rv	CGGCGACAACGGAGTTC
*MAB_1135c-1134c*_RA_Fw	GCTGATGCGAACCGAAGAT
*MAB_1135c-1134c*_RA_Rv (MfeI)	CAGACAATTGTGGTCGATCACCACCTCAT
PCR confirmation of pUX1-*katG* knock-out	
*1136*KOscrnU_Fw	ATACACTCGGATCGGTGCTC
*1136*KOscrnU_ Rv	GTGCGTTATGGGCAACCTAC
*1136*KOscrnD_ Fw	CGTTGGACTGCTACTCGACA
*1136*KOscrnD_ Rv	ATGTCACCGGAGAGGTTCAC
*1135c-1134c*KOscrnU_ Fw	GGCGACGATGGAATCGAAA
*1135c-1134c*KOscrnU_ Rv	CGGATTCGCGGCATCTT
*1135c-1134c*KOscrnD_ Fw	TGGAGTGGTTCGGTCTAGTA
*1135c-1134c*KOscrnD_ Rv	ATGTCGAGCGCACCTTC
Sequencing	
pMV5'	CGCCCGGCCAGCGTAAGTAGC
pMV3'	GCCTGGCAGTCGATCGTACG
pMV3' Ext	TTGAGACACAACGTCGCTTT
NheIpUX1	ACGGCATGGACGAGCTGTAC
qRT-PCR	
sigA	Fw: CACATGGTCGAGGTCATCAA Rv: TGGATTTCCAGCACCTTCTC
MAB_3551c (tgs1)	Fw: CACCGTCTACTACGGAATCAAC Rv: TGCGCAGCCTCCAATAAT
MAB_0478	Fw: CCACTCCGCAGATGATTACT Rv: GCGATGGTGGCATGAAATAG
MAB_0855	Fw: TCAGGCATCAACATCGTCAA Rv: CGGTCGTCGTATCCGAATTT
MAB_0937c	Fw: GAACCAGTCCATCGTGTTCTT Rv: CGGCTTGGTCGTAGTTCTTAC
MAB_0987c	Fw: CCGCCTATCAGACGATGTATAAG Rv: CGTGTGAACGACAGACAGAA
MAB_1134c	Fw: CCGGAAGGTCTTTCGCATATC Rv: CGAGTTCGATCTTGGCATCTT
MAB_1137c	Fw: CTCGGGCTACCTCAATAACATC Rv: GCCTTGTGGCGGTAGATAAA
MAB_1287	Fw: AACAACAGCTCCACCAACT Rv: CTCCTTGACGTCCTCGATATTC
MAB_1520c	Fw: TGCGATTGGGTTTCGATGA Rv: CGATACAATCTCCGGCAACA

MAB_2037	Fw: GGGACAATGGAGGAGATGAAG Rv: GTGCGGTTCCCAGTAGTAATAG
MAB_2210c	Fw: CCAAGCGGTACAAGGCATTA Rv: GCTGACCATCTCGGCTATTT
MAB_2275	Fw: CTCCATGTCACGATGCTTACT Rv: GCAAGCGACTTCAGCAAATAC
MAB_2301	Fw: CAGCTCCATCCCATTCCTTATC Rv: TCGGCCTGGACCTTCATA
MAB_2303	Fw: ACATTCTCTGTCCCGATCATTC Rv: GTGCTCTTTACCGACCTCTTC
MAB_2570c	Fw: GGCTCAAGGAAGTAATGGAGAA Rv: GTGTGGCTCCCAATACAGATAG
MAB_2571c	Fw: CTCTTGTTGGCGTGTTGATTAC Rv: CGAACGACGAGATTCCAATGA
MAB_2650	Fw: GAAAGCGGACTCGGGTATTT Rv: TTGGGCTTGTATGTCGGAAG
MAB_3150	Fw: ACTGGTCATCCTGGTGATTG Rv: CATCCGCCTTCGTCATACTT
MAB_3201	Fw: CCGATTCTCGATACCCATTCTC Rv: GTGCTGCTTGATCACTGTTTC
MAB_3562c	Fw: GGGAGTTTGTTCGGGCTATT Rv: GCACCCACCATGACGATAAT
MAB_4115c	Fw: CGTATGGCGTGATGAAGAAGA Rv: GGAGGAAGTCGTCAAAGAGTG
MAB_4116c	Fw: CATCTGCGGCATACAGATCAA Rv: CATTCGTGAGACCAGCAACA
MAB_4240c	Fw: CTCGATGAAGGAGATGGGAAAG Rv: GCTCGATCAACGCCGAATA
MAB_4263	Fw: CTGATTCCGACCTCGATGATG Rv: GCCGATGAAGAAGATGGAGTAG
MAB_4310c	Fw: AAGCCCAACAGCAAGAATTG Rv: GAATACATCGGGCGGTAGATAG
MAB_4382c	Fw: GGGCTATCACACCACCTAT Rv: CGGGTTCATCTTGGCTTTA
MAB_4508	Fw: GGTATCGGTTCATCGTCGTT Rv: GCCTTGACTGACTCACTGTT
MAB_4529	Fw: GGGTGCTTCGATATTCCTACTG Rv: GTCGGATCTCGTGTGATGAAT
MAB_4703c	Fw: CAGATGCAGCACACCTATGA Rv: GATGTAATCTCGCAGCCTATCC
MAB_4746	Fw: CAGAGGTATCGTCGCAATTCTC Rv: CCGATGAGAAAGATCGCGTAAT
MAB_4768c	Fw: CGGTATGACGCTGATGATGT Rv: TCGTAATGGCATCGGGAAAG
MAB_2300	Fw: GAGAAGCATGACCGACGACAAA Rv: CACACCCTTCCTTGTCGATGTAGTT
MAB_1135c	Fw: GTCGATCGAGATCATCACCAC Rv: CGTTGGTATACCTCTCGTCTTT
MAB_1136	Fw: GCTCGAACACGACTTCAGTAA Rv: CTACTTGGCCGCACCAAT

Eletrophoretic Mobility Shift Assay (EMSA)	
Probe A_Fw	AAACATATGAAGCATTCAATTCTTAACGCATGGCATGTGCGTTATGGG CAACCTACCAGCGGGT
Probe A_Rv	ACCCGCTGGTAGGTTGCCCATAACGCACATGCCATGCGTTAAGAATTG AATGCTTCATATGTTT
Probe B_Fw	GTGCGTAACGCACGCTACCGGGTGGTTCGTTGGCTCGCAAATCACAC GCCGTGCGTTATCCTCG
Probe B_Rv	CACGCATTGCGTGCGATGGCCCACCAAGCAACCGAGCGTTTAGTGTG CGGCACGCAATAGGAGC
Probe C_Fw	AAACATATGAAGCATTCAATTCTTAGTAGATGGCATGTTGCATATGGG CAACCTACCAGCGGGT
Probe C_Rv	ACCCGCTGGTAGGTTGCCCATATGCAACATGCCATCTACTAAGAATTG AATGCTTCATATGTTT
Non-specific probe_Fw	CACTTCGCCATAAGTGGATTGACTCTATCCACTTTTACCCATAGA
Non-specific probe_Rv	TCTATGGGTAAAAGTGGATAGAGTCAATCCACTTATGGCGAAGTG

Restriction sites are underlined and specified inside brackets.

Table S3. Conservation of the *MAB_2299c-2301* and *MAB_1136-34c* loci in the *M. abscessus* complex.

Strain (source)	*MAB_1136-1135c-1134c*				*MAB_2299c-2300-2301*			
	% ID locus	% ID TetR	% ID MmpS	% ID MmpL	% ID locus	% ID TetR	% ID MmpS	% ID MmpL
M. abscessus subsp. abscessus								
CIP 104536/ ATCC 19977 (type strain)								
% ID to *MAB_2299c-2300-2301*	83.0	60.5	99.3	79.2	-	-	-	-
GZ01 (China, lung (S), 2015)	100	100	100	100	100	100	100	100
GZ002 (China, lung (S), 2015)	100	100	100	100	100	100	100	100
FLAC013 (USA, 2012)	100	100	100	100	100	100	100	100
FLAC028 (USA, 2013)	100	100	100	100	100	100	100	100
FLAC029 (USA, 2013)	100	100	100	100	100	100	100	100
FLAC046 (USA, 2015)	100	100	100	100	100	100	100	100
FLAC003 (USA, 2011)	98.4	98.6	100	99.7	97	99.7	99.5	100
7C (Malaysia, 2016)	100	100	100	100	100	100	100	100
NOV0213 (Russia, sputum, 2013)	100	100	100	100	100	100	100	100
M. abscessus subsp. bolletii								
50594 (South Korea, 2014)	98.7	99.5	100	99.7	97.3	99.7	100	100
G122 (China, sputum, 2017)	99.3	98.6	100	99.7	100	100	100	100
199 (China, sputum, 2017)	99.8	100	100	100	99.7	100	100	100
BD (Japan, 2017)	98.3	98.6	100	99.7	96.8	99.7	99.5	100
FLAC049 (USA, 2015)	100	100	100	100	99.7	100	100	100
FLAC008 (USA, 2012)	98.6	99.5	100	99.7	97.4	99.7	100	100
GD01B (UK, 2017)	98.5	99.5	100	99.6	97.1	99.6	100	100
M. abscessus subsp. massiliense								
FLAC047 (USA, 2015)	98.5	99.5	100	99.6	97.1	99.6	100	100
GO 06 (Brazil, 2012)	98.7	99.5	100	99.7	97.4	99.7	100	100
M. chelonae								
ATCC 35752	89.1	83.5	95.5	93.7	81.8	93.7	91.4	96.2

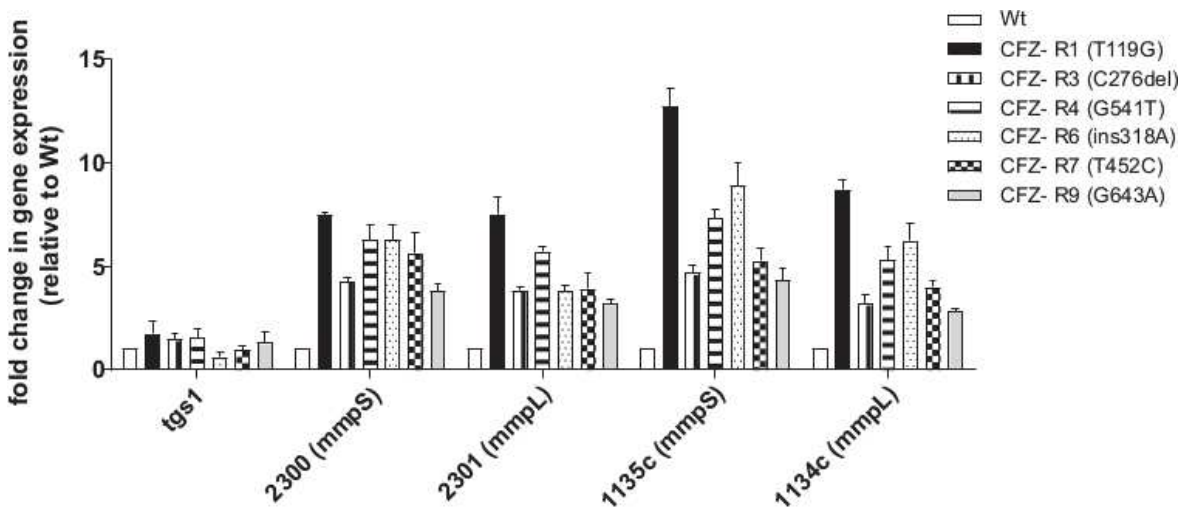

Figure S1. Transcriptional expression of the *MAB_2300-2301* and *MAB_1135c-1134c* gene couples in the parental *M. abscessus* strain and in 6 spontaneous CFZ-resistant mutants harbouring mutations in MAB_2299c. The results are expressed as the fold change in mRNA levels between the mutant strains and the parental strain. Error bars indicate standard deviation. Relative gene expression was calculated using the $2^{-\Delta\Delta Ct}$ method with E correction.

Article 4

« **Dissecting *erm(41)* – Mediated Macrolide Inducible Resistance in *Mycobacterium abscessus*** ». Richard M., Gutiérrez AV., Kremer L. Antimicrob Agents Chemother 64:e01879-19

La résistance inductible aux macrolides est particulièrement problématique car elle contribue grandement aux échecs thérapeutiques observés dans les traitements à *M. abscessus*. Les données sur l'utilisation de l'azithromycine (AZM) en faveur de la clarithromycine (CLR) sont discutables et varient considérablement en fonction des travaux réalisés précédemment par diverses équipes. Dans notre étude, nous avons démontré que l'AZM induisait une résistancemédiée par Erm(41) plus forte que celle provoquée par la CLR *in vitro*. Ces résultats ont été confirmés en mesurant l'activité β-galactosidase exprimée par le gène *lacZ* sous le contrôle du promoteur d'*erm(41)*. La troncation progressive du promoteur d'*erm(41)* a permis d'identifier précisément les éléments génétiques responsables de l'induction de cette résistance et d'en confirmer le principal protagoniste, WhiB7, connu comme un activateur transcriptionnel central chez les mycobactéries. Le remplacement de *lacZ* par le marqueur de fluorescence *tdTomato* sous le contrôle du promoteur complet d'*erm(41)* a montré que l'induction de la résistance aux macrolides se produit également *in vivo* chez le modèle d'infection du zebrafish. Ces observations pourraient refléterun mécanisme ayant lieu chez un patient infecté par *M. abscessus* et sous traitement aux macrolides. Nous avons finalement mis en évidence la complexité de cette régulation en observant une activation plus rapide d'Erm(41) conduisant ainsi à une résistance plus intense chez des souches traitées au préalable avec de la CLR et de l'AZM. Ces souches prétraitées aux macrolides exhibent par ailleurs un antagonisme avec l'amikacine *in vitro*, ce qui pourrait en partie expliquer les nombreux échecs thérapeutiques, car les macrolides et l'amikacine sont utilisés en association dans l'antibiothérapie classique contre *M. abscessus*. Les souches rapportrices *lacZ* et/ou *tdTomato* générées au cours de ces travaux pourraient constituer des outils de choix pour la mise en place d'une nouvelle approche de criblage de molécules actives contre *M. abscessus* et capables de contourner la résistance induite médiée par Erm(41).

AMERICAN SOCIETY FOR MICROBIOLOGY | Antimicrobial Agents and Chemotherapy®

MECHANISMS OF RESISTANCE

Dissecting *erm*(41)-Mediated Macrolide-Inducible Resistance in *Mycobacterium abscessus*

Matthias Richard,[a] Ana Victoria Gutiérrez,[a] Laurent Kremer[a,b]

[a]Institut de Recherche en Infectiologie de Montpellier (IRIM), Université de Montpellier, CNRS UMR, Montpellier, France
[b]INSERM, IRIM, Montpellier, France

ABSTRACT Macrolides are the cornerstone of *Mycobacterium abscessus* multidrug therapy, despite that most patients respond poorly to this class of antibiotics due to the inducible resistance phenotype that occurs during drug treatment. This mechanism is driven by the macrolide-inducible ribosomal methylase encoded by *erm*(41), whose expression is activated by the transcriptional regulator WhiB7. However, it has been debated whether clarithromycin and azithromycin differ in the extent to which they induce *erm*(41)-mediated macrolide resistance. Herein, we show that macrolide resistance is induced more rapidly in various *M. abscessus* isolates upon exposure to azithromycin than to clarithromycin, based on MIC determination. Macrolide-induced expression of *erm*(41) was assessed *in vivo* using a strain carrying *tdTomato* placed under the control of the *erm*(41) promoter. Visualization of fluorescent bacilli in infected zebrafish demonstrates that azithromycin and clarithromycin activate *erm*(41) expression *in vivo*. That azithromycin induces a more rapid expression of *erm*(41) was confirmed by measuring the β-galactosidase activity of a reporter strain in which *lacZ* was placed under the control of the *erm*(41) promoter. Shortening the promoter region in the *lacZ* reporter plasmid identified DNA elements involved in the regulation of *erm*(41) expression, particularly an AT-rich motif sharing partial conservation with the WhiB7-binding site. Mutation of this motif abrogated the macrolide-induced and WhiB7-dependent expression of *erm*(41). This study provides new mechanistic information on the adaptive response to macrolide treatment in *M. abscessus*.

KEYWORDS *Mycobacterium abscessus*, WhiB7, beta-galactosidase, *erm*(41), inducible resistance, macrolides, therapeutic activity, zebrafish

Members of the *Mycobacterium abscessus* complex are rapidly growing nontuberculous mycobacteria (NTM) of increasing clinical significance due to the rising burden of associated pulmonary disease, particularly in cystic fibrosis (CF) patients (1). In CF patients, infection with *M. abscessus* correlates with a more rapid decline in lung function and can represent an obstacle to subsequent lung transplantation (2–4). The possible person-to-person transmission of virulent clones among the CF population makes this situation even more worrisome (5, 6). From a taxonomic view, the complex currently comprises three subspecies: *M. abscessus* subsp. *abscessus*, *M. abscessus* subsp. *bolletii*, and *M. abscessus* subsp. *massiliense* (7). These subspecies exhibit different clinical outcomes and drug susceptibility profiles with respect to antibiotic treatments. *M. abscessus* subsp. *abscessus* is notoriously acknowledged as the most drug-resistant mycobacterial species, characterized by a wide panel of acquired and innate drug-resistance mechanisms against nearly all antitubercular drugs, as well as to most classes of antibiotics (8). These mechanisms rely largely on the expression of enzymes able to modify and inactivate rifamycins (9), aminoglycosides (10), tetracyclines (11), or β-lactams (12) or on the presence of multiple efflux pumps of the MmpL family, which

Citation Richard M, Gutiérrez AV, Kremer L. 2020. Dissecting *erm*(41)-mediated macrolide-inducible resistance in *Mycobacterium abscessus*. Antimicrob Agents Chemother 64:e01879-19. https://doi.org/10.1128/AAC.01879-19.

Address correspondence to Laurent Kremer, laurent.kremer@irim.cnrs.fr.

Received 16 September 2019
Returned for modification 11 November 2019
Accepted 25 November 2019
Accepted manuscript posted online 2 December 2019
Published 27 January 2020

afford low-level resistance to clofazimine and bedaquiline (13, 14). Therapeutic treatments require prolonged courses of multiple antibiotics, usually combining a macrolide, a β-lactam (cefoxitin or imipenem), and an aminoglycoside (15). Macrolides represent the cornerstone of *M. abscessus* subsp. *abscessus* multidrug therapy (15), but treatment success rates are poor, particularly in macrolide-resistant strains. Acquired resistance to macrolides usually occurs at low rates through point mutations at positions 2058 or 2059 of the 23S rRNA *rrl* gene (16). In addition, *M. abscessus* subsp. *abscessus* harbors an inducible ribosomal methylase encoded by *erm*(41), which represents the primary mechanism of intrinsic resistance against macrolides (17). This adaptive resistance mechanism can be manifested by prolonged incubation of the bacilli up to 14 days in drug-susceptible testing assays, rather than the typical 3 to 4 days of exposure to other drugs. A single nucleotide exchange (of T28C, resulting in a Trp10Arg replacement) in *erm*(41) is associated with a loss of methylase activity in *M. abscessus* subsp. *abscessus*, abrogating the inducible resistance mechanism and thereby resulting in a macrolide-susceptible phenotype (18, 19). This T28C polymorphism is found in 15 to 20% of clinical isolates (20, 21). In contrast to *M. abscessus* subsp. *abscessus* or *M. abscessus* subsp. *bolletii*, *M. abscessus* subsp. *massiliense* has been associated with clarithromycin (CLR) susceptibility due to deletions (bases 64 to 65 and 159 to 432) within *erm*(41) (17, 22), explaining the more favorable clinical outcomes upon CLR treatment (23). However, the role and contribution of the Erm(41)-dependent mechanism in azithromycin (AZM) resistance is less clear and has been the subject of discrepancies between studies. In accordance with an early report of Brown et al. (24), it was subsequently reported that MICs of AZM for the *M. abscessus* complex tend to be higher than those of CLR (18). In contrast to these studies, Choi et al. reported that AZM is a poor inducer of *erm*(41) gene expression compared to CLR and, therefore, should be preferred in antibiotic therapy for *M. abscessus* infections (25). However, this work was inconsistent with another study in which both molecules provoked a comparable resistance phenotype in *M. abscessus* (19). A recent study also showed that *erm*(41) expression increased after exposure to either macrolide for 7 days and it was proposed that this should not be an argument for choosing between CLR and AZM for therapy (26). However, most studies are based on the *in vitro* determination of the MIC to cultures exposed to macrolides and data reporting the Erm(41)-dependent inducible mechanisms in the infected host are scarce. Except for a study reporting the increased expression of *erm*(41) transcripts in *M. abscessus*-infected mice treated with CLR, but not with AZM (25), it remains to be fully established whether macrolide-inducible resistance occurs *in vivo*, and whether induction occurs rapidly upon drug treatment in the infected host.

In the context of this long debate, the present study aimed at revisiting the *erm*(41) inducible mechanisms through the following means: (i) evaluation of the *in vitro* drug susceptibility of clinical isolates belonging to the *M. abscessus* complex to CLR and AZM; (ii) visualization of induced expression of *erm*(41) in zebrafish infected with an *M. abscessus* reporter strain in which a fluorescent marker has been placed under the control of the *erm*(41) promoter region; and (iii) dissection of the *erm*(41) promoter to uncover important DNA regions that participate directly in this regulatory process.

RESULTS

Macrolide-inducible resistance of smooth and rough *M. abscessus* CIP104536^T is medium independent. The current debate regarding the level of resistance induced by CLR or AZM has been hypothesized to be dependent on the composition of the medium used for the determination of the MICs of the two drugs. In particular, Choi et al. (25) used Middlebrook 7H9, which contains a large amount of inorganic salts and has a slightly acidic pH (pH 6.8), whereas Bastian et al. (18), following the Clinical and Laboratory Standards Institute (CLSI) recommendations, used cation-adjusted Mueller-Hinton broth (CaMHB), which has a higher pH (pH 7.4) than 7H9. Because macrolide activity is sensitive to pH (27), it was hypothesized that the different media used in various studies may have influenced the MIC values. Herein, we evaluated and com-

pared macrolide-induced resistance to both drugs at various time points (3, 5, 7, 10, and 14 days posttreatment [dpt]) in three different media (CaMHB, 7H9, and Sauton's). When assaying the smooth (S) morphotype of the reference strain CIP104536^T, we consistently found that AZM induced a more rapid upshift of the MIC than CLR in all three media (Fig. S1A in the supplemental material). The increase in MIC of AZM started after 3 dpt and rose progressively to reach a MIC of 256 μg/ml at 10 dpt. The same MIC value was reached at 14 dpt with CLR, indicating that, although the intensity of induced resistance is comparable for both macrolides, the kinetics of resistance was delayed with CLR compared to AZM *in vitro*. As expected, amikacin (AMK), used as a nonrelevant control drug, failed to show a similar drug-induced phenotype upon a prolonged exposure time. As observed with the S variant, the kinetics of resistance to AZM in the rough (R) variant was more rapid than that with CLR and this macrolide-induced resistance was independent of the medium used (Fig. S1B). Overall, these results indicate that both S and R morphotypes respond similarly to macrolide treatment regardless of the medium.

Resistance to macrolides is rapidly induced in the *M. abscessus* complex strains upon exposure to CLR and AZM. We next investigated the kinetics of macrolide-inducible resistance in clinical strains isolated from cystic fibrosis (CF) and non-CF patients in CaMHB. Clinical *M. abscessus* subsp. *abscessus* strains 2069 and 3022, from non-CF patients, were characterized by a more rapid increase in the MIC values for AZM than for CLR, similar to the reference strain CIP104536^T (Fig. S2A and S2B). However, in the case of strain 2069, the resistance to CLR reached a plateau at 128 μg/ml at 10 dpt, whereas for strain 3022 the MIC continued to rise up to 256 μg/ml at 14 dpt, sharing a profile similar to the CF strain 2648. In contrast, strain 1298 failed to show inducible resistance to either macrolide (Fig. S2A). Due to the important contribution of the polymorphism at the 28th nucleotide of *erm*(41), where the T28 sequevar (Trp10) shows inducible resistance while the C28 sequevar (Arg10) remains susceptible to macrolides (18), we sequenced *erm*(41) in *M. abscessus* subsp. *abscessus* strains 1298, 2069, 2648, 3022, *M. abscessus* subsp. *bolletii*, and *M. abscessus* subsp. *massiliense*. All *M. abscessus* subsp. *abscessus* strains possess an *erm*(41) gene identical to the *M. abscessus* CIP104536^T reference strain, with a Trp in position 10, except for strain 1298 carrying a Leu residue instead of a Phe in position 34 (not shown). To our knowledge, this point mutation, presumably inactivating Erm(41) and conferring susceptibility to macrolides, has not been yet reported (20). The *M. abscessus* subsp. *bolletii* S strain carrying the T28 sequevar also showed inducible resistance to macrolides, similarly to *M. abscessus* subsp. *abscessus* (Fig. S2C). As anticipated, *M. abscessus* subsp. *massiliense* was found to be intrinsically susceptible to CLR and AZM due to a genetic lesions in *erm*(41) that renders the enzyme nonfunctional (18) (Fig. S2D). We next constructed an unmarked deletion mutant of *erm*(41) using a recently developed strategy based on a new suicide vector, pUX1-*katG*, which allows the easy and rapid generation of genetic deletions in the *M. abscessus* chromosome, facilitated by the presence of the brightly red fluorescent tdTomato positive selectable marker and the *katG* counter selectable marker (10, 13, 28) (Fig. S3). In agreement with a previous report (25), this mutant remained fully susceptible to CLR and AZM, confirming the direct involvement of Erm(41) in macrolide-inducible resistance (Fig. S2E).

Together, these results confirm that *M. abscessus* subsp. *abscessus* clinical isolates and *M. abscessus* subsp. *bolletii* carry a functional Erm(41) methylase undergoing a faster increase in resistance to AZM than to CLR, and that the newly discovered F34L substitution in Erm(41) abrogates the macrolide-induced resistance.

Inducible resistance to macrolides occurs in infected zebrafish. The vast majority of studies related to macrolide-inducible resistance are based on MIC determination and/or determination by quantitative reverse transcriptase PCR (qRT-PCR) of the level of *erm*(41) transcripts *in vitro* (18, 19, 26). Despite the clinical importance, reports describing whether macrolide-inducible resistance occurs during patient therapy are scarce. However, one study reported increased expression of *erm*(41) transcripts in *M.*

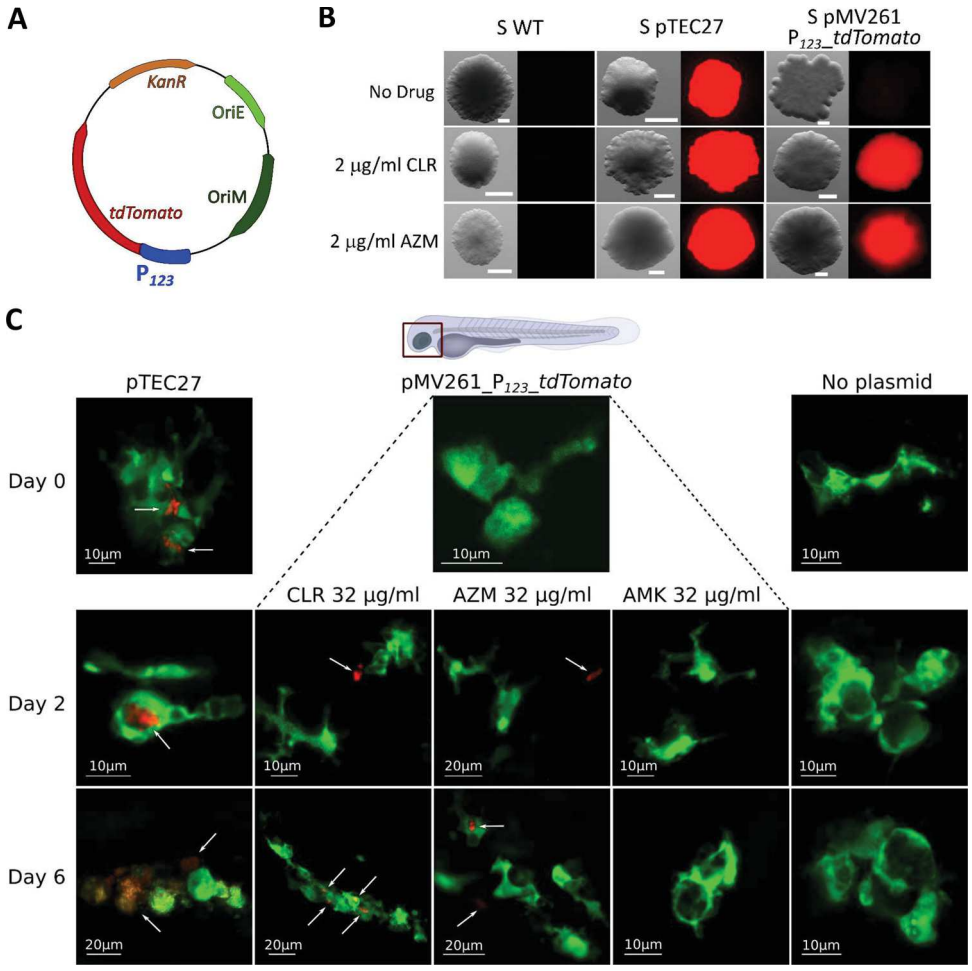

FIG 1 *In vivo* induction of macrolide resistance in *M. abscessus*-infected zebrafish embryos. (A) Schematic representation of the plasmid pMV261_P_{123}_*tdTomato* used to transform *M. abscessus* smooth (S) variant CIP104536^T, where P_{123} represents the full-length promoter region of *erm*(41). (B) Bacteria with no plasmid (WT), with the pTEC27 plasmid which constitutively expresses the red fluorescent protein tdTomato, or with the pMV261_P_{123}_*tdTomato* plasmid for monitoring macrolide-inducible expression of tdTomato were plated on 7H10^{OADC} supplemented or not with 2 μg/ml CLR or AZM. Plates were incubated at 37°C for 5 days and observed under a fluorescence microscope. Scale bars represent 0.200 μm. (C) Macrolide-inducible resistance by CLR and AZM occurs *in vivo*. Tg(*mpeg1:GFP-CAAX*) zebrafish embryos, harboring green fluorescent macrophages, were injected in the caudal vein with 900 to 1,000 CFU of the three *M. abscessus* strains described in panel B. At 24 hpi, embryos were exposed to osmotic water supplemented with 32 μg/ml CLR, AZM, or AMK (day 0 of treatment) and fluorescence was monitored at 2 and 6 days posttreatment. Shown is representative confocal live imaging. White arrows indicate red fluorescent bacteria.

abscessus-infected mice treated with CLR but not with AZM (25). We took advantage of the transparency of zebrafish embryos to visualize and monitor the induced expression of *erm*(41) during macrolide treatment of larvae infected with *M. abscessus*. Indeed, this recently developed animal model allows easy assessment of the suitability and sensitivity of clinically relevant drugs, along with the ability to visualize, in a dose- and time-dependent manner, the dynamics of infection in the presence of an active compound (12, 29–31). To do so, a fluorescent reporter *M. abscessus* strain was designed, carrying the plasmid pMV261_P_{123}_*tdTomato*, in which the *tdTomato* gene was cloned under the control of the 123 bp promoter region of *erm*(41) (Fig. 1A). To verify the usefulness of this construct, the recombinant strain was first plated onto Middlebrook 7H10 medium containing 100 μg/ml kanamycin supplemented or not with 2 μg/ml CLR or AZM. Examination of the plates under a fluorescence microscope revealed the presence of red fluorescent colonies in the presence of either macrolide, while no fluorescence was detected on plates lacking these drugs (Fig. 1B). As a positive

control for fluorescence, a strain harboring pTEC27, which allows constitutive expression of *tdTomato* in *M. abscessus* (32), was also included in these experiments (Fig. 1B). These results clearly highlight the potential of this reporter strain to monitor macrolide-inducible *erm*(41) expression in an infected host. Whether red fluorescent bacilli can be visualized directly in *M. abscessus*-infected embryos upon treatment with macrolides was next investigated. Around 1000 CFU of the reporter strain were microinjected into the caudal vein of the *mpeg:GFP-CAAX* transgenic embryos harboring green fluorescent macrophages (33) which, after 96 h, were exposed to 32 μg/ml CLR or AZM (directly added to the water). Fish were observed under the fluorescence microscope at 0, 2, and 6 dpt. Red fluorescent bacilli could be detected at 2 dpt with either macrolide, while no signal was detected in control embryos (*M. abscessus* without plasmid) or embryos treated with AMK as a nonrelevant drug, indicating that expression of *tdTomato* occurred very rapidly during infection in a living animal and was specifically induced by macrolides (Fig. 1C). At later time points (6 dpt), red fluorescent bacilli were detected inside individualized macrophages or inside aggregated macrophages forming granulomas. Red bacilli could also be observed outside macrophages, although they may reside inside neutrophils (which cannot be visualized in this transgenic zebrafish line harboring only fluorescent macrophages), shown to rapidly engulf *M. abscessus* (34). It remains, however, difficult to explain at this stage whether already fluorescent bacteria are phagocytosed by macrophages or whether macrolides penetrate macrophages/granulomas to induce *tdTomato* expression in intracellular bacilli.

Overall, these results indicate that macrolide-inducible resistance occurs in the zebrafish model of infection.

Low macrolide concentrations induce a more rapid expression of *erm*(41) than high concentrations in *M. abscessus*. The pMV261_P_{123}_*lacZ* plasmid containing the *lacZ* gene encoding the β-galactosidase (β-Gal) gene under the control of the *erm*(41) promoter was designed to tackle the fluctuations in *erm*(41) gene expression during exposure of the culture to various drug treatments (Fig. 2A). This strain was exposed to 2, 8, 64, and 128 μg/ml of either CLR or AZM and *lacZ* expression was determined by measuring β-Gal activity using 2-nitrophenyl β-D-galactopyranoside (ONPG) at different time points over a 14-day period (Fig. 2B). Exposure to 2 μg/ml of CLR induced rapid β-Gal activity during the first 2 days of treatment, which plateaued thereafter. Increasing the drug concentration resulted in similar but delayed specific activity curves. At the highest concentration tested, the lag phase lasted for 7 days prior to the induction of *lacZ* expression. This is unlikely to be linked to the impaired growth of the cultures treated with high concentrations of macrolide as the specific activity is expressed in relation to the total amount of soluble proteins. The maximum specific activity was, however, lower than the β-Gal activity produced when *lacZ* was placed under the control of the strong constitutive *hsp60* promoter (Fig. 2C, left). As expected, when the promoterless construct was introduced in *M. abscessus*, this resulted in the loss of β-Gal activity. Moreover, in another strain in which the *erm*(41) promoter region was substituted by the promoter region of *MAB_4384*, encoding a TetR protein previously characterized (35), no activity was detected. This further supports that CLR-dependent expression of *lacZ* was specific to the *erm*(41) promoter region. Treatment with increasing concentrations of AZM showed slightly different trends, characterized by a faster induction of *lacZ* expression at low concentrations (2 and 8 μg/ml) than at high concentrations (64 and 128 μg/ml) and a significantly shorter lag phase with AZM than with CLR (Fig. 2C, right). Cultures treated with 64 μg/ml of AZM reached a β-Gal activity of approximately 8,000 units in only 3 days, whereas 10 days were needed for cultures treated with the same CLR concentration to reach this level of activity. Together, these results suggest that *erm*(41) transcriptional expression is more rapidly induced by AZM than by CLR, in agreement with the MIC results (Fig. S1 and S2).

To ask whether the rapid increase in AZM-dependent expression of *lacZ* was restricted to the reference strain, the influence of both macrolides on *lacZ* expression was assessed in clinical strains (*M. abscessus* subsp. *abscessus* strains 2069, 2648, 3022 and *M. abscessus* subsp. *bolletii*) transformed with pMV261_P_{123}_*lacZ*. In all cases,

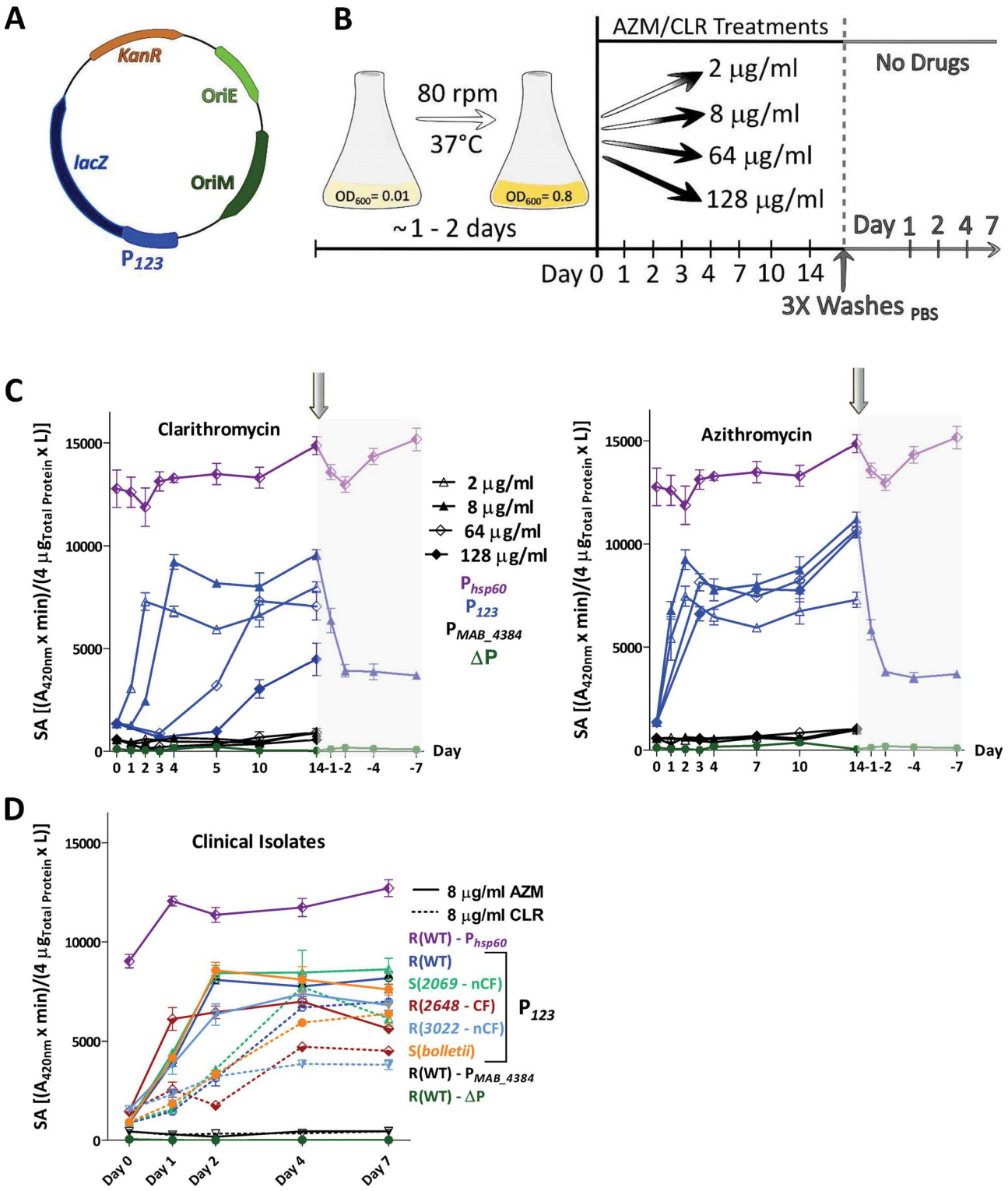

FIG 2 Kinetics of macrolide-induced expression of *erm*(41) using *lacZ* reporter strains. (A) Schematic representation of the pMV261_P_{123}_*lacZ* used to transform the *M. abscessus* CIP104536^T rough variant. (B) Schematic protocol of the β-Gal assay to evaluate the kinetics of macrolide-induced resistance. (C) The *M. abscessus* strain carrying the pMV261_P_{123}_*lacZ* was first exposed to various concentrations of CLR and AZM for 14 days. Antibiotics were then removed by washing the bacterial pellets several times with PBS prior to β-Gal activity measurements for the next 7 days. (C) The β-Gal activity profile of *M. abscessus* CIP104536^T rough variant exposed to 2, 8, 64, and 128 µg/ml CLR (left) or AZM (right). A pMV261 derivative containing *lacZ* cloned under the control of the constitutive *hsp60* promoter (P_{hsp60}) was used as a positive control. A promoterless construct (ΔP) and a pMV261_*lacZ* construct carrying the promoter of an unrelated gene (P_{MAB_4384}) were included as negative controls. (D) Similar experiments as in panel C were carried out using different *M. abscessus* subsp. *abscessus* clinical strains (2069, 2648, and 3022) as well as *M. abscessus* subsp. *bolletii* transformed with pMV261_P_{123}_*lacZ* and exposed to either CLR or AZM (8 µg/ml) for 7 days. All experiments were performed on 2 separate occasions with a total of 6 technical replicates. The specific activity of β-Gal is given in (A_{420nm} × min)/(4 $\mu g_{Total\ protein}$ × liters) as described in the Materials and Methods section ± standard deviation.

TABLE 1 Enduring resistance levels to macrolides and amikacin following preexposure of *M. abscessus* to CLR or AZM

	MIC μg/ml														
	Day 3			Day 5			Day 7			Day 10			Day 14		
Growth conditions[a]	CLR	AZM	AMK	CLR	AZM	AMK	CLR	AZM	AMK	CLR	AZM	AMK	CLR	AZM	AMK
Untreated	1	4	16	16	64	16	64	128	16	128	256	32	256	>256	32
CLR pretreated	64	128	16	256	>256	32	>256	>256	32	>256	>256	64	>256	>256	64
AZM pretreated	128	256	32	>256	>256	64	>256	>256	64	>256	>256	64	>256	>256	64

[a]*M. abscessus* CIP104536^T (rough variant) was pretreated or not with 8 μg/ml of either CLR or AZM for 4 days, washed, and incubated in macrolide-free medium for 2 additional days. MIC of CLR, AZM, and AMK were determined according to the CLSI guidelines at different time points. The MICs are given in μg/ml. Results are representative from three individual experiments with similar values.

treatment with 8 μg/ml AZM induced a more rapid induction of *lacZ* expression than treatment with 8 μg/ml CLR, although the intensity of the response varied from one strain to another and was always below the activity associated with the *hsp60* promoter (Fig. 2D). For instance, *lacZ* induction in strain 3022 was significantly slower than in strain 2069.

Overall, these results confirm that, although both macrolides induce a potent transcriptional expression of *erm*(41), AZM induces a more rapid response than does CLR.

Both CLR and AZM reduce the efficacy of AMK in *M. abscessus*. Drug-inducible resistance is a mechanism of adaptive response to antibiotic treatment that is not genetically programed. As such, this reversible phenomenon is expected to disappear after stopping the drug treatment. Our reporter strain allowed us to ask whether *erm*(41) expression is reversed after removal of the drugs. In the experimental protocol used, bacteria were treated for 14 days with 8 μg/ml CLR (Fig. 2C, left) or with 8 μg/ml AZM (Fig. 2C, right), after which the cultures were extensively washed with phosphate-buffered saline (PBS) and the β-Gal activity further monitored for 7 days in the absence of drugs (Fig. 2B). Rapidly after washing, *lacZ* expression dropped during the next 2 days and then remained unchanged until the end of the experiment (7 days post washing) at significantly higher levels (around 4,000 units) than prior to drug addition. To assess the possibility that macrolide-pretreated cultures are more tolerant than unexposed cultures, bacteria containing pMV261_P_{123}_*lacZ* were first preexposed or not with 8 μg/ml of CLR or AZM for 4 days. Once the optimal β-Gal activity was reached, the cultures were carefully washed with 1× PBS and bacterial pellets were resuspended and incubated in macrolide-free Sauton's medium for two more days, a time point at which a β-Gal activity of 4,000 units was measured (not shown). From this stage (considered day 0), the MIC of CLR, AZM, and AMK were determined in Sauton's medium at 3, 5, 7, 10, and 14 days (Table 1). At day 3, the untreated cultures exhibited MIC values of 1, 4, and 16 μg/ml for CLR, AZM, and AMK, respectively, while the macrolide-pretreated cultures exhibited higher MIC values. The CLR-treated culture displayed MICs of 64, 128, and 16 μg/ml against CLR, AZM, and AMK, respectively. This effect was even more pronounced with the AZM-treated culture (128, 256, and 32 for CLR, AZM, and AMK, respectively) and further increased at day 5 and day 7, with MIC values exceeding 256 μg/ml. While the MIC of AMK remained unchanged for the untreated culture (16 to 32 μg/ml), pretreatment with CLR induced cross-resistance to AMK (64 g/ml), as previously reported (36). We found this was also true with AZM (Table 1), indicating that, like CLR, exposure to AZM reduces the activity of AMK.

Identification of a *whiB7* box upstream of *erm*(41) required for macrolide-induced expression. Careful examination of the promoter region using the MEME software identified two pairs of conserved repetitive sequences. To gain further insights into the regulatory DNA elements responsible for macrolide induction, the P_{123} promoter region in pMV261_ P_{123}_*lacZ* was replaced by DNA fragments of 92 bp, 61 bp, and 38 bp derived from the original P_{123}. The segment sizes were chosen to progressively shorten the degenerated inverted repeats (Fig. 3A and B). These DNA motifs may eventually represent the target of transcriptional factors that contribute to *erm*(41) transcriptional regulation. Cultures were exposed to various concentrations of AZM or

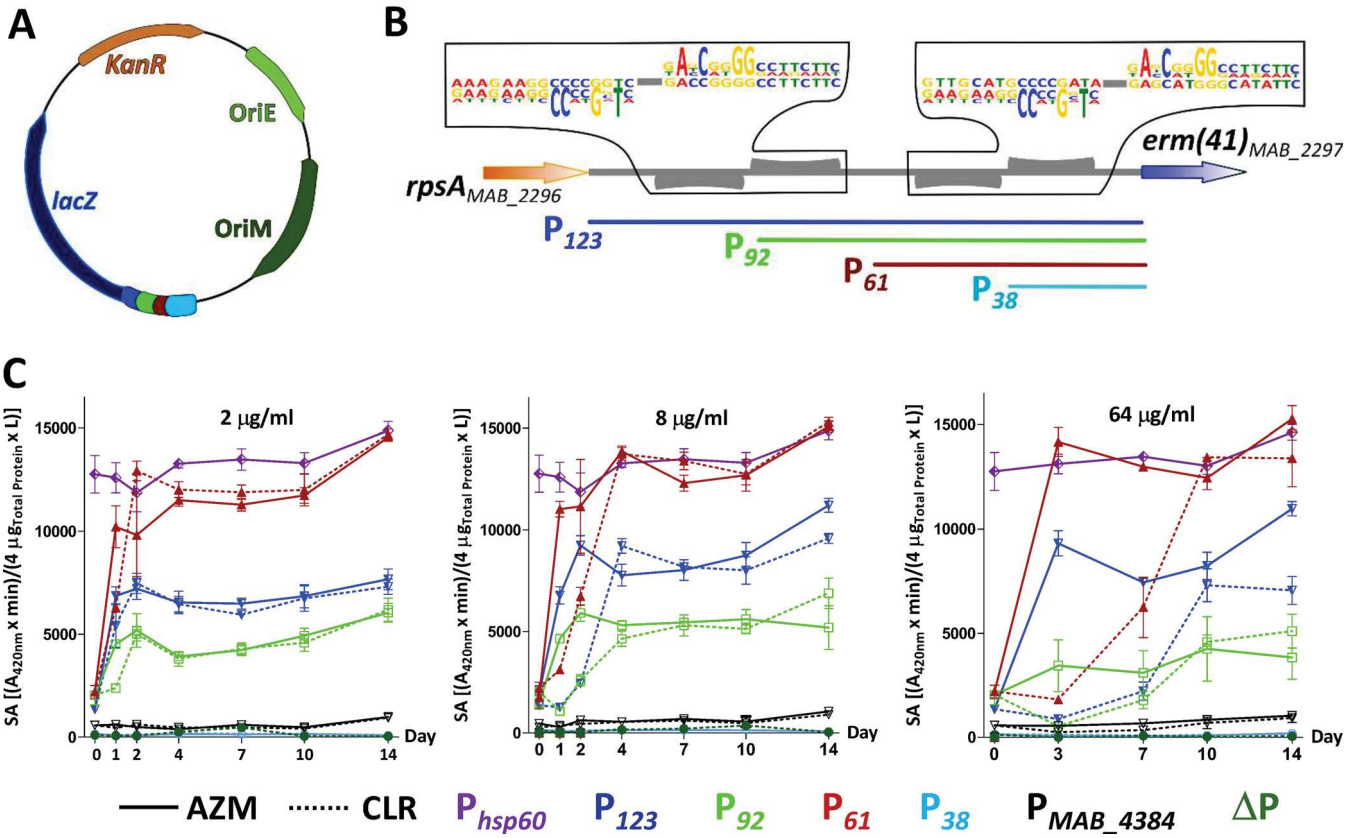

FIG 3 Dissection of the *erm*(41) promoter region and impact on *lacZ* expression. (A) Schematic representation of the intergenic region between *rpsA* and *erm*(41). Two pairs of weakly conserved palindromes were identified using the MEME Suite 4.20.0 online tool. (B) Derivatives of pMV261_*lacZ* containing various truncated intergenic regions (where P_{123}, P_{92}, P_{61}, and P_{38} correspond to the size of the promoter region in base pairs) were generated according to this bioinformatics analysis and shown using a color code. (B) Schematic representation of the intergenic region between *rpsA* and *erm*(41). Two pairs of weakly conserved palindromes were identified using the MEME Suite 4.20.0 online tool. (C) β-Gal activity profile of the *M. abscessus* strains transformed with the various *lacZ* reporter constructs monitored over a period of 14 days and exposed to 2 μg/ml (left), 8 μg/ml (middle), or 64 μg/ml (right) of either CLR (dotted lines) or AZM (normal lines). A pMV261 derivative containing *lacZ* cloned under the control of the constitutive *hsp60* promoter was used as a positive control (P_{hsp60}). A promoterless construct (ΔP) and a pMV261_*lacZ* construct carrying the promoter of an unrelated gene (P_{MAB_4384}) were included as negative controls. The results were obtained from two separate experiments with a total of 6 technical replicates. The specific activity of β-Gal is given in $(A_{420nm} \times min)/(4\ \mu g_{Total\ protein} \times liters)$ as described in the Materials and Methods section ± standard deviation.

CLR and *lacZ* expression was monitored over time by measuring the β-Gal activity. In the presence of 2 μg/ml of either macrolide, the optimal specific activity of the full-length construct (123 bp) plateaued at around 7,000 units, while the 92-bp construct was associated with a reduction in activity, to around 5,000 units (Fig. 3C, left). This indicates that the construct lacks an important regulatory element that is required for normal transcriptional levels. Unexpectedly, further shortening the promoter region down to 61 bp led to an opposite effect, with a much more pronounced β-Gal activity than with P_{123}, reaching the levels of the strong *hsp60* promoter. As shown earlier, these effects were always more rapid when the various strains were exposed to AZM than to CLR. Similar profiles were obtained by treating the various strains with 8 μg/ml (Fig. 3C, middle) or 64 μg/ml (Fig. 3C, right) of macrolides. In sharp contrast, the strain carrying pMV261_P_{38}_*lacZ* failed to express any β-Gal activity, indicating that P_{38} is missing important regulatory information. As expected, when either the promoterless construct (ΔP) or the pMV261_P_{MAB_4384}_*lacZ* were introduced in *M. abscessus*, no β-Gal activity was detected (Fig. 3C). This suggests the presence of two important regulatory sequences in P_{123}: one located between the 5′ end of the P_{61} construct and the 5′ end of the P_{38} construct that positively regulates the expression and one located at the 5′ end of the 92 bp segment that possibly participates in the downregulation of *erm*(41) expression.

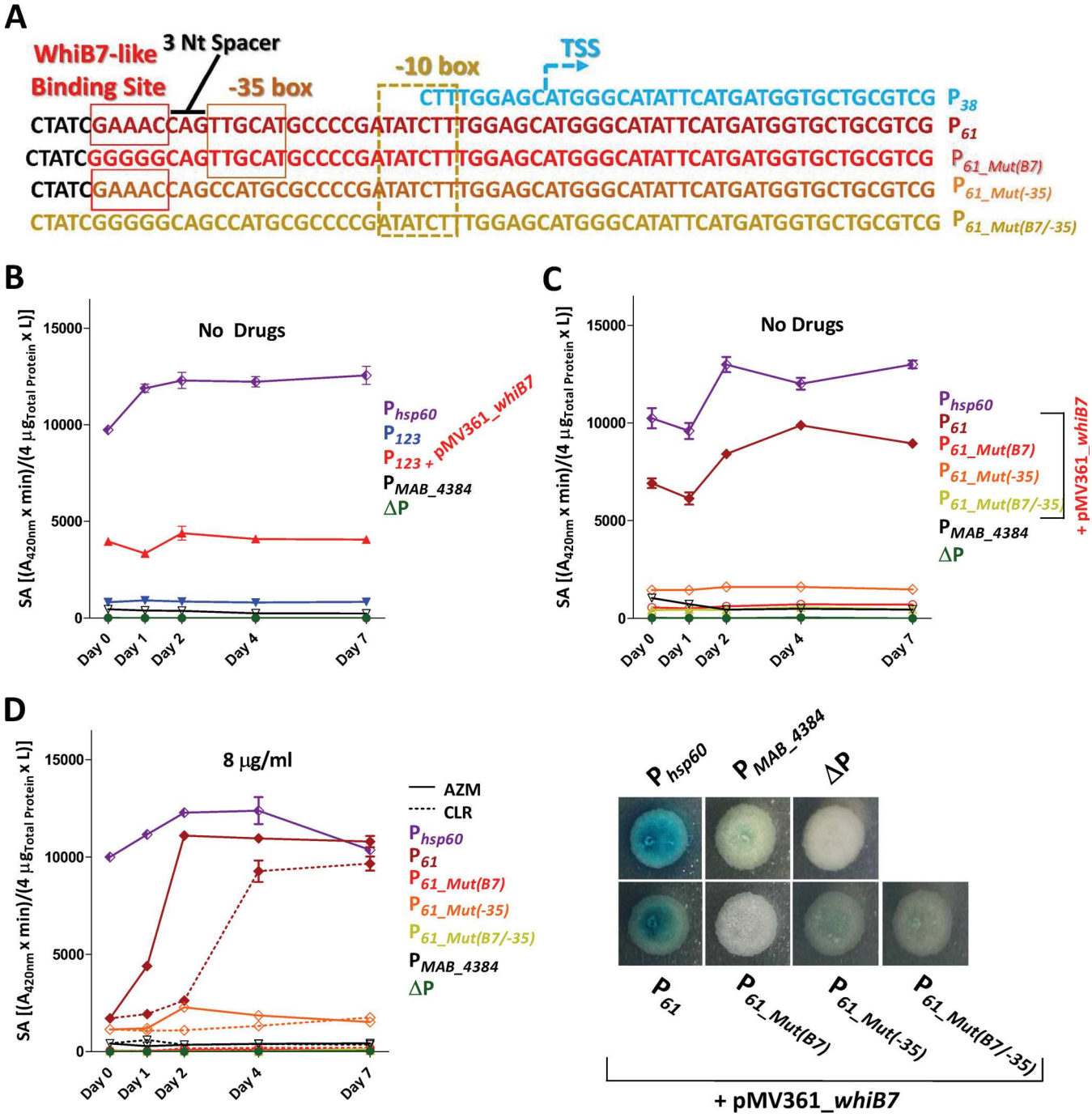

FIG 4 Implications of a WhiB7-binding site required for macrolide-inducible expression of *erm*(41). (A) DNA sequences of P_{38} and P_{61} as well as three mutated constructs of the P_{61} promoter region were introduced into the *lacZ* reporter strains. These nucleotide changes were introduced in the putative WhiB7-binding site ($P_{61\_Mut(B7)}$) and the *erm*(41) putative −35 box ($P_{61\_Mut(-35)}$), either individually or together ($P_{61\_Mut(B7/-35)}$). All constructs were used to transform *M. abscessus* CIP104536^T rough variant. The transcriptional starting site (TSS) has been determined previously (17). (B) In the absence of macrolides, constitutive expression of *whiB7* (provided by the integrative pMV361_*whiB7*, red) in *M. abscessus* pMV261_P_{123}_*lacZ* correlates with a significantly stronger β-Gal activity than in a strain carrying pMV261_P_{123}_*lacZ* alone, implicating WhiB7 as a positive regulator of P_{123}. (C) *M. abscessus* rough variant containing the P_{61}, $P_{61\_Mut(B7)}$, $P_{61\_Mut(-35)}$, or $P_{61\_Mut(B7/-35)}$ derivatives fused to *lacZ* were transformed with pMV361_*whiB7*. All these mutations abrogated the β-Gal activity in liquid cultures (upper) and on solid medium (lower). Exponentially growing *M. abscessus* cultures were spotted onto 7H10 plates containing 50 µg/ml X-Gal. The plates were subsequently incubated for 3 days at 37°C and bacteria visualized for their blue/white coloration. (D) The presence of macrolides failed to induce β-Gal activity in the mutated promoter constructs as evidenced by monitoring the *lacZ* activity in the presence of 8 µg/ml of CLR or AZM. A pMV261 derivative containing *lacZ* cloned under the control of the constitutive *hsp60* promoter was used as positive control (P_{hsp60}). A promoterless construct (ΔP) and a pMV261_*lacZ* construct carrying the promoter of an unrelated gene (P_{MAB_4384}) were included as negative controls. The results were obtained from two separate experiments with a total of 6 technical replicates. The specific activity of β-Gal is given in (A_{420nm} × min)/(4 $\mu g_{Total\ protein}$ × liters) as described in the Materials and Methods section ± standard deviation.

By analyzing the sequence of P_{61} missing in P_{38}, we identified a putative −35 box (Fig. 4A). In addition, WhiB7 is known as a master regulator that activates transcription of many different genes involved in resistance to macrolides and amikacin (36, 37), but its direct implication in this process remains to be defined. We therefore scrutinized more thoroughly the DNA sequence of P_{61} and found a sequence that resembles the typical AT-rich DNA sequence recognized by WhiB7. This sequence displays partial conservation with a motif located in the region upstream of *whiB7* in various mycobacterial species (38) and which is missing in P_{38} (Fig. 4A). This putative 5 bp WhiB7-binding site (GAAAC) is located 3 nucleotides upstream of a potential −35 box, similarly to the sites and sequences defining the *whiB7* promoter (38, 39). However, the optimal distance of 16 to 19 nucleotides between the −35 and −10 hexamers is not conserved, as they are separated by only 7 nucleotides (Fig. 4A). Mycobacterial promoters have been identified with hexamer distances of between 6 and 35 bp (40). To test whether WhiB7 influences *erm*(41) expression by binding to this motif, the integrative plasmid pMV361_*whiB7* was introduced into *M. abscessus* carrying pMV261_P_{123}_*lacZ* and β-Gal activity was followed for 7 days in the absence of drug treatment. Fig. 4B clearly shows that *lacZ* was constitutively expressed at much higher levels in the strain containing pMV361_*whiB7*, indicating that WhiB7 is a positive regulator of *erm*(41) expression, in accordance with previous findings (36, 37). To further illuminate the contribution of the GAAAC motif as a potential WhiB7-binding site, this sequence was mutated in pMV261_P_{61}_*lacZ*, (designated $P_{61\_Mut(B7)}$), as illustrated in Fig. 4A. Introduction of the mutation abrogated *lacZ* expression both in liquid cultures (Fig. 4C, upper) and on agar plates (Fig. 4C, lower). In addition, mutating the putative −35 box was accompanied by a sharp drop in β-Gal activity and mutations in both the *whiB7* and the −35 boxes abrogated *lacZ* expression, suggesting that both regions are required for regulation and the transcriptional expression of *erm*(41) (Fig. 4C). To conclusively demonstrate the importance of the GAAAC motif for macrolide-inducible resistance, we treated the three mutated strains (pMV261_$P_{61_Mut(B7)}$_*lacZ*, pMV261_$P_{61_Mut(-35)}$_*lacZ*, and pMV261_$P_{61_Mut(B7/-35)}$_*lacZ*) with either 8 μg/ml CLR or AZM for 7 days. This almost completely abolished the β-Gal activity upon treatment with either drug, compared to the pMV261_P_{61}_*lacZ* control strain carrying the intact motifs (Fig. 4D).

Collectively, these results indicate that the 61 bp promoter region comprises a critical WhiB7 binding motif that is necessary for macrolide-inducible *erm*(41) expression.

DISCUSSION

M. abscessus is a challenging pathogen that causes severe respiratory infections in patients with underlying lung disorders and these infections have become more common recently. This is of particular concern due to the natural resistance of *M. abscessus* to most conventional antibiotics (8). Macrolides are important components of the multidrug therapy against *M. abscessus sensu lato* and the American Thoracic Society/Infectious Diseases Society of America guidelines for the treatment of nontuberculous mycobacteria (NTM) recommend use of one of these agents as part of a multidrug regimen (15). It was previously shown that clarithromycin (CLR) is a stronger inducer of Erm(41) than azithromycin (AZM), with higher mRNA expression and a more rapid increase in MICs during prolonged incubation (25), leading to the conclusion that AZM may be preferred to CLR for the treatment of *M. abscessus* infections. It was then reported that the median MICs of AZM for *M. abscessus sensu lato* were markedly higher than those of CLR (41), while both macrolides induce resistance similarly (26). The present results confirm that *M. abscessus* subsp. *bolletii* and *M. abscessus* subsp. *abscessus* clinical isolates carrying a functional Erm(41) methylase undergo a more rapid increase in the MIC for AZM than for CLR, which was linked neither to the composition of the medium nor to the morphotype of the strains. Based on these results, induction of resistance cannot be a criterion for choosing between CLR and AZM for *M. abscessus* subsp. *abscessus* and *M. abscessus* subsp. *bolletii* drug treatment.

In one case only, macrolide-induced resistance was abrogated (clinical strain 1298)

due to a F34L substitution in Erm(41), a mutation that was not previously reported to our knowledge, that presumably inactivates enzymatic activity. MIC data were also corroborated with transcriptional data through the development of a *lacZ* reporter strain exposed to various doses of either macrolide and supporting the view that expression of *erm*(41) is more rapidly induced with AZM than with CLR. This reporter strain provides a means to better understand the differential effect of AZM and CLR on promoter activity when bacteria are exposed to various stress conditions, such as antibiotic combinations and medium composition. Importantly, through the development of a *tdTomato* reporter strain, we were able to image macrolide-induced resistance in infected animals. Thanks to the optical transparency of zebrafish embryos, individual bacilli expressing tdTomato could be detected very early after exposing the embryos to either CLR or AZM (2 dpt). Although qualitative, these results indicate that CLR- and AZM-inducible resistance occurs very rapidly in the infected host, likely explaining the poor effectiveness of macrolide therapy in patients infected with *M. abscessus* subsp. *abscessus* or *M. abscessus* subsp. *bolletii* (42, 43). While the zebrafish model appears well adapted to monitor the *in vivo* induction of *erm*(41), it presents some limitations to study the reverse phenomenon following removal of the drugs. Drugs are likely to accumulate in the embryos and, even after their removal from the water, their presence in fish will sustain the expression of tdTomato. Hence, this would lead to *erm*(41) expression kinetics that differ from those observed *in vitro*. However, this *tdTomato* reporter strain may be particularly suitable to assay next-generation macrolide antibiotics that do not induce the *erm*(41)-based resistance mechanism and retain activity against *M. abscessus*. It is conceivable to develop a microbiological assay based on the *M. abscessus* strain containing pMV261_P_{123}_*tdTomato* in a 96-well plate format that couples MIC determination with fluorimetric readings, enabling simultaneous assessment *in vitro* of the activity of a compound and the degree of macrolide-induced resistance. Such an approach could be adapted to the high-throughput screening of large libraries of macrolide scaffolds (44) in a short time frame.

Penetration of drugs into the bacterial cytoplasmic compartment induces an important transcriptional reprograming that results in changes in growth rate, metabolism, and induction of genes involved in drug resistance, such as enzymes that modify either the antibiotic or its target as well as efflux pumps. Interestingly, *erm*(41), also known as *MAB_2297*, is located in close proximity to a gene cluster participating in the intrinsic resistance to clofazimine and bedaquiline in *M. abscessus*, comprising a TetR transcriptional repressor (*MAB_2299c*) that regulates the transcription of an MmpS/MmpL efflux pump system encoded by *MAB_2300/MAB_2301* (13). This gene cluster also possesses a second MmpS/MmpL pair (*MAB_2302/MAB_2303*) whose role in resistance to antibiotics has yet to be established. These observations point to a multidrug resistance island that participates in the intrinsic resistance to different classes of antibiotics in *M. abscessus*.

WhiB7 represents one of the best-studied transcriptional activators of the reprograming circuit that belongs to the WhiB family of regulators conserved in actinomycetes (39, 45). The *whiB7* gene is induced upon treatment of mycobacteria with several structurally unrelated antibiotics, as well as compounds that can perturb respiration, redox balance, and iron starvation (38, 39, 46, 47). Recently, *MAB_3508c*, which is 75% identical to the *Mycobacterium smegmatis* and *Mycobacterium tuberculosis whiB7* genes, has been shown to be involved in intrinsic resistance of *M. abscessus* to various antibiotics, as deletion of this gene results in hypersusceptibility to erythromycin, clarithromycin, streptomycin, spectinomycin, amikacin, and tetracycline (37). In addition, RNA-seq data to determine the *whiB7* regulon of *M. abscessus* identified 128 genes, including *erm*(41) and *eis2* (39). In another study, it was shown that WhiB7 was induced by CLR and was needed for *erm*(41) induction in *M. abscessus* (36). This is supported by our study, where constitutive overexpression of WhiB7 led to increased *lacZ* expression when it was cloned under the control of the *erm*(41) promoter. In addition, we identified a putative WhiB7-binding site which, when mutated, prevented macrolide-induced resistance, proving that the direct binding of WhiB7 to the specific

AT-rich motif is necessary to induce *erm*(41) expression. This confirms WhiB7 as a primary determinant in transcriptional reprograming in macrolide-inducible resistance in *M. abscessus*.

As a nongenetically programed mechanism, macrolide-inducible resistance reflects an adaptive response to antibiotic treatment, thought to be reversible upon drug removal. We found that the β-Gal activity, mirroring *erm*(41) transcriptional expression, rapidly decreased during the 2 days following removal of CLR or AZM from cultures and then remained constant for the 5 following days at levels that were significantly higher than prior to drug addition. This suggests that induced macrolide resistance is only partially reversible, at least under the conditions used, since the specific activity at 7 days postwashing remained significantly higher than the basal level of *lacZ* expression prior to drug treatment. This phenomenon implies that, even after several rounds of division, the bacteria remain in an activated metabolic state conferring an enduring resistance phenotype. In this particular physiological stage, *M. abscessus* exhibits very high resistance levels to CLR and AZM and, to a lesser extent, to AMK, compared to previously unexposed bacteria at days 3, 5, 7, and 10. It can be inferred that pretreatment with CLR or AZM sensitizes the cultures, which will respond more efficiently upon reexposure to the drugs. This may confer the bacilli a protective advantage during subsequent drug therapy. This scenario appears to involve the transfer of signaling events through the subsequent generations and may possibly implicate epigenetic regulation by providing newly formed bacteria the capacity to stay in an "on" state for macrolide-inducible resistance. A simple explanation is that during treatment, the bacilli adapt their metabolism so as to continue producing *erm*(41) transcripts at higher basal levels. That bacteria previously exposed to either CLR or AZM express higher basal levels of *erm*(41) transcripts (and show higher resistance levels to macrolides and amikacin) may have important clinical consequences. Indeed, recent surveys have identified *M. abscessus* as a major threat in many CF centers worldwide and epidemiological studies are documenting the transmission from patient to patient of dominant circulating *M. abscessus* clones that have spread globally between hospitals (6). If this happens, it is possible that patients infected with previously macrolide-exposed bacilli may be more refractory to subsequent macrolide and AMK treatment, complicating the antibiotic-based therapy.

MATERIALS AND METHODS

Strains and growth conditions. *M. abscessus* subsp. *abscessus* CIP104536^T reference strain and clinical isolates are listed in Table S1 in the supplemental material. Strains were grown either in Middlebrook 7H9 broth (BD Difco) supplemented with 0.05% Tween 80 (Sigma-Aldrich) and 10% oleic acid, albumin, dextrose, catalase (OADC enrichment; BD Difco) (7H9$^{T/OADC}$), Sauton's medium, or cation-adjusted Mueller-Hinton broth (CaMHB; Sigma-Aldrich) at 30°C. On plates, colonies were selected either on Middlebrook 7H10 agar (BD Difco) supplemented with 10% OADC enrichment (7H10^{OADC}) or on LB agar. Antibiotics were purchased from Sigma-Aldrich.

Drug susceptibility assessment. The MICs were determined according to the Clinical and Laboratory Standards Institute (CLSI) guidelines (48).

Construction of the *lacZ* and *tdTomato* reporter strains. The full-length intergenic region (IR) (designated P_{123}) as well as its truncated versions (designated P_{92}, P_{61}, and P_{38}) were PCR amplified from the *M. abscessus* CIP104536^T genomic DNA using the Phusion polymerase (Thermo Fisher Scientific) with the primers listed in Table S2. To generate the mutated IRs ($P_{61\_Mut(B7)}$, $P_{61\_Mut(-35)}$, and $P_{61\_Mut(B7/-35)}$), complementary single-stranded DNA segments containing the XbaI and BamHI sites (Table S2) were first denaturated for 15 min at 95°C and then annealed together. All DNA fragments were restricted with XbaI and BamHI and ligated to the linearized pMV261_*lacZ* (35), digested with the same restriction enzymes, leading to a panel of *lacZ* reporter constructs, as listed in Table S3. To generate pM261_P_{123}_*tdTomato*, pMV261_P_{123}_*lacZ* was digested with BamHI and HindIII to replace *lacZ* by a linearized BamHI/HindIII-restricted *tdTomato* gene which was amplified by PCR from pTEC27 using the primers listed in Table S2. The pMV361 containing an apramycin resistance cassette was linearized with the XmnI blunt cutter and ligated to the double-blunt *whiB7* PCR product to generate the pMV361_*whiB7* construct, allowing constitutive overexpression of *whiB7*. Plasmids were electroporated into an electrocompetent *M. abscessus* S strain for the *tdTomato* reporter construct and *M. abscessus* R strains for the *lacZ* constructs.

β-Galactosidase assay. The quantification in liquid medium of the β-Gal activity was performed as previously reported (35). Briefly, bacterial cultures were adjusted to an optical density at 600 nm (OD_{600}) of 0.8 in Sauton's medium supplemented with 0.025% tyloxapol containing the appropriate antibiotics to maintain the plasmids. The β-Gal activity was determined at various time points after the initial addition of CLR or AZM ($t = 0$). At each time point, 1 ml cultures were centrifuged (4,000 × *g* for 10 min

at room temperature) and the pellets were resuspended in 700 μl 1× phosphate-buffered saline (PBS). Bacterial suspensions were lysed by bead beating for 3 min at 30 Hz. Lysates were centrifuged (16,000 × *g* for 10 min at room temperature) and the supernatant collected for measuring the OD_{280} with a NanoDrop 2000c. Four micrograms of the total protein amount present in the supernatant were coincubated with 100 μl of a reaction buffer containing 60 mM Na_2HPO_4, 40 mM NaH_2PO_4, 10 mM KCl, 1 mM $MgSO_4$, and 50 mM β-mercaptoethanol in 96-well plates at 37°C for 30 min. Thirty-five microliters of a 4 mg/ml solution of 2-nitrophenyl β-D-galactopyranoside (ONPG, Sigma-Aldrich) were added and the absorbance at 420 nm was measured at 30 to 34°C for 30 min using a multimode microplate reader POLARstar Omega (BMG Labtech). The specific β-Gal activity ($SA_{\beta\text{-}Gal}$) was defined as follows: ($absorbance_{420nm}$ × min)/(4 μg of total protein × liter of culture). To discard macrolides from bacterial cultures after 14 days of treatment, bacteria were centrifuged at 4000 × *g* for 10 min at room temperature and washed three times in PBS. The pellets were finally resuspended in Sauton's medium supplemented with 0.025% tyloxapol containing the appropriate antibiotics to maintain the plasmids. β-Gal activity on solid medium was directly observed by spotting 2.5 μl of cultures at an OD_{600} of 0.8 onto $7H10^{OADC}$ and following incubation of the plates at 37°C for 3 days.

Unmarked deletion of *erm*(41) in *M. abscessus*. The pUX1-*katG-erm*(41) was generated following the same strategy as previously described (13, 14) using the primers listed in Table S2 and introduced into *M. abscessus* S. Selection of bacteria having undergone the first homologous recombination was done by screening for red fluorescent colonies on $7H10^{OADC}$ supplemented with 200 μg/ml kanamycin. To promote the second homologous recombination event, the selected clones were subcultured overnight in $7H9^{OADC}$ in the absence of kanamycin. Cultures were 10-fold-serially diluted and plated onto $7H10^{OADC}$ containing 50 μg/ml isoniazid (INH) to select for isoniazid-resistant, kanamycin-sensitive, and nonfluorescent colonies. Following genomic DNA preparation of selected colonies, a PCR screening was set up using primer sets binding upstream of the left arm (LA) and inside the right arm (RA) or binding inside the LA and downstream of the RA. Amplicons were subsequently sequenced to confirm the junction between LA and RA and proper deletion of *erm*(41).

Zebrafish infections and visualization of macrolide inducible resistance. All zebrafish experiments were conducted in accordance with the guidelines from the European Union for handling of laboratory animals (http://ec.europa.eu/environment/chemicals/lab_animals/home_en.htm) and approved by the Direction Sanitaire et Vétérinaire de l'Hérault et Comité d'Ethique pour l'Expérimentation Animale de la région Languedoc Roussillon under the reference number CEEA-LR-1145. Experiments were conducted using the transgenic Tg(*mpeg1:GFP-CAAX*) zebrafish line carrying green fluorescent macrophages (33). Ages of embryos are expressed as hours post fertilization (hpf). *M. abscessus* S left untransformed (as a negative control) or carrying either pTEC27 (with constitutive expression of *tdTomato*) or pMV261-P_{123}-*tdTomato* (with macrolide-inducible expression of *tdTomato*) were injected into zebrafish embryos and monitored for fluorescence expression, according to protocols reported previously (49). Briefly, infections were performed by intravenous microinjection of 900 to 1,000 CFU in dechorionated and anesthetized 30 hpf embryos. At 96 hours postinfection (hpi), infected embryos were exposed to either 32 μg/ml CLR or AZM in osmotic water and this treatment was renewed on a daily basis. Red fluorescence was assessed by immobilizing anesthetized embryos in 1% low-melting-point agarose and performing life imaging by confocal microscopy (LSM 880 Airyscan) at day 0, day 2, and day 6 post treatment (dpt). 2D reconstructions of image stacks were done with the ZEN 2 software.

SUPPLEMENTAL MATERIAL

Supplemental material is available online only.

SUPPLEMENTAL FILE 1, PDF file, 1 MB.

ACKNOWLEDGMENTS

This work was supported by the Fondation pour la Recherche Médicale (FRM) (grant number DEQ20150331719 to L.K.; grant number ECO20160736031 to M.R.) and the InfectioPôle Sud for funding the Ph.D. fellowship of A.V.G.

We have no conflicts of interest to declare.

REFERENCES

1. Cowman S, van Ingen J, Griffith DE, Loebinger MR. 2019. Non-tuberculous mycobacterial pulmonary disease. Eur Respir J 54:1900250. https://doi.org/10.1183/13993003.00250-2019.
2. Jönsson BE, Gilljam M, Lindblad A, Ridell M, Wold AE, Welinder-Olsson C. 2007. Molecular epidemiology of *Mycobacterium abscessus,* with focus on cystic fibrosis. J Clin Microbiol 45:1497–1504. https://doi.org/10.1128/JCM.02592-06.
3. Esther CR, Esserman DA, Gilligan P, Kerr A, Noone PG. 2010. Chronic *Mycobacterium abscessus* infection and lung function decline in cystic fibrosis. J Cyst Fibros 9:117–123. https://doi.org/10.1016/j.jcf.2009.12.001.
4. Catherinot E, Roux A-L, Macheras E, Hubert D, Matmar M, Dannhoffer L, Chinet T, Morand P, Poyart C, Heym B, Rottman M, Gaillard J-L, Herrmann J-L. 2009. Acute respiratory failure involving an R variant of *Mycobacterium abscessus*. J Clin Microbiol 47:271–274. https://doi.org/10.1128/JCM.01478-08.
5. Bryant JM, Grogono DM, Greaves D, Foweraker J, Roddick I, Inns T, Reacher M, Haworth CS, Curran MD, Harris SR, Peacock SJ, Parkhill J, Floto RA. 2013. Whole-genome sequencing to identify transmission of *Mycobacterium abscessus* between patients with cystic fibrosis: a retrospective cohort study. Lancet 381:1551–1560. https://doi.org/10.1016/S0140-6736(13)60632-7.
6. Bryant JM, Grogono DM, Rodriguez-Rincon D, Everall I, Brown KP, Moreno P, Verma D, Hill E, Drijkoningen J, Gilligan P, Esther CR, Noone PG, Giddings O, Bell SC, Thomson R, Wainwright CE, Coulter C, Pandey S, Wood ME, Stockwell RE, Ramsay KA, Sherrard LJ, Kidd TJ, Jabbour N,

Johnson GR, Knibbs LD, Morawska L, Sly PD, Jones A, Bilton D, Laurenson I, Ruddy M, Bourke S, Bowler IC, Chapman SJ, Clayton A, Cullen M, Daniels T, Dempsey O, Denton M, Desai M, Drew RJ, Edenborough F, Evans J, Folb J, Humphrey H, Isalska B, Jensen-Fangel S, Jönsson B, Jones AM, Katzenstein TL, Lillebaek T, MacGregor G, Mayell S, Millar M, Modha D, Nash EF, O'Brien C, O'Brien D, Ohri C, Pao CS, Peckham D, Perrin F, Perry A, Pressler T, Prtak L, Qvist T, Robb A, Rodgers H, Schaffer K, Shafi N, van Ingen J, Walshaw M, Watson D, West N, Whitehouse J, Haworth CS, Harris SR, Ordway D, Parkhill J, Floto RA. 2016. Emergence and spread of a human-transmissible multidrug-resistant nontuberculous mycobacterium. Science 354:751–757. https://doi.org/10.1126/science.aaf8156.

7. Adekambi T, Sassi M, van Ingen J, Drancourt M. 2017. Reinstating *Mycobacterium massiliense* and *Mycobacterium bolletii* as species of the *Mycobacterium abscessus* complex. Int J Syst Evol Microbiol 67:2726–2730. https://doi.org/10.1099/ijsem.0.002011.
8. Nessar R, Cambau E, Reyrat JM, Murray A, Gicquel B. 2012. *Mycobacterium abscessus*: a new antibiotic nightmare. J Antimicrob Chemother 67:810–818. https://doi.org/10.1093/jac/dkr578.
9. Rominski A, Roditscheff A, Selchow P, Böttger EC, Sander P. 2017. Intrinsic rifamycin resistance of *Mycobacterium abscessus* is mediated by ADP-ribosyltransferase MAB_0591. J Antimicrob Chemother 72:376–384. https://doi.org/10.1093/jac/dkw466.
10. Rominski A, Selchow P, Becker K, Brülle JK, Dal Molin M, Sander P. 2017. Elucidation of *Mycobacterium abscessus* aminoglycoside and capreomycin resistance by targeted deletion of three putative resistance genes. J Antimicrob Chemother 72:2191–2200. https://doi.org/10.1093/jac/dkx125.
11. Rudra P, Hurst-Hess K, Lappierre P, Ghosh P. 2018. High levels of intrinsic tetracycline resistance in *Mycobacterium abscessus* are conferred by a tetracycline-modifying monooxygenase. Antimicrob Agents Chemother 62:e00119-18. https://doi.org/10.1128/AAC.00119-18.
12. Dubée V, Bernut A, Cortes M, Lesne T, Dorchene D, Lefebvre A-L, Hugonnet J-E, Gutmann L, Mainardi J-L, Herrmann J-L, Gaillard J-L, Kremer L, Arthur M. 2015. β-Lactamase inhibition by avibactam in *Mycobacterium abscessus*. J Antimicrob Chemother 70:1051–1058. https://doi.org/10.1093/jac/dku510.
13. Richard M, Gutiérrez AV, Viljoen A, Rodriguez-Rincon D, Roquet-Baneres F, Blaise M, Everall I, Parkhill J, Floto RA, Kremer L. 2019. Mutations in the MAB_2299c TetR regulator confer cross-resistance to clofazimine and bedaquiline in *Mycobacterium abscessus*. Antimicrob Agents Chemother 63:e01316-18. https://doi.org/10.1128/AAC.01316-18.
14. Gutiérrez AV, Richard M, Roquet-Banères F, Viljoen A, Kremer L. 2019. The TetR-family transcription factor MAB_2299c regulates the expression of two distinct MmpS-MmpL efflux pumps involved in cross-resistance to clofazimine and bedaquiline in *Mycobacterium abscessus*. Antimicrob Agents Chemother 63:e01000-19. https://doi.org/10.1128/AAC.01000-19.
15. Griffith DE, Aksamit T, Brown-Elliott BA, Catanzaro A, Daley C, Gordin F, Holland SM, Horsburgh R, Huitt G, Iademarco MF, Iseman M, Olivier K, Ruoss S, von Reyn CF, Wallace RJ, Winthrop K, ATS Mycobacterial Diseases Subcommittee, American Thoracic Society, Infectious Disease Society of America. 2007. An official ATS/IDSA statement: diagnosis, treatment, and prevention of nontuberculous mycobacterial diseases. Am J Respir Crit Care Med 175:367–416. https://doi.org/10.1164/rccm.200604-571ST.
16. Wallace RJ, Meier A, Brown BA, Zhang Y, Sander P, Onyi GO, Böttger EC. 1996. Genetic basis for clarithromycin resistance among isolates of *Mycobacterium chelonae* and *Mycobacterium abscessus*. Antimicrob Agents Chemother 40:1676–1681. https://doi.org/10.1128/AAC.40.7.1676.
17. Nash KA, Brown-Elliott BA, Wallace RJ. 2009. A novel gene, *erm(41)*, confers inducible macrolide resistance to clinical isolates of *Mycobacterium abscessus* but is absent from *Mycobacterium chelonae*. Antimicrob Agents Chemother 53:1367–1376. https://doi.org/10.1128/AAC.01275-08.
18. Bastian S, Veziris N, Roux A-L, Brossier F, Gaillard J-L, Jarlier V, Cambau E. 2011. Assessment of clarithromycin susceptibility in strains belonging to the *Mycobacterium abscessus* group by *erm(41)* and *rrl* sequencing. Antimicrob Agents Chemother 55:775–781. https://doi.org/10.1128/AAC.00861-10.
19. Maurer FP, Rüegger V, Ritter C, Bloemberg GV, Böttger EC. 2012. Acquisition of clarithromycin resistance mutations in the 23S rRNA gene of *Mycobacterium abscessus* in the presence of inducible *erm(41)*. J Antimicrob Chemother 67:2606–2611. https://doi.org/10.1093/jac/dks279.
20. Brown-Elliott BA, Vasireddy S, Vasireddy R, Iakhiaeva E, Howard ST, Nash K, Parodi N, Strong A, Gee M, Smith T, Wallace RJ. 2015. Utility of sequencing the *erm(41)* gene in isolates of *Mycobacterium abscessus* subsp. *abscessus* with low and intermediate clarithromycin MICs. J Clin Microbiol 53:1211–1215. https://doi.org/10.1128/JCM.02950-14.
21. Mougari F, Amarsy R, Veziris N, Bastian S, Brossier F, Berçot B, Raskine L, Cambau E. 2016. Standardized interpretation of antibiotic susceptibility testing and resistance genotyping for *Mycobacterium abscessus* with regard to subspecies and *erm41* sequevar. J Antimicrob Chemother 71:2208–2212. https://doi.org/10.1093/jac/dkw130.
22. Kim H-Y, Kim BJ, Kook Y, Yun Y-J, Shin JH, Kim B-J, Kook Y-H. 2010. *Mycobacterium massiliense* is differentiated from *Mycobacterium abscessus* and *Mycobacterium bolletii* by erythromycin ribosome methyltransferase gene (*erm*) and clarithromycin susceptibility patterns. Microbiol Immunol 54:347–353. https://doi.org/10.1111/j.1348-0421.2010.00221.x.
23. Roux A-L, Catherinot E, Soismier N, Heym B, Bellis G, Lemonnier L, Chiron R, Fauroux B, Le Bourgeois M, Munck A, Pin I, Sermet I, Gutierrez C, Véziris N, Jarlier V, Cambau E, Herrmann J-L, Guillemot D, Gaillard J-L, OMA group. 2015. Comparing *Mycobacterium massiliense* and *Mycobacterium abscessus* lung infections in cystic fibrosis patients. J Cyst Fibros 14:63–69. https://doi.org/10.1016/j.jcf.2014.07.004.
24. Brown BA, Wallace RJ, Onyi GO, De Rosas V, Wallace RJ. 1992. Activities of four macrolides, including clarithromycin, against *Mycobacterium fortuitum, Mycobacterium chelonae*, and *M. chelonae*-like organisms. Antimicrob Agents Chemother 36:180–184. https://doi.org/10.1128/aac.36.1.180.
25. Choi G-E, Shin SJ, Won C-J, Min K-N, Oh T, Hahn M-Y, Lee K, Lee SH, Daley CL, Kim S, Jeong B-H, Jeon K, Koh W-J. 2012. Macrolide treatment for *Mycobacterium abscessus* and *Mycobacterium massiliense* infection and inducible resistance. Am J Respir Crit Care Med 186:917–925. https://doi.org/10.1164/rccm.201111-2005OC.
26. Schildkraut JA, Pennings LJ, Ruth MM, de Brouwer AP, Wertheim HF, Hoefsloot W, de Jong A, van Ingen J. 2019. The differential effect of clarithromycin and azithromycin on induction of macrolide resistance in *Mycobacterium abscessus*. Future Microbiol 14:749–755. https://doi.org/10.2217/fmb-2018-0310.
27. Peters DH, Friedel HA, McTavish D. 1992. Azithromycin. A review of its antimicrobial activity, pharmacokinetic properties and clinical efficacy. Drugs 44:750–799. https://doi.org/10.2165/00003495-199244050-00007.
28. Viljoen A, Gutiérrez AV, Dupont C, Ghigo E, Kremer L. 2018. A simple and rapid gene disruption strategy in *Mycobacterium abscessus*: on the design and application of glycopeptidolipid mutants. Front Cell Infect Microbiol 8:69. https://doi.org/10.3389/fcimb.2018.00069.
29. Dupont C, Viljoen A, Thomas S, Roquet-Banères F, Herrmann J-L, Pethe K, Kremer L. 2017. Bedaquiline inhibits the ATP synthase in *Mycobacterium abscessus* and is effective in infected zebrafish. Antimicrob Agents Chemother 61:e01225-17. https://doi.org/10.1128/AAC.01225-17.
30. Dupont C, Viljoen A, Dubar F, Blaise M, Bernut A, Pawlik A, Bouchier C, Brosch R, Guérardel Y, Lelièvre J, Ballell L, Herrmann J-L, Biot C, Kremer L. 2016. A new piperidinol derivative targeting mycolic acid transport in *Mycobacterium abscessus*. Mol Microbiol 101:515–529. https://doi.org/10.1111/mmi.13406.
31. Bernut A, Le Moigne V, Lesne T, Lutfalla G, Herrmann J-L, Kremer L. 2014. *In vivo* assessment of drug efficacy against *Mycobacterium abscessus* using the embryonic zebrafish test system. Antimicrob Agents Chemother 58:4054–4063. https://doi.org/10.1128/AAC.00142-14.
32. Bernut A, Herrmann J-L, Kissa K, Dubremetz J-F, Gaillard J-L, Lutfalla G, Kremer L. 2014. *Mycobacterium abscessus* cording prevents phagocytosis and promotes abscess formation. Proc Natl Acad Sci U S A 111:E943–952. https://doi.org/10.1073/pnas.1321390111.
33. Keatinge M, Bui H, Menke A, Chen Y-C, Sokol AM, Bai Q, Ellett F, Da Costa M, Burke D, Gegg M, Trollope L, Payne T, McTighe A, Mortiboys H, de Jager S, Nuthall H, Kuo M-S, Fleming A, Schapira AHV, Renshaw SA, Highley JR, Chacinska A, Panula P, Burton EA, O'Neill MJ, Bandmann O. 2015. Glucocerebrosidase 1 deficient *Danio rerio* mirror key pathological aspects of human Gaucher disease and provide evidence of early microglial activation preceding alpha-synuclein-independent neuronal cell death. Hum Mol Genet 24:6640–6652. https://doi.org/10.1093/hmg/ddv369.
34. Bernut A, Nguyen-Chi M, Halloum I, Herrmann J-L, Lutfalla G, Kremer L. 2016. *Mycobacterium abscessus*-induced granuloma formation is strictly dependent on TNF signaling and neutrophil trafficking. PLoS Pathog 12:e1005986. https://doi.org/10.1371/journal.ppat.1005986.
35. Richard M, Gutiérrez AV, Viljoen AJ, Ghigo E, Blaise M, Kremer L. 2018. Mechanistic and structural insights into the unique TetR-dependent regulation of a drug efflux pump in *Mycobacterium abscessus*. Front Microbiol 9:649. https://doi.org/10.3389/fmicb.2018.00649.

36. Pryjma M, Burian J, Kuchinski K, Thompson CJ. 2017. Antagonism between front-line antibiotics clarithromycin and amikacin in the treatment of *Mycobacterium abscessus* infections is mediated by the *whiB7* gene. Antimicrob Agents Chemother 61:e01353-17. https://doi.org/10.1128/AAC.01353-17.
37. Hurst-Hess K, Rudra P, Ghosh P. 2017. *Mycobacterium abscessus* WhiB7 regulates a species-specific repertoire of genes to confer extreme antibiotic resistance. Antimicrob Agents Chemother 61:e01347-17. https://doi.org/10.1128/AAC.01347-17.
38. Burian J, Ramón-García S, Sweet G, Gómez-Velasco A, Av-Gay Y, Thompson CJ. 2012. The mycobacterial transcriptional regulator *whiB7* gene links redox homeostasis and intrinsic antibiotic resistance. J Biol Chem 287:299–310. https://doi.org/10.1074/jbc.M111.302588.
39. Burian J, Ramón-García S, Howes CG, Thompson CJ. 2012. WhiB7, a transcriptional activator that coordinates physiology with intrinsic drug resistance in *Mycobacterium tuberculosis*. Expert Rev Anti Infect Ther 10:1037–1047. https://doi.org/10.1586/eri.12.90.
40. Newton-Foot M, Gey van Pittius NC. 2013. The complex architecture of mycobacterial promoters. Tuberculosis (Edinb) 93:60–74. https://doi.org/10.1016/j.tube.2012.08.003.
41. Maurer FP, Castelberg C, Quiblier C, Böttger EC, Somoskövi A. 2014. Erm(41)-dependent inducible resistance to azithromycin and clarithromycin in clinical isolates of *Mycobacterium abscessus*. J Antimicrob Chemother 69:1559–1563. https://doi.org/10.1093/jac/dku007.
42. Rollet-Cohen V, Roux A-L, Le Bourgeois M, Sapriel G, El Bahri M, Jais J-P, Heym B, Mougari F, Raskine L, Véziris N, Gaillard J-L, Sermet-Gaudelus I. 2019. *Mycobacterium bolletii* lung disease in cystic fibrosis. Chest 156:247–254. https://doi.org/10.1016/j.chest.2019.03.019.
43. Koh W-J, Jeon K, Lee NY, Kim B-J, Kook Y-H, Lee S-H, Park YK, Kim CK, Shin SJ, Huitt GA, Daley CL, Kwon OJ. 2011. Clinical significance of differentiation of *Mycobacterium massiliense* from *Mycobacterium abscessus*. Am J Respir Crit Care Med 183:405–410. https://doi.org/10.1164/rccm.201003-0395OC.
44. Pavlović D, Fajdetić A, Mutak S. 2010. Novel hybrids of 15-membered 8a- and 9a-azahomoerythromycin A ketolides and quinolones as potent antibacterials. Bioorg Med Chem 18:8566–8582. https://doi.org/10.1016/j.bmc.2010.10.024.
45. Soliveri JA, Gomez J, Bishai WR, Chater KF. 2000. Multiple paralogous genes related to the *Streptomyces coelicolor* developmental regulatory gene *whiB* are present in Streptomyces and other actinomycetes. Microbiology (Reading, Engl) 146:333–343. https://doi.org/10.1099/00221287-146-2-333.
46. Geiman DE, Raghunand TR, Agarwal N, Bishai WR. 2006. Differential gene expression in response to exposure to antimycobacterial agents and other stress conditions among seven *Mycobacterium tuberculosis whiB*-like genes. Antimicrob Agents Chemother 50:2836–2841. https://doi.org/10.1128/AAC.00295-06.
47. Morris RP, Nguyen L, Gatfield J, Visconti K, Nguyen K, Schnappinger D, Ehrt S, Liu Y, Heifets L, Pieters J, Schoolnik G, Thompson CJ. 2005. Ancestral antibiotic resistance in *Mycobacterium tuberculosis*. Proc Natl Acad Sci U S A 102:12200–12205. https://doi.org/10.1073/pnas.0505446102.
48. Woods GL, Brown-Elliott BA, Conville PS, Desmond EP, Hall GS, Lin G, Pfyffer GE, Ridderhof JC, Siddiqi SH, Wallace RJ. 2011. Susceptibility testing of mycobacteria, nocardiae and other aerobic actinomycetes: approved standard 2nd ed M24-A2. Clinical and Laboratory Standards Institute, Wayne, PA.
49. Bernut A, Dupont C, Sahuquet A, Herrmann J-L, Lutfalla G, Kremer L. 2015. Deciphering and imaging pathogenesis and cording of *Mycobacterium abscessus* in zebrafish embryos. J Vis Exp 103:e53130. https://doi.org/10.3791/53130.

Table S1. List of bacterial strains used in this study.

Name	Description/genotype	Marker	Reference
Strains			
M. abscessus Smooth (S)	*M. abscessus sensu stricto*, strain CIP104536^T, S morphotype	_	Laboratoire de Référence des Mycobactéries
M. abscessus Rough (R)	*M. abscessus sensu stricto*, strain CIP104536 ^{T}, R morphotype	_	Laboratoire de Référence des Mycobactéries
M. massiliense (R)	*M. abscessus massiliense*, strain CIP108297^T, R morphotype	_	Laboratoire de Référence des Mycobactéries
M. bolletii (S)	*M. abscessus bolletii*, strain CIP108541^T, S morphotype	_	Laboratoire de Référence des Mycobactéries
M. abscessus S 1298 (S)	*M. abscessus sensu stricto,* clinical isolate from a cystic fibrosis (CF) patient, S morphotype	_	(1)
M. abscessus S 2069 (S)	*M. abscessus sensu stricto,* clinical isolate from a non-CF patient, S morphotype	_	(1)
M. abscessus R 2648 (R)	*M. abscessus sensu stricto,* clinical isolate from a CF patient, R morphotype	_	(1)
M. abscessus R 3022 (R)	*M. abscessus sensu stricto,* clinical isolate from a non-CF patient, R morphotype	_	(1)
M. abscessus S - Δ*erm(41)*	*erm(41)* unmarked deletion mutant in the S variant *of* CIP104536^T	-	This study
E. coli XL1-Blue	*recA1 endA1 gyrA96 thi-1 hsdR17 supE44 relA1 lac* [F′ *proAB lacI*q*Z*Δ*M15* Tn*10* (Tetr)].	Tet	Stratagene

Table S2. PCR primers used in this study. Fow and Rev stand for forward and reverse, respectively.

Primers	5' to 3' sequence
Cloning in pMV261_*lacZ* derivatives	
P_{123} Fow	GGTATATCTAGAGCGCACGTTCTGACGAAAGAA (XbaI)
P_{123} Rev	GGTATAGGATCCGACGCAGCACCATCATGAATA (BamHI)
P_{92} Fow	GGTATATCTAGAATGGCGACCGGGGCCTTCTTCGTG (XbaI)
P_{61} Fow	GGTATATCTAGAGAAACCAGTTGCATGCCCCGATAT (XbaI)
P_{38} Fow	CTAGATCTTTGGAGCATGGGCATATTCATGATGGTGCTGCGTCG (XbaI)
P_{38} Rev	GATCCGACGCAGCACCATCATGAATATGCCCATGCTCCAAAGAT (BamHI)
$P_{Mut(B7)}$ Fow	CTAGAG**GGGG**CAGTTGCATGCCCCGATATCTTTGGAGCATGGGC ATATTCATGATGGTGCTGCGTCG (XbaI)
$P_{Mut(B7)}$ Rev	GATCCGACGCAGCACCATCATGAATATGCCCATGCTCCAAAGATA TCGGGGCATGCAACTG**CCCC**CT (BamHI)
$P_{Mut(-35)}$ Fow	CTAGAGAAACCAG**CCATGC**GCCCCGATATCTTTGGAGCATGGGCA TATTCATGATGGTGCTGCGTCG (XbaI)
$P_{Mut(-35)}$ Rev	GATCCGACGCAGCACCATCATGAATATGCCCATGCTCCAAAGATA TCGGGGC**GCATGG**CTGGTTTCT (BamHI)
$P_{Mut(B7/-35)}$ Fow	CTAGAG**GGGG**CAG**CCATGC**GCCCCGATATCTTTGGAGCATGGGC ATATTCATGATGGTGCTGCGTCG (XbaI)
$P_{Mut(B7/-35)}$ Rev	GATCCGACGCAGCACCATCATGAATATGCCCATGCTCCAAAGATA TCGGGGC**GCATGG**CTG**CCCC**CT (BamHI)
Cloning in pMV361-ApraR	
361-*whiB7* Fow	ACTTCGCAATGATGACCGTTGAAGTGGAG
361-*whiB7* Rev	CTAAGCGTAATCTGGAACATCGTATGGGTATGCCGCGGCGGTGTC GGCGTC
Cloning in pMV261_P_{123}_*tdTomato*	
261-td*Tomato* Fow	GAGAGAGGATCCGTGAGCAAGGGCGAGGAG (BamHI)
261-td*Tomato* Rev	GAGAGAAAGCTTCTACTTGTACAGCTCGTC (HindIII)
Cloning in pUX1-*katG*	
*erm(41)*KO_U_F	GAGAGACAATTGCGCGATCTGCAGCCGTATATC (MfeI)
*erm(41)*KO_U_R	CCGTTGGCCGGACACGAC
*erm(41)*KO_D_F	TGGTGCTGCGTCGTGTCCGGCCAACGGGTGCTGGTGATCAGGCG GCGCTGA
*erm(41)*KO_D_R	GAGAGAGCTAGCTGCACCAGAACGGCGCGT (XbaI)
Sequencing	
pMV5' Ext	CGCCCGGCCAGCGTAAGTAGC
l*acZ* intern Rev	GATACAGCGCGTCGTGATTA
erm(41) Fow	ACGCCGAGGCCGAGCGCCGTCACA
erm(41) Rev	CGCAGTATCGTTTCTCCAAAGGCC

[a]Restriction sites are underlined and specified inside brackets.

[b]Mutagenized bases are shown in bold.

Tables S3. List of the plasmids used in this study.

Plasmids			
pTEC27	Multicopy *E. coli*/mycobacterial shuttle vector to express *tdTomato* under the control of a strong mycobacterial promoter	Hyg	Addgene (plasmid 30182)
pMV261	Multicopy *E. coli*/mycobacterial shuttle vector	Kan	(2)
pMV261_P_{hsp60}_*lacZ*	The *hsp60* promoter region is cloned upstream of *lacZ* into pMV261.	Kan	(3)
pMV261_P_{123}_*lacZ*	The full intergenic region of *erm(41)* of 123 bp is cloned upstream of *lacZ* into pMV261.	Kan	This study
pMV261_P_{92}_*lacZ*	A truncated version of 92 bp of the *erm(41)* intergenic region is cloned upstream of *lacZ* into pMV261.	Kan	This study
pMV261_P_{61}_*lacZ*	A truncated version of 61 bp of the *erm(41)* intergenic region is cloned upstream of *lacZ* into pMV261.	Kan	This study
pMV261_P_{38}_*lacZ*	A truncated version of 38 bp of the *erm(41)* intergenic region is cloned upstream of *lacZ* into pMV261.	Kan	This study
pMV261_ $P_{61_Mut(B7)}$_*lacZ*	A truncated version of 61 bp of the *erm(41)* intergenic region containing mutations in the *whiB7* binding site is cloned upstream of *lacZ* into pMV261.	Kan	This study
pMV261_ $P_{61_Mut(-35)}$_*lacZ*	A truncated version of 61 bp of the *erm(41)* intergenic region containing mutation in the putative *erm(41)* -35 box is cloned upstream of *lacZ* into pMV261.	Kan	This study
pMV261_ $P_{61_Mut(B7/-35)}$_*lacZ*	A truncated version of 61 bp of the *erm(41)* intergenic region containing mutation into the *whiB7* binding site and in the putative *erm(41)* -35 box is cloned upstream of *lacZ* into pMV261.	Kan	This study
pMV261_*lacZ*	The *lacZ* reporter gene is cloned into a promoter-less pMV261.	Kan	(3)
pMV261_P_{MAB_4384}_*lacZ*	pMV261_*lacZ* carrying the promoter region of *MAB_4384* cloned upstream of *lacZ*	Kan	(3)
pMV261_ P_{123}_*tdTomato*	The red fluorescent marker td*Tomato* is cloned into the pMV261 under the control of the full/123bp *erm(41)* intergenic region.	Kan	This study
pMV361_*whiB7*	*whiB7* cloned into the integrative vector pMV361 under the control of the strong and constitutive *hsp60* promoter.	Apra	This study

Hyg, hygromycin; Kan, kanamycin; Apra, apramycin.

References

1. Singh S, Bouzinbi N, Chaturvedi V, Godreuil S, Kremer L. 2014. In vitro evaluation of a new drug combination against clinical isolates belonging to the Mycobacterium abscessus complex. Clin Microbiol Infect 20:O1124–O1127.

2. Stover CK, de la Cruz VF, Fuerst TR, Burlein JE, Benson LA, Bennett LT, Bansal GP, Young JF, Lee MH, Hatfull GF. 1991. New use of BCG for recombinant vaccines. Nature 351:456–460.

3. Richard M, Gutiérrez AV, Viljoen AJ, Ghigo E, Blaise M, Kremer L. 2018. Mechanistic and Structural Insights Into the Unique TetR-Dependent Regulation of a Drug Efflux Pump in Mycobacterium abscessus. Front Microbiol 9:649.

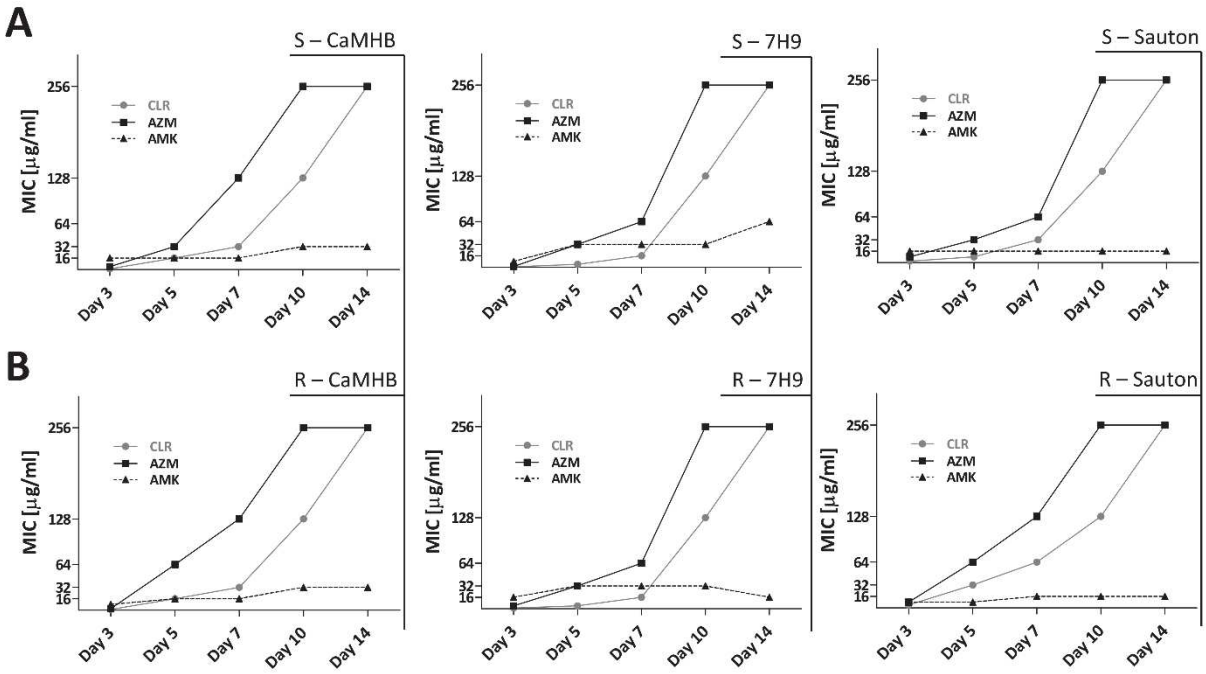

Figure S1. Macrolide-induced resistance profile of *M. abscessus* CIP104536^T smooth (A) and rough (B) variants in different broth media. MICs of the two morphotypes were assessed over a period of 14 days in CaMHB, Sauton's medium and Middlebrook 7H9-Glycerol broth. AMK was included as a non-related control drug.

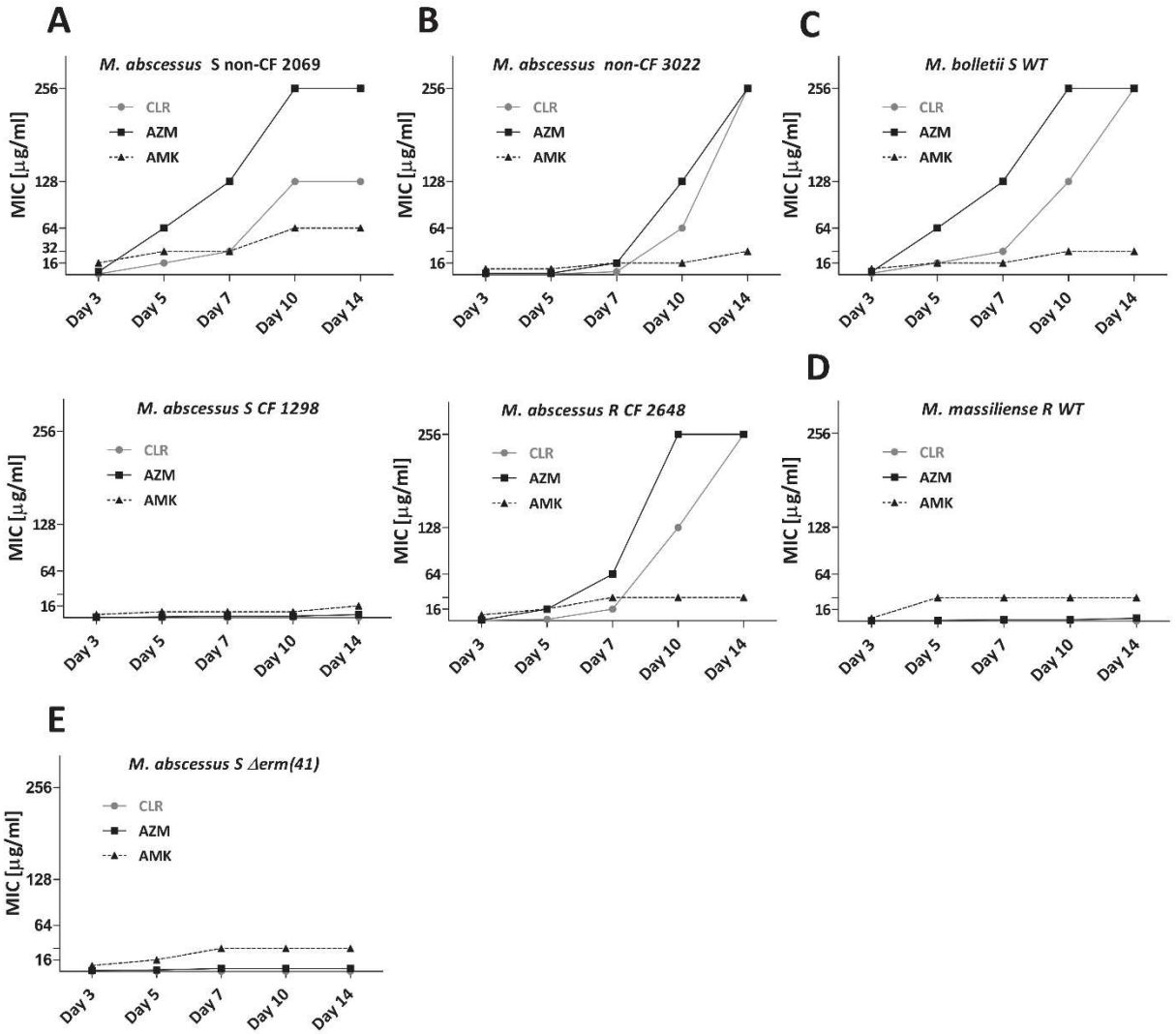

Figure S2. Macrolide-induced resistance profile of clinical isolates in CaMHB. (A) Smooth *M. abscessus* clinical isolates. **(B)** Rough *M. abscessus* clinical isolates. **(C)** Smooth *M. bolletii* CIP108541^{T}. **(D)** Rough *M. massiliense* CIP108297^{T}. **(E)** Smooth *M. abscessus* CIP104536^{T} in which the *erm(41)* gene has been deleted by double homologous recombination using the suicide-vector pUX1-*katG*. AMK was included as a non-related control drug.

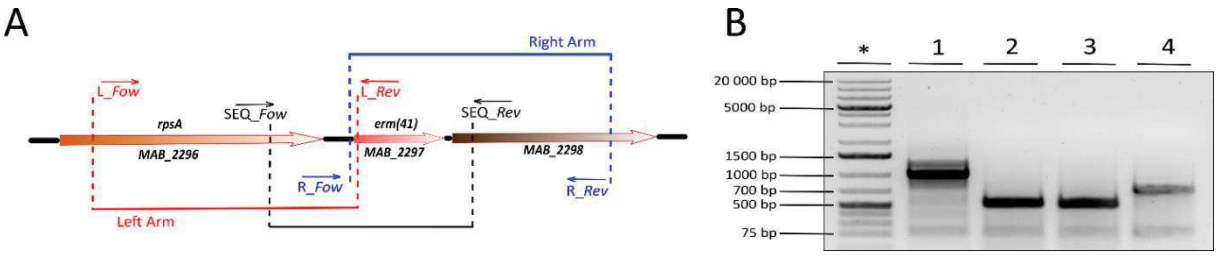

Figure S3. Unmarked deletion of the *erm(41)* gene. (A) Genomic environment of *erm(41)*. The L_*Fow*/L_*Rev* and the R_*Fow*/R_*Rev* primer sets were used to produce left and right arms, respectively, which were subsequently used to generate pUX1_*katG-erm(41)* to delete *erm(41)* by double homologous recombination. **(B)** 1 % agarose gel of the amplicons using the SEQ_Fow an SEQ_Rev primers. The expected sizes are: *M. abscessus* WT (1034 bp; lane 1), *M. abscessus* Δ*erm(41*) Clone 1 (509 bp; lane 2), *M. abscessus* Δ*erm(41)* Clone 2 (509 bp; lane 3) and *M. massiliense* WT (758 bp; lane 4). (*) GeneRuler^{TM} 1 kb Plus DNA Ladder.

Discussion

L'apparition et l'expansion de résistances à la plupart des classes d'antibiotiques n'ont cessé d'accroître la morbidité et la mortalité causées par les infections bactériennes. Certaines autorités sanitaires comme l'OMS (Organisation Mondiale de la Santé) ou le PHE (Public Health England) estiment que, d'ici 2050, le nombre global de décès lié à des infections causées par des bactéries multi-résistantes sera de 10 millions chaque année (PHE 2015). Ce constat s'applique également aux mycobactéries. Concernant *M. tuberculosis* par exemple, la moitié des 580 000 personnes souffrant de tuberculose multi-résistante ont trouvé la mort en 2017 (WHO 2017). Tout comme *M. tuberculosis*, certaines MNT provoquent également de plus en plus d'infections multi-résistantes, comme par exemple *M. avium* chez les personnes séropositives aux VIH (Daley 2017). Des observations alarmantes concernent aussi *M. abscessus*. Bryant et al. ont mis en évidence la transmission à l'échelle mondiale d'un clone dominant de *M. abscessus* avec une virulence accrue dans les modèles macrophagique et murin. L'émergence de ce clone dans les centres hospitaliers pourrait sérieusement engager le pronostique des patients infectés et souffrant de mucoviscidose. L'apparition de résistance est en soit un phénomène naturel chez une bactérie. Cependant, une étude récente souligne la plasticité du génome de *M. abscessus*, permettant une évolution rapide et une acquisition aisée de matériel génétique exogène (Choo et al. 2014). Ceci suggère que cette bactérie peut potentiellement hériter de nouveaux facteurs de virulences et/ou de gènes de résistance aux antibiotiques. Deux exemples faisant références à ces transferts génétiques horizontaux sont *MAB_0555* et *MAB_3593* (Ripoll et al. 2009). *MAB_0555* code pour la Phospholipase C, une enzyme capable de moduler des voies signalétiques de l'hôte favorisant la survie intracellulaire et capable aussi de lyser les cellules eucaryotes ainsi que leurs sécrétions (Schmiel et Miller 1999). MAB_0855 pourrait jouer un rôle dans la dégradation du mucus et l'établissement d'une infection aigüe chez les personnes saines comme celles atteintes de mucoviscidose (Bakala N'Goma et al. 2015). *MAB_3593* code pour la protéine MgtC, décrite pour la première fois chez *Salmonella typhimurium* mais présente chez de nombreux pathogènes intracellulaires (Moncrief et Maguire 1998). Cette protéine fait partie d'un système d'import d'ion Mg^{2+} au sein du phagosome favorisant la survie intramacrophagique des bactéries (Alix et Blanc-Potard 2007). Ces deux gènes non-mycobactériens ne sont pas répandus chez les MNT et offrent à *M. abscessus* un avantage en termes de virulence.

Les travaux de cette thèse ont montré que le génome de *M. abscessus* renferme l'information génétique jouant un rôle déterminant dans son antibiorésistance intrinsèque, en l'occurrence des gènes qui codent les pompes à efflux de type MmpL. Ce génome est également très riche en régulateur de la famille TetR et près de la moitié des MmpL (13/31) sont couplés à ce type de répresseur, offrant un éventuel contrôle de l'expression des protéines MmpL. Ces transporteurs

participent indirectement à l'antibiorésistance en exportant à travers la membrane plasmique des lipides qui confèrent à la paroi mycobactérienne son extrême hydrophobicité (Viljoen et al. 2017). Cette propriété biochimique empêche l'entrée d'un grand nombre de molécules hydrophiles et de certains antibiotiques. Ces mêmes MmpL peuvent aussi exporter des antibiotiques ayant pénétrés la bactérie et deviennent alors des acteurs à part entière du résistome de *M. abscessus*.

Partie I – Régulation

C'est dans le but d'identifier des pompes à efflux participant à la résistance aux antibiotiques que nous avons initié trois études combinant à la fois des approches biochimiques et génétiques. Ainsi, ces stratégies nous ont permis d'identifier le TetR MAB_4384 contrôlant la pompe à efflux MAB_4383c/MAB_4382c impliquée dans de hauts niveaux de résistance aux TACa. Nous avons également identifié MAB_2299c comme étant un TetR contrôlant l'expression de deux paires MmpS/MmpL distinctes et indépendantes, MAB_1135c/MAB_1134c et MAB_2300/MAB_2301, lesquelles participent dans la résistance croisée à la BDQ et à la CFZ. Afin d'identifier ces MmpL, nous nous sommes basés sur la capacité de *M. abscessus* à acquérir des mutations chromosomiques capables de conférer une résistance. Plus particulièrement, des mutations situées dans des gènes codants des régulateurs transcriptionnels qui induiront une perte de leur fonction de répresseur et devenant incapables de se lier à leurs ADN cibles. Les mutations étudiées dans le cas présent englobent des substitutions d'acides aminés impliquées soit dans la reconnaissance de la séquence palindromique du gène cible (dans le domaine HTH, D14N et F57L pour MAB_4384 et L40W pour MAB_2299c) soit dans l'organisation structurale de la protéine (dans le domaine C-terminal, L151P et G215W pour MAB_2299c). Ces altérations conduisent à une surexpression du régulome, et dans ce cas précis des paires MmpS/MmpL.

La structure cristallographique de MAB_4384 et les prédictions des structures secondaires de MAB_2299c ont révélé que leurs domaines HTH sortent de l'ordinaire. En effet, les hélices h1 à h3 sont composées de 56 et 58 acides aminés pour MAB_4384 et MAB_2299c, respectivement. Une autre particularité de MAB_4384, de MAB_2299c et d'EthR (impliqué dans la résistance de *M. tuberculosis* à l'ETH) réside dans la longueur de leur hélice h1. En moyenne, les HTH comprennent 41 résidus, les h1 sont constituées de 11 aminoacides et les TetR reconnaissent des ADN_{op} de 15 pb (Yu et al. 2010). MAB_4384 (h1 = 21 résidus) reconnait un palindrome de 27 pb mais requiert des nucléotides supplémentaires aspécifiques de part et d'autre de son DNA_{op} pour une fixation optimale. Le motif palindromique atypique d'EthR (h1 = 25 résidus) mesure 35 pb mais le *footprinting* de sa région intergénique révèle que ce TetR recouvre en réalité une séquence de 55 pb (Engohang-Ndong et al. 2004)(Figure 36B). Le motif reconnu en amont de *MAB_2300/2301* par

MAB_2299c (h1 = 22-25) est composé d'un couple de palindromes de 7 pb séparé par un long *spacer* de 39 nucléotides menant à un motif de 53 pb. La taille du domaine HTH et la longueur de l'hélice h1 pourrait permettre la reconnaissance d'ADN cible de plusieurs dizaines de nucléotides composés de grands palindromes et/ou séparés par un long *spacer*. Une étude bio-informatique est cependant requise pour confirmer ces observations. Par ailleurs, d'autres facteurs que la morphologie du domaine HTH peuvent influencer la capacité à reconnaitre ces ADN cibles longs comme par exemple l'envergure du mouvement pendulaire réalisé lors de la fixation à l'ADN. L'amplitude de ce mouvement pourrait permettre à des TetR possédant une h1 de petite taille de reconnaitre de longues séquences et inversement, ce qui est peut-être le cas de MAB_2299c lorsqu'il s'ancre à l'ADN_{op} en amont de *MAB_1135c/1134c* (Voir Figure 4A de l'**Article 3**).

L'expression de protéines recombinantes TetR natives et des mutants des domaines HTH chez *E. coli* a été possible ce qui atteste de leurs solubilités. En revanche, il a été impossible de purifier les protéines recombinantes MAB_2299c possédant les mutations L151P et G215W, car ces résidus doivent être impliqués dans le maintien de l'intégrité structurale du domaine C-terminal ou de l'interface monomère – monomère.

Malgré l'absence de co-structures TetR - DNA_{op} pour MAB_4384 et MAB_2299c, il est possible de déduire le type de ces TetR (Type I-II-III, Figure 33) et leur stœchiométrie pour leurs ADN cibles respectifs. MAB_4384 est un TetR de type I ne régulant que l'opéron en orientation opposée le plus proche. MAB_2299c contrôle l'opéron voisin orienté dans la direction opposée mais aussi un autre opéron plus éloigné, faisant de lui un TetR de type III. La plasticité de MAB_2299c pour ces ADN cible suggère une interaction dimère – ADN alors qu'étant donné la spécificité de MAB_4384 pour sa séquence palindromique, deux dimères interagiraient avec l'ADN cible. Les différents ratios concentrations TetR/ADN utilisés dans les EMSA supportent également ces hypothèses. En effet, le ratio TetR/ADN de MAB_4384 est deux fois supérieur à celui de MAB_2299c, suggérant la nécessité d'avoir deux dimères pour avoir formation du complexe. La spécificité de MAB_4384 est également plus importante que celle de MAB_2299c. En effet, une quantité 100 fois plus importante d'ADN non-spécifique froid (non fluorescent) n'est pas suffisante pour dissocier le complexe MAB_4384/DNA_{op}, tandis qu'avec un tel ratio MAB_2299c se dissocie de sa cible. La spécificité de MAB_4384 et la puissance du promoteur de *MAB_4383c/4382c* suggère que ce cluster est finement contrôlé.

Les souches surexprimant MAB_4383c/4382c ne présentent aucun défaut de croissance *in vitro* ni une virulence accrue dans le zebrafish, excluant l'implication de ce MmpS/MmpL dans l'homéostasie des bacilles et/ou dans leur virulence dans les conditions expérimentales testées

(Halloum et al. 2017). L'expression de cette pompe à efflux se produit en réalité uniquement dans un contexte bien précis. Une analyse transcriptomique a révélé que ce transporteur est légèrement surexprimé dans un milieu mimétique recréant les conditions nutritives du mucus d'une personne atteinte de mucoviscidose, le milieu SCFM (Miranda-CasoLuengo et al. 2016). La forte surexpression de MAB_4383c/4382c dans le milieu SCFM pourrait augmenter le taux de croissance et la capacité à former des biofilms. Si ces caractéristiques phénotypiques sont en effet dépendantes de l'environnement, la surexpression de MAB_4383c/4382c pourrait conférer un avantage en termes de virulence dans le mucus pulmonaire pathologique. Dans ce contexte, *MAB_4384* pourrait représenter un marqueur de résistance et/ou de sévérité de l'infection utilisable en diagnostic clinique. De la même façon, en présence d'un isolat clinique résistant à la CFZ et/ou à la BDQ, *MAB_2299c* est un marqueur de résistance à prendre en considération. Cependant, contrairement aux mutants *MAB_4384*, le variant S ∆*MAB_2299c* possède un léger défaut de survie au sein du macrophage selon un mécanisme qui reste à définir. Un des scénarios possibles est que la surexpression de MAB_1135c/1134c et de MAB_2300/2301 mène à l'export trop important d'une molécule ou d'un lipide qui se retrouverait piégé à la surface de la paroi bactérienne interagissant avec la cellule hôte. La fonction de modulation normale de la réponse immunitaire exercée par les GPL serait altérée. Il est également possible que MAB_2299c régule d'autres gènes que cespaires *mmpS*/*mmpL* et que ces derniers participent directement dans la survie intracellulaire de *M. abscessus*. L'utilisation du gène rapporteur *lacZ* ainsi que d'une nouvelle technique de délétion génétique non-marquée nous ont permis de découvrir que ces couples MmpS/MmpL sont responsables de résistances basales chez *M. abscessus*.

La régulation, l'intensité et la spécificité de la résistance induite par les macrolides chez *M. abscessus* ont été investigués *in vitro* et *in vivo*à l'aide d'autres souches rapportrices. Ce phénomène nuit grandement à la prise en charge des patients et la sensibilité aux macrolides est ainsi un facteur déterminant dans le pronostic en faveur d'une guérison.Une caractéristique frappante est que le pourcentage de succès thérapeutique est étroitement lié à la proportion d'infections causées par la sous-espèce *M. massiliense* pour laquelle Erm(41) est non-fonctionnelle (Won-Jung Koh et al. 2011)(J. Park et al. 2017). Cette corrélation fait de cette enzyme une cible thérapeutique particulièrement attractive. Notre étude a permis de réfuter les conclusions de travaux antérieurs indiquant que l'AZM n'est pas un inducteur de la résistance médiée par Erm(41). L'AZM semble en réalité déclencher une résistance plus rapide et plus intense que la CLR. L'activité de *lacZ* sous le contrôle du promoteur d'*erm(41*) complet et tronqués en plusieurs segments a révélé que WhiB7 exerce une régulation complexe et atypique. L'architecture du motif de liaison de WhiB7 sur le promoteur d'*erm(41)* de *M. abscessus* est unique. Chez d'autres mycobactéries, les motifs de

reconnaissance de WhiB7 pour son propre gène et pour *erm(41)* semblent beaucoup plus conservés. D'après les distances entre les boites -35 et -10, ces autres protéines WhiB7 interagiraient avec le facteur de transcription végétatif SigA. Cet écart est beaucoup plus faible chez *M. abscessus* et ne correspond à aucune distance typique de facteur σ connu (Newton-Foot et Gey van Pittius 2013). Cependant, l'interaction de protéines WhiB avec les parties C-terminales de facteurs σ pourraient provoquer chez eux un réarrangement structural. Ces complexes facteurs σ/WhiB seraient alors capables de reconnaitre des promoteurs avec une architecture variée, leur offrant un régulome élargie. WhiB7 interagit peut-être avec SigA comme chez les autres espèces et éventuellement avec d'autres facteurs σ alternatifs.

Par définition, un évènement inductible est un phénomène transitoire temporaire concomitant à un signal spécifique faisant passer un système d'un état « *Off* » à un état « *ON* ». En absence de signal, l'induction disparait et le système redevient *Off*. Ce schéma ne semble toutefois pas s'appliquer totalement à *M. abscessus* et à sa résistance inductible aux macrolides due à Erm(41). Ceci est suggèré par nos expériences où la résistance à l'AZM et à la CLR est prolongée dans son état *On* en l'absence de ces antibiotiques. Cette régulation est peut-être d'ordre épigénétique car elle implique la modification du profil d'expression de protéines sans altération du génome transmise aux cellules filles. Ces mécanismes peuvent être composés, entre autres, de boucles de rétroaction positive (*positive feedback loop*) ou de méthylation de l'ADN (Casadesús et Low 2006). WhiB7 pourrait alors être activé de manière constitutive chez les futures bactéries en absence de signal par l'un de ces deux mécanismes. La régulation épigénétique reste encore à être explorée chez les mycobactéries mais certaines études fournissent quelques indices en faveur d'un tel contrôle de l'expression génique chez ces microorganismes (Balleza et al. 2009)(Shell et al. 2013)(Bowman et Ghosh 2014).

Partie II – Nouvelles Cibles, Molécules et Stratégies Thérapeutiques

Les études à la base de cette thèse confortent non seulementl'importance de pompes à efflux, d'Erm(41) mais aussi de WhiB7 dans l'antibiorésistance naturelle de *M. abscessus* mais soulignent également leur intérêt en tant que cibles thérapeutiques à exploiter. En effet, des inhibiteurs spécifiques de MmpL permettraient potentiellement d'inverser la balance succès/échecs thérapeutiques. MmpL3 est le seul MmpL essentiel chez les mycobactéries car il assure le transport des acides mycoliques qui sont nécessaires à la formation de la paroi et à la croissance mycobactérienne (Grzegorzewicz et al. 2012). Ainsi, l'essentialité de MmpL3 rend *M. abscessus* vulnérable aux molécules inhibant spécifiquement ce transporteur. Ces inhibiteurs permettraient de contourner les phénomènes de résistances inductibles aux macrolides et aux aminoglycosides. De

tels composés ont récemment été décrits chez *M. abscessus*, notamment un dérivé du pipéridinol désigné PIPD1 (Dupont et al. 2016) et des indoles-2-carboxamides (voir l'article en **Annexe 1,** Kozikowski et al. 2017). Les co-structures de MmpL3 de *M. smegmatis* avec PIPD1 et un indolcarboxamide montrent que les inhibiteurs se nichent de la même manière entre les TM4, 5, 6, 10, 11 et 12 bloquant le passage des protons (Zhang et al. 2019). Ces données cristallographiques ouvrent la voie vers la synthèse de nouveaux dérivés de ces inhibiteurs. Ces co-structures protéine/inhibiteur permettent l'optimisation de composés en fonction de leurs structures chimiques et de leurs activités biologiques. Ces inhibiteurs de MmpL3 sont bactéricides *in vitro* et réduisent la charge bactérienne *ex vivo* dans le macrophage. PIPD1 réduit significativement la mortalité des embryons de zebrafish infectés par *M. abscessus*, les symptômes liés à l'infection ainsi que la charge bactérienne. Néanmoins, d'autres études sont nécessaires pour intégrer ces molécules dans une multi-thérapie excluant les macrolides et les aminoglycosides. En effet, l'IPM et la CFX ont aussi un effet bactéricide *in vitro* mais sont peu efficaces en monothérapie. Une combinaison d'antibiotiques optimale comprendrait des molécules : (i) ciblant des enzymes ou des compartiments subcellulaires distincts, (ii) qui ne soient pas inactivées des enzymes du régulome de WhiB7. Une trithérapie inhibiteur de MmpL3 – MOX – TGC/LNZ s'avérerait intéressante à étudier, car même si les tétracyclines et le LNZ induisent l'expression de *whiB7*, aucune de ces molécules n'est *a priori* sensibles à une enzyme activée par WhiB7. Un antibiotique visant plusieurs MmpL autre que MmpL3 ciblerait des voies métaboliques non-essentielles mais requises pour une infection efficace ou un export basal d'antibiotiques faisant de cette molécule un pharmacophore très efficace. Les acteurs du métabolisme dérivant des acides mycoliques transportés par MmpL3 sont aussi de bonnes cibles antibiotiques. Ainsi, le complexe Antigène 85 est un complexe enzymatique particulièrement attractif non seulement en tant que cible thérapeutique mais également pour le développement de vaccin et de nouveaux tests diagnostiques(Babaki et al 2017) . Il catalyse la formation du TDM et la mycolyltation de l'arabinogalactane (Belisle et al. 1997). Dans ce contexte, l'article en **Annexe 2** rapporte la caractérisation d'une nouvelle activité enzymatique pour trois des membres de ce complexe ainsi que de leurs inhibitions *in vitro* et *in vivo* par des analogues de cyclipostines et cyclophostines chez *M. tuberculosis* (Viljoen, Richard et al. 2018). Cette étude est étayée par des travaux plus récents démontrant que les cyclipostines et cyclophostines sont des inhibiteurs très efficaces contre *M. abscessus* (Madani et al. 2019). Ces composés sont prometteurs car ils ciblent un résidu ultra-conservé du site actif des trois enzymes, diminuant de manière considérable les chances d'apparition d'une résistance croisée. La liaison covalente établie avec la sérine du site catalytique est irréversible et ne pourrait donc pas être détruite par une enzyme modifiant la cible d'antibiotiques, comme Erm(41).

L'utilisation de kétolides au lieu de la CLR et l'AZM pourrait permettre de palier à la résistance inductible aux macrolides. L'une des particularités des kétolides est l'absence de cladinose dans leurs structures. Ce sucre est remplacé par un groupement cétone, ce qui fait normalement de ces macrolides des faibles inducteurs des résistances médiées par des méthyltransférases (Douthwaite 2001). Malheureusement cette particularité ne semble pas se vérifier chez *M. abscessus*. Nash et al. ont montré une forte augmentation des niveaux de transcrits d'*erm(41)* suite à une exposition à la télithromycine, le seul kétolide actuellement approuvé pour un usage clinique. Une autre particularité des kétolides est la présence d'un groupement carbamate permettant à ces molécules d'interagir avec d'autres nucléotides de l'ARNr 23S comme la paire A752 – U2609 (Chellat et al. 2016). Un nouveau kétolide est en cours d'essai clinique pour le traitement de pneumopathies communautaires bactériennes, la solithromycine (Zhanel et al. 2016). Une de ces particularité est qu'un atome de fluor est présent en position 2 de son cycle lactone lui offrant un troisième site de liaison à l'ARNr 23S (Fernandes et al. 2016). Comme la télithromycine, la solithromycine pourrait induire l'expression d'Erm(41) mais son troisième site de fixation ribosomique pourrait lui procurer une meilleure pharmacocinétique et un pouvoir antimicrobien plus prononcé. Néanmoins, on ne peut exclure la possibilité qu'Erm(41) ne soit capable de modifier d'autres nucléotides de l'ARNr 23S. En l'absence de donnée cristallographique et d'un test d'activité enzymatique, une manière de répondre à cette question consisterait à générer des mutants résistants spontanés contre la télithromycine et la solithromycine chez une souche de *M. abscessus* Δ*erm(41)* ou chez *M. massiliense* soumis à des doses croissantes d'antibiotiques et de séquencer leur génome (Martinez et Baquero 2000). La découverte de nouveaux dérivés de macrolide n'induisant pas Erm(41) représenterait une avancée majeure dans la thérapie contre *M. abscessus* mais aussi contre d'autres MNT possédant un système de résistance inductible aux macrolides. La recherche de telles molécules peut s'avérer longue et fastidieuse en l'absence d'outils appropriés. Dans ce contexte, la souche rapportrice exprimant le marqueur de fluorescence *tdTomato* sous le contrôle du promoteur d'*erm(41)* pourrait être décisive dans le criblage de ce type d'antibiotiques. En effet, il est techniquement possible de coupler la détermination de la CMI en plaque 96 puits en respectant les directives du CLSI avec une mesure de l'émission de fluorescence due à l'activation transcriptionnelle d'*erm(41)* reflétée par l'expression de tdTomato. Ainsi, il apparait tout à fait envisageable d'évaluer simultanément le pouvoir bactéricide et l'incapacité à déclencher le système *erm(41)* de molécules en criblant une banque de dérivés de macrolides en un temps réduit.

Une autre alternative au développement de nouveaux antibiotiques serait de générer des *boosters* qui augmenteraient l'activité de ces antibiotiques en déstabilisant les mécanismes de résistances intrinsèques et inductibles. Certains composés de ce type ont déjà été testés sur des

MmpL *in vitro* et *in vivo*. Ces molécules seules n'ont pas ou peu d'effets antimicrobiens mais sont capables d'améliorer fortement l'activité de certains antibiotiques, parmi lesquels font partis la réserpine, le CCCP (CarbonylCyanure m-ChloroPhénylhydrazone) et le vérapamil (VPM). La réserpine est utilisée pour traiter l'hypertension ou certains troubles psychiatriques et comme le VPM, est utilisée dans le traitement de l'hypertension. Ces molécules perturbent le potentiel de membrane en inhibant les canaux calciques. Le CCCP est un protonophore qui va directement cibler la force proto-motrice en séquestrant les H^+ bloquant leur flux transmembranaire. Ces trois molécules impactent ainsi le fonctionnement de pompes à efflux en générant un stress membranaire ou énergétique (Li et al. 2016)(Ramis et al. 2019), et améliorent l'efficacité d'antibiotiques expulsés hors du cytoplasme ou ciblant des voies métaboliques dépendantes du gradient électrochimique membranaire comme la BDQ (Viljoen et al. 2019). Cette combinaison BDQ/VPM est synergique *in vitro* sur des isolats cliniques de *M. abscessus* et dans le macrophage. Cette association est également efficace contre la souche Δ*MAB_2299c* (technique pUX1-*katG* développée au cours de cette thèse) indiquant que cette combinaison est efficace en présence d'une surexpression des deux transporteurs impliqués dans la résistance croisée à la CFZ et à la BDQ. La réserpine et le VPM inhibent les canaux calciques mais le mécanisme moléculaire précis de cette inhibition n'est pas connu chez les mycobactéries. En admettant qu'elles ciblent des protéines différentes impliquées dans le transport de Ca^{2+}, elles pourraient donc avoir un effet additif ou même synergique. Les inhibiteurs de pompes à efflux utilisés en parallèle avec les aminoglycosides mèneraient potentiellement à une meilleure activité de ces antibiotiques, qui génèrent indirectement un stress énergétique membranaire (Kohanskie et al. 2010). Les aminoglycosides ciblent la sous-unité 30S du ribosome et provoquent la synthèse de protéines mal repliées et notamment des protéines membranaires. L'incorporation de protéines transmembranaires mal repliées va augmenter la perméabilité de la paroi à ces antibiotiques mais aussi activer un système à deux composants (Cpx/Arc) qui dérèglera la chaine de transporteurs d'électrons présent dans la membrane plasmique. Ces changements biochimiques perturberaient en théorie les fonctions exercées par les MmpL. L'apramycine serait un bon candidat car elle n'est pas inactivée par *M. abscessus*, possède une toxicité réduite (Rominski, Selchow, et al. 2017). Tout autre antibiotique visant la chaine de transport d'électrons pourrait être utilisé avec ces inhibiteurs, comme la CFZ activée par la NDH-2 et les imidazopyridines qui visent le complexe cytochrome bc_1(Bald et al. 2017). Ces molécules donnent un regain d'originalité et de nouveauté dans des stratégies alternatives au traitement de *M. abscessus*, d'autant plus que la BDQ, le VPM et la réserpine sont approuvés pour un usage clinique.

On retrouve sur le même modèle l'avibactam, un inhibiteur de β-lactamase désarmant les bactéries (Lefebvre et al. 2017). Un inhibiteur de MabTetX permettrait d'utiliser une large variété de

tétracyclines inactivées par cette enzyme. L'inhibition d'Eis2 et d'Erm(41) impliquerait la découverte de deux molécules distinctes tandis qu'une molécule ciblant spécifiquement WhiB7 ferait d'une pierre deux coups, en réglant ces deux problèmes de résistance en une seule fois. Le remplacement de la région intergénique d'*erm(41)* par le promoteur de *whiB7* dans le plasmide rapporteur *tdTomato* permettrait un criblage à large spectre de molécules en tout genre ne déclenchant pas l'expression du régulome de WhiB7. Ce test permettrait de cribler des banques d'inhibiteurs potentiels en combinaison avec un antibiotique très sensible à WhiB7 comme l'AZM. Ces antibiotiques très inducteurs permettre un fort contraste lorsque l'inhibiteur est actif contre WhiB7. Ces inhibiteurs de WhiB7 peuvent présenter *a minima* deux mécanismes d'action : (i) un contact direct avec WhiB7, (ii) un contact avec la région promotrice du régulome. La région entre les domaines fer – soufre et l'AT-Hook est conservée et relativement unique aux protéines WhiB et serait alors un bon candidat. La protéine WhiBTM4 produite par le mycobactériophage TM4 est très proche structuralement de WhiB2 de *M. tuberculosis*. Elle se lie au motif reconnu par WhiB2 et de ce fait inhibe sa transcription et celles des gènes de son régulome (Rybniker et al. 2010). Imiter ce bactériophage en produisant une protéine recombinante structuralement proche de WhiB7 permettrait d'inhiber sa transcription et celle de son régulome. Un groupe brésilien a récemment rapporté *via* deux études la découverte de nouveaux inhibiteurs de pompes à efflux dérivés de tétrahydropyridines (Vianna et al. 2019a)(Vianna et al. 2019b). Ces molécules bloquent effectivement l'efflux chez *M. abscessus* mais les baisses des CMI de la CLR et d'AMK en combinaison avec leurs composés laissent à penser que ces molécules pourraient en fait inhiber WhiB7. En effet, la résistance à ces deux composés est majoritairement due à Eis2 et Erm(41), l'efflux d'AMK par MAB_{tap}étant un mécanisme de résistance basale de faible intensité et celui de la CLR n'est pas prouvé expérimentalement. Nos lignées rapportrices représenteraient une application rapide afin d'en avoir le cœur net.

La découverte de nouvelles molécules qu'elles soient des antibiotiques ou des inhibiteurs de de facteurs de résistance n'est probablement pas à elle seule la solution contre *M. abscessus* et l'émergence d'épidémies en milieu hospitalier. Un nouveau concept apparu ces dernières années permet une prise de recul entre de la résistance antibiotique et la persistance antibiotique (Balaban et al. 2019). Ce dernier phénomène n'est pas pleinement appréhendé mais il pourrait être responsable de récidives lors d'un traitement à *M. abscessus*. La persistance antibiotique est caractérisée principalement par la présence d'une sous-population au sein d'un même isolat qui n'est pas tuée à la même vitesse par le même antibiotique que le reste de la population. Ceci s'oppose à la tolérance qui est caractérisée par un changement métabolique de toute la population bactérienne menant à une résistance temporaire ou à un retard dans l'élimination par un

antibiotique. Il est possible qu'au terme d'une infection à *M. abscessus*, cet infime nombre de bactéries persistantes soit toujours présent mais non-détectable. Le traitement sera alors arrêté en l'absence de symptômes ou de preuves microbiologiques de la présence de ces bactéries. Ces « *persistors* » perdureront pour finalement à nouveau se multiplier et générer une rechute. Ces récidives sont communes et très problématiques lorsqu'elles se produisent, notamment chez une personne atteinte de mucoviscidose et/ou ayant subi une greffe pulmonaire (Smibert et al. 2016)(Osmani et al. 2018). Un suivi de ces patients et l'élaboration d'une thérapie supportable à long terme sont primordiaux pour anticiper ces réinfections récalcitrantes.

En conclusion, les travaux de cette thèse ont fourni des informations inédites concernant les mécanismes de résistance intrinsèques à deux molécules actuellement évaluées cliniquement, la BDQ et la CFZ, et concernant la résistance inductible aux macrolides. Ces études proposent également de nouveaux marqueurs de résistance ainsi que des outils génétiques originaux pour étudier la virulence/résistance de *M. abscessus*. La voie semble toute tracée pour le développement de méthodes de criblage à haut débit de nouveaux macrolides et de molécules bloquant les mécanismes de la multi-résistance intrinsèque de *M. abscessus*.

Références

Abrahams A., et Besra G. 2018. « Mycobacterial cell wall biosynthesis: a multifaceted antibiotic target ». *Parasitology* 145 (2): 116‑33. https://doi.org/10.1017/S0031182016002377.

Adekambi, Toidi, Mohamed Sassi, Jakko van Ingen, et Michel Drancourt. 2017. « Reinstating Mycobacterium Massiliense and Mycobacterium Bolletii as Species of the Mycobacterium Abscessus Complex ». *International Journal of Systematic and Evolutionary Microbiology* 67 (8): 2726‑30. https://doi.org/10.1099/ijsem.0.002011.

Alcaide, F, G E Pfyffer, et A Telenti. 1997. « Role of embB in natural and acquired resistance to ethambutol in mycobacteria. » *Antimicrobial Agents and Chemotherapy* 41 (10): 2270‑73.

Alderwick, Luke J., James Harrison, Georgina S. Lloyd, et Helen L. Birch. 2015. « The Mycobacterial Cell Wall—Peptidoglycan and Arabinogalactan ». *Cold Spring Harbor Perspectives in Medicine* 5 (8). https://doi.org/10.1101/cshperspect.a021113.

Alix, Eric, et Anne-Béatrice Blanc-Potard. 2007. « MgtC: A Key Player in Intramacrophage Survival ». *Trends in Microbiology* 15 (6): 252‑56. https://doi.org/10.1016/j.tim.2007.03.007.

American Lung Association. 2018. « Pneumoconiosis Symptoms, Causes and Risk Factors ». American Lung Association. 2018. https://www.lung.org/lung-health-and-diseases/lung-disease-lookup/pneumoconiosis/pneumoconiosis-symptoms-causes-risks.html.

Auboyer, C., G. Beaucaire, H. Drugeon, F. Gouin, J.C. Granry, V. Jarlier, A.M. Korinek, et al. 2000. « Associations d'antibiotiques ou monothérapie en réanimation chirurgicale et en chirurgie ». *Réanimation Urgences* 9 (4): 305‑10. https://doi.org/10.1016/S1164-6756(00)80011-0.

Aziz, Dinah B., Jeanette W. P. Teo, Véronique Dartois, et Thomas Dick. 2018. « Teicoplanin - Tigecycline Combination Shows Synergy Against Mycobacterium Abscessus ». *Frontiers in Microbiology* 9: 932. https://doi.org/10.3389/fmicb.2018.00932.

Aziz, Dinah Binte, Jian Liang Low, Mu-Lu Wu, Martin Gengenbacher, Jeanette W. P. Teo, Véronique Dartois, et Thomas Dick. 2017. « Rifabutin Is Active against Mycobacterium abscessus Complex ». *Antimicrobial Agents and Chemotherapy* 61 (6). https://doi.org/10.1128/AAC.00155-17.

Bakala N'Goma, Jean Claude, Vincent Le Moigne, Nathalie Soismier, Laura Laencina, Fabien Le Chevalier, Anne-Laure Roux, Isabelle Poncin, et al. 2015. « Mycobacterium Abscessus Phospholipase C Expression Is Induced during Coculture within Amoebae and Enhances M. Abscessus Virulence in Mice ». *Infection and Immunity* 83 (2): 780‑91. https://doi.org/10.1128/IAI.02032-14.

Baker, Arthur W., Sarah S. Lewis, Barbara D. Alexander, Luke F. Chen, Richard J. Wallace, Barbara A. Brown-Elliott, Pamela J. Isaacs, et al. 2017. « Two-Phase Hospital-Associated Outbreak of Mycobacterium Abscessus: Investigation and Mitigation ». *Clinical Infectious Diseases: An Official Publication of the Infectious Diseases Society of America* 64 (7): 902‑11. https://doi.org/10.1093/cid/ciw877.

Balaban, Nathalie Q., Sophie Helaine, Kim Lewis, Martin Ackermann, Bree Aldridge, Dan I. Andersson, Mark P. Brynildsen, et al. 2019. « Definitions and Guidelines for Research on Antibiotic Persistence ». *Nature Reviews. Microbiology* 17 (7): 441‑48. https://doi.org/10.1038/s41579-019-0196-3.

Bald, Dirk, Cristina Villellas, Ping Lu, et Anil Koul. 2017. « Targeting Energy Metabolism in Mycobacterium Tuberculosis, a New Paradigm in Antimycobacterial Drug Discovery ». *MBio* 8 (2). https://doi.org/10.1128/mBio.00272-17.

Balleza, Enrique, Lucia N López-Bojorquez, Agustino Martínez-Antonio, Osbaldo Resendis-Antonio, Irma Lozada-Chávez, Yalbi I Balderas-Martínez, Sergio Encarnación, et Julio Collado-Vides. 2009. « Regulation by transcription factors in bacteria: beyond description ». *Fems Microbiology Reviews* 33 (1): 133-51. https://doi.org/10.1111/j.1574-6976.2008.00145.x.

Barkay, Tamar, Susan M. Miller, et Anne O. Summers. 2003. « Bacterial Mercury Resistance from Atoms to Ecosystems ». *FEMS Microbiology Reviews* 27 (2-3): 355-84. https://doi.org/10.1016/S0168-6445(03)00046-9.

Baulard, A. R., J. C. Betts, J. Engohang-Ndong, S. Quan, R. A. McAdam, P. J. Brennan, C. Locht, et G. S. Besra. 2000. « Activation of the Pro-Drug Ethionamide Is Regulated in Mycobacteria ». *The Journal of Biological Chemistry* 275 (36): 28326-31. https://doi.org/10.1074/jbc.M003744200.

Baysarowich, Jennifer, Kalinka Koteva, Donald W. Hughes, Linda Ejim, Emma Griffiths, Kun Zhang, Murray Junop, et Gerard D. Wright. 2008. « Rifamycin Antibiotic Resistance by ADP-Ribosylation: Structure and Diversity of Arr ». *Proceedings of the National Academy of Sciences of the United States of America* 105 (12): 4886-91. https://doi.org/10.1073/pnas.0711939105.

Bechara, Chadi, Edouard Macheras, Beate Heym, Adele Pages, et Nicole Auffret. 2010. « Mycobacterium Abscessus Skin Infection after Tattooing: First Case Report and Review of the Literature ». *Dermatology (Basel, Switzerland)* 221 (1): 1-4. https://doi.org/10.1159/000313974.

Belardinelli, Juan Manuel, Gérald Larrouy-Maumus, Victoria Jones, Luiz Pedro Sorio de Carvalho, Michael R. McNeil, et Mary Jackson. 2014. « Biosynthesis and Translocation of Unsulfated Acyltrehaloses in Mycobacterium Tuberculosis ». *The Journal of Biological Chemistry* 289 (40): 27952-65. https://doi.org/10.1074/jbc.M114.581199.

Belisle, J. T., V. D. Vissa, T. Sievert, K. Takayama, P. J. Brennan, et G. S. Besra. 1997. « Role of the Major Antigen of Mycobacterium Tuberculosis in Cell Wall Biogenesis ». *Science (New York, N.Y.)* 276 (5317): 1420-22. https://doi.org/10.1126/science.276.5317.1420.

Bellinzoni, Marco, Silvia Buroni, Francis Schaeffer, Giovanna Riccardi, Edda De Rossi, et Pedro M. Alzari. 2009. « Structural Plasticity and Distinct Drug-Binding Modes of LfrR, a Mycobacterial Efflux Pump Regulator ». *Journal of Bacteriology* 191 (24): 7531-37. https://doi.org/10.1128/JB.00631-09.

Benwill, Jeana L., et Richard J. Wallace. 2014. « Mycobacterium Abscessus: Challenges in Diagnosis and Treatment ». *Current Opinion in Infectious Diseases* 27 (6): 506-10. https://doi.org/10.1097/QCO.0000000000000104.

Bernut, Audrey, Christian Dupont, Nikolay V. Ogryzko, Aymeric Neyret, Jean-Louis Herrmann, R. Andres Floto, Stephen A. Renshaw, et Laurent Kremer. 2019. « CFTR Protects against Mycobacterium Abscessus Infection by Fine-Tuning Host Oxidative Defenses ». *Cell Reports* 26 (7): 1828-1840.e4. https://doi.org/10.1016/j.celrep.2019.01.071.

Bernut, Audrey, Jean-Louis Herrmann, Karima Kissa, Jean-François Dubremetz, Jean-Louis Gaillard, Georges Lutfalla, et Laurent Kremer. 2014. « Mycobacterium abscessus cording prevents phagocytosis and promotes abscess formation ». *Proceedings of the National Academy of Sciences of the United States of America* 111 (10): E943-52. https://doi.org/10.1073/pnas.1321390111.

Bernut, Audrey, Jean-Louis Herrmann, Diane Ordway, et Laurent Kremer. 2017. « The Diverse Cellular and Animal Models to Decipher the Physiopathological Traits of Mycobacterium Abscessus

Infection ». *Frontiers in Cellular and Infection Microbiology* 7: 100. https://doi.org/10.3389/fcimb.2017.00100.
Bernut, Audrey, Mai Nguyen-Chi, Iman Halloum, Jean-Louis Herrmann, Georges Lutfalla, et Laurent Kremer. 2016. « Mycobacterium Abscessus-Induced Granuloma Formation Is Strictly Dependent on TNF Signaling and Neutrophil Trafficking ». *PLoS Pathogens* 12 (11): e1005986. https://doi.org/10.1371/journal.ppat.1005986.
Bernut, Audrey, Albertus Viljoen, Christian Dupont, Guillaume Sapriel, Mickaël Blaise, Christiane Bouchier, Roland Brosch, Chantal de Chastellier, Jean-Louis Herrmann, et Laurent Kremer. 2016. « Insights into the Smooth-to-Rough Transitioning in Mycobacterium Bolletii Unravels a Functional Tyr Residue Conserved in All Mycobacterial MmpL Family Members ». *Molecular Microbiology* 99 (5): 866-83. https://doi.org/10.1111/mmi.13283.
Beveridge, T. J. 1999. « Structures of Gram-Negative Cell Walls and Their Derived Membrane Vesicles ». *Journal of Bacteriology* 181 (16): 4725-33.
Bhukya, Hussain, et Ruchi Anand. 2017. « TetR Regulators: A Structural and Functional Perspective ». *Journal of the Indian Institute of Science* 97 (2): 245-59. https://doi.org/10.1007/s41745-017-0025-5.
Bhukya, Hussain, Ruchika Bhujbalrao, Aruna Bitra, et Ruchi Anand. 2014. « Structural and Functional Basis of Transcriptional Regulation by TetR Family Protein CprB from S. Coelicolor A3(2) ». *Nucleic Acids Research* 42 (15): 10122-33. https://doi.org/10.1093/nar/gku587.
Blair, Jessica M. A., Mark A. Webber, Alison J. Baylay, David O. Ogbolu, et Laura J. V. Piddock. 2015. « Molecular Mechanisms of Antibiotic Resistance ». *Nature Reviews. Microbiology* 13 (1): 42-51. https://doi.org/10.1038/nrmicro3380.
Blondiaux, Nicolas, Martin Moune, Matthieu Desroses, Rosangela Frita, Marion Flipo, Vanessa Mathys, Karine Soetaert, et al. 2017. « Reversion of Antibiotic Resistance in Mycobacterium Tuberculosis by Spiroisoxazoline SMARt-420 ». *Science (New York, N.Y.)* 355 (6330): 1206-11. https://doi.org/10.1126/science.aag1006.
Bolinger, Hannah, et Sophia Kathariou. 2017. « The Current State of Macrolide Resistance in Campylobacter Spp.: Trends and Impacts of Resistance Mechanisms ». *Applied and Environmental Microbiology* 83 (12). https://doi.org/10.1128/AEM.00416-17.
Bowman, Joshua, et Pallavi Ghosh. 2014. « A Complex Regulatory Network Controlling Intrinsic Multidrug Resistance in Mycobacterium Smegmatis ». *Molecular Microbiology* 91 (1): 121-34. https://doi.org/10.1111/mmi.12448.
Brown, Stephanie, John P. Santa Maria, et Suzanne Walker. 2013. « Wall Teichoic Acids of Gram-Positive Bacteria ». *Annual Review of Microbiology* 67: 313-36. https://doi.org/10.1146/annurev-micro-092412-155620.
Brown-Elliott, Barbara A., Sruthi Vasireddy, Ravikiran Vasireddy, Elena Iakhiaeva, Susan T. Howard, Kevin Nash, Nicholas Parodi, et al. 2015. « Utility of Sequencing the erm(41) Gene in Isolates of Mycobacterium abscessus subsp. abscessus with Low and Intermediate Clarithromycin MICs ». *Journal of Clinical Microbiology* 53 (4): 1211-15. https://doi.org/10.1128/JCM.02950-14.
Bryant, Josephine M., Dorothy M. Grogono, Daniela Rodriguez-Rincon, Isobel Everall, Karen P. Brown, Pablo Moreno, Deepshikha Verma, et al. 2016. « Emergence and Spread of a Human-Transmissible Multidrug-Resistant Nontuberculous Mycobacterium ». *Science (New York, N.Y.)* 354 (6313): 751-57. https://doi.org/10.1126/science.aaf8156.
Burbaud, Sophie, Françoise Laval, Anne Lemassu, Mamadou Daffé, Christophe Guilhot, et Christian Chalut. 2016. « Trehalose Polyphleates Are Produced by a Glycolipid Biosynthetic Pathway Conserved across Phylogenetically Distant Mycobacteria ». *Cell Chemical Biology* 23 (2): 278-89. https://doi.org/10.1016/j.chembiol.2015.11.013.
Burian, Ján, Santiago Ramón-García, Charles G. Howes, et Charles J. Thompson. 2012. « WhiB7, a Transcriptional Activator That Coordinates Physiology with Intrinsic Drug Resistance in Mycobacterium Tuberculosis ». *Expert Review of Anti-Infective Therapy* 10 (9): 1037-47. https://doi.org/10.1586/eri.12.90.

Burian, Ján, Santiago Ramón-García, Gaye Sweet, Anaximandro Gómez-Velasco, Yossef Av-Gay, et Charles J. Thompson. 2012. « The Mycobacterial Transcriptional Regulator WhiB7 Gene Links Redox Homeostasis and Intrinsic Antibiotic Resistance ». *The Journal of Biological Chemistry* 287 (1): 299-310. https://doi.org/10.1074/jbc.M111.302588.

Burian, Ján, Grace Yim, Michael Hsing, Peter Axerio-Cilies, Artem Cherkasov, George B. Spiegelman, et Charles J. Thompson. 2013. « The Mycobacterial Antibiotic Resistance Determinant WhiB7 Acts as a Transcriptional Activator by Binding the Primary Sigma Factor SigA (RpoV) ». *Nucleic Acids Research* 41 (22): 10062-76. https://doi.org/10.1093/nar/gkt751.

Bush, Karen. 2013. « The ABCD's of β-Lactamase Nomenclature ». *Journal of Infection and Chemotherapy: Official Journal of the Japan Society of Chemotherapy* 19 (4): 549-59. https://doi.org/10.1007/s10156-013-0640-7.

Buss, W. C., E. Reyes, et T. D. Barela. 1977. « Metal Ion Catalyzed Oxidation of the Antibiotic Rifampicin ». *Research Communications in Chemical Pathology and Pharmacology* 17 (3): 547-50.

Camacho, L. R., P. Constant, C. Raynaud, M. A. Laneelle, J. A. Triccas, B. Gicquel, M. Daffe, et C. Guilhot. 2001. « Analysis of the Phthiocerol Dimycocerosate Locus of Mycobacterium Tuberculosis. Evidence That This Lipid Is Involved in the Cell Wall Permeability Barrier ». *The Journal of Biological Chemistry* 276 (23): 19845-54. https://doi.org/10.1074/jbc.M100662200.

Campbell, E. A., N. Korzheva, A. Mustaev, K. Murakami, S. Nair, A. Goldfarb, et S. A. Darst. 2001. « Structural Mechanism for Rifampicin Inhibition of Bacterial Rna Polymerase ». *Cell* 104 (6): 901-12. https://doi.org/10.1016/s0092-8674(01)00286-0.

Carvalho, Natalia F. G. de, Fernando Pavan, Daisy N. Sato, Clarice Q. F. Leite, Robert D. Arbeit, et Erica Chimara. 2018. « Genetic Correlates of Clarithromycin Susceptibility among Isolates of the Mycobacterium Abscessus Group and the Potential Clinical Applicability of a PCR-Based Analysis of Erm(41) ». *The Journal of Antimicrobial Chemotherapy* 73 (4): 862-66. https://doi.org/10.1093/jac/dkx476.

Casadesús, Josep, et David Low. 2006. « Epigenetic Gene Regulation in the Bacterial World ». *Microbiology and Molecular Biology Reviews: MMBR* 70 (3): 830-56. https://doi.org/10.1128/MMBR.00016-06.

Casonato, Stefano, Axel Cervantes Sánchez, Hirohito Haruki, Monica Rengifo González, Roberta Provvedi, Elisa Dainese, Thomas Jaouen, et al. 2012. « WhiB5, a Transcriptional Regulator That Contributes to Mycobacterium Tuberculosis Virulence and Reactivation ». *Infection and Immunity* 80 (9): 3132-44. https://doi.org/10.1128/IAI.06328-11.

Catherinot, Emilie, Anne-Laure Roux, Edouard Macheras, Dominique Hubert, Moussa Matmar, Luc Dannhoffer, Thierry Chinet, et al. 2009. « Acute Respiratory Failure Involving an R Variant of Mycobacterium Abscessus ». *Journal of Clinical Microbiology* 47 (1): 271-74. https://doi.org/10.1128/JCM.01478-08.

Chadha, R., M. Grover, A. Sharma, A. Lakshmy, M. Deb, A. Kumar, et G. Mehta. 1998. « An Outbreak of Post-Surgical Wound Infections Due to Mycobacterium Abscessus ». *Pediatric Surgery International* 13 (5-6): 406-10.

Chalut, Christian. 2016. « MmpL Transporter-Mediated Export of Cell-Wall Associated Lipids and Siderophores in Mycobacteria ». *Tuberculosis (Edinburgh, Scotland)* 100: 32-45. https://doi.org/10.1016/j.tube.2016.06.004.

Chater, K. F. 1972. « A Morphological and Genetic Mapping Study of White Colony Mutants of Streptomyces Coelicolor ». *Journal of General Microbiology* 72 (1): 9-28. https://doi.org/10.1099/00221287-72-1-9.

Chawla, Manbeena, Pankti Parikh, Alka Saxena, Mohamedhusen Munshi, Mansi Mehta, Deborah Mai, Anup K. Srivastava, et al. 2012. « Mycobacterium Tuberculosis WhiB4 Regulates Oxidative Stress Response to Modulate Survival and Dissemination in Vivo ». *Molecular Microbiology* 85 (6): 1148-65. https://doi.org/10.1111/j.1365-2958.2012.08165.x.

Chellat, Mathieu F., Luka Raguž, et Rainer Riedl. 2016. « Targeting Antibiotic Resistance ». *Angewandte Chemie (International Ed. in English)* 55 (23): 6600-6626. https://doi.org/10.1002/anie.201506818.

Cheng, Aristine, Yi-Tzu Tsai, Shu-Yuan Chang, Hsin-Yun Sun, Un-In Wu, Wang-Huei Sheng, Yee-Chun Chen, et Shan-Chwen Chang. 2019. « In Vitro Synergism of Rifabutin with Clarithromycin, Imipenem, and Tigecycline against the Mycobacterium Abscessus Complex ». *Antimicrobial Agents and Chemotherapy* 63 (4). https://doi.org/10.1128/AAC.02234-18.

Chiaradia, Laura, Cyril Lefebvre, Julien Parra, Julien Marcoux, Odile Burlet-Schiltz, Gilles Etienne, Maryelle Tropis, et Mamadou Daffé. 2017. « Dissecting the mycobacterial cell envelope and defining the composition of the native mycomembrane ». *Scientific Reports* 7 (octobre). https://doi.org/10.1038/s41598-017-12718-4.

Chim, Nicholas, Rodrigo Torres, Yuqi Liu, Joe Capri, Gaëlle Batot, Julian P. Whitelegge, et Celia W. Goulding. 2015. « The Structure and Interactions of Periplasmic Domains of Crucial MmpL Membrane Proteins from Mycobacterium Tuberculosis ». *Chemistry & Biology* 22 (8): 1098-1107. https://doi.org/10.1016/j.chembiol.2015.07.013.

Chmiel, J. F., M. W. Konstan, J. E. Knesebeck, J. B. Hilliard, T. L. Bonfield, D. V. Dawson, et M. Berger. 1999. « IL-10 Attenuates Excessive Inflammation in Chronic Pseudomonas Infection in Mice ». *American Journal of Respiratory and Critical Care Medicine* 160 (6): 2040-47. https://doi.org/10.1164/ajrccm.160.6.9901043.

Choi, Go-Eun, Ki-Nam Min, Choul-Jae Won, Kyeongman Jeon, Sung Jae Shin, et Won-Jung Koh. 2012. « Activities of Moxifloxacin in Combination with Macrolides against Clinical Isolates of Mycobacterium Abscessus and Mycobacterium Massiliense ». *Antimicrobial Agents and Chemotherapy* 56 (7): 3549-55. https://doi.org/10.1128/AAC.00685-12.

Choi, W. S., M. J. Kim, D. W. Park, S. W. Son, Y. K. Yoon, T. Song, S. M. Bae, J. W. Sohn, H. J. Cheong, et M. J. Kim. 2011. « Clarithromycin and Amikacin vs. Clarithromycin and Moxifloxacin for the Treatment of Post-Acupuncture Cutaneous Infections Due to Mycobacterium Abscessus: A Prospective Observational Study ». *Clinical Microbiology and Infection: The Official Publication of the European Society of Clinical Microbiology and Infectious Diseases* 17 (7): 1084-90. https://doi.org/10.1111/j.1469-0691.2010.03395.x.

Choo, Siew Woh, Wei Yee Wee, Yun Fong Ngeow, Wayne Mitchell, Joon Liang Tan, Guat Jah Wong, Yongbing Zhao, et Jingfa Xiao. 2014. « Genomic reconnaissance of clinical isolates of emerging human pathogen Mycobacterium abscessus reveals high evolutionary potential ». *Scientific Reports* 4 (février). https://doi.org/10.1038/srep04061.

Clary, Gillian, Smitha J. Sasindran, Nathan Nesbitt, Laurel Mason, Sara Cole, Abul Azad, Karen McCoy, Larry S. Schlesinger, et Luanne Hall-Stoodley. 2018. « Mycobacterium Abscessus Smooth and Rough Morphotypes Form Antimicrobial-Tolerant Biofilm Phenotypes but Are Killed by Acetic Acid ». *Antimicrobial Agents and Chemotherapy* 62 (3). https://doi.org/10.1128/AAC.01782-17.

Cole, Stewart T., et Pedro M. Alzari. 2005. « Microbiology. TB--a New Target, a New Drug ». *Science (New York, N.Y.)* 307 (5707): 214-15. https://doi.org/10.1126/science.1108379.

Compain, Fabrice, Daria Soroka, Beate Heym, Jean-Louis Gaillard, Jean-Louis Herrmann, Delphine Dorchène, Michel Arthur, et Vincent Dubée. 2018. « In Vitro Activity of Tedizolid against the Mycobacterium Abscessus Complex ». *Diagnostic Microbiology and Infectious Disease* 90 (3): 186-89. https://doi.org/10.1016/j.diagmicrobio.2017.11.001.

Converse, Scott E., Joseph D. Mougous, Michael D. Leavell, Julie A. Leary, Carolyn R. Bertozzi, et Jeffery S. Cox. 2003. « MmpL8 Is Required for Sulfolipid-1 Biosynthesis and Mycobacterium Tuberculosis Virulence ». *Proceedings of the National Academy of Sciences of the United States of America* 100 (10): 6121-26. https://doi.org/10.1073/pnas.1030024100.

Cook, Gregory M., Michael Berney, Susanne Gebhard, Matthias Heinemann, Robert A. Cox, Olga Danilchanka, et Michael Niederweis. 2009. « Physiology of Mycobacteria ». *Advances in microbial physiology* 55: 81-319. https://doi.org/10.1016/S0065-2911(09)05502-7.

Cowman, Steven, Jakko van Ingen, David E. Griffith, et Michael R. Loebinger. 2019. « Non-Tuberculous Mycobacterial Pulmonary Disease ». *The European Respiratory Journal* 54 (1). https://doi.org/10.1183/13993003.00250-2019.

Coxon, Geoffrey D., Derek Craig, Rosa Milagros Corrales, Emilie Vialla, Laila Gannoun-Zaki, et Laurent Kremer. 2013. « Synthesis, Antitubercular Activity and Mechanism of Resistance of Highly Effective Thiacetazone Analogues ». *PloS One* 8 (1): e53162. https://doi.org/10.1371/journal.pone.0053162.

Cremades, Rosa, Ana Santos, Juan Carlos Rodríguez, Eduardo Garcia-Pachón, Montserrat Ruiz, et Gloria Royo. 2009. « Mycobacterium Abscessus from Respiratory Isolates: Activities of Drug Combinations ». *Journal of Infection and Chemotherapy: Official Journal of the Japan Society of Chemotherapy* 15 (1): 46-48. https://doi.org/10.1007/s10156-008-0651-y.

Cuthbertson, Leslie, et Justin R. Nodwell. 2013. « The TetR Family of Regulators ». *Microbiology and Molecular Biology Reviews : MMBR* 77 (3): 440-75. https://doi.org/10.1128/MMBR.00018-13.

Daffé, Mamadou, et Hedia Marrakchi. 2019. « Unraveling the Structure of the Mycobacterial Envelope ». *Microbiology Spectrum* 7 (4). https://doi.org/10.1128/microbiolspec.GPP3-0027-2018.

Dal Molin, Michael, Myriam Gut, Anna Rominski, Klara Haldimann, Katja Becker, et Peter Sander. 2018. « Molecular Mechanisms of Intrinsic Streptomycin Resistance in Mycobacterium Abscessus ». *Antimicrobial Agents and Chemotherapy* 62 (1). https://doi.org/10.1128/AAC.01427-17.

Daley, Charles L. 2017. « Mycobacterium Avium Complex Disease ». *Microbiology Spectrum* 5 (2). https://doi.org/10.1128/microbiolspec.TNMI7-0045-2017.

Davidson, Lisa B., Rachid Nessar, Prakasha Kempaiah, Douglas J. Perkins, et Thomas F. Byrd. 2011. « Mycobacterium Abscessus Glycopeptidolipid Prevents Respiratory Epithelial TLR2 Signaling as Measured by HβD2 Gene Expression and IL-8 Release ». *PloS One* 6 (12): e29148. https://doi.org/10.1371/journal.pone.0029148.

De Groote, Mary Ann, Norman R. Pace, Kayte Fulton, et Joseph O. Falkinham. 2006. « Relationships between Mycobacterium Isolates from Patients with Pulmonary Mycobacterial Infection and Potting Soils ». *Applied and Environmental Microbiology* 72 (12): 7602-6. https://doi.org/10.1128/AEM.00930-06.

Donoghue, Helen D., Oona Y.-C. Lee, David E. Minnikin, Gurdyal S. Besra, John H. Taylor, et Mark Spigelman. 2010. « Tuberculosis in Dr Granville's mummy: a molecular re-examination of the earliest known Egyptian mummy to be scientifically examined and given a medical diagnosis ». *Proceedings of the Royal Society B: Biological Sciences* 277 (1678): 51-56. https://doi.org/10.1098/rspb.2009.1484.

Douthwaite, S. 2001. « Structure-Activity Relationships of Ketolides vs. Macrolides ». *Clinical Microbiology and Infection: The Official Publication of the European Society of Clinical Microbiology and Infectious Diseases* 7 Suppl 3: 11-17.

Dover, Lynn G., Anuradha Alahari, Paul Gratraud, Jessica M. Gomes, Veemal Bhowruth, Robert C. Reynolds, Gurdyal S. Besra, et Laurent Kremer. 2007. « EthA, a Common Activator of Thiocarbamide-Containing Drugs Acting on Different Mycobacterial Targets ». *Antimicrobial Agents and Chemotherapy* 51 (3): 1055-63. https://doi.org/10.1128/AAC.01063-06.

Dubée, Vincent, Audrey Bernut, Mélanie Cortes, Tiffany Lesne, Delphine Dorchene, Anne-Laure Lefebvre, Jean-Emmanuel Hugonnet, et al. 2015. « β-Lactamase Inhibition by Avibactam in Mycobacterium Abscessus ». *The Journal of Antimicrobial Chemotherapy* 70 (4): 1051-58. https://doi.org/10.1093/jac/dku510.

Dubois, Violaine, Alexandre Pawlik, Anouchka Bories, Vincent Le Moigne, Odile Sismeiro, Rachel Legendre, Hugo Varet, et al. 2019. « Mycobacterium Abscessus Virulence Traits Unraveled by Transcriptomic Profiling in Amoeba and Macrophages: Supplementary Tables and Figures ». Preprint. Microbiology. https://doi.org/10.1101/529057.

Dubois, Violaine, Albertus Viljoen, Laura Laencina, Vincent Le Moigne, Audrey Bernut, Faustine Dubar, Mickaël Blaise, et al. 2018. « MmpL8MAB Controls Mycobacterium Abscessus Virulence and Production of a Previously Unknown Glycolipid Family ». *Proceedings of the National Academy of Sciences of the United States of America* 115 (43): E10147-56. https://doi.org/10.1073/pnas.1812984115.

Dudek, Marta, Julia Romanowska, Tomasz Wituła, et Joanna Trylska. 2014. « Interactions of Amikacin with the RNA Model of the Ribosomal A-Site: Computational, Spectroscopic and Calorimetric Studies ». *Biochimie* 102 (juillet): 188-202. https://doi.org/10.1016/j.biochi.2014.03.009.

Dupont, Christian, Albertus Viljoen, Faustine Dubar, Mickaël Blaise, Audrey Bernut, Alexandre Pawlik, Christiane Bouchier, et al. 2016. « A New Piperidinol Derivative Targeting Mycolic Acid Transport in Mycobacterium Abscessus ». *Molecular Microbiology* 101 (3): 515-29. https://doi.org/10.1111/mmi.13406.

Dupont, Christian, Albertus Viljoen, Sangeeta Thomas, Françoise Roquet-Banères, Jean-Louis Herrmann, Kevin Pethe, et Laurent Kremer. 2017. « Bedaquiline Inhibits the ATP Synthase in Mycobacterium Abscessus and Is Effective in Infected Zebrafish ». *Antimicrobial Agents and Chemotherapy* 61 (11). https://doi.org/10.1128/AAC.01225-17.

Eid, Albert J., Elie F. Berbari, Irene G. Sia, Nancy L. Wengenack, Douglas R. Osmon, et Raymund R. Razonable. 2007. « Prosthetic Joint Infection Due to Rapidly Growing Mycobacteria: Report of 8 Cases and Review of the Literature ». *Clinical Infectious Diseases: An Official Publication of the Infectious Diseases Society of America* 45 (6): 687-94. https://doi.org/10.1086/520982.

Engohang-Ndong, Jean, David Baillat, Marc Aumercier, Flore Bellefontaine, Gurdyal S. Besra, Camille Locht, et Alain R. Baulard. 2004. « EthR, a Repressor of the TetR/CamR Family Implicated in Ethionamide Resistance in Mycobacteria, Octamerizes Cooperatively on Its Operator ». *Molecular Microbiology* 51 (1): 175-88. https://doi.org/10.1046/j.1365-2958.2003.03809.x.

Falkinham, Joseph O. 2011. « Nontuberculous Mycobacteria from Household Plumbing of Patients with Nontuberculous Mycobacteria Disease ». *Emerging Infectious Diseases* 17 (3): 419-24. https://doi.org/10.3201/eid1703.101510.

Fennelly, Kevin P., Carolyn Ojano-Dirain, Qingping Yang, Lin Liu, Li Lu, Ann Progulske-Fox, Gary P. Wang, Patrick Antonelli, et Gregory Schultz. 2016. « Biofilm Formation by Mycobacterium Abscessus in a Lung Cavity ». *American Journal of Respiratory and Critical Care Medicine* 193 (6): 692-93. https://doi.org/10.1164/rccm.201508-1586IM.

Fernandes, Prabhavathi, Evan Martens, Daniel Bertrand, et David Pereira. 2016. « The Solithromycin Journey-It Is All in the Chemistry ». *Bioorganic & Medicinal Chemistry* 24 (24): 6420-28. https://doi.org/10.1016/j.bmc.2016.08.035.

Ferro, Beatriz E., Shashikant Srivastava, Devyani Deshpande, Jotam G. Pasipanodya, Dick van Soolingen, Johan W. Mouton, Jakko van Ingen, et Tawanda Gumbo. 2016. « Tigecycline Is Highly Efficacious against Mycobacterium Abscessus Pulmonary Disease ». *Antimicrobial Agents and Chemotherapy* 60 (5): 2895-2900. https://doi.org/10.1128/AAC.03112-15.

Feßler, Andrea T., Yang Wang, Congming Wu, et Stefan Schwarz. 2018. « Mobile Macrolide Resistance Genes in Staphylococci ». *Plasmid* 99: 2-10. https://doi.org/10.1016/j.plasmid.2018.05.001.

Floto, R. Andres, Kenneth N. Olivier, Lisa Saiman, Charles L. Daley, Jean-Louis Herrmann, Jerry A. Nick, Peadar G. Noone, et al. 2016. « US Cystic Fibrosis Foundation and European Cystic Fibrosis Society Consensus Recommendations for the Management of Non-Tuberculous Mycobacteria in Individuals with Cystic Fibrosis ». *Thorax* 71 Suppl 1 (janvier): i1-22. https://doi.org/10.1136/thoraxjnl-2015-207360.

Foerstner, Konrad U., Christian von Mering, Sean D. Hooper, et Peer Bork. 2005. « Environments Shape the Nucleotide Composition of Genomes ». *EMBO Reports* 6 (12): 1208-13. https://doi.org/10.1038/sj.embor.7400538.

Fox, Lindy Peta, Adam S. Geyer, Sameera Husain, Phyllis Della-Latta, et Marc E. Grossman. 2004. « Mycobacterium Abscessus Cellulitis and Multifocal Abscesses of the Breasts in a

Transsexual from Illicit Intramammary Injections of Silicone ». *Journal of the American Academy of Dermatology* 50 (3): 450-54. https://doi.org/10.1016/j.jaad.2003.09.008.
Francisco, Estela Miranda. 2018. « Disabling and Potentially Permanent Side Effects Lead to Suspension or Restrictions of Quinolone Fluoroquinolone Antibiotics ». Text. European Medicines Agency. 16 novembre 2018. https://www.ema.europa.eu/en/news/disabling-potentially-permanent-side-effects-lead-suspension-restrictions-quinolone-fluoroquinolone.
Ganapathy, Uday S., Véronique Dartois, et Thomas Dick. 2019. « Repositioning Rifamycins for Mycobacterium Abscessus Lung Disease ». *Expert Opinion on Drug Discovery* 14 (9): 867-78. https://doi.org/10.1080/17460441.2019.1629414.
Garza-Ramos, G., L. Xiong, P. Zhong, et A. Mankin. 2001. « Binding Site of Macrolide Antibiotics on the Ribosome: New Resistance Mutation Identifies a Specific Interaction of Ketolides with RRNA ». *Journal of Bacteriology* 183 (23): 6898-6907. https://doi.org/10.1128/JB.183.23.6898-6907.2001.
Geiman, Deborah E., Tirumalai R. Raghunand, Nisheeth Agarwal, et William R. Bishai. 2006. « Differential Gene Expression in Response to Exposure to Antimycobacterial Agents and Other Stress Conditions among Seven Mycobacterium Tuberculosis WhiB-like Genes ». *Antimicrobial Agents and Chemotherapy* 50 (8): 2836-41. https://doi.org/10.1128/AAC.00295-06.
Genilloud, Olga. 2017. « Actinomycetes: Still a Source of Novel Antibiotics ». *Natural Product Reports* 34 (10): 1203-32. https://doi.org/10.1039/c7np00026j.
Ghosh, Soumitra, Bhavna Padmanabhan, Chinmay Anand, et Valakunja Nagaraja. 2016. « Lysine Acetylation of the Mycobacterium Tuberculosis HU Protein Modulates Its DNA Binding and Genome Organization ». *Molecular Microbiology* 100 (4): 577-88. https://doi.org/10.1111/mmi.13339.
Gibson, Justine S., Rowland N. Cobbold, Myat T. Kyaw-Tanner, Peter Heisig, et Darren J. Trott. 2010. « Fluoroquinolone Resistance Mechanisms in Multidrug-Resistant Escherichia Coli Isolated from Extraintestinal Infections in Dogs ». *Veterinary Microbiology* 146 (1-2): 161-66. https://doi.org/10.1016/j.vetmic.2010.04.012.
Giovannenze, Francesca, Vito Stifano, Giancarlo Scoppettuolo, Fernando Damiano, Federico Pallavicini, Giovanni Delogu, Ivana Palucci, Alessandro Rapisarda, Cosimo Sturdà, et Angelo Pompucci. 2018. « Incidental Intraoperative Diagnosis of Mycobacterium Abscessus Meningeal Infection: A Case Report and Review of the Literature ». *Infection* 46 (5): 591-97. https://doi.org/10.1007/s15010-018-1141-5.
Griffith, D. E., W. M. Girard, et R. J. Wallace. 1993. « Clinical Features of Pulmonary Disease Caused by Rapidly Growing Mycobacteria. An Analysis of 154 Patients ». *The American Review of Respiratory Disease* 147 (5): 1271-78. https://doi.org/10.1164/ajrccm/147.5.1271.
Grzegorzewicz, Anna E., Ha Pham, Vijay A. K. B. Gundi, Michael S. Scherman, Elton J. North, Tamara Hess, Victoria Jones, et al. 2012. « Inhibition of Mycolic Acid Transport across the Mycobacterium Tuberculosis Plasma Membrane ». *Nature Chemical Biology* 8 (4): 334-41. https://doi.org/10.1038/nchembio.794.
Guillemin, I., V. Jarlier, et E. Cambau. 1998. « Correlation between Quinolone Susceptibility Patterns and Sequences in the A and B Subunits of DNA Gyrase in Mycobacteria ». *Antimicrobial Agents and Chemotherapy* 42 (8): 2084-88.
Gutiérrez, Ana Victoria, Albertus Viljoen, Eric Ghigo, Jean-Louis Herrmann, et Laurent Kremer. 2018. « Glycopeptidolipids, a Double-Edged Sword of the Mycobacterium Abscessus Complex ». *Frontiers in Microbiology* 9: 1145. https://doi.org/10.3389/fmicb.2018.01145.
Halloum, Iman, Séverine Carrère-Kremer, Mickael Blaise, Albertus Viljoen, Audrey Bernut, Vincent Le Moigne, Catherine Vilchèze, et al. 2016. « Deletion of a Dehydratase Important for Intracellular Growth and Cording Renders Rough Mycobacterium Abscessus Avirulent ». *Proceedings of the National Academy of Sciences of the United States of America* 113 (29): E4228-4237. https://doi.org/10.1073/pnas.1605477113.

Halloum, Iman, Albertus Viljoen, Varun Khanna, Derek Craig, Christiane Bouchier, Roland Brosch, Geoffrey Coxon, et Laurent Kremer. 2017. « Resistance to Thiacetazone Derivatives Active against Mycobacterium Abscessus Involves Mutations in the MmpL5 Transcriptional Repressor MAB_4384 ». *Antimicrobial Agents and Chemotherapy* 61 (4). https://doi.org/10.1128/AAC.02509-16.

Hartkoorn, Ruben C., Swapna Uplekar, et Stewart T. Cole. 2014. « Cross-Resistance between Clofazimine and Bedaquiline through Upregulation of MmpL5 in Mycobacterium Tuberculosis ». *Antimicrobial Agents and Chemotherapy* 58 (5): 2979-81. https://doi.org/10.1128/AAC.00037-14.

Hoch, J. A. 2000. « Two-Component and Phosphorelay Signal Transduction ». *Current Opinion in Microbiology* 3 (2): 165-70.

Homolka, Susanne, Stefan Niemann, David G. Russell, et Kyle H. Rohde. 2010. « Functional Genetic Diversity among Mycobacterium Tuberculosis Complex Clinical Isolates: Delineation of Conserved Core and Lineage-Specific Transcriptomes during Intracellular Survival ». *PLoS Pathogens* 6 (7): e1000988. https://doi.org/10.1371/journal.ppat.1000988.

Howard, Susan T., Elizabeth Rhoades, Judith Recht, Xiuhua Pang, Anny Alsup, Roberto Kolter, C. Rick Lyons, et Thomas F. Byrd. 2006. « Spontaneous Reversion of Mycobacterium Abscessus from a Smooth to a Rough Morphotype Is Associated with Reduced Expression of Glycopeptidolipid and Reacquisition of an Invasive Phenotype ». *Microbiology (Reading, England)* 152 (Pt 6): 1581-90. https://doi.org/10.1099/mic.0.28625-0.

Huang, Chien-Wen, Jiann-Hwa Chen, Shiau-Ting Hu, Wei-Chang Huang, Yen-Chung Lee, Chen-Cheng Huang, et Gwan-Han Shen. 2013. « Synergistic Activities of Tigecycline with Clarithromycin or Amikacin against Rapidly Growing Mycobacteria in Taiwan ». *International Journal of Antimicrobial Agents* 41 (3): 218-23. https://doi.org/10.1016/j.ijantimicag.2012.10.021.

Hurst-Hess, Kelley, Paulami Rudra, et Pallavi Ghosh. 2017. « Mycobacterium Abscessus WhiB7 Regulates a Species-Specific Repertoire of Genes To Confer Extreme Antibiotic Resistance ». *Antimicrobial Agents and Chemotherapy* 61 (11). https://doi.org/10.1128/AAC.01347-17.

Ingen, Jakko van, Sarah E. Totten, Niels K. Helstrom, Leonid B. Heifets, Martin J. Boeree, et Charles L. Daley. 2012. « In Vitro Synergy between Clofazimine and Amikacin in Treatment of Nontuberculous Mycobacterial Disease ». *Antimicrobial Agents and Chemotherapy* 56 (12): 6324-27. https://doi.org/10.1128/AAC.01505-12.

Izaki, K., K. Kiuchi, et K. Arima. 1966. « Specificity and Mechanism of Tetracycline Resistance in a Multiple Drug Resistant Strain of Escherichia Coli ». *Journal of Bacteriology* 91 (2): 628-33.

Jarand, Julie, Adrah Levin, Lening Zhang, Gwen Huitt, John D. Mitchell, et Charles L. Daley. 2011. « Clinical and Microbiologic Outcomes in Patients Receiving Treatment for Mycobacterium Abscessus Pulmonary Disease ». *Clinical Infectious Diseases: An Official Publication of the Infectious Diseases Society of America* 52 (5): 565-71. https://doi.org/10.1093/cid/ciq237.

Jeon, Kyeongman, O. Jung Kwon, Nam Yong Lee, Bum-Joon Kim, Yoon-Hoh Kook, Seung-Heon Lee, Young Kil Park, Chang Ki Kim, et Won-Jung Koh. 2009. « Antibiotic Treatment of Mycobacterium Abscessus Lung Disease: A Retrospective Analysis of 65 Patients ». *American Journal of Respiratory and Critical Care Medicine* 180 (9): 896-902. https://doi.org/10.1164/rccm.200905-0704OC.

Jönsson, Bodil E., Marita Gilljam, Anders Lindblad, Malin Ridell, Agnes E. Wold, et Christina Welinder-Olsson. 2007. « Molecular Epidemiology of Mycobacterium abscessus, with Focus on Cystic Fibrosis ». *Journal of Clinical Microbiology* 45 (5): 1497-1504. https://doi.org/10.1128/JCM.02592-06.

Kana, Bavesh D., Bhavna G. Gordhan, Katrina J. Downing, Nackmoon Sung, Galina Vostroktunova, Edith E. Machowski, Liana Tsenova, et al. 2008. « The Resuscitation-Promoting Factors of Mycobacterium Tuberculosis Are Required for Virulence and Resuscitation from Dormancy but Are Collectively Dispensable for Growth in Vitro ». *Molecular Microbiology* 67 (3): 672-84. https://doi.org/10.1111/j.1365-2958.2007.06078.x.

Karbalaei Zadeh Babaki, Mohsen, Saman Soleimanpour, et Seyed Abdolrahim Rezaee. 2017. « Antigen 85 Complex as a Powerful Mycobacterium Tuberculosis Immunogene: Biology, Immune-Pathogenicity, Applications in Diagnosis, and Vaccine Design ». *Microbial Pathogenesis* 112 (novembre): 20-29. https://doi.org/10.1016/j.micpath.2017.08.040.

Kaushik, Amit, Nicole C. Ammerman, Olumide Martins, Nicole M. Parrish, et Eric L. Nuermberger. 2019. « In Vitro Activity of New Tetracycline Analogs Omadacycline and Eravacycline against Drug-Resistant Clinical Isolates of Mycobacterium Abscessus ». *Antimicrobial Agents and Chemotherapy* 63 (6). https://doi.org/10.1128/AAC.00470-19.

Kaushik, Amit, Chhavi Gupta, Stefanie Fisher, Elizabeth Story-Roller, Christos Galanis, Nicole Parrish, et Gyanu Lamichhane. 2017. « Combinations of Avibactam and Carbapenems Exhibit Enhanced Potencies against Drug-Resistant Mycobacterium Abscessus ». *Future Microbiology* 12: 473-80. https://doi.org/10.2217/fmb-2016-0234.

Kaushik, Amit, Nayani Makkar, Pooja Pandey, Nicole Parrish, Urvashi Singh, et Gyanu Lamichhane. 2015. « Carbapenems and Rifampin Exhibit Synergy against Mycobacterium Tuberculosis and Mycobacterium Abscessus ». *Antimicrobial Agents and Chemotherapy* 59 (10): 6561-67. https://doi.org/10.1128/AAC.01158-15.

Kehrmann, Jan, Nermin Kurt, Kai Rueger, Franz-Christoph Bange, et Jan Buer. 2016. « GenoType NTM-DR for Identifying Mycobacterium Abscessus Subspecies and Determining Molecular Resistance ». *Journal of Clinical Microbiology* 54 (6): 1653-55. https://doi.org/10.1128/JCM.00147-16.

Kehrmann, Jan, Sarah Wessel, Roshni Murali, Annegret Hampel, Franz-Christoph Bange, Jan Buer, et Frank Mosel. 2016. « Principal Component Analysis of MALDI TOF MS Mass Spectra Separates M. Abscessus (Sensu Stricto) from M. Massiliense Isolates ». *BMC Microbiology* 16 (mars): 24. https://doi.org/10.1186/s12866-016-0636-4.

Kim, Kyoung Hoon, Doo Ri An, Jinsu Song, Ji Young Yoon, Hyoun Sook Kim, Hye Jin Yoon, Ha Na Im, et al. 2012. « Mycobacterium Tuberculosis Eis Protein Initiates Suppression of Host Immune Responses by Acetylation of DUSP16/MKP-7 ». *Proceedings of the National Academy of Sciences of the United States of America* 109 (20): 7729-34. https://doi.org/10.1073/pnas.1120251109.

Kim, Su-Young, Byung Woo Jhun, Seong Mi Moon, Sun Hye Shin, Kyeongman Jeon, O. Jung Kwon, In Young Yoo, et al. 2018. « Mutations in GyrA and GyrB in Moxifloxacin-Resistant Mycobacterium Avium Complex and Mycobacterium Abscessus Complex Clinical Isolates ». *Antimicrobial Agents and Chemotherapy* 62 (9). https://doi.org/10.1128/AAC.00527-18.

Koh, W.-J., J. E. Stout, et W.-W. Yew. 2014. « Advances in the Management of Pulmonary Disease Due to Mycobacterium Abscessus Complex ». *The International Journal of Tuberculosis and Lung Disease: The Official Journal of the International Union Against Tuberculosis and Lung Disease* 18 (10): 1141-48. https://doi.org/10.5588/ijtld.14.0134.

Koh, Won-Jung, Kyeongman Jeon, Nam Yong Lee, Bum-Joon Kim, Yoon-Hoh Kook, Seung-Heon Lee, Young Kil Park, et al. 2011. « Clinical Significance of Differentiation of Mycobacterium Massiliense from Mycobacterium Abscessus ». *American Journal of Respiratory and Critical Care Medicine* 183 (3): 405-10. https://doi.org/10.1164/rccm.201003-0395OC.

Koh, Won-Jung, Jun Haeng Lee, Yong Soo Kwon, Kyung Soo Lee, Gee Young Suh, Man Pyo Chung, Hojoong Kim, et O. Jung Kwon. 2007. « Prevalence of Gastroesophageal Reflux Disease in Patients with Nontuberculous Mycobacterial Lung Disease ». *Chest* 131 (6): 1825-30. https://doi.org/10.1378/chest.06-2280.

Kohanski, Michael A., Daniel J. Dwyer, et James J. Collins. 2010. « How Antibiotics Kill Bacteria: From Targets to Networks ». *Nature Reviews. Microbiology* 8 (6): 423-35. https://doi.org/10.1038/nrmicro2333.

Koteva, Kalinka, Georgina Cox, Jayne K. Kelso, Matthew D. Surette, Haley L. Zubyk, Linda Ejim, Peter Stogios, Alexei Savchenko, Dan Sørensen, et Gerard D. Wright. 2018. « Rox, a Rifamycin Resistance Enzyme with an Unprecedented Mechanism of Action ». *Cell Chemical Biology* 25 (4): 403-412.e5. https://doi.org/10.1016/j.chembiol.2018.01.009.

Kowalski, Regis P., Lisa M. Karenchak, et Eric G. Romanowski. 2003. « Infectious Disease: Changing Antibiotic Susceptibility ». *Ophthalmology Clinics of North America* 16 (1): 1-9.

Kozikowski, Alan P., Oluseye K. Onajole, Jozef Stec, Christian Dupont, Albertus Viljoen, Matthias Richard, Tridib Chaira, et al. 2017. « Targeting Mycolic Acid Transport by Indole-2-Carboxamides for the Treatment of Mycobacterium Abscessus Infections ». *Journal of Medicinal Chemistry* 60 (13): 5876-88. https://doi.org/10.1021/acs.jmedchem.7b00582.

Kundu, Subhashri, Goran Biukovic, Gerhard Grüber, et Thomas Dick. 2016. « Bedaquiline Targets the ε Subunit of Mycobacterial F-ATP Synthase ». *Antimicrobial Agents and Chemotherapy* 60 (11): 6977-79. https://doi.org/10.1128/AAC.01291-16.

Laencina, Laura, Violaine Dubois, Vincent Le Moigne, Albertus Viljoen, Laleh Majlessi, Justin Pritchard, Audrey Bernut, et al. 2018. « Identification of Genes Required for Mycobacterium Abscessus Growth in Vivo with a Prominent Role of the ESX-4 Locus ». *Proceedings of the National Academy of Sciences of the United States of America* 115 (5): E1002-11. https://doi.org/10.1073/pnas.1713195115.

Lambert, P. A. 2002. « Cellular Impermeability and Uptake of Biocides and Antibiotics in Gram-Positive Bacteria and Mycobacteria ». *Journal of Applied Microbiology* 92 Suppl: 46S-54S.

Le Run, Eva, Michel Arthur, et Jean-Luc Mainardi. 2018. « In Vitro and Intracellular Activity of Imipenem Combined with Rifabutin and Avibactam against Mycobacterium Abscessus ». *Antimicrobial Agents and Chemotherapy* 62 (8). https://doi.org/10.1128/AAC.00623-18.

———. 2019. « In Vitro and Intracellular Activity of Imipenem Combined with Tedizolid, Rifabutin, and Avibactam against Mycobacterium Abscessus ». *Antimicrobial Agents and Chemotherapy* 63 (4). https://doi.org/10.1128/AAC.01915-18.

Le, Tung B. K., Clare E. M. Stevenson, Hans-Peter Fiedler, Anthony Maxwell, David M. Lawson, et Mark J. Buttner. 2011. « Structures of the TetR-like Simocyclinone Efflux Pump Repressor, SimR, and the Mechanism of Ligand-Mediated Derepression ». *Journal of Molecular Biology* 408 (1): 40-56. https://doi.org/10.1016/j.jmb.2011.02.035.

Lee, Meng-Rui, Aristine Cheng, Yi-Chieh Lee, Ching-Yao Yang, Chih-Cheng Lai, Yu-Tsung Huang, Chao-Chi Ho, Hao-Chien Wang, Chong-Jen Yu, et Po-Ren Hsueh. 2012. « CNS Infections Caused by Mycobacterium Abscessus Complex: Clinical Features and Antimicrobial Susceptibilities of Isolates ». *The Journal of Antimicrobial Chemotherapy* 67 (1): 222-25. https://doi.org/10.1093/jac/dkr420.

Lee, Meng-Rui, Wang-Huei Sheng, Chien-Ching Hung, Chong-Jen Yu, Li-Na Lee, et Po-Ren Hsueh. 2015. « Mycobacterium Abscessus Complex Infections in Humans ». *Emerging Infectious Diseases* 21 (9): 1638-46. https://doi.org/10.3201/2109.141634.

Lee, Wonsik, Brian C. VanderVen, Ruth J. Fahey, et David G. Russell. 2013. « Intracellular Mycobacterium Tuberculosis Exploits Host-Derived Fatty Acids to Limit Metabolic Stress ». *The Journal of Biological Chemistry* 288 (10): 6788-6800. https://doi.org/10.1074/jbc.M112.445056.

Lefebvre, Anne-Laure, Vincent Dubée, Mélanie Cortes, Delphine Dorchêne, Michel Arthur, et Jean-Luc Mainardi. 2016. « Bactericidal and Intracellular Activity of β-Lactams against Mycobacterium Abscessus ». *The Journal of Antimicrobial Chemotherapy* 71 (6): 1556-63. https://doi.org/10.1093/jac/dkw022.

Lefebvre, Anne-Laure, Vincent Le Moigne, Audrey Bernut, Carole Veckerlé, Fabrice Compain, Jean-Louis Herrmann, Laurent Kremer, Michel Arthur, et Jean-Luc Mainardi. 2017. « Inhibition of the β-Lactamase BlaMab by Avibactam Improves the In Vitro and In Vivo Efficacy of Imipenem against Mycobacterium Abscessus ». *Antimicrobial Agents and Chemotherapy* 61 (4). https://doi.org/10.1128/AAC.02440-16.

Leitch, A. E., et H. C. Rodgers. 2013. « Cystic Fibrosis ». *The Journal of the Royal College of Physicians of Edinburgh* 43 (2): 144-50. https://doi.org/10.4997/JRCPE.2013.212.

Levy, Isaac, Galia Grisaru-Soen, Liat Lerner-Geva, Eitan Kerem, Hana Blau, Lea Bentur, Micha Aviram, et al. 2008. « Multicenter Cross-Sectional Study of Nontuberculous Mycobacterial Infections

among Cystic Fibrosis Patients, Israel ». *Emerging Infectious Diseases* 14 (3): 378-84. https://doi.org/10.3201/eid1403.061405.

Li, Guilian, Jingrui Zhang, Chao Li, Qian Guo, Yi Jiang, Jianhao Wei, Yan Qiu, et al. 2016. « Antimycobacterial Activity of Five Efflux Pump Inhibitors against Mycobacterium Tuberculosis Clinical Isolates ». *The Journal of Antibiotics* 69 (3): 173-75. https://doi.org/10.1038/ja.2015.101.

Liu, Weijia, Bing Li, Haiqing Chu, Zhemin Zhang, Liulin Luo, Wei Ma, Shiyi Yang, et Qi Guo. 2017. « Rapid Detection of Mutations in Erm(41) and Rrl Associated with Clarithromycin Resistance in Mycobacterium Abscessus Complex by Denaturing Gradient Gel Electrophoresis ». *Journal of Microbiological Methods* 143: 87-93. https://doi.org/10.1016/j.mimet.2017.10.010.

Llorens-Fons, Marta, Míriam Pérez-Trujillo, Esther Julián, Cecilia Brambilla, Fernando Alcaide, Thomas F. Byrd, et Marina Luquin. 2017. « Trehalose Polyphleates, External Cell Wall Lipids in Mycobacterium Abscessus, Are Associated with the Formation of Clumps with Cording Morphology, Which Have Been Associated with Virulence ». *Frontiers in Microbiology* 8: 1402. https://doi.org/10.3389/fmicb.2017.01402.

Locher, Kaspar P. 2009. « Structure and mechanism of ATP-binding cassette transporters ». *Philosophical Transactions of the Royal Society B: Biological Sciences* 364 (1514): 239-45. https://doi.org/10.1098/rstb.2008.0125.

Louw, G. E., R. M. Warren, N. C. Gey van Pittius, C. R. E. McEvoy, P. D. Van Helden, et T. C. Victor. 2009. « A Balancing Act: Efflux/Influx in Mycobacterial Drug Resistance ». *Antimicrobial Agents and Chemotherapy* 53 (8): 3181-89. https://doi.org/10.1128/AAC.01577-08.

Lubelski, Jacek, Wil N. Konings, et Arnold J. M. Driessen. 2007. « Distribution and Physiology of ABC-Type Transporters Contributing to Multidrug Resistance in Bacteria ». *Microbiology and Molecular Biology Reviews: MMBR* 71 (3): 463-76. https://doi.org/10.1128/MMBR.00001-07.

Luthra, Sakshi, Anna Rominski, et Peter Sander. 2018. « The Role of Antibiotic-Target-Modifying and Antibiotic-Modifying Enzymes in Mycobacterium Abscessus Drug Resistance ». *Frontiers in Microbiology* 9: 2179. https://doi.org/10.3389/fmicb.2018.02179.

Madani, Abdeldjalil, Jeremy N. Ridenour, Benjamin P. Martin, Rishi R. Paudel, Anosha Abdul Basir, Vincent Le Moigne, Jean-Louis Herrmann, et al. 2019. « Cyclipostins and Cyclophostin Analogues as Multitarget Inhibitors That Impair Growth of Mycobacterium Abscessus ». *ACS Infectious Diseases* 5 (9): 1597-1608. https://doi.org/10.1021/acsinfecdis.9b00172.

Mahapatra, Sebabrata, Hataichanok Scherman, Patrick J. Brennan, et Dean C. Crick. 2005. « N Glycolylation of the Nucleotide Precursors of Peptidoglycan Biosynthesis of Mycobacterium Spp. Is Altered by Drug Treatment ». *Journal of Bacteriology* 187 (7): 2341-47. https://doi.org/10.1128/JB.187.7.2341-2347.2005.

Maiga, Mamoudou, Sophia Siddiqui, Souleymane Diallo, Bassirou Diarra, Brehima Traoré, Yvonne R. Shea, Adrian M. Zelazny, et al. 2012. « Failure to Recognize Nontuberculous Mycobacteria Leads to Misdiagnosis of Chronic Pulmonary Tuberculosis ». *PloS One* 7 (5): e36902. https://doi.org/10.1371/journal.pone.0036902.

Maravić, G. 2004. « Macrolide Resistance Based on the Erm-Mediated RRNA Methylation ». *Current Drug Targets. Infectious Disorders* 4 (3): 193-202.

Martinez, J. L., et F. Baquero. 2000. « Mutation Frequencies and Antibiotic Resistance ». *Antimicrobial Agents and Chemotherapy* 44 (7): 1771.

Matrat, Stéphanie, Alexandra Aubry, Claudine Mayer, Vincent Jarlier, et Emmanuelle Cambau. 2008. « Mutagenesis in the Alpha3alpha4 GyrA Helix and in the Toprim Domain of GyrB Refines the Contribution of Mycobacterium Tuberculosis DNA Gyrase to Intrinsic Resistance to Quinolones ». *Antimicrobial Agents and Chemotherapy* 52 (8): 2909-14. https://doi.org/10.1128/AAC.01380-07.

Maurer, Florian P., Vera L. Bruderer, Claudio Castelberg, Claudia Ritter, Dimitri Scherbakov, Guido V. Bloemberg, et Erik C. Böttger. 2015. « Aminoglycoside-Modifying Enzymes Determine the Innate Susceptibility to Aminoglycoside Antibiotics in Rapidly Growing Mycobacteria ». *The Journal of Antimicrobial Chemotherapy* 70 (5): 1412-19. https://doi.org/10.1093/jac/dku550.

Maurer, Florian P., Claudio Castelberg, Chantal Quiblier, Erik C. Böttger, et Akos Somoskövi. 2014. « Erm(41)-Dependent Inducible Resistance to Azithromycin and Clarithromycin in Clinical Isolates of Mycobacterium Abscessus ». *The Journal of Antimicrobial Chemotherapy* 69 (6): 1559-63. https://doi.org/10.1093/jac/dku007.

Medjahed, Halima, Jean-Louis Gaillard, et Jean-Marc Reyrat. 2010. « Mycobacterium Abscessus: A New Player in the Mycobacterial Field ». *Trends in Microbiology* 18 (3): 117-23. https://doi.org/10.1016/j.tim.2009.12.007.

Melly, Geoff, et Georgiana E. Purdy. 2019. « MmpL Proteins in Physiology and Pathogenesis of M. tuberculosis ». *Microorganisms* 7 (3). https://doi.org/10.3390/microorganisms7030070.

Mendum, Tom A., Huihai Wu, Andrzej M. Kierzek, et Graham R. Stewart. 2015. « Lipid Metabolism and Type VII Secretion Systems Dominate the Genome Scale Virulence Profile of Mycobacterium Tuberculosis in Human Dendritic Cells ». *BMC Genomics* 16 (mai): 372. https://doi.org/10.1186/s12864-015-1569-2.

Mignard, Sophie, et Jean-Pierre Flandrois. 2008. « A Seven-Gene, Multilocus, Genus-Wide Approach to the Phylogeny of Mycobacteria Using Supertrees ». *International Journal of Systematic and Evolutionary Microbiology* 58 (Pt 6): 1432-41. https://doi.org/10.1099/ijs.0.65658-0.

Milano, Anna, Maria Rosalia Pasca, Roberta Provvedi, Anna Paola Lucarelli, Giulia Manina, Ana Luisa de Jesus Lopes Ribeiro, Riccardo Manganelli, et Giovanna Riccardi. 2009. « Azole Resistance in Mycobacterium Tuberculosis Is Mediated by the MmpS5-MmpL5 Efflux System ». *Tuberculosis (Edinburgh, Scotland)* 89 (1): 84-90. https://doi.org/10.1016/j.tube.2008.08.003.

Miranda-CasoLuengo, Aleksandra A., Patrick M. Staunton, Adam M. Dinan, Amanda J. Lohan, et Brendan J. Loftus. 2016. « Functional characterization of the Mycobacterium abscessus genome coupled with condition specific transcriptomics reveals conserved molecular strategies for host adaptation and persistence ». *BMC Genomics* 17 (août). https://doi.org/10.1186/s12864-016-2868-y.

Mirnejad, Reza, Arezoo Asadi, Saeed Khoshnood, Habibollah Mirzaei, Mohsen Heidary, Lanfranco Fattorini, Arash Ghodousi, et Davood Darban-Sarokhalil. 2018. « Clofazimine: A Useful Antibiotic for Drug-Resistant Tuberculosis ». *Biomedicine & Pharmacotherapy = Biomedecine & Pharmacotherapie* 105 (septembre): 1353-59. https://doi.org/10.1016/j.biopha.2018.06.023.

Mishra, Arun K, Nicole N Driessen, Ben J Appelmelk, et Gurdyal S Besra. 2011. « Lipoarabinomannan and related glycoconjugates: structure, biogenesis and role in Mycobacterium tuberculosis physiology and host–pathogen interaction ». *Fems Microbiology Reviews* 35 (6): 1126-57. https://doi.org/10.1111/j.1574-6976.2011.00276.x.

Miyasaka, Tomomitsu, Hiroyuki Kunishima, Mayumi Komatsu, Kiyoko Tamai, Kotaro Mitsutake, Keiji Kanemitsu, Yoshiharu Ohisa, Hideji Yanagisawa, et Mitsuo Kaku. 2007. « In Vitro Efficacy of Imipenem in Combination with Six Antimicrobial Agents against Mycobacterium Abscessus ». *International Journal of Antimicrobial Agents* 30 (3): 255-58. https://doi.org/10.1016/j.ijantimicag.2007.05.003.

Moncrief, M. B., et M. E. Maguire. 1998. « Magnesium and the Role of MgtC in Growth of Salmonella Typhimurium ». *Infection and Immunity* 66 (8): 3802-9.

Morris, Rowan P., Liem Nguyen, John Gatfield, Kevin Visconti, Kien Nguyen, Dirk Schnappinger, Sabine Ehrt, et al. 2005. « Ancestral Antibiotic Resistance in Mycobacterium Tuberculosis ». *Proceedings of the National Academy of Sciences of the United States of America* 102 (34): 12200-205. https://doi.org/10.1073/pnas.0505446102.

Mougari, Faiza, Lorenzo Guglielmetti, Laurent Raskine, Isabelle Sermet-Gaudelus, Nicolas Veziris, et Emmanuelle Cambau. 2016. « Infections Caused by Mycobacterium Abscessus: Epidemiology, Diagnostic Tools and Treatment ». *Expert Review of Anti-Infective Therapy* 14 (12): 1139-54. https://doi.org/10.1080/14787210.2016.1238304.

Mougari, Faiza, Jade Loiseau, Nicolas Veziris, Christine Bernard, Béatrice Bercot, Wladimir Sougakoff, Vincent Jarlier, Laurent Raskine, Emmanuelle Cambau, et French National Reference Center for Mycobacteria. 2017. « Evaluation of the New GenoType NTM-DR Kit for the Molecular

Detection of Antimicrobial Resistance in Non-Tuberculous Mycobacteria ». *The Journal of Antimicrobial Chemotherapy* 72 (6): 1669-77. https://doi.org/10.1093/jac/dkx021.
Mukherjee, Devika, Mu-Lu Wu, Jeanette W. P. Teo, et Thomas Dick. 2017. « Vancomycin and Clarithromycin Show Synergy against Mycobacterium Abscessus In Vitro ». *Antimicrobial Agents and Chemotherapy* 61 (12). https://doi.org/10.1128/AAC.01298-17.
Nash, Kevin A., Barbara A. Brown-Elliott, et Richard J. Wallace. 2009. « A Novel Gene, Erm(41), Confers Inducible Macrolide Resistance to Clinical Isolates of Mycobacterium Abscessus but Is Absent from Mycobacterium Chelonae ». *Antimicrobial Agents and Chemotherapy* 53 (4): 1367-76. https://doi.org/10.1128/AAC.01275-08.
Nataraj, Vijayashankar, Cristian Varela, Asma Javid, Albel Singh, Gurdyal S. Besra, et Apoorva Bhatt. 2015. « Mycolic acids: deciphering and targeting the Achilles' heel of the tubercle bacillus ». *Molecular Microbiology* 98 (1): 7-16. https://doi.org/10.1111/mmi.13101.
Nessar, Rachid, Emmanuelle Cambau, Jean Marc Reyrat, Alan Murray, et Brigitte Gicquel. 2012. « Mycobacterium Abscessus: A New Antibiotic Nightmare ». *The Journal of Antimicrobial Chemotherapy* 67 (4): 810-18. https://doi.org/10.1093/jac/dkr578.
Newton-Foot, Mae, et Nicolaas C. Gey van Pittius. 2013. « The Complex Architecture of Mycobacterial Promoters ». *Tuberculosis (Edinburgh, Scotland)* 93 (1): 60-74. https://doi.org/10.1016/j.tube.2012.08.003.
NHS. 2017. « Chronic Obstructive Pulmonary Disease (COPD) ». Nhs.Uk. 20 octobre 2017. https://www.nhs.uk/conditions/chronic-obstructive-pulmonary-disease-copd/.
NORD. 2015. « Nontuberculous Mycobacterial Lung Disease ». *NORD (National Organization for Rare Disorders)* (blog). 2018 2015. https://rarediseases.org/rare-diseases/nontuberculous-mycobacterial-lung-disease/.
Oh, Chun-Taek, Cheol Moon, Ok Kyu Park, Seung-Hae Kwon, et Jichan Jang. 2014. « Novel Drug Combination for Mycobacterium Abscessus Disease Therapy Identified in a Drosophila Infection Model ». *The Journal of Antimicrobial Chemotherapy* 69 (6): 1599-1607. https://doi.org/10.1093/jac/dku024.
Orth, P., D. Schnappinger, W. Hillen, W. Saenger, et W. Hinrichs. 2000. « Structural Basis of Gene Regulation by the Tetracycline Inducible Tet Repressor-Operator System ». *Nature Structural Biology* 7 (3): 215-19. https://doi.org/10.1038/73324.
Osmani, Morsal, David Sotello, Salvador Alvarez, John A. Odell, et Mathew Thomas. 2018. « Mycobacterium Abscessus Infections in Lung Transplant Recipients: 15-Year Experience from a Single Institution ». *Transplant Infectious Disease: An Official Journal of the Transplantation Society* 20 (2): e12835. https://doi.org/10.1111/tid.12835.
Ostash, Iryna, Bohdan Ostash, Andriy Luzhetskyy, Andreas Bechthold, Suzanne Walker, et Victor Fedorenko. 2008. « Coordination of Export and Glycosylation of Landomycins in Streptomyces Cyanogenus S136 ». *FEMS Microbiology Letters* 285 (2): 195-202. https://doi.org/10.1111/j.1574-6968.2008.01225.x.
O'Sullivan, Mary E., Frédéric Poitevin, Raymond G. Sierra, Cornelius Gati, E. Han Dao, Yashas Rao, Fulya Aksit, et al. 2018. « Aminoglycoside Ribosome Interactions Reveal Novel Conformational States at Ambient Temperature ». *Nucleic Acids Research* 46 (18): 9793-9804. https://doi.org/10.1093/nar/gky693.
Owens, Cedric P., Nicholas Chim, Amanda B. Graves, Christine A. Harmston, Angelina Iniguez, Heidi Contreras, Matthew D. Liptak, et Celia W. Goulding. 2013. « The Mycobacterium Tuberculosis Secreted Protein Rv0203 Transfers Heme to Membrane Proteins MmpL3 and MmpL11 ». *The Journal of Biological Chemistry* 288 (30): 21714-28. https://doi.org/10.1074/jbc.M113.453076.
Pacheco, Sophia A., Fong-Fu Hsu, Katelyn M. Powers, et Georgiana E. Purdy. 2013. « MmpL11 Protein Transports Mycolic Acid-Containing Lipids to the Mycobacterial Cell Wall and Contributes to Biofilm Formation in Mycobacterium Smegmatis ». *The Journal of Biological Chemistry* 288 (33): 24213-22. https://doi.org/10.1074/jbc.M113.473371.

Palmer, Mitchell V., Michael D. Welsh, et Jesse M. Hostetter. 2011. « Mycobacterial Diseases of Animals ». *Veterinary Medicine International* 2011. https://doi.org/10.4061/2011/292469.

Park, In Kwon, Amy P. Hsu, Hervé Tettelin, Shamira J. Shallom, Steven K. Drake, Li Ding, Un-In Wu, et al. 2015. « Clonal Diversification and Changes in Lipid Traits and Colony Morphology in Mycobacterium Abscessus Clinical Isolates ». *Journal of Clinical Microbiology* 53 (11): 3438-47. https://doi.org/10.1128/JCM.02015-15.

Park, Jimyung, Jaeyoung Cho, Chang-Hoon Lee, Sung Koo Han, et Jae-Joon Yim. 2017. « Progression and Treatment Outcomes of Lung Disease Caused by Mycobacterium Abscessus and Mycobacterium Massiliense ». *Clinical Infectious Diseases: An Official Publication of the Infectious Diseases Society of America* 64 (3): 301-8. https://doi.org/10.1093/cid/ciw723.

Pasca, Maria R., Paola Guglierame, Edda De Rossi, Francesca Zara, et Giovanna Riccardi. 2005. « MmpL7 Gene of Mycobacterium Tuberculosis Is Responsible for Isoniazid Efflux in Mycobacterium Smegmatis ». *Antimicrobial Agents and Chemotherapy* 49 (11): 4775-77. https://doi.org/10.1128/AAC.49.11.4775-4777.2005.

Passemar, Charlotte, Ainhoa Arbués, Wladimir Malaga, Ingrid Mercier, Flavie Moreau, Laurence Lepourry, Olivier Neyrolles, Christophe Guilhot, et Catherine Astarie-Dequeker. 2014. « Multiple Deletions in the Polyketide Synthase Gene Repertoire of Mycobacterium Tuberculosis Reveal Functional Overlap of Cell Envelope Lipids in Host-Pathogen Interactions ». *Cellular Microbiology* 16 (2): 195-213. https://doi.org/10.1111/cmi.12214.

Pawlik, Alexandre, Guillaume Garnier, Mickael Orgeur, Pin Tong, Amanda Lohan, Fabien Le Chevalier, Guillaume Sapriel, et al. 2013. « Identification and Characterization of the Genetic Changes Responsible for the Characteristic Smooth-to-Rough Morphotype Alterations of Clinically Persistent Mycobacterium Abscessus ». *Molecular Microbiology* 90 (3): 612-29. https://doi.org/10.1111/mmi.12387.

Periti, P., T. Mazzei, E. Mini, et A. Novelli. 1992. « Pharmacokinetic Drug Interactions of Macrolides ». *Clinical Pharmacokinetics* 23 (2): 106-31. https://doi.org/10.2165/00003088-199223020-00004.

Pier, G. B., M. Grout, T. S. Zaidi, J. C. Olsen, L. G. Johnson, J. R. Yankaskas, et J. B. Goldberg. 1996. « Role of Mutant CFTR in Hypersusceptibility of Cystic Fibrosis Patients to Lung Infections ». *Science (New York, N.Y.)* 271 (5245): 64-67. https://doi.org/10.1126/science.271.5245.64.

Prammananan, T., P. Sander, B. A. Brown, K. Frischkorn, G. O. Onyi, Y. Zhang, E. C. Böttger, et R. J. Wallace. 1998. « A Single 16S Ribosomal RNA Substitution Is Responsible for Resistance to Amikacin and Other 2-Deoxystreptamine Aminoglycosides in Mycobacterium Abscessus and Mycobacterium Chelonae ». *The Journal of Infectious Diseases* 177 (6): 1573-81. https://doi.org/10.1086/515328.

Preiss, Laura, Julian D. Langer, Özkan Yildiz, Luise Eckhardt-Strelau, Jérôme E. G. Guillemont, Anil Koul, et Thomas Meier. 2015. « Structure of the Mycobacterial ATP Synthase Fo Rotor Ring in Complex with the Anti-TB Drug Bedaquiline ». *Science Advances* 1 (4): e1500106. https://doi.org/10.1126/sciadv.1500106.

Pryjma, Mark, Ján Burian, Kevin Kuchinski, et Charles J. Thompson. 2017. « Antagonism between Front-Line Antibiotics Clarithromycin and Amikacin in the Treatment of Mycobacterium Abscessus Infections Is Mediated by the WhiB7 Gene ». *Antimicrobial Agents and Chemotherapy* 61 (11). https://doi.org/10.1128/AAC.01353-17.

Pryjma, Mark, Ján Burian, et Charles J. Thompson. 2018. « Rifabutin Acts in Synergy and Is Bactericidal with Frontline Mycobacterium Abscessus Antibiotics Clarithromycin and Tigecycline, Suggesting a Potent Treatment Combination ». *Antimicrobial Agents and Chemotherapy* 62 (8). https://doi.org/10.1128/AAC.00283-18.

Public Health Egland. s. d. « Health Matters: Antimicrobial Resistance ». GOV.UK. Consulté le 16 septembre 2019. https://www.gov.uk/government/publications/health-matters-antimicrobial-resistance/health-matters-antimicrobial-resistance.

pubmeddev, et Burian J. al et. s. d. « The Mycobacterial Antibiotic Resistance Determinant WhiB7 Acts as a Transcriptional Activator by Binding the Primary Sigma Factor SigA (RpoV). -

PubMed - NCBI ». Consulté le 6 septembre 2019a. https://www.ncbi.nlm.nih.gov/pubmed/?term=burian+2013+sigA.
———. s. d. « WhiB7, a Transcriptional Activator That Coordinates Physiology with Intrinsic Drug Resistance in Mycobacterium Tuberculosis. - PubMed - NCBI ». Consulté le 6 septembre 2019b. https://www.ncbi.nlm.nih.gov/pubmed/23106278.
Pym, Alexander S., Priscille Brodin, Roland Brosch, Michel Huerre, et Stewart T. Cole. 2002. « Loss of RD1 Contributed to the Attenuation of the Live Tuberculosis Vaccines Mycobacterium Bovis BCG and Mycobacterium Microti ». *Molecular Microbiology* 46 (3): 709-17. https://doi.org/10.1046/j.1365-2958.2002.03237.x.
Ramis, Ivy B., Júlia S. Vianna, Lande Silva Junior, Andrea von Groll, Daniela F. Ramos, Nilo Zanatta, Miguel Viveiros, et Pedro E. Almeida da Silva. 2019. « In Silico and in Vitro Evaluation of Tetrahydropyridine Compounds as Efflux Inhibitors in Mycobacterium Abscessus ». *Tuberculosis (Edinburgh, Scotland)* 118 (juillet): 101853. https://doi.org/10.1016/j.tube.2019.07.004.
Ramón-García, Santiago, Virginie Mick, Elisa Dainese, Carlos Martín, Charles J. Thompson, Edda De Rossi, Riccardo Manganelli, et José A. Aínsa. 2012. « Functional and Genetic Characterization of the Tap Efflux Pump in Mycobacterium Bovis BCG ». *Antimicrobial Agents and Chemotherapy* 56 (4): 2074-83. https://doi.org/10.1128/AAC.05946-11.
Ramón-García, Santiago, Carol Ng, Pernille R. Jensen, Manisha Dosanjh, Jan Burian, Rowan P. Morris, Marc Folcher, et al. 2013. « WhiB7, an Fe-S-Dependent Transcription Factor That Activates Species-Specific Repertoires of Drug Resistance Determinants in Actinobacteria ». *The Journal of Biological Chemistry* 288 (48): 34514-28. https://doi.org/10.1074/jbc.M113.516385.
Ramón-García, Santiago, Isabel Otal, Carlos Martín, Rafael Gómez-Lus, et José A. Aínsa. 2006. « Novel Streptomycin Resistance Gene from Mycobacterium Fortuitum ». *Antimicrobial Agents and Chemotherapy* 50 (11): 3920-22. https://doi.org/10.1128/AAC.00223-06.
Ramos, Juan L., Manuel Martínez-Bueno, Antonio J. Molina-Henares, Wilson Terán, Kazuya Watanabe, Xiaodong Zhang, María Trinidad Gallegos, Richard Brennan, et Raquel Tobes. 2005. « The TetR Family of Transcriptional Repressors ». *Microbiology and Molecular Biology Reviews: MMBR* 69 (2): 326-56. https://doi.org/10.1128/MMBR.69.2.326-356.2005.
Ratjen, Felix, et Gerd Döring. 2003. « Cystic Fibrosis ». *Lancet (London, England)* 361 (9358): 681-89. https://doi.org/10.1016/S0140-6736(03)12567-6.
Rawat, Mamta, Gerald L. Newton, Mary Ko, Gladys J. Martinez, Robert C. Fahey, et Yossef Av-Gay. 2002. « Mycothiol-Deficient Mycobacterium Smegmatis Mutants Are Hypersensitive to Alkylating Agents, Free Radicals, and Antibiotics ». *Antimicrobial Agents and Chemotherapy* 46 (11): 3348-55. https://doi.org/10.1128/aac.46.11.3348-3355.2002.
Recht, J., A. Martínez, S. Torello, et R. Kolter. 2000. « Genetic Analysis of Sliding Motility in Mycobacterium Smegmatis ». *Journal of Bacteriology* 182 (15): 4348-51. https://doi.org/10.1128/jb.182.15.4348-4351.2000.
Renna, Maurizio, Catherine Schaffner, Karen Brown, Shaobin Shang, Marcela Henao Tamayo, Krisztina Hegyi, Neil J. Grimsey, et al. 2011. « Azithromycin Blocks Autophagy and May Predispose Cystic Fibrosis Patients to Mycobacterial Infection ». *The Journal of Clinical Investigation* 121 (9): 3554-63. https://doi.org/10.1172/JCI46095.
Rhoades, Elizabeth R., Angela S. Archambault, Rebecca Greendyke, Fong-Fu Hsu, Cassandra Streeter, et Thomas F. Byrd. 2009. « Mycobacterium Abscessus Glycopeptidolipids Mask Underlying Cell Wall Phosphatidyl-Myo-Inositol Mannosides Blocking Induction of Human Macrophage TNF-Alpha by Preventing Interaction with TLR2 ». *Journal of Immunology (Baltimore, Md.: 1950)* 183 (3): 1997-2007. https://doi.org/10.4049/jimmunol.0802181.
Richey, L. E., J. Bahadorani, et D. Mushatt. 2013. « Endovascular Mycobacterium Abscessus Infection in a Heart Transplant Recipient: A Case Report and Review of the Literature ». *Transplant Infectious Disease: An Official Journal of the Transplantation Society* 15 (2): 208-13. https://doi.org/10.1111/tid.12024.

Ripoll, Fabienne, Sophie Pasek, Chantal Schenowitz, Carole Dossat, Valérie Barbe, Martin Rottman, Edouard Macheras, et al. 2009. « Non Mycobacterial Virulence Genes in the Genome of the Emerging Pathogen Mycobacterium Abscessus ». *PloS One* 4 (6): e5660. https://doi.org/10.1371/journal.pone.0005660.

Rominski, Anna, Anna Roditscheff, Petra Selchow, Erik C. Böttger, et Peter Sander. 2017. « Intrinsic Rifamycin Resistance of Mycobacterium Abscessus Is Mediated by ADP-Ribosyltransferase MAB_0591 ». *The Journal of Antimicrobial Chemotherapy* 72 (2): 376-84. https://doi.org/10.1093/jac/dkw466.

Rominski, Anna, Bettina Schulthess, Daniel M. Müller, Peter M. Keller, et Peter Sander. 2017. « Effect of β-Lactamase Production and β-Lactam Instability on MIC Testing Results for Mycobacterium Abscessus ». *The Journal of Antimicrobial Chemotherapy* 72 (11): 3070-78. https://doi.org/10.1093/jac/dkx284.

Rominski, Anna, Petra Selchow, Katja Becker, Juliane K. Brülle, Michael Dal Molin, et Peter Sander. 2017. « Elucidation of Mycobacterium Abscessus Aminoglycoside and Capreomycin Resistance by Targeted Deletion of Three Putative Resistance Genes ». *The Journal of Antimicrobial Chemotherapy* 72 (8): 2191-2200. https://doi.org/10.1093/jac/dkx125.

Roux, Anne-Laure, Aurélie Ray, Alexandre Pawlik, Halima Medjahed, Gilles Etienne, Martin Rottman, Emilie Catherinot, et al. 2011. « Overexpression of Proinflammatory TLR-2-Signalling Lipoproteins in Hypervirulent Mycobacterial Variants ». *Cellular Microbiology* 13 (5): 692-704. https://doi.org/10.1111/j.1462-5822.2010.01565.x.

Roux, Anne-Laure, Albertus Viljoen, Aïcha Bah, Roxane Simeone, Audrey Bernut, Laura Laencina, Therese Deramaudt, et al. 2016. « The distinct fate of smooth and rough Mycobacterium abscessus variants inside macrophages ». *Open Biology* 6 (11). https://doi.org/10.1098/rsob.160185.

Rudra, Paulami, Kelley Hurst-Hess, Pascal Lappierre, et Pallavi Ghosh. 2018. « High Levels of Intrinsic Tetracycline Resistance in Mycobacterium abscessus Are Conferred by a Tetracycline-Modifying Monooxygenase ». *Antimicrobial Agents and Chemotherapy* 62 (6). https://doi.org/10.1128/AAC.00119-18.

Ruth, Mike M., Jasper J. N. Sangen, Lian J. Pennings, Jodie A. Schildkraut, Wouter Hoefsloot, Cecile Magis-Escurra, Heiman F. L. Wertheim, et Jakko van Ingen. 2018. « Minocycline Has No Clear Role in the Treatment of Mycobacterium Abscessus Disease ». *Antimicrobial Agents and Chemotherapy* 62 (10). https://doi.org/10.1128/AAC.01208-18.

Rybniker, Jan, Angela Nowag, Edeltraud van Gumpel, Nicole Nissen, Nirmal Robinson, Georg Plum, et Pia Hartmann. 2010. « Insights into the Function of the WhiB-like Protein of Mycobacteriophage TM4--a Transcriptional Inhibitor of WhiB2 ». *Molecular Microbiology* 77 (3): 642-57. https://doi.org/10.1111/j.1365-2958.2010.07235.x.

Sanchez, M. R. 2000. « Miscellaneous Treatments: Thalidomide, Potassium Iodide, Levamisole, Clofazimine, Colchicine, and D-Penicillamine ». *Clinics in Dermatology* 18 (1): 131-45.

Sandhu, Padmani, et Yusuf Akhter. 2017. « Siderophore Transport by MmpL5-MmpS5 Protein Complex in Mycobacterium Tuberculosis ». *Journal of Inorganic Biochemistry* 170: 75-84. https://doi.org/10.1016/j.jinorgbio.2017.02.013.

Sarpe, Vikram A., Michael G. Pirrone, Klara Haldimann, Sven N. Hobbie, Andrea Vasella, et David Crich. 2019. « Synthesis of Saccharocin from Apramycin and Evaluation of Its Ribosomal Selectivity ». *MedChemComm* 10 (4): 554-58. https://doi.org/10.1039/C9MD00093C.

Sarro, Yeya DS, Bourahima Kone, Bassirou Diarra, Alisha Kumar, Ousmane Kodio, Djeneba B Fofana, Chad J Achenbach, et al. 2018. « Simultaneous diagnosis of tuberculous and non-tuberculous mycobacterial diseases: Time for a better patient management ». *Clinical microbiology and infectious diseases* 3 (3). https://www.ncbi.nlm.nih.gov/pmc/articles/PMC6319944/.

Sauvage, Eric, Frédéric Kerff, Mohammed Terrak, Juan A. Ayala, et Paulette Charlier. 2008. « The Penicillin-Binding Proteins: Structure and Role in Peptidoglycan Biosynthesis ». *FEMS Microbiology Reviews* 32 (2): 234-58. https://doi.org/10.1111/j.1574-6976.2008.00105.x.

Schmalstieg, Aurelia M., Shashikant Srivastava, Serkan Belkaya, Devyani Deshpande, Claudia Meek, Richard Leff, Nicolai S. C. van Oers, et Tawanda Gumbo. 2012. « The Antibiotic Resistance Arrow of Time: Efflux Pump Induction Is a General First Step in the Evolution of Mycobacterial Drug Resistance ». *Antimicrobial Agents and Chemotherapy* 56 (9): 4806-15. https://doi.org/10.1128/AAC.05546-11.

Schmiel, D. H., et V. L. Miller. 1999. « Bacterial Phospholipases and Pathogenesis ». *Microbes and Infection* 1 (13): 1103-12.

Schroeder, Max R., et David S. Stephens. 2016. « Macrolide Resistance in Streptococcus Pneumoniae ». *Frontiers in Cellular and Infection Microbiology* 6: 98. https://doi.org/10.3389/fcimb.2016.00098.

Schué, Mathieu, Lynn G. Dover, Gurdyal S. Besra, Julian Parkhill, et Nigel L. Brown. 2009. « Sequence and Analysis of a Plasmid-Encoded Mercury Resistance Operon from Mycobacterium Marinum Identifies MerH, a New Mercuric Ion Transporter ». *Journal of Bacteriology* 191 (1): 439-44. https://doi.org/10.1128/JB.01063-08.

Schumacher, Maria A., Marshall C. Miller, Steve Grkovic, Melissa H. Brown, Ronald A. Skurray, et Richard G. Brennan. 2002. « Structural basis for cooperative DNA binding by two dimers of the multidrug-binding protein QacR ». *The EMBO Journal* 21 (5): 1210-18. https://doi.org/10.1093/emboj/21.5.1210.

Seeliger, Jessica C., Cynthia M. Holsclaw, Michael W. Schelle, Zsofia Botyanszki, Sarah A. Gilmore, Sarah E. Tully, Michael Niederweis, Benjamin F. Cravatt, Julie A. Leary, et Carolyn R. Bertozzi. 2012. « Elucidation and Chemical Modulation of Sulfolipid-1 Biosynthesis in Mycobacterium Tuberculosis ». *The Journal of Biological Chemistry* 287 (11): 7990-8000. https://doi.org/10.1074/jbc.M111.315473.

Seeliger, Jessica, et D. Branch Moody. 2016. « Monstrous Mycobacterial Lipids ». *Cell Chemical Biology* 23 (2): 207-9. https://doi.org/10.1016/j.chembiol.2016.02.004.

Shakil, Shazi, Rosina Khan, Raffaele Zarrilli, et Asad U. Khan. 2008. « Aminoglycosides versus Bacteria--a Description of the Action, Resistance Mechanism, and Nosocomial Battleground ». *Journal of Biomedical Science* 15 (1): 5-14. https://doi.org/10.1007/s11373-007-9194-y.

Shell, Scarlet S., Erin G. Prestwich, Seung-Hun Baek, Rupal R. Shah, Christopher M. Sassetti, Peter C. Dedon, et Sarah M. Fortune. 2013. « DNA Methylation Impacts Gene Expression and Ensures Hypoxic Survival of Mycobacterium tuberculosis ». *PLoS Pathogens* 9 (7). https://doi.org/10.1371/journal.ppat.1003419.

Shen, Gwan-Han, Bo-Da Wu, Shiau-Ting Hu, Chen-Fu Lin, Kun-Ming Wu, et Jiann-Hwa Chen. 2010. « High Efficacy of Clofazimine and Its Synergistic Effect with Amikacin against Rapidly Growing Mycobacteria ». *International Journal of Antimicrobial Agents* 35 (4): 400-404. https://doi.org/10.1016/j.ijantimicag.2009.12.008.

Shin, Dong-Min, Bo-Young Jeon, Hye-Mi Lee, Hyo Sun Jin, Jae-Min Yuk, Chang-Hwa Song, Sang-Hee Lee, et al. 2010. « Mycobacterium Tuberculosis Eis Regulates Autophagy, Inflammation, and Cell Death through Redox-Dependent Signaling ». *PLoS Pathogens* 6 (12): e1001230. https://doi.org/10.1371/journal.ppat.1001230.

Singh, Amit, David K. Crossman, Deborah Mai, Loni Guidry, Martin I. Voskuil, Matthew B. Renfrow, et Adrie J. C. Steyn. 2009. « Mycobacterium Tuberculosis WhiB3 Maintains Redox Homeostasis by Regulating Virulence Lipid Anabolism to Modulate Macrophage Response ». *PLoS Pathogens* 5 (8): e1000545. https://doi.org/10.1371/journal.ppat.1000545.

Singh, Amit, Loni Guidry, K. V. Narasimhulu, Deborah Mai, John Trombley, Kevin E. Redding, Gregory I. Giles, Jack R. Lancaster, et Adrie J. C. Steyn. 2007. « Mycobacterium Tuberculosis WhiB3 Responds to O2 and Nitric Oxide via Its [4Fe-4S] Cluster and Is Essential for Nutrient Starvation Survival ». *Proceedings of the National Academy of Sciences of the United States of America* 104 (28): 11562-67. https://doi.org/10.1073/pnas.0700490104.

Smibert, O., G. I. Snell, H. Bills, G. P. Westall, et C. O. Morrissey. 2016. « Mycobacterium Abscessus Complex - a Particular Challenge in the Setting of Lung Transplantation ». *Expert Review of Anti-Infective Therapy* 14 (3): 325-33. https://doi.org/10.1586/14787210.2016.1138856.

Smith, J. J., S. M. Travis, E. P. Greenberg, et M. J. Welsh. 1996. « Cystic Fibrosis Airway Epithelia Fail to Kill Bacteria Because of Abnormal Airway Surface Fluid ». *Cell* 85 (2): 229-36. https://doi.org/10.1016/s0092-8674(00)81099-5.

Smith, Laura J., Melanie R. Stapleton, Gavin J. M. Fullstone, Jason C. Crack, Andrew J. Thomson, Nick E. Le Brun, Debbie M. Hunt, et al. 2010. « Mycobacterium Tuberculosis WhiB1 Is an Essential DNA-Binding Protein with a Nitric Oxide-Sensitive Iron-Sulfur Cluster ». *The Biochemical Journal* 432 (3): 417-27. https://doi.org/10.1042/BJ20101440.

Sondén, Berit, Dana Kocíncová, Caroline Deshayes, Daniel Euphrasie, Lamya Rhayat, Françoise Laval, Claude Frehel, Mamadou Daffé, Gilles Etienne, et Jean-Marc Reyrat. 2005. « Gap, a Mycobacterial Specific Integral Membrane Protein, Is Required for Glycolipid Transport to the Cell Surface ». *Molecular Microbiology* 58 (2): 426-40. https://doi.org/10.1111/j.1365-2958.2005.04847.x.

Soroka, Daria, Vincent Dubée, Olivia Soulier-Escrihuela, Guillaume Cuinet, Jean-Emmanuel Hugonnet, Laurent Gutmann, Jean-Luc Mainardi, et Michel Arthur. 2014. « Characterization of Broad-Spectrum Mycobacterium Abscessus Class A β-Lactamase ». *The Journal of Antimicrobial Chemotherapy* 69 (3): 691-96. https://doi.org/10.1093/jac/dkt410.

Sriram, Raghu, A.K. Sahni, Vaibhav L. Dudhat, et A.K. Pujahari. 2018. « Matrix-assisted laser desorption ionization-time of flight mass spectrometry (MALDI-TOF MS) for rapid identification of Mycobacterium abscessus ». *Medical Journal, Armed Forces India* 74 (1): 22-27. https://doi.org/10.1016/j.mjafi.2017.02.006.

Surette, Michael G. 2014. « The Cystic Fibrosis Lung Microbiome ». *Annals of the American Thoracic Society* 11 Suppl 1 (janvier): S61-65. https://doi.org/10.1513/AnnalsATS.201306-159MG.

Szumowski, John D., Kristin N. Adams, Paul H. Edelstein, et Lalita Ramakrishnan. 2013. « Antimicrobial Efflux Pumps and Mycobacterium Tuberculosis Drug Tolerance: Evolutionary Considerations ». *Current Topics in Microbiology and Immunology* 374: 81-108. https://doi.org/10.1007/82_2012_300.

Tahlan, Kapil, Sang Kyun Ahn, Anson Sing, Tetyana D. Bodnaruk, Andrew R. Willems, Alan R. Davidson, et Justin R. Nodwell. 2007. « Initiation of Actinorhodin Export in Streptomyces Coelicolor ». *Molecular Microbiology* 63 (4): 951-61. https://doi.org/10.1111/j.1365-2958.2006.05559.x.

Thanna, Sandeep, et Steven J. Sucheck. 2016. « Targeting the Trehalose Utilization Pathways of Mycobacterium Tuberculosis ». *MedChemComm* 7 (1): 69-85. https://doi.org/10.1039/C5MD00376H.

Thomson, Rachel, Carla Tolson, Robyn Carter, Chris Coulter, Flavia Huygens, et Megan Hargreaves. 2013. « Isolation of Nontuberculous Mycobacteria (NTM) from Household Water and Shower Aerosols in Patients with Pulmonary Disease Caused by NTM ». *Journal of Clinical Microbiology* 51 (9): 3006-11. https://doi.org/10.1128/JCM.00899-13.

Torraca, Vincenzo, Samrah Masud, Herman P. Spaink, et Annemarie H. Meijer. 2014. « Macrophage-Pathogen Interactions in Infectious Diseases: New Therapeutic Insights from the Zebrafish Host Model ». *Disease Models & Mechanisms* 7 (7): 785-97. https://doi.org/10.1242/dmm.015594.

Torraca, Vincenzo, et Serge Mostowy. 2018. « Zebrafish Infection: From Pathogenesis to Cell Biology ». *Trends in Cell Biology* 28 (2): 143-56. https://doi.org/10.1016/j.tcb.2017.10.002.

Tortoli, Enrico, Thomas A. Kohl, Barbara A. Brown-Elliott, Alberto Trovato, Sylvia Cardoso Leão, Maria Jesus Garcia, Sruthi Vasireddy, et al. 2016. « Emended Description of Mycobacterium Abscessus, Mycobacterium Abscessus Subsp. Abscessus and Mycobacteriumabscessus Subsp. Bolletii and Designation of Mycobacteriumabscessus Subsp. Massiliense Comb. Nov ». *International Journal of Systematic and Evolutionary Microbiology* 66 (11): 4471-79. https://doi.org/10.1099/ijsem.0.001376.

Tran, Tung, Kevin Chiem, Saumya Jani, Brock A. Arivett, David L. Lin, Rupali Lad, Verónica Jimenez, et al. 2018. « Identification of a Small Molecule Inhibitor of the Aminoglycoside 6'-N-Acetyltransferase Type Ib [AAC(6')-Ib] Using Mixture-Based Combinatorial Libraries ».

International Journal of Antimicrobial Agents 51 (5): 752-61. https://doi.org/10.1016/j.ijantimicag.2018.01.019.

Ulrich, Luke E., Eugene V. Koonin, et Igor B. Zhulin. 2005. « One-component systems dominate signal transduction in prokaryotes ». *Trends in microbiology* 13 (2): 52-56. https://doi.org/10.1016/j.tim.2004.12.006.

Ung, Kien Lam, Husam M. A. B. Alsarraf, Vincent Olieric, Laurent Kremer, et Mickaël Blaise. 2019. « Crystal Structure of the Aminoglycosides N-Acetyltransferase Eis2 from Mycobacterium Abscessus ». *The FEBS Journal*, juin. https://doi.org/10.1111/febs.14975.

Vaghaiwalla, Tanaz, Shevonne S. Satahoo, Rolla Zarifa, Marc Dauer, James S. Davis, Doreann Dearmas, Nicholas Namias, Louis R. Pizano, et Carl I. Schulman. 2014. « Mycobacterium Abscessus Infection in a Burn Intensive Care Unit Patient ». *Surgical Infections* 15 (6): 847-49. https://doi.org/10.1089/sur.2014.052.

Vianna, Júlia S., Diana Machado, Ivy B. Ramis, Fábia P. Silva, Dienefer V. Bierhals, Michael Andrés Abril, Andrea von Groll, et al. 2019. « The Contribution of Efflux Pumps in Mycobacterium Abscessus Complex Resistance to Clarithromycin ». *Antibiotics (Basel, Switzerland)* 8 (3). https://doi.org/10.3390/antibiotics8030153.

Vianna, Júlia S., Ivy B. Ramis, Dienefer Bierhals, Andrea von Groll, Daniela F. Ramos, Nilo Zanatta, Maria Cristina Lourenço, Miguel Viveiros, et Pedro E. Almeida da Silva. 2019. « Tetrahydropyridine Derivative as Efflux Inhibitor in Mycobacterium Abscessus ». *Journal of Global Antimicrobial Resistance* 17 (juin): 296-99. https://doi.org/10.1016/j.jgar.2018.12.020.

Vilchèze, Catherine, et Laurent Kremer. 2017. « Acid-Fast Positive and Acid-Fast Negative Mycobacterium Tuberculosis: The Koch Paradox ». *Microbiology Spectrum* 5 (2). https://doi.org/10.1128/microbiolspec.TBTB2-0003-2015.

Viljoen, Albertus, Violaine Dubois, Fabienne Girard-Misguich, Mickaël Blaise, Jean-Louis Herrmann, et Laurent Kremer. 2017. « The Diverse Family of MmpL Transporters in Mycobacteria: From Regulation to Antimicrobial Developments ». *Molecular Microbiology* 104 (6): 889-904. https://doi.org/10.1111/mmi.13675.

Viljoen, Albertus, Clement Raynaud, Matt D. Johansen, Françoise Roquet-Banères, Jean-Louis Herrmann, Wassim Daher, et Laurent Kremer. 2019. « Improved Activity of Bedaquiline by Verapamil against Mycobacterium Abscessus in Vitro and in Macrophages ». *Antimicrobial Agents and Chemotherapy*, juin. https://doi.org/10.1128/AAC.00705-19.

Viljoen, Albertus, Matthias Richard, Phuong Chi Nguyen, Patrick Fourquet, Luc Camoin, Rishi R. Paudal, Giri R. Gnawali, et al. 2018. « Cyclipostins and Cyclophostin Analogs Inhibit the Antigen 85C from Mycobacterium Tuberculosis Both in Vitro and in Vivo ». *The Journal of Biological Chemistry* 293 (8): 2755-69. https://doi.org/10.1074/jbc.RA117.000760.

Villanueva, A., R. V. Calderon, B. A. Vargas, F. Ruiz, S. Aguero, Y. Zhang, B. A. Brown, et R. J. Wallace. 1997. « Report on an Outbreak of Postinjection Abscesses Due to Mycobacterium Abscessus, Including Management with Surgery and Clarithromycin Therapy and Comparison of Strains by Random Amplified Polymorphic DNA Polymerase Chain Reaction ». *Clinical Infectious Diseases: An Official Publication of the Infectious Diseases Society of America* 24 (6): 1147-53. https://doi.org/10.1086/513656.

Wee, Wei Yee, Avirup Dutta, et Siew Woh Choo. 2017. « Comparative Genome Analyses of Mycobacteria Give Better Insights into Their Evolution ». *PloS One* 12 (3): e0172831. https://doi.org/10.1371/journal.pone.0172831.

Weisblum, B. 1995. « Erythromycin Resistance by Ribosome Modification ». *Antimicrobial Agents and Chemotherapy* 39 (3): 577-85. https://doi.org/10.1128/aac.39.3.577.

Wells, Ryan M., Christopher M. Jones, Zhaoyong Xi, Alexander Speer, Olga Danilchanka, Kathryn S. Doornbos, Peibei Sun, Fangming Wu, Changlin Tian, et Michael Niederweis. 2013. « Discovery of a Siderophore Export System Essential for Virulence of Mycobacterium Tuberculosis ». *PLoS Pathogens* 9 (1): e1003120. https://doi.org/10.1371/journal.ppat.1003120.

Werf, Tjip S. van der, Ymkje Stienstra, R. Christian Johnson, Richard Phillips, Ohene Adjei, Bernhard Fleischer, Mark H. Wansbrough-Jones, et al. 2005. « Mycobacterium Ulcerans Disease ».

Bulletin of the World Health Organization 83 (10): 785-91. https://doi.org//S0042-96862005001000016.

Whang, Jake, Yong Woo Back, Kang-In Lee, Nagatoshi Fujiwara, Seungwha Paik, Chul Hee Choi, Jeong-Kyu Park, et Hwa-Jung Kim. 2017. « Mycobacterium Abscessus Glycopeptidolipids Inhibit Macrophage Apoptosis and Bacterial Spreading by Targeting Mitochondrial Cyclophilin D ». *Cell Death & Disease* 8 (8): e3012. https://doi.org/10.1038/cddis.2017.420.

WHO. 2017. « Tuberculosis (TB) ». 2017. https://www.who.int/news-room/fact-sheets/detail/tuberculosis.

« WHO | Global tuberculosis report 2018 ». s. d. WHO. Consulté le 26 août 2019. http://www.who.int/tb/publications/global_report/en/.

Willems, A. R., K. Tahlan, T. Taguchi, K. Zhang, Z. Z. Lee, K. Ichinose, M. S. Junop, et J. R. Nodwell. 2008. « Crystal Structures of the Streptomyces Coelicolor TetR-like Protein ActR Alone and in Complex with Actinorhodin or the Actinorhodin Biosynthetic Precursor (S)-DNPA ». *Journal of Molecular Biology* 376 (5): 1377-87. https://doi.org/10.1016/j.jmb.2007.12.061.

Wilson, Daniel N., Frank Schluenzen, Joerg M. Harms, Agata L. Starosta, Sean R. Connell, et Paola Fucini. 2008. « The Oxazolidinone Antibiotics Perturb the Ribosomal Peptidyl-Transferase Center and Effect TRNA Positioning ». *Proceedings of the National Academy of Sciences of the United States of America* 105 (36): 13339-44. https://doi.org/10.1073/pnas.0804276105.

Wiseman, Ben, Xavi Carpena, Miguel Feliz, Lynda J. Donald, Miquel Pons, Ignacio Fita, et Peter C. Loewen. 2010. « Isonicotinic Acid Hydrazide Conversion to Isonicotinyl-NAD by Catalase-Peroxidases ». *The Journal of Biological Chemistry* 285 (34): 26662-73. https://doi.org/10.1074/jbc.M110.139428.

Worlitzsch, Dieter, Robert Tarran, Martina Ulrich, Ute Schwab, Aynur Cekici, Keith C. Meyer, Peter Birrer, et al. 2002. « Effects of Reduced Mucus Oxygen Concentration in Airway Pseudomonas Infections of Cystic Fibrosis Patients ». *The Journal of Clinical Investigation* 109 (3): 317-25. https://doi.org/10.1172/JCI13870.

Wu, Mingyan, Bing Li, Qi Guo, Liyun Xu, Yuzhen Zou, Yongjie Zhang, Mengling Zhan, et al. 2019. « Detection and Molecular Characterization of Amikacin-Resistant Mycobacterium Abscessus Isolated from Patients with Pulmonary Disease ». *Journal of Global Antimicrobial Resistance*, mai. https://doi.org/10.1016/j.jgar.2019.05.016.

Wu, Mu-Lu, Dinah B. Aziz, Véronique Dartois, et Thomas Dick. 2018. « NTM Drug Discovery: Status, Gaps and the Way Forward ». *Drug Discovery Today* 23 (8): 1502-19. https://doi.org/10.1016/j.drudis.2018.04.001.

Yadav, Gitanjali, Rajesh S. Gokhale, et Debasisa Mohanty. 2003. « Computational Approach for Prediction of Domain Organization and Substrate Specificity of Modular Polyketide Synthases ». *Journal of Molecular Biology* 328 (2): 335-63. https://doi.org/10.1016/s0022-2836(03)00232-8.

Yagi, Kazuma, Makoto Ishii, Ho Namkoong, Takahiro Asami, Osamu Iketani, Takanori Asakura, Shoji Suzuki, et al. 2017. « The Efficacy, Safety, and Feasibility of Inhaled Amikacin for the Treatment of Difficult-to-Treat Non-Tuberculous Mycobacterial Lung Diseases ». *BMC Infectious Diseases* 17 (1): 558. https://doi.org/10.1186/s12879-017-2665-5.

Yang, Grace, Joanna Trylska, Yitzhak Tor, et J. Andrew McCammon. 2006. « Binding of Aminoglycosidic Antibiotics to the Oligonucleotide A-Site Model and 30S Ribosomal Subunit: Poisson-Boltzmann Model, Thermal Denaturation, and Fluorescence Studies ». *Journal of Medicinal Chemistry* 49 (18): 5478-90. https://doi.org/10.1021/jm060288o.

Yano, Takahiro, Sacha Kassovska-Bratinova, J. Shin Teh, Jeffrey Winkler, Kevin Sullivan, Andre Isaacs, Norman M. Schechter, et Harvey Rubin. 2011. « Reduction of Clofazimine by Mycobacterial Type 2 NADH:Quinone Oxidoreductase: A Pathway for the Generation of Bactericidal Levels of Reactive Oxygen Species ». *The Journal of Biological Chemistry* 286 (12): 10276-87. https://doi.org/10.1074/jbc.M110.200501.

Ye, Meiping, Liyun Xu, Yuzhen Zou, Bing Li, Qi Guo, Yongjie Zhang, Mengling Zhan, et al. 2019. « Molecular Analysis of Linezolid-Resistant Clinical Isolates of Mycobacterium Abscessus ». *Antimicrobial Agents and Chemotherapy* 63 (2). https://doi.org/10.1128/AAC.01842-18.

Yu, Zhou, Sean E. Reichheld, Alexei Savchenko, John Parkinson, et Alan R. Davidson. 2010. « A Comprehensive Analysis of Structural and Sequence Conservation in the TetR Family Transcriptional Regulators ». *Journal of Molecular Biology* 400 (4): 847-64. https://doi.org/10.1016/j.jmb.2010.05.062.

Zaunbrecher, M. Analise, R. David Sikes, Beverly Metchock, Thomas M. Shinnick, et James E. Posey. 2009. « Overexpression of the Chromosomally Encoded Aminoglycoside Acetyltransferase Eis Confers Kanamycin Resistance in Mycobacterium Tuberculosis ». *Proceedings of the National Academy of Sciences of the United States of America* 106 (47): 20004-9. https://doi.org/10.1073/pnas.0907925106.

Zhai, Le, Ke-Wu Yang, Cheng-Cheng Liu, Hui-Zhou Gao, Xia Yang, Ying Shi, et Jing Wen. 2012. « Thermokinetic characterization of imipenem hydrolysis with metallo-β-lactamase CcrA from Bacteroides fragilis ». *Thermochimica Acta* 539 (juillet): 67-70. https://doi.org/10.1016/j.tca.2012.04.003.

Zhanel, George G., Erika Hartel, Heather Adam, Sheryl Zelenitsky, Michael A. Zhanel, Alyssa Golden, Frank Schweizer, et al. 2016. « Solithromycin: A Novel Fluoroketolide for the Treatment of Community-Acquired Bacterial Pneumonia ». *Drugs* 76 (18): 1737-57. https://doi.org/10.1007/s40265-016-0667-z.

Zhang, Bing, Jun Li, Xiaolin Yang, Lijie Wu, Jia Zhang, Yang Yang, Yao Zhao, et al. 2019. « Crystal Structures of Membrane Transporter MmpL3, an Anti-TB Drug Target ». *Cell* 176 (3): 636-648.e13. https://doi.org/10.1016/j.cell.2019.01.003.

Zhang, Nannan, Jordi B. Torrelles, Michael R. McNeil, Vincent E. Escuyer, Kay-Hooi Khoo, Patrick J. Brennan, et Delphi Chatterjee. 2003. « The Emb Proteins of Mycobacteria Direct Arabinosylation of Lipoarabinomannan and Arabinogalactan via an N-Terminal Recognition Region and a C-Terminal Synthetic Region ». *Molecular Microbiology* 50 (1): 69-76. https://doi.org/10.1046/j.1365-2958.2003.03681.x.

Zhang, Zhijian, Jie Lu, Min Liu, Yufeng Wang, Yanlin Zhao, et Yu Pang. 2017. « In vitro activity of clarithromycin in combination with other antimicrobial agents against Mycobacterium abscessus and Mycobacterium massiliense ». *International Journal of Antimicrobial Agents* 49 (3): 383-86. https://doi.org/10.1016/j.ijantimicag.2016.12.003.

Zhang, Zhijian, Jie Lu, Yuanyuan Song, et Yu Pang. 2018. « In Vitro Activity between Linezolid and Other Antimicrobial Agents against Mycobacterium Abscessus Complex ». *Diagnostic Microbiology and Infectious Disease* 90 (1): 31-34. https://doi.org/10.1016/j.diagmicrobio.2017.09.013.

Annexes

Annexe 1

« Targeting Mycolic Acid Transport by Indole-2-carboxamides for the Treatment of Mycobacterium abscessus Infections. » Kozikowski AP, Onajole OK, Stec J, Dupont C, Viljoen A, Richard M, Chaira T, Lun S, Bishai W, Raj VS, Ordway D, Kremer L. J Med Chem. 2017 Jul 13;60(13):5876-5888.

Journal of Medicinal Chemistry

Article

pubs.acs.org/jmc

Targeting Mycolic Acid Transport by Indole-2-carboxamides for the Treatment of *Mycobacterium abscessus* Infections

Alan P. Kozikowski,[*,†] Oluseye K. Onajole,[†,‡,+] Jozef Stec,[§,∥,+] Christian Dupont,[⊥,+] Albertus Viljoen,[⊥] Matthias Richard,[⊥] Tridib Chaira,[#,▽] Shichun Lun,[○] William Bishai,[○] V. Samuel Raj,[#] Diane Ordway,[◆] and Laurent Kremer[*,⊥,¶]

[†]Drug Discovery Program, Department of Medicinal Chemistry and Pharmacognosy, College of Pharmacy, University of Illinois at Chicago, 833 South Wood Street, Chicago, Illinois 60612, United States

[‡]Department of Biological, Chemical and Physical Sciences, Roosevelt University, 425 South Wabash Avenue, Chicago, Illinois 60605, United States

[§]Department of Pharmaceutical Sciences, College of Pharmacy, Chicago State University, 9501 South King Drive, Chicago, Illinois 60628, United States

[∥]Department of Pharmaceutical Sciences, College of Pharmacy, Marshall B. Ketchum University, 2575 Yorba Linda Boulevard, Fullerton, California 92831, United States

[⊥]Institut de Recherche en Infectiologie (IRIM), CNRS, UMR 9004, Université de Montpellier, Montpellier Cedex 5 34 293, France

[#]Centre for Drug Design Discovery and Development (C4D), SRM University, Delhi-NCR, Rajiv Gandhi Education City, Sonepat 131 029, Haryana India

[▽]Daiichi Sankyo India Pharma Private Limited, Sector 18, Gurgaon 122 015, Haryana India

[○]JHU Center for TB Research, Johns Hopkins School of Medicine, 1550 Orleans Street, Baltimore, Maryland 21231-1001, United States

[◆]Department of Microbiology, Immunology & Pathology, Mycobacteria Research Laboratory, Colorado State University, Fort Collins, Colorado 80523 United States

[¶]IRIM, INSERM, 34293 Montpellier, France

Supporting Information

ABSTRACT: *Mycobacterium abscessus* is a fast-growing, multidrug-resistant organism that has emerged as a clinically significant pathogen in cystic fibrosis (CF) patients. The intrinsic resistance of *M. abscessus* to most commonly available antibiotics seriously restricts chemotherapeutic options. Herein, we report the potent activity of a series of indolecarboxamides against *M. abscessus*. The lead compounds, **6** and **12**, exhibited strong activity in vitro against a wide panel of *M. abscessus* isolates and in infected macrophages. High resistance levels to the indolecarboxamides appear to be associated with an A309P mutation in the mycolic acid transporter MmpL3. Biochemical analyses demonstrated that while de novo mycolic acid synthesis remained unaffected, the indolecarboxamides strongly inhibited the transport of trehalose monomycolate, resulting in the loss of trehalose dimycolate production and abrogating mycolylation of arabinogalactan. Our data introduce a hereto unexploited chemical structure class active against *M. abscessus* infections with promising translational development possibilities for the treatment of CF patients.

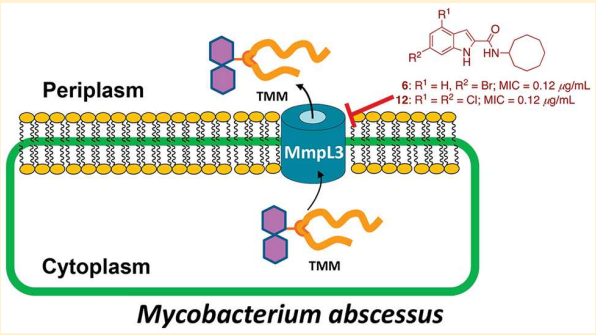

INTRODUCTION

Fighting multidrug-resistant bacteria requires repurposing of existing drugs or the development of new more rapidly acting and cost-effective antibiotics. Chronic obstructive pulmonary disease (COPD) and cystic fibrosis (CF) are associated with unresolved therapeutic needs resulting from severe and even fatal infections by multidrug-resistant bacteria. Lung infections in CF patients represent the most frequent and most serious manifestations because they are responsible for more than 90% of CF patient deaths.[1] In the context of CF and COPD, *Mycobacterium abscessus*, a fast-growing mycobacterial species, has emerged in recent years as an important opportunistic pathogen increasingly responsible for mortality.[2] The incidence

Received: April 14, 2017
Published: June 2, 2017

DOI: 10.1021/acs.jmedchem.7b00582
J. Med. Chem. 2017, 60, 5876−5888

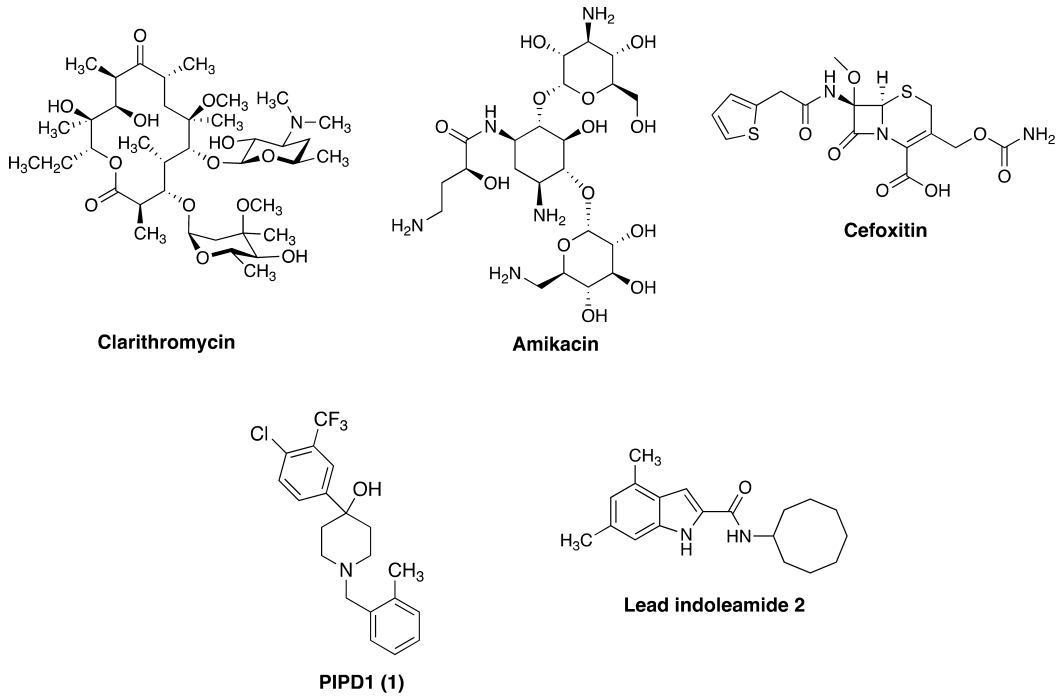

Figure 1. Structures of clarithromycin, amikacin, cefoxitin, PIPD1 (**1**), and our lead indolecarboxamide **2**.

of *M. abscessus* infection in the CF population rises, suggesting a potential link between a genetic defect in the cystic fibrosis transmembrane conductance regulator (CFTR) and *M. abscessus* lung infection. In this population, *M. abscessus* accelerates inflammatory lung damage, leading to increased morbidity and mortality.[3] A recent genomic study of a global collection of clinical isolates indicated that the majority of *M. abscessus* infections are acquired through aerosol transmission of recently emerged dominant circulating clones.[4]

Although a rapid grower, *M. abscessus* shares important physiopathologic features with pathogenic slow-growing mycobacteria such as the ability to persist silently for years and even decades[5] in the human host and to induce lung disease associated with caseous lesions and granuloma formation in lung parenchyma.[6,7] Infections caused by *M. abscessus* are difficult to treat and to eradicate because *M. abscessus* is naturally resistant to most antibiotics, including nearly all current antitubercular drugs.[8] The recommended treatment for pulmonary infections includes a combination of a macrolide (clarithromycin or azithromycin), an aminoglycoside (amikacin), and an intravenous β-lactam (cefoxitin or imipenem) to be taken for at least 12 months[9,10] (Figure 1). The cure rate is estimated to only 25−40% in the case of resistance to macrolides, which appears in 40−60% of the isolates.[11] In addition, unsuccessful eradication of *M. abscessus* represents a contraindication for lung transplantation by several CF centers, leaving patients without therapeutic options. Therefore, more specific, active, and at the same time less toxic antimicrobial agents are urgently needed.

Despite being a formidable respiratory mycobacterial pathogen, little is known with respect to the molecular and cellular mechanisms leading to immunopathogenesis and infection. However, recent genomic data highlighted the considerable sequence similarity between *Mycobacterium tuberculosis* and *M. abscessus*,[12,13] suggesting that these species may share common biochemical pathways. From this, it can be inferred that compounds inhibiting biosynthetic pathways in *M. tuberculosis* may also be active against *M. abscessus* and that already existing data generated during previous tuberculosis (TB) drug discovery programs would be useful to identify new chemotypes with strong activity against *M. abscessus*, an approach that would obviate the need to initiate chemical screens de novo. Indeed, we have recently validated this approach and undertaken an *M. abscessus* "cross-screen" with a confirmed chemical series arising from a known set of potent nontoxic antitubercular hits.[14] This led to the discovery of a new piperidinol-based compound **1** (PIPD1) (Figure 1), showing selective activity against *M. abscessus* both in vitro and in vivo.[15] This success prompted us to further explore this strategy by testing a small library of indole-2-carboxamide derivatives, previously shown to exhibit strong activity against *M. tuberculosis*.[16−18]

In the recent past, we have designed a series of indolecarboxamides with potent activity against both drug-susceptible and drug-resistant strains of *M. tuberculosis* by targeting the putative mycolic acid transporter MmpL3.[18] We identified a single point mutation in MmpL3, which confers high resistance to the indolecarboxamide class while remaining susceptible to currently used first- and second-line TB drugs, signifying a lack of cross-resistance. The lead compound **2** (Figure 1) was found to be active against *M. abscessus*, thus prompting further investigation of other indolecarboxamide analogues. The bioavailability of the indolecarboxamides, combined with their ability to kill tubercle bacilli as well as nontubercular mycobacteria (NTM), indicates great potential for the translational development of this structural class for the treatment of *M. abscessus* infections in CF patients. Herein, we describe SAR studies of a series of indolecarboxamide analogues against *M. abscessus* and provide biological evidence

DOI: 10.1021/acs.jmedchem.7b00582
J. Med. Chem. 2017, 60, 5876−5888

Scheme 1. Synthesis of Compounds 2−29[a]

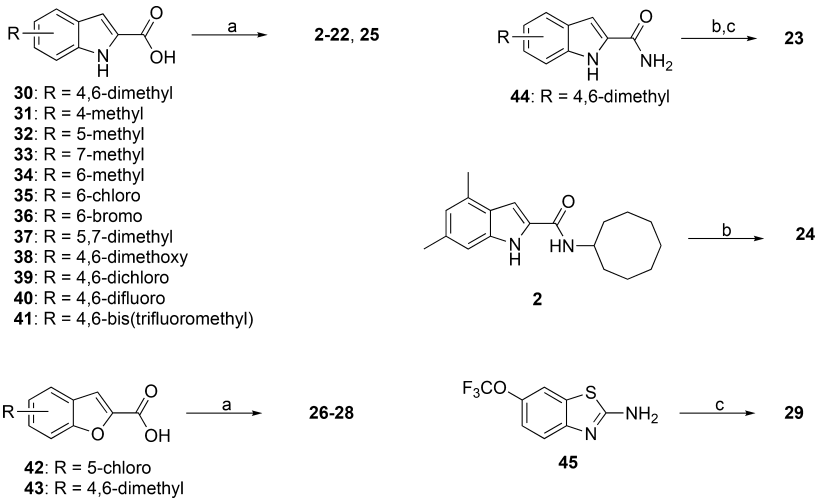

[a]Reagents and conditions: (a) EDC·HCl, corresponding amines, Et_3N, CH_2Cl_2, rt, 12−16 h; (b) $LiAlH_4$, THF, reflux, overnight; (c) cycloheptanecarbonyl chloride, CH_2Cl_2, rt, overnight.

that they are working through inhibition of mycolic acid transport.

RESULTS

The synthesis of compounds **2−29** was carried out by following procedures reported previously.[16−18] Briefly, starting from the appropriate indole-2-carboxylic acid, a standard amide coupling protocol (Scheme 1) was performed to furnish the amides **2−23** and **25−28**. Compound **24** was obtained by $LiAlH_4$ reduction of the amide **2**, whereas compound **29** was prepared by coupling intermediate **45** with cycloheptanecarbonyl chloride.

Structure−Activity Relationship of New Indole-2-carboxamides against *M. abscessus*. The indoles **2−29** were initially screened in vitro against the *M. tuberculosis*[16,17] and *M. abscessus* strains to obtain their respective MIC values (Table 1). The lead compound **2**, with a cyclooctyl group, displayed excellent activity against both *M. tuberculosis* and *M. abscessus*. Presence of only a single methyl at positions 4, 5, or 6 of the indole ring (compounds **3−5**) resulted in a 2-fold decrease in activity against *M. abscessus* in comparison to **2**. A similar trend in activity was observed when these compounds were screened against *M. tuberculosis*,[16] thus indicating that the presence of two nonpolar substituents in the indole ring helps to improve activity. Likewise, compound **6** that possesses a lipophilic bromine atom at position 6 displayed a 2-fold increase in activity when compared to its 6-methyl counterpart, compound **5**. Compound **7**, bearing an *N*-adamantyl group, was nearly 130-fold less active than compounds **6** and **8**. These findings further support the notion that the activity of these compounds is driven by their lipophilicity and that the tolerance for steric bulk at the amide N is fairly high but limited. Additionally, the effect of a single methyl group at position 7, as in compound **9**, was evaluated. Compound **9** showed a large loss in activity against *M. tuberculosis* and *M. abscessus* as compared to other monosubstituted compounds with methyl groups at positions 4, 5, or 6 (**3−5**), indicating that substitution at this position is unfavorable. Next, we investigated the effect of disubstitution at other positions of the indole ring. The 5,7-dimethylindole **10** showed 16- and 2-fold loss of activity against the *M. tuberculosis* and *M. abscessus* strains, respectively, as compared to its 4,6-dimethyl counterpart **2**. In this case, both molecules have equal CLogP values, and the differential activities observed are thus a consequence of the substitution pattern in the indole ring.

After finding that substituents at the 4- and 6-positions of the indole ring were optimal for activity, other 4,6-disubstituted derivatives, such as the 4,6-dimethoxy, 4,6-dichloro, 4,6-difluoro, and 4,6-bis(trifluoro)methyl analogues, were investigated for their activity against *M. abscessus*. Compound **11** bearing the 4,6-dimethoxyindole moiety displayed an 8-fold loss of activity compared to compound **2** (4,6-dimethyl substitution), suggesting that the more polar methoxy substituents are less favorable compared to methyl due to their reduced lipophilicity. Next, we replaced the two methyl groups of **2** with more lipophilic and metabolically stable halogen atoms to afford compounds **12** (4,6-dichloroindole analogue; CLogP = 6.16) and **13** (4,6-difluoroindole analogue; CLogP = 5.02). Both of these compounds showed activities identical (0.12 μg/mL) to that of the lead compound **2** against *M. abscessus*. In the case of *M. tuberculosis*, compound **12** displayed the same activity as did the lead **2**, while compound **13** was approximately 8-fold less active than compound **2**. Of interest is the fact that while compound **12** is more lipophilic than **13**, this property did not enhance its activity in the *M. abscessus* screening assay in contrast to the result that was observed in the case of the *M. tuberculosis* assay. Both compounds **14** and **15** were inactive against *M. abscessus* while retaining activity against *M. tuberculosis*.

Next, the activities of the 4,6-dichloroindole analogues **16−22** bearing different substituents on the amide nitrogen were explored. Compounds **16** (containing a *N*-adamantyl group) and **17** (containing a *N*-(*R*)-(+)-bornyl group) showed poor activities (MIC > 32 μg/mL) against *M. abscessus*. These modifications thus resulted in an at least 256-fold decrease in activity of **16** and **17** as compared to lead compound **2**. Introduction of a simple *n*-octyl group or a *trans*-geranyl group on the amide nitrogen yielded the compounds **18** and **19**. Again, both of these compounds were found to be inactive (MIC > 32 μg/mL) against *M. abscessus*, suggesting that these

DOI: 10.1021/acs.jmedchem.7b00582
J. Med. Chem. 2017, 60, 5876−5888

Table 1. MIC Values of Indole-2-carboxamides against *M. tuberculosis* and the *M. abscessus* CIP 104536 Reference Strain, and the Compounds' CLogP Values (Data for Compounds 6 and 12 Are in Bold)

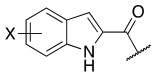
2-22, 25

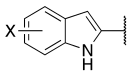
23-24

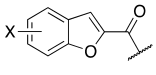
26-28

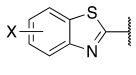
29

Compd	X	R	MIC$_{M.\ tb.}$[a] (μg/mL)	MIC$_{M.\ abs.}$[b] (μg/mL)	IC$_{50\ VERO}$ (μg/mL)	SI $_{M.\ tb.}$[c]	SI $_{M.\ abs.}$[d]	CLogP[e]
2	4,6-dimethyl	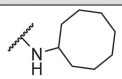	0.0039	0.125	16	4100	128	5.59
3	4-methyl	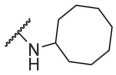	0.0313	0.25				5.10
4	5-methyl	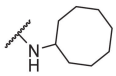	0.250	0.25				5.10
5	6-methyl	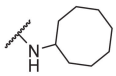	0.0313	0.25				5.10
6	**6-Br**	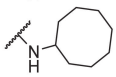	**0.0313**	**0.125**	**≥64**	**≥2050**	**≥512**	**5.56**
7	6-Br	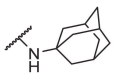	0.0156	16.0	≥64	≥4100	≥4	5.07
8	6-Br	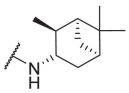	0.0039	0.125				6.28
9	7-methyl	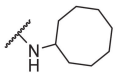	1.00	16.0				5.10
10	5,7-dimethyl	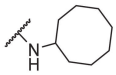	0.0625	0.250				5.59
11	4,6-dimethoxy	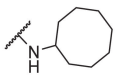	0.0625	1.00				4.57
12	**4,6-dichloro**	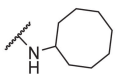	**0.0039**	**0.125**	**8-16**	**2050-4100**	**64-128**	**6.16**
13	4,6-difluoro	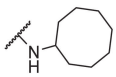	0.031	0.125				5.03
14	4,6-dichloro	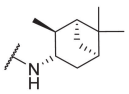	0.0078	128	16	2050	0.125	6.88
15	4,6-difluoro	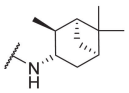	0.0039	32.0	≥64	≥16400	≥2	5.74
16	4,6-dichloro	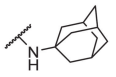	0.0039	>32.0	≥32	≥8210	≥1	5.67

DOI: 10.1021/acs.jmedchem.7b00582
J. Med. Chem. 2017, 60, 5876−5888

Table 1. continued

Compd	X	R	MIC$_{M.\ tb.}$[a] (μg/mL)	MIC$_{M.\ abs.}$[b] (μg/mL)	IC$_{50\ VERO}$ (μg/mL)	SI $_{M.\ tb.}$[c]	SI $_{M.\ abs.}$[d]	CLogP[e]
17	4,6-dichloro		0.0156	>32.0	8	513	0.25	6.88
18	4,6-dichloro	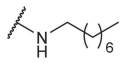	128	>32.0				6.72
19	4,6-dichloro	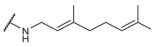	4.00	>32.0				6.75
20	4,6-dichloro	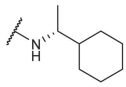	2.00	0.50				5.97
21	4,6-dichloro	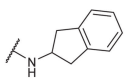	0.250	>32.0				5.00
22	4,6-dichloro	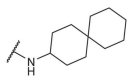	0.001953	>32.0	≥64	≥32800	≥2	7.04
23	4,6-dimethyl	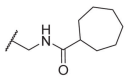	16.0	>32.0				4.53
24	4,6-dimethyl	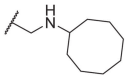	0.125	0.50				5.65
25	4,6-bis(trifluoro-methyl)	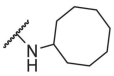	0.0156	0.50				6.64
26	5-chloro	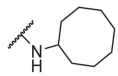	8.00	0.50				5.43
27	4,6-dimethyl	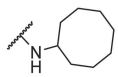	8.00	0.50				5.57
28	4,6-dimethyl	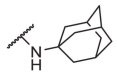	1.00	1.00				5.54
29	5-trifluoro-methoxy	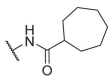	128	>32.0				5.99
INH			0.04		>256	>6400		
RIF			0.125		>256	>2050		

[a]The lowest concentration of drug leading to at least a 90% reduction of bacterial growth signal by the microplate AlamarBlue assay (MABA), as previously reported.[16,17] MIC values are reported as an average of three individual measurements. [b]MIC values (μg/mL) were determined using the microdilution method and cation-adjusted Mueller−Hinton broth according to the Clinical and Laboratory Standards Institute guidelines.[39] [c]SI = $IC_{50\ VERO}/MIC_{M.\ tb.}$. [d]SI = $IC_{50\ VERO}/MIC_{M.\ abs.}$. [e]Calculated using ChemBioDraw Ultra 13.0. INH, isoniazid; RIF, rifampicin.

lipophilic alkyl and alkenyl chains are likely unable to bind to the target site. The analogue **20** bearing an α-branched cyclohexylmethyl group (MIC = 0.5 μg/mL) was moderately active, whereas compound **21** bearing the indanyl group proved to be inactive against *M. abscessus*. The spiro compound **22** (CLogP = 7.04) proved to be the most active compound against *M. tuberculosis* (MIC = 0.00098 μg/mL) in the in vitro assay; disappointingly, this excellent activity was not duplicated in the *M. abscessus* screening (MIC > 32 μg/mL). Furthermore, the reverse amide derivative **23** was inactive against *M. abscessus*, while the amine **24** exhibited a 4-fold drop in activity compared to **2**. Compound **25**, containing a 4,6-bis-(trifluoromethyl)indole, and the benzofuran derivatives **26**–**28**[17] showed MIC values between 0.5 and 1.0 μg/mL, while the benzothiazole derivative **29** was inactive against the susceptible strain of *M. abscessus*.

Overall, the SAR of these indole-2-carboxamides reveals some parallels in their activity against *M. tuberculosis* and *M. abscessus*, but this is not strictly true for all of the analogues that were studied. In most cases, the indole analogues reported herein are more active against *M. tuberculosis* than against *M. abscessus*. Also, it is apparent that, on the basis of the limited number of compounds studied so far, the cyclooctyl group is preferred for activity against *M. abscessus* and that in a few cases

DOI: 10.1021/acs.jmedchem.7b00582
J. Med. Chem. 2017, 60, 5876−5888

these cyclooctyl analogues are more active against *M. abscessus* than *M. tuberculosis*. We believe that the present data provide fertile ground to inspire the generation of a host of improved analogues that may show even better activity against *M. abscessus*.

Activity of Compounds 12 and 6 against *M. abscessus* Clinical Isolates. The two lead compounds, **12** and **6**, were further evaluated in in vitro and in vivo assays. Both exhibited an MIC of 0.125 μg/mL against the smooth (S) as well as the rough (R) variants of the reference *M. abscessus* strain CIP104536 (Table 2). Notably, both compounds were similarly active against nine different clinical strains isolated from CF and non-CF patients. The *M. abscessus* complex is classified into three subspecies: *Mycobacterium. abscessus* subsp. *abscessus*, *Mycobacterium abscessus* subsp. *bolletii*, and *Mycobacterium abscessus* subsp. *massiliense*,[19,20] and the distinction between these subspecies is clinically relevant because they can respond differently to antibiotics.[20] We found that 30 clinical isolates comprising 11 isolates of *M. abscessus* subsp. *abscessus*, 11 of *M. abscessus* subsp. *massiliense*, and 8 of *M. abscessus* subsp. *bolletii* with different susceptibility profiles to amikacin were equally sensitive to **12** and **6**, generally exhibiting MICs of 0.125 μg/mL (Table 2). The lack of cross-resistance between the indolecarboxamides and amikacin suggests that these compounds inhibit a different biological function, which is not targeted by amikacin.

Table 2. MICs (μg/mL) of Compounds 12 and 6 in Cation-Adjusted Mueller−Hinton Broth for 30 Clinical Isolates from CF and Non-CF Patients Belonging to the *M. abscessus* Complex

strain	morphotype	source	12	6	AMK[a]
M. abscessus subsp. *abscessus*					
CIP104536	R	non-CF	0.125	0.0625	12.5
2524	R	CF	0.125	0.125	25
2648	R	CF	0.125	0.125	12.5
3022	R	non-CF	0.125	0.125	12.5
CF	R	CF	0.125	0.125	12.5
CIP104536	S	non-CF	0.125	0.125	25
3321	S	non-CF	0.125	0.125	25
1298	S	CF	0.125	0.125	12.5
2587	S	CF	0.125	0.25	25
2069	S	non-CF	0.125	0.125	25
CF	S	CF	0.125	0.125	12.5
M. abscessus subsp. *massiliense*					
CIP108297	R	Addison's disease	0.125	0.125	12.5
210	R	CF	0.125	0.125	12.5
CIP108297	S	Addison's disease	0.125	0.25	25
111	S	CF	0.125	0.125	25
212	S	CF	0.125	0.125	25
185	S	CF	0.125	0.125	25
140	S	CF	0.125	0.125	25
100	S	CF	0.125	0.125	>100
107	S	CF	0.25	0.25	12.5
122	S	CF	0.125	0.125	12.5
120	S	CF	0.125	0.125	12.5
M. abscessus subsp. *bolletii*					
19	R	non-CF	0.125	0.125	50
108	R	CF	0.25	0.5	12.8
112	R	CF	0.125	0.0625	>100
CIP108541	S	not reported	0.125	0.125	25
17	S	non-CF	0.125	0.125	12.5
97	S	CF	0.125	0.25	12.5
114	S	CF	0.125	0.125	12.5
116	S	CF	0.25	1	12.5

[a]AMK, amikacin; MIC values are from the literature.[27]

To further understand the properties of the indolecarboxamides, exposure of *M. abscessus* 104536 (S) in exponential growth phase to 0.125 μg/mL of compound **12**, corresponding to 1 × MIC, resulted in a notable reduction in viable colony-forming units (CFU) of about 2 orders of magnitude in 3 days as compared to the initial inoculum. This in vitro killing effect of compound **12** was even more pronounced than the one obtained when exposing the cultures to 8 μg/mL imipenem (2 × MIC) (Figure 2A). A comparable killing effect was obtained when cultures were treated with the same dose of compound **6** (Figure 2A).

Activity of Compound 12 against Intracellular *M. abscessus*. The intracellular killing activity of **12** was next assessed after infection of PMA-activated THP-1 macrophages. To avoid growth of extracellular mycobacteria, cells were extensively washed and treated with amikacin. When left untreated for 4 days, the number of intracellular *M. abscessus* was increased by more than 2 orders of magnitude while exposure to compound **12** (3 μg/mL, 24 × MIC) prevented any multiplication within the macrophages (Figure 2B). Treatment with imipenem (96 μg/mL, 24 × MIC) also significantly reduced the intracellular *M. abscessus* load, similar to compound **12**. The intracellular activity of both compounds was further confirmed by counting the number of macrophages infected with *M. abscessus* expressing tdTomato at day 4 post-treatment. A significant decrease in the percentage of infected cells treated with either imipenem or compound **12** was found (Figure 2C). Overall, these results clearly indicate that compound **12** is able to enter human macrophages and to stop bacterial replication.

The A309P Mutation in *MAB_4508* Confers High Resistance Levels to Compound 12. To search for the molecular mechanism of action of the inhibitor, we first selected a spontaneous mutant of *M. abscessus* resistant to compound **12**, designated CIP_OK4−10^{R}, which was subsequently found to exhibit high resistance levels to both compounds **12** and **6** (MIC values of 32 μg/mL) (Table 3). Gene sequencing identified a single g925c single nucleotide polymorphism in *MAB_4508*, encoding MmpL3, which results in an amino acid replacement at position 309 (A309P). Interestingly, we had previously identified the same mutation in a compound **1**-resistant mutant (CIP_PIPD1^{R}),[15] which showed cross-resistance with compounds **12** and **6**. As anticipated, the A309P mutant selected on compound **12** was found to be resistant to compound **1** (Table 3).

To further validate the A309P mutation as the mechanistic basis for resistance to the indolecarboxamides, both the wild-type *MAB_4508* gene and the *MAB_4508* allele harboring the A309P mutation were cloned in pMV261 under the control of the constitutive *hsp60* promoter to allow overexpression of the wild-type and mutated versions of the protein in *M. abscessus*. Whereas overproduction of the wild-type protein failed to result in increased resistance to compounds **6** or **12** as compared to the control drug-susceptible strain, overexpression of the mutated protein resulted in high resistance levels when plated on 7H10^{OADC} media (Figure 3). This indicates that transferring the single point mutation identified in the

DOI: 10.1021/acs.jmedchem.7b00582
J. Med. Chem. 2017, 60, 5876−5888

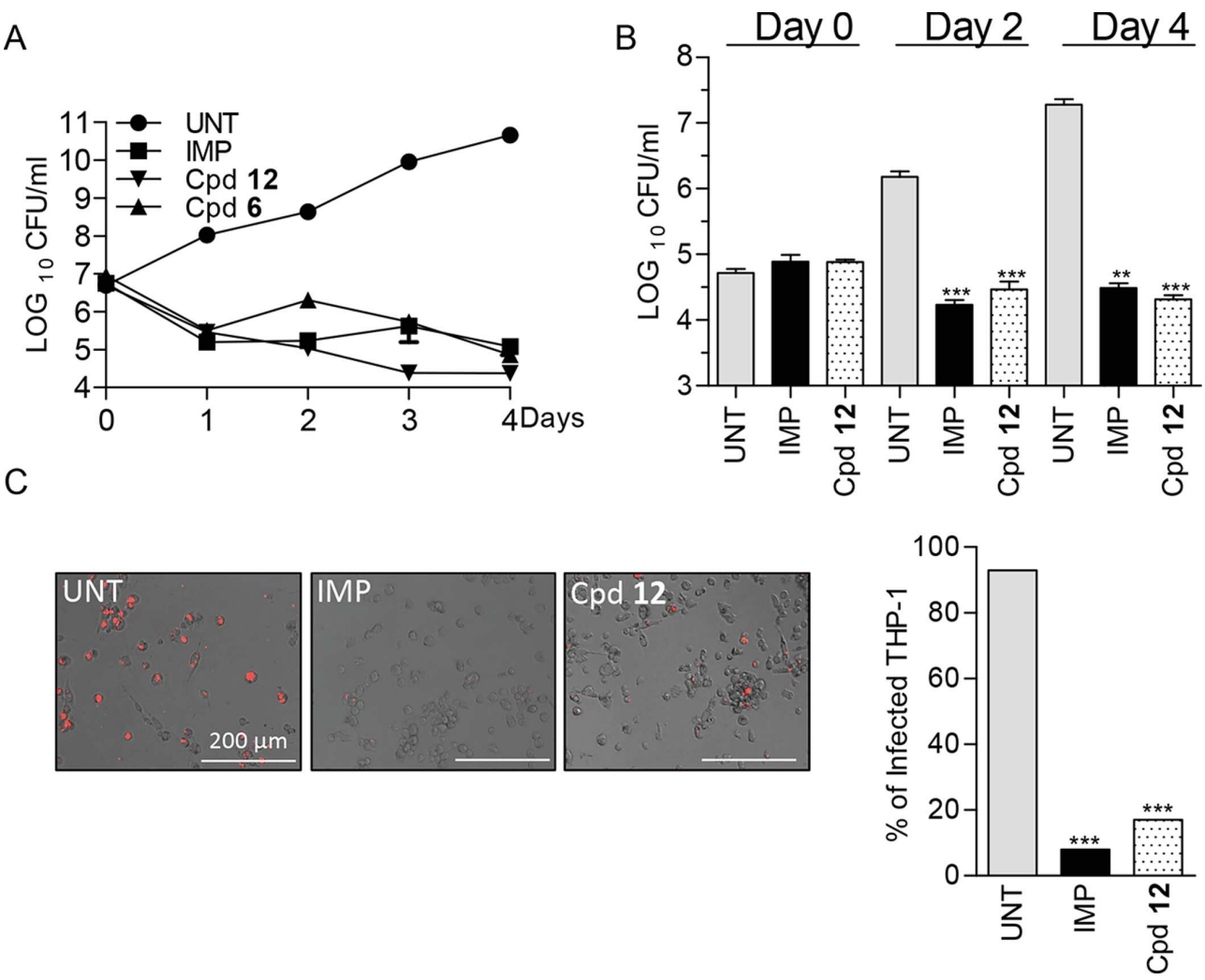

Figure 2. In vitro and intracellular activity of indole-2-carboxamides. (A) In vitro killing curves of *M. abscessus* CIP 104536 (smooth strain) exposed to 8 μg/mL imipenem (IMP) (2 × MIC), 0.125 μg/mL compound **12** (1 × MIC), or 0.125 μg/mL compound **6** (1 × MIC) in CaMH broth at 37 °C. Results are expressed as mean of triplicate Log10 values ± SEM. UNT, untreated cultures. The results for each drug concentration are representative of three independent experiments. (B) THP-1 macrophages were infected with *M. abscessus* CIP 104536. After removal of the extracellular bacteria by extensive washing and treatment with amikacin, cells were treated with IMP at 96 μg/mL (24 × MIC) or compound **12** at 3 μg/mL (24 × MIC). Cells were washed with PBS, and fresh medium containing the different drugs was renewed every 24 h. CFUs were determined at 0, 2, and 4 days post-treatment. Results are expressed as mean of triplicates from two independent experiments, and error bars represent the SEM. One-tailed Mann−Whitney's *t* test comparing the values with the day 0 was applied with $^{**}P < 0.01$, $^{***}P < 0.001$, and $^{****}P < 0.0001$. (C) Following infection with *M. abscessus* expressing tdTomato (red fluorescence), macrophages were treated with either IMP or compound **12** (each at 24 × MIC) and observed under the microscope at day 4 post-treatment (4297 total cells were counted) to determine the percentage of infected cells. Corresponding microscopy captures are also shown. Fisher exact test, $^{***}P < 0.001$.

Table 3. MIC of a Spontaneous Resistant Strain Carrying the A309P Mutation in *MAB_4508*[a]

				mutation in *MAB_4508*	
strain	MIC **1**	MIC **12**	MIC **6**	SNP	AA change
CIP104536 (S)	0.125	0.125	0.125		
CIP_OK4-10^{R}	8	32	32	g925c	A309P
CIP_PIPD1^{R}	8	32	32	g925c	A309P

[a]MIC values (μg/mL) were determined in cation-adjusted Mueller−Hinton broth. The resistant strain, designated CIP_OK4-10^{R}, was derived from the *M. abscessus* CIP104536 (S) parental strain. The CIP_PIPD1^{R} mutant was reported previously.[15].

spontaneously resistant mutant to a susceptible strain is sufficient to confer resistance to compounds **6** and **12**.

Together, these results implicate the A309P mutation as critical in conferring high resistance levels to indole-2-carboxamides in *M. abscessus* and present evidence for the involvement of MmpL3 in the mode of action of this family of inhibitors.

Lead Compound 12 Inhibits Mycolic Acid Transport in *M. abscessus*. Indolecarboxamides have previously been proposed to target the mycolic acid transporter MmpL3 in *M. tuberculosis*,[18] and it has been reported that a mutation in MmpL3 correlates with resistance in *M. abscessus*. To explore whether compound **12** may alter this pathway in *M. abscessus*, untreated and **12**-treated cultures were metabolically labeled

DOI: 10.1021/acs.jmedchem.7b00582
J. Med. Chem. 2017, 60, 5876−5888

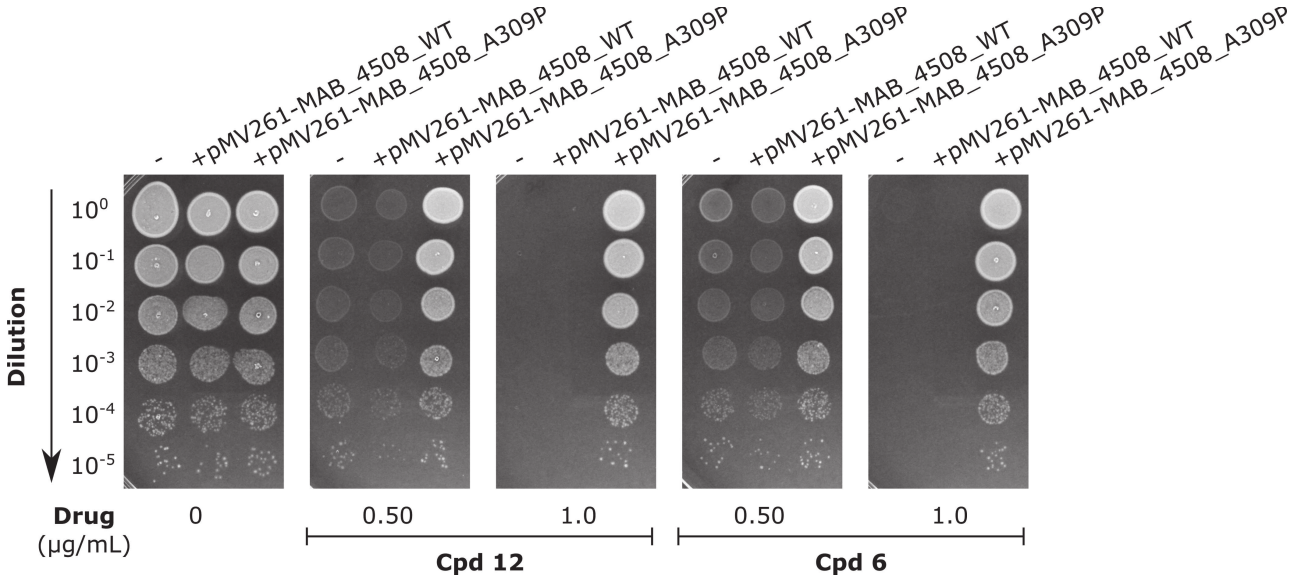

Figure 3. Overexpression of the *MAB_4508* A309P mutated allele in *M. abscessus* renders the bacterium resistant to compounds **12** and **6**. Exponentially growing wild-type *M. abscessus*, or *M. abscessus* carrying either the pMV261_*MAB_4508*_WT or the pMV261_*MAB_4508*_A309P constructs, were grown in $7H9^{OADC}$ and serially diluted and spotted (5 μL) on $7H10^{OADC}$ media containing different concentrations of compounds **12** and **6**. Plates were incubated at 30 °C for 3 days prior to growth inspection.

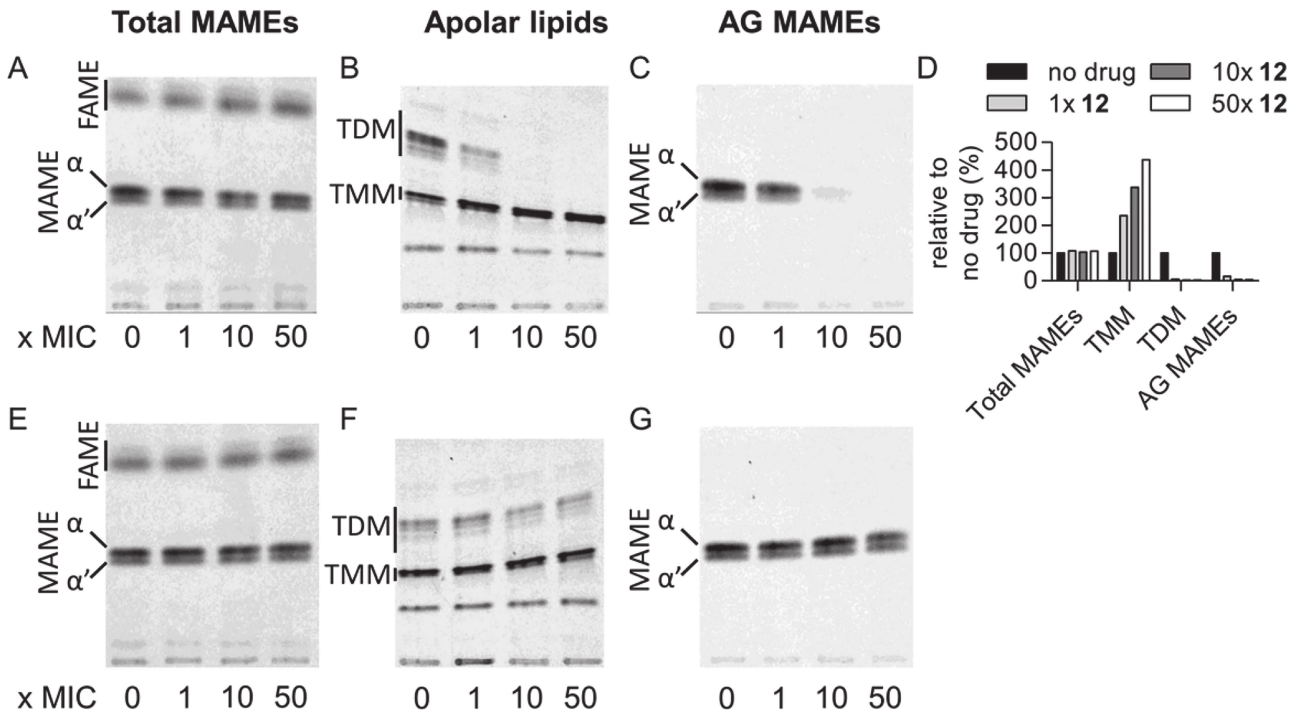

Figure 4. Treatment with compound **12** prevents TMM transport in *M. abscessus* and involves the Ala309 residue in MmpL3. Exponentially growing *M. abscessus*, wild-type (A–D) or carrying the A309P mutation in MmpL3 (E–G), were incubated with increasing concentrations of compound **12** in $7H9^{OADC}$ at 37 °C with agitation for 1 h. Subsequently, bacteria were labeled with [^{14}C]acetate for 2 h at 37 °C with agitation. The cultures were split and from the first volume were extracted the total methyl esters of mycolates (MAME) and methyl esters of fatty acids (FAME). From the second volume, apolar and polar fractions were obtained prior to derivatization of arabinogalactan (AG) mycolate methyl esters. (A,E) Equal counts (50000 cpm) of the MAME and FAME fraction were loaded on a TLC plate and resolved once using the solvent system petroleum ether/acetone (95:5, v/v). (B,F) The apolar fraction was loaded (50000 cpm), and TMM/TDM were visualized on a 1D TLC plate using the solvent system chloroform/methanol/water (40:8:1, v/v/v). (C,G) Equal volumes of the arabinogalactan MAME fractions were loaded, and α- and α'-mycolic acids were visualized on a 1D TLC plate using the solvent system petroleum ether/acetone (95:5, v/v). (D) Densitometric analysis of the TLC plates shown in A–C.

DOI: 10.1021/acs.jmedchem.7b00582
J. Med. Chem. 2017, 60, 5876–5888

with [^{14}C]acetic acid to monitor (glyco)lipid synthesis. When applied at concentrations of up to 50 × MIC (6.2 μg/mL), compound **12** had no effect on de novo mycolic acid biosynthesis (Figure 4A). However, following apolar lipid extraction and their subsequent separation by thin layer chromatography (TLC), a dramatic inhibition of trehalose dimycolate (TDM) synthesis was observed concomitantly with an accumulation of trehalose monomycolate (TMM) (Figure 4B,D), the latter being the substrate of MmpL3 for the transport of mycolic acids onto the mycobacterial surface where TDM is formed. To test whether treatment with compound **12** also impacts mycolylation of arabinogalactan (AG), radiolabeled mycolic acids were extracted from delipidated bacteria.[15,21] The dose-dependent inhibition of [^{14}C]acetic acid incorporation suggests that compound **12** inhibits AG mycolylation with a pronounced decrease of cell wall-bound α- and α′-mycolic acids (Figure 4C,D). The two types of mycolic acids (i.e., α and α′) correspond to long-chain (C_{77-79}) and short-chain (C_{62-64}) mycolic acids, respectively, as reported earlier.[22] Indeed, compound **12** behaved similarly to compound **1**, an unrelated compound that inhibits the transport of mycolic acid transport in *M. abscessus* by targeting MmpL3.[15] Importantly, the mutant strain carrying the *MAB_4508*(A309P) allele was found to be totally refractory to the inhibition of TMM transport and to obstruction of AG mycolylation as compared to the parental strain, even in the presence of high concentrations of compound **12** (Figure 4E–G). In addition, very similar TLC profiles were obtained when treating *M. abscessus* cultures with increasing doses of compound **6** (Supporting Information, Figure S1), indicating that both analogues target the same biosynthetic pathway. To exclude the possibility that compounds **12** and **6** may inhibit the synthesis of TDM and mycolylated arabinogalactan directly rather than the mycolic acid transport by targeting the mycolyltransferase activity of the antigen 85 complex,[23] both compounds were tested for their potential inhibitory activity in an in vitro enzymatic assay using purified Ag85C.[24] This assay is based on a fluorescent probe (resorufin butyrate) that produces a direct measurement of the Ag85C enzymatic activity. Concentrations ranging from 2.5 to 50 μM of compounds **6** or **12** failed to inhibit the Ag85C activity (Supporting Information, Figure S2). In sharp contrast, ebselen inhibited the activity of Ag85C in a dose-dependent manner, as reported previously.[24]

Taken collectively, these biochemical data underline a mode of action that results in the abolition of mycolic acid translocation from the cytoplasm where they are synthesized to the periplasmic side of the plasma membrane for subsequent use in the biogenesis of TDM and transfer onto the essential AG component of the mycobacterial cell wall.

Preliminary ADME Studies on Compound 12. On the basis of the encouraging biological results described above, selected ADME studies were conducted on compound **12** to assess its drug-like properties (Table 4). The cell permeability of compound **12** was measured in the PAMPA cell line assay system. Compound **12** showed a low permeability with 0.2 × 10^{-6} cm/s at pH 7.4 and 0.3 × 10^{-6} cm/s at pH 5.0, respectively. In mouse and rat liver microsomes, compound **12** showed a high intrinsic clearance of 4.8 mL/min/g liver and 6.3 mL/min/g liver, respectively. Compound **12** showed a low propensity to inhibit CYP 1A2, 2C8 2C9, 2C19, 2D6, and 3A4 with an IC_{50} value of ≤20 μM. The compound exhibited high plasma protein binding in mouse (98.9%) and rat (99.2%). On the basis of the AMES mutagenicity assay, compound **12** showed no mutagenic potential in the histidine auxotrophic strains of *Salmonella typhimurium* TA98 and TA100 at 0.24–500 μg/well. Because the compound showed less than a 2-fold increase in the number of revertant colonies compared to the negative controls in either the presence or absence of S9, it can be inferred that it has no mutagenic potential under the test conditions. The compound showed precipitation at 500 and 250 μg/well.

Table 4. ADME Data for Compound 12

assay	values
permeability (PAMPA)	low (0.2 × 10^{-6} cm/s and 0.3 × 10^{-6} cm/s at pH 7.4 and 5.0, respectively)
plasma protein binding (%), mouse/rat	98.9/99.2
CYP inhibition (% inhibition at 10 μM)	
CYP1A2	19
CYP2C8	20
CYP2C9	6
CYP2C19	4
CYP2D6	10
CYP3A4	1
CL_{int} in LM[a], mL/min/g liver (mouse/rat)	high (4.8/6.3)
Ames	negative

[a]LM: Liver microsomes.

DISCUSSION AND CONCLUSIONS

M. abscessus is an emerging causative agent of chronic lung disease, particularly in patients with altered host defenses or disrupted airway clearance mechanisms, such as in CF. *M. abscessus* infection represents a threat to patients with CF with increased prevalence in recent years.[25,26] Among mycobacterial species, *M. abscessus* is regarded as one of the most drug-resistant species, and chemotherapeutic options are very limited.[8] The fact that most available treatments are often unsuccessful or poorly tolerated by patients emphasizes the urgent need for developing more active and better-tolerated drugs. As originally conjectured, the notion of screening drugs that had previously demonstrated activity against *M. tuberculosis* for possible efficacy against *M. abscessus* has been shown to provide good lead candidates for combating *M. abscessus* infections.[15,27] Following this cross-screen approach, we have screened a library of indole-2-carboxamides, reported to be highly active against *M. tuberculosis*.[16,17] This allowed us to define a new structural class of compounds exhibiting promising activity against *M. abscessus*, further validating the value of utilizing data obtained from prior TB screens to directly identify new chemotypes with strong activity against *M. abscessus*. Our lead compounds **6** and **12** display very low MIC values against a vast panel of clinical strains with different susceptibility profiles to antibiotics, regardless of whether they were isolated from CF or non-CF patients. Moreover, the efficacy of compounds **6** and **12** was not dependent on the smooth or rough morphotype of the *M. abscessus* subspecies, which is of particular interest because *M. abscessus* subsp. *abscessus*, *M. abscessus* subsp. *massiliense*, and *M. abscessus* subsp. *bolletii* infections can present various drug sensitivity test results, responses to antibiotics, and clinical symptoms.[28,29] Additionally, compound **12** exhibited appreciable activity in infected macrophages.

DOI: 10.1021/acs.jmedchem.7b00582
J. Med. Chem. 2017, 60, 5876–5888

To pinpoint the possible molecular mechanism of action of these inhibitors, we identified a spontaneous mutant which exhibited a high resistance phenotype to both lead compounds. Gene sequencing identified a single g925c single nucleotide polymorphism in *MAB_4508*, encoding MmpL3. This mutation resulted in an A309P amino acid replacement also previously identified in a compound **1**-resistant mutant,[15] which itself showed cross-resistance to compounds **6** and **12**. Consistent with these findings, compounds **6** and **12** inhibited the translocation of TMM, resulting in the abolition of both TDM formation and mycolylation of AG. Our analyses also revealed that compounds **6** and **12** were not capable of inhibiting the activity of Ag85C in vitro. Together, our combined genetic and biochemical data reflect the inaccessibility of the intracellularly generated TMM to the Ag85 family of mycolyltransferases,[23] similarly to other MmpL3 inhibitors, such as compound **1**,[15] the adamantyl-urea AU1235,[21] or *N*-geranyl-*N*′-(2-adamantyl)ethane-1,2-diamine (SQ109).[30]

Furthermore, sequence analysis indicates that the MmpL3 protein of *M. abscessus* (MAB_4508) and its counterpart in *M. tuberculosis* (Rv0206c)[18,31] show high similarity in multiple aspects. In addition to similar gene sizes, 3006 and 2835 base pairs, respectively, amino acid sequence blasting also revealed 56% identity and 69% similarity. Bioinformatic analysis indicates that both MAB_4508 and Rv0206c are transmembrane proteins comprising 12 transmembrane helices. Currently, MmpL3 appears to be one of the most promising antimycobacterial pharmacological targets as multiple chemical entities have recently been shown to inhibit MmpL3 activity not only in *M. tuberculosis* but also in *M. abscessus*, thus opening a new field centered on the inhibition of mycolic acid transport.[15,18,21,30−34] Interestingly, recent findings indicate that MmpL3 inhibitors can also act synergistically with other antitubercular drugs, which is of interest to efforts aiming at reducing the length of treatments.[35] Whether indole-2-caboxamides may also act in synergy with drugs used for the treatment of *M. abscessus* infections remains to be investigated.

Tetrahydropyrazo[1,5-*a*]pyrimidine-3-carboxamide (THPP) has recently been reported to inhibit the biogenesis of mycolic acids by targeting the enoyl-coenzyme A (CoA) hydratase EchA6 rather than the previously assumed MmpL3 target,[36] even though several mutations identified in *mmpL3* had been proposed to confer resistance to THPP.[37] It was subsequently demonstrated that THPP competes with CoA-binding so as to arrest mycolic acid production, leading to the conclusion that spontaneous resistance-conferring mutations in *mmpL3* can potentially obscure the actual target identification of small inhibitors. Our results failed to show an inhibition of mycolic acid biosynthesis, even in the presence of high concentrations of compounds **6** or **12**, and clearly demonstrated a dose-dependent inhibition of TDM synthesis with a concomitant accumulation of TMM. In addition, overexpression of the MmpL3 (A309P) variant in a genetically susceptible strain correlated with high resistance levels to compounds **6** and **12** and rendered the strain refractory to TMM transport inhibition. Together, these results extend the results obtained previously in *M. tuberculosis* that indole-2-carboxamides act by altering the transport of TMM across the membrane in pathogenic, fast-growing nontubercular mycobacteria.

How compound **1** and our indole-2-carboxamides inhibit MmpL3, and whether they have access to the same or different binding cavities in MmpL3, remains to be established. The design of further improved indolecarboxamides targeting mycolic acid transport would also greatly benefit from future structural and functional studies on MmpL3. Moreover, details as to whether the activity of the indolecarboxamides results from specific inhibition of the MmpL3 transporter functions or through indirect mechanisms, for example, involving the dissipation of the proton-motive force as recently suggested,[38] require additional investigations. In summary, our indole-2-carboxamides represent a very promising chemotype that is able to alter the mycolic acid profile in *M. abscessus*, a species that is naturally resistant to most mycolic acid biosynthesis inhibitors. Of particular interest for medicinal chemistry and drug development, these indole analogues are easy to prepare and generally show reasonably good ADME properties as reported earlier[16] and as further investigated herein for compound **12**. This work, along with previous findings using compound **1**, support the view that targeting the transport of mycolic acids rather than their biosynthesis, has significant translational potential for development of these chemotypes into real drugs for *M. abscessus* treatment and control. Research is currently underway to assess their efficacy in *M. abscessus* animal models.

EXPERIMENTAL SECTION

Chemistry: General Information. The tested 28 compounds were synthesized and characterized as reported in literature.[16,17] Purities of final compounds were confirmed to be ≥95% by analytical HPLC, which was carried out using an Agilent 1100 HPLC system with a Synergi 4 μm Hydro-RP 80A column and a variable wavelength detector G1314A; method 1, flow rate 1.4 mL/min, gradient elution over 20 min, from 30% MeOH−H_2O to 100% MeOH with 0.05% TFA added to both solvents; method 2, flow rate 1.4 mL/min, gradient elution over 20 min, from 50% MeOH−H_2O to 70% MeOH−H_2O with 0.05% TFA added to both solvents.

Bacterial Strains. *M. abscessus* subsp. *abscessus* CIP104536^T, *M. abscessus* subsp. *bolletii* CIP108541^T, and *M. abscessus* subsp. *massiliense* CIP108297^T reference strains were used along with a series of clinical isolates as reported previously.[27] Strains were routinely grown and maintained at 30 °C in Middlebrook 7H9 broth (BD Difco) supplemented with 0.05% Tween 80 (Sigma-Aldrich) and 10% oleic acid, albumin, dextrose, and catalase (OADC enrichment; BD Difco) (7H9$^{T/OADC}$), or on Middlebrook 7H10 agar (BD Difco) containing 10% OADC enrichment (7H10^{OADC}), and in the presence of antibiotics when required. For drug susceptibility testing, bacteria were grown in cation-adjusted Mueller−Hinton broth (CaMHB; Sigma-Aldrich).

Drug Susceptibility Testing. The minimal inhibitory concentrations (MIC) were determined according to the Clinical and Laboratory Standards Institute (CLSI) guidelines.[39] The broth microdilution method was used in CaMHB with an inoculum of 5 × 10^6 CFU/mL in the exponential growth phase. Briefly, the bacterial suspension was seeded in 100 μL volumes in all of the wells of a 96-well plate, except for the first column to which 198 μL of the bacterial suspension was added to each well. In the first column, 2 μL of compound at its highest concentration was added in six wells (the solvent used to dissolve the compound was added to the two outermost wells as a control). Two-fold serial dilutions were then carried out by transferring 100 μL from the wells in the first column to the next column and repeating this for each successive column. Plates were subsequently incubated at 30 °C for 3−5 days. MICs were recorded by visual inspection and by absorbance at 560 nm to confirm visual recordings. Experiments were done in triplicate on three independent occasions.

Time-Kill Assay. Microtiter plates were set up as for the MIC determination. Serial dilutions of the bacterial suspensions from these microtiter plates were plated after 0, 24, 48, 72, and 96 h of exposure to different drug concentrations. Colony-forming units (CFU) were counted after 4 days of incubation at 30 °C.

DOI: 10.1021/acs.jmedchem.7b00582
J. Med. Chem. 2017, 60, 5876−5888

Intramacrophage Killing Assay. THP-1 cells were grown in RPMI medium containing 10% fetal bovine serum ($RPMI^{FBS}$) and differentiated with 20 ng/mL phorbol myristate acetate (PMA) in 12-well flat-bottom tissue culture microplates (1×10^5 cells/well) and incubated for 48 h at 37 °C. Cells were infected with a multiplicity of infection (MOI) of 1:2 and incubated at 37 °C in the presence of 5% CO_2 for 2 h. Wells were carefully washed three times with 1× PBS, re-fed with $RPMI^{FBS}$ supplemented with 200 μg/mL amikacin, reincubated at 37 °C in the presence of 5% CO_2 for 1 h, and washed again three times with PBS prior to the addition of 1 mL of $RPMI^{FBS}$ supplemented with either 3 μg/mL compound **12** or 96 μg/mL imipenem. Media were changed on a daily basis with fresh drug preparations. At various time points (0, 48, and 96 h), cells were washed three times with PBS and lysed by adding 100 μL of 1% Triton X100. Cell lysis was stopped after 2 min by adding 900 μL of PBS, and serial dilutions were plated to monitor the intracellular bacterial counts. Experiments were done two times independently. For determining the percentage of infected macrophages, THP-1 cells were prepared and infected with *M. abscessus* expressing tdTomato and treated with drugs, as described above. Untreated and drug-treated infected cells (96 h time point) were observed under a fluorescence microscope to count the number of bacteria-containing macrophages, as previously described.[15]

Selection of a Compound 12-Resistant Mutant. Exponentially growing *M. abscessus* cultures were plated on $7H10^{OADC}$ containing 6 μg/mL of compound **12**. After 1 week of incubation at 30 °C, a single colony was selected and grown in liquid medium, assessed by MIC determination, and subsequently scored for resistance to compound **12**. Identification of putative SNPs in the *MAB_4508* (*mmpL3*) gene was carried out by PCR amplification using the *MAB_4508seq1* (5′-GGCCACCGTCTTTACCAATA-3′) and *MAB_4508seq7* (5′-GTGCCGTACCTGAATGTCCT-3′) primers to produce a 3549 bp amplicon to gain full coverage sequencing of *MAB_4508*, as done previously.[15] The SNP was confirmed by at least two independent sequencing reactions. To overexpress the *MAB_4508* (*A309P*) allele, the *MAB_4508* open reading frame was PCR-amplified using as template purified genomic DNA of CIP_OK4-10^R, Phusion DNA polymerase (Finnzymes, Finland) and the primers *MAB_4508f* and *MAB_4508r*, as previously described.[15] The obtained PCR product was subsequently digested with *Hin*dIII and ligated to MscI/*Hin*dIII linearized pMV261.

Whole-Cell Radiolabeling Experiments and Lipid Analysis. For visualizing drug-induced changes in the lipid profile, increasing concentrations of compound **12** were added to exponentially growing cultures for 1 h, and metabolic labeling of lipids was performed by adding 1 μCi/mL of [^{14}C]acetate (56 mCi/mmol) for an additional 2 h at 37 °C. Cells were harvested and either delipidated or used immediately to extract mycolic acids, as previously described.[22,40] The apolar lipid fraction containing trehalose monomycolate (TMM) and trehalose dimycolate (TDM) was separated on a one-dimensional thin layer chromatography (TLC) plate using chloroform/methanol/water (40:8:1, v/v/v) and revealed after exposure to a film. Delipidated cells were further processed to extract the mycolic acids,[41] which were analyzed by TLC/autoradiography using petroleum ether/acetone (95:5, v/v) and exposure to a film to reveal ^{14}C-labeled mycolic acid methyl esters (MAME).

Cell Permeability. The permeability of compound **12** was measured at two pH values (pH 7.4 and pH 5.0) in Prisma HT aqueous buffer (pION Inc.). The pH was adjusted with 0.5 N NaOH. The test compound in buffer solutions (25 μM) was added to the PAMPA donor plate (in triplicate). The acceptor plate was painted with 4 μL of GIT-0 lipid solution (pION Inc.), and ASB (acceptor sink buffer, pION Inc.) was added. The acceptor and donor plates were stacked, sealed with a rubber plate, and incubated for 4 h at 25 ± 2 °C. The donor and acceptor plate solutions were analyzed by an LC-MS (UPLC) system.

In Vitro Study: CYP Inhibition. Inhibition of CYP by compound **12** was evaluated using pooled human liver microsomes (catalogue no. 452118, BD-Biosciences). Ten μM compound **12** or the positive control was preincubated with human liver microsomes for 5 min at 37 °C. The reaction was initiated by addition of an NADPH regenerating system and incubated at 37 °C with gentle agitation for the specified time recommended for each of the CYP's (5 min for CYP3A4, 10 min for CYP1A2, 2C8, 2C9, and 2D6, and 40 min for CYP2C19). The samples were vacuum-filtered using Captiva 96-well plates followed by LC-MS/MS analysis. The formation of standard metabolite (concentration/peak area ratio) was estimated. The percentage of inhibition of the test compound and the positive control in comparison to a negative control (DMSO) were determined using the equation:

$$\%\text{inhibition} = 100 - \{[(\text{average metabolite concentration of test compound/positive control})/\text{average metabolite concentration of no inhibitor control}] \times 100\}$$

Plasma Protein Binding. Plasma protein binding studies were performed using an ultracentrifuge method. A 5 μM solution of compound **12** was prepared in mouse or rat plasma using 500 μM stock solution (in DMSO) and incubated for 10 min at 37 °C. For determination of total plasma concentration, 5 μL of incubated plasma was mixed thoroughly with 50 μL of saline, 50 μL of acetonitrile, and 100 μL of 1 μM niflumic acid. For determination of unbound concentrations, the incubated plasma sample was centrifuged at 200000*g* for 4.5 h, and 50 μL of supernatant from the middle layer was taken after removing the upper layer with a Beckmann Coulter slicer. To this solution, 5 μL of blank plasma, 50 μL of acetonitrile, and 100 μL of 1 μM niflumic acid were added. The samples were filtered into a 96-deep well storage plate with a Captiva 0.45 μm 96-well filter plate, and appropriate volumes of all samples were analyzed by LC-MS/MS.

Metabolic Stability. Compound **12** (0.5 μM) was incubated in a reaction mixture consisting of mouse or rat liver microsomes and an NADPH regenerating system. Aliquots were withdrawn at 3 min intervals for 30 min and analyzed for the parent compound by LC-MS/MS. The loss of parent was expressed as the percentage of the test compound remaining, and the rate of decay was estimated by monoexponential decay kinetics. The rate of decay was normalized to microsomal protein expressed as mL/min/g liver.

AMES Mutagenicity Assay. Compound **12** was evaluated for its mutagenic potential in the presence and absence of the S9 fraction by investigating its ability to induce reverse mutations at the histidine locus in the genome of *Salmonella typhimurium* strains. Two histidine auxotrophic strains of *Salmonella typhimurium* were used, namely the TA98 strain carrying a frame shift mutation and the TA100 strain carrying a base-pair substitution. Plates were incubated at 37 ± 2 °C for 72 h, and the experiments were carried out in triplicates. DMSO was used as vehicle control. Sodium azide, 2-nitrofluorene (2NF), and 2-aminoanthracene (2AA) were used as positive controls. A compound was considered positive if the number of revertants increased by ≥2-fold over the negative control in a dose-dependent manner.

■ ASSOCIATED CONTENT

Supporting Information

The Supporting Information is available free of charge on the ACS Publications website at DOI: 10.1021/acs.jmedchem.7b00582.

Mycolic acid profile is affected by treatment with compound **6**; effect of inhibitors on Ag85C activity (PDF)

Molecular formula strings and some data (CSV)

■ AUTHOR INFORMATION

Corresponding Authors

*For A.P.K.: phone, 312-996-5972; fax, 312-996-7107; E-mail, alankozikowski@gmail.com (medicinal chemistry).

*For L.K.: E-mail: laurent.kremer@irim.cnrs.fr (biological screening).

DOI: 10.1021/acs.jmedchem.7b00582
J. Med. Chem. 2017, 60, 5876−5888

ORCID

Alan P. Kozikowski: 0000-0003-4795-5368

Author Contributions

[+]O.K.O., J.S., and C.D. contributed equally

Notes

The authors declare no competing financial interest.

■ ACKNOWLEDGMENTS

We thank F. Roquet-Banères for technical assistance. We are indebted to the Howard Hughes Foundation for providing funds that allowed us to initiate this work. O.K.O. acknowledges Roosevelt University for generous financial support. J.S. acknowledges Chicago State University (CSU) College of Pharmacy and CSU Center for Teaching and Research Excellence (Faculty Seed Grant) for financial support. A Faculty Development Stipend (J.S.) from the Marshall B. Ketchum University College of Pharmacy is also acknowledged. We thank the Association Gregory Lemarchal and Vaincre La Mucoviscidose (RF20130500835) for funding C.D. L.K. also acknowledges the support by the Fondation pour la Recherche Médicale (FRM) (DEQ20150331719). This work was funded in whole or in part with federal funds from the National Institute of Allergy and Infectious Diseases, National Institutes of Health, Department of Health and Human Services, AIO99534-02, NIH/NIAID services under contracts HHSN272201000009I/HHSN27200001 and HHSN272201000009I/HHSN27200005, principal investigator Dr. A.J. Lenaerts, coprincipal investigator, D.O.

■ ABBREVIATIONS USED

CF, cystic fibrosis; COPD, chronic obstructive pulmonary disease; CFTR, cystic fibrosis transmembrane conductance regulator; TB, tuberculosis; NTM, nontubercular mycobacteria; CaMHB, cation-adjusted Mueller–Hinton broth; MIC, minimal inhibitory concentration; CLSI, Clinical Laboratory Standards Institute; CFU, colony-forming units; PMA, phorbol myristate acetate; SAR, structural–activity relationship; TMM, trehalose monomycolate; TDM, trehalose dimycolate; TLC, thin layer chromatography; MAME, mycolic acid methyl ester; DMSO, dimethyl sulfoxide; 2NF, 2-nitrofluorene; 2AA, 2-aminoanthracene; AG, arabinogalactan; THPP, tetrahydropyrazo[1,5-*a*]pyrimidine-3-carboxamide

■ REFERENCES

(1) Rowe, S. M.; Miller, S.; Sorscher, E. J. Cystic fibrosis. *N. Engl. J. Med.* **2005**, *352*, 1992–2001.

(2) Brode, S. K.; Daley, C. L.; Marras, T. K. The epidemiologic relationship between tuberculosis and non-tuberculous mycobacterial disease: a systematic review. *Int. J. Tuberc. Lung Dis.* **2014**, *18*, 1370–1377.

(3) Esther, C. R.; Esserman, D. A.; Gilligan, P.; Kerr, A.; Noone, P. G. Chronic *Mycobacterium abscessus* infection and lung function decline in cystic fibrosis. *J. Cystic Fibrosis* **2010**, *9*, 117–123.

(4) Bryant, J. M.; Grogono, D. M.; Rodriguez-Rincon, D.; Everall, I.; Brown, K. P.; Moreno, P.; Verma, D.; Hill, E.; Drijkoningen, J.; Gilligan, P.; Esther, C. R.; Noone, P. G.; Giddings, O.; Bell, S. C.; Thomson, R.; Wainwright, C. E.; Coulter, C.; Pandey, S.; Wood, M. E.; Stockwell, R. E.; Ramsay, K. A.; Sherrard, L. J.; Kidd, T. J.; Jabbour, N.; Johnson, G. R.; Knibbs, L. D.; Morawska, L.; Sly, P. D.; Jones, A.; Bilton, D.; Laurenson, I.; Ruddy, M.; Bourke, S.; Bowler, I.; Chapman, S. J.; Clayton, A.; Cullen, M.; Dempsey, O.; Denton, M.; Desai, M.; Drew, R. J.; Edenborough, F.; Evans, J.; Folb, J.; Daniels, T.; Humphrey, H.; Isalska, B.; Jensen-Fangel, S.; Jonsson, B.; Jones, A. M.; Katzenstein, T. L.; Lillebaek, T.; MacGregor, G.; Mayell, S.; Millar, M.; Modha, D.; Nash, E. F.; O'Brien, C.; O'Brien, D.; Ohri, C.; Pao, C. S.; Peckham, D.; Perrin, F.; Perry, A.; Pressler, T.; Prtak, L.; Qvist, T.; Robb, A.; Rodgers, H.; Schaffer, K.; Shafi, N.; van Ingen, J.; Walshaw, M.; Watson, D.; West, N.; Whitehouse, J.; Haworth, C. S.; Harris, S. R.; Ordway, D.; Parkhill, J.; Floto, R. A. Emergence and spread of a human-transmissible multidrug-resistant nontuberculous mycobacterium. *Science* **2016**, *354*, 751–757.

(5) Cullen, A. R.; Cannon, C. L.; Mark, E. J.; Colin, A. A. *Mycobacterium abscessus* infection in cystic fibrosis: Colonization or infection? *Am. J. Respir. Crit. Care Med.* **2000**, *161*, 641–645.

(6) Medjahed, H.; Gaillard, J. L.; Reyrat, J. M. Mycobacterium abscessus: a new player in the mycobacterial field. *Trends Microbiol.* **2010**, *18*, 117–123.

(7) Tomashefski, J. F.; Stern, R. C.; Demko, C. A.; Doershuk, C. F. Nontuberculous mycobacteria in cystic fibrosis: An autopsy study. *Am. J. Respir. Crit. Care Med.* **1996**, *154*, 523–528.

(8) Nessar, R.; Cambau, E.; Reyrat, J. M.; Murray, A.; Gicquel, B. *Mycobacterium abscessus*: a new antibiotic nightmare. *J. Antimicrob. Chemother.* **2012**, *67*, 810–818.

(9) Floto, R. A.; Olivier, K. N.; Saiman, L.; Daley, C. L.; Herrmann, J. L.; Nick, J. A.; Noone, P. G.; Bilton, D.; Corris, P.; Gibson, R. L.; Hempstead, S. E.; Koetz, K.; Sabadosa, K. A.; Sermet-Gaudelus, I.; Smyth, A. R.; van Ingen, J.; Wallace, R. J.; Winthrop, K. L.; Marshall, B. C.; Haworth, C. S. US Cystic Fibrosis Foundation and European Cystic Fibrosis Society consensus recommendations for the management of non-tuberculous mycobacteria in individuals with cystic fibrosis: executive summary. *Thorax* **2016**, *71*, 88–90.

(10) Novosad, S. A.; Beekmann, S. E.; Polgreen, P. M.; Mackey, K.; Winthrop, K. L. Treatment of *Mycobacterium abscessus* infection. *Emerging Infect. Dis.* **2016**, *22*, 511–514.

(11) Roux, A. L.; Catherinot, E.; Soismier, N.; Heym, B.; Bellis, G.; Lemonnier, L.; Chiron, R.; Fauroux, B.; Le Bourgeois, M.; Munck, A.; Pin, I.; Sermet, I.; Gutierrez, C.; Veziris, N.; Jarlier, V.; Cambau, E.; Herrmann, J. L.; Guillemot, D.; Gaillard, J. L. Comparing *Mycobacterium massiliense* and *Mycobacterium abscessus* lung infections in cystic fibrosis patients. *J. Cystic Fibrosis* **2015**, *14*, 63–69.

(12) Choo, S. W.; Wee, W. Y.; Ngeow, Y. F.; Mitchell, W.; Tan, J. L.; Wong, G. J.; Zhao, Y. B.; Xiao, J. F. Genomic reconnaissance of clinical isolates of emerging human pathogen *Mycobacterium abscessus* reveals high evolutionary potential. *Sci. Rep.* **2015**, *4*, 4061.

(13) Ripoll, F.; Pasek, S.; Schenowitz, C.; Dossat, C.; Barbe, V.; Rottman, M.; Macheras, E.; Heym, B.; Herrmann, J. L.; Daffe, M.; Brosch, R.; Risler, J. L.; Gaillard, J. L. Non mycobacterial virulence genes in the genome of the emerging pathogen *Mycobacterium abscessus*. *PLoS One* **2009**, *4* (6), e5660.

(14) Ballell, L.; Bates, R. H.; Young, R. J.; Alvarez-Gomez, D.; Alvarez-Ruiz, E.; Barroso, V.; Blanco, D.; Crespo, B.; Escribano, J.; Gonzalez, R.; Lozano, S.; Huss, S.; Santos-Villarejo, A.; Martin-Plaza, J. J.; Mendoza, A.; Rebollo-Lopez, M. J.; Remuinan-Blanco, M.; Lavandera, J. L.; Perez-Herran, E.; Gamo-Benito, F. J.; Garcia-Bustos, J. F.; Barros, D.; Castro, J. P.; Cammack, N. Fueling Open-Source Drug Discovery: 177 Small-molecule leads against tuberculosis. *ChemMedChem* **2013**, *8*, 313–321.

(15) Dupont, C.; Viljoen, A.; Dubar, F.; Blaise, M.; Bernut, A.; Pawlik, A.; Bouchier, C.; Brosch, R.; Guerardel, Y.; Lelievre, J.; Ballell, L.; Herrmann, J. L.; Biot, C.; Kremer, L. A new piperidinol derivative targeting mycolic acid transport in *Mycobacterium abscessus*. *Mol. Microbiol.* **2016**, *101*, 515–529.

(16) Stec, J.; Onajole, O. K.; Lun, S. C.; Guo, H. D.; Merenbloom, B.; Vistoli, G.; Bishai, W. R.; Kozikowski, A. P. Indole-2-carboxamide-based MmpL3 inhibitors show exceptional antitubercular activity in an animal model of tuberculosis infection. *J. Med. Chem.* **2016**, *59*, 6232–6247.

(17) Onajole, O. K.; Pieroni, M.; Tipparaju, S. K.; Lun, S.; Stec, J.; Chen, G.; Gunosewoyo, H.; Guo, H. D.; Ammerman, N. C.; Bishai, W. R.; Kozikowski, A. P. Preliminary structure-activity relationships and biological evaluation of novel antitubercular indolecarboxamide derivatives against drug-susceptible and drug-resistant *Mycobacterium tuberculosis* strains. *J. Med. Chem.* **2013**, *56*, 4093–4103.

DOI: 10.1021/acs.jmedchem.7b00582
J. Med. Chem. 2017, 60, 5876–5888

(18) Lun, S. C.; Guo, H. D.; Onajole, O. K.; Pieroni, M.; Gunosewoyo, H.; Chen, G.; Tipparaju, S. K.; Ammerman, N. C.; Kozikowski, A. P.; Bishai, W. R. Indoleamides are active against drug-resistant. *Nat. Commun.* **2013**, *4*, 2907.
(19) Adekambi, T.; Reynaud-Gaubert, M.; Greub, G.; Gevaudan, M. J.; La Scola, B.; Raoult, D.; Drancourt, M. Amoebal coculture of "*Mycobacterium massiliense*" sp nov from the sputum of a patient with hemoptoic pneumonia. *J. Clin. Microbiol.* **2004**, *42*, 5493−5501.
(20) Bastian, S.; Veziris, N.; Roux, A. L.; Brossier, F.; Gaillard, J. L.; Jarlier, V.; Cambau, E. Assessment of clarithromycin susceptibility in strains belonging to the *Mycobacterium abscessus* group by *erm(41)* and *rrl* sequencing. *Antimicrob. Agents Chemother.* **2011**, *55*, 775−781.
(21) Grzegorzewicz, A. E.; Pham, H.; Gundi, V.; Scherman, M. S.; North, E. J.; Hess, T.; Jones, V.; Gruppo, V.; Born, S. E. M.; Kordulakova, J.; Chavadi, S. S.; Morisseau, C.; Lenaerts, A. J.; Lee, R. E.; McNeil, M. R.; Jackson, M. Inhibition of mycolic acid transport across the *Mycobacterium tuberculosis* plasma membrane. *Nat. Chem. Biol.* **2012**, *8*, 334−341.
(22) Halloum, I.; Carrere-Kremer, S.; Blaise, M.; Viljoen, A.; Bernut, A.; Le Moigne, V.; Vilcheze, C.; Guerardel, Y.; Lutfalla, G.; Herrmann, J. L.; Jacobs, W. R.; Kremer, L. Deletion of a dehydratase important for intracellular growth and cording renders rough *Mycobacterium abscessus* avirulent. *Proc. Natl. Acad. Sci. U. S. A.* **2016**, *113*, E4228−E4237.
(23) Belisle, J. T.; Vissa, V. D.; Sievert, T.; Takayama, K.; Brennan, P. J.; Besra, G. S. Role of the major antigen of *Mycobacterium tuberculosis* in cell wall biogenesis. *Science* **1997**, *276*, 1420−1422.
(24) Favrot, L.; Grzegorzewicz, A. E.; Lajiness, D. H.; Marvin, R. K.; Boucau, J.; Isailovic, D.; Jackson, M.; Ronning, D. R. Mechanism of inhibition of *Mycobacterium tuberculosis* antigen 85 by ebselen. *Nat. Commun.* **2013**, *4*, 2748.
(25) Prevots, D. R.; Shaw, P. A.; Strickland, D.; Jackson, L. A.; Raebel, M. A.; Blosky, M. A.; Montes de Oca, R.; Shea, Y. R.; Seitz, A. E.; Holland, S. M.; Olivier, K. N. Nontuberculous mycobacterial lung disease prevalence at four integrated health care delivery systems. *Am. J. Respir. Crit. Care Med.* **2010**, *182*, 970−976.
(26) Martiniano, S. L.; Nick, J. A.; Daley, C. L. Nontuberculous mycobacterial infections in cystic fibrosis. *Clin. Chest Med.* **2016**, *37*, 83−96.
(27) Halloum, I.; Viljoen, A.; Khanna, V.; Craig, D.; Bouchier, C.; Brosch, R.; Coxon, G.; Kremer, L. Resistance to thiacetazone derivatives active against *Mycobacterium abscessus* involves mutations in the MmpL5 transcriptional repressor MAB_4384. *Antimicrob. Agents Chemother.* **2017**, *61* (4), e02509-16.
(28) Koh, W. J.; Jeon, K.; Lee, N. Y.; Kim, B. J.; Kook, Y. H.; Lee, S. H.; Park, Y. K.; Kim, C. K.; Shin, S. J.; Huitt, G. A.; Daley, C. L.; Kwon, O. J. Clinical significance of differentiation of *Mycobacterium massiliense* from *Mycobacterium abscessus*. *Am. J. Respir. Crit. Care Med.* **2011**, *183*, 405−410.
(29) Harada, T.; Akiyama, Y.; Kurashima, A.; Nagai, H.; Tsuyuguchi, K.; Fujii, T.; Yano, S.; Shigeto, E.; Kuraoka, T.; Kajiki, A.; Kobashi, Y.; Kokubu, F.; Sato, A.; Yoshida, S.; Iwamoto, T.; Saito, H. Clinical and microbiological differences between *Mycobacterium abscessus* and *Mycobacterium massiliense* lung diseases. *J. Clin. Microbiol.* **2012**, *50*, 3556−3561.
(30) Tahlan, K.; Wilson, R.; Kastrinsky, D. B.; Arora, K.; Nair, V.; Fischer, E.; Barnes, S. W.; Walker, J. R.; Alland, D.; Barry, C. E.; Boshoff, H. I. SQ109 Targets MmpL3, a membrane transporter of trehalose monomycolate involved in mycolic acid donation to the cell wall core of *Mycobacterium tuberculosis*. *Antimicrob. Agents Chemother.* **2012**, *56*, 1797−1809.
(31) Rao, S. P. S.; Lakshminarayana, S. B.; Kondreddi, R. R.; Herve, M.; Camacho, L. R.; Bifani, P.; Kalapala, S. K.; Jiricek, J.; Ma, N. L.; Tan, B. H.; Ng, S. H.; Nanjundappa, M.; Ravindran, S.; Seah, P. G.; Thayalan, P.; Lim, S. H.; Lee, B. H.; Goh, A.; Barnes, W. S.; Chen, Z.; Gagaring, K.; Chatterjee, A. K.; Pethe, K.; Kuhen, K.; Walker, J.; Feng, G.; Babu, S.; Zhang, L. J.; Blasco, F.; Beer, D.; Weaver, M.; Dartois, V.; Glynne, R.; Dick, T.; Smith, P. W.; Diagana, T. T.; Manjunatha, U. H. Indolecarboxamide is a preclinical candidate for treating multidrug-resistant tuberculosis. *Sci. Transl. Med.* **2013**, *5* (214), 214ra168.
(32) Viljoen, A.; Dubois, V.; Girard-Misguich, F.; Blaise, M.; Herrmann, J. L.; Kremer, L. The diverse family of MmpL transporters in mycobacteria: from regulation to antimicrobial developments. *Mol. Microbiol.* **2017**, *104*, 889−904.
(33) La Rosa, V.; Poce, G.; Canseco, J. O.; Buroni, S.; Pasca, M. R.; Biava, M.; Raju, R. M.; Porretta, G. C.; Alfonso, S.; Battilocchio, C.; Javid, B.; Sorrentino, F.; Ioerger, T. R.; Sacchettini, J. C.; Manetti, F.; Botta, M.; De Logu, A.; Rubin, E. J.; De Rossi, E. MmpL3 is the cellular target of the antitubercular pyrrole derivative BM212. *Antimicrob. Agents Chemother.* **2012**, *56*, 324−331.
(34) Bailo, R.; Bhatt, A.; Ainsa, J. A. Lipid transport in *Mycobacterium tuberculosis* and its implications in virulence and drug development. *Biochem. Pharmacol.* **2015**, *96*, 159−167.
(35) Li, W.; Sanchez-Hidalgo, A.; Jones, A.; Calado Nogueira de Moura, V.; North, E. J.; Jackson, M. Synergistic interactions of MmpL3 inhibitors with antitubercular compounds in vitro. *Antimicrob. Agents Chemother.* **2017**, *61* (4), e02399-16.
(36) Cox, J. A. G.; Abrahams, K. A.; Alemparte, C.; Ghidelli-Disse, S.; Rullas, J.; Angulo-Barturen, I.; Singh, A.; Gurcha, S. S.; Nataraj, V.; Bethell, S.; Remuinan, M. J.; Encinas, L.; Jervis, P. J.; Cammack, N. C.; Bhatt, A.; Kruse, U.; Bantscheff, M.; Futterer, K.; Barros, D.; Ballell, L.; Drewes, G.; Besra, G. S. THPP target assignment reveals EchA6 as an essential fatty acid shuttle in mycobacteria. *Nat. Microbiol.* **2016**, *1*, 15006.
(37) Remuinan, M. J.; Perez-Herran, E.; Rullas, J.; Alemparte, C.; Martinez-Hoyos, M.; Dow, D. J.; Afari, J.; Mehta, N.; Esquivias, J.; Jimenez, E.; Ortega-Muro, F.; Fraile-Gabaldon, M. T.; Spivey, V. L.; Loman, N. J.; Pallen, M. J.; Constantinidou, C.; Minick, D. J.; Cacho, M.; Rebollo-Lopez, M. J.; Gonzalez, C.; Sousa, V.; Angulo-Barturen, I.; Mendoza-Losana, A.; Barros, D.; Besra, G. S.; Ballell, L.; Cammack, N. Tetrahydropyrazolo[1,5-*a*]pyrimidine-3-carboxamide and *N*-benzyl-6′,7′-dihydrospiro[piperidine-4,4′-thieno[3,2-*c*]pyran] analogues with bactericidal efficacy against *Mycobacterium tuberculosis* targeting MmpL3. *PLoS One* **2013**, *8* (4), e60933.
(38) Li, W.; Upadhyay, A.; Fontes, F. L.; North, E. J.; Wang, Y. H.; Crans, D. C.; Grzegorzewicz, A. E.; Jones, V.; Franzblau, S. G.; Lee, R. E.; Crick, D. C.; Jackson, M. Novel insights into the mechanism of inhibition of MmpL3, a target of multiple pharmacophores in *Mycobacterium tuberculosis*. *Antimicrob. Agents Chemother.* **2014**, *58*, 6413−6423.
(39) Woods, G. L.; Brown-Eliott, B. A.; Conville, P. S.; Desmond, E. P.; Hall, G. S.; Lin, G.; Pfyffer, G. E.; Ridderhof, J. C.; Siddiqi, S. H.; Wallace, R. J. *Susceptibility Testing of Mycobacteria, Nocardiae and Other Aerobic Actinomycetes*, 2nd ed.; Approved Standard M24-A2; Clinical and Laboratory Standards Institute: Wayne, PA, 2011.
(40) Kremer, L.; Guerardel, Y.; Gurcha, S. S.; Locht, C.; Besra, G. S. Temperature-induced changes in the cell-wall components of *Mycobacterium thermoresistibile*. *Microbiology* **2002**, *148*, 3145−3154.
(41) Coxon, G. D.; Craig, D.; Corrales, R. M.; Vialla, E.; Gannoun-Zaki, L.; Kremer, L. Synthesis, antitubercular activity and mechanism of resistance of highly effective thiacetazone analogues. *PLoS One* **2013**, *8* (1), e53162.

DOI: 10.1021/acs.jmedchem.7b00582
J. Med. Chem. 2017, 60, 5876−5888

SUPPORTING INFORMATION

Targeting Mycolic Acid Transport by Indole-2-carboxamides for the Treatment of *Mycobacterium abscessus* Infections

Alan P. Kozikowski[a], Oluseye K. Onajole[a,b,#], Jozef Stec[c,d,#], Christian Dupont[e,#], Albertus Viljoen[e], Matthias Richard[e], Tridib Chaira[f,g], Shichun Lun[h], William Bishai[h], V. Samuel Raj[f], Diane Ordway[i], and Laurent Kremer[e,j*]*

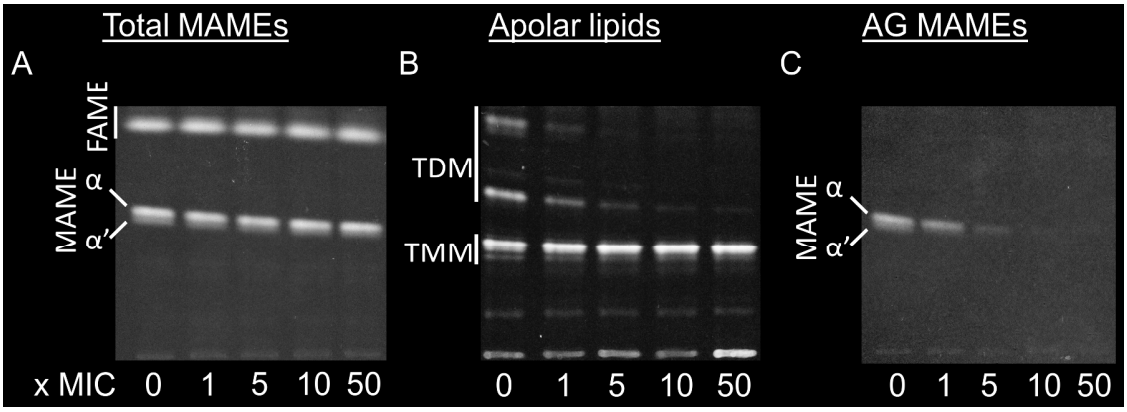

Figure S1. Mycolic acid profile is affected by treatment with compound 6. Exponentially growing *M. abscessus* S was incubated with increasing concentrations of **6** in 7H9^{OADC} at 37 °C with agitation for 1 h. Subsequently bacteria were labeled with [^{14}C]acetate for 2 h at 37 °C with agitation. The cultures were split, and from the first volume were extracted the total methyl esters of mycolates (MAME) and fatty acids (FAME). From the second volume, apolar and polar fractions were obtained prior to derivatization of arabinogalactan MAME. **A:** Equal counts (50,000 cpm) of the MAME and FAME fractions was loaded on a TLC plate and resolved once using the solvent system petroleum ether/acetone (95:5, v/v). **B:** The apolar fraction was loaded (50,000 cpm), and TMM/TDM were visualized on a 1D TLC plate using the solvent system chloroform/methanol/water (40:8:1, v/v/v). **C:** Equal volumes of the arabinogalactan MAME fractions were loaded, and α- and α'-mycolic acids were visualized on a 1D TLC plate using the solvent system petroleum ether/acetone (95:5, v/v).

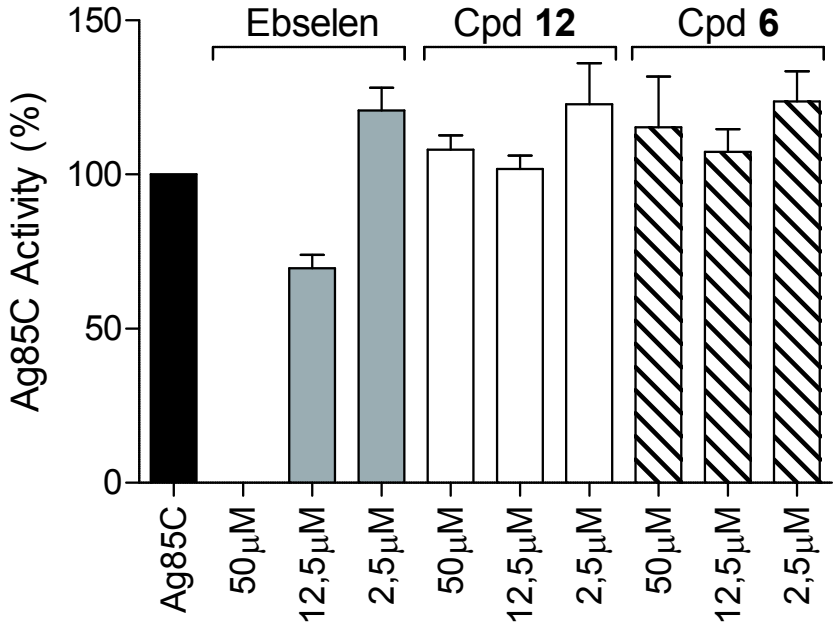

Figure S2. Effect of inhibitors on Ag85C activity. Purified Ag85C (FbpC2) containing a C-terminal His tag was produced in *E. coli* C41(DE3) carrying pET23b_*fbpC2*[34] and incubated with 2.5, 12.5, and 50 µM of compound **6**, compound **12**, or ebselen at room temperature for 1 h. The enzymatic activity of Ag85C in the presence or absence of the different inhibitors was tested using a fluorescence-based assay performed at 35 °C for 15 min in 50 mM sodium phosphate buffer (pH 6.0) containing 4 mM trehalose, 12.5 µM resorufin butyrate, and 5.5 µM of Ag85C. The inhibitory effect was determined at the maximum rate of the reaction. The activity of the enzyme in the absence of inhibitor was arbitrarily placed at 100%. Error bars represent standard error of the mean calculated from three independent experiments.

Annexe 2

« Cyclipostins and cyclophostin analogs inhibit the antigen 85C from *Mycobacterium tuberculosis* both *in vitro* and *in vivo*. »Viljoen A *, Richard M *, Nguyen PC, Fourquet P, Camoin L, Paudal RR, Gnawali GR, Spilling CD, Cavalier JF, Canaan S, Blaise M, Kremer L. (* = contribution égale) J Biol Chem. 2018 Feb 23;293(8):2755-2769

JBC ARTICLE

Cyclipostins and cyclophostin analogs inhibit the antigen 85C from *Mycobacterium tuberculosis* both *in vitro* and *in vivo*

Received for publication, November 2, 2017, and in revised form, December 5, 2017 Published, Papers in Press, January 4, 2018, DOI 10.1074/jbc.RA117.000760

Albertus Viljoen[‡1], Matthias Richard[‡1], Phuong Chi Nguyen[§¶2], Patrick Fourquet[‖], Luc Camoin[‖], Rishi R. Paudal[**], Giri R. Gnawali[**], Christopher D. Spilling[**], Jean-François Cavalier[§¶], Stéphane Canaan[§¶], Mickael Blaise[‡3], and Laurent Kremer[‡ ‡‡4]

From the [‡]Institut de Recherche en Infectiologie de Montpellier (IRIM), Université de Montpellier, CNRS UMR9004, 34293 Montpellier, France, [‡‡]INSERM, IRIM, 34293 Montpellier, France, [§]Aix-Marseille Université, CNRS, EIPL, IMM FR3479, 13009 Marseille, France, [¶]Aix-Marseille Université, CNRS, LISM, IMM FR3479, 13009 Marseille, France, [‖]Aix Marseille Université, CNRS, INSERM, Institut Paoli-Calmettes, CRCM, Marseille Protéomique, 13009 Marseille, France, and the [**]Department of Chemistry and Biochemistry, University of Missouri, St. Louis, Missouri 63121

Edited by Chris Whitfield

An increasing prevalence of cases of drug-resistant tuberculosis requires the development of more efficacious chemotherapies. We previously reported the discovery of a new class of cyclipostins and cyclophostin (CyC) analogs exhibiting potent activity against *Mycobacterium tuberculosis* both *in vitro* and in infected macrophages. Competitive labeling/enrichment assays combined with MS have identified several serine or cysteine enzymes in lipid and cell wall metabolism as putative targets of these CyC compounds. These targets included members of the antigen 85 (Ag85) complex (*i.e.* Ag85A, Ag85B, and Ag85C), responsible for biosynthesis of trehalose dimycolate and mycolylation of arabinogalactan. Herein, we used biochemical and structural approaches to validate the Ag85 complex as a pharmacological target of the CyC analogs. We found that $CyC_{7\beta}$, $CyC_{8\beta}$, and CyC_{17} bind covalently to the catalytic Ser^{124} residue in Ag85C; inhibit mycolyltransferase activity (*i.e.* the transfer of a fatty acid molecule onto trehalose); and reduce triacylglycerol synthase activity, a property previously attributed to Ag85A. Supporting these results, an X-ray structure of Ag85C in complex with $CyC_{8\beta}$ disclosed that this inhibitor occupies Ag85C's substrate-binding pocket. Importantly, metabolic labeling of *M. tuberculosis* cultures revealed that the CyC compounds impair both trehalose dimycolate synthesis and mycolylation of arabinogalactan. Overall, our study provides compelling evidence that CyC analogs can inhibit the activity of the Ag85 complex *in vitro* and in mycobacteria, opening the door to a new strategy for inhibiting Ag85. The high-resolution crystal structure obtained will further guide the rational optimization of new CyC scaffolds with greater specificity and potency against *M. tuberculosis*.

This work was supported by Fondation pour la Recherche Médicale (FRM) Grants DEQ20150331719 (to L. K.) and ECO20160736031 (to M. R.) and by CNRS and INSERM. The authors declare that they have no conflicts of interest with the contents of this article.

The atomic coordinates and structure factors (code 5OCJ) have been deposited in the Protein Data Bank (http://wwpdb.org/).

[1] Both authors contributed equally to this work.

[2] Supported by the Ph.D. Training program of the University of Science and Technology of Hanoi.

[3] To whom correspondence may be addressed. Tel.: 33-4-34-35-94-47; E-mail: mickael.blaise@irim.cnrs.fr.

[4] To whom correspondence may be addressed. Tel.: 33-4-34-35-94-47; E-mail: laurent.kremer@irim.cnrs.fr.

With 10.4 million new cases and 1.8 million deaths in 2016, tuberculosis (TB)[5] continues to be a major global health problem. TB is caused by *Mycobacterium tuberculosis*, a resilient microorganism that persists through long courses of antibiotics and years of dormancy within the host. The emergence of multidrug-resistant and extensively drug-resistant TB has contributed to the difficulties in treating this bacterial infection (1). Chemotherapeutic treatments against TB remain very challenging and complicated, essentially because of the slow rate of growth of the bacilli and the presence of a thick, greasy, and relatively drug-impermeable cell wall (2). This mycobacterial cell wall consists of a complex skeleton comprising covalently linked macromolecules, such as peptidoglycan, arabinogalactan, and mycolic acids, in which non-covalently associated glycolipids are interspersed (3). The mycolic acid portion of the envelope is composed of very long fatty acids (C70–90) that are either covalently attached to the arabinan moiety of the arabinogalactan (AG) polymer or found esterified to trehalose as trehalose monomycolate (TMM) or trehalose dimycolate (TDM). Because several key antitubercular drugs, such as isoniazid, SQ109, delamanid, or ethambutol, target different aspects of the biosynthetic steps responsible for the cell wall attachment of mycolic acids (4–7), this pathway is of particular interest from a drug discovery perspective.

The three functionally and structurally related members of the antigen 85 complex, designated Ag85A, -B, and -C, are among the most abundantly secreted proteins in *M. tuberculosis* (8). These enzymes are responsible for the biosynthesis of TMM and TDM as well as the covalent attachment of mycolic acids to AG (9–11). Deletion of *fbpC2*, encoding Ag85C, resulted in a 40% decrease in the AG-bound mycolic acids but failed to affect the production of non-covalently linked myco-

[5] The abbreviations used are: TB, tuberculosis; AG, arabinogalactan; CyC, cyclipostins and cyclophostin; DGAT, diacylglycerol acyltransferase; FAME, fatty acid methyl ester; MAME, mycolic acid methyl ester(s); MIC, minimal inhibitory concentration; TAG, triacylglycerol; TDM, trehalose dimycolate; TLC, thin layer chromatography; TMM, trehalose monomycolate; x_{150}, inhibitor molar excess leading to 50% inhibition; FP, fluorophosphonate; DTNB, 5,5′-dithio-bis-(2-nitrobenzoic acid); DEP, *p*-nitrophenyl phosphate; TAMRA, carboxytetramethylrhodamine; ILI, intracellular lipid inclusion; r.m.s., root mean square; PDB, Protein Data Bank.

lates (10), whereas deletion of *fbpA* or *fbpB*, encoding Ag85A and Ag85B, respectively, led to reduced TDM levels (12–14), implying that although a level of functional redundancy exists *in vivo* between the three members, the contribution of each member is significant. The lack of double and triple knockout mutants might indicate that the loss of two or more Ag85 enzymes is detrimental to *M. tuberculosis* viability. An additional isoform, designated Ag85D or MPT51, has been characterized but found to be inactive due to the lack of catalytic elements required for mycolyltransferase activity (11, 15, 16). Ag85A/B/C share the same mycolic acid donor TMM, and their crystal structures present a highly conserved catalytic site, which further supports their similar enzymatic role (17–19).

Due to their importance in mycolic acid metabolism, the Ag85 enzymes have often been proposed as attractive targets for future chemotherapeutic developments against TB (9, 20–22). Because of their high structural conservation, it can be inferred that a single compound may inhibit all three enzymes of the complex at the same time and would make improbable the development of resistance to inhibitors, because resistant mutants would require the simultaneous acquisition of mutations in at least two *fbp* genes. In addition, because these proteins are secreted, targeting the Ag85 complex will minimize the effect of efflux mechanisms that may result in resistance phenotypes. Early inhibitors, such as trehalose analogs, were first designed as Ag85 inhibitors but were found to exhibit relatively poor activity on whole mycobacterial cells (9, 23). Another potentially selective fluorophosphonate α,α-D-trehalose inhibitor of the three antigen 85 enzymes has been reported to form a stable, covalent complex with the Ag85 enzyme following nucleophilic attack on the phosphorus atom of the catalytic Ser^{124} (24). In the same manner, the 2-amino-6-propyl-4,5,6,7-tetrahydro-1-benzothiophene-3-carbonitrile, designated I3-AG85, inhibits Ag85C, and exposure of *M. tuberculosis* to this compound was associated with reduced survival rates in broth medium and in infected primary macrophages. Moreover, I3-AG85 was active against a panel of multidrug-resistant/extensively drug-resistant strains, although it exhibited an MIC of 100 μM (25). By combining fragment-based drug discovery with early whole cell antibacterial screening, tetrahydro-1-benzothiophene analogs were discovered as potent Ag85C inhibitory molecules against drug-susceptible and drug-resistant *M. tuberculosis* strains (26). The selenazole compound ebselen (2-phenyl-1,2-benzisoselenazol-3(2H)-one) was found to inhibit the activity of Ag85C through an original mechanism by reacting with the conserved Cys^{209} residue located near the active site of the enzyme but not involved in the catalytic activity (27, 28). Ebselen was shown to directly impede the production of TDM and mycolylation of AG (27).

Recently, cyclipostins and cyclophostin (CyC), representing a new class of monocyclic enolphosph(on)ate compounds, have been discovered to act as powerful antitubercular agents affecting growth of *M. tuberculosis* both *in vitro* and in infected macrophages (29). Among the set of 27 CyC analogs previously evaluated against *M. tuberculosis* H37Rv, eight compounds exhibited potent anti-tubercular activities, particularly the cyclophostin analogs $CyC_{7\beta}$ and $CyC_{8\beta}$ as well as the cyclipostins-related molecule CyC_{17}. Whereas $CyC_{7\beta}$ exhibited a strong activity against extracellular and intracellular mycobacteria (MIC_{50} of 16.6 and 3.1 μM, respectively), $CyC_{8\beta}$ was mostly found to be active against intracellular bacteria (MIC_{50} ~ 11.7 μM). In contrast, CyC_{17} was a potent inhibitor of *in vitro* growth (MIC_{50} ~ 0.5 μM) but failed to show activity against intracellular bacilli (29). To identify the putative target(s) of the CyC inhibitors, an activity-based protein profiling approach was used based on TAMRA-FP and desthiobiotin-FP probes and mass spectrometry analyses. This led to the capture of several active serine/cysteine enzymes in a complex proteome before mass spectrometry identification, among which Ag85A (Rv3804c) and Ag85C (Rv0129c) were identified.

The present study was undertaken to further explore and validate, through a combination of biochemical and structural approaches, the specificity of inhibition of the Ag85 activity by the CyC analogs, to determine their mode of action and to describe how they affect the mycolic acid profile in *M. tuberculosis*.

Results

CyC analogs inhibit TDM biosynthesis and transfer of mycolic acids to arabinogalactan in M. tuberculosis

CyCs are a new class of compounds demonstrating potent antitubercular activity, presumably involving inhibition of the Ag85 activity (29). The chemical structures of the cyclophostin analogs $CyC_{7\beta}$ and $CyC_{8\beta}$ and the cyclipostins CyC_{17} used in this study are provided in Fig. 1*A*. To test whether treatment with these CyCs alters the mycolic acid composition of *M. tuberculosis* mc^26230, cultures were exposed to increasing concentrations of CyC_{17} or $CyC_{7\beta}$, the two inhibitors most active against extracellularly replicating *M. tuberculosis* (29), followed by metabolic labeling with sodium [2-^{14}C]acetate and lipid analysis. Extraction and separation of the total mycolic acid methyl esters (MAME) by thin layer chromatography (TLC) revealed that neither CyC_{17} nor $CyC_{7\beta}$ altered the *de novo* biosynthesis of mycolic acid (Fig. 1 (*B* and *C*), *left*). In contrast, separation of the apolar lipid fraction by TLC showed a dose-dependent decrease in TDM levels associated with a concomitant increase in the production of TMM, which is the natural substrate of the Ag85 proteins (Fig. 1 (*B* and *C*), *middle*). To address whether CyC treatment also impacts the cell wall-bound mycolic acids, radiolabeled mycolic acids were extracted from delipidated bacteria (30). The autoradiography/TLC analysis confirmed a dose-dependent inhibition of [2-^{14}C]acetate incorporation into all three forms of the AG-attached mycolic acids (α, methoxy, and keto), suggesting that treatment with CyC_{17} or $CyC_{7\beta}$ inhibits AG mycolylation at low concentrations (Fig. 1 (*B* and *C*), *right*). A quantitative analysis of these effects is provided in the corresponding graphs (Fig. 1, *B* and *C*).

Overall, this suggests that *in vivo* inhibition of the mycolyltransferase activity by the CyC compounds results in decreased formation of the virulence-associated TDM and reduced transfer of mycolic acids onto the essential cell wall AG.

Covalent inhibition of the Ag85C mycolyltransferase activity

All three members of the Ag85 complex, sharing between 65 and 75% sequence identity, have been shown to possess a serine

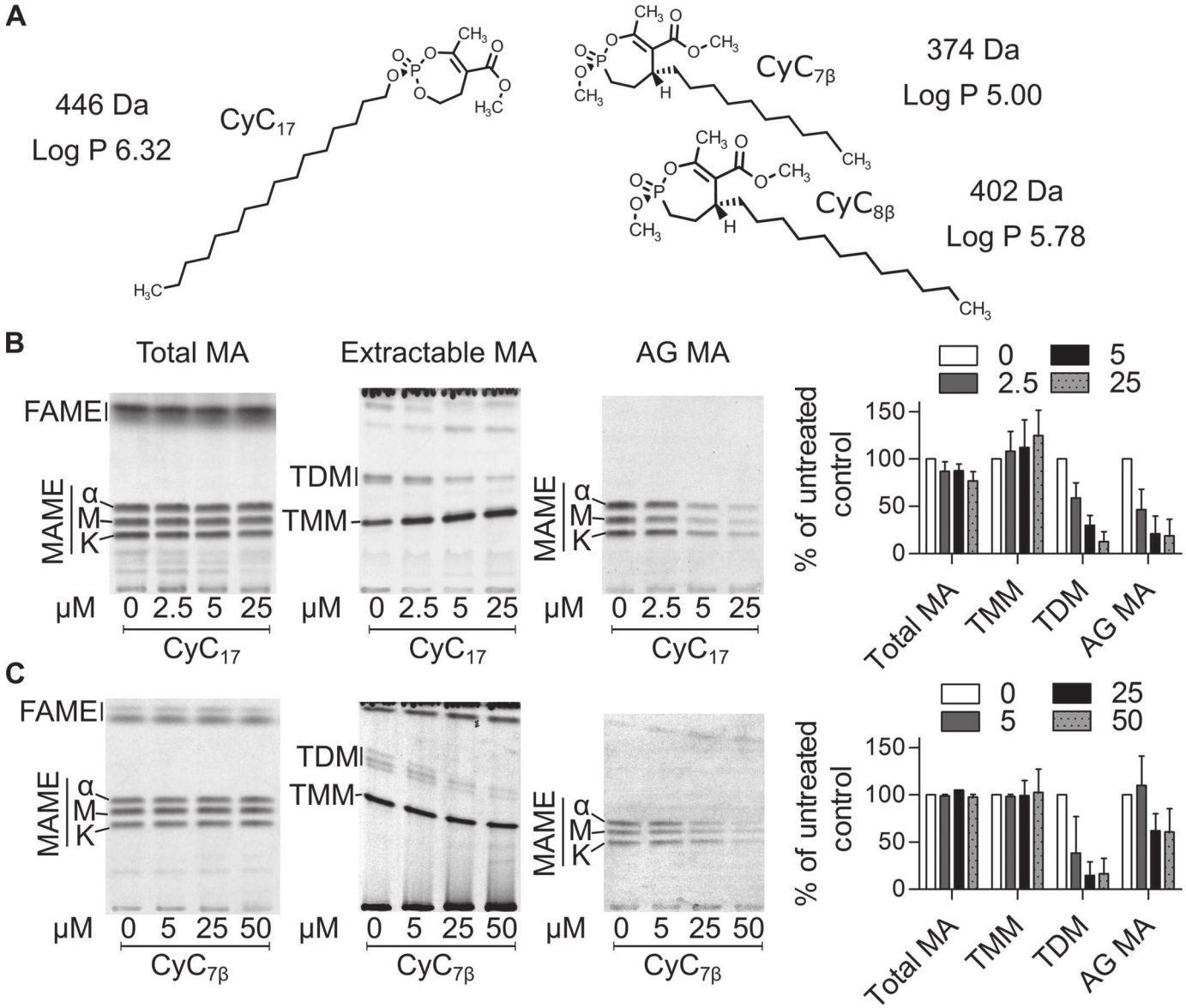

Figure 1. Ag85 complex mycolyltransferase activity is inhibited by CyC analogs *in vivo*. Exponentially growing *M. tuberculosis* mc^{2}6230 was incubated with increasing concentrations of CyC_{17} or $CyC_{7\beta}$ in 7H9$^{OADC/Tween\ 80}$ at 37 °C with agitation for 1 h. Subsequently, bacteria were labeled with sodium [2-^{14}C]acetate for 6 h at 37 °C with agitation. The cultures were split, and from the first volume were extracted the total methyl esters of mycolates (MAME) and fatty acids (FAME). From the second volume, apolar and polar lipid fractions were obtained before derivatization of arabinogalactan MAME. *A*, chemical structures of the CyC analogs used in this study. *B* and *C*, effect of CyC_{17} (*B*) or $CyC_{7\beta}$ (*C*) treatment on the mycolic acid profiles of *M. tuberculosis* mc^{2}6230. Equal counts (50,000 cpm) of MAME + FAME fraction were loaded on a TLC plate and resolved once using the solvent system hexane/ethyl acetate (95:5, v/v) run twice (*far left*). The apolar fraction was loaded (50,000 cpm), and TMM and TDM were visualized on a 1D TLC plate using the solvent system chloroform/methanol/water (40:8:1, v/v/v) (*middle left*). Equal volumes of arabinogalactan MAME fraction were loaded, and α, methoxy, and keto mycolic acids were visualized on a 1D TLC plate using the solvent system hexane/ethyl acetate (95:5, v/v) run twice (*middle right*). Densitometric analysis (*far right*) was performed on the TLCs shown in the left panels. *Histograms* and *error bars*, means and S.D. values calculated from at least two independent experiments.

hydrolase mycolyl esterase/transferase activity (17–19). To test the hypothesis that CyC analogs inhibit the activity of the three Ag85 members, we first cloned *Ag85C* (*fbpcC2*) into pET23b, and the recombinant protein was produced in *Escherichia coli*. The protein was then purified from lysates of *E. coli* by successive nickel-affinity, anion-exchange, and size-exclusion chromatography steps, leading to 3 mg of pure protein/liter of culture. Using a recently developed fluorescent assay based on resorufin butyrate as the acyl donor for Ag85C and trehalose as the acyl acceptor (27), we investigated whether $CyC_{7\beta}$, $CyC_{8\beta}$, and CyC_{17} inhibit the acyltransferase activity onto trehalose. In each case, a dose-dependent inhibition was observed with all three compounds, with $CyC_{8\beta}$ being the most efficient inhibitor (IC_{50} of 15 ± 5 μM), followed by $CyC_{7\beta}$ (IC_{50} of 43 ± 3 μM) and CyC_{17} (IC_{50} of 98 ± 6 μM) (Fig. 2*A*). Moreover, in terms of molar excess of inhibitor ($x_{150} = IC_{50}/[Ag85C]$) (31), all three CyCs react almost in stoichiometry with pure Ag85C, as judged by their respective x_{150} values of around 0.3, 0.8, and 1.8, respectively.

To address the inhibitory effect on the mycolyltransferase assay, Ag85C (55 μM) was next incubated for 30 min in its native form with 500 μM (*i.e.* enzyme/inhibitor molar ratio of 1:9) of each CyC compound. As expected, the complete loss of activity was confirmed by comparing the pretreated *versus* non-treated

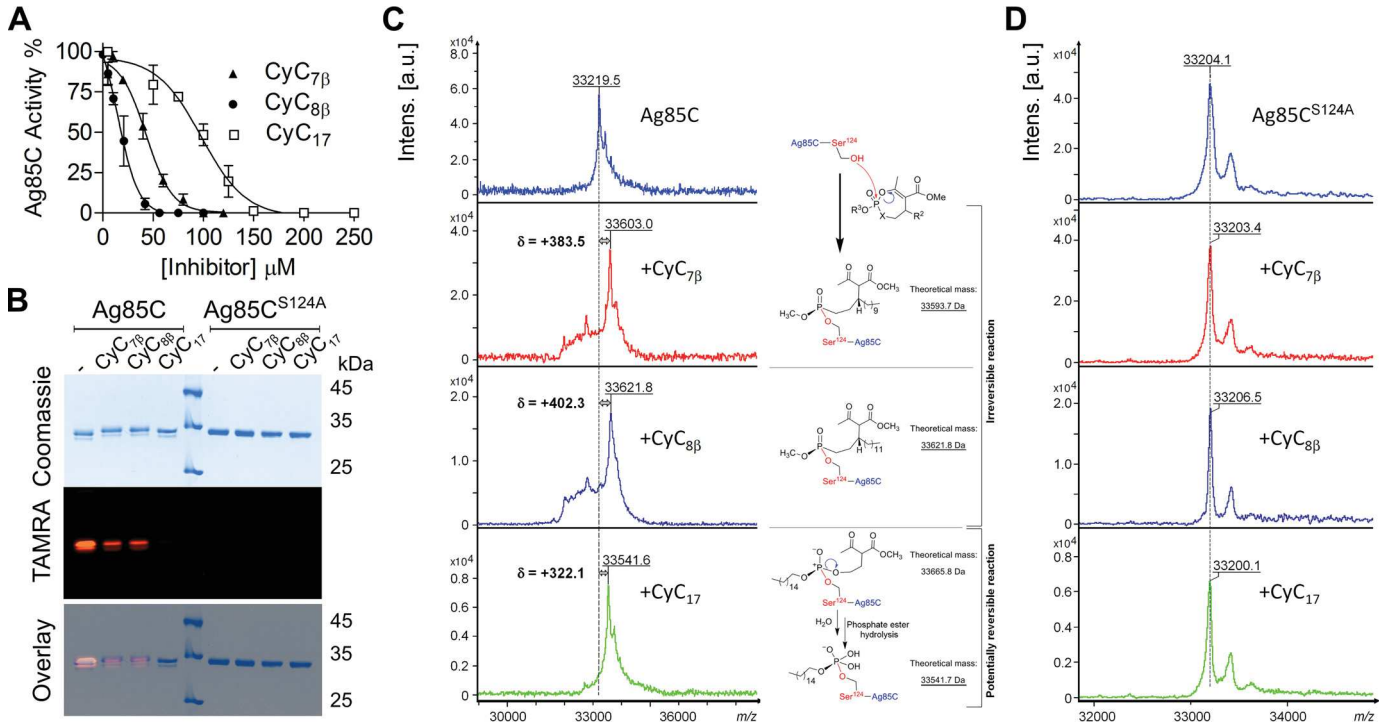

Figure 2. Inhibition of the Ag85C mycolyltransferase activity is mediated by the covalent binding of CyC analogs. *A*, the enzymatic activity of Ag85C was tested using a fluorescence-based assay in the presence of different concentrations of $CyC_{7\beta}$, $CyC_{8\beta}$, and CyC_{17}. The inhibitory effect was determined at the maximum rate of the reaction. *Error bars*, S.D. calculated from three independent experiments. *Curves* for $CyC_{7\beta}$, $CyC_{8\beta}$, and CyC_{17} were fitted using the EC_{50} shift non-linear regression model in GraphPad Prism with R^2 values of 0.9675, 0.9508, and 0.9415, respectively. *B*, equal amounts of either Ag85C or $Ag85C^{S124A}$ were pretreated with $CyC_{7\beta}$, $CyC_{8\beta}$, and CyC_{17}; incubated with TAMRA-FP, separated by SDS-PAGE; and visualized by Coomassie Blue staining (*top*) or in-gel fluorescence visualization (*middle*). The *merged image* is shown at the *bottom*. TAMRA labeling of Ag85C is prevented by the covalent binding of the CyC analogs to the catalytic Ser^{124}. No TAMRA-FP labeling is seen for the $Ag85C^{S124A}$ variant, confirming Ser^{124} as the TAMRA-binding site. *C* and *D*, global mass modification of Ag85C (*C*) and $Ag85C^{S124A}$ (*D*) preincubated with $CyC_{7\beta}$, $CyC_{8\beta}$, and CyC_{17} as determined using an Ultraflex III mass spectrometer (Bruker Daltonics) in linear mode with the LP_66 kDa method. The mechanism of action of the phosphonates $CyC_{7\beta}$ and $CyC_{8\beta}$ and of the phosphate analog CyC_{17} based on mass spectrometry analyses is illustrated in *C*. *a.u.*, arbitrary units.

Ag85C. All three Ag85C-CyC adducts were treated with 10 μM TAMRA-FP fluorescent probe, known to bind to serine enzymes (32), for 1 h, and equal amounts of proteins were separated by SDS-PAGE and visualized by Coomassie staining (Fig. 2*B*, *top*) or in-gel fluorescence for TAMRA detection (Fig. 2*B*, *middle*). Pretreatment with either $CyC_{7\beta}$ or $CyC_{8\beta}$ resulted in a significant loss in fluorescence intensity (about 75%) as compared with the non-treated protein, whereas incubation with CyC_{17} abrogated TAMRA labeling. This suggests that reaction with the TAMRA probe is strongly impaired in the Ag85C-CyC adducts, resulting in a decrease/loss of fluorescence emission. To determine the implication of the conserved catalytic Ser^{124} in Ag85C in TAMRA labeling, this residue was replaced by an Ala residue, and the mutated protein was purified (Fig. 2*B*, *top*). Exposure of TAMRA to $Ag85C^{S124A}$ failed to produce a fluorescence signal (Fig. 2*B*, *middle*), indicating that the catalytic Ser^{124} is required for binding of the probe. As expected, no fluorescence emission was observed when pretreating the mutated protein with the CyC analogs (Fig. 2*B*, *bottom*).

MALDI-TOF mass spectrometry was further used to study the (covalent) nature of the inhibition. Mass increments of +383.5 and +402.3 Da in the presence of $CyC_{7\beta}$ and $CyC_{8\beta}$, respectively, were observed within the global mass of treated Ag85C as compared with the global mass of untreated Ag85C (Fig. 2*C*). In contrast, no changes in the global mass were observed with the inactive $Ag85C^{S124A}$ protein (Fig. 2*D*). These data thus support the formation of a covalent Ag85C-CyC complex, as the reaction between the catalytic Ser^{124} and either $CyC_{7\beta}$ or $CyC_{8\beta}$ is expected to yield mass increases of +374.2 or +402.25 Da, respectively. Moreover, such results are consistent with the known and irreversible classical mechanism of action of phosphonate compounds, as demonstrated using pure mycobacterial lipolytic enzymes (31).

With respect to CyC_{17}, the observed 322.1-Da mass shift increment was 124.18 Da lower than its expected theoretical molecular mass of 446.28 Da (Fig. 2*C*). This size difference may arise from the specific chemical properties of phosphate (*i.e.* CyC_{17}) *versus* phosphonate (*i.e.* $CyC_{7\beta}$ and $CyC_{8\beta}$) chemical groups. In all cases, the nucleophilic attack of catalytic Ser^{124} at the phosphorus center induces ring opening. However, the reaction with CyC_{17} is very likely to form a new phosphate triester, which in turn becomes susceptible to hydrolysis. From these findings, it can be inferred that once the CyC_{17}-Ser^{124} adduct is formed, it becomes rapidly hydrolyzed in the presence of water, resulting in the cleavage and release of the methyl 2-acetyl-4-hydroxybutyrate (*i.e.* 124.1 Da), accounting exactly for the molecular mass discrepancy observed experimentally (Fig. 2*C*).

Taken together, these findings conclusively indicate that Ag85C is covalently modified by CyC analogs, leading to the inhibition of the mycolyltransferase activity and thus supporting the *in vivo* alteration of the mycolic acid pattern by these compounds.

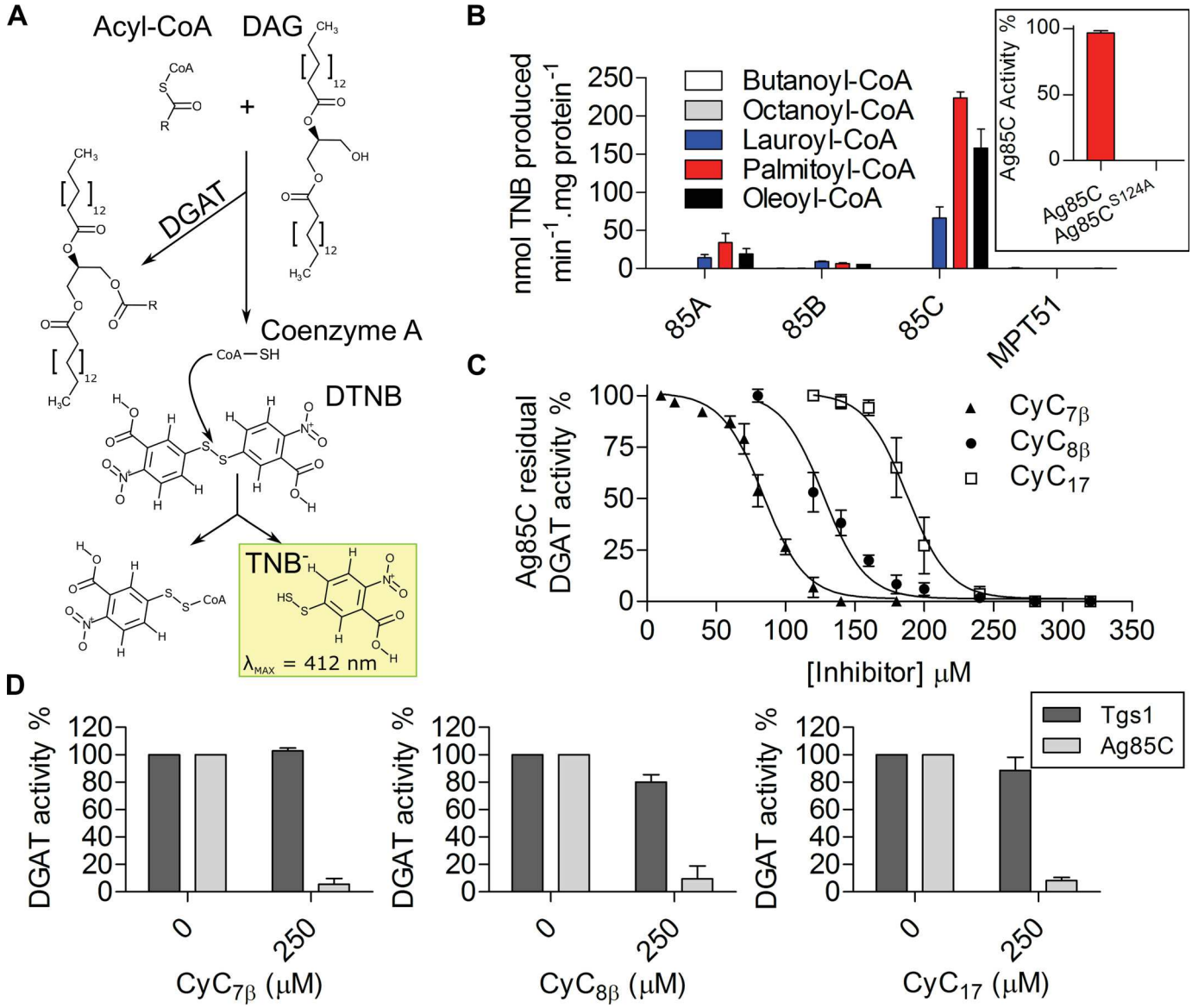

Figure 3. DGAT activity of the antigen 85 complex and inhibition by CyC analogs. *A*, chemical reaction occurring while determining the DGAT activity. DTNB reacts with the free-thiol group coming from the release of SH-CoA during the formation of TAG from 1,2-dipalmitoylglycerol (*DAG*) and a molecule of acyl-CoA. *B*, comparison of the DGAT activity of Ag85A, Ag85B, Ag85C, and MPT51. Enzymatic activity was determined by the colorimetry-based assay illustrated in *A*. *Inset*, activity of the wildtype and S124A Ag85C proteins using palmitoyl-CoA (*C16*) as acyl donor molecule. *Error bars*, S.D. calculated from three independent experiments. *C*, inhibitory effect of CyC analogs on Ag85C DGAT activity. Inhibition was performed with increasing concentrations of $CyC_{7\beta}$, $CyC_{8\beta}$, and CyC_{17} using the colorimetry-based assay illustrated in *A*. The inhibitory effect was determined after 1 h of reaction. *Error bars*, S.D. calculated from three independent experiments. Curves for $CyC_{7\beta}$, $CyC_{8\beta}$, and CyC_{17} were fitted using the EC_{50} shift non-linear regression model on GraphPad with R^2 values of 0.9755, 0.9641, and 0.9422, respectively. *D*, comparison of the DGAT activity of Ag85C and Tgs1 in the absence or presence of $CyC_{7\beta}$, $CyC_{8\beta}$, and CyC_{17}.

Ag85A, -85B, and -85C express DGAT activity

Although the mycolyltransferase activity of the Ag85 complex has been established for a long time (8, 9), more recent work suggested that Ag85A mediates the transesterification of diacylglycerol using long-chain acyl-CoA to produce triglycerides (TAG), which act as storage compounds for energy and carbon (33). Ag85A contains the same catalytic triad as Ag85C or Ag85B, formed by residues Ser^{126}, His^{262}, and Glu^{230}, and possesses a deep substrate-binding groove near the active-site serine, suggesting that Ag85B and Ag85C, similarly to Ag85A, may also express diacylglycerol acyltransferase (DGAT) activity. To test this hypothesis, all of the genes were cloned into pET23b, and the recombinant proteins were produced in *E. coli* and purified from lysates by successive nickel-affinity, anion-exchange, and size-exclusion chromatography steps. Because Ag85B was poorly expressed in *E. coli*, a synthetic gene was produced by replacing low-usage codons with high-usage codons, as reported previously (34) and subsequently cloned into pET23a. All three proteins were assayed for DGAT activity in the presence of acyl-CoA with various chain lengths (from C4 to C18) as acyl donors and 1,2-dipalmitoyl-*sn*-glycerol (1,2-dipalmitin) as the acyl acceptor, as illustrated in Fig. 3*A*. Transesterification in the presence of 5,5′-dithio-bis-(2-nitrobenzoic acid) (DTNB) leads to the formation of TNB, which can readily be measured at 412 nm (33, 35). In agreement with previous findings, Ag85A was found to express DGAT activity, but such

an activity was only detected with C12-C18 acyl-CoAs (Fig. 3*B*). Whereas Ag85B demonstrated lower activity than Ag85A, Ag85C showed the highest activity, which was optimal in the presence of C16-CoA. No activity was detected with the C4- or C8-containing acyl chains. We also expressed and purified the Ag85 complex-related MPT51 (FbpC1) protein, which possesses an overall structure similar to that of the Ag85 complex members but is defective in the catalytic elements required for mycolyltransferase activity (11, 16). As anticipated, MPT51 failed to express any DGAT activity, suggesting that residues important for mycolyltransferase activity are also key players in the DGAT activity, as proposed earlier for the Ser^{126} in Ag85A (33). Purified $Ag85C^{S124A}$ was next assayed with various acyl-CoA substrates, and, as shown in Fig. 3*B* (*inset*), the DGAT activity was abrogated in the mutant protein, implying that Ser^{124} plays a critical role in the enzymatic reaction.

Overall, these data extend insights from previous findings and indicate that all three members of the Ag85 complex express DGAT activity, with Ag85C exhibiting the most pronounced activity. This suggests that Ag85C may also make an important contribution in TAG synthesis in *M. tuberculosis*.

CyC analogs inhibit the in vitro DGAT activity of Ag85C but not of Tgs1

The above-mentioned results prompted us to investigate whether CyC analogs alter the DGAT activity of Ag85C. This was achieved by incubating the purified enzyme in the presence of increasing concentrations of $CyC_{7\beta}$, $CyC_{8\beta}$, and CyC_{17} using the colorimetric activity assay described in the legend to Fig. 3*A*. As expected from the previous results on the inhibition of mycolyltransferase activity, a dose-dependent inhibition of the DGAT activity with all three compounds was also observed (Fig. 3*C*). $CyC_{7\beta}$ appeared as the most potent inhibitor, with an IC_{50} value of 85 ± 2 μM (*i.e.* $x_{I50} = 2.8$), followed by $CyC_{8\beta}$ and CyC_{17} exhibiting IC_{50} values of 121 ± 4 μM (*i.e.* $x_{I50} = 4.0$) and 187 ± 3 μM (*i.e.* $x_{I50} = 6.2$), respectively.

Because the TAG synthase *tgs1* in *M. tuberculosis* and *Mycobacterium abscessus* has been reported as the major contributor of TAG accumulation in the form of intracellular lipid inclusions (ILIs) in these two species (35, 36), we addressed whether the DGAT activity of Tgs1 may also be targeted by the CyC analogs. Tgs1 from *M. tuberculosis* (Rv3130c) was expressed and purified from *E. coli* and subsequently used in a DGAT assay in the absence or presence of either $CyC_{7\beta}$, $CyC_{8\beta}$, or CyC_{17} (Fig. 3*D*). Whereas the activity of Tgs1 remained intact even in the presence of a 250 μM concentration of each compound, the DGAT activity of Ag85C assayed in the same conditions was almost abrogated, suggesting that Tgs1 activity is not impacted by CyC treatment.

These results indicate that CyC analogs specifically inhibit the DGAT activity of Ag85C but not of Tgs1 *in vitro*, in agreement with the fact that members of the Tgs family were not identified in our original proteomic profiling study (29).

Overexpressing Ag85C in M. tuberculosis is associated with reduced inhibition of TAG production by CyC_{17}

That Ag85C expresses the highest DGAT activity among the three members of the Ag85 complex prompted us to address whether overexpression of Ag85C in *M. tuberculosis* affects the TAG content. *M. tuberculosis* was first transformed with either pMV261-Ag85C or pMV261-$Ag85C^{S124A}$. Overexpression of either the wildtype or the catalytically dead proteins was checked by quantitative real-time PCR (Fig. 4*A*, *left*) and by immunoblotting using two different monoclonal antibodies and purified Ag85A, -B, and -C as positive controls (Fig. 4*A*, *right*). The 17/4 monoclonal antibody recognizes a well-conserved epitope present in Ag85A and Ag85B but not in Ag85C (37). In contrast, the 32/15 antibody revealed all three antigens and the presence of more pronounced bands in the pMV261-Ag85C and pMV261-$Ag85C^{S124A}$ lysates, which, by comparison with the 17/4 blot, could clearly be attributed to Ag85C (Fig. 4*B*, *right*). This indicates that both Ag85C variants were overproduced at comparable transcriptional and translational levels and allowed us to investigate whether this may affect the intracellular TAG content of *M. tuberculosis* (38). TAGs are often stored in the form of ILIs, which can be visualized by staining with Nile Red (39, 40). As shown in Fig. 4*B* (*left*), although a punctiform labeling corresponding to ILIs is observed in the control strain carrying the empty pMV261, Nile Red straining was much more pronounced in the strain overproducing Ag85C, and the effect returned to control levels in the strain harboring pMV261-$Ag85C^{S124A}$. Quantification of the fluorescence intensity over the entire length of the individual bacilli from each strain clearly indicates that large and numerous ILIs were present in the Ag85C-overexpressing strain, as compared with the control and $Ag85C^{S124A}$ strains (Fig. 4*B*, *right*).

To check whether enhanced ILI formation coincided with increased *de novo* biosynthesis of TAG, metabolic labeling of *M. tuberculosis* cultures with sodium [2-^{14}C]acetate was performed, followed by extraction and separation of the apolar lipid fraction by TLC. In the absence of CyC treatment, the strain carrying pMV261-Ag85C produced moderately higher amounts of TAGs than the control strain containing the empty pMV261 or the strain overexpressing $Ag85C^{S124A}$ (Fig. 4*C*, *left*), supporting the *in vivo* contribution of Ag85C in TAG production. Importantly, exposure to CyC_{17} inhibited TAG biosynthesis in a dose-dependent manner in the control strain, thus implying that the *de novo* biosynthesis of TAG is also targeted by CyC_{17} (Fig. 4*C*). In addition, a less pronounced decrease in TAG production occurred in the strain overexpressing Ag85C as compared with the control strain, presumably because of the inherent capacity of this strain to synthesize more TAG that partially overcomes CyC_{17} inhibition (Fig. 4*C*). Collectively, these results suggest that TAG production in *M. tuberculosis* is inhibited by CyC_{17} and that this is dependent upon Ag85C DGAT activity.

Crystal structure of the $CyC_{8\beta}$-bound Ag85C

To gain insight into the mode of action of the CyC compounds, crystallization studies of Ag85C were undertaken in the presence of the three CyC inhibitors. However, diffracting crystals were only obtained with $CyC_{8\beta}$ for which the X-ray structure of Ag85C bound to $CyC_{8\beta}$ was solved at a resolution of 1.8 Å (Table 1). The asymmetric unit contains two molecules of Ag85C (Fig. 5*A*). Residues 6–282 and 8–282 for each subunit

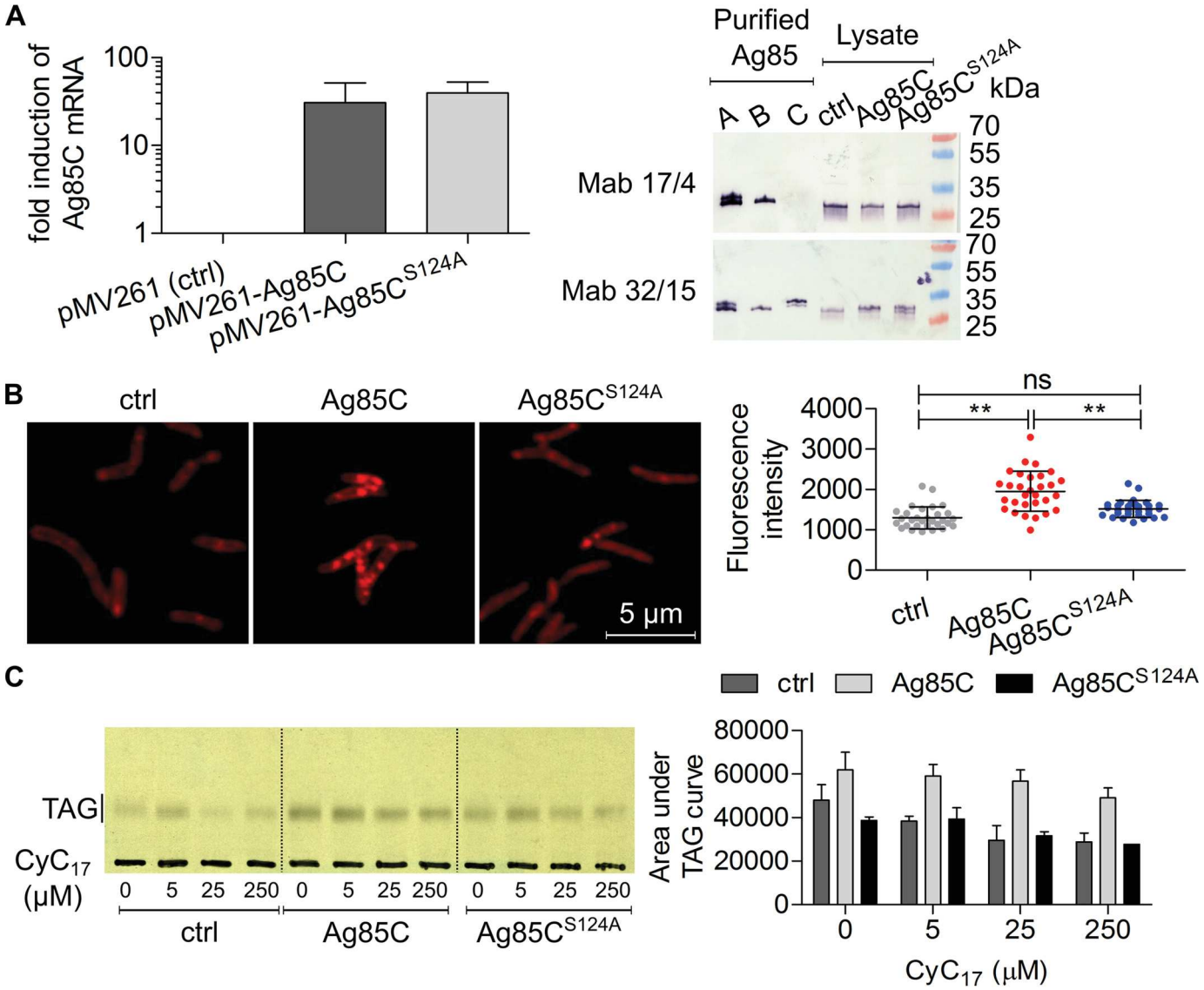

Figure 4. Biosynthesis of TAG in *M. tuberculosis* is inhibited by CyC_{17} and is dependent upon Ag85C expression. *A*, quantitative real-time PCR analysis showing the -fold increase in the Ag85C transcripts in *M. tuberculosis* mc^{2}6230 containing either pMV261 (*ctrl*), pMV261-Ag85C, or pMV261-Ag85C^{S124A} (*left*). Western blotting using the 32/15 and 17/4 monoclonal antibodies probed against purified Ag85A/B/C and crude lysates of *M. tuberculosis* mc^{2}6230 containing either pMV261, pMV261-Ag85C, or pMV261-Ag85C^{S124A} (*right*). *B*, Nile Red staining of *M. tuberculosis* strains growing exponentially (*left*) with the corresponding fluorescence quantification (*right*). Fluorescence quantification was performed on 30 bacilli of each group. Shown are the mean fluorescence and S.D. values. Means were compared by the two-tailed Mann–Whitney test. *ns*, non-significant; **, $p < 0.01$. Results shown are representative of two independent experiments. *C*, cultures were exposed to increasing concentrations of CyC_{17} in 7H9$^{OADC/Tween\ 80}$ and labeled with sodium [2-^{14}C]acetate for 4 h at 37 °C with agitation. The apolar fraction was extracted to analyze *de novo* synthesis of TAG. Equal counts (50,000 cpm) of apolar fraction were loaded, and TAG was visualized on a 1D TLC plate using the solvent system petroleum ether/diethyl ether (90:10, v/v) (*left*). *Right*, densitometric analysis of TLCs. *Histograms* and *error bars*, means and S.D. values calculated from four independent experiments.

could be built, implying that the last 14 residues as well as the polyhistidine tag in the C terminus were not modeled. The structure of Ag85C has been extensively reported (17). In brief, the protein adopts a typical α/β hydrolase fold made of a central β-sheet surrounded by α-helices. The two monomers are nearly identical, as their superposition over 274 residues gives an r.m.s. deviation of 0.24 Å. However, whereas a clear electron density could be seen for the entire structure of $CyC_{8\beta}$ in one monomer, this was only the case for the headgroup of the second molecule (Fig. 5*B*). It is noteworthy that the extra but non-interpretable electron density (Fig. 5*B*) in the vicinity of $CyC_{8\beta}$, observed in all data sets collected from either co-crystallization or soaking experiments and in various crystallization conditions (data not shown), appears as a possible molecule interacting with Phe^{150} and could be seen in both monomers. As Phe^{150} was shown to be involved in stacking of the lipid chain of octylglucoside in the Ag85C-octylglucoside crystal structure (PDB entry 1VA5 (19)), we tried to place the acyl chain of $CyC_{8\beta}$ in this extra electron density, but refinement of this alternate conformation of $CyC_{8\beta}$ did not converge. Therefore, further modeling of this electron density blob was not pursued. Although $CyC_{8\beta}$ has clearly reacted, as evidenced by the presence of an opened ring and the MALDI-TOF data, no covalent bond between the catalytic Ser^{124} residue and the phosphonate group of $CyC_{8\beta}$ was observed (Fig. 5, *B* and *D*). Therefore, $CyC_{8\beta}$ was modeled in an opened conformation (Fig. 5, *B* and *D*). $CyC_{8\beta}$

Table 1
Data collection and refinement statistics

Data collection statistics	
Beamline	ESRF-ID23.1
Wavelength (Å)	0.972
Resolution range (Å)	48.09–1.8 (1.86–1.8)[a]
Space group	$P\,2_1\,2_1\,2_1$
Unit cell	
Å	67.39, 75.77, 137.32
Degrees	90, 90, 90
Total reflections	528,844 (50,342)
Unique reflections	65,871 (6486)
Completeness (%)	99.92 (99.85)
Mean $I/\sigma(I)$	16.66 (2.24)
Wilson *B*-factor (Å^2)	24.34
R_{meas}	0.0968 (1.049)
Refinement statistics	
Reflections used in refinement	65,862 (6486)
R_{work}	0.151 (0.232)
R_{free}	0.175 (0.269)
No. of non-hydrogen atoms	4895
Macromolecules	4308
Ligands	54
Solvent	533
No. of r.m.s. deviations	
Bonds (Å)	0.006
Angles (degrees)	0.84
Ramachandran favored (%)	96.7
Ramachandran allowed (%)	3.3
Ramachandran outliers (%)	0.00
Rotamer outliers (%)	1.12
Clashscore	1.07
Average *B*-factor	29.13
Macromolecules	27.22
Ligands	50.05
Solvent	42.43
PDB accession number	5OCJ

[a] The values in parenthesis are for the highest-resolution shell.

interacts through residues at the entrance of the Ag85C active site (Fig. 5, *C* and *D*). The polar head of $CyC_{8\beta}$ is recognized through hydrogen bonds with the catalytic Ser^{124} side chain as well as with the main chain of Leu^{40} and the Asp^{38} side chain via two water molecules. The Arg^{41} side chain completes the interaction with the headgroup of $CyC_{8\beta}$ by van der Waals interaction (Fig. 5*D*). The long aliphatic chain of $CyC_{8\beta}$ is stabilized by hydrophobic interactions involving the Ile^{222}, Pro^{223}, Phe^{226}, and Leu^{227} side chains (Fig. 5*D*). The distance between the phosphate of $CyC_{8\beta}$ and Ser^{124} of 3.6 Å clearly attests that in this crystal, the ligand is not covalently bound. Importantly, this loss of covalent binding was observed in multiple data sets collected, obtained either by soaking or co-crystallization experiments. However, the lack of covalent binding in the crystal structure does not rule out the well-known covalent inhibitory mechanism of the CyC analogs supported by MALDI-TOF mass spectrometry analyses (Fig. 2, *C* and *D*).

Furthermore, the polar headgroup of $CyC_{8\beta}$ is located where trehalose, the natural substrate of the Ag85 proteins, binds, as seen in the crystal of the trehalose-bound structure of Ag85B (PDB entry 1F0P (18)) (Fig. 6*A*). Interestingly, the fatty acyl chain of $CyC_{8\beta}$ is placed in a very hydrophobic cavity that was proposed to be part of the TDM/TMM fatty chain recognition site (17). In addition, structural comparison indicated that the important residues in Ag85C interacting with $CyC_{8\beta}$ are fully conserved in Ag85B and Ag85A (Fig. 6*B*), strongly suggesting that $CyC_{8\beta}$, and presumably all of the other CyC analogs, may inhibit the three members of the Ag85 complex.

Discussion

Toward the generation of new lead compounds with unexplored modes of action in *M. tuberculosis*, the CyC analogs were initially designed to inhibit mycobacterial lipases (31). In particular, by covalently binding to the catalytic serine, they fully inactivated the monoacylglycerol lipase Rv0183 and the triacylglycerol lipase LipY from *M. tuberculosis* but not the mammalian gastric and pancreatic lipases (31). Subsequent biochemical studies involving the selective labeling and enrichment of captured enzymes using appropriate fluorophosphonate probes in combination with CyC_{17} resulted in the identification of 23 potential target lipolytic enzymes, all of which comprise catalytic serine or cysteine residues (29). Because they are multitarget-inhibitory compounds in mycobacteria, the use of CyC analogs could prevent the selection of drug resistance mechanisms. In addition, the lack of cytotoxicity in human cells (29) makes them attractive hits to be further evaluated.

Herein, we provide compelling evidence that at least some of the CyC analogs primarily act by inhibition of the Ag85 complex, resulting in decreased TDM formation and reduced mycolylation of AG, an essential polymer of the mycobacterial cell wall. Although one cannot rule out the possibility that the killing effect of the CyC on *M. tuberculosis* results from the simultaneous and net effect on multiple physiological targets, the inhibition of TMM and AG mycolylation is very likely to represent the major cause of growth inhibition of *M. tuberculosis*, at least in *in vitro* growing cultures. We demonstrate here that all three Ag85 members express DGAT activity *in vitro*, with Ag85C being the most active, thereby extending previous work reporting the DGAT activity of Ag85A (33). Importantly, the S124A site-directed mutation of the active site of Ag85C proved that this residue is involved in the DGAT activity of this enzyme and TAG synthesis. Although the synthesis of TAG relies on the presence of multiple TAG synthases, such as the well-characterized Tgs1 (Rv3130c) (36), our work extends the growing list of enzymes displaying DGAT activity in *M. tuberculosis*. The Ag85 proteins do not belong to the known DGAT families and do not possess the characteristic conserved heptapeptide acyltransferase motif of the mycobacterial Tgs enzymes involved in TAG biosynthesis (35, 41). Nevertheless, the DGAT activity of Ag85C, similarly to Ag85A (33), includes two consecutive reactions, the fatty acyl-CoA hydrolysis (thioesterification) and the subsequent transfer of the acyl chain to the diacylglycerol (transesterification). Overexpressing Ag85C in *M. tuberculosis* was correlated with an increase in *de novo* TAG production and formation of lipid storage inclusions. These findings establish for the first time a connection between cell wall and TAG biosynthesis by Ag85C and expand our understanding of this important enzyme in the physiology of *M. tuberculosis.* However, a direct implication of the DGAT activity of Ag85C in pathogenesis and persistence of *M. tuberculosis* requires further studies. In addition, under conditions where Ag85C is overexpressed, *M. tuberculosis* was more refractory to TAG inhibition by CyC_{17}, further emphasizing the yet unexpected contribution of Ag85C as a player in TAG biosynthesis. Inhibition of the DGAT activity of Ag85C, and therefore TAG inhibition, by the CyC compounds is very unlikely to

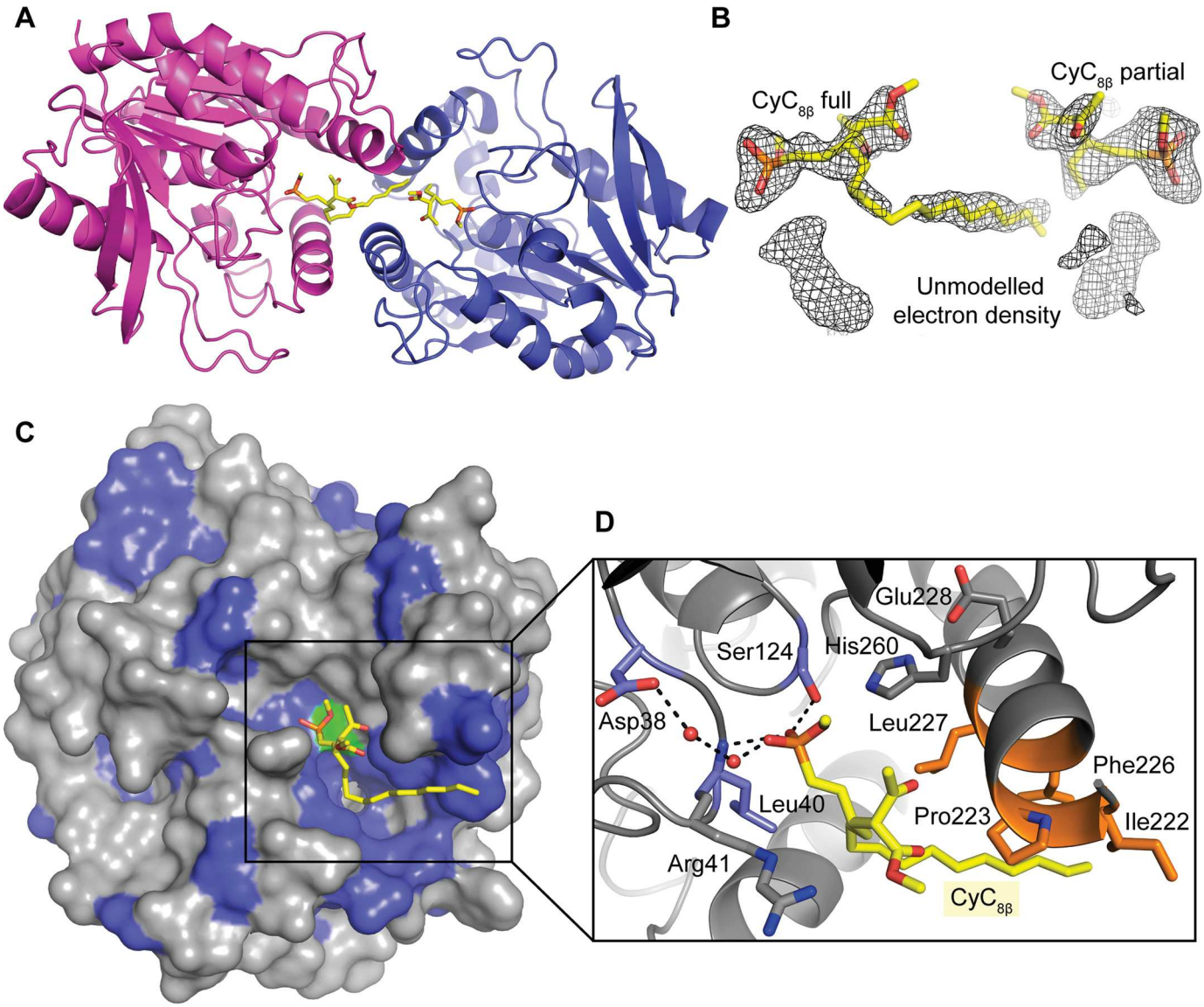

Figure 5. Structural basis for Ag85C inhibition by $CyC_{8\beta}$. *A*, crystal structure of Ag85C in complex with $CyC_{8\beta}$. The figure displays the overall asymmetric unit with the two monomers represented as *blue* and *magenta schematics*. $CyC_{8\beta}$ is shown as *sticks* and *colored* in *yellow*. *B*, simulated annealing $F_o - F_c$ OMIT map contoured at 3σ attesting to the presence of two $CyC_{8\beta}$ that could be entirely modeled for one molecule and partially for the second one. The map also reveals the presence of an extra, but non-interpretable, electron density in the vicinity of the $CyC_{8\beta}$ molecule. *C*, surface representation of the Ag85C structure bound to $CyC_{8\beta}$. The hydrophobic residues are *colored* in *blue*, and the catalytic Ser^{124} is shown in *green*. *D*, $CyC_{8\beta}$ binding site. Ag85C residues involved in $CyC_{8\beta}$ recognition are displayed as *blue sticks* for those involved in hydrogen bond (*black dashes*) formation. Residues in *orange* are involved in hydrophobic interactions with the acyl chain of $CyC_{8\beta}$, and Arg^{41} in *gray* contributes to the recognition of the $CyC_{8\beta}$ headgroup by van der Waals interaction. Ser^{124}, Glu^{228}, and His^{260} form the catalytic triad. *Red spheres*, water molecules.

participate in growth inhibition of *M. tuberculosis in vitro*, but it may have important consequences for *in vivo* survival and/or for maintaining the bacilli in a non-replicating growth phase, such as in foamy macrophages in which *M. tuberculosis* is able to hydrolyze the host-derived TAGs from lipid bodies to fatty acids, which are then reprocessed as TAGs and stored within ILIs (42, 43). In these subcellular structures, TAGs represent the primary storage source of carbon and energy, allowing the bacteria to survive in a non-replicating state and to persist inside these foamy cells, which usually line the necrotic centers of tubercle granulomas and have been proposed to be the intracellular niche of *M. tuberculosis* during latent infection (42). Although this requires further exploration, inhibiting the DGAT activity of Ag85C may help in designing new classes of molecules that restrict entry of *M. tuberculosis* into dormancy, a strategy that would overcome mycobacterial persistence and prolonged chronic infections.

Biochemical studies involving the TAMRA-FP probe that binds to serine hydrolases along with mass spectrometry and structural analyses indicate that, in addition to covalently binding to the catalytic Ser^{124}, the CyC analogs could also be competing with the binding of Ag85 substrate (*i.e.* the trehalose and the acyl chain moieties of TMM). As the Ag85 complex members share similar substrate specificities, our results suggest that CyC analogs could target not only Ag85C but also Ag85B and Ag85A, an assertion reinforced by the fact that Ag85A was also identified as a potential target in the original proteomic screen approach (29). Comparison of the three structures

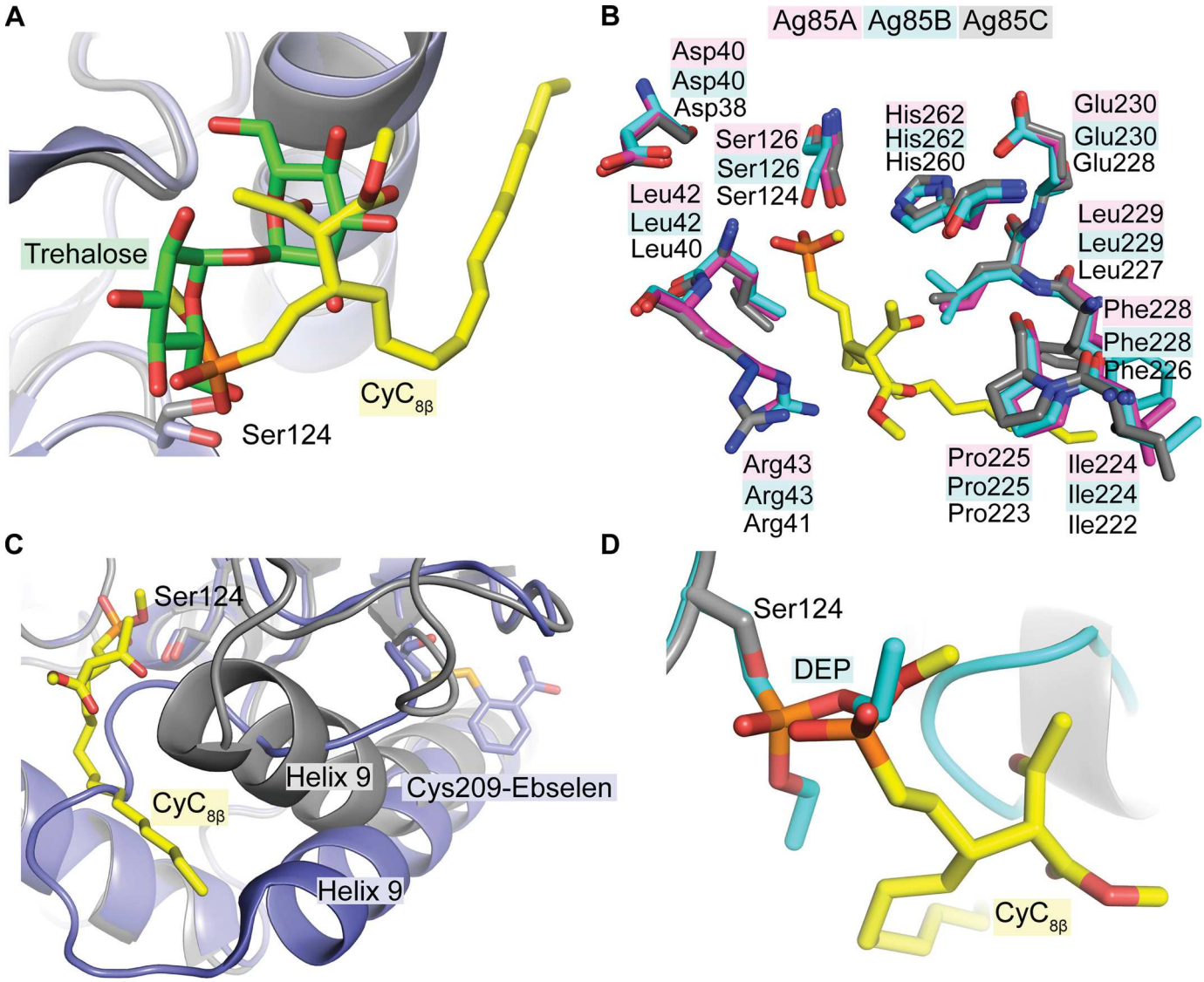

Figure 6. Mode of inhibition of the Ag85 complex by $CyC_{8\beta}$. *A*, superposition of the Ag85B-trehalose (PDB code 1F0P, *blue*) and Ag85C-$CyC_{8\beta}$ (*gray*) crystal structures. The headgroup of $CyC_{8\beta}$ (*yellow*) occupies the same site as trehalose (*green*). *B*, Ag85C residues (*gray*) involved in the recognition of $CyC_{8\beta}$ are all strictly conserved in Ag85B (*cyan*) and Ag85A (*magenta*). *C*, superposition of the Ag85C-ebselen (PDB code 4QDU; *blue*) and Ag85C-$CyC_{8\beta}$ (*gray*) crystal structures. $CyC_{8\beta}$ binds far away from the ebselen-binding site and does not trigger structural rearrangement of helix α9. *D*, superposition of the Ag85C-DEP (PDB code 1DQY; *cyan*) and Ag85C-$CyC_{8\beta}$ (*gray*) crystal structures. $CyC_{8\beta}$ presents a similar mode of inhibition as DEP (*cyan stick*), a nonspecific σ/β hydrolase inhibitor.

strongly supports this hypothesis, as residues contacting $CyC_{8\beta}$ in Ag85C are strictly conserved in Ag85A and Ag85B. This is of interest, as the inhibitor I3-AG85 binding to the active site of Ag85C exhibits only strict specificity toward Ag85C and does not bind Ag85A and -B (25). Moreover, given their low x_{150} values, the three CyC compounds are able to act in near stoichiometry and alter both the mycolyltransferase and DGAT activities of Ag85C. It is noteworthy that, among the three CyCs investigated, the phosphate CyC_{17}, which appears as the best inhibitor against extracellular *M. tuberculosis*, was the least efficient when assayed on pure recombinant enzyme. However, when assayed on living bacteria, CyC_{17} clearly affected TDM synthesis and mycolylation of AG. The differences in activity with $CyC_{7\beta}$ and $CyC_{8\beta}$ may be related to the chemical properties of the phosphate *versus* phosphonate chemical groups. On the other hand, despite their high activity, phosphate inhibitors can be subjected to hydrolysis, rendering their covalent binding potentially reversible, as shown here in the case of the CyC_{17}-Ser^{124} adduct (29). Interestingly, using a chemical proteomic approach, the EZ120 β-lactone compound exhibiting strong antitubercular activity and resembling an electrophilic mimic of mycolic acids was recently found to block several serine hydrolases essential for the mycomembrane biosynthesis (44). The polyketide synthase Pks13, whose β-keto mycolate is transferred onto trehalose and reduced to yield TMM, as well as Ag85A were identified as primary targets of EZ120. However, whether this β-lactone acts similarly to the CyC inhibitors in Ag85 awaits structural determination.

Comparison of the Ag85C-$CyC_{8\beta}$ structure with that of Ag85C-ebselen (PDB entry 4QDU (27)) shows that the mode of inhibition triggered by $CyC_{8\beta}$ is different. Ebselen indeed covalently modifies Cys^{209}, which is 13 Å away from the catalytic

Ser^{124} (Fig. 6*C*). Inhibition by ebselen and its derivatives (azido ebselen and adamantyl ebselen) is mediated by inducing structural rearrangements of helix α9 and the loop between helices 9 and 10 that ends in destabilizing the hydrogen bond network of the active site (27, 28, 45). Comparison of the crystal structures of Ag85C-$CyC_{8\beta}$ and the Ag85C native structure (PDB entry 3HRH) possessing the same space group and crystallized in similar conditions shows that the two structures are identical. The superposition of the two structures yields an overall r.m.s. deviation over 251 residues of about 0.19 Å. Furthermore, no local structural rearrangement was observed (data not shown). As expected, the mode of inhibition of $CyC_{8\beta}$ consists of blocking the active site (31) and not of destabilizing the overall structure and stability of the protein as reported for ebselen and its analogs (27, 45). Furthermore, the mode of action of $CyC_{8\beta}$ is more related to that of the diethyl *p*-nitrophenyl phosphate (DEP), a nonspecific α/β hydrolase inhibitor that covalently modifies the Ser^{124} catalytic residue (17). Superposition of the Ag85C-DEP (PDB entry 1DQY) and Ag85C-$CyC_{8\beta}$ structures highlights the similar positioning of the phosphonate groups of the two inhibitors (Fig. 6*D*).

In summary, the data reported here offer a first look at the potent inhibition of the *M. tuberculosis* Ag85C by cyclipostins and cyclophostin analogs, compounds that effectively inhibit growth of extracellularly and intracellularly replicating *M. tuberculosis* and their mechanism of action. Interestingly, a recent study indicated that these compounds were also effective against clinical isolates of the *M. abscessus* complex (46), mostly encountered in cystic fibrosis patients, and known to be intrinsically resistant to most antitubercular drugs. We anticipate that the high-resolution crystal structure of Ag85C-$CyC_{8\beta}$ will now open the way to the development, through structure-based drug design, of improved inhibitors that target the Ag85 complex in various pathogenic mycobacteria.

Experimental procedures

Mycobacterial strains and growth conditions

M. tuberculosis mc^26230 (47) was grown on Middlebrook 7H10 agar plates containing OADC (oleic acid, albumin, dextrose, catalase) enrichment (Difco) and supplemented with 24 μg/ml pantothenic acid. Liquid cultures were obtained by growing mycobacteria in Middlebrook 7H9 (Difco) supplemented with 10% OADC enrichment, 0.2% (v/v) glycerol, 0.05% (v/v), Tween 80 (Sigma), 24 μg/ml pantothenic acid, and 25 μg/ml kanamycin when required.

Plasmids and DNA manipulations

The *fbpC2* gene, encoding Ag85C, was amplified by PCR from *M. tuberculosis* H37Rv genomic DNA using the forward primer 5′-CTA CTT **CAT ATG** TTC TCT AGG CCC GGT CTT CCA G-3′ (NdeI site in boldface type) and the reverse primer 5′-GAG ATT **CTC GAG** AGC AGC AGG CGC AGC AGG GG-3′ (XhoI site in boldface type). The PCR product was cloned into pET23b cut with NdeI and XhoI (New England Biolabs), enabling the incorporation of a polyhistidine tag in the C terminus of the Ag85C protein. The pET23b-*fbpA* and pET23b-*fbpC1* constructs carrying the genes encoding Ag85A and MPT51, respectively, were described previously (11). A codon-optimized version of the *fbpB* gene, encoding Ag85B, was synthesized (GenScript) and introduced within the pET23a plasmid thanks to the NdeI and XhoI restriction sites, enabling also the incorporation of a polyhistidine tag in the C terminus of the Ag85B protein. The $Ag85C^{S124A}$ mutant was obtained by using the PCR-driven overlap extension method (48). Briefly, two separate PCRs were set up with the Phusion® DNA polymerase (Thermo Fisher Scientific). The first one was set up with the forward primer used to amplify the wildtype *fbpC2* gene and the reverse internal primer 5′-AAG ACC CAC CGC CGC GTT-3′. The second one was set up with a forward internal primer, 5′-AAC GCG GCG GTG GGT CTT **G**CG ATG TCG GGC GGT TCC G-3′, overlapping the internal reverse primer and containing the nucleotide substitution (changed nucleotide in boldface type) with the reverse primer used to amplify the wildtype *fbpC2* gene. The purified PCR products were heterodimerized by heating to 95 °C for 1 min, followed by cooling to 60 °C for 10 min in the presence of Phusion® DNA polymerase and dNTPs to generate a double-stranded hybrid. A last step of PCR was performed with the primers used to amplify the wildtype *fbpC2* gene with the hybrid product obtained in the previous step as template. The mutated *fbpC2* gene was finally cloned like the wildtype gene into pET23b and subjected to DNA sequencing to confirm the proper introduction of the mutation. The coding sequence of the gene *Rv3130c*, which encodes Tgs1 from *M. tuberculosis*, was PCR-amplified using the forward primer 5′-GAG GAG **CCA TGG** aga atc tgta ctt cca ggg AAT GAA TCA CCT AAC GAC ACT TGA CGC-3′ (NcoI site in boldface type, tobacco Etch virus protease cleavage site in lowercase type) and the reverse primer 5′-ACG AGG **AAG CTT** TCA CAC AAC CAG CGA TAG CGC T-3′ (HindIII site in boldface type). The PCR amplicon was treated with NcoI and HindIII and ligated to NcoI-HindIII–linearized pET32a. This plasmid containing the polyhistidine and thioredoxin as fusion tags in the N-terminal position was used to produce soluble recombinant Tgs1.

Expression and purification of the individual Ag85 antigens and MPT51

All four plasmids harboring the *fbpA*, *fbpB*, *fbpC2*, and *fbpC1* genes were used to transform the *E. coli* C41 (DE3) expression strain. Transformed bacteria were grown in Luria-Bertani medium containing ampicillin (200 μg/ml) until the A_{600} reached 0.6. Bacterial cultures were then placed on icy water for 30 min before induction with 1 mM isopropyl β-D-1-thiogalactopyranoside and further incubated at 16 °C for 20 h. Bacterial pellets were collected by centrifugation (6,000 × *g*, 4 °C, 1 h) and resuspended in lysis buffer (50 mM Tris, pH 8.0, 200 mM NaCl, 20 mM imidazole, 5 mM β-mercaptoethanol, 1 mM benzamidine). Lysates were sonicated and clarified by centrifugation (27,000 × *g*, 4 °C, 45 min) before purification by nickel-affinity chromatography with nickel-nitrilotriacetic acid–Sepharose beads and elution with lysis buffer containing 250 mM imidazole without benzamidine (GE Healthcare). Proteins were next dialyzed against 50 mM Tris-HCl, pH 8.0, and 5 mM β-mercaptoethanol buffer and loaded on an anion-exchange HiTrap® Q Fast Flow column (GE Healthcare). The protein was eluted with a linear NaCl gradient. The final step of purification was by

size-exclusion chromatography using a Superdex^{TM} 75 10/300 GL column (GE Healthcare). Proteins were eluted in potassium phosphate buffer (50 mM KH_2PO_4/K_2HPO_4, pH 7.6) for DGAT activity assessments. Ag85C was eluted in a sodium phosphate buffer (50 mM NaH_2PO_4/Na_2HPO_4, pH 6.0) for mycolyltransferase activity assessments and in 50 mM Tris-HCl, pH 8.0, 200 mM NaCl for crystallization experiments and stored at 4 °C.

Expression and purification of Tgs1

The *M. tuberculosis* Tgs1 was overproduced in *E. coli* and purified. Briefly, *E. coli* BL21 Rosetta^{TM} 2 was freshly transformed with pET32a-*tgs1*. Exponentially growing bacteria cultured in 2 liters of NYZ Broth (BD Biosciences) were cooled on icy water for 30 min, and 1 mM isopropyl β-D-1-thiogalactopyranoside was added before incubation at 16 °C for 16 h with agitation (200 rpm). Bacteria were then collected by centrifugation, the medium was discarded, and the pellet was resuspended in lysis buffer containing 10% glycerol, which was maintained for all subsequent buffers used. Lysates were produced and subjected to purification via nickel affinity chromatography. His-tagged tobacco etch virus protease was added to the eluted protein solution at a 1:50 (w/w) ratio, and the mixture was dialyzed overnight before again being subjected to nickel-affinity chromatography. The fraction that flowed through the nickel-nitrilotriacetic acid column, containing tagless Tgs1, was concentrated and subjected to size-exclusion chromatography using a Bio-rad ENrich SEC 650 (Bio-rad) and as buffer 100 mM K_2HPO_4/KH_2PO_4, pH 7.5, supplemented with 400 mM NaCl and 10% glycerol. The fractions containing active Tgs1 were pooled and concentrated to 0.1 mg/ml.

RNA extraction, cDNA production, and quantitative real-time PCR

Mycobacterial RNA was purified using the Nucleospin RNA kit (Macherey Nagel) and assessed for purity on a NanoDrop spectrometer and for integrity using a BioAnalyzer (Agilent). Subsequently, RNA was treated by DNase I (Life Technologies) and converted to cDNA using the SuperScript V reverse transcriptase kit (Life Technologies). Quantitative real-time PCR was performed using the LightCycler 480 SYBR Green master mix (Roche Applied Science) and primers specific to the housekeeping control gene *sigA* (forward, 5′-TGT ACT CGT GCG CAG TAA AG-3′; reverse, 5′-GTC GAA TGT CGG CGT TGA TA-3′) and *fbpC2* (forward, 5′-CAG TTT CTA CAC CGA CTG GTA TC-3′; reverse, 5′-TCT CTC TGG TAA GGA AGG TCT C-3′). Triplicate data were analyzed by the $\Delta\Delta Cp$ method with correction for PCR efficiency.

Western blotting

Lysates of *M. tuberculosis* mc^26230 wildtype or overexpressing Ag85C were prepared and subjected to Western blot analysis as described previously (49).

DGAT and mycolyltransferase assays

The DGAT activity assay was performed for 1 h at 37 °C using a protocol reported earlier (33). Briefly, the reaction mixture was composed of 400 μM 1,2-dipalmitoyl-*sn*-glycerol and a 500 μM concentration of the different acyl donor molecules tested (butanoyl-CoA, octanoyl-CoA, lauroyl-CoA, palmitoyl-CoA, and oleoyl-CoA (Sigma-Aldrich)) in 50 mM potassium phosphate buffer, pH 7.6, containing 2% DMSO. The enzyme concentration in the reaction was 3 μM (0.5 μM in the case of Tgs1). At the end of the assay, an equal volume of DTNB (360 μg/ml) was added to the reaction, and the absorbance was measured at 412 nm with a NanoDrop 2000c spectrophotometer (Thermo Fisher Scientific), enabling the calculation of the specific activity of the enzymes (nmol of TNB produced × min^{-1} × mg of $protein^{-1}$).

The mycolyltransferase activity assay was performed for 15 min at 35 °C based on a procedure described previously (27). Measurements were taken every 15 s using a Multimode Microplate Reader POLARstar® Omega (BMG Labtech), and the activity of Ag85C was calculated at the maximum rate of the reaction. The reaction mixture was composed of 50 mM sodium phosphate (pH 6.0) containing 2% DMSO, 4 mM trehalose, and 12.5 μM resorufin butyrate (Sigma-Aldrich). The resorufin butyrate was dissolved in DMSO and diluted 100-fold in the reactions. The enzyme concentration in each reaction was 5.5 μM. Data presented were obtained from three independent experiments and analyzed by non-linear regression using GraphPad Prism version 5 software.

Inhibition of the DGAT and mycolyltransferase activity

$CyC_{7\beta}$, $CyC_{8\beta}$, and CyC_{17} were synthesized as described previously (31, 50). To study the inhibitory effect on DGAT activity, a 30 μM concentration of either Ag85A, Ag85B, Ag85C, or MPT51 was co-incubated with increasing concentrations of $CyC_{7\beta}$, $CyC_{8\beta}$, and CyC_{17} for 1 h at room temperature in a reaction mixture containing 50 mM potassium phosphate buffer (pH 7.6), 10% DMSO, and 0.5 times the critical micelle concentration of *n*-dodecyl β-D-maltoside. Inhibition of the mycolyltransferase activity was determined using 55 μM of Ag85C co-incubated with increasing concentrations of $CyC_{7\beta}$, $CyC_{8\beta}$, and CyC_{17} for 30 min at room temperature in 50 mM sodium phosphate buffer (pH 6.0), 10% DMSO, and 0.5 times the critical micelle concentration of *n*-dodecyl β-D-maltoside. Ag85C and $Ag85C^{S124A}$ pretreated or not with the CyC analogs were further incubated with 10 μM ActivX TAMRA-FP probe (Thermo Fisher Scientific) for 1 h at room temperature in the darkness. The reaction was stopped by adding 5× Laemmli reducing buffer followed by boiling, and proteins were separated by 12% SDS-PAGE. Subsequently, TAMRA FP-labeled proteins were detected by fluorescent gel scanning (TAMRA: λ_{ex} 557 nm, λ_{em} 583 nm) using the Cy®3 filter of a ChemiDoc MP Imager (Bio-Rad) before staining of the gels with Coomassie Brilliant Blue dye.

Overexpression of Ag85C variants in M. tuberculosis

The *Rv0129c* gene was amplified by PCR from *M. tuberculosis* H37Rv genomic DNA using the forward primer 5′-CCC AGC TTG TTG ACA GGG TTC GTG-3′ and the reverse primer 5′-ACC AT**G GAT CC**C TAG GCG CCC TGG GGC GCG-3′ (BamHI site in boldface type). After amplification, the PCR product was digested with BamHI (Promega) and cloned into MscI/BamHI- digested pMV261, thus placing the Rv0129c open reading frame under control of the *hsp60* promoter to yield pMV261-Ag85C. The pMV261-$Ag85C^{S124A}$ mutant plasmid was constructed by the QuikChange method using

pMV261-Ag85C as template, Phusion® DNA polymerase (Thermo Fisher Scientific), the forward primer 5′-GCG GCG GTG GGT CTT **GCG** ATG TCG GGC GGT TCC-3′, and the reverse primer 5′-GGA ACC GCC CGA CAT **CGC** AAG ACC CAC CGC CG-3′ (Ser → Ala mutation in boldface type). The DNA sequence was confirmed by DNA sequencing. *M. tuberculosis* mc^{2}6230 was subsequently electrotransformed with pMV261 as a control, pMV261-Ag85C, or pMV261-Ag85C^{S124A}.

Whole-cell radiolabeling experiments and lipid analysis

To investigate the CyC-induced changes in the lipid profile, increasing drug concentrations were added to exponentially growing *M. tuberculosis* mc^{2}6230 cultures grown in Middlebrook 7H9 supplemented with OADC enrichment and Tween 80 and 20 μg/ml pantothenate for 1 h. Subsequently, metabolic labeling of lipids was performed by adding 1 μCi/ml sodium [2-^{14}C]acetate (56 mCi/mmol; American Radio Chemicals) for an additional 6 h at 37 °C. Cells were harvested and delipidated, as described previously (51). The apolar lipid fraction containing TMM and TDM was separated on a 1D TLC plate using the solvent system chloroform/methanol/water (40:8:1, v/v/v) and revealed after exposure to a film. Similarly, the apolar lipid fraction, which also contains TAG, was separated on a 1D TLC plate using the solvent system petroleum ether/diethyl ether (90:10, v/v) and revealed after exposure to film. Delipidated cells were further processed to extract the arabinogalactan-bound mycolic acids (52) and analyzed by TLC/autoradiography using hexane/ethyl acetate (95:5, v/v) run twice in the first dimension followed by exposure to a film to reveal ^{14}C-labeled mycolic acid methyl esters.

Fluorescent microscopy experiments

Wildtype *M. tuberculosis* mc^{2}6230 or strains harboring either the pMV261-Ag85C or its variant pMV261-Ag85C^{S124A} were stained with Nile Red fluorescent probe (Interchim), as described previously (40). Approximately 7.5 × 10^7 cells (OD 1.5) were collected at 9,000 × *g* for 3 min, washed twice with 500 μl of PBS-Tween 0.05%, and resuspended in 300 μl of PBS. Nile Red (15 μl of a solution at 0.5 mg/ml solubilized in ethanol) was added to the bacterial suspension, which was further incubated for 30 min at 37 °C in the darkness. Cells were then centrifuged, washed twice with PBS-Tween 0.05%, and resuspended in 300 μl of PBS. Bacteria were spotted between a 170-μm-thick coverslip and a 1.5% agarose-PBS pad. Image acquisition was performed with an OLYMPUS FV1000 confocal microscope at $\lambda_{ex}\backslash\lambda_{em}$ = 530/590 ± 10 nm, and images were processed and analyzed using ImageJ.

Mass spectrometry

Mass analyses were performed on a MALDI-TOF-TOF Bruker Ultraflex III spectrometer (Bruker Daltonics, Wissembourg, France) controlled by the Flexcontrol version 3.0 package (Build 51). This instrument was used at a maximum accelerating potential of 25 kV and was operated in linear mode using the *m*/*z* range from 20,000 to 100,000 (LP_66 kDa method). Five external standards (Protein Calibration Standard II, Bruker Daltonics) were used to calibrate each spectrum to a mass accuracy within 200 ppm. Peak picking was performed with Flexanalysis version 3.0 software (Bruker) with an adapted analysis method. To eliminate salts from the samples, 10 μl of each preparation was submitted to a desalting step on a C4 Zip-Tip μcolumn (Millipore). 1 μl of desalted sample was mixed with 1 μl of α-cyano-4-hydroxycinnamic acid matrix in a 50% acetonitrile, 0.3% TFA mixture (1:1, v/v). 1 μl was spotted on the target, dried, and analyzed with the LP_66 kDa method. Peak picking was performed with Flexanalysis version 3.0 software (Bruker) with an adapted analysis method. Parameters used were as follows: SNAP peak detection algorithm, S/N threshold fixed to 6, and a quality factor threshold of 30.

Crystallization, data collection, structure determination, and refinement

Crystals were grown in sitting drops at 18 °C by mixing 0.8 μl of protein (in 50 mM Tris-HCl, pH 8.0, and 200 mM NaCl) at a concentration of 8 mg/ml with 0.8 μl of reservoir solution consisting of 0.2 M magnesium chloride hexahydrate, 0.1 M sodium citrate tribasic dihydrate, pH 5.0, and 10% (w/v) polyethylene glycol 20,000. 1-month-old crystals were then soaked for 24 h with a final concentration in the drop of 5 mM $CyC_{8\beta}$. Crystals were fished with a litholoop and flash-cooled in liquid nitrogen without any cryoprotection. Data collection was performed at the ID-23.1 beamline at the ESRF synchrotron (Grenoble, France). Data were processed with *XDS* (53), and the structure was solved by molecular replacement with the structure of Ag85C as search model (PDB code 3HRH (54)) and using *Phaser* from the *PHENIX* software suite (55). Manual adjustments of the model were performed with *Coot* (56), and the structure was refined to 1.8 Å with *PHENIX*. PDB coordinates and structure factors were deposited in the Protein Data Bank under accession number 5OCJ. Data collection and refinement statistics are displayed in Table 1.

Author contributions—A.V., J.-F.C., S.C., M.B., and L.K. conceptualization; A.V., M.R., P.F., and L.C. data curation; A.V., M.R., P.C.N., P.F., L.C., R.R.P., G.R.G., J.-F.C., S.C., and M.B. investigation; A.V., M.R., P.C.N., P.F., L.C., R.R.P., G.R.G., J.-F.C., S.C., and M.B. methodology; A.V., M.R., P.F., L.C., C.D.S., J.-F.C., S.C., M.B., and L.K. writing-review and editing; P.C.N. visualization; C.D.S. and S.C. resources; M.B. and L.K. supervision; L.K. funding acquisition; L.K. validation; L.K. writing-original draft; L.K. project administration.

Acknowledgments—We thank K. Huygen for kindly providing the 17/4 and 32/15 monoclonal antibodies, W. R. Jacobs, Jr., for M. tuberculosis mc^{2}6230, and P. Santucci for help in fluorescent microscopy experiments. This work benefited from the facilities and expertise of the Platform for Microscopy of IMM. We thank the ESRF and SLS beamline staffs for support during data collection. Mass spectrometry analyses were done using the mass spectrometry facility of Marseille Proteomics, supported by IBISA (Infrastructures Biologie Santé et Agronomie), the Cancéropôle PACA, the Provence-Alpes-Côte d'Azur Region, the Institut Paoli-Calmettes, and the Centre de Recherche en Cancérologie de Marseille.

References

1. Dheda, K., Gumbo, T., Maartens, G., Dooley, K. E., McNerney, R., Murray, M., Furin, J., Nardell, E. A., London, L., Lessem, E., Theron, G., van Helden, P., Niemann, S., Merker, M., Dowdy, D., *et al.* (2017) The epidemiology,

pathogenesis, transmission, diagnosis, and management of multidrug-resistant, extensively drug-resistant, and incurable tuberculosis. *Lancet Respir. Med.* **5,** 291–360 CrossRef Medline
2. Barry, C. E., 3rd, and Mdluli, K. (1996) Drug sensitivity and environmental adaptation of mycobacterial cell wall components. *Trends Microbiol.* **4,** 275–281 CrossRef Medline
3. Brennan, P. J., and Nikaido, H. (1995) The envelope of mycobacteria. *Annu. Rev. Biochem.* **64,** 29–63 CrossRef Medline
4. Mikusová, K., Slayden, R. A., Besra, G. S., and Brennan, P. J. (1995) Biogenesis of the mycobacterial cell wall and the site of action of ethambutol. *Antimicrob. Agents Chemother.* **39,** 2484–2489 CrossRef Medline
5. Vilchèze, C., Wang, F., Arai, M., Hazbón, M. H., Colangeli, R., Kremer, L., Weisbrod, T. R., Alland, D., Sacchettini, J. C., and Jacobs, W. R. (2006) Transfer of a point mutation in *Mycobacterium tuberculosis inhA* resolves the target of isoniazid. *Nat. Med.* **12,** 1027–1029 CrossRef Medline
6. Matsumoto, M., Hashizume, H., Tomishige, T., Kawasaki, M., Tsubouchi, H., Sasaki, H., Shimokawa, Y., and Komatsu, M. (2006) OPC-67683, a nitro-dihydro-imidazooxazole derivative with promising action against tuberculosis *in vitro* and in mice. *PLoS Med.* **3,** e466 CrossRef Medline
7. Tahlan, K., Wilson, R., Kastrinsky, D. B., Arora, K., Nair, V., Fischer, E., Barnes, S. W., Walker, J. R., Alland, D., Barry, C. E., 3rd, and Boshoff, H. I. (2012) SQ109 targets MmpL3, a membrane transporter of trehalose monomycolate involved in mycolic acid donation to the cell wall core of *Mycobacterium tuberculosis*. *Antimicrob. Agents Chemother.* **56,** 1797–1809 CrossRef Medline
8. Harth, G., Lee, B. Y., Wang, J., Clemens, D. L., and Horwitz, M. A. (1996) Novel insights into the genetics, biochemistry, and immunocytochemistry of the 30-kilodalton major extracellular protein of *Mycobacterium tuberculosis*. *Infect. Immun.* **64,** 3038–3047 Medline
9. Belisle, J. T., Vissa, V. D., Sievert, T., Takayama, K., Brennan, P. J., and Besra, G. S. (1997) Role of the major antigen of *Mycobacterium tuberculosis* in cell wall biogenesis. *Science* **276,** 1420–1422 CrossRef Medline
10. Jackson, M., Raynaud, C., Lanéelle, M. A., Guilhot, C., Laurent-Winter, C., Ensergueix, D., Gicquel, B., and Daffé, M. (1999) Inactivation of the antigen 85C gene profoundly affects the mycolate content and alters the permeability of the *Mycobacterium tuberculosis* cell envelope. *Mol. Microbiol.* **31,** 1573–1587 CrossRef Medline
11. Kremer, L., Maughan, W. N., Wilson, R. A., Dover, L. G., and Besra, G. S. (2002) The *M. tuberculosis* antigen 85 complex and mycolyltransferase activity. *Lett. Appl. Microbiol.* **34,** 233–237 CrossRef Medline
12. Armitige, L. Y., Jagannath, C., Wanger, A. R., and Norris, S. J. (2000) Disruption of the genes encoding antigen 85A and antigen 85B of *Mycobacterium tuberculosis* H37Rv: effect on growth in culture and in macrophages. *Infect. Immun.* **68,** 767–778 Medline
13. Nguyen, L., Chinnapapagari, S., and Thompson, C. J. (2005) FbpA-dependent biosynthesis of trehalose dimycolate is required for the intrinsic multidrug resistance, cell wall structure, and colonial morphology of *Mycobacterium smegmatis*. *J. Bacteriol.* **187,** 6603–6611 CrossRef Medline
14. Puech, V., Guilhot, C., Perez, E., Tropis, M., Armitige, L. Y., Gicquel, B., and Daffé, M. (2002) Evidence for a partial redundancy of the fibronectin-binding proteins for the transfer of mycoloyl residues onto the cell wall arabinogalactan termini of *Mycobacterium tuberculosis*: redundancy of fibronectin-binding proteins in *M. tuberculosis*. *Mol. Microbiol.* **44,** 1109–1122 CrossRef Medline
15. Wilson, R. A., Rai, S., Maughan, W. N., Kremer, L., Kariuki, B. M., Harris, K. D. M., Wagner, T., Besra, G. S., and Fütterer, K. (2003) Crystallization and preliminary X-ray diffraction data of *Mycobacterium tuberculosis* FbpC1 (Rv3803c). *Acta Crystallogr. D Biol. Crystallogr.* **59,** 2303–2305 CrossRef Medline
16. Wilson, R. A., Maughan, W. N., Kremer, L., Besra, G. S., and Fütterer, K. (2004) The structure of *Mycobacterium tuberculosis* MPT51 (FbpC1) defines a new family of non-catalytic α/β hydrolases. *J. Mol. Biol.* **335,** 519–530 CrossRef Medline
17. Ronning, D. R., Klabunde, T., Besra, G. S., Vissa, V. D., Belisle, J. T., and Sacchettini, J. C. (2000) Crystal structure of the secreted form of antigen 85C reveals potential targets for mycobacterial drugs and vaccines. *Nat. Struct. Biol.* **7,** 141–146 CrossRef Medline
18. Anderson, D. H., Harth, G., Horwitz, M. A., and Eisenberg, D. (2001) An interfacial mechanism and a class of inhibitors inferred from two crystal structures of the *Mycobacterium tuberculosis* 30 kDa major secretory protein (Antigen 85B), a mycolyl transferase. *J. Mol. Biol.* **307,** 671–681 CrossRef Medline
19. Ronning, D. R., Vissa, V., Besra, G. S., Belisle, J. T., and Sacchettini, J. C. (2004) *Mycobacterium tuberculosis* antigen 85A and 85C structures confirm binding orientation and conserved substrate specificity. *J. Biol. Chem.* **279,** 36771–36777 CrossRef Medline
20. Daffé, M. (2000) The mycobacterial antigens 85 complex: from structure to function and beyond. *Trends Microbiol.* **8,** 438–440 CrossRef Medline
21. Favrot, L., and Ronning, D. R. (2012) Targeting the mycobacterial envelope for tuberculosis drug development. *Expert Rev. Anti Infect. Ther.* **10,** 1023–1036 CrossRef Medline
22. Jackson, M., McNeil, M. R., and Brennan, P. J. (2013) Progress in targeting cell envelope biogenesis in *Mycobacterium tuberculosis*. *Future Microbiol.* **8,** 855–875 CrossRef Medline
23. Rose, J. D., Maddry, J. A., Comber, R. N., Suling, W. J., Wilson, L. N., and Reynolds, R. C. (2002) Synthesis and biological evaluation of trehalose analogs as potential inhibitors of mycobacterial cell wall biosynthesis. *Carbohydr. Res.* **337,** 105–120 CrossRef Medline
24. Barry, C. S., Backus, K. M., Barry, C. E., 3rd, and Davis, B. G. (2011) ESI-MS assay of *M. tuberculosis* cell wall antigen 85 enzymes permits substrate profiling and design of a mechanism-based inhibitor. *J. Am. Chem. Soc.* **133,** 13232–13235 CrossRef Medline
25. Warrier, T., Tropis, M., Werngren, J., Diehl, A., Gengenbacher, M., Schlegel, B., Schade, M., Oschkinat, H., Daffe, M., Hoffner, S., Eddine, A. N., and Kaufmann, S. H. E. (2012) Antigen 85C inhibition restricts *Mycobacterium tuberculosis* growth through disruption of cord factor biosynthesis. *Antimicrob. Agents Chemother.* **56,** 1735–1743 CrossRef Medline
26. Scheich, C., Puetter, V., and Schade, M. (2010) Novel small molecule inhibitors of MDR *Mycobacterium tuberculosis* by NMR fragment screening of antigen 85C. *J. Med. Chem.* **53,** 8362–8367 CrossRef Medline
27. Favrot, L., Grzegorzewicz, A. E., Lajiness, D. H., Marvin, R. K., Boucau, J., Isailovic, D., Jackson, M., and Ronning, D. R. (2013) Mechanism of inhibition of *Mycobacterium tuberculosis* antigen 85 by ebselen. *Nat. Commun.* **4,** 2748 Medline
28. Favrot, L., Lajiness, D. H., and Ronning, D. R. (2014) Inactivation of the *Mycobacterium tuberculosis* antigen 85 complex by covalent, allosteric inhibitors. *J. Biol. Chem.* **289,** 25031–25040 CrossRef Medline
29. Nguyen, P. C., Delorme, V., Bénarouche, A., Martin, B. P., Paudel, R., Gnawali, G. R., Madani, A., Puppo, R., Landry, V., Kremer, L., Brodin, P., Spilling, C. D., Cavalier, J.-F., and Canaan, S. (2017) Cyclipostins and cyclophostin analogs as promising compounds in the fight against tuberculosis. *Sci. Rep.* **7,** 11751 CrossRef Medline
30. Dupont, C., Viljoen, A., Dubar, F., Blaise, M., Bernut, A., Pawlik, A., Bouchier, C., Brosch, R., Guérardel, Y., Lelièvre, J., Ballell, L., Herrmann, J.-L., Biot, C., and Kremer, L. (2016) A new piperidinol derivative targeting mycolic acid transport in *Mycobacterium abscessus*. *Mol. Microbiol.* **101,** 515–529 CrossRef Medline
31. Point, V., Malla, R. K., Diomande, S., Martin, B. P., Delorme, V., Carriere, F., Canaan, S., Rath, N. P., Spilling, C. D., and Cavalier, J.-F. (2012) Synthesis and kinetic evaluation of cyclophostin and cyclipostins phosphonate analogs as selective and potent inhibitors of microbial lipases. *J. Med. Chem.* **55,** 10204–10219 CrossRef Medline
32. Liu, Y., Patricelli, M. P., and Cravatt, B. F. (1999) Activity-based protein profiling: the serine hydrolases. *Proc. Natl. Acad. Sci. U.S.A.* **96,** 14694–14699 CrossRef Medline
33. Elamin, A. A., Stehr, M., Spallek, R., Rohde, M., and Singh, M. (2011) The *Mycobacterium tuberculosis* Ag85A is a novel diacylglycerol acyltransferase involved in lipid body formation. *Mol. Microbiol.* **81,** 1577–1592 CrossRef Medline
34. Lakey, D. L., Voladri, R. K., Edwards, K. M., Hager, C., Samten, B., Wallis, R. S., Barnes, P. F., and Kernodle, D. S. (2000) Enhanced production of recombinant *Mycobacterium tuberculosis* antigens in *Escherichia coli* by replacement of low-usage codons. *Infect. Immun.* **68,** 233–238 CrossRef Medline

35. Viljoen, A., Blaise, M., de Chastellier, C., and Kremer, L. (2016) MAB_3551c encodes the primary triacylglycerol synthase involved in lipid accumulation in *Mycobacterium abscessus*. *Mol. Microbiol.* **102,** 611–627 CrossRef Medline
36. Daniel, J., Deb, C., Dubey, V. S., Sirakova, T. D., Abomoelak, B., Morbidoni, H. R., and Kolattukudy, P. E. (2004) Induction of a novel class of diacylglycerol acyltransferases and triacylglycerol accumulation in *Mycobacterium tuberculosis* as it goes into a dormancy-like state in culture. *J. Bacteriol.* **186,** 5017–5030 CrossRef Medline
37. Huygen, K., Lozes, E., Gilles, B., Drowart, A., Palfliet, K., Jurion, F., Roland, I., Art, M., Dufaux, M., and Nyabenda, J. (1994) Mapping of TH1 helper T-cell epitopes on major secreted mycobacterial antigen 85A in mice infected with live *Mycobacterium bovis* BCG. *Infect. Immun.* **62,** 363–370 Medline
38. Daniel, J., Maamar, H., Deb, C., Sirakova, T. D., and Kolattukudy, P. E. (2011) *Mycobacterium tuberculosis* uses host triacylglycerol to accumulate lipid droplets and acquires a dormancy-like phenotype in lipid-loaded macrophages. *PLoS Pathog.* **7,** e1002093 CrossRef Medline
39. Garton, N. J., Christensen, H., Minnikin, D. E., Adegbola, R. A., and Barer, M. R. (2002) Intracellular lipophilic inclusions of mycobacteria *in vitro* and in sputum. *Microbiol. Read. Engl.* **148,** 2951–2958 CrossRef Medline
40. Dhouib, R., Ducret, A., Hubert, P., Carrière, F., Dukan, S., and Canaan, S. (2011) Watching intracellular lipolysis in mycobacteria using time lapse fluorescence microscopy. *Biochim. Biophys. Acta* **1811,** 234–241 CrossRef Medline
41. Kalscheuer, R., and Steinbüchel, A. (2003) A novel bifunctional wax ester synthase/acyl-CoA:diacylglycerol acyltransferase mediates wax ester and triacylglycerol biosynthesis in *Acinetobacter calcoaceticus* ADP1. *J. Biol. Chem.* **278,** 8075–8082 CrossRef Medline
42. Peyron, P., Vaubourgeix, J., Poquet, Y., Levillain, F., Botanch, C., Bardou, F., Daffé, M., Emile, J.-F., Marchou, B., Cardona, P.-J., de Chastellier, C., and Altare, F. (2008) Foamy macrophages from tuberculous patients' granulomas constitute a nutrient-rich reservoir for *M. tuberculosis* persistence. *PLoS Pathog.* **4,** e1000204 CrossRef Medline
43. Santucci, P., Bouzid, F., Smichi, N., Poncin, I., Kremer, L., De Chastellier, C., Drancourt, M., and Canaan, S. (2016) Experimental models of foamy macrophages and approaches for dissecting the mechanisms of lipid accumulation and consumption during dormancy and reactivation of tuberculosis. *Front. Cell. Infect. Microbiol.* **6,** 122 Medline
44. Lehmann, J., Cheng, T.-Y., Aggarwal, A., Park, A. S., Zeiler, E., Raju, R. M., Akopian, T., Kandror, O., Bach, N. C., Sacchettini, J. C., Moody, D. B., Rubin, E. J., and Sieber, S. A. (2018) An antibacterial β-lactone kills *Mycobacterium tuberculosis* by infiltrating mycolic acid biosynthesis. *Angew. Chem. Int. Ed. Engl.* **57,** 348–353 Medline
45. Goins, C. M., Dajnowicz, S., Thanna, S., Sucheck, S. J., Parks, J. M., and Ronning, D. R. (2017) Exploring covalent allosteric inhibition of antigen 85C from *Mycobacterium tuberculosis* by ebselen derivatives. *ACS Infect. Dis.* **3,** 378–387 CrossRef Medline
46. Nguyen, P. C., Madani, A., Santucci, P., Martin, B. P., Paudel, R., Delattre, S., Herrmann, J.-L., Spilling, C. D., Kremer, L., Canaan, S., and Cavalier, J.-F. (2017) Cyclophostin and cyclipostins analogs, new promising molecules to treat mycobacterial-related diseases. *Int. J. Antimicrob. Agents* 10.1016/j.ijantimicag.2017.12.001 CrossRef Medline
47. Sambandamurthy, V. K., Derrick, S. C., Hsu, T., Chen, B., Larsen, M. H., Jalapathy, K. V., Chen, M., Kim, J., Porcelli, S. A., Chan, J., Morris, S. L., and Jacobs, W. R. (2006) *Mycobacterium tuberculosis* ΔRD1 ΔpanCD: a safe and limited replicating mutant strain that protects immunocompetent and immunocompromised mice against experimental tuberculosis. *Vaccine* **24,** 6309–6320 CrossRef Medline
48. Heckman, K. L., and Pease, L. R. (2007) Gene splicing and mutagenesis by PCR-driven overlap extension. *Nat. Protoc.* **2,** 924–932 CrossRef Medline
49. Kremer, L., Dover, L. G., Morbidoni, H. R., Vilchèze, C., Maughan, W. N., Baulard, A., Tu, S.-C., Honoré, N., Deretic, V., Sacchettini, J. C., Locht, C., Jacobs, W. R., Jr., and Besra, G. S. (2003) Inhibition of InhA activity, but not KasA activity, induces formation of a KasA-containing complex in mycobacteria. *J. Biol. Chem.* **278,** 20547–20554 CrossRef Medline
50. Vasilieva, E., Dutta, S., Malla, R. K., Martin, B. P., Spilling, C. D., and Dupureur, C. M. (2015) Rat hormone sensitive lipase inhibition by cyclipostins and their analogs. *Bioorg. Med. Chem.* **23,** 944–952 CrossRef Medline
51. Kremer, L., Guérardel, Y., Gurcha, S. S., Locht, C., and Besra, G. S. (2002) Temperature-induced changes in the cell-wall components of *Mycobacterium thermoresistibile*. *Microbiol. Read. Engl.* **148,** 3145–3154 CrossRef Medline
52. Coxon, G. D., Craig, D., Corrales, R. M., Vialla, E., Gannoun-Zaki, L., and Kremer, L. (2013) Synthesis, antitubercular activity and mechanism of resistance of highly effective thiacetazone analogues. *PLoS One* **8,** e53162 CrossRef Medline
53. Kabsch, W. (2010) Integration, scaling, space-group assignment and post-refinement. *Acta Crystallogr. D Biol. Crystallogr.* **66,** 133–144 CrossRef Medline
54. Sanki, A. K., Boucau, J., Umesiri, F. E., Ronning, D. R., and Sucheck, S. J. (2009) Design, synthesis and biological evaluation of sugar-derived esters, α-ketoesters and α-ketoamides as inhibitors for *Mycobacterium tuberculosis* antigen 85C. *Mol. Biosyst.* **5,** 945–956 CrossRef Medline
55. Adams, P. D., Afonine, P. V., Bunkóczi, G., Chen, V. B., Echols, N., Headd, J. J., Hung, L.-W., Jain, S., Kapral, G. J., Grosse Kunstleve, R. W., McCoy, A. J., Moriarty, N. W., Oeffner, R. D., Read, R. J., Richardson, D. C., *et al.* (2011) The Phenix software for automated determination of macromolecular structures. *Methods* **55,** 94–106 CrossRef Medline
56. Emsley, P., Lohkamp, B., Scott, W. G., and Cowtan, K. (2010) Features and development of Coot. *Acta Crystallogr. D Biol. Crystallogr.* **66,** 486–501 CrossRef Medline

Mycobacterium abscessus est une bactérie environnementale non-tuberculeuse causant des infections pulmonaires sévères chez les patients atteints de mucoviscidose. Sa résistance intrinsèque aux antibiotiques rend les infections à *M. abscessus* extrêmement difficiles à traiter. Ses mécanismes de résistance sont variés et incluent des pompes à efflux expulsant les antibiotiques ainsi que des enzymes modifiant leurs cibles. La trithérapie standard contre *M. abscessus* implique un aminoglycoside (amikacine (AMK)), une β-lactamine (imipénème (IPM)) et un macrolide (clarithromycine (CLR) ou azithromycine (AZM). Ma thèse a porté sur la régulation de nouveaux mécanismes d'antibiorésistance *via* des pompes à efflux de la famille MmpL ainsi que sur une enzyme modifiant la cible des macrolides. La sélection de mutants résistants aux dérivés du thiacétazone (TACd) et à la clofazimine (CFZ) a permis d'identifier des mutations dans les régulateurs TetR MAB_4384 et MAB_2299c, respectivement. Les mutants CFZ, également co-résistants à la bédaquiline (BDQ), surexpriment deux MmpS/MmpL distincts, MAB_1135c/1134c et MAB_2300/2301 tandis que les mutants TACd surproduisent le système MmpS/MmpL MAB_4383c/4382c. Des approches biochimiques, génétiques et structurales ont confirmé le rôle de ces protéines dans la résistance à ces composés et ont permis de disséquer le mode de régulation. Ainsi, MAB_2299c représenterait un marqueur de résistance à exploiter chez des patients traités par CFZ ou BDQ. La méthyltransférase Erm(41) modifie l'adénosine 2058 de l'ARNr 23S du ribosome, bloquant l'action des macrolides. WhiB7 serait l'activateur de cette résistance inductible observée chez 40% des isolats cliniques, conduisant souvent à l'échec thérapeutique. Nous avons confirmé le rôle de WhiB7 dans ce mécanisme et montré que la résistance inductible opérait *in vivo* chez le modèle zebrafish. Nos résultats indiquent que l'AZM induit une résistance plus rapide et forte que la CLR *in vitro* et qu'elles exercent un effet antagoniste sur l'AMK, réduisant l'efficacité du traitement. Ces travaux décrivent l'export d'antibiotique *via* des MmpL et la résistance adaptative aux macrolides chez *M. abscessus*. Enfin, ils apportent des nouveaux outils génétiques performants pour étudier la fonction de protéines d'intérêt *via* une nouvelle technique de délétion génique et pour tester rapidement de nouveaux antibiotiques contournant la résistance induite aux macrolides.

Mycobacterium abscessus is an environmental non-tuberculous mycobacteria causing severe lung infections in cystic fibrosis patients. Its intrinsic resistance to antibiotics renders treatments extremely challenging. This pathogen has developed a wide panel of strategies to resist to antibiotics, including efflux pumps and target-modifying enzymes. Standard antibiotherapy combines an aminoglycoside (amikacin (AMK)), β-lactams (imipenem (IPM)) and macrolides (clarithromycin (CLR) or azithromycin (AZM)). My thesis was focusing on the regulation of antibiotic resistance mechanisms involving efflux pumps from the MmpL family as well as an enzyme modifying the macrolide target. Selection of resistant mutants against thiacetazone derivatives (TACd) and clofazimine (CFZ) unraveled mutations in the TetR regulators MAB_4384 and MAB_2299c, respectively. The CFZ-mutants, also co-resistant to bedaquiline (BDQ), overexpress two distinct MmpS/MmpL, MAB_135c/1134c and MAB_2300/2301 while the TACd mutants overproduce the MAB_4383c/4382c efflux pump. Biochemical, genetic and structural approaches confirmed their involvement in drug resistance mechanisms. MAB_2299c could therefore represent a potential resistance marker to monitor in strains isolated from patients under CFZ/BDQ therapy. The methyltransferase Erm(41) modifies the adenosine 2058 of the ribosomal 23S rRNA, protecting the ribosome from the macrolides. WhiB7 may represent a major actor in inducible resistance, observed in 40% of clinical cases, often leading to treatment failure. We confirmed the role of WhiB7 in this process and showed that inducible resistance occurred also *in vivo* in the zebrafish model. Our data suggest that AZM is a stronger and faster resistance inducer than CLR *in vitro* and that both drugs show antagonism with AMK, thus reducing drugs' efficacy. This work enriched our knowledge regarding both MmpL-mediated and macrolides inducible resistance mechanism against *M. abscessus*. It also provides new efficient tools to investigate the function of proteins through a novel unmarked gene deletion approach and to rapidly assay new antibiotics to counteract inducible macrolide resistance.